NHMFL

National High Magnetic Field Laboratory

1996 Annual Report

Operated by:
Florida State University
University of Florida
Los Alamos National Laboratory

Supported by:
National Science Foundation
State of Florida

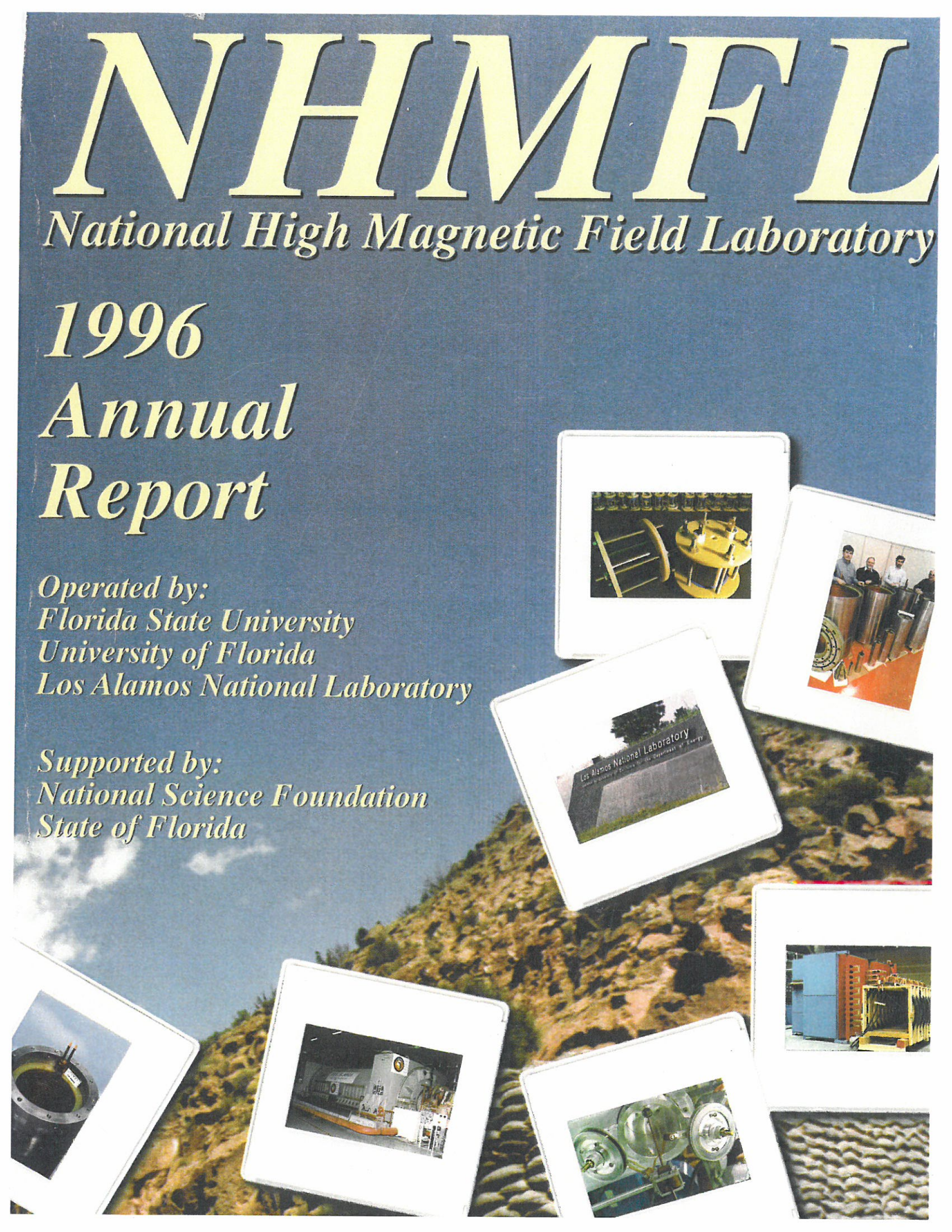

NHMFL

National High Magnetic Field Laboratory

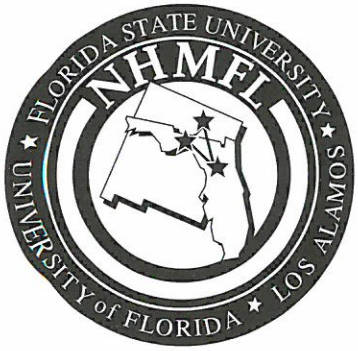

1996 Annual Report

Operated by:
Florida State University
University of Florida
Los Alamos National Laboratory

Supported by:
National Science Foundation
State of Florida

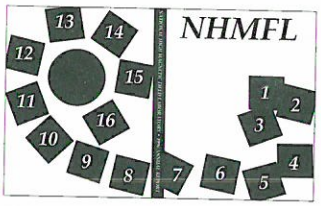

ON THE COVER:
Pulsed magnet activities at the Los Alamos and Tallahassee sites.

1. Two 50 T pulsed field coils with a series of small test coils in the background.

2. The complete set of nine coils for the 60 T quasi-continuous magnet are ready for nested assembly. From left to right are Jim Sims, Don Parkin, Larry Campbell, and Dwight Rickel.

3. Los Alamos National Laboratory, site of the NHMFL Pulsed Field Facility.

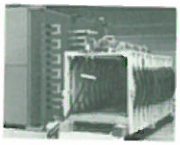

4. Massive inductance and resistance loads used to commission the 560 MW pulsed power converters at NHMFL, Los Alamos.

5. Rotating bobbins wrap insulation on a high strength, high conductivity conductor prior to it being wound into a pulsed magnet.

6. The 1.43 GVA motor-generator at Los Alamos. The generator will be used to power the 60 T quasi-continuous and non-destructive 100 T magnets.

7. The fifth coil of the nested nine-coil quasi-continuous magnet. The complete magnet system will store 90 MJ when energized to 60 T.

8. The seal of the NHMFL, a symbol of multi-university – national laboratory cooperation.

9. One of the seven 80 MW pulsed power converters to be used for the 60 T quasi-continuous and non-destructive 100 T magnets.

10. Prototype pulsed magnet being built for Pegasus Tokamak fusion reactor, University of Wisconsin.

11. George Schmiedeshoff, Alex Lacerda, and Jeff Goettee review preparations in the underground bunker control room at Los Alamos prior to their flux compression shot.

12. The volcanic tuff cliffs surrounding the explosive flux compression site at Los Alamos. The cavities are a result of both natural erosion and occupation by earlier peoples.

13. Fiberglass reinforcement being applied to a pulsed field test magnet.

14. Bob Clark, Director of the National Pulsed Magnet Laboratory of Australia, lowering the He-4 cryostat into the 1,000 tesla MC-1 flux compression generator during the Dirac series at Los Alamos.

15. Entrance to the designated NHMFL bunker at Los Alamos that is used for explosive flux compression shots. The bunker contains full life-support systems.

16. Prototype pulsed magnet tested to destruction to verify code predictions and test strengthening options.

This document is available upon request in alternative formats for individuals with print-related disabilities.

National High Magnetic Field Laboratory
1800 East Paul Dirac Drive
Tallahassee, Florida 32310

Phone: (904) 644-0311
Fax: (904) 644-9462
e-mail: *patten@magnet.fsu.edu*
World Wide Web: *http://www.magnet.fsu.edu/*

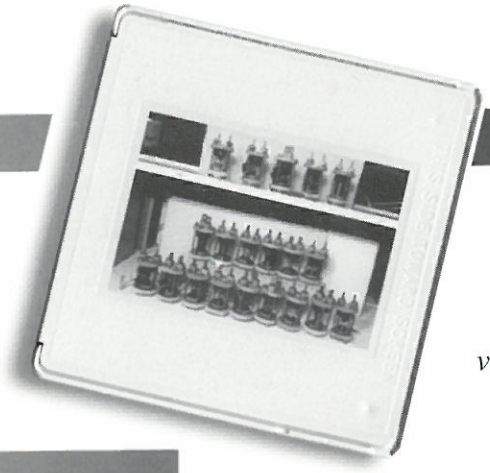

TABLE OF CONTENTS

APPENDIXES

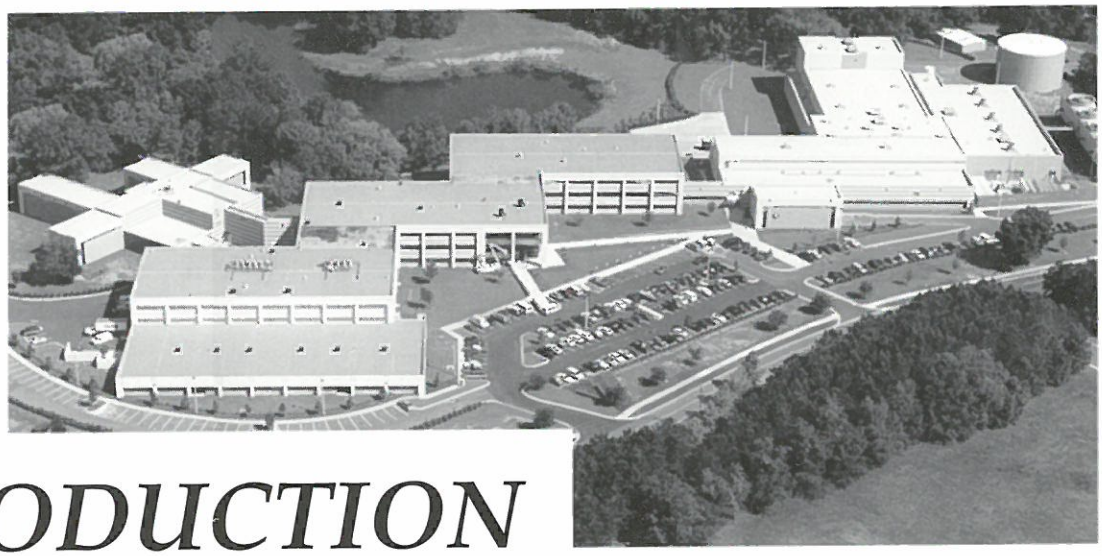

INTRODUCTION

If they build the laboratory, will they build it right? Can they attract truly outstanding in-house faculty? Will they be able to design and build state-of-the-art magnets? When the laboratory is built, will the users come to conduct their research? Can this unique federal/state and multi-institutional partnership be successful?

These were some of the frequently asked questions just five to six years ago after the National High Magnetic Field Laboratory (NHMFL) was awarded to the consortium of Florida State University, the University of Florida, and Los Alamos National Laboratory. As the NHMFL completes its sixth year of existence and its second year of full operations, the answers to the above questions are a resounding *yes*.

The year 1996 began with the successful renewal of the core grant for the next five years from the National Science Foundation (NSF), and with it came the recognition that the NHMFL had come into its own. The stage is set for a challenging and exciting second phase to push the frontiers of science and technology in the highest available magnetic fields. The panel of peers commissioned by the NSF to review the NHMFL renewal proposal was unanimous in its praise of the laboratory: "In a short period of time, the NHMFL already has become an internationally respected institution. The scientific potential is enormous." The NSF renewal grant represents an increase of almost fifty percent over the initial award and sustains the extraordinary and model partnership that the NHMFL has forged with federal and state governments, multiple federal agencies and academic institutions, and the private sector.

There are almost fifty more research reports in this year's annual report as compared to last year's document. Users are responding to increased demand by making more effective use of their magnet time, and they are getting more data at higher fields in less time. Some of the research featured in this report are:

- advances in very high field solid state NMR to 25 T, including high T_c superconductors and low dimension organic materials;

The NHMFL will ensure the science and technology competitiveness of the United States in high magnetic field research well into the next century. Its scientific potential is enormous.

—William Harris, NSF's Former Assistant Director for Mathematical and Physical Sciences, February 23, 1996

- new evidence for quantum Hall behavior at high fields in quasi-three dimensional materials;
- millimeter wave spectroscopy to measure cyclotron resonance and magneto-conductivity in highly anisotropic metals.

The year also began with the NHMFL setting its third world record for the highest continuous magnetic field produced by a resistive magnet attaining 33.6 tesla (T) in a 32 millimeter (mm) diameter bore on February 5, 1996. Within hours of commissioning this new resistive magnet, an in-house research team led by FSU physicist James Brooks used a dysprosium probe to concentrate the flux, enhance the field to 36.2 T, and measure the Shubnikov-de Haas effect in an organic superconductor κ-(BEDT-TTF)$_2$Cu(NCS)$_2$ in its normal state. The 33 T has continued to run routinely throughout the year.

The resistive magnetic field record was made possible through two successful developments: the new technology of the "Florida-Bitter" design applied in a poly-Bitter configuration; and the equally important cooperation between the Japanese National Research Institute for Metals (NRIM) and the NHMFL that resulted in a very advanced Cu alloy, consisting of Ag nanofilaments in CuAg matrix, that could be used as conductor material for the two innermost coils. This material combines, in a unique manner, high mechanical strength with high electrical and thermal conductivity and is the ideal conductor for very high field magnets. The material was developed by NRIM and made available to the NHMFL in the framework of a continuing cooperation.

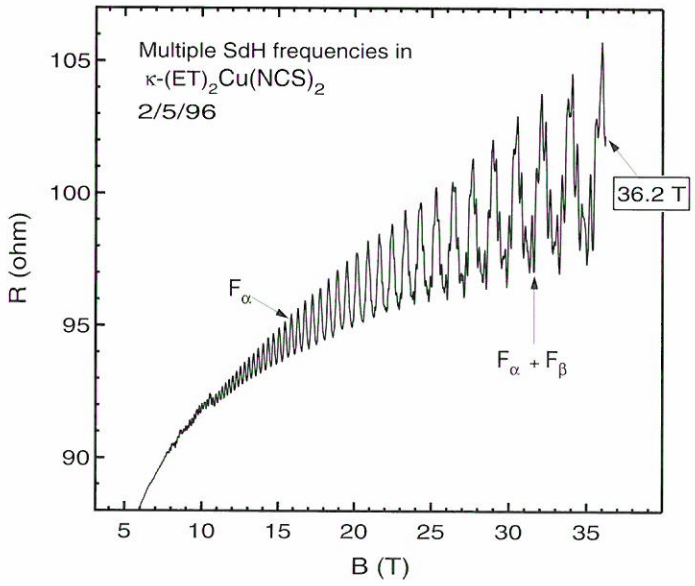

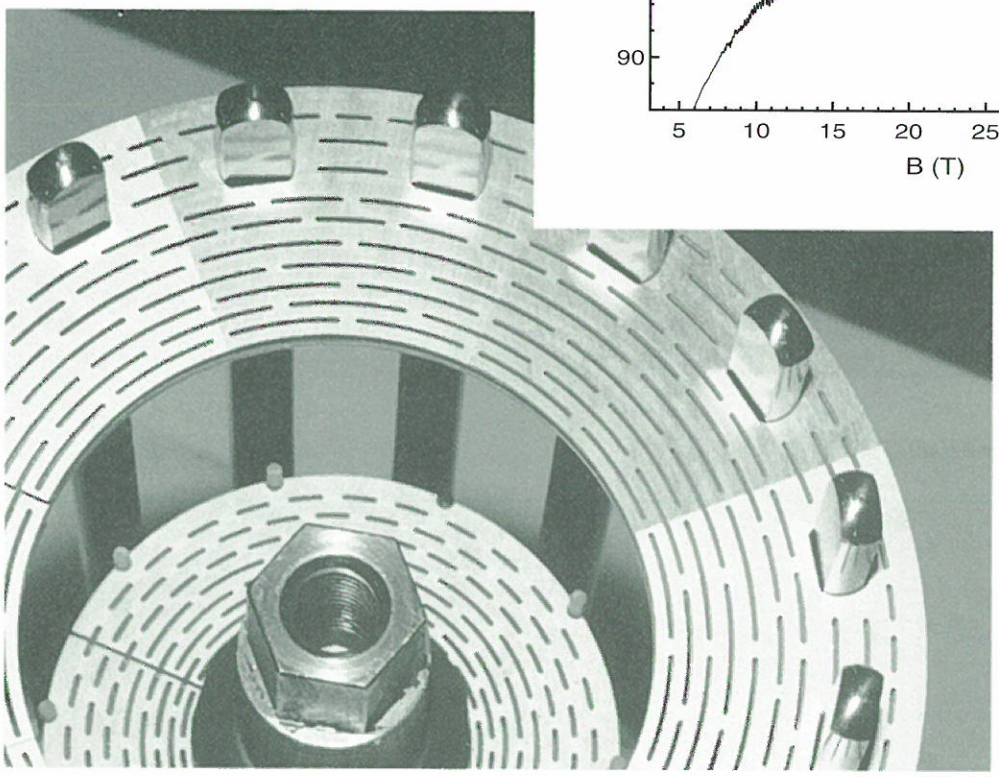

Measurements of the Shubnikov-de Haas effect to 36.2 T (above). These results were attained by using a dysprosium probe to concentrate the flux in the record-setting 33 T resistive magnet that used the "Florida-Bitter" coil design (left).

The resistive magnets developed by the NHMFL have achieved extraordinary longevity in their usage. For example, the two 30 T magnets have now performed continuously without interruption: one for over 1,900 hours of operation (6,500 megawatt (MW) hours) and the other for 1,500 hours (6,300 MW hours).

The NHMFL has opened a new capability for condensed matter physics by using high field resistive magnets to perform NMR studies of high T_c superconductors, quantum wells, glassy structures, and other solid state systems. These new research opportunities have been made possible by the high level of stability and low ripple and noise (approximately 5 parts per million (ppm)) of the 40 MW DC power supply and better temperature control of the coolant water. The re-engineering of existing resistive magnet designs has achieved improved homogeneity of 2 ppm over a 2 millimeter (mm) diameter sample volume. Physicists at the NHMFL led by William Moulton have extended condensed matter NMR research to fields of 25 T to 30 T in resistive magnets—higher than at any other laboratory in the world. Users from the United States and Europe have been lining up to use this unique NMR magnet system.

World record high magnetic fields, however, were not limited to resistive magnets. The National Center for Ion Cyclotron Resonance (ICR) Mass Spectrometry commissioned and made available to users the world's highest field ICR system, a 9.4 T, 210 mm warm bore magnet. The State of Florida, in the spirit of its official partnership with the NSF, appropriated $1.5 million to develop and build a new world-record 15/17 T, ICR magnet to be delivered in 1998. The NHMFL also has established the world's highest field, high resolution electron magnetic resonance (EMR) spectrometer, 15/17 T, and sixteen research groups with scientific interests in physics, chemistry, and biology used the EMR facility during the first year of operation.

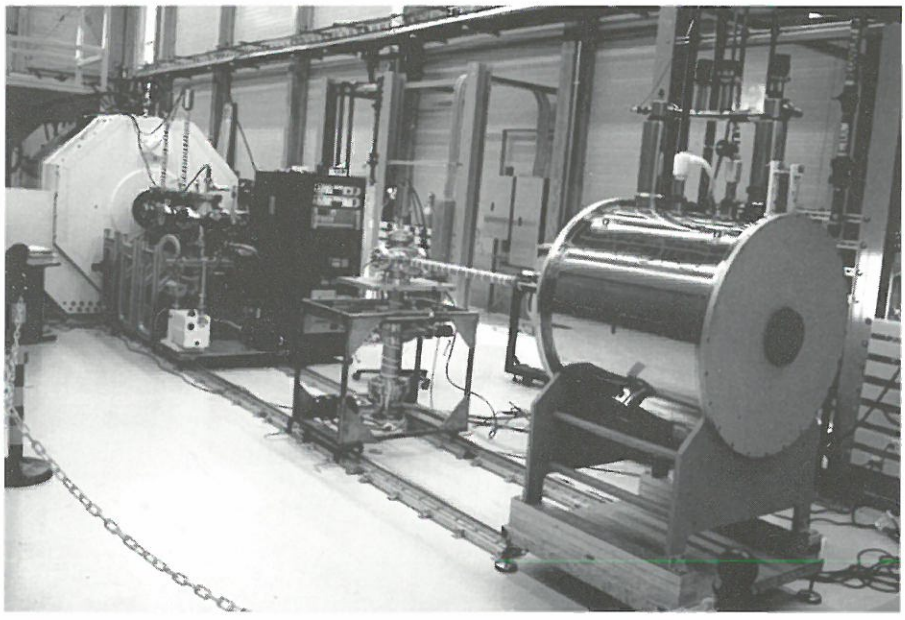

The 9.4 T FT-ICR mass spectrometer at the NHMFL. The large object just left of center is the shielded 9.4 T magnet. The darker objects in the center are the electrospray ion source and system controls. A 6 T, 150 mm bore magnet is shown on the right.

Furthermore, in-house faculty member and FSU chemist, Alan Marshall, demonstrated that Fourier transform ion cyclotron resonance (FT-ICR) could be achieved at twice the world record high-field *superconducting* FT-ICR magnet strength (9.4 T at the NHMFL) in a *resistive* 20 T magnet. Although a resistive magnet has a low spatial homogeneity (1000 ppm) and narrow bore (50 mm diameter), Marshall was able to produce mass

resolving power of 10,000 at mass-to-charge (m/Z) of 1185 from a peptide, luteinizing-releasing hormone. These results provide additional inspiration for pursuit of truly high-performance FT-ICR mass spectrometry at 20 T and above.

The preliminary successes with exploratory research projects using the powered magnets for magnetic resonance studies help demonstrate the unique potential at the NHMFL in providing facilities in support of magnetic resonance beyond the capacity presently available anywhere. This new opportunity was the basis of a successful proposal submitted to the W.M. Keck Foundation to partially fund the establishment of a dedicated magnet for high resolution studies. The W.M. Keck Foundation of Los Angeles, California, in June awarded $600,000 to Florida State University and the University of Florida for a state-of-the-art, high-field, resistive magnet system that will be designed, built, and used at the NHMFL. The Keck grant will be matched by over $1.5 million from the NHMFL and the universities. The magnet system will feature an innovatively-designed 25 T, high resolution, resistive magnet equipped with new specialized instruments for nuclear magnetic resonance (NMR), EMR, and ICR. Until now, NMR, EMR, and ICR research has generally been conducted in superconducting magnet systems that could reach only about 17 T.

The NHMFL Pulsed Field Facility at Los Alamos can now accommodate four concurrent experiments with the installation of new equipment. The newest pulsed magnet produces 40 T in 24 mm over a long pulse length of 500 milliseconds. Los Alamos has continually provided outside users access to flux compression experiments. This year the NHMFL assisted in hosting a group of international scientists with the unprecedented opportunity to perform experiments in fields approaching 1000 T in the *Dirac Series.* These experiments originated from an international collaboration of scientists from Russia, Japan, Australia, and the United States, including NHMFL experimentalists James Brooks and Alex Lacerda. The experiments were sponsored by an inter-agency cooperation comprising the U.S. State Department, Department of Energy, and the NSF. Some of the initial planning for the *Dirac Series* occurred at a 1995 workshop, *Science Opportunities At and Beyond 1000 T*, hosted by the NHMFL in Tallahassee. The series used specially-designed flux compression Russian MC-1 generators (1000 T generators) provided by Arzamas-16 laboratory. The NHMFL Pulsed Field staff and the 50 T magnets provided important set-up, staging, and calibration for most of the *Dirac* experiments.

Bob Clark, Director of the National Pulsed Magnet Laboratory of Australia, prepares a Dirac Series experiment at LANL.

Six main experiments were pursued in the *Dirac Series*: (1) a search for quantum limit phenomena in two-dimensional organic metals and the search for new phenomena beyond that limit; (2) an attempt to observe high-magnetic-field-induced superconductivity, a theoretically predicted phenomena that is yet to be validated by experiment; (3) several experiments to observe a field-induced transition to metallic behavior in several Kondo insulators; (4) use of the Zeeman effect to break one bond of a quadruple bonded transition metal complex, a novel use of magnetism in chemistry;

(5) exploration of the Faraday rotation in samples containing the ions Eu^{3+} and Sm^{3+}, which should provide level-crossing benchmarks for calibrating ultra-high magnetic fields, independent of the media in which the ions are embedded; and (6) an exploration of the nonlinear Faraday rotation in CdMnTe at low temperatures and ultra-high fields. The Russian collaborators from Arzamas propose to furnish an additional twelve 1000 T generators over the next two years, with six experiments to be conducted at Arzamas and six at Los Alamos.

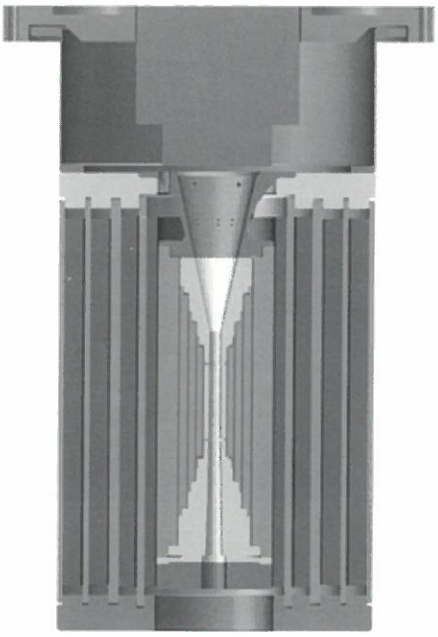

The 60 T quasi-continuous magnet at LANL.

The nine coils for the 60 T quasi-continuous magnet have been assembled and this new magnet system will be tested in early 1997. The commissioning is being completed for three AC-DC power converters. A total of seven converters will be installed and will energize the 60 T quasi-continuous magnet at Los Alamos. These converters are powered by the Los Alamos 1430 MVA motor-generator and have a combined DC power rating of 240 MVA for two seconds. When connected to the magnet, these converters will generate new science opportunities by providing controlled pulse shapes for long durations, approximately 100-200 milliseconds, at the extremes of magnetic fields only previously available in capacitive-driven magnets and only for short intervals. This formidable power capacity will more than double with the addition of four more converters that will arrive in 1997. A cooperative program also has been established between the NSF and the Department of Energy to develop a non-destructive 100 T magnet with a 24 mm liquid nitrogen bore for the NHMFL Pulsed Field Facility. A combined design team including engineers from the NHMFL and Los Alamos National Laboratory have initiated an engineering design of this new, unique, and extremely challenging magnet system. To achieve this goal of a non-destructive 100 T magnetic field for increased time durations (approximately 1,000 times longer than previously available) and in larger volumes than generally available, will require innovative designs and the utilization of extremely high-strength materials.

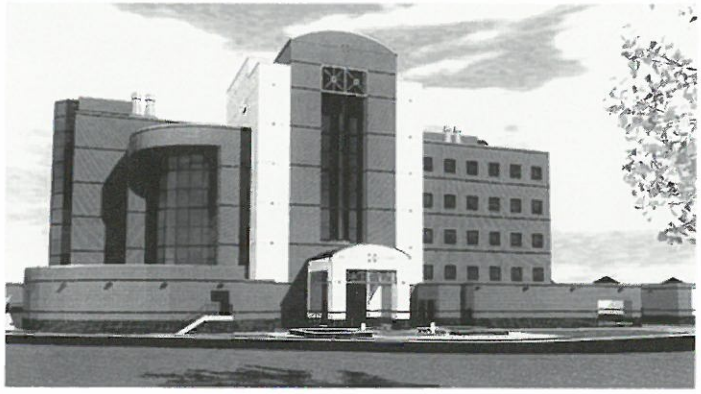

Architectural rendering of the University of Florida Brain Institute, scheduled for completion in 1998.

At the University of Florida, the Brain Institute, in cooperation with the NHMFL, has secured $5 million in supplemental funding to support the development and fabrication of the 12 T, 40 centimeter (cm) warm bore, magnetic resonance system for small animal imaging and spectroscopy research. A new 3 T, 80 cm bore whole-body system for magnetic resonance imaging (MRI) and MRI spectroscopy was installed in the fall of 1996 in cooperation with the Brain Institute. The system already has given exquisite head images and angiograms of unrivaled resolution during its testing and development phase. The

NHMFL Ultra-High B/T Facility in Gainesville put its dilution refrigerator into operation and installed many small parts that will allow immediate use of the facility as soon as the high field magnet is delivered, which is anticipated in 1997.

At the NHMFL in Tallahassee, the world's only wide bore 600 MHz NMR spectrometer was installed. This unique warm bore (89 mm) research instrument has produced significant analysis in high resolution, multinuclear studies of liquids, and *in vivo* spectroscopy of biological preparations. A new 400 MHz, 89 mm bore, high sensitivity spectrometer was delivered and is available to users. Varian and Conductus have designated the NHMFL as a beta test site for a new, jointly developed, two-channel spectrometer that uses a detector made of high T_c superconducting material that will enhance the signal to noise of this spectrometer to five to ten times that available in conventional spectrometers of this size. There are many exciting opportunities to improve the capacity of magnetic resonance technology through the development of innovative probes, detector systems, and experimental techniques, for example, optically enhanced polarization, which is proving so effective in both medical and non-medical applications. The NHMFL looks forward to expanding its cooperation with the private sector and to responding further to the scientific and technological challenges for advanced instrumentation and systems.

An in-house research program, which was included in the NSF charges to the laboratory, was initiated this year that (1) utilizes the NHMFL facilities to carry out high quality research at the forefront of science and engineering; and (2) advances the NHMFL facilities and scientific and technical capabilities. The in-house research program, which funds projects for one to two years, encourages collaborations across host-institutional boundaries and between internal and external investigators. It also encourages high risk research projects that have significant opportunities to extend scientific experimentation into new areas. All proposals are peer reviewed by the NHMFL In-house Research Program Committee and by a panel of external reviewers. The peer-review process was developed and conducted in cooperation with the NSF. Sixty-seven research proposals were submitted by the three participating institutions and fifteen were selected for the first year of funding. Program solicitations will be at least once yearly.

The science and technological impact of the NHMFL continues to grow at a remarkable pace. Individual reports summarizing the science activities and previewing the scientific output of the researchers and users of the NHMFL are contained in *Part One: Research Reports* of this NHMFL Annual Report (Chapter 1: Science Research Reports and Chapter 2: Magnet Science & Technology Reports). This year, the second year of operation of the NHMFL, also has seen significant growth in user driven science activities. This growth is reflected in the increased number of reports submitted by users for this Annual Report. Within the magnet science and technology area, there have been significant accomplishments beyond the ongoing successes associated with magnet development projects initiated in previous years, for example, the 45 T hybrid magnet project; Phase I of the 1.1 GHz (25 T) high resolution NMR magnet development effort which has completed the engineering design study for the ultra wide bore 900 MHz NMR magnet; the near completion of the 60 T quasi-continuous pulsed magnet; and continued advancement of the resistive magnet program. A significant new challenge, the 100 T, 24 mm bore non-destructive pulsed magnet project, represents a new and expanded partnership between the NSF and the Department of Energy built around the Florida-Los Alamos partnership.

The NHMFL has set as one of its strategic goals for the next five years the expansion of cooperative efforts with the private sector by enhancing the effectiveness of the NHMFL's Industrial Affiliates Program as a bridge to instituting important public-private sector partnerships. The NHMFL and its participating institutions have developed unique research and development capacity for exploring new science frontiers, testing and characterization of new materials, and advancing magnet technology in response to science and technology driven challenges. This unique R&D capacity, along with the human resources within the laboratory consortium, represents an unequaled asset that can respond effectively to technological opportunities in magnet-related areas.

The NHMFL continues to foster partnerships with the private sector that promote economic competitiveness and technology transfer. This commitment to public-private sector partnerships is symbolized by the cooperative research and development agreement (CRADA) established this year between the NHMFL and EURUS Technologies, Inc.® EURUS, which represents state-of-the-art expertise in high temperature superconductor (HTS) current leads and materials technology, and the NHMFL initiated a program to co-develop and test an ultra-high current lead utilizing the remarkable properties of high temperature superconductivity. Successful tests were conducted at the NHMFL on a 10,000-amp-class, encapsulated, high temperature superconducting current lead that will culminate in the production of the world's first commercially available lead of this class. These HTS leads will be suitable for deployment in ultra-high magnetic field applications, such as in magnetic energy storage and in new magnet systems for materials processing. EURUS will be relocating its headquarters to Tallahassee in early 1997 and will be located directly across the street from the NHMFL.

The NHMFL's Industrial Affiliates Program is a bridge to instituting important public-private sector partnerships. Pictured are representatives of EURUS Technologies, Inc. and NHMFL.

In addition to the CRADA with EURUS, a cooperative development contract with Intermagnetics General Corporation (IGC) was negotiated and signed that provides a $1 million contribution to the 900 MHz large bore NMR magnet system. The 900 MHz will achieve the highest field attainable with commercially available conventional superconductors (NbTi and Nb_3Sn) in an extra-large and room temperature bore (110 mm).

The NHMFL is building a 30 T resistive Florida-Bitter magnet for the National Research Institute for Metals (NRIM) in Tsukuba, Japan, through a contract with Toshiba America, Inc. The main difference between this new magnet and 30 T magnets at the NHMFL is that the coils are designed to match the pumps and power supplies of the NRIM. The innermost coil is constructed of a copper-silver alloy sheet developed at NRIM and is similar to those used in the initial world record testing of the 33.6 T powered magnet at the NHMFL earlier in 1996.

Early in the year the laboratory co-hosted an international workshop with the NRIM on *High Magnetic Fields: Industry, Materials & Technology.* The Tallahassee conference was the second in an ongoing series of deliberations with the Japanese laboratory on magnet science and technology. The workshop explored magnet technologies with a look to future opportunities for promoting new applications, such as energy storage, particle accelerators, fusion, magnetic separation, materials processing, and magnetic imaging of materials. Many industry representatives participated in the conference, including Lockheed-Martin, Bechtel, Intermagnetics General, Siemens, Kobe Steel, Toshiba, Hitachi, and Oxford Instruments. The proceedings of this conference will be published by World Scientific Publications.

This year also was noteworthy in recognizing the accomplishments and achievements of the faculty and staff of the NHMFL.

- Zachary Fisk, NHMFL faculty member and physics professor at FSU was elected to the National Academy of Sciences.
- Robert Schrieffer, NHMFL Chief Scientist and the University System's First Eminent Scholar, was appointed by President Clinton to serve on the Committee on the National Medal of Science. Dr. Schrieffer also served as the President of the American Physical Society during 1996.
- Alan Marshall, director of the National FT-ICR Mass Spectrometry Facility at the NHMFL, was selected to receive the 1997 Maurice F. Hasler Award given by the Spectroscopy Society of Pittsburgh.
- Don Parkin, the NHMFL co-principal investigator, was awarded a Los Alamos Distinguished Performance Award for his leadership of LANL's materials science efforts over the past ten years, including the development of new initiatives such as the Many-body Theory Fellows program in correlated electron materials, and other new programs developed in cooperation with Department of Energy/Office of Basic Sciences.
- Pierre Ramond, a member of the NHMFL extended faculty at the University of Florida and director of the Institute for Fundamental Theory, was recognized with the university's highest internal award, Scholar/Teacher of the Year.
- Russ Bowers, also of the University of Florida, was one of only four experimental physical chemists (out of seventeen nominees) to win an NSF Career Award.
- Nick Bonesteel, NHMFL faculty and FSU assistant professor of physics, received a Sloan Research Fellowship.
- NHMFL faculty and collaborators at the University of Florida, FSU, and Florida Agricultural and Mechanical University submitted five proposals to the NSF's peer-reviewed Academic Research Infrastructure program and all five were funded for a total of $2,230,000 with the state and institutions providing matching funds in excess of this figure.

Educational activities and public outreach have always been high in priority among faculty and staff of the laboratory. This year, however, the NHMFL officially inaugurated its K-12 educational outreach programs with the hiring of a science educator, Sam Spiegel, to direct its many activities. It was an *outstanding* first year. Approximately 12,000 individuals toured the NHMFL in 1996, and a large percentage of these were K-12 students. Our educational tours include a lecture with hands-on demonstrations and an overview of the general science and technology being investigated at the facility. Many of the K-12 visitors came from outside the immediate area and throughout Florida. A new outreach effort takes the science and resources of the laboratory to K-12 schools in the region, allowing us to extend and enhance scientific awareness well beyond the NHMFL. With a series of

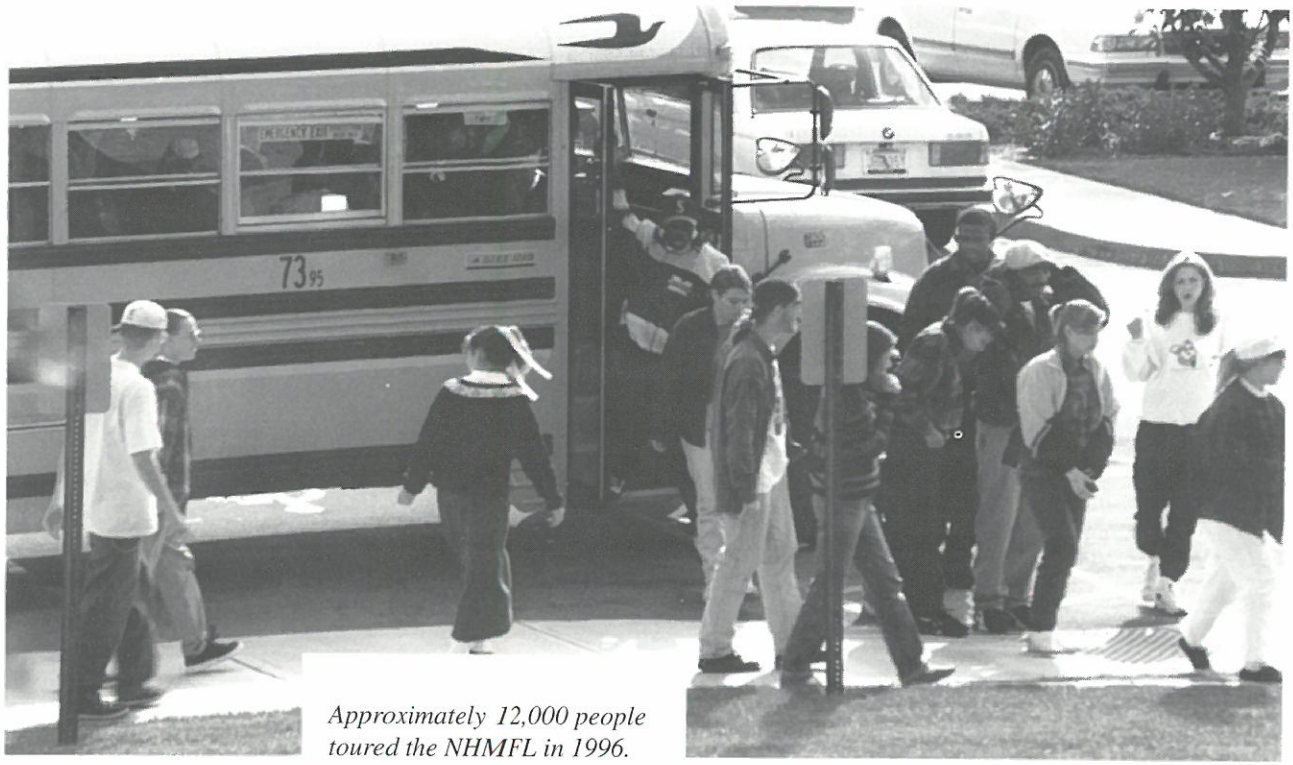

Approximately 12,000 people toured the NHMFL in 1996.

presentations and workshops such as *What Does a Scientist Do?, Magnets — What's the Attraction?,* and *What's Matter — Molecules, Resistance, and Superconductivity,* the NHMFL challenged over 3,000 young students this year to "look, think, ask, and solve" as they explore the magnetic world around them.

For the second consecutive year we participated in a middle school mentorship program in which twenty-four local students spent one morning a week for a semester at the NHMFL working with a scientist mentor on a research project. As one parent stated, "My daughter entered the program hesitantly, but after the first week she was so enthralled that she is now considering a career in computers or science." After completing their research projects, the students will present their research results in a mini-science conference in early January 1997. The students will give ten to fifteen minute oral presentations, and the conference will be attended by partners, school administrators, and the press.

This past summer, we initiated the STAR TREE program (**S**cience **T**eachers **a**nd **R**esearchers **T**ranslating **R**esearch **E**xperiences into **E**ducational Materials) with a grant from the Florida Department of Education. Nine master middle school science teachers came to NHMFL to work alongside scientists, educators, and staff. They produced a comprehensive program of prototype middle school materials that guides educators and students to a greater understanding of magnetism and related concepts. In conjunction with this grant, the NHMFL developed a teacher/student resource laboratory with state-of-the-art multimedia development equipment, manipulative experiments, curriculum materials, and instructional resources. This laboratory has become a popular instructional and development resource for regional schools.

Keiko Harris participated in the 1996 NHMFL Minority/Women Summer Internship Program.

For the fourth consecutive year, the NHMFL sponsored its Minority/Women Summer Internship Program. Interest in the program has continued to grow significantly, with applications coming from twenty-seven states. Twenty candidates for the summer research program were selected and sixteen undergraduate students accepted offers and participated in the program at all three consortium sites. One of the interns worked with a condensed matter experimentalist, James Brooks, and is listed as a second author on a paper to be published in *Application of High Magnetic Fields in Semiconductor Physics* (World Press, 1997).

The NHMFL and Florida A&M University co-hosted the Fourth Annual NSF Alliances for Minority Participation (AMP) Student Research Conference during the summer. Over 150 college students from throughout the United States and Puerto Rico, along with AMP project directors and NSF officials, attended the three-day conference in Tallahassee. The conference included thirty-four research presentations by the college students along with a few invited lectures given by distinguished scientists. The research presentations were judged and awards given to some of the most significant projects.

A new course for college science educators, *Magnetic Fields in Science and Technology*, was offered at the NHMFL as a part of NSF's National Chautauqua Short Course. Twenty-one individuals received lectures on the generation of magnetic fields, the application of magnet technology, and various magnetic resonance techniques. This program will be continued in future years.

Overall this has been another outstanding year for the NHMFL. The renewal was awarded during a time of great uncertainly in federal budget considerations, the users programs continued to grow, the In-House Research Program was initiated, new facilities were commissioned, and private sector partners continued to develop. This Annual Report provides a comprehensive summary of these activities and has been structured to aid the reader in locating areas of interest. The faculty and staff of the NHMFL would like to thank the NSF and members of the NSF Review Committee for their vote of confidence in our efforts to respond to the scientific and technological needs of our users. We also want to thank the State of Florida for its continued support of this unique federal-state partnership, and to acknowledge the growing inter-agency partnership reflected in the support provided by the Department of Energy.

PART ONE
Research Reports

SCIENCE RESEARCH REPORTS

Chapter 1

Overview

The year 1996 witnessed continued rapid growth in the scope and level of activity of research on all three sites of the NHMFL. The number of Science Program reports continued to increase, from 136 in 1995 to 180 in 1996, a growth of 32%. The total number of reports, including the Science Research and Magnet Science and Technology reports found in the next chapter, also increased, from 193 to 239 in this period.

More impressive than the number, however, is the increase in the range of topics under investigation and the importance of the results being obtained, both by users of the facilities and by in-house scientists. While it is impossible to present a balanced summary of these reports in several pages, we have chosen a few nuggets to illustrate the breadth and excellence of the Science Program at the NHMFL. The reader is encouraged to browse through the individual reports to gain a more complete impression of the richness and creative importance of these works, which in many cases interface strongly with the Magnet Science and Technology Program.

1. One of the leading challenges in modern molecular biology is understanding how proteins fold up into their highly ordered active conformations. Although protein conformations in aqueous solution are heavily studied, much less is known about proteins in non-aqueous situations, e.g. biological cell membranes. By use of multinuclear NMR, Cross *et al.* (page 3) have characterized the small peptide, gramicidin, in various non-polar organic solvents and conclude that proteins may be trapped in many more possible shapes in cell membranes than in solution because of slow conformational rearrangements in non-aqueous environments.

2. Drug companies are increasingly using combinatorial synthesis to generate large libraries of peptides as potential new drug families. Eyler *et al.* (page 9) have used electrospray Fourier transform ion cyclotron resonance mass spectroscopy as a new means for resolving such mixtures, without prior chemical separation. Working with NHMFL's world-record 9.4 T FT-ICR instrument, their pilot results show that it will be possible to assess the diversity and degeneracy of such combinatorial libraries.

3. Heavy metal pollution, especially mercury, has resulted in a ban on the human consumption of several types of fresh water fish from south and central Florida. Odom *et al.* (page 15) have measured the lead isotopic composition of rain waters from south Florida to determine the sources of lead, and by inference mercury, in the atmosphere. Using this nuclear fingerprint, they find that a significant part of the lead and mercury in this region is brought from Europe and north Africa by the prevailing winds.

4. While Landau's theory of a Fermi liquid has for four decades been the foundation for understanding the properties of metals and semiconductors, recent advances have uncovered materials such as intermetallic compounds, alloys, and oxides that exhibit exotic non-Fermi liquid behavior. One such system is $UCu_{5-x}Pd_x$, studied by Aronson *et al.* (page 41), in which anomalous temperature dependences of the electrical resistivity, magnetic susceptibility, and specific heat were observed. At issue is whether single U site spin scattering or cooperative multisite scattering is responsible for the observed effects. Experiments were carried out in 33 T down to temperature of 0.8 K to determine the

temperature scaling of the data and whether a crossover from single to multisite scattering was evident.

In a related theoretical study, Miranda and Dobrosavljevic (page 48) investigated the role of disorder produced by the alloying in causing the non-Fermi liquid behavior. They conclude that for a broad range of types of disorder, local fluctuations of the characteristic (Kondo) temperature, below which the U spins are dynamically quenched, accurately account for the experimental data.

5. There has been intense interest in so called Kondo insulators, compounds in which a small semiconductor-like (charge) energy gap opens at the Fermi level due to coherent spin scattering. This only occurs for even integer electron count per unit cell of the material. In addition to the charge gap, these materials exhibit a gap in their spin excitation spectrum. Thompson *et al.* (page 51) have studied the magnetic field dependence of the spin gap in $Ce_3Bi_4Pt_3$ and have found it to be weakly dependent on field up to 50 T at temperatures between 4 and 150 K. This is in sharp contrast with earlier measurements of the charge gap, which appears to vanish above 50 T. Related tunneling experiments were carried out by Amsler *et al.* (page 40).

6. Quasi one dimensional organic conductors are fascinating materials on the border of chemistry and physics. Using among the highest field/frequency studies ever carried out in solid state NMR (24 T), the nature of the spin density wave ground state of these materials was studied by Clark *et al.* (page 61) in $(TMTSF)_2AsF_6$ and by Valfells *et al.* (page 75) on $(TMTSF)_2PF_6$. The first work is directed at developing 1 GHz NMR techniques to explore the collective phase dynamics of the SDW, with measurements to be made in 1997. In the second work, ^{77}Se NMR from 24 K to 1.5 K show that a portion of the Fermi surface remains down to 4 K, but activated behavior occurs below this temperature. What is responsible for this very low temperature transition remains a challenging theoretical problem.

7. Turning to semiconductors, the fractional quantum Hall effect in high mobility heterostructures is one of the most remarkable discoveries of this decade in physics. As in superconductivity, many body quantum effects are the essence here. A recent integrating concept in this field is that of composite fermions, i.e., pseudo particles composed of an electron to which is attached one or more quantized flux tubes. Du *et al.* (page 77) have studied such structures in high magnetic field at low temperature as a function of the tilt angle of the field relative to the plane of the heterostructure. The results to date are consistent with the composite fermion approach, extending this scheme to conditions where the spins are not fully polarized in the field.

8. Blue-green lasers, important for applications, have interesting electron-hole interaction effects. Song and Nurmikko (page 85) have studied the mechanism for lasing in a ZnCdSe/ZnSSe quantum well diode. With increasing magnetic field, the laser frequency increases by discrete mode hops, consistent with the exciton diamagnetic response, indicating the importance of electron-hole coupling in these devices.

9. ^3He is one of the purest and simplest materials in nature, yet it exhibits extremely complex behavior at low temperature, including superfluidity in the liquid phase. Studies of solid ^3He below one micro degree kelvin show that it becomes magnetically ordered at ambient pressure, in the bcc phase. Theoretical predictions suggest that the ordering temperature will increase under pressure to near 20 microkelvin in the hcp phase. Using direct demagnetization cooling, Adams *et al.* (page 89) have provided the first clear evidence for ferromagnetic ordering in the hcp phase.

10. The magnetic excitations of an antiferromagnetic spin chain are known from the work of Haldane to exhibit a gap for integer spin on each site. The first evidence of a Haldane gap in an S = 2 antiferromagnetic chain was observed in the quasi linear compound $MnCl_3C_{10}H_8N_2$ by Granroth *et al.* (page 95). The results indicate a non magnetic ground state in weak field, with the continuous onset of a magnetic state for fields above a critical value of 1 to 2 T, depending on the orientation of the field. These results are most naturally explained by the Haldane gap effect in contrast to single ion magnetic anisotropy.

In summary, the above are but a few of the exciting scientific projects underway at the NHMFL. Clearly, many of these studies have implications for advanced technology, as well as advancing the forefront of science as a whole. The intellectual unity of the laboratory, both in-house and with its users, is one of its strongest attributes, and we intend to enhance this aspect in the future.

Biology

Protein Structure and Stability in a Membrane Environment by Solid-State NMR

Cross, T.A., NHMFL/FSU, Chemistry, and Institute of Molecular Biophysics
Cotten, M., NHMFL/FSU, Chemistry
Xu, F., NHMFL/FSU, Chemistry

One of the primary goals of our research effort is to understand the unique properties of the lipid bilayer as an environment for proteins. Tryptophans are much more common in membrane proteins than in water soluble proteins. To study the role of this amino acid in a membrane protein, we have characterized the structure and dynamics of the ion channel forming polypeptide dimer of gramicidin A. Among its 15 amino acids it has four indoles near the carboxy terminus. These indoles appear to hydrogen bond to the surface of the bilayer, thereby orienting the channel with respect to the bilayer normal.

The replacement of four tryptophans in gramicidin A by four phenylalanines (gramicidin M) causes no change in the molecular fold of this peptide dimer in a low dielectric isotropic organic solvent, but the molecular folds are dramatically different in a lipid bilayer environment. The indoles of gramicidin A interact with the anisotropic bilayer environment to induce a change in the molecular fold. The intertwined double-helical fold of gramicidin M dimer as opposed to the single-stranded dimer of gramicidin A is not compatible with ion conductance. Gramicidin A/gramicidin M hybrid structures also have been prepared and like gramicidin M homodimers these hybrids appear to have a double helical fold suggesting that a couple of indoles are being buried in the bilayer interstices. To achieve this equilibrium structure (i.e. minimum energy conformation), incubation at 68 °C for two days is required. Kinetically trapped metastable structures may be more common in lipid bilayers then in an aqueous isotropic environment. Regulation of protein function is one of the key features of metabolic activities in living systems. Furthermore, regulation is often achieved by structural modification of the proteins. In membranes where metastable states can be achieved more easily than in aqueous environments, it is possible that this will prove to be a regulatory mechanism with numerous ramifications for the field of biochemistry.

Structural characterizations in the bilayers were achieved with solid-state NMR derived orientational constraints from uniformly aligned lipid bilayer samples. With this relatively new form of structural constraint, it has been demonstrated that high resolution three-dimensional structures can be achieved. Moreover, detailed dynamic characterizations can be achieved with a combination of powder pattern spectral analysis as a function of temperature and with field-dependent relaxation parameters. Structural characterizations in organic solvents were accomplished by solution NMR using standard NOE-based techniques.

Multinuclear NMR Studies of Intracellular Sodium Homeostasis in Isolated Muscle Fibers

Ellington, W.R., FSU, Biology
Combs, C.A., FSU, Biology

A key feature of cells is the maintenance of asymmetry of ion distribution between the intracellular and extracellular compartments. This distribution is maintained by the presence of ion transport proteins that are directly (or indirectly) driven by the hydrolysis of ATP. The amount of energy available from ATP hydrolysis is best quantified as the effective free energy change ($dG/d\xi_{ATP}$), which represents the extent of displacement of the reaction away from equilibrium. Kammermeier[1,2] has suggested that the above ion transport ATPases may be sensitive

to reductions in $dG/d\xi_{ATP}$ associated with metabolic lesions.

We have investigated the impact of $dG/d\xi_{ATP}$ reductions on intracellular sodium homeostasis in isolated crustacean muscle fibers. Bundles of muscle fibers (25 to 50 mg wet weight) were mounted in a home-built probe consisting of a five-turn micro solenoid coil wrapped around a glass tube (1.9 mm ID) that served as a superfusion chamber. The coil was dual tuned to ^{31}P (243 MHz) and ^{23}Na (158 MHz). Spectra were acquired using a wide bore Bruker DMX-600 equipped with XYZ gradients (max. 100 G/cm). ^{31}P NMR spectra were acquired to obtain information on high energy phosphate levels, intracellular pH and intracellular free Mg^{2+} concentrations. These data were used to calculate $dG/d\xi_{ATP}$ in all experimental treatments. In order to isolate the intracellular sodium signal, ^{23}Na NMR spectra were acquired using a diffusion-weighted pulse gradient spin echo sequence.[3] Since extracellular sodium has higher mobility (both convective and diffusive), it was possible to use the diffusion-weighting protocol to eliminate the extracellular sodium contribution.

The efficacy of this protocol was evaluated by following the attenuation of signal amplitude as gradient strength was increased—a biexponential decay curve resulted displaying high and low mobility sodium contributions. Using the shift reagent Tm(DOTP-5) we showed that the rapidly decaying component was extracellular sodium. Isolated fiber bundles displayed extraordinary stability as ^{31}P- and ^{23}Na-NMR spectra were unchanged for up to 8 to 10 hours of superfusion. As expected, metabolic inhibition (cyanide/iodoacetate) produced dramatic effects on $dG/d\xi_{ATP}$ values, which declined from -61 KJ/mole (controls) to -48 KJ/mole after 3 hours of inhibition. The final $dG/d\xi_{ATP}$ value was well above the predicted "threshold" $dG/d\xi_{ATP}$ value of 44 KJ/mole at which the Na^+:K^+-ATPase should become compromised. Surprisingly, ^{23}Na spectra showed that intracellular sodium levels increased progressively during metabolic inhibition. At the end of 3 hours, intracellular sodium had increased 270% indicating severe erosion of the transmembrane sodium gradient. Our results show that even small reductions in $dG/d\xi_{ATP}$ disrupt intracellular sodium homeostasis. (This research is supported by NSF grant IBN-9104548.)

References:

1 Kammermeier, H., Basic Res. Cardiol., **83**, 31 (1987).

2 Kammermeier, H., Basic Res. Cardiol., **88**, 380 (1993).

3 van Zihl, P.C.M., *et al.*, Proc. Nat. Acad. Sci. U.S.A., **88**, 3228 (1991).

Conformational Study of Adenosine Nucleotides Bound to *E. Coli.* Adenylate Kinase by NMR Spectroscopy

Lin, Y., Indiana Univ. Purdue Univ. Indianapolis (IUPUI), Physics

Murali, N., NHMFL

Rao, B.D.N., IUPUI, Physics

Adenylate kinase catalyses the reversible reaction MgATP+AMP<->MgADP+ADP, where AMP, ADP, and ATP are adenosine 5'-mono-, di-, and tri-phosphate, respectively. In order to contribute to the understanding of the catalytic mechanism of this enzyme, we have been investigating the conformations of adenosine nucleotides in the enzyme-bound complexes. There are three internal motions of adenosine nucleotides in solution: the glycosidic rotation, the sugar pucker, and the mobility of phosphate chain. Previous study has shown that these internal motions are significantly restricted or arrested when adenosine nucleotides bind to ATP-utilizing enzymes, which provides the possibility of determining the conformation of enzyme-bound complexes in solution by nuclear magnetic resonance (NMR) spectroscopy.

Two-dimensional ^1H transferred nuclear Overhauser effect spectroscopy (TRNOESY) experiments have been conducted on the 720 MHz NMR spectrometer at NHMFL from June 23 to July 1, and from November 14 to December 2, 1996. The data were analyzed by the full relaxation matrix method. The conformation of the adenosine moiety

was obtained by energy-minimization with the NOE-determined distances as constraints using QUANTA. The glycosidic angle in the AMP complex agrees with those previously determined for other enzymes where the glycosidic angle is in the range of 51°±8° irrespective of whether the enzymes catalyze phosphoryl transfer, adenylyl transfer, or pyrophosphoryl transfer reactions. This narrow range of glycosidic angle obtained for these different enzymes suggests a possible common motif for the recognition and binding of the adenine moiety at the active sites of ATP-utilizing enzymes. The results for ATP complex have been variable, however, which conforms to the fact that for adenylate kinase only the AMP site is adenine-specific. The results of the experiments on 720 MHz spectrometer have been encouraging. The complete conformation of the bound adenosine nucleotides will be established after the conformation of the phosphate chain is determined by other NMR methods, such as the relaxation effects on labeled ^{13}C and ^{15}N position on the nucleotides arising from the substituent activating cation.

Analysis of Transdermal Drug Delivery by Pulsed Field Gradient Nuclear Magnetic Resonance

Locke, B.R., FAMU-FSU Chemical Engineering
Moerland, T.S., FSU, Biology
Kinsey, S.T., FSU, Biology/NHMFL
McFadden, L., FSU, Biology
Galban, C., FAMU-FSU Chemical Engineering

This project utilizes pulsed field gradient NMR spectroscopy (PFGNMR) and diffusion weighted NMR microscopy to analyze the transport of solutes through skin under conditions of constant (iontophoresis) and pulsed (electroporation) electrical fields. In addition to analysis by NMR, structural analysis of the skin is being investigated by electron microscopy (EM) and stereological measurements of skin structure. This project is supported by a grant from the Whitaker Foundation for Biomedical Engineering Research. Information from NMR and EM will characterize structural changes induced by the electrical fields on the skin. NMR is uniquely suited for making these measurements since it provides reliable, accurate, and most importantly, direct *in-situ* measurements of probe transport.

A specific goal of the research on iontophoresis includes measurement of the rates of transport of charged and uncharged molecules across skin. Hair follicles and sweat pores are considered to be the major pathways for iontophoretic transport across human skin, and the current resolution of diffusion-weighted NMR microscopy permits a quantitative analysis of transport through these routes.

Work in the previous year, which was the first year of this project, included obtaining preliminary diffusion-weighted MR images of skin samples. These data were acquired using the wide-bore 600 MHz Bruker DMX spectrometer at the NHMFL. Resolution of 23.4 x 23.4 x 200 μm was obtained with sufficient contrast to visualize the components of skin that are relevant to the measurement of transdermal motion. Additional effort in the previous year includes developing stereological methods to analyze the effects of electrical fields on skin structure, and developing mathematical models of transdermal drug delivery via electrophoresis and electroosmosis in hair follicles and sweat glands.

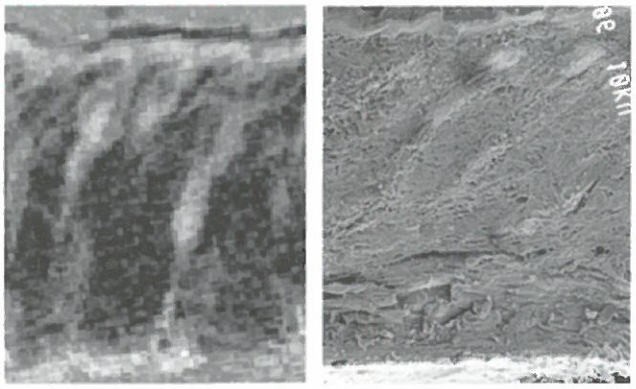

Figure 1. Magnetic resonance image (left panel) of hairless rat skin obtained with a resolution of 23.4 x 23.4 x 200 μm showing clearly the stratum corneum at the top and the hair follicles oriented diagonally to the vertical axis. Shown for comparison is a scanning electron microscope image (right panel) of a similar sample at the same scale.

Two-Way Conversation with a Mass Spectrometer: Non-Destructive Interactive Mass Spectrometry

Marshall, A.G., NHMFL/FSU, Chemistry
Guan, S., NHMFL/FSU, Chemistry
Solouki, T., NHMFL
Pasa-Tolic, L., NHMFL
Jackson, G.S., FSU, Chemistry

Most mass spectrometers employ destructive detection, so that it is necessary to create another sample in order to vary even one parameter. In contrast, Fourier transform ion cyclotron resonance (FT-ICR) mass spectrometry offers *non-destructive* detection, so that ions remain available for further manipulation and re-detection. In 1996, we showed for the first time how to perform mass spectrometry interactively.[1,2] Following each elementary experimental stage, such as ion generation, isolation, dissociation, or detection, the operator is free to choose and tailor the next stage without creating a fresh supply of ions. For example, we can test the effect of varying one parameter over several values without having to repeat the entire experimental event sequence each time, much like varying one letter or word in a sentence without having to rewrite the whole sentence. Alternatively, Figure 1 shows a series of experiments performed on the *same* batch of oligosaccharide ions, in which we stopped at each stage (while keeping the ions trapped) while deciding what to do next. Such interactive control promises to speed development of complex experimental event sequences, as for optimizing the sequencing and structural analysis of tiny amounts (e.g., femtomoles or less) of biomacromolecules (peptides, nucleic acids, oligosaccharides).

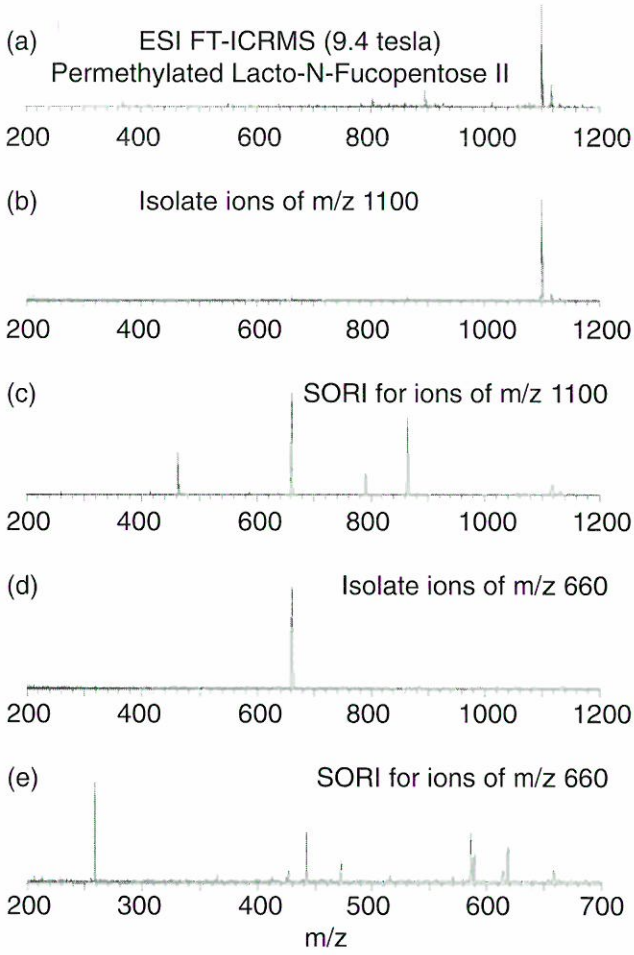

Figure 1. Electrospray ionization FT-ICR mass spectra of permethylated lacto-N-fucopentose II, obtained interactively. (a) Detection after ion accumulation and transfer to ion trap. (b) Detection after subsequent isolation of singly-charged sodiated pseudomolecular ions. Several interactively-selected ejection commands were executed to obtain the desired isolation. (c) MS/MS detection after interactively-selected collisional dissociation of quasimolecular ions of *m/z* 1100 during a pulse of Ar collision gas. (d) Detection after interactively selected isolation of MS/MS fragment ions of *m/z* 660. (e) MS/MS/MS detection after interactively selected dissociation of ions of *m/z* 660.

References:

1 Guan, S., *et al.*, Anal. Chem., **69**, 1 (1997).

2 Solouki, T., *et al.*, Anal. Chem., **68**, 3718 (1996).

Intracellular Diffusive Mobility of Phosphorous Metabolites in Striated Muscle

Moerland, T.S., FSU, Biology
Locke, B.R., FAMU-FSU Chemical Engineering
Kinsey, S., FSU, Biology
Penke, B., FAMU-FSU Chemical Engineering

This project is a systematic investigation of the intracellular diffusive mobility (D) of an energetically important phosphorous metabolite (phosphocreatine, PCr) in skeletal and cardiac muscle. This work is supported by a grant from the Florida Affiliate of the American Heart Association. Specific goals are (1) to determine the time-dependence of D_{PCr} in muscle as a quantitative probe of restricted diffusion for this metabolite, and (2) to determine if the D_{PCr} in muscle is anisotropic. Experiments are conducted with the wide-bore 600 MHz Bruker DMX nuclear magnetic resonance spectrometer at the NHMFL, using pulsed field gradient ^{31}P NMR.

Effort in 1996, which was the first year of this project, has resulted in two very significant findings. First, we have been able to show conclusively that D_{PCr} is a function of time. Second, the temporal dependence of D_{PCr} is highly anisotropic. These findings are depicted in Figure 1, which shows results obtained from a preparation of glycolytic ("white") muscle from goldfish. The apparent diffusion coefficient for PCr (D_{PCr}) is plotted as a function of the square root of the time over which the diffusion measurements were performed. The lower panel is a detailed view of time-dependence at lower diffusion times.

The data show that diffusion of PCr in the radial dimension is hindered or restricted to a greater degree than it is in the longitudinal dimension. A focus of effort in the coming year of the project will be to understand the structural determinants of this difference.

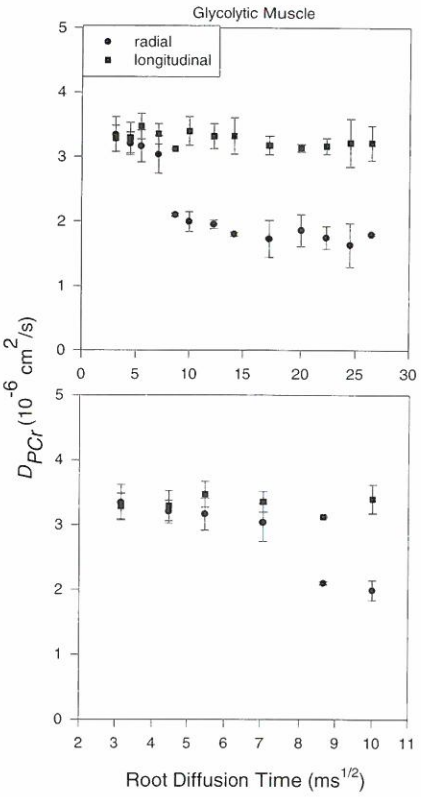

Figure 1. The apparent diffusion coefficient for phosphocreatine (D_{PCr}) as a function of the root diffusion time in pulsed field gradient NMR experiments. The sample investigated in these experiments is glycolytic (white) skeletal muscle of common goldfish. "Radial" denotes results when diffusion was measured across the radius of cylindrical fibers of muscle, and "longitudinal" shows results when diffusion was measured along the long axis. The lower panel is an expanded view at brief diffusion times.

Invoking Polymer Order: High Magnetic Field Orientation of Liquid Crystalline Thermosets

Benicewicz, B.C., LANL
Smith, M.E., LANL
Douglas, E.P., UF, Materials Science and Engineering
Earls, J.D., Dow Chemical
Priester, R.D. Jr., Dow Chemical

Liquid crystalline thermosets (LCT's) provide a unique opportunity to produce anisotropic solids of varying degree. LCT's can be defined as low molar mass liquid crystals that contain crosslinking endgroups. Our laboratory has been very involved the synthesis and characterization of LCT's and their specific properties. Our current work at the NHMFL is focused on using high magnetic fields to create highly oriented polymers, and then controlling the processing parameters to translate the high orientation into high mechanical properties. Maximum enhancement in properties of LCT's depends on the ability to create orientation in a preferred loading direction. The material used in experiments at the NHMFL is 4,4'-diglycidyloxy-alpha-methylstilbene cured with sulfanilamide. The initially isotropic material forms a smectic liquid crystalline phase during the crosslinking process.

Experiments were conducted to define the effects of high magnetic fields on the orientation and mechanical properties of LCT's cured in the fields. The thermoset formulation was prepared by dissolving 1 equivalent of sulfanilamide and 2 milliequivalents of an organophosphonium catalyst into 1 equivalent of the epoxy at elevated temperature. The mixture was then poured into a mold for the magnetic field experiments. Transformation of the isotropic liquid into the smectic liquid crystalline phase occurred during the exposure of the material to the magnetic field. The material was also reacted sufficiently in the magnetic field to reach the gel state. The final cure was conducted in a conventional oven (not in the magnetic field) for an additional three hours at 150 °C, 1 hour at 175 °C, and 4 hours at 200 °C. Figure 1 shows the variation of tensile modulus with field strength. There is a rapid increase in modulus at low field strength reaching a plateau at approximately 9 tesla. The plateau modulus values of approximately 1200 kpsi are extremely high and exceed normal values for unfilled epoxies by a factor of about 3.

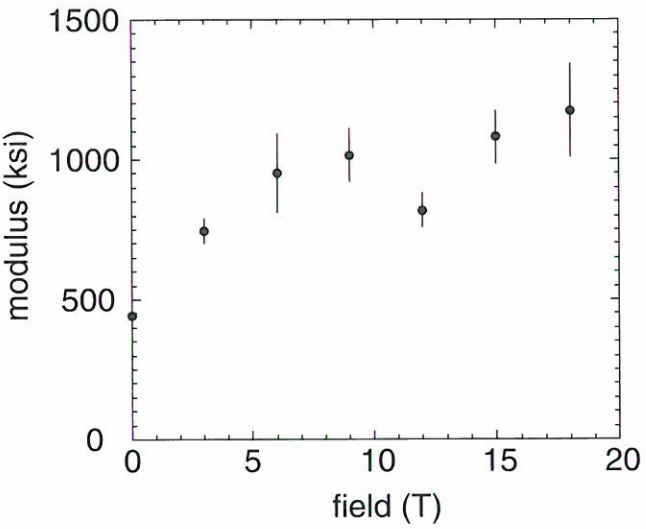

Figure 1. The variation of tensile modulus with field strength.

We have processed LCT's in high magnetic fields and measured the resulting mechanical properties on standard tensile test specimens. This work has clearly defined the effects of high magnetic fields on the processing and properties of high magnetic fields, with substantial improvements over non-magnetically processed materials.

Solvent Catalysis of Polypeptide Structural Rearrangements by Solution NMR

Cross, T.A., NHMFL/FSU, Chemistry, and Institute of Molecular Biophysics
Xu, F., NHMFL/FSU, Chemistry
Vaughn, J., NHMFL/FSU, Chemistry, and Institute of Molecular Biophysics

Many water soluble proteins can fold into their native conformation from an extended chain structure very rapidly (1 s timescale or less). In part, this is due to the nature of the weak interactions that stabilize protein structures. In part, this is due to the nature of the solvent environment. Water is a protic solvent that can compete for the intramolecular hydrogen bonds in a protein structure. In this role water destabilizes protein structure and in so doing water facilitates structural rearrangements. Many of these rearrangements are necessary for the protein to search its conformational space to find its minimum energy conformation, known as the native conformation.

Membrane proteins have protic solvents restricted from much of their environment, and it is not clear how conformational rearrangements are facilitated and how the minimum energy conformation is achieved. To gain insight into this question we have studied a hydrophobic polypeptide, gramicidin, in non-polar organic solvents. This peptide forms a variety of dimeric structures in organic solvents, and it is possible to study the interconversion between these dimers. By high field solution NMR, it is possible to identify the various conformers and to monitor their concentration as a function of time. By choosing a dry non-protic solvent (dioxane or benzene) the conformational distribution is fixed and conformational rearrangements do not occur for weeks. The addition of a small amount of protic solvent facilitates the conformational rearrangements. The binding sites for these protic solvent molecules on one of the dimeric structures have been extensively characterized. These binding sites position the solvent so as to destabilize the intermolecular hydrogen bonds between gramicidin monomers. The solvents are also positioned so as to stabilize conformational intermediates in which these intermolecular hydrogen bonds would be broken and the partial charge of the amides groups exposed to the solvent environment. In other words, the protic solvent molecules would be acting as a catalyst. This novel concept has just been published in the *Journal of the American Chemical Society* (Xu *et al.*, 118:9176-9177).

It was anticipated that more than one protic solvent molecule would be needed in order to facilitate the conformational rearrangements. Kinetic studies have generated preliminary data supporting this anticipation. First the kinetic rates are not enhanced with just a few solvent molecules per gramicidin dimer. Secondly the kinetic rate has a concentration dependence on the protic solvent that is ≥ 6, suggesting that at least 6 molecules of protic solvent must be bound to facilitate these structural rearrangements.

The implications of this effort for membrane proteins are that non-minimum energy conformational states may be trapped in membrane environments and that conformational rearrangements will be both slow and dependent on the presence of a small concentration of protic solvent. The concentration of protic solvent in the membrane, bound to the surface of membrane proteins is not known, but there is hope that such measurements can be made.

Analysis of Combinatorial Libraries Using Electrospray Fourier Transform Ion Cyclotron Resonance Mass Spectrometry

Eyler, J.R., NHMFL/UF, Chemistry
Nawrocki, J.P., UF, Chemistry
Watson, C.H., UF, Chemistry
Hayes, T.W., UF, Chemistry
Benner, S.A., UF, Chemistry, and Swiss Federal Institute of Technology, Chemistry
Wigger, M., Swiss Federal Institute of Technology, Chemistry
Senko, M.W., NHMFL

Electrospray ionization (ESI) coupled with Fourier transform ion cyclotron resonance (FT-

ICR) mass spectrometry has been used to provide information about complete combinatorial libraries of small peptides containing 10^3 - 10^4 components. The fidelity of attempted synthesis steps can be ascertained rapidly, and, when the extremely high resolution FT-ICR mass spectra are combined with appropriate computer simulation, both diversity and degeneracy of the libraries as synthesized can be assessed. Experiments were carried out at both the University of Florida Department of Chemistry and at the NHMFL in Tallahassee. Figure 1 shows a high resolution mass spectrum obtained on the 9.4 T ESI-FT-ICR instrument at the NHMFL's National High Field ICR Facility that covers only a small mass range from a H-Xxx-Xxx-Xxx-Xxx-pTyr-Cys-OH combinatorial library (Cys and Trp excluded) and that exhibits baseline resolution between peaks of the same nominal mass.

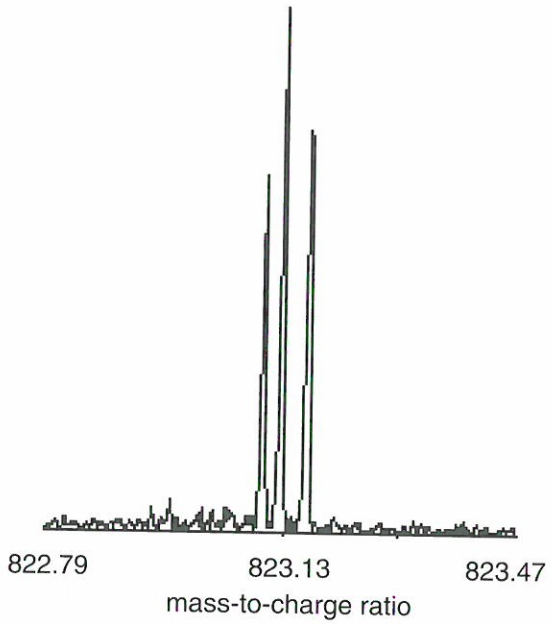

Figure 1. High resolution mass spectrum obtained on the 9.4 T ESI-FT-ICR instrument at the NHMFL's National High Field ICR Facility.

Application of Deuterium Solid State NMR to the Study of Molecular Dynamics in Metal Organo-Phosphonates

Fanucci, G.E., UF, Chemistry
Hughes, E., UF, Chemistry
Talham, D.R., UF, Chemistry
Bowers, C.R., UF, Chemistry

Langmuir-Blodgett (LB) films of metal organo-phosphonates offer an ideal way to control formation of mixed organic/inorganic assemblies. By incorporating phenoxy or other π-moieties into the aliphatic portion of these organo-phosphonic acids, it is possible to construct LB films that possess the composite physical properties of the separate organic and metal phosphonate inorganic components. By producing films that contain specialized organic moieties, it becomes possible to construct materials with specialized chemical and physical properties, such as magnetism, propensity for electron transfer, conductivity and even superconductivity. Before the fabrication of materials with these diverse properties can be achieved, however, the influence of the structure and dynamics of the organic substituents on the packing patterns and organization must be fundamentally understood. One aspect of the dual-network films that has yet to be explored is the dynamics of the phenyl or other functional groups in the hydrophobic regions.

Selective deuteration of the functionalized organic groups makes it possible to study the dynamical processes on the time-scale of milliseconds to tens of microseconds using deuterium quadrupole echo NMR spectroscopy. In the present work, deuterated samples of both cadmium and magnesium phenyl- phosphonates ($M(O_3PC_6D_5) \cdot H_2O$ M = Cd, Mg), the bulk solid state powders that possess the same inorganic extended lattice structure as LB metal phosphonate films, have been studied. The motion of the phenyl groups has been characterized by measuring the deuterium NMR spectra of the deuterated phenyl groups at a series of temperatures, ranging from the essentially static limit at low temperature to the fast motion regime where the nuclear quadrupole

interaction obtains its time-averaged value. Theoretical simulation of the spectra and comparison with experiment allow analysis of the particular type of motion present, as well as a quantitative determination of the rate constant for the process. It turns out that the motion is well described by simple 180 degree flips of the phenyl ring. Figure 1 presents the experimental spectra over a range of temperatures along with the simulated spectra obtained by simplex fitting with the exchange rate and the quadrupole coupling constant as the fitted parameters.

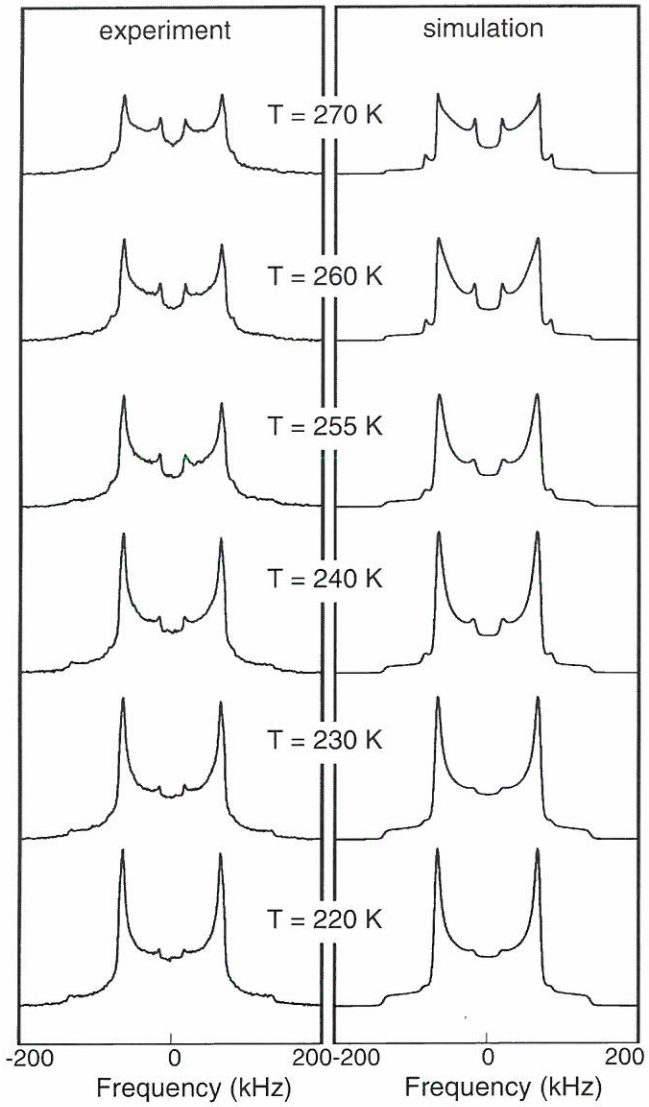

Figure 1. Experimental and simulated solid state deuterium NMR spectra of $Cd(O_3PC_6D_5).H_20$ acquired as a function of temperature.

Furthermore, the free energy of the flipping process can be obtained from the temperature dependence if Arrhenius behavior is assumed. This assumption is justified by the linear relationship between 1/T and In(k) as shown in Figure 2.

Ultimately, the ring flipping rates and energetics in the cadmium and magnesium phenylphosphonates will be compared. Although the analysis of the magnesium data has not yet been completed, the larger van der Waals radius of the cadmium ion is expected to open up the inorganic lattice, making the phenyl ring motion less constrained than in the magnesium compound. The extension of this work to LB multilayers is anticipated to be possible with the goal of studying packing and molecular organization of amphipathic molecules that contain phenoxy groups in these planar assemblies which approaches a 2D limit.

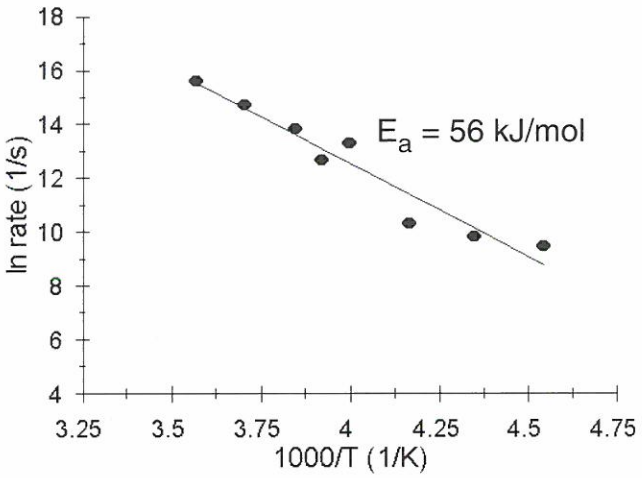

Figure 2. Arrhenius plot using the rate constants extracted by fitting the simulated deuterium lineshape to the experimental spectra at varying temperatures. Linear regression yields an activation energy of 56kJ/mol for the 180 degree flipping motion of the phenyl rings.

Multifrequency High Field EPR of Mn(III) Porphyrazines

Hoffman, B.M., Northwestern Univ., Chemistry
Krzystek, J., NHMFL
Goldberg, D.P., Northwestern Univ., Chemistry
Pardi, L., NHMFL
Brunel, L.-C., NHMFL

As part of an ongoing program targeted at the development of new porphyrazine systems, we have been pursuing a detailed magnetic

characterization of manganese porphyrazine complexes. These novel macrocycles are of potential interest for such diverse applications as contrast agents in biomedical magnetic resonance imaging, or as building blocks for molecular magnetic materials. In order to tailor the magnetic properties of these compounds for a particular application, we need to correlate structure with magnetic properties. In case of compounds containing Mn(III) as central ion, magnetic investigations have usually been limited to susceptibility studies since that particular ion is known to be "EPR-silent" in most cases at conventional frequencies (X- to Q-band) due to large zero field splitting and unfavorable relaxation properties.

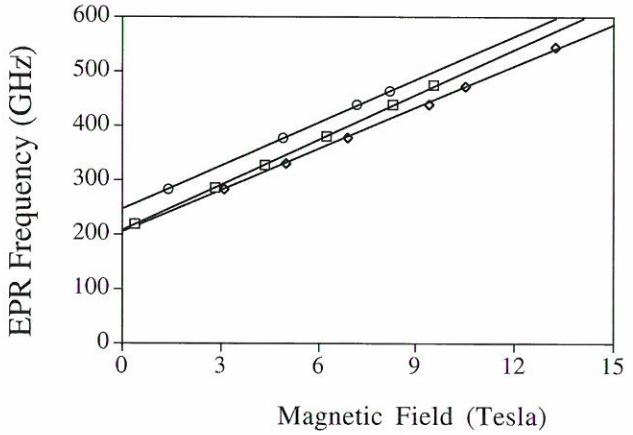

Figure 1. Frequency vs. field dependence of the M_S |±1> to |±2> EPR transition in three compounds under study: Mn(Cl)ODMAPz (squares), Mn(Et_2dtc)ODMAPz (circles, Et_2dtc = diethyldithiocarbamate), and Mn(Cl)TPP (diamonds, TPP = meso-tetraphenyl porphine). The linear fit yields the splitting between both zero field levels, which is equal to 3D.

We used the multifrequency (200 to 550 GHz) and high field (up to 15 tesla) capability of the EMR spectrometer at NHMFL to study two manganese porphyrazine complexes for which the crystal structure has been determined. The ligand was the newly synthesized octakis(dimethylamino)-porphyrazine (H_2ODMAPz).[1] Additionally we examined commercial Mn tetraphenylporphyrin. EPR transitions were observed in all three compounds at frequencies above 200 GHz. The data from these experiments are providing a detailed description of the spin ground state for these new molecules. In particular, we were able to measure directly the zero-field splitting parameter D, which varies between 2.2 and 2.7 cm^{-1} depending on the axial ligand of the manganese ion. Such information is the first of its kind to be reported for a manganese(III) porphyrin-type molecule. Future work will include theoretical simulations of the EPR spectra as well as measurements of related porphyrazine derivatives.

References:

1 Mani, N.S., *et al.*, J. Chem. Soc. Chem. Comm., 2095 (1994).

A New Radical Detected by HF-EPR, ENDOR, and Pulsed EPR in a Room Temperature Irradiated Single Crystal of Glycine

Maniero, A.L., NHMFL
Brunel, L.-C., NHMFL
Brustolon, M., Univ. of Padova, Italy, Physical Chemistry
Chis, V., Univ. of Padova, Italy, Physical Chemistry

The different radicals produced by high energy irradiation of solid glycine have been the subject of many studies since the beginning of EPR spectroscopy age.[1] This aminoacid gives rise to a large variety of different radicals and the nature of the stable observed radicals depends on the temperature of irradiation and on the thermal history of the irradiated crystal. The cw-X band EPR spectrum has been attributed to the superposition of the spectra of two radicals: $^{+}NH_3$-CH-COO^{-} (radical A), and CH_2-COO^{-} (radical B). These two types of radicals are commonly formed in irradiated aminoacids by deprotonation and deamination, respectively. A third type of radical might be the one produced by decarboxylation, but this radical was not observed in room temperature irradiated glycine until now.

High field EPR experiments have been performed on room temperature γ irradiated glycine. This technique is important to gain insight

into systems where more than one radical is formed. X band EPR spectra of freshly irradiated and aged crystals of glycine show only slight differences. Our HF-EPR spectra show that in the aged crystals two radicals are present [radical A and one giving rise to the low field triplet (Figure 1 spectrum A)]. In the freshly irradiated crystals a third radical can be detected, as indicated by arrows in the figure (spectrum B). The hyperfine splitting of the low field triplet is about 11 G, whereas that of the triplet indicated by arrows is of 21 G, so the latter triplet can be attributed to radical B.

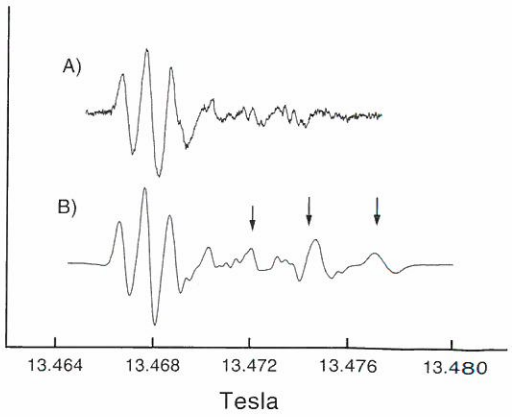

Figure 1. 380 GHz EPR spectra of irradiated single crystals of glycine. A) aged crystal. B) freshly irradiated crystal.

By ENDOR and pulsed EPR techniques the third radical has been identified as the radical CH_2-NH_2 produced by decarboxylation of the primary radical anion, and it has not been previously detected. Whereas radicals A and C are stable for months, radical B decays in weeks.

Reference:

1 Morton, J.R., J. Amer. Chem. Soc., **86**, 2325 (1964).

High Field EPR Spectra of a Tetranuclear Cluster Containing Exchange Coupled Gadolinium(III) and Copper(II) Ions

Pardi, L., NHMFL
Gatteschi, D., Univ. of Florence, Chemistry
Benelli, C., Univ. of Florence, Chemistry
Caneschi, A., Univ. of Florence, Chemistry
Brunel, L.-C., NHMFL

The 188.9 GHz EPR spectra of powdered $[Gd(hfac)_3CuSatnOH]_2$ (hfac = hexafluoro acetylacetonate, CuSatn = [N - (3-aminopropyl) salicyl - aldiminato] copper(II)) reported in Figure 1 show the EPR signals coming from the different states thermally populated at different temperatures. The fine structure resolved in the 100 to 10 K range is originated from the transition within a high-spin level (S = 5 or higher) close to the ground state. Other states are populated and a simulation of these

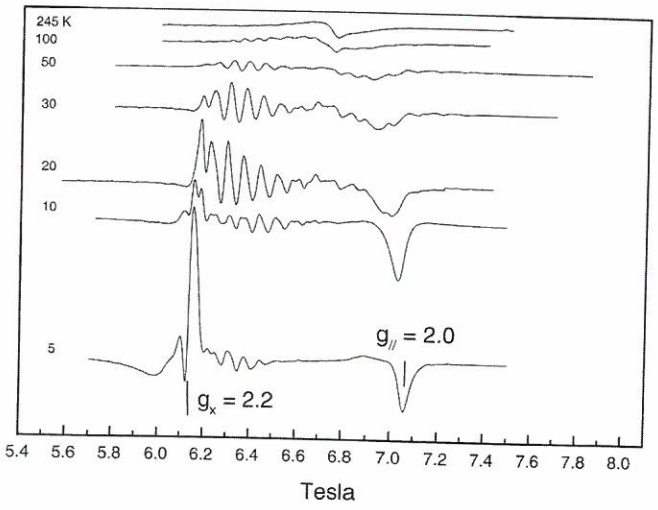

Figure 1. 188.9 GHz EPR spectra of powdered $[Gd(hfac)_3CuSatnOH]_2$.

spectra requires a superposition of the spectra originating from the different spin states including the forbidden transition. The S dependence of the transition probability is also to be taken into account. By lowering the temperature, the high spin state is depopulated while signals originated by lower spin states come out. Remarkable also is the resolution of the parallel from the perpendicular

components of the spectra, which was not achieved in the 9 GHz spectra.[1]

Reference:

1 Benelli, C., *et al.*, Inorg. Chem., **29**, 1750 (1990).

Calculation of Electronic and Geometric Properties of Some Small Molecules in High Magnetic Fields

Sabin, J.R., UF, Physics/NHMFL
Runge, K., UF, Physics/NHMFL

Advances in magnet construction technology have made magnets available with continuous fields of nearly 50 tesla and with bores of sufficient diameter for experiments. In addition to these magnets, already in use at the NHMFL, semi-continuous pulsed sources of 100 T are anticipated in the near future. At its Los Alamos facility, the NHMFL has detonated pulsed magnets of over 1000 T. It thus becomes possible to investigate the behavior of molecules in strong fields with an eye to field-induced changes in such quantities as geometrical and electronic properties, spectroscopic properties, and reactivities. Theory is a useful probe for these quantities and serves to screen among possible candidates for experiments.

In this work, we make use of a transformation of integrals calculated with respect to an ordinary Gaussian atomic function basis to those calculated with respect to a basis of gauge origin independent atomic functions, ξ, composed of the commonly chosen normalized Gaussian basis functions, χ, multiplied by gauge origin independence factors

$$\xi_\mu = \exp(i[\vec{\mathbf{B}} \times \vec{\mathbf{R}}] \bullet \vec{r}_i)\chi_\mu$$

This allows us to bring to bear on the current problem all the accumulated experience and techniques of quantum chemical calculational technology.

We have made some preliminary calculations of electronic properties of some simple molecules in magnetic fields, including, for example, *LiH* (see Figure 1). Initial indications are that for increasing applied field strength, molecular bond lengths decrease and binding energies increase, as expected, with concomitant increases in vibrational frequencies. Field-induced changes in these quantities, as well as in ground state molecular potential energy surfaces are discussed, and further investigations, both theoretical and experimental are suggested.

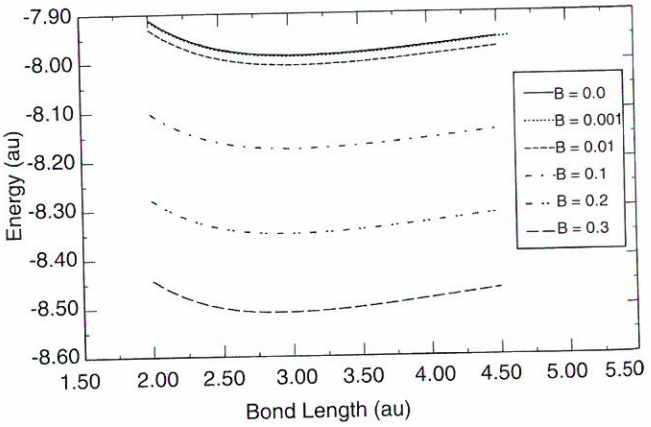

Figure 1. Ground state energy of lithium hydride in the parallel orientation as a function of applied field strength.

Geochemistry

Pb-Isotope Study of Rainwater from South Florida

Odom, A.L., NHMFL/FSU, Geology
Salters, V.J.M., NHMFL/FSU, Geology
Landing, W., FSU, Oceanography

We determined the Pb-isotopic composition of the rainwater from several locations in south Florida. The aim of this study is to determine the source of the metals, especially mercury, in rainwaters. Fish and other wildlife in certain regions in Florida, especially the Everglades, show evidence of mercury pollution. It has been our objective to find the sources of mercury for the Florida ecosystems, so that we might take action to restrict the input. Previously, mercury deposition has been determined and analyzed with respect to seasonal and regional trends that might identify sources. The deposition of mercury during the summer is the highest as this coincides with the time of largest amounts of rainfall. In naturally low pH waters, like those of the Everglades, metallic mercury, which is the dominant form in the atmosphere, is rapidly oxidized and accumulates in the waters and sediments. It has been shown that the atmospheric mercury deposition rate is high enough to explain the elevated mercury levels in the Everglades. Furthermore, the mercury levels in the atmosphere are uniform across south Florida and are not associated with any of the potential point sources as like urban emissions or coal burning power plants.

The Pb-isotopic composition of the rainwaters from south Florida (see Figure 1) have compositions identical to Atlantic aerosols as they were sampled on Barbados. The prevailing winds on Barbados and south Florida are from the east and northeast and the Barbados aerosols have been interpreted as coming from Europe and north Africa. The principle difference between the lead isotopic compositions from Europe and the United States is the different Pb-ore that is used for leaded gasoline as well as for other lead containing products. The U.S. lead is Mississippi Valley type and has higher $^{206}Pb/^{204}Pb$ values than the lead used in Europe which originates from the Broken Hill orebody which is of much older age than the Mississippi Valley deposits. The similarity in Pb-isotopic composition between the Barbados aerosols and Florida rainwaters is evidence that the Pb in these rainwaters comes from across the Atlantic. By inference, those heavy metals that cannot be attributed to specific point sources (mercury for example) are thus thought also to find their source in Europe and north Africa.

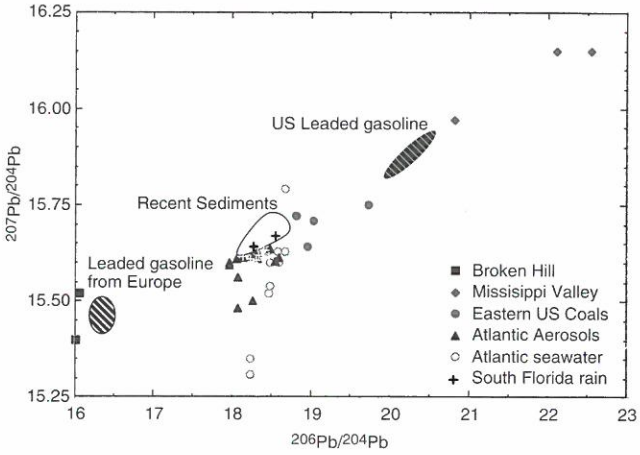

Figure 1. The Pb-isotopic composition of the rainwaters from south Florida have compositions identical to Atlantic aerosols as they were sampled on Barbados.

Hafnium Isotope Ratios in Seawater: Indicators of Paleo-Hydrothermal Activity

Salters, V.J.M., NHMFL/FSU, Geology
Godfrey, L.V., Cornell Univ., Geosciences
White, W.M., Cornell Univ., Geosciences

Previous work of our group has shown that the residence time of Hf in seawater is in the order of several thousand years, that is, a factor two to four larger to the ocean water mixing time. Preliminary

Hf-isotopic work indicates that approximately 50% of the Hf budget in the oceans is derived from hydrothermal activity. This research is aimed and obtaining detailed knowledge of the behavior of Hf in seawater. With this knowledge in hand Hf-isotopes in sediments have the potential to be an indicator of paleo-hydrothermal activity with a time resolution similar to its residence time. No other indicator of hydrothermal activity is available with this high an age resolution.

Dissolved Hf in seawater was originally thought to be at a concentration of 20 pmol/kg. Our results for Atlantic seawater show that the concentration of Hf is 20 to 50 times lower than these early measurements—the range is 0.4 to 1.0 pmol/kg. Sampling profiles across a shelf break across the NE Atlantic show that variations in Hf and Zr concentrations with depth are similar to nutrients, removal in the surface ocean and regeneration at depth. In contrast to the Zr and nutrients, Hf concentrations decrease from the mid-depth maximum to the seafloor. Zr/Hf ratios indicate that fractionation between these two elements occurs in solution, most probably due to stronger particle interactions for Hf than for Zr. The similarity of Hf and Zr concentration profiles with other hydroxyllated trace metals allows an estimate of their oceanic residence time of several thousand years. The inter-basin variation in Hf-isotope ratios also requires a residence time of a couple of thousand years.

Large volume water samples (each ~50 liters) from the equatorial Pacific were analyzed for their Hf isotopic composition. This represents the first direct analysis of Hf-isotopes in seawater. The data does show that ε_{Hf} varies as a function of depth between mid-ocean ridge basalt (MORB)-like values and values close to average continental crust (Figure 1). The sample closest to MORB is from the same depth as the neutrally buoyant plume from the East Pacific Rise. As the concentrations of Hf in seawater were considerably lower than what we assumed, the amount of isotope data that could be produced was a lot smaller than we had expected.

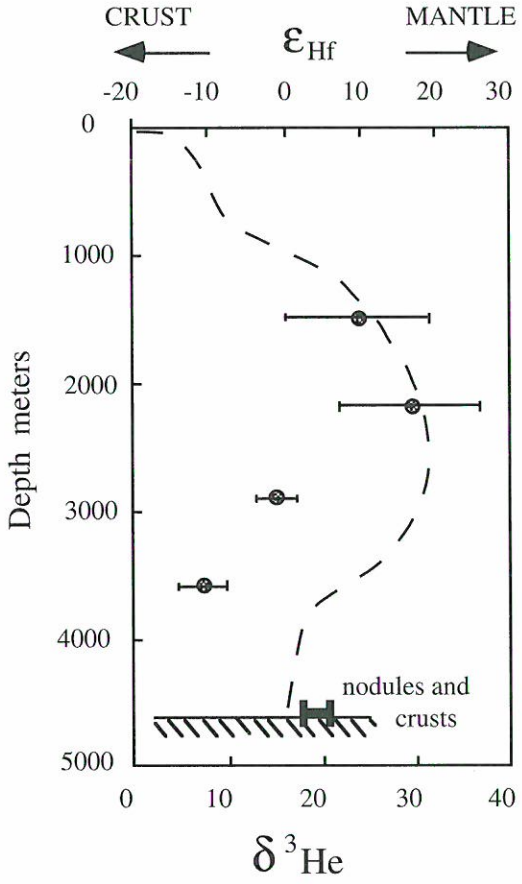

Figure 1. Hf isotope data for unfiltered seawater from 140W on the equator. The dashed line refers to He-3 and was taken from GEOSECS data. Error bars are 2 std error. Samples were supplied by Bob Anderson of Lamont Doherty Earth Observatory. Further samples for all 4 depths are available.

The behavior of Zr and Hf in hydrothermal settings also was addressed since we propose to use the isotopic composition of Hf as a tracer of hydrothermal activity. The concentration in many hydrothermal phases (e.g. sulfides, anhydrite) is low, less than 10 ppb. Where these minerals have undergone alteration, or where some minerals are thought also to form from seawater or low temperature fluids, the concentration of Hf is somewhat higher: up to 200 ppb. Analyses of hydrothermal manganese deposits and comparison to the rare earth element (REE) show that the removal of Hf at hydrothermal venting sites is less efficient for Hf than for the REE leading to longer residence times of Hf in hydrothermal venting sites, even though they have similar overall residence time in the oceans.

Trace Element Partitioning During the Initial Stages of Melting Beneath a Mid-Ocean Ridge

Salters, V.J.M., NHMFL/FSU, Geology
Longhi, J., Lamont Doherty Earth Observatory

We have determined the partition coefficients between clinopyroxene, orthopyroxene, garnet, and melt at a range of pressures (2.8 to 1.0 GPa) and temperatures (1570 °C to 1375 °C) and compositions in an effort to mimic as closely as possible the conditions under which primary mid-ocean ridge basalts (MORB) melts are formed.

The experiments were run in two steps. First, the multi-saturated liquidus phase relations of upper mantle minerals (olivine, orthopyroxene, clinopyroxene, and garnet or spinel) were determined for relevant portions of a synthetic peridotite bulk system. These lherzolitic melts can be assigned a percent mantle melt by assuming a reference mantle composition (e.g., primitive mantle minus 1% basalt) and then using the K concentration in the synthetic melt to calculate percent melt. Second, after determining the phase relations, the starting materials that produced multi-saturated assemblages with the highest melt/crystal ratios were doped with U, Th, Nb, Hf, Y, Zr, Ce, Nd, Sm, Er, Yb, and Lu and run to yield run products on which mineral melt distribution coefficients were determined.

Experiments show that at high pressures and temperatures low-Ca clinopyroxene (6wt% CaO) coexists with olivine, orthopyroxene, garnet, and a range of liquids corresponding to 7, 2, and 0.7% melts of reference mantle. Melt reactions derived from phase compositions show that orthopyroxene is produced during melting in the garnet stability field, which results in an increased rate of depletion of clinopyroxene relative to eutectic melting. The orthopyroxene production rate increases with decreasing percent of melting. The low Ca-clinopyroxene has significantly lower partition coefficients (Ds) for most of the trace elements than high CaO-clinopyroxene produced in experiments on basaltic starting materials.

Garnets in our study have a limited range in composition, but garnet-melt partition coefficients vary predictably with melt composition. Furthermore, D_U and D_{Th} for garnet are higher than previous studies and are higher than those in clinopyroxene. Consequently, garnet has a larger effect on the U-Th disequilibria than previously assumed. These new Ds now relax the requirement that ^{230}Th-excesses are the result of extremely small degrees of melting (low porosity) and very rapid transport to the surface. ^{230}Th-excesses of 10% and higher can be created by fractional melting with porosities up to 1% (see Figure 1).

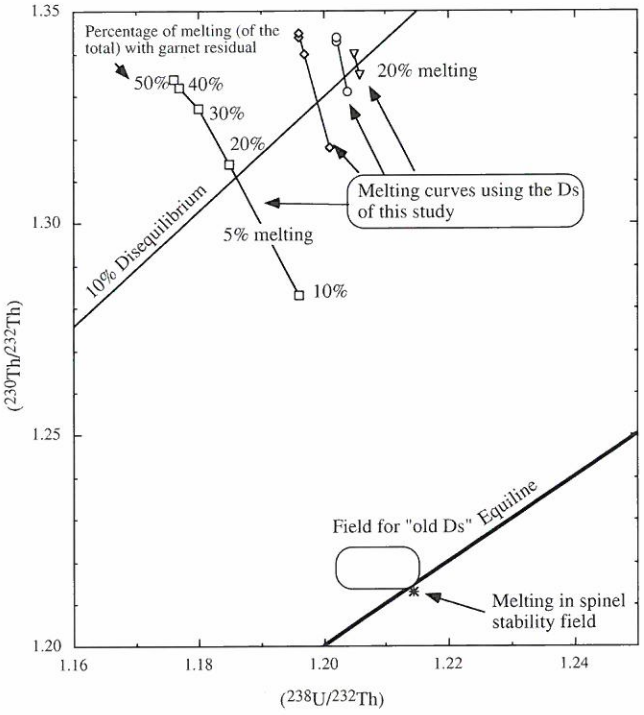

Figure 1. ^{230}Th-excesses of 10% and higher can be created by fractional melting with porosities up to 1%.

The Impact of Climate and Land Use Change on Carbon Turnover in Soils

Wang, Y., NHMFL/FSU, Geology
Amundson, R., Univ. of California at Berkeley, Environmental Science, Policy and Management
Trumbore, S., Univ. of California at Irvine, Earth System Science

Climate and land use impact soil by altering the soil environment, which may well affect C

storage and turnover in soils. In this study, we monitored the soil temperature, moisture, and soil CO_2 flux of paired natural and disturbed soils along an elevation transect throughout an annual cycle. In addition, we analyzed the C and ^{14}C content of organic matter in both pre- and post-bomb samples of these soils. The natural soils displayed strong seasonal variations of soil temperature, moisture, and soil CO_2 flux, with the highest CO_2 fluxes in the late fall and in the spring in response to soil moisture variation. In contrast, adequate moisture was available year-round in one of the disturbed soils because of irrigation, and soil CO_2 flux varied in response to changes in both temperature and moisture. Large differences in the inventory and ^{14}C content of soil organic C are also observed in these soils representing natural and disturbed systems.

By using a time-dependent box model to best fit the observed changes in C and ^{14}C content from pre-bomb to post-bomb soils, we estimated the turnover time and the sizes of soil organic C pools. Our modeling results suggest that the majority (>90%) of the organic C in the upper horizons (upper 20 cm) is in the fast-cycling C pool with an apparent turnover time of 25 years or less in the natural soil. In the disturbed soil, the amount of C in the fast-cycling C pool is smaller compared to the natural soil. The relative size of fast-cycling C pool decreases drastically with depth in both natural and disturbed soils. The annual CO_2 flux out of soil ranges from 1.4 kg C/m^2/yr. for the native soil and 1.2 kg C/m^2/yr. for the disturbed soil at the lowest elevation to 0.7 kg C/m^2/yr. at the highest elevation, based on monthly field measurements. Our study shows that conversion of grassland to agriculture land has resulted in ~24% decrease in total soil C in 22 years and an increase in ^{14}C age due to the accelerated decomposition of organic matter in the fast cycling C pool, which is consistent with observations in other agricultural soils. Additionally, logging appears to have altered soil temperature and reduced the amount of C stored in soil.

Mid-Ocean Ridge Basalts Melting Revisited

Zindler, A., NHMFL/FSU, Geology
Salters, V.J.M., NHMFL/FSU, Geology
Elliott, T., Faculteit Aardwetenschappen, Vrije Universiteit, Amsterdam, The Netherlands, Laboratory for Isotope Geology
Bourdon, B., Institut du Physique du Globe, Univ. of Paris, France, Laboratorie de Geochimie et Cosmochimie

The major and trace element, as well as, the isotope systematics of mid-ocean ridge basalts (MORB) have resulted in a number of estimates of degree and depth of melting. The variations in MORB along the ridge, as a function of ridge depth has been interpreted differently by these different estimators. In terms of major element chemistry, MORBs and abyssal peridotites show systematic variations with distance from a hot spot and ridge depth. Shallow ridges are thought to represent a high degree of melting with a relatively deep integrated depth of melting. Deep ridges segments are thought to represent small degrees of relatively shallow level melts. Salters (1996) has argued that ridge-segment-averaged $\delta_{(Lu/Hf)}$ and $\delta_{(Sm/Nd)}$ correlate with ridge depth, but suggest, in contrast to the $Fe_{8.0}$ data, that larger proportions of melt at deep ridges are generated in the garnet stability field.

Bourdon, *et al.* (1996), present a similar argument, but with contradictory conclusion, based on their identification of a global, negative correlation between MORB ($^{230}Th/^{238}U$) and ridge depth, which they interpret as reflecting greater depths for the initiation of melting beneath shallow ridges, due to the greater potential for Th-U fractionation by garnet.

The validity of all of these arguments hinges on the assumption of compositional similarity or regularity between all MORB sources. The correlations themselves are "rough," and therefore, strict chemical homogeneity is not a requirement, but systematic compositional variation with ridge depth (or $Na_{8.0}$, $Fe_{8.0}$, δ(Sm/Nd), or ($^{230}Th/^{238}U$))

undermines the basis for the interpretations of the correlations. If the extent to which the "normal" MORB source is polluted with plume components is a function of any of these parameters, then source heterogeneity may play a very important role in producing the observed correlations. In this case, it becomes difficult to draw simple inferences concerning the depth or extent of melting.

We have examined data for MORBs from the literature and find that global correlations between MORB isotope and trace element ratios, and between these parameters and ridge depth, do indeed exist. Our study suggests that an important component of variation is due to variable pollution of the MORB source by plume-like source materials with a range of compositions (as observed in ocean island basalts, OIBs). This is not to say that the extent and depth of melting do not play a role in producing chemical variations in MORBs, but that these must be considered in the context of systematic source variations.

A clue toward reconciliation of these apparently contradictory signals can be found in a new trace element partition study that found a compositional dependence of the garnet partition coefficients such that at conditions similar to the onset of melting for MORB U and Th in garnet are less incompatible than previously assumed. With these new Ds the ^{230}Th excesses in MORB can be explained at higher porosities and higher degrees of melting. In addition, it was found that the compositional dependence of the Ds in clinopyoroxene is such that DU and DTh are lower than previously reported. This new study is applicable to the melting in garnet peridotite while the previous studies are in P,T,X space closer to melting of garnet pyroxenite at lower pressures. The Th-Hf and major element signatures can be reconciled by melting of a mixed peridotite-garnet pyroxenite lithology. The porosities during melting are high enough that the garnet pyroxenite has no influence on the ^{230}Th-excesses, while it does effect the Lu-Hf signature.

SCIENCE RESEARCH REPORTS

Superconductivity – Basic & Applied

d-Wave Pairing from the Spin-Gap Proximity Effect

Bonesteel, N.E., NHMFL/FSU, Physics

The observation of frozen anti-phase domain walls in the LaNdSrCuO system by Tranquada *et al.*[1] has renewed interest in the idea that electrons in the CuO_2 layers of high-T_c superconductors have a tendency to phase separate into conducting hole-rich and insulating antiferromagnetic phases. While the long-range Coulomb interaction frustrates complete phase separation, a tendency to form insulating antiferromagnetic "droplets," or in the case of LaNdSrCuO, "stripes," may remain. It has recently been suggested by Emery *et al.*[2] that the existence of such a state exhibiting frustrated phase separation suggests a potential pairing mechanism—the "spin-gap proximity effect." The idea is that the antiferromagnetic insulating phase, if it has a spin gap, can induce superconductivity in the conducting hole-rich phase via an analog of the conventional superconductor-normal metal proximity effect.

A simple model has been considered that exhibits the spin-gap proximity effect. In this model, the frustrated phase separation envisioned by Emery *et al.* is enforced "by hand." The model consists of an array of 2x2 insulating antiferromagnet "droplets" with a criss-cross pattern of conducting phase running between the droplets. The ground state of each 2x2 droplet is the simplest example of a short-range "resonating-valence bond" state with a spin gap. Tunneling of Cooper pairs into and out of the 2x2 droplets leads to an effective pairing interaction between electrons in the conducting phase, providing a simple

example of the spin-gap proximity effect. Because this model has tetragonal symmetry it is possible to address the question of the symmetry of the order parameter induced in the conducting phase by the insulating droplets. It has been shown that the order parameter has d-wave symmetry. The connection between this result and the possibility of spin-gap proximity effect induced superconductivity in the cuprates is still being investigated.

References:

1 Tranquada, J.M., *et al.*, Nature, **375**, 561 (1995).

2 Emery, V., *et al.*, preprint (cond-mat/9610094).

Surprises on the Way From 1D to 2D Quantum Magnets: The Novel Ladder Materials

Dagotto, E., FSU, Physics/NHMFL

Rice, T.M., Theoretische Physik, ETH, Zurich, Switzerland

One way of making the transition between the quasi-long range order in a chain of S=1/2 spins coupled antiferromagnetically and the true long range order that occurs in a plane, is by assembling chains to make ladders of increasing width. Surprisingly this crossover between one and two dimensions is not at all smooth. Ladders with an even number of legs have purely short range magnetic order and a finite energy gap to all magnetic excitations. Predictions of this novel groundstate have now been verified experimentally. Holes doped into these ladders are predicted to pair, and possibly superconduct.[1]

Reference:

1 Dagotto, E., *et al.*, Science, **271**, 618 (1996).

High Field Magnetoresistivity in Thin Films of the Electron-Doped High-T_c Superconductor $Nd_{1.85}Ce_{0.15}CuO_{4\pm\delta}$

Dickey, R.P., Univ. of California, San Diego (UCSD), Physics, and Institute for Pure and Applied Physical Sciences

Herrmann, J., UCSD Institute for Pure and Applied Physical Sciences

de Andrade, M.C., UCSD Institute for Pure and Applied Physical Sciences

Maple, M.B., UCSD, Physics, and Institute for Pure and Applied Physical Sciences

Jiang, W., Univ. Maryland, College Park, Center for Superconductivity Research

Mao, S.N., Univ. Maryland, College Park, Center for Superconductivity Research

Greene, R.L., Univ. Maryland, College Park, Center for Superconductivity Research

Superconductor-insulator transitions have been induced in disordered 2D thin films by changing the amount of disorder[1] as well as by application of external magnetic fields[2,3]. The observed behavior was considered to be a manifestation of a transition between a superconducting vortex-glass phase with localized vortices and Bose-condensed electron pairs and an insulating Bose-glass phase of localized electron pairs and condensed vortices. According to theoretical predictions,[4] these two phases are separated by a Bose-metal characterized by a zero-temperature universal sheet resistance $R_{\square}^{*} = h/4e^2 = 6.45\ k\Omega$. This behavior has been verified experimentally in several systems including the electron-doped high–T_c superconductor $Nd_{1.85}Ce_{0.15}CuO_{4-\delta}$ (NCCO).[5,6] These studies, however, have been restricted to temperatures $T > 1.7$ K, inferring the critical magnetic field corresponding to the intermediate metallic state either from the condition $d\rho/dT = 0$ at their minimum temperature (1.7K),[5] or from the crossing of $\rho(B)$ curves taken at four different temperatures (with the minimum temperature being 2.2K).[6] In measurements at UCSD of the low-temperature resistivity of a superconducting thin film of NCCO with an optimum T_c of 22 K in magnetic fields up to 6 T,[7] we observed saturation of $\rho(T)$ only for $T \ll 500$ mK.

Preliminary measurements of the transverse electrical resistivity in two of the films measured in Reference 7 were made at the NHMFL-LANL in magnetic fields B in the range $0T \leq B \leq 18$ T at low temperatures T in the range 85 mK $\leq T \leq$ 700 mK. The $\rho(B)$ curves for an over-oxygenated sample with a reduced $T_c \approx 10K$ show a universal crossing point at the critical field $B^{cr} = (2.2 \pm 0.1)$ T, and a characteristic sheet resistance $R_{\square}^{cr} = (4.9 \pm 0.3)$ kΩ, where $R_{\square}$ is given by $R_{\square} = \rho/d$ and d = 0.603 nm is the lattice spacing between CuO_2 layers.[5] The $\rho(B)$ curves for the optimally doped sample with a $T_c \approx 22$ K seem to indicate a similar type of behavior, with an approximate crossing point at $B^{cr} = 6.5$ T and $R_{\square}^{cr} = 840$ Ω. In addition, the $\rho(B)$ curves from both samples show a maximum at high fields, followed by a decrease in the resistance at higher fields. Comparing $\rho(B)$ curves taken at different temperatures, we see that at fields above the crossing point, the resistance increases with decreasing temperature, possibly indicative of 2D weak localization behavior suggested in previous work.[8-10] It has recently been argued, however, that a similar normal state $\rho(T)$ behavior observed in $La_{2-x}Sr_xCuO_4$ is due to unusual anisotropic 3D transport rather than 2D Anderson localization.[11] Further measurements are needed to characterize the magnetoresistance in high magnetic fields and at low temperatures to resolve these issues.

References:

1 Paalanen, M.A., *et al.*, Phys. Rev. Lett., **69**, 1604 (1992).

2 Hebard, A.F., *et al.*, Phys. Rev. Lett., **65**, 927 (1990).

3 Yazdani, A., *et al.*, Phys. Rev. Lett., **74**, 3037 (1995).

4 Fisher, M.P.A., *et al.*, Phys. Rev. Lett., **64**, 587 (1990); Fisher, M.P.A., Phys. Rev. Lett., **65**, 923 (1990).

5 Tanda, S., *et al.*, Phys. Rev. Lett., **69**, 530 (1992).

6 Ichikawa, F., *et al.*, Solid State Comm., **98**, 139 (1996).

7 Herrmann, J., *et al.*, Phys. Rev. B, **54**, 3610 (1996).

8 Hidaka, Y., *et al.*, J. Phys. Soc. Jpn., **60**, 1185 (1991).

9 Tanda, S., *et al.*, Phys. Rev. B, **43**, 8725 (1991).

10 Hagen, S.J., *et al.*, Phys. Rev. B, **45**, 515 (1992).

11 Ando, Y., *et al.*, Phys. Rev. Lett., **75**, 4662 (1995).

Specific Heat of the 2D Hubbard Model

Duffy, D., NHMFL
Moreo, A., FSU/Physics, NHMFL, and MARTECH

Quantum Monte Carlo results for the specific heat c of the 2D Hubbard model are presented. At half-filling, $c \approx T^2$ at low temperature and two distinct features are observed: a low temperature peak related to the spin degrees of freedom and a higher temperature feature related to the charge degrees of freedom. Away from half-filling the spin feature slowly disappears as a function of doping while the charge feature moves to lower temperature. Comparisons with experimental results for the high temperature cuprates are made.

Effect of Li-Doping in La_2CuO_4 and La_2NiO_4

Fisk, Z., NHMFL/FSU, Physics
Sarrao, J.L., NHMFL
Hammel, P.C., LANL
Yoshinari, Y., LANL
Suh, B.J., LANL
Thompson, J.D., LANL

La_2CuO_4, the prototypic single layer cuprate, can be hole-doped in two ways chemically: out-of-plane Sr-doping and in-plane Li-doping. In both cases, one hole is added to the CuO_2-planes per dopant atom. In the Li case, the doped material is insulating for all x. It is therefore remarkable that the Li-doping in other respects is identical to Sr-doping. The in-plane plaquette size, as determined by lattice constant measurements, depends only on x. The magnetism of La_2CuO_4 is suppressed at essentially the same rate for Sr or Li substitution.

The rate of suppression of T_c in optimally-doped $La_{1.85}Sr_{0.15}CuO_4$ by added Li is relatively weak, being similar to that due to excess Sr doping and being several times smaller than that found for Zn substitutions.[1]

We have also studied $La_2Cu_{0.5}Li_{0.5}O_4$, which is an atomically ordered, diamagnetic, insulating material. Each Cu connects in-plane through an O to a Li, and vice versa. Despite the observed diamagnetism, Cu NQR measurements reveal a magnetic relaxation mechanism with an activation energy of 1500 K.[2] Thus, the ground state appears to be a magnetic singlet, involving the Cu spins and the one doped hole per Cu that is present, with a triplet excitation whose characteristic energy is 1500 K. This appears to be a new and unexpected result in the physics of the doped CuO_2-planes.

Recently, we have begun similar experiments on Li-doped La_2NiO_4. In this compound the Ni ions form a spin-1 lattice. Here, as Li is substituted, the effective magnetic moment per Ni ion increases, and for $La_2Ni_{0.5}Li_{0.5}O_4$, the Ni appears to be in a rather unexpected low-spin d^7 configuration. More work remains to be done, but the similarities and differences between this system and the spin-1/2 La_2CuO_4 case should provide valuable insight into the detailed interaction of spin and charge in these layered materials.

References:

1 Sarrao, J.L., *et al.*, Phys. Rev. B, **54**, 12014 (1996).

2 Yoshinari, Y., *et al.*, Phys. Rev. Lett., **72**, 2069 (1996).

De Haas Van Alphen Measurements on Superconductors and Heavy Fermions

Goodrich, R.G., LSU, Physics
Lowndes, D.H., Oak Ridge National Laboratory
Hall, D., LSU, Physics
Godbole, M.G., Oak Ridge National Laboratory

During 1996 we spent six weeks at the NHMFL in Tallahassee and Los Alamos taking data on several superconducting materials and one heavy Fermion compound. The materials studied are $YBa_2Cu_3O_7$ (YBCO), $Ba_{0.6}K_{0.4}BiO_3$ (BKBO), and CeB_6. Most of the measurements both in the resistive and pulsed field magnets were made below 0.5 K in a ^{3}He refrigerator. A continuing problem at Tallahassee for this work is the lack of adequate field modulation of the resistive magnets.

$YBa_2Cu_3O_7$ (YBCO). We again attempted measurements of dHvA on YBCO, a continuation of the first ever such measurement on patterned epitaxial films. For the detection of signals we had produced several sample-coil sandwiches at ORNL, in addition to an astatic balancing coil. During cool-down the sample becomes superconducting, and 4.2 K *in situ* balancing of the coil pair becomes necessary. We accomplish this by placing the balancing coil on a rotator so that the area exposed to the modulation field can be reduced and balance achieved. Many data sets from 10 to 50 T, using both steady and pulsed fields and at temperatures between 0.5 and 4.2 K, were collected and we are in the process of analyzing the data. After converting to a 1/B scale a Discrete Fourier Transform (DFT) is performed. Several peaks appear in each of the transforms, some of which are not reproducible, and some of which correspond to dHvA frequencies and their harmonics. With nearly 100 data sets now in hand, the analysis becomes a time consuming process.

$Ba_{0.6}K_{0.4}BiO_3$ (BKBO). During one of our runs at Tallahassee this year we made extensive measurements on a sample that had been ground into a sphere to eliminate phase smearing due to demagnetizing effects. We now are in the process of analyzing this data. We are using a sample rotator in the resistive magnets at the NHMFL in order to collect complete angular data on this material. More measurements need to be made on this material before a complete Fermi surface can be established. This work will form part of the basis of the Ph.D. thesis of Mr. Donavan Hall who is a Graduate Research Assistant at LSU.

CeB_6. A considerable amount of data on the dHvA effect in CeB_6 at 0.5 K and in fields from 20 to 32 tesla was obtained this year. The frequencies and effective masses for the 8.6 kT orbit with the field along the [100] were determined. When added to

the data between 6 and 15 T taken between 0.025 and 0.2 K at LSU we are able to trace the field dependence of both the frequency and effective mass over a considerable range. The fact that both the mass and the dHvA frequency are field dependent is unique to this material. In addition we began measurements of two lower frequency orbits in CeB_6. For these measurements much higher modulation amplitudes are required than we are able to achieve with the small modulation coil wound on the tail of the dewar. Therefore we made measurements at 2 Hz by modulating the entire magnet power supply. This technique is not really satisfactory because of the considerable 1/f noise at 2 Hz and the fact that we are limited to first harmonic detection, lacking a 2 Hz filter. Reasonably strong signals from two orbits were observed in this manner, however. Our initial analysis of this data shows that there are either strong magnetic interaction effects, or magnetic breakdown is occurring. We will return in January 1997 to continue with these measurements. This work will be another part of the Ph.D. thesis for Mr. Donavan Hall.

Force Magnetometer Measurements on $Ba_{0.6}K_{0.4}BiO_4$.

M. Chaparala, M.L. Norton, D. Hall, and R.G. Goodrich

As a supplementary experiment to our dHvA work on BKBO we have measured the force on a sample as a function of field and temperature using the cantilever force magnetometer at the NHMFL. The ranges covered were fields from 0 to 25 tesla and temperatures from 1.5 to 20 K. While the data does not show oscillations, there is a very interesting effect showing up in the data. Measurements of H_{c2} and the reversibility field, H_r, are obtained from the data. We find that at temperatures below about 13 K these two fields coincide. Above 13 K there are two distinct fields for the two transitions. Thus it appears that in this material a critical point in the superconducting magnetic phase diagram is observed. This data is currently being added to the extensive SQUID magnetometer data we have taken at LSU and a paper on the results is being written.

De Haas-Van Alphen Effect and Excitation Spectrum in s- and d-Wave Superconductors in Intermediate Strength Magnetic Fields

Gor'kov, L.P., NHMFL
Schrieffer, J.R., NHMFL/FSU, Physics

We have studied the problem of pairing in a magnetic field whose strength is such that the penetration depth is larger than the vortex spacing, which in turn is larger than the coherence length. In this regime, B and the magnitude of the gap are essentially uniform in space. Making a gauge transformation to remove phase fluctuations of the gap, we find the resulting problem can be treated within the semiclassical approximation for an arbitrary Fermi surface. The observable properties of this system are being worked out, including the de Haas-van Alphen amplitude in both s- and d-wave phases as well as the quasiparticle excitation spectrum.

Spectrum of Lightly Doped Cuprates

Gor'kov, L.P., NHMFL
Kumar, P., UF, Physics

Electronic spectrum of CuO_2-planes in cuprates is derived[1] in the framework of a three band model. The basic ingredient of this model is the charge-transfer (CT) gap seen optically in the insulating state of all cuprates. Spectrum[1] consists of two branches having a degeneracy at the (0,0)-point. One branch (the lowest one in the hole language) is completely flat in absence of the direct oxygen-oxygen overlap, hence indicating immediate formation of an extended spin-polaron, once a hole is doped into the insulating antiferromagnetic state. The second band may correspond to itinerant carriers. The degeneracy in the (0,0)-point provides a link between localized holes trapped into polaronic states at T=0, and their thermal excitation into itinerant band. This model explains very well non-exponential (in temperature) behavior of resistivity in low-doped 214-samples (x~.025 and .05), as seen experimentally. In reference 2, it is shown that the ARPES results[3] for $Sr_2CuO_2Cl_2$ can be well described in a mean field approximation,

if a weak direct oxygen-oxygen overlap is added into the model[1]. It is argued that ARPES results[3] are not affected by the polaronic effects above.

References:

1 Gor'kov, L.P., *et al.*, "Hole Spectrum in Three Band Model," to be published in Proceedings of the 10th Anniversary HTS Workshop, Houston, 1996.

2 Gor'kov, L.P., *et al.*, "Back to a Mean Field Hole Spectrum in the Three Band Model," Phyl. Mag., to be published, 1996.

3 Wells, B.O., *et al.*, Phys. Rev. Lett., **74**, 964 (1995).

Spin Fluctuations in Two Dimension

Ha, Z.N.C., NHMFL
Schrieffer, J.R., NHMFL/FSU, Physics

It is generally agreed that the spin fluctuations in the 2D CuO layers of the high T_c superconductors play an important role even though exactly what role they play is not well understood. The goal of this project is to understand the nature of the spin fluctuations in the two-dimensional system.

We discovered that the 2D antiferromagnetic (AF) spin system on square lattice with moderate frustrations (i.e. $J_2/J_1 \approx 0.34$) can be described by a variational ansatz based on the singlet $\nu = 1/2$ FQHE wavefunction without the chirality condition (in contrast to the Kalmeyer-Laughlin wavefunction[1]). In particular, we find its overlap close to 0.94 with the true numerically found ground state for 4 x 4 lattice with $J_2/J_1 = 0.34$. This ansatz can be improved by acting the Hamiltonian on the ansatz several times. (Typically, the overlap of 0.98 can easily be achieved by few applications of the Hamiltonian.) The frustration basically increases the spin fluctuations in the 2D system and destroys the long range AF spin order, and only the short range AF correlation survives. The importance of this short range AF correlation in the high T_c cuprates is stressed in Reference 2.[2]

It is also possible that in the itinerant electron systems without the explicit spin frustration the holes injected induce the frustration and allow the spin sector to be described by the variational ansatz we constructed. (If the density of holes is small enough then the system might also like to phase separate.) We hope to resolve some of these issues by using the analytic wavefunction combined with the numerical technique. The coupling between the spin fluctuation and the charge in the itinerant electron systems is also currently under investigation using our technique and an analytic method based on the quantum field theory in curved space.[3]

References:

1 Kalmeyer, V., *et al.*, Phys. Rev. Lett., **59**, 2095 (1987).

2 Schrieffer, J.R., (unpublished).

3 Schrieffer, J.R., *et al.*, (in progress).

Studies of the Cuprate Spin Gap in High Magnetic Fields

Hammel, P.C., LANL
Martindale, J.A., Ohio State Univ., Physics
Pennington, C.H., Ohio State Univ., Physics
Recchia, C., Ohio State Univ., Physics
Nandor, V., Ohio State Univ., Physics
Suh, B.J., LANL
Kuhns, P.L., NHMFL
Kleinhammes, A., NHMFL
Moulton, W.G., NHMFL

Our interest has been understanding the spin gap in the superconducting cuprates. To accomplish this we are measuring the temperature dependence of the magnetic spin susceptibility of $YBa_2Cu_3O_{6.96}$ and $YBa_2Cu_3O_{6.63}$ in fields of 16 tesla (T) and 24 T, as determined from the ^{17}O Knight shift with field oriented parallel to the crystal c-axis, $^{17}K_c$. These data are being compared with our existing data[1,2] for same quantities measured at 8 T. Our present interest is primarily in normal state properties. Based on determinations[3] of dH_{c2}/dT, we expect that T_c is suppressed to ~78 K ($YBa_2Cu_3O_{6.96}$) and ~50 K ($YBa_2Cu_3O_{6.63}$). Measurements have been made

down to 77 K ($YBa_2Cu_3O_{6.96}$) and 45 K ($YBa_2Cu_3O_{6.63}$). One important feature of this work has been careful calibration of the applied field in order to ensure that the values of the Knight shift can be compared with measurements made in well-calibrated superconducting solenoids. This has been achieved through measurement of the Cs resonance in CsCl as a reference marker.

References:

1 Martindale, J.A., *et al.*, Phil. Mag. B (in press).

2 Takigawa, M., *et al.*, *Phys. Rev. B*, **43**, 247 (1991).

3 Welp, U., *et al.*, *Physical Phenomena at High Magnetic Fields*, ed. E. Manousakis, (Addison - Wesley, 1991).

Superconductor-Insulator Transition in the Electron Doped Superconductor $Pr_{1.85}Ce_{0.15}CuO_{4-y}$

Han, S.H., UCSD, Institute for Pure and Applied Physical Sciences

de Andrade, M.C., UCSD, Institute for Pure and Applied Physical Sciences

Herrmann, J., UCSD, Institute for Pure and Applied Physical Sciences

Maple, M.B., UCSD, Physics, and Institute for Pure and Applied Physical Sciences

We have performed magnetoresistance measurements at the NHMFL-Tallahassee, using a ^3He-^4He dilution refrigerator in the temperature range 30 mK $\leq$ T $\leq$ 500 mK and a 18 T superconducting magnet. The measurements were made on a superconducting single crystal sample of the electron-doped compound $Pr_{1.85}Ce_{0.15}CuO_{4-y}$. This high T_c cuprate superconductor has a rich magnetic field temperature (H-T) phase diagram that includes a possible magnetic filed induced superconductor-insulator transition. Recent measurements on $Nd_{1.85}Ce_{0.15}CuO_{4-y}$, another electron-doped cuprate superconductor, show a much lower upper critical field H_{c2} when compared to other cuprate superconductors. Our results at the NHMFL showed that the upper critical field, determined from the resistivity drop, for magnetic fields applied along the c-axis of the crystal (H||c), is 12 T at 30 mK and 11.2 T at 600 mK. This value is the highest observed among the electron-doped cuprates. In the normal state at 30 mK, the electrical resistivity shows positive magnetoresistance for applied fields 14 T $\leq$ H $\leq$ 17.5 T. The temperature dependence of the electrical resistivity after quenching the superconductivity by a magnetic field at 17 T shows a gradual increase with decreasing temperature. Additional magneto-resistance measurements in these electron-doped cuprate superconductors are planned in order to investigate the magnetic-field induced superconductor-insulator transition and the different regions in the mixed state at very low temperatures and high magnetic fields.

Disorder and Transport in d-Wave Superconductors

Hirschfeld, P., UF, Physics

Putikka, W.O., Univ. of Ohio, Mansfield, Physics

Ziegler, K., MPI-Stuttgart, Germany

Hettler, M., UF, Physics

Theory of Thermal Conductivity in YBCO7.[1]

The electronic thermal conductivity in a d-wave superconductor was calculated, including both the effect of impurity scattering and inelastic scattering by antiferromagnetic spin fluctuations. Existing experiments on YBCO were analyzed, particularly with regard to the question of the relative importance of electronic and phononic contributions to the heat current, and to the influence of disorder on low-temperature properties. Phonons were found to dominate heat transport near T_c, but electrons were responsible for most of the peak observed in clean samples, in agreement with a recent analysis of Krishana *et al.* In agreement with recent data from L. Taillefer on YBC(Zn)O, the peak position was found to vary nonmonotonically with disorder and a simple explanation for this behavior was given. Quantitative fits to this data were obtained for all temperatures and Zn concentrations.

Non-Zero Fermi Level Density of States for a Disordered d-Wave Superconductor in Two Dimensions.[2]

In 3D, arbitrarily weak disorder in superconductors with line nodes gives rise to a nonzero Fermi level density of states N(0), leading to characteristic low-temperature thermodynamics similar to that observed in cuprate and heavy-fermion systems. In a strictly 2D-model possibly appropriate for the cuprates, it has been argued that N(0) vanishes, based on a mapping of the problem to one of Dirac fermions in a random gauge field. An exact calculation was performed for a 2D d-wave superconductor with Lorenzian disorder and found a nonzero N(0). For other continuous distributions exact nonzero lower bounds for N(0) were obtained. The reasons for this disagreement with earlier work were discussed.

References:

1 Hirschfeld, P., *et al.*, *Theory of Thermal Conductivity in YBCO7,* Phys. Rev. Lett., **77**, 3903 (1996).

2 Ziegler, K., *et al.*, *Non-Zero Fermi Level Density of States for a Disordered d-Wave Superconductor in Two Dimensions*, Phys. Rev. Lett., **77**, 3013 (1996).

High Field Critical Currents in Nb_3Sn Multifilamentary Composites

Hong, S., Oxford Instruments, Inc.
Hentges, R., Oxford Instruments, Inc.
Marken, K., Oxford Instruments, Inc.
McKinnell, J., Oxford Instruments, Inc.
Zhang, Y., Oxford Instruments Inc.

Various multifilamentary composites fabricated at Oxford Superconducting Technology were tested for critical current values in magnetic fields up to 27 T and at temperatures between 1.8 and 4.2 K. Test samples included bronze processed and internal tin processed wires. The purpose of the study was understanding and optimizing the Jc performance of these materials with respect to conductor fabrication, processing, and heat treatment.

Engineering current density (current normalized to overall wire cross section) attained in internal tin wire at 1.8 K was greater than 200 A/mm^2 at 18 T and greater than 110 A/mm^2 at 20 T, suggesting that this type of wire is suitable for NMR spectrometer magnets operating above 900 MHz. At 4.2 K, engineering Jc measured in internal tin wire was greater than 110 A/mm^2 at 18 T.

The optimized bronze process wire measured in this study has been used successfully in NMR spectroscopy magnets operated at 4.2 K as high as 800 MHz.

High Field Hysteresis and Flux Matching Effects in Superconducting $YBCO_7$

Hope, A.P., SUNY Buffalo, Physics
Leone, M.J., SUNY Buffalo, Physics
Petrov, D.K., SUNY Buffalo, Physics
Chaparala, M.V., NHMFL
Gajewski, D.A., UCSD, Physics
Han, S., UCSD, Physics
Maple, M.B., UCSD, Physics
Naughton, M.J., SUNY Buffalo and NHMFL

The high temperature superconductors have a layered crystalline structure, with this feature reflected in the superconducting properties. The various cuprate superconductors differ in the magnitude of their anisotropy, quantified by the ratio $\Gamma = (m_\perp/m_{//})^{1/2}$, where $m_{//}$ ($m_\perp$) is the effective mass of the superconducting electrons in (normal to) the layers. This quasi-two-dimensional nature gives rise to interesting anisotropic electronic and magnetic phenomena. When these superconductors are in a magnetic field $H_{c1} < H < H_{c2}$, quantized vortices penetrate the sample. As one might expect, the interplay of the crystalline anisotropy and the vortices yields many interesting angular dependent phenomena.

$YBa_2Cu_3O_{7-\delta}$ ($YBCO_7$, $\Gamma \sim 8$) is considered weakly anisotropic in comparison to other cuprates, such as the Bi- and Tl-based systems ($\Gamma \geq 10^2$). This anisotropy is manifest in the irreversible as well as the reversible component of the magnetization. Here, we report on high field

(20 T) torque measurements on detwinned single crystal $YBCO_7$ in the mixed state, using silicon cantilever magnetometry. Magnetic field sweeps were conducted for various field orientations with respect to the c-axis, the normal to the layers.

Depicted in Figure 1 is a set of field sweeps at different temperatures above and below T_c taken with the magnetic field aligned 4° from the a-b plane. The largest of the "butterfly" curves is at the lowest temperature (85 K), where hysteresis due to pinned flux is the strongest. On individual curves at higher temperature, the measurement becomes non-hysteretic or reversible. The point at which hysteresis starts is interpreted as marking the irreversibility line. A monotonic background term is observed above T_c, likely due to a combination of normal state anisotropy and measurement background. Looking at the field sweeps for temperatures near 89 ± 2 K, a multi-peak structure appears. We have highlighted such distinguishing features for B>0. These inflection points are yet to be explained, but we are investigating the possibility that we are observing the vortex liquid-vortex solid melting line, and its bifurcation at lower T.

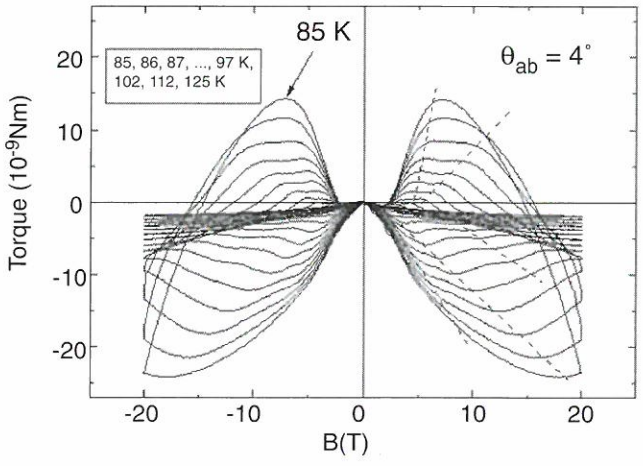

Figure 1. Torque magnetization for various temperatures in single crystal $YBCO_7$ for magnetic field tilted 4° from the a-b layers. The dashed lines serve to highlight the features described in the text.

We show in Figure 2 a set of field sweeps taken with the magnetic field tilted ~26° from the a-b plane. The overall shape of the butterfly curves is altered in appearance as compared to the much smaller tilt in Figure 1, but the main features are similar. In Figure 2, hysteresis is observed only up to 10 T, above which the system enters the reversible, presumed vortex liquid, state. For data just below T_c, inflection points akin to those in Figure 1 persist, but are not readily apparent on this scale. This is likely due to the fact that the overall torque signal (reversible and irreversible) is much increased at this orientation, as is expected with the larger c-axis component.

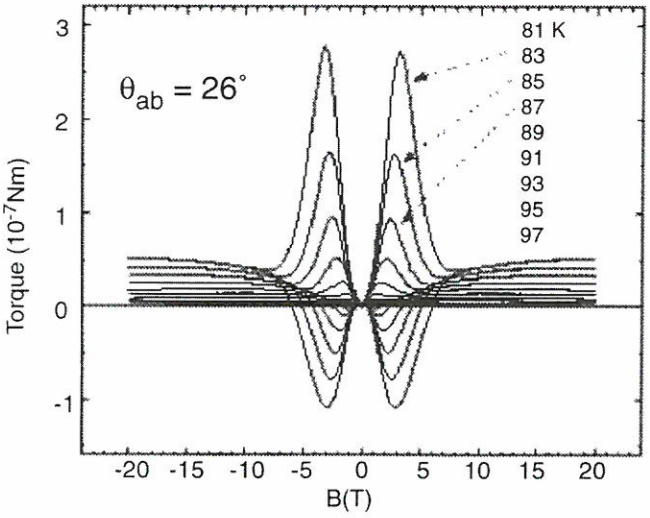

Figure 2. Torque magnetization for the sample of Figure 1 for field tilted 26° from the a-b layers.

Additional studies are planned throughout a larger (T,B,θ) space to investigate the nature of the substructure in Figure 1.

This work was supported by the New York State Energy Research and Development Authority.

Long-Range Order Near H_{c2} in Disordered Type II Superconductors

Hu, J., NHMFL
MacDonald, A.H., Indiana Univ., Physics
Girvin, S.M., Indiana Univ., Physics

Because of the combination of high transition temperatures, strong anisotropy, and short coherence lengths that occurs in high temperature superconductors, strong thermal fluctuations are present over a wide temperature interval in these

materials, which gives us a qualitatively new accessible regime in the phenomenology of type-II superconductivity. The key elements governing the statistical mechanics and the dynamics of the vortex system are the thermal fluctuations and the quenched disorders.[1] Thermal fluctuations are especially important in a magnetic field where they are responsible for the melting of the Abrikosov vortex lattice at temperatures below the mean-field critical temperature giving rise to a vortex liquid state. In the strong field limit, the fluctuating spectrum of the superconducting order parameter exhibits Landau level degeneracy that greatly enhances fluctuations. We employed Lowest Landau Level approximations to study the long-range superconducting order in the Ginzburg-Landau and Lawrence-Doniach models for layered superconductors in a strong magnetic field[2] with the quenched disorders modeled as random local T_c pinning potentials. Due to the extreme slow dynamics of this system, the usual methods to look at the superconducting state by making an analogy with spin glass systems seem difficult to apply. The disorder effects and superconducting order are currently studied by evaluation of the gauge-invariant eigenvalues of density matrix of the order parameter. The distributions of these eigenvalues and corresponding eigenvectors can give us important information in the system. For the clean system at the zero-temperature, the system will be in the Abrikosov lattice state that exhibits both broken translational symmetry and off-diagonal long-range order (ODLRO), which is indicated by all eigenvalues being zero but one becoming macroscopic. In the vortex liquid state, all eigenvalues are microscopic. By studying the ratio of largest eigenvalue to sum of all eigenvalues and its size dependence for the finite systems, we are able to be in a better position to answer the question of whether or not true long-range superconducting order occurs in this system.

References:

1 Fisher, D.S., *et al.*, Phys. Rev. B, **43**, 130 (1991).

2 Hu, J., *et al.*, Phys. Rev. Lett., **71**, 432 (1993).

^{7}Li NMR Studies of $La_2Cu_{1-x}Li_xO_4$ at High Magnetic Fields

Kuhns, P.L., NHMFL
Kleinhammes, A., NHMFL
Moulton, W.G., NHMFL/FSU, Physics
Sarrao, J.L., NHMFL
Fisk, Z., NHMFL/FSU, Physics
Sullivan, N.S., NHMFL/UF, Physics

La_2CuO_4, with its many doped versions has been considered as a model system for studying the interplay between magnetism and superconductivity determined by the holes introduced by doping, and the localized moments on the Cu. Questions which must be answered to understand the behavior of the doped cuprates concerns the interaction of the holes with the Cu and O and the effect on the exchange, the spin correlation excitation spectrum, and the magnitude of the hole delocalization. The objectives of this research are to use NMR studies as a function of temperature and field to provide new insights into these questions. Data have been taken in the new 5 ppm/mm magnet on a x = 0.015 powder sample. The spin-lattice relaxation rate, $1/T_1$ as a function of temperature is shown in Figure 1.

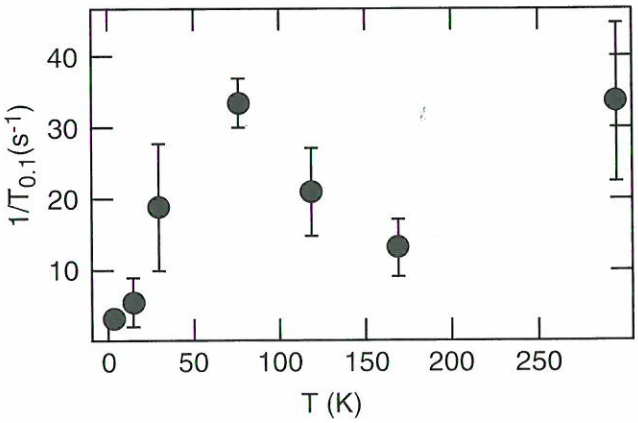

Figure 1. Inverse spin-lattice relaxation time as a function of temperature in $La_2Cu_{0.985}Li_{0.015}O_4$.

We speculate that the peak in $1/T_1$ is due to a Mott variable range hopping mechanism in 2D[1]. Assuming that the peak in $1/T_1$ corresponds to the matching of the variable range hopping frequency to the Larmor frequency, the data fits with a high temperature phonon frequency $\nu=10^{14}$ sec^{-1}. Data at different fields (different frequencies) will test

this model. Another striking aspect of the data is the lack of any broadening of the ^{7}Li line in the ordered state, while the ^{139}La shows the expected splitting from the two sublattices. A dipole calculation gives a broadening of 220 G, which should have easily been seen in the data, even if there is no transferred hyperfine field at the Li site. This can be understood if the holes suppress the moment on the nearest neighbor Cu's to the Li ions. Further experimental work will test this hypothesis by using NMR to measure the spin-spin correlations between the Li and the NN Cu. In particular, work at high fields will provide new information on the effect of field on the spin fluctuations and the spin couplings.

Reference:

1 Kastner, M.A., *et al.*, Phys. Rev B, **37**, 111 (1988).

Activation Energies for Vortex Motion in the Vortex-Liquid State of $YBa_2Cu_3O_7$

López, D., IBM Yorktown Heights
Safar, H., Univ. of Illinois at Chicago, Physics
Krusin-Elbaum, L., IBM Yorktown Heights
Maley, M.P., LANL–STC

The novel vortex-liquid phase observed in the mixed state of high temperature superconductors poses many interesting problems. In particular, it was suggested[1] that in this phase there is a possibility of topological entanglement of the vortex lines. In the present project we investigated this possibility by measuring the field dependence of the activation energy for vortex motion in the liquid state of clean, untwinned single crystalline YBaCuO.

The activation energy U_0 can be extracted from a fit of the temperature and field dependence of the electrical resistivity in the vortex-liquid state to a thermally-activated temperature dependence of the form $\rho = \rho_0 \exp(U_0(T,H) / kT)$. Theoretical models based on the energy necessary to break the vortex entanglement predict[2] a magnetic field and temperature dependence of the form $U_0 \sim U_0(T) / H^{0.5}$. On the other hand, the activation energy of a system of two-dimensional vortex pancakes is expected[3] to have a similar temperature dependence, but with a 1 / H magnetic field dependence instead.

We experimentally determined temperature and field dependence of the activation energy. In the inset of Figure 1 is shown the temperature dependence of U_0 at a field of 18 T. At high temperatures U_0 rises smoothly, and reaches a plateau at about 60 K, following the expected temperature dependence. At lower temperatures U_0 is seen to diverge, due to the proximity of the vortex liquid-to-solid phase transition, which was not considered in the theoretical models. The value of the activation energy at the plateau is shown in the main panel of Figure 1 as a function of the magnetic field. It is seen to decay as a power law of H, as shown by the full line. The exponent in the power law is found to be 0.78 ± 0.05. The value of the power law exponent, found to be the same in three samples investigated, is not predicted by any of the theoretical models considered. Further investigations of the dependence of the activation energy on the vortex dimensionality and crystallographic disorder are being pursued.

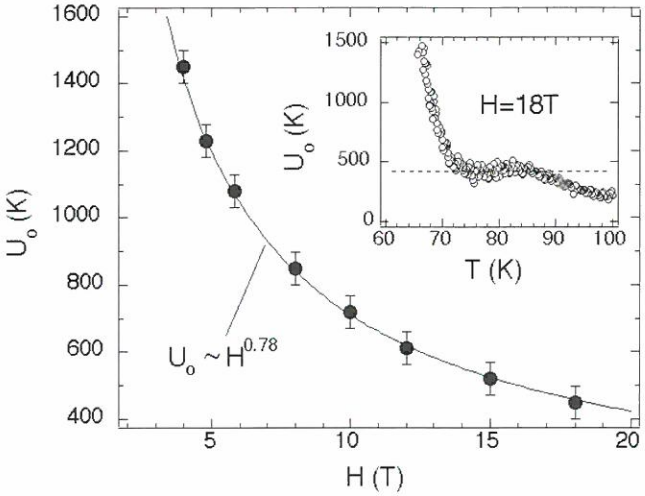

Figure 1. Magnetic field dependence of the activation energy U_0. The values shown in the figure are extracted from the plateau seen in the temperature dependence of U_0 at the different magnetic fields. Inset: Temperature dependence of U_0 at a magnetic field of 18 T as obtained from a fit of the electrical resistance to a thermally-activated model.

References:

1 Nelson, D.R., Phys. Rev. Lett., **60**, 1973 (1988).

2 Vinokur, V.M., Phys. Rev. Lett., **65**, 259 (1990).

3 Bulaevskii, L.N., private communication.

Local Enhancement of Antiferromagnetic Correlations by Nonmagnetic Impurities

Martins, G.B., NHMFL
Laukamp, M., NHMFL
Riera, J., Instituto de Física Rosario, Argentina
Dagotto, E., NHMFL

The enhancement of antiferromagnetic (AF) correlations near vacancies observed experimentally[1] and numerically[2] in a variety of spin systems is analyzed in a single framework. It is argued that the Resonant Valence Bond (RVB)[3] short distance character of the spin correlations is responsible for the enhancement. Independently of the long distance properties of the model being studied, the small distance behavior, at least for small S, is dominated by the formation of short spin singlets resonating in all their possible arrangements. The key detail to understand the AF enhancement is to note that in the absence of a vacancy (a nonmagnetic ion) each spin resonates with all its neighbors (2 in one dimensional systems); with the introduction of the vacancy there is one less neighbor to resonate, so the spin in question forms singlets more times with the remaining spins, actually enhancing the average correlation at short distances. At long distances the correlations should be virtually the same as for the undoped system. Numerical results for uniform spin chains, with and without frustration, dimerized chains, ladders, and two dimensional clusters are in quantitative agreement with our conjecture. This local phenomenon occurs independently of the long distance behavior of the spin correlation in the undoped system.

References:

1 Azuma, M., *et al.*, preprint; Hase, M., *et al.*, Phys. Rev. Lett., **70**, 3651 (1993); Oseroff, S.B., *et al.*, Phys. Rev. Lett., **74**, 1450 (1995); Regnault, L.P., *et al.*, Europh. Lett., **32**, 579 (1995).

2 Martins, G.B., *et al.*, to appear in Phys. Rev. B.

3 Anderson, P.W., Mater. Res. Bull., **8**, 153 (1973).

Many-Body Basis-Set Reduction Applied to the Two-Dimensional t-J Model with Holes

Martins, G.B., NHMFL
Riera, J., Instituto de Física Rosario, Argentina
Dagotto, E., NHMFL

We apply the systematically expanded Hilbert space technique[1] to the study of the t-J model in 2 X 20 and 4 X 8 ladders with 0, 2, and 4 holes. Even though the complete Hilbert space for these systems cannot fit in present-day computer memories, only a small percentage of the total number of states is enough to describe accurately their physical behavior. Starting with just one state, and applying an iterative process of expansion and truncation, the majority of these more "representative" states can be sorted out of the complete Hilbert space, forming a truncated basis. The advantage of using this technique, along with the Lanczos Method,[2] lies in the possibility of calculating dynamic properties.

Further improvement can be obtained by a change of basis: Instead of using as basis states the direct product of the eigenstates of individual S_z operators, a change is made to a new basis that is a product of previously coupled S_z eigenstates, e.g., singlets and triplets along the rungs of a 2 X N ladder. The use of this new basis makes the number of "representative" states even smaller, allowing the study of bigger systems and increasing the accuracy of the method.

References:

1 Riera, J., *et al.*, Phys. Rev. B, **47**, 15346 (1993).

2 Dagotto, E., Rev. Mod. Phys., **66**, 763 (1994).

3DXY vs. Lowest Landau Level Fluctuations in Deoxygenated $YBa_2Cu_3O_7$ Thin Films

McElfresh, M.W., Purdue Univ., Physics
Moloni, K., Purdue Univ., Physics
Friesen, M., Purdue Univ., Physics
Li, S., Purdue Univ., Physics
Souw, V., Purdue Univ., Physics
Metcalf, P., Purdue Univ., Physics
Hou, L., Purdue Univ., Physics

The continuous vortex solid melting transition is investigated in three deoxygenated $YBaCu_3O_{7-\delta}$ thin films with stoichiometries of $\delta \sim 0.24$, 0.57 and 0.59. The films were patterned into 100 μm x 2000 μm bridges. Isothermal current-voltage and resistivity curves were obtained using a conventional four-point geometry. Glass transition temperatures, T_g, were obtained, using the scaling analysis of Fisher, Fisher and Huse,[1] in the field range $0 < H \leq 26$ T. The glass scaling exponents ν_g and z_g are found to be independent of field, with values $\nu_g = 1.8\text{-}1.95$ and $z_g = 4.0 - 4.1$.

The phase boundaries $H_g(T)$ [inverse of $T_g(H)$] are shown in Figure 1. As shown in the inset, power law behavior of the form $H_g(T) = H^*(1\text{-}T/Tc)^{2\nu_{xy}}$ is observed for low fields, in the temperature range $.5T_c \leq T \leq T_c$, in accordance with the 3DXY prediction.[1] The exponent $\nu_{xy} = 0.63 \pm 0.4$, determined from the figure, is in good agreement with the expected value of 0.669.[2]

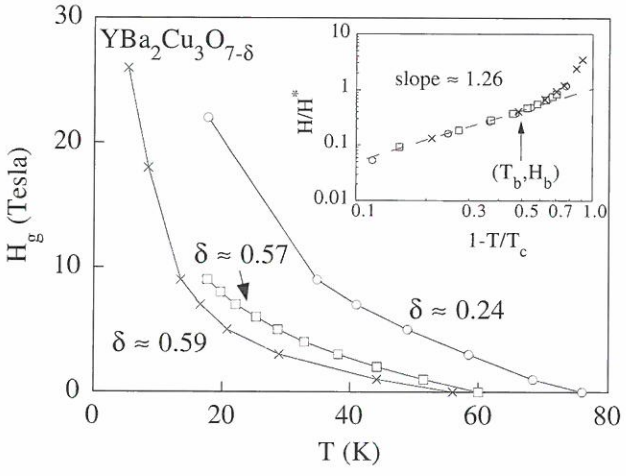

Figure 1. Phase boundaries $H_g(T)$ [inverse of $T_g(H)$].

In addition to glass scaling, multicritical 3DXY and LLL scaling theories were also used to study the ohmic conductivity. In agreement with the power law of Figure 1 (inset), excellent 3DXY scaling is observed for fields $H \leq H_b$ [$= H_g(.5T_c)$]. This low-field analysis yields a dynamic 3DXY exponent $z_{xy} = 1.25 \pm 0.05$, which disagrees with the expected result of $z_{xy} = 2$.[1] For high fields $H \geq H_b$, the ohmic conductivity scales self-consistently according to the LLL theory, in contrast to previous experiments suggesting LLL scaling at low fields.[3] This analysis yields the temperature dependence of $H_{c2}(T)$ curves, which are found to exhibit positive curvature.

References:

1 Fisher, D.S., *et al.*, Phys. Rev B, **43**, 130 (1991).

2 Salamon, M.B., *et al.*, Phys. Rev. B, **47**, 5520 (1993).

3 Welp, U., *et al.*, Phys Rev. Lett., **67**, 3180 (1991).

Monte Carlo Studies of the Two Dimensional Electron Gas in a Magnetic Field

Melik-Alaverdian, V., NHMFL/FSU, Physics
Ortiz, G., LANL, Theoretical Division
Bonesteel, N.E., NHMFL/FSU, Physics

The "fixed-phase" diffusion Monte Carlo (FPDMC) method of Ortiz *et al.*[1] is a promising new numerical technique for studying electrons in a magnetic field. The FPDMC has been applied to the problem of interacting electrons on the "Haldane sphere," *i.e.*, electrons on the surface of a sphere with a uniform magnetic field normal to its surface. It has been shown that the so-called "quantum corrections"[2] to the propagator or Green's function must be included when simulating electrons by diffusion Monte Carlo on a curved manifold. These corrections have been worked out for the case of a general metric. Specializing to the sphere, the test case of a charge-monopole system has been solved and compared with the exact result. The FPDMC method also has been used to study the effect of Landau level mixing on the quasielectron and quasihole excitation gaps in the

fractional quantum Hall effect, again using the spherical geometry. The results are an "unbiased" improvement on earlier variational calculation.[3]

References:

1 Ortiz, G., *et al.*, Phys. Rev. Lett., **17**, 2777 (1993).

2 DeWitt, B.S., Rev. Mod. Phys., **29**, 377 (1957).

3 Melik-Alaverdian, V., *et al.*, Phys. Rev. B, **52**, 17032-17035 (1995).

Spin-Fluctuation Mechanism for High-T_c Superconductivity

Monthoux, P., FSU, Physics/NHMFL

We have calculated, within perturbation theory, the correction to the Eliashberg approximation for nearly antiferromagnetic Fermi liquids. The vertex corrections to the effective interaction that determine the normal state properties of the model result in an increase of the quasiparticle spin-fluctuation coupling for spin-fluctuation momenta near the antiferromagnetic wavevector $\vec{Q} = (\pi, \pi)$ for a large Fermi surface. This increase gets larger as the antiferromagnetic correlation length increases and is very anisotropic. It is most important for points on the Fermi surface where the $d_{x^2-y^2}$ gap is large. These higher order corrections also result in a stronger pairing potential in the $d_{x^2-y^2}$ channel relative to the one-loop Eliashberg contribution.[1]

We provide a detailed numerical comparison between various approaches to the problem of antiferromagnetically correlated metals. We study the strength of the shadow band peak in the spectral function and the depth of the pseudogap in the density of states as a function of the spin-fluctuation spectrum. We show that a well developed pseudogap and a strong shadow band peak should only be experimentally observable for large antiferromagnetic enhancements of the effective low-energy interaction.[2]

References:

1 Monthoux, P., submitted to Phys. Rev. B.

2 Monthoux, P., submitted to Phys. Rev. B.

Fluctuation Diamagnetism in Single Crystal Hg-1223

Naughton, M.J., SUNY Buffalo, Physics, and NHMFL

Hope, A.P., SUNY Buffalo, Physics

Janossy, B., INSA, Toulouse, France

Fruchter, L., Univ. of Paris-Sud, Orsay, France, LPS

Torque magnetization measurements on single crystal $HgBa_2Ca_2Cu_3O_x$ (T_c = 132 K) were undertaken between 80 K and 240 K, in magnetic fields to 30 T, employing silicon cantilever magnetometry. A diamagnetic signal was detected at temperatures above as well as below T_c in the high field regime (B>1 T), the former assumed to arise from superconducting fluctuations into the normal state.

There are a few notable features. (1) After accounting for an anisotropic, paramagnetic component to the normal state susceptibility, a diamagnetic magnetization signal appears to persist to at least 200 K at 30 T. (2) Two-dimensional and three-dimensional scaling functions unexpectedly fail to provide distinguishing information on the dimensionality of the superconductivity in this layered cuprate system. Essentially, both scaling functions work equally well (or, equally poorly). (3) Finally, an anticipated crossover point in magnetization - temperature space at (M*,T*), where the magnetization is independent of magnetic field, is found to exist for low fields only (i.e. below 10 T), with the apparent T* decreasing at higher fields.

In Figure 1 we show data from representative temperature sweeps at constant magnetic fields of 10, 20, and 30 T, with the crystal c-axis tilted 15° from the field direction. These data include within them a signal due to the normal state anisotropy of the material, which should be (and is, as best we can tell) independent of temperature. Also included in the figure are 30 T points taken from fixed temperature field sweeps up to 270 K. There appears to remain a diamagnetic signal to greater than 200 K. It must be stated that the

superconducting fluctuation signal depends sensitively on the background, normal state signal, and so we remain cautious in attributing the data in Figure 1 to fluctuations at such elevated temperatures. Further studies on other samples should help to clarify the situation.

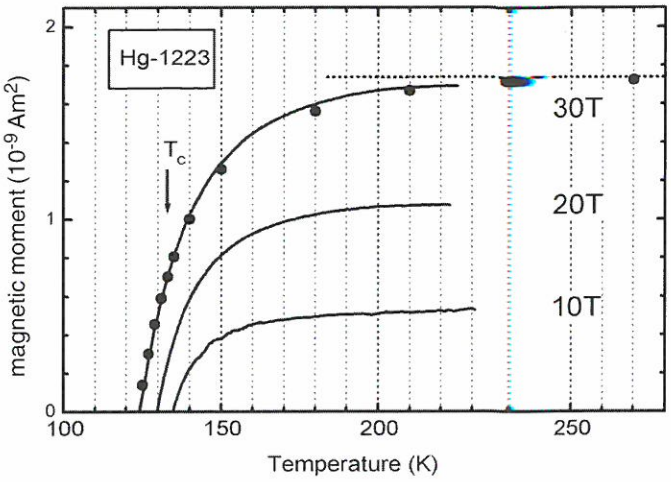

Figure 1. Magnetization versus temperature at 10 T, 20 T and 30 T for a $HgBa_2Ca_2Cu_3O_{8+\delta}$ (Hg-1223) single crystal in the fluctuation regime at temperatures well above T_c = 132 K. The solid points are taken from fixed T field sweeps up to 270 K. The dashed line simply extends the 270 K, 30 T point to lower temperatures to highlight that the diamagnetic signal persists to above 200 K.

Regarding the crossover at (M*,T*), anticipated in thermal fluctuation theories,[1] and reportedly observed in several cuprate systems,[2] we do observe a general crossover of M(T) curves, with a common moment. This can be seen in Figure 2, where we plot magnetic moment derived from magnetic torque measurements (again, with H tilted 15° from c) vs. temperature at several values of magnetic field, namely 2, 4, 6, ..., 30 T. The crossover can be seen near T*~127 K, with magnetic moment at T* of -m*~1.5 nAm^2 (0.15 emu/cm^3). However, as can be seen in the inset, this T* is *not* independent of field above a few tesla, such that the 28 T and 30 T lines cross at 122.5 K, with -m*=1.8 nAm^2. Thus, the crossover breaks down, implying that the energy loss from fluctuation vortices is able to exceed the free energy of the undistorted lattice at these high magnetic fields.

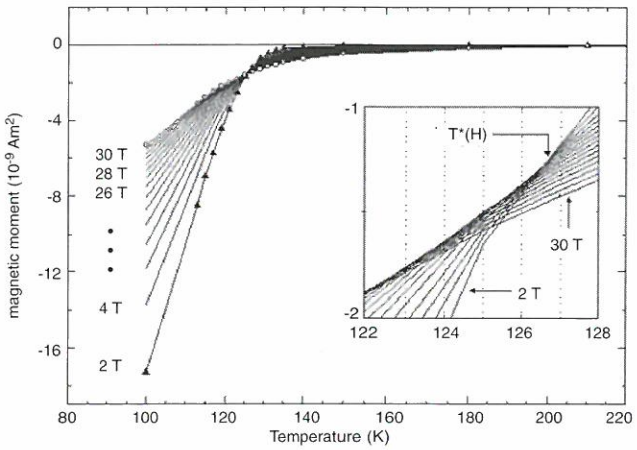

Figure 2. M(T) at constant H between 2 T and 30 T, showing a "crossover" near (M*,T*) = ($1.5x10^{-9}$ Am^2, 127 K), as well as the large fluctuation regime above T*. These data have a normal state paramagnetic component removed. This component is assumed to be independent of temperature (see dashed line in Figure 1). The inset shows that, in fact, the crossing point depends on the field strength, with T* falling to ~123 K at the highest field.

References:

1 Bulaevskii, L.N., *et al.*, Phys. Rev. Lett., **61**, 3773 (1991); Tesanovic, Z., *et al.*, Phys. Rev. B, **49**, 4064 (1994); Koshelev, A.E., Phys. Rev. B., **50**, 506 (1994).

2 Tesanovic, Z., *et al.*, Phys Rev. Lett., **69**, 3563 (1992); Bae, M-K., *et al.*, Physica C, **228**, 195 (1994); Vulcanescu, V., *et al.*, Physica C, **259**, 131 (1996).

A Possible Phononic Mechanism for d-Wave Superconductivity in the Presence of Short-Range Antiferromagnetic Correlations

Nazarenko, A., Boston College, Physics
Dagotto, E., FSU, Physics/NHMFL

We discuss the high temperature superconductors in a regime where the antiferromagnetic (AF) correlation length is only a couple of lattice spacings.[1] In the model proposed here, these short-range AF fluctuations play an essential role in the dressing of the carriers, but the attraction needed for superconductivity arises from a transverse phonon oxygen mode with a finite

buckling angle as it appears in YBCO. A simple fermion-phonon model analog to the Holstein model is introduced to account for this effect. We argue that the model has a d-wave superconducting groundstate. The critical temperature (T_c) and the O-isotope effect coefficient vs. hole density are in qualitative agreement with experiments for the cuprates. The minimum (maximum) of the O-isotope coefficient (T_c) at optimal doping is caused by a large peak in the density of states of holes dressed by AF fluctuations, as discussed in previous van Hove scenarios.

Reference:

1 Nazarenko, A., *et al.*, Phys. Rev. B, **53**, R2987 (1996).

Hole Dispersion and Symmetry of the Superconducting Order Parameter for Underdoped CuO_2 Bilayers and 3D Antiferromagnets

Nazarenko, A., Boston College, Physics
Dagotto, E., FSU, Physics/NHMFL

We calculate the dispersion of a hole in CuO_2 bilayers and 3D antiferromagnets, using the self-consistent Born approximation to the t-J model.[1] Superconductivity and the symmetry of its order parameter are studied introducing a nearest-neighbor density-density attraction induced by short range antiferromagnetic fluctuations, as described in recent studies for the single layer cuprates. The well-known pairing in the $d(x^2-y^2)$ channel observed for one plane remains robust when three-dimensional interactions are turned on. In bilayers, as the exchange along the direction perpendicular to the planes grows, eventually a transition to a "s-wave" state is observed with an order parameter mixture of $d(3z^2-r^2)$ and $s(x^2+y^2+z^2)$. For an isotropic 3D antiferromagnet the $d(x^2-y^2)$ and $d(3z^2-r^2)$ channels are degenerate. Our results are compared with other predictions in the literature.

Reference:

1 Nazarenko, A., *et al.*, to appear in Phys. Rev. B.

Influence of Hole Doping on Antiferromagnetic Real-Space Approaches for the High-T_c Cuprates

Nazarenko, A., Boston College, Physics
Haas, S., Theoretische Physik, ETH, Zurich, Switzerland
Riera, J., Rosario Univ., Physics, Rosario, Argentina
Moreo, A., FSU, Physics/NHMFL
Dagotto, E., FSU, Physics/NHMFL

Recently proposed scenarios for the cuprates make extensive use of a "flat" quasiparticle (q.p.) dispersion and short-range hole-hole interactions in real-space, both caused by strong antiferromagnetic (AF) correlations. The density of states (DOS) at half-filling has a robust peak, which, in a simple BCS approach, boosts the superconducting critical temperature T_c to large values as holes are introduced into the (rigid) q.p. band. Here, the stability of such scenarios is studied after a finite but small hole density is introduced.[1] In spite of substantial modifications in the photoemission spectra induced by doping, the overall conclusion is that the main features of real-space AF-based approaches remain qualitatively similar, namely a large T_c is found and superconductivity (SC) appears in the $d(x^2-y^2)$ channel. As the hole density grows the chemical potential crosses a broad peak in the DOS. We also observe that extended s-wave SC may compete with d-wave in the overdoped regime.

Reference:

1 Nazarenko, A., *et al.*, submitted to Phys. Rev. B.

Characterization of Internal-Tin Nb_3Sn at Variable Temperature and Magnetic Field

Pyon, T., IGC Advanced Superconductors
Wheatley, R., Intermagnetics General Corporation
Gregory, E., IGC Advanced Superconductors

Internal tin processed Nb_3Sn wires have been fabricated to investigate the effects of titanium on strand performances. Improvements were found in

hysteresis losses and n-values as well as changes in the current carrying capacity. The principal goal of this study is to establish experimentally the temperature dependence of J_c for internal-tin Nb_3Sn at 3.5 K to 12.0 K and 4 T to 18 T using the 20 T superconducting magnet at the NHMFL–Los Alamos Facility. Two full scaled-up billets were processed. One with titanium in the copper matrix and the other with titanium in the tin core. The ease with which these materials can be fabricated and the resulting properties are discussed. In some applications, conductors are required to have a high n-value and to exhibit an outstanding degree of persistency during operation in the high field region. A conductor was designed to give such properties, and the results of measurements made on it are discussed.

This work has been supported by the U.S. Department of Energy.

Vortex Melting in Poly-Crystalline $YBa_2Cu_3O_7$ from ^{17}O NMR

Reyes, A.P., Northwestern Univ., Physics, and Science and Technology Center for Superconductivity
Bachman, H.N., Northwestern Univ., Physics, and Science and Technology Center for Superconductivity
Halperin, W.P., Northwestern Univ., Physics, and Science and Technology Center for Superconductivity
Hammel, P.C., LANL
Kuhns, P.L., NHMFL
Kleinhammes, A., NHMFL
Moulton, W.G., NHMFL/FSU, Physics

We have extended measurements of the H-T vortex phase diagram up to 24 T for aligned $YBa_2Cu_3O_7$ powder as observed by ^{17}O NMR. Our measurements[1] at fields up to 8.5 T have shown that motional narrowing of the ^{17}O NMR line persists below T_c to a melting line T_m (H) consistent with previous work based on resistivity[2] and torque measurements on high quality single crystals. In our new work we have determined that from ~10 T to 24 T the melting transition temperature is field-independent, occurring at T_m = 80 K. ^{17}O NMR spectra, such as that shown for 18.7 T (Figure 1), were also obtained at fields of 14, 21, and 24 T.

At sufficiently low temperatures it is expected that the magnetic field in the mixed state of a superconductor is characterized by a static vortex solid. For superconductors with high transition temperatures, T_c, this solid "melts" at a temperature $T_m < T_c$ when the amplitude of vortex fluctuations becomes comparable to the intervortex spacing. Vortex melting may be detected from the NMR spectrum, obtained from Fourier transformation of the spin-echo. When the field fluctuations are fast compared to the spin echo formation time, as would be expected for a liquid, the NMR linewidth is reduced due to motional narrowing. If the fluctuations are slow, as would be expected for a solid, averaging does not occur and the NMR line is broad, reflecting the distribution of fields in the vortex state.

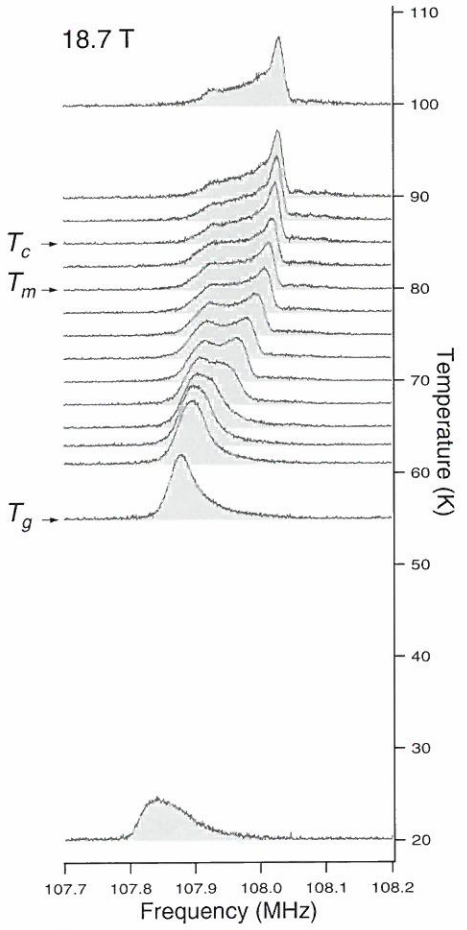

Figure 1. ^{17}O NMR spectra between 20 and 100 K for $YBa_2Cu_3O_7$ at 18.7 T.

We have found that the spectrum shows onset of broadening at the melting transition, T_m, where vortices become pinned. Below T_m there is a coexistence region of liquid and solid vortices, indicated by the appearance of an additional component in the spectrum at lower frequency. The lower bound on this coexistence region, T_g, is marked by the disappearance of the high frequency peak. Below T_g the spectrum is consistent with a solid vortex structure.

Work at Northwestern University is supported by the NSF (DMR 91-20000) through the Science and Technology Center for Superconductivity. Work at LANL is performed under the auspices of U.S. DOE. The NHMFL is supported through the NSF and the State of Florida.

References:

1 Reyes, A.P., *et al.*, Phys. Rev. Lett. (submitted).

2 Kwok, W.K., *et al.*, Phys. Rev. Lett. **69**, 3370 (1992); *ibid.* **72**, 1092 (1994).

Upper Critical Magnetic Field of $LuNi_2B_2C$

Schmiedeshoff, G.M., Occidental College, Physics
Lacerda, A., NHMFL/LANL
Buford, C.M., North Carolina A&T State Univ., Physics
Braje, T., UF, Physics
Canfield, P.C., Iowa State Univ./Ames Laboratory
Smith, J.L., LANL

We have measured the temperature dependence of the upper critical magnetic field of single crystal and polycrystal samples of $LuNi_2B_2C$. This nonmagnetic compound exhibits the highest T_c of any member of the $RENi_2B_2C$ (RE = rare earth) family of superconductors.[1] The upper critical field, H_{c2}, was determined as the midpoint of an isothermal resistive transition. The samples had superconducting transition temperatures of about 15.8 K for the polycrystal and 16.2 K for the single crystal. The single crystal sample exhibits an anisotropic upper critical field: With the field perpendicular to the c-axis, H_{c2} is about 1.3 times larger than with the field parallel to the c-axis. The observation of anisotropy is somewhat surprising since band structure calculations suggest that a three-dimensional Fermi surface and the existence of an anisotropic H_{c2} in nonmagnetic YNi_2B_2C is controversial.[1]

Reference:

1 Hilscher, G., *et al.*, Physica B, **206** & **207**, 542 (1995); and references therein.

Momentum, Temperature, and Doping Dependence of Photoemission Lineshape and Implications for the Nature of the Pairing Potential in HTS Materials

Schrieffer, J.R., NHMFL/FSU, Physics
Shen, Z.X., Stanford Univ., Applied Physics

We have shown that the anomalous momentum and temperature dependence of the spectral lineshape in data from underdoped $Bi_2Sr_2CaCu_2O_{8+\delta}$ (Bi2212) indicates that the quasiparticles are strongly coupled to collective excitations centered near $q=(\pi, \pi)$. The doping dependence of the spectral lineshape and its correlation with the size of the superconducting gap indicate these collective excitations are related to the pairing interaction in high-T_c materials. For electron momentum k near $(\pi, 0)$ the presence of a large inelastic hump centered near 150 mev is interpreted in terms of collective mode shakeoff. This effect is suppressed for k near $(\frac{\pi}{2}, \frac{\pi}{2})$ because of momentum conservation and the peaking of the dynamic spin susceptibility near (π, π).

Spectral Properties of Quasiparticle Excitations Induced by Magnetic Moments in Superconductors

Schrieffer, J.R., NHMFL/FSU, Physics
Salkola, M.I., Stanford Univ., Physics
Balatsky, A.V., LANL

The consequences of localized, classical magnetic moments in superconductors are explored and their effect on the spectral properties of the

intragap bound states is studied. Above an exchange coupling moment, a localized quasiparticle excitation in an s-wave superconductor is spontaneously created near a magnetic impurity, inducing a zero-temperature quantum transition. In this transition, the spin quantum number of the ground state changes from zero to 1/2, while the total charge remains the same. In contrast, the spin-unpolarized ground state of a d-wave superconductor is found to be stable for any value of the magnetic moment when the normal-state energy spectrum possesses particle-hole symmetry. The effect of impurity scattering on the quasiparticle states is interpreted in the spirit of relevant symmetries of the clean superconductor. The results obtained by the nonself-consistent (T matrix) and the self-consistent mean-field approximations are compared and qualitative agreement between the two schemes is found in the regime where the coherence length is longer than the Fermi length.

Magnetization Experiments on the Superconducting Oxide $Bi_2Sr_2CaCu_2O_8$

Triscone, G., Univ. of California, San Diego, Physics
Maple, M.B., Univ. of California, San Diego, Physics

We have measured the magnetization (M(H)) of the superconducting oxide $Bi_2Sr_2CaCu_2O_8$ from 0 to 18 T at fifteen different temperatures below T_c at the NHMFL-Los Alamos Facility. The objective was to determine the variation of dM/dln(H) vs. H at very high magnetic fields in order to test existing theories. To determine dM/dln(H), we have to be certain that the magnetization data are reversible, and special care has to be taken regarding the sample temperature. To characterize the system well, we first used a 7 T SQUID magnetometer at the University of California, San Diego, and then used the 20 T VSM magnetometer at the NHMFL-Los Alamos Facility.

EPR Study of Linewidth and g-Anisotropy of $Y_{1-x}RxBa_2Cu_3O_{6+\delta}$

Whitaker, H., FSU, Physics/NHMFL
Martins, G.B., NHMFL
Pardi, L., NHMFL
Hassan, A., FSU, Physics/NHMFL
Cao, G., NHMFL
Brunel, L.-C., NHMFL

The high Tc superconductor, YBCO, is EPR silent but may be studied by doping with rare earth, magnetic impurities, $Y_{1-x}RxBa_2Cu_3O_{6+\delta}$. In order to simulate results for this system, the authors used a Hamiltonian for $HoBa_2Cu_3O_6$ modified by scaling crystal field parameters (cfp) obtained via Inelastic Neutron Scattering (INS) measurements of HoBaCuO.[1,2] To simplify the cfp and to allow EPR measurements at low temperatures (below T_c), the tetragonal (insulating) phase was studied. The angular dependence of g for $Y_{0.94}Er_{0.06}Ba_2Cu_3O_{6+\delta}$ was determined by rotation in the a-c plane (Figure 1). The differences between the simulation and the experimental results at $\theta = 0°$ and 180° may be due to the replacement of Ho ions by Y (and a small concentration of Er) ions.

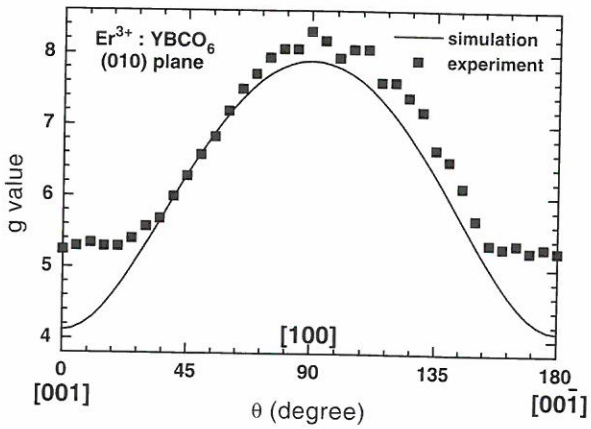

Figure 1. g anisotropy of $Y_{0.94}Er_{0.06}Ba_2Cu_3O_{6+\delta}$ in the a-c plane, $\nu = 9.4$ GHz, $T = 5$ K.

The linewidth was also found to be anisotropic in the a-c plane. Our results are consistent with straightforward crystal field theory, and we will next apply the INS Ho model with scaled crystal field parameters to Dy doped YBCO and Tb doped

YBCO. There is much interest in understanding Tb doped YBCO as the system exhibits some interesting phenomena (e.g., affects resistivity above T_c and will not form pure TbBaCuO).

References:

1 Furrer, A., *et al.*, Physica C, **153-155**, 164 (1988).

2 Simizu, S., *et al.*, Phys. Rev. B, **39**, 9099 (1989).

High-Field Magnetoresistance in Amorphous Superconducting Thin Films of Mo_3Si and Nb_3Ge

Yeh, N.-C., California Institute of Technology, Physics

Samoilov, A.V., California Institute of Technology, Physics

Tsuei, C.C., IBM, Thomas J. Watson Research Center

We have investigated the low-temperature and high-magnetic-field state of three-dimensional disordered superconductors,[1] amorphous Mo_3Si and Nb_3Ge films, whose normal resistivities increase upon cooling, a behavior known to be associated with weak localization[2]. The superconducting transitions of amorphous Mo_3Si and Nb_3Ge films are tracked by the resistivity-vs.-magnetic field measurements, and the transitions are followed by a resistivity decrease at further increase of the field H up to 30 tesla. The high-field resistivity is found to increase with the decreasing temperature, and eventually approaches a constant value at low temperatures, down to 25 mK. This behavior is attributed to the destructive influence of both the increasing magnetic field and increasing temperature on the interference effects of carrier wave functions, and is in contrast to the magnetic-field-tuned superconductor-insulator transition[3] at T=0 in two-dimensional amorphous films[4].

References:

1 Samoilov, A.V. *et al.*, Czec. J. Phys., **46** Suppl., 2, 761 (1996).

2 Lee, P.A., *et al.*, Rev. Mod. Phys., **57**, 287 (1985).

3 Fisher, M.P.A., Phys. Rev. Lett., **65**, 923 (1990).

4 Hebard, A.F., *et al.*, Phys. Rev. Lett. **65**, 927 (1990); Yazdani, *et al.*, Phys. Rev. Lett., **74**, 3037 (1995).

Josephson Vortex Lattice Melting in Highly Anisotropic Superconductors

Zettl, A., Univ. of California, Berkeley, Physics

Fuhrer, M.S., Univ. of California, Berkeley, Physics

Ino, K., Electrotechnical Laboratory, Tsukuba, Japan

Oka, K., Electrotechnical Laboratory, Tsukuba, Japan

Nishihara, Y., Electrotechnical Laboratory, Tsukuba, Japan

The Josephson vortex state (H || ab-plane) of the highly anisotropic superconductors $Bi_2Sr_2CaCu_2O_x$ and iodine-intercalated-$Bi_2Sr_2CaCu_2O_x$ has been probed by measurements of the out-of-plane (c-axis) resistivity as a function of temperature, current density, magnetic field strength H, and magnetic field orientation angle θ. Unlike $YBa_2Cu_3O_x$, in which anisotropic-effective-mass scaling theory can well explain the variation of transport properties with magnetic field angle, these materials exhibit qualitatively different properties in magnetic fields oriented parallel and perpendicular to the CuO_2 planes. In particular, it was recently discovered[1] that the melting transition of the vortex lattice may easily be observed in the resistivity with the field oriented parallel to the layers, but not in the perpendicular configuration, where the melting transition occurs at extremely low dissipation levels. We have investigated this melting transition in fields up to 18 T, at different field orientations with respect to the ab-plane. The data cannot be explained by three-dimensional vortex melting, but are better fit by a model of Kosterlitz-Thouless-like depairing of interlayer vortex/anti-vortex pairs.

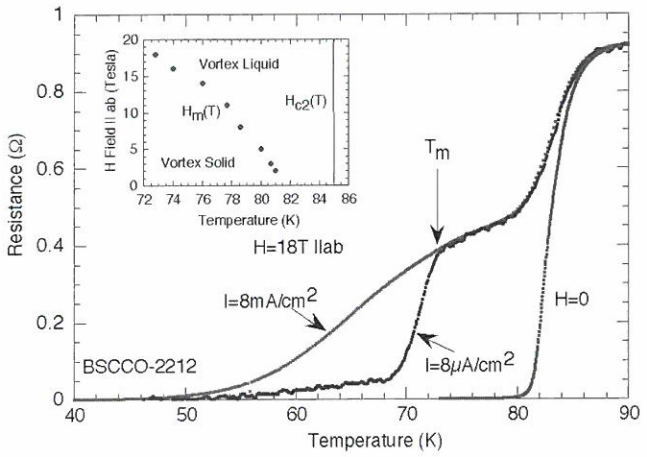

Figure 1. The resistance versus temperature of $Bi_2Sr_2CaCu_2O_x$ at H = O and H = 18 T oriented parallel to the ab-plane. Two current densities are shown for H=18 T. The kink in the low current density curve marks the melting transition of the Josephson vortex lattice. The inset shows the H-T phase diagram for this material.

Reference:

1 Fuhrer, M.S, *et al.* to be published in Solid State Communications.

NMR Study of $YBa_2Cu_4O_8$ at High Magnetic Field

Zheng, G.-q., UCLA, Physics and Osaka Univ.
Clark, W.G., UCLA, Physics
Kuhns, P.L., NHMFL
Kleinhammes, A., NHMFL
Moulton, W.G., NHMFL/FSU, Physics

$YBa_2Cu_4O_8$ is one of the high-T_c cuprates that shows clear "spin-gap" behavior; i.e., the uniform spin susceptibility decreases with decreasing temperature. This feature of the susceptibility remains when the superconductivity is suppressed by non-magnetic impurities doped into the CuO_2 plane.[1]

We have performed ^{17}O NMR measurements at high magnetic field up to 23.3 T to study the features of the spin gap. The sample is placed in epoxy and cured at the highest field available in the UCLA superconducting magnet, which results in a preferential orientation of the crystallites along c-axis. Because of the small oscillating field H_1 limitation during our run, we made a small step frequency-sweep to record the spin echo at respective frequencies, and reconstructed the Fourier-transformed spectrum to obtain the whole spectrum where the NMR lines are well separated.[2]

In addition to the four-sets of lines observed at 11 T previously, which arise from four distinct crystal sites (O(2,3) in the CuO_2 plane, O(1) in the CuO chain and O(4) in the BaO plane), we observed a set of lines that has the same quadrupolar frequency as O(2,3), but with a different Knight shift. The reconstruction of the spectra needed to obtain the detailed temperature dependence and field dependence of this signal is in progress.

References:

1 Zheng, G.-q., *et al.*, J. Phys. Soc. Jpn., **62**, 154 (1992).

2 Clark, W.G., *et al.*, Rev. Sci. Instrum., **66**, 2453 (1995).

Infrared Measurements in High Magnetic Fields

Zibold, A., UF, Physics
Liu, H.L., UF, Physics
Tanner, D.B., UF, Physics
Wang, Y.J., NHMFL
Grüninger, M., Univ. of Karlsruhe, Germany, Physics
Geserich, H.P., Univ. of Karlsruhe, Germany, Physics
Kopp, T., Univ. of Karlsruhe, Germany, Physics
Wolf, Th., Forschungszentrum Karlsruhe, Germany
Li, M.Y., National Tsing Hua Univ., Taiwan
Wu, M.K., National Tsing Hua Univ., Taiwan
Burns, M.J., Jet Propulsion Laboratory, Pasadena, CA

1. Midgap infrared absorption in the insulating phases of the cuprate superconductors.

Infrared measurements and linear-spin-wave calculations for single-crystal $Y_{1-x}Pr_xBa_2Cu_3O_6$ (x = 0., 0.4, 1.) in magnetic fields up to 30 T show

that absorption features that have been ascribed to magnon excitations are very insensitive to the applied field. The substitution of Pr^{3+} for Y^{3+} leads to an additional absorption feature, which does have a strong field dependence. This excitation is assigned to an intermultiplet transition in the Pr^{3+} ion. The zero-field temperature dependence of this absorption shows clear evidence of an interaction between Cu and Pr spins.

2. Far-infrared studies of high-T_c films in high magnetic fields.

We have measured the reflectance and transmittance of thin $YBa_2Cu_3O_7$ films in the far-infrared region of the spectrum. The transmittance was studied at fields up to 30 T (perpendicular to the ab-plane) using resistive magnets and at temperatures between 4.2 K and 100 K. The reflectance was measured at fields up to 17 T in a superconducting magnet at 4.2 K. The magnetotransmittance measurements using unpolarized light did not show any discernible field dependence at low temperatures, in contradiction to several previous reports. At temperatures where the DC resistance was not zero–on account of flux motion–there is a corresponding change in infrared transmittance that can be understood as related to the finite DC resistance in this temperature-field region and allows measurement of the relaxation time of the states in the vortex cores.

SCIENCE RESEARCH REPORTS

Kondo/Heavy Fermion Systems

Electron Tunneling Studies of the Kondo Insulators SmB_6 and EuB_6

Amsler, B., UF, Physics
Meisel, M.W., UF, Physics
Sharifi, F., UF Physics
Sarrao, J.L., NHMFL
Fisk, Z., NHMFL

We have performed a series of tunneling measurements on the hexaboride Kondo insulators SmB_6 and EuB_6. The anomalous electrical transport properties of these materials have been attributed to the formation of a small gap in the density of states, possibly arising from the hybridization of the f-electrons.[1,2] These materials exhibit qualitatively similar transport and magnetic properties with the important exception that EuB_6 orders ferromagnetically at approximately 16 K, where a decrease in the resistivity is also observed. Previously, Raman scattering techniques have been used to measure the size and temperature dependence of this gap in both SmB_6 and EuB_6.[3] In addition, there has been one report of a tunneling measurement, using planar junctions, on SmB_6.[4] We have fabricated planar tunnel junctions on these materials using Pb counter-electrodes. The observation of the Pb superconducting gap structure along with Pb phonons, provides a quality check on our junctions.

Our measurements on SmB_6 show a highly asymmetric density of states, N(E), with a reduction in the number of available states with decreasing temperature. The background conductance also increases linearly with increasing energy, a feature that is common to systems exhibiting electron correlation effects. We have extracted a "gap" value of 8 meV, and the missing spectral weight appears exclusively on the hole side of the spectrum, above the Fermi level. By measuring the zero-bias conductance as a function of temperature, we have found that the gap begins to form at 40 K. We note that within the gap region, there is only a partial depletion in N(E). Since there are still available states within the gap region at temperatures significantly below 40 K, we do not believe that thermal excitations can solely account for this incomplete depletion.

EuB_6 exhibits a qualitatively similar excitation spectrum above its ordering temperature. Although the gap value (40 meV) is substantially larger than

SmB_6, the reduction in N(E) in the gap region is substantially smaller. This result correlates with previous transport measurements on these two materials, which show that SmB_6 exhibits stronger semi-conducting behavior.[5] When EuB_6 orders magnetically, however, there is a dramatic change in the shape of the density of states. We see the formation of strong zero-bias anomalies corresponding to inelastic tunneling channels. The anomalies exist in all of our EuB_6 tunnel junctions, although their shape and temperature dependence vary greatly from junction to junction. Nevertheless, in all cases, the background tunnel conductance increases and becomes roughly flat, and no longer varies linearly with energy. The change in N(E) correlates with the drop in resistivity that is seen in EuB_6 as it orders.

We are indebted to S. von Molnar, S.L. Cooper, and S. Hershfield for numerous enlightening discussions.

References:

1 Aeppli, G., *et al.*, Comments Cond. Mat. Phys., **16**, 155 (1992).

2 Millis, A.J., in *Physical Phenomena at High Magnetic Fields* (Addison-Wesley, Reading, MA 1992).

3 Nyhus, P., *et al.*, Phys. Rev. B, **52**, 14308 (1995), and to be published.

4 Batlogg, B., *et al.*, in *Valence Fluctuations in Solids*, p. 267 (North-Holland, Amsterdam, 1981).

5 von Molnar, S., *et al.*, in *Valence Instabilities*, p. 389 (North-Holland, Amsterdam, 1982). Guy, C.N., *et al.*, Solid State Comm., **33**, 1055 (1980).

The De Haas-Van Alphen Effect in Heavy Fermion Systems

Arko, A.J., LANL
Cornelius, A.L., LANL
Smith, J.L., LANL

The de Haas-van Alphen (dHvA) effect is one of the most powerful experimental tools to determine the electronic structure of metals. By measuring the oscillations in the magnetization of a sample as a function of varying strong applied magnetic fields, the dHvA effect yields a great deal of information about the Fermi surface of a given metal. In a heavy fermion compound, the effective mass of the conduction electrons can be increased as much as 1000 times over the normal electron mass. As the electron mass becomes larger, a stronger magnetic field is required to observe the dHvA effect. Because of this, very few experiments have been performed on heavy fermion systems. We have done preliminary measurements on the heavy fermion compounds UAl_3, $YbAl_3$ and UBe_{13} at temperatures down to 300 mK and magnetic fields to 50 T. Though these measurements were only preliminary, evidence of oscillations in the magnetization were detected. Because of this, further, more detailed measurements are merited and are planned for the future.

High Field Magnetization of the Non-Fermi-Liquid System $UCu_{5-x}Pd_x$

Aronson, M.C., Univ. of Michigan, The Harrison M. Randall Laboratory of Physics
Chau, R., Univ. of California, San Diego, Physics, IPAPS
Maple, M.B., Univ. of California, San Diego, Physics, IPAPS

Over the past few years, an emerging new class of f-electron materials has been found experimentally to have strong deviations from Fermi-liquid behavior in their low temperature physical properties.[1] These non-Fermi-liquid materials exhibit weak power law or logarithmic divergences in the low temperature electrical resistivity, DC magnetic susceptibility, and specific heat. Various models have been proposed to explain non-Fermi-liquid (NFL) behavior that range from a single impurity description (e.g., multichannel Kondo effect)[2] to collective behavior,[3] and, possibly, disorder.[4]

The $UCu_{5-x}Pd_x$ system ($1 \leq x < 2$) is one of the most studied NFL systems because of its lattice of U ions.[5,6] One of the key issues for the $UCu_{5-x}Pd_x$ system is whether the underlying mechanism for

NFL behavior is single impurity or collective. Early measurements on $UCu_{3.5}Pd_{1.5}$ found that the magnetization curves could be superimposed by plotting them as $M/HT^{0.27}$ vs. $H/T^{1/3}$ and a magnetic field scaling dimension greater than one indicating nonsingle impurity behavior.[5] More recently, the scaling behavior was predicted to scale as $H/T^{2/3}$ for single impurity behavior for sufficiently low temperatures and high fields ($T = 10$ K, $H > 10$ T).[7]

To investigate this question, we performed high field magnetization measurements for several compounds in the $UCu_{5-x}Pd_x$ system ($x = 0.7$, 1, 1.5, 2) using a vibrating sample magnetometer in the 33 T resistive magnet down to 0.8 K at the NHMFL DC field facility in Tallahassee. M vs. H curves were measured in order to determine the scaling and to look for possible crossover between single ion and collective behavior. We found a linear temperature dependence for all samples at high temperatures. As the temperature is decreased, the magnetization begins to exhibit a strong non-linear temperature dependence. Further analysis is underway to determine the scaling behavior.

References:

1 Maple, M.B., *et al.*, J. Low Temp. Phys., **99**, 223 (1995).

2 Nozieres, P., *et. al.*, J. Phys., 41 (1980); Ludwig, A.W.N., *et al.*, Phys. Rev. Lett., **67**, 31606 (1991); Cox, D.L., Phys. Rev. Lett., **59**, 1240 (1982).

3 Millis, A.J., Phys. Rev. B, **48**, 7183 (1993); Tsevelik, A.M., *et al.*, Phys. Rev. B, **48**, 9887 (1993); Continentino, M.A., Phys. Rev. B, **47**, 11587 (1993).

4 Bernal, O.O., *et al.*, Phys. Rev. Lett., **75**, 2023 (1995); Miranda, E., *et al.*, J. Phys. Cond. Mat., **48**, 9871 (1996).

5 Aronson, M.C., *et al.*, Phys. Rev. Lett., **75**, 725 (1995).

6 Aronson, M.C., *et al.*, J. Phys. Cond. Mat., **48**, 9815 (1996).

7 Andraka, B., *et. al* ., Phys. Rev. B, **47**, 32081 (1993).

High Field Magnetoresistance of Non-Fermi-Liquid Alloys $Y_{1-x}U_xPd_3$ and $U_{1-x}Th_xPd_2Al_3$

Dickey, R.P., Univ. California-San Diego (UCSD), Physics, and Institute for Pure and Applied Physical Sciences

Gajewski, D.A., UCSD, Physics, and Institute for Pure and Applied Physical Sciences

de Andrade, M.C., UCSD Institute for Pure and Applied Physical Sciences

Maple, M.B., UCSD, Physics, and Institute for Pure and Applied Physical Sciences

We have performed magnetoresistance measurements at the NHMFL-LANL, using a ^3He - ^4He dilution refrigerator in the temperature range $80\ mK \leq T \leq 800\ mK$ and a 20 T superconducting magnet. Measurements were made on two different kinds of uranium-based materials that exhibit non-Fermi-liquid behavior in their physical properties at low temperatures, $Y_{1-x}U_xPd_3$ and $U_{1-x}Th_xPd_2Al_3$. Previous measurements on the $Y_{1-x}U_xPd_3$ system in conjunction with this work reveal a crossover from a small negative linear magnetoresistance at large U concentrations ($x = 0.15$ and $x = 0.20$) to a small positive magnetoresistance with a field dependence $\Delta\rho/\rho \sim H^2$ for the $x = 0.10$ sample. Additional magnetoresistance measurements are needed to characterize the detailed behavior of this crossover as a function of x and provide a basis for subtracting off the non-magnetic contributions. Magnetoresistance measurements on the $U_{1-x}Th_xPd_2Al_3$ samples show a negative magnetoresistance with negative curvature at low fields and an inflection point at high fields. This result is suggestive of a contribution from single ion Kondo scattering. Magnetoresistance measurements on additional samples in this system are required to determine how the non-Fermi-liquid behavior is reflected in properties like the magnetoresistance.

High Field Magnetization Measurements on the Heavy Electron Material UPt_3

Dorsey, B., Univ. of Virginia, Physics
Shivaram, B.S., Univ. of Virginia, Physics
Chaparala, M.V., NHMFL and Univ. of Virginia, Physics
Hinks, D.G., Argonne National Laboratories

We have performed high resolution torque magnetization measurements in a single crystal of the heavy electron material UPt_3 in magnetic fields up to 30 tesla with the field oriented both along the c-axis and the a-axis of the hexagonal crystal. The interaction of the spins in the hexagonal plane with the ambient field generates a torque, which is measured using a cantilever magnetometer. For fields oriented along the a-axis a pronounced metamagnetic transition around 19.9 tesla was observed (Figure 1). The sharpness of this transition

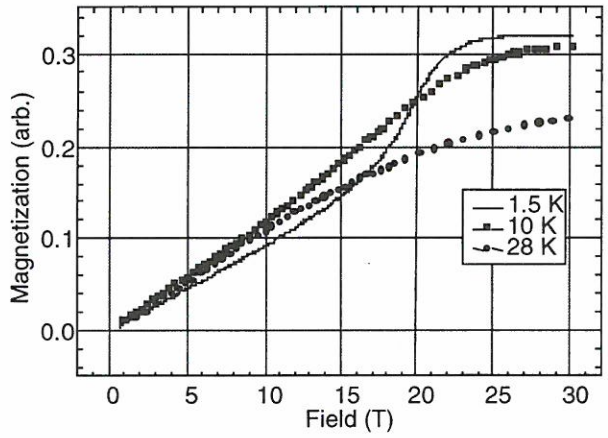

Figure 1. Metamagnetic transition of UPt_3 at around 19.9 tesla.

weakens gradually as the temperature is raised above 10 K with no apparent discontinuities observed near 5 K, which is the temperature where the antiferromagnetic order apparently sets in. As the temperature is raised the susceptibility peak corresponding to the metamagnetic transition moves to a lower field (Figure 2). This temperature dependence has not been observed before and is novel to these measurements. The metamagnetic transition is not expected for the perpendicular orientation. Our measurements are consistent with this expectation. These observations of the metamagnetic transition are consistent with the ultrasonic measurements (see *High Field Ultrasonic Measurements in the Heavy Electron Material UPt_3*, by Ulrich, *et al.*).

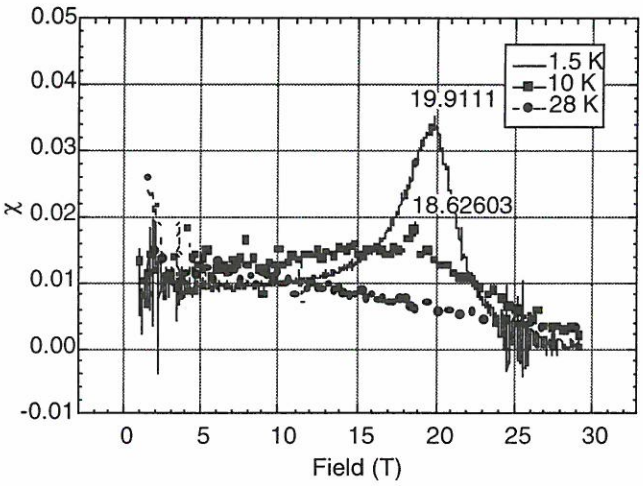

Figure 2. As the temperature increases, the susceptibility peak corresponding to the metamagnetic transition of UPt_3 moves to a lower field.

Reference:

[1] Dorsey, B., *et al.*, submitted to Phys. Rev. B, Dec. 1996.

The Physics of $YbInCu_4$

Fisk, Z., NHMFL/FSU, Physics
Sarrao, J.L., NHMFL
Immer, C.D., NHMFL/FSU, Physics
Lawrence, J.M., Univ. California-Irvine, Physics
Lacerda, A., NHMFL/LANL
Thompson, J.D., LANL

$YbInCu_4$ is a cubic intermetallic compound that has a first-order isostructural valence transition to a non-magnetic ground state at T = 42 K.[1] We study this γ-α Ce-type transition using single crystals that show particularly clean properties. This type of first-order structural change bears a number of similarities to a gas-liquid phase transition, and part of our motivation for studying this system is to determine the extent to which we can regard the development of the so-called "coherent" ground state in heavy Fermion materials as a gas-liquid phase transition, but generally one beyond the critical point.

We have alloyed the system into the region beyond the first order range. In particular we have synthesized the full range of compounds $YbIn_{1-x}Ag_xCu_4$ ($0 \leq x \leq 1$) as single crystals, and we observe a smooth evolution of physical properties from $YbInCu_4$ to $YbAgCu_4$, a "normal" heavy Fermion material.[2]

The high temperature state carries the full Yb J = 7/2 magnetic moment, so there is a strong field dependence in the phase diagram. We have performed high-field magnetoresistance measurements in DC and pulsed fields for both stoichiometric and doped samples at ambient pressure and under applied pressures of up to 10 kbar. We observe a field-induced first-order transition whose critical field depends on temperature. By properly scaling the (H_c,T_c) data extracted from the resistance measurements, we can collapse all of the data onto a single universal H-T phase diagram. These data provide valuable insight into the underlying thermodynamics of this system.

We also are performing high pressure experiments in ambient field: pressure suppresses the transition temperature. What we have not been able to determine yet is whether the phase transition can be pushed to T = 0 K, or whether it becomes continuous at high enough pressure. The initial indications are that this second possibility is what happens.

References:

1 Sarrao, J.L., *et al.*, Physica B, **223&224**, 366 (1996).

2 Sarrao, J.L., *et al.*, Phys. Rev. B, **54**, 12207 (1996).

Physical Properties of the $Ce(Ru_{1-x}Fe_x)_2Ge_2$ Series

Fontes, M.B., CBPF–Brazil
Bud'ko, S.L., CBPF–Brazil
El-Massalami, M., CBPF–Brazil
Sampaio, L.C., CBPF–Brazil
Guimaraes, A.P., CBPF–Brazil
Baggio-Saitovitch, E., CBPF–Brazil
Continentino, M., UFF–Brazil
Hundley, M.F., LANL
Lacerda, A., NHMFL/LANL

The $CeRu_2Ge_2$ compound is a ferromagnetic material with $T_c \sim 7.5$ K, while the $CeFe_2Ge_2$, was recently characterized as a moderate heavy fermion ($\gamma \sim 210$ mJ/molK^2). They belong to the same family of compounds that has attracted great attention after the discovery of the heavy fermion properties of $CeRu_2Si_2$ and the superconductivity of $CeCu_2Si_2$. It was suggested that by applying either chemical or hydrostatic pressure, the $CeRu_2Ge_2$ could be driven to a state with strong enhancement of the electronic effective mass. Mapping the passage to this state could give us the opportunity to observe the existence of the critical point in this family of compounds, where the system would present a non-Fermi-liquid behavior, as predicted by Continentino, *et al.*[1]

In the present work we study the evolution of the physical properties of the $Ce(Ru_{1-x}Fe_x)_2Ge_2$ series, using resistivity under hydrostatic pressure, magnetization, specific heat, and Mössbauer spectroscopy.[2] The specific heat showed that above x - Fe = 0.7 the system present a moderated enhancement of the electronic mass. Our results strongly suggest that at x - Fe = 0.9 the system present non-Fermi-liquid behavior. A tentative phase diagram is proposed to represent the physical picture of this series. The variation of the hybridization strength between f and p/d orbitals due to the change of the volume was investigated.

References:

1 Continentino, M.A. *et al.*, Phys. Rev. B, **39**, 9734 (1989).

2 Fontes, M.B. *et al.*, Phys. Rev. B, **53**, 11678 (1996).

Kondo Effect and RKKY Interactions in Alloys

Gor'kov, L.P., NHMFL
Kim, J.H., NHMFL

In continuation of our previous studies[1-3] of diluted Kondo system, we derived expressions for an effective RKKY interaction between two paramagnetic centers in case when the centers are embedded into a metal with some short mean free path, l. The familiar expression for the RKKY interaction is known to become cut off exponentially on distances, R, of order of the mean free path. Therefore, one may expect that the picture of two independent Kondo centers would persist at low temperatures (T ~ Tk) right up until R ~ l in dirty metals. In references 2 and 3, it was shown that in a pure metallic matrix, properties of dilute paramagnetic alloys start to deviate drastically from those of a collection of independent centers already at quite a low concentration, if Tk itself is low enough. These results indicate that attempts to describe the physics of heavy fermions in terms of the solution for single center Kondo problem cannot be justified. Importance of the RKKY-like contribution even at T << Tk follows from the fact that fluctuations of a given spin, say, at the site R_1, would induce electron-hole pairs coupling S_1 and S_2, at R_2 if the "propagation time," R_{12}/v, becomes comparable with 1/Tk, i.e., already at rather large distances. In the case that two centers are imbedded into an alloy, and l<<R, the information regarding mutual spin orientations can only propagate as diffusion mode. We have derived the corresponding S-matrix that substitutes for coupling between two spins through the ballistic propagation of the e-h pairs. It is unknown yet how large the effect is on, say, the magnetic susceptibility of the two-center system. Generalization of the problem to other models, such as the Anderson model of a single center, would be straightforward but has not been completed.

References:

1 NHMFL Annual Report, 1995, p. 36.

2 Gor'kov, L.P., *et al.*, Phyl. Mag. B, **74**, 447 (1996).

3 Gor'kov, L.P., *et al.*, in *Proceedings of Physical Phenomena at High Magnetic Fields-II*, eds. Z. Fisk, *et al.*, p. 197, (World Scientific, Singapore, 1996).

Lattice Effects in Mixed Valence Problem

Gor'kov, L.P., NHMFL

An attempt is made to improve the standard approach to mixed valence (MV) phenomenon by a more careful account of the lattice degrees of freedom. The MV problem is usually formulated in terms of fluctuating occupation of the 4f-/5f-shells for the atomic orbitals. Thus, it is difficult to understand the origin of rather small energy scales of order of 10-100 K, typical for the heavy fermion and mixed valence physics. We assume that fluctuating configurations are formed with some essential involvement of lattice deformations, which would then produce a characteristic time scale of order of inverse phonon frequency. To realize such an idea, a polaronic model is adopted in reference 1 to describe one of the two configurations. Polaronic displacements in this model lower the level's energy for one of the configurations in such a manner that the adiabatic potential decreases and touches the chemical potential of the conducting electrons. In this range of deformations calculations of the adiabatic potential reduce to the solution of an Anderson model with an effective on-site interaction which depends on the deformation itself. It is known (see, e.g., reference 2) that polaronic effects may dramatically reduce the hybridization width of the level in the Anderson model. Simple classical model is considered to demonstrate that at a proper choice of parameters, the local level of the effective Anderson model may also become pinned in the vicinity of the chemical potential of electrons in the conduction sea. Therefore, the smallness of energy scales in heavy fermion and mixed valence

phenomena might be ascribed to renormalization of bare parameters by polaronic effects of the lattice.

References:

1 Gor'kov, L.P., Physica B, **223** & **224**, 245, (1996).

2 Sherrington, D., *et al.*, Solid State Comm., **16**, 1347 (1975).

Magnetoresistance in the Heavy Fermion Compound $YbNi_2B_2C$

Lacerda, A., NHMFL/LANL
Yatskar, A., Univ. of California-Riverside, Physics, and NHMFL
Mielke, C.H., NHMFL/LANL
Beyermann, W.P., Univ. of California-Riverside, Physics
Canfield, P.C., Iowa State Univ./Ames Laboratory

An interesting interplay exists between superconductivity and local moment magnetism in the series of intermetallic borocarbides RNi_2B_2C (R = Y, Gd-Tm, and Lu). Unlike every other member of the series, $YbNi_2B_2C$ has a heavy Fermi-liquid ground state without long-range order.[1] An enhanced electronic contribution to the specific heat is observed with a Sommerfeld coefficient of ~ 530 mJ/mol K^2, implying the Kondo temperature is ~ 10 K. The large separation between the Kondo temperature and the crystal-electric-field levels makes this an ideal system for studying correlated-electron behavior.

The transverse and longitudinal magnetoresistances were measured on single crystals of $YbNi_2B_2C$ in magnetic fields up to 50 T and at temperatures down to ~ 70 mK. At high temperatures, the magnetoresistance curves are negative. For a J = 1/2 Coqblin-Schrieffer model, the magnetoresistance can be described by a universal function.[2] It is possible to scale our high temperature data with $(T+T_0)/B$ where T_0 ~ 10 K, which is the same as the Kondo temperature determined from thermodynamic measurements.

A large anisotropic transverse magnetoresistance is observed depending on whether the field is applied perpendicular or parallel to the c-axis. A pronounced maximum develops at 10 T below 4 K in the transverse magnetoresistance when the field is perpendicular to the c-axis. Below ~ 2 K, the resistivity in zero field has a quadratic temperature dependence with a magnitude that is consistent with the enhanced specific heat. Both the T^2 coefficient and the impurity contribution the resistivity are field dependent, and quantitatively match the theoretical prediction by Chen *et al.*[3] Experiments are planned to examine the field dependence of the low-temperature specific heat and compare this to the magnetoresistance.

References:

1 Yatskar, A., *et al.*, Phys. Rev. B, **54**, R3772 (1996).

2 Batlogg, *et al.*, J. Magn. Mat., **63** & **64**, 441 (1987).

3 Chen, C., *et al.*, J. Phys. Condens. Matter, **6**, 2957 (1994).

Magnetotransport Measurements to 125 T in FeSi

Lacerda, A., NHMFL/LANL
Goettee, J.D., LANL–DX
Rickel, D.G., NHMFL/LANL
Schmiedeshoff, G.M., Occidental College, Physics
Sarrao, J.L., NHMFL
Fisk, Z., NHMFL/FSU, Physics

The effects of a strong magnetic field on the energy gap of FeSi is of great deal of interest. Previously we performed magnetotransport measurements at 4 K to 50 T in this compound with no indication of a gap closure at the maximum field investigated. Recently, using the flux compression technique, we attempted to measure the transverse magnetoresistance of this compound to 125 T. Although, our results are still preliminary and more measurements are needed, our measurements indicate that a substantial change in the magnetoresistance was observed at 90 T.

Pulsed Magnetic Field Investigation of the Fermi Surface of $SmSb_2$

Mielke, C.H., NHMFL/LANL
Harrison, N., NHMFL/LANL
Lacerda, A., NHMFL/LANL
Salo, L., South Plains College, TX, Physics
Canfield, P.C., Iowa State Univ./Ames Laboratory
Bud'ko, S.L., Iowa State Univ./Ames Laboratory

The rare earth compound $SmSb_2$ has recently been synthesized[1] and yields very high quality single crystals with a residual resistance ratio of 450. Zero field temperature dependent resistivity indicates a phase transition to an antiferromagnetic ground state at 12.6 K (onset). The antiferromagnetic transition is accompanied by a sharp drop in resistivity due to the loss of spin disorder scattering. Clear Shubnikov-de Haas and de Haas-van Alphen oscillations have been measured in pulsed magnetic fields to 50 tesla (T) at temperatures as low as 420 mK (see Figure 1). A determination of the Fermi surface from the spectral analysis of the quantum oscillations indicates closed pockets of 65 T and several higher frequency pockets of 575, 700, and 760 T dominating the Fermi surface. The effective mass of the carriers also has been determined by analysis of the temperature dependence of the quantum oscillations. An effective mass of 1.3 m_e results from analysis of the quantum oscillations.

Magnetoresistance measurements were performed above and below the antiferromagnetic transition (T_{AF}). Analysis indicates that the background magnetoresistance is not temperature dependent for $T < T_{AF}$ however, a saturation is observed at $20 < H < 40$ T. Above T_{AF} the saturation in background magnetoresistance is not observed for fields less than 50 T. Spectral analysis indicates that the Fermi surface is not affected by the antiferromagnetic ordering since the measured frequencies are identical both above and below T_{AF}. It is especially evident in the magnetization measurements that the Fermi surface is strongly fragmented, indicated by the large number of low frequencies, i.e. small pockets (see Figure 2). Temperature dependent magnetization measurements[1] indicate a "knee-like" feature at T ~ 100 K. The feature at 100 K is believed to be the signature of a density wave transition that is responsible for reconstructing the high temperature Fermi surface.

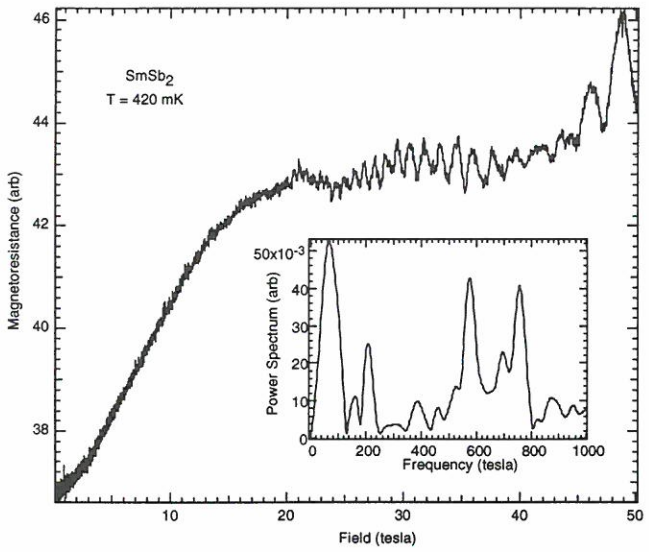

Figure 1. Magnetoresistance of $SmSb_2$ at 420 mK to 50 T.

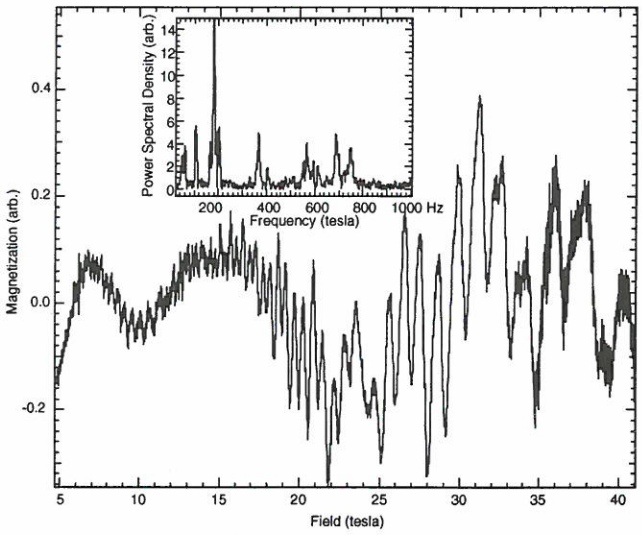

Figure 2. Magnetization of $SmSb_2$ at T = 450 mK.

Reference:

[1] S. Bud'ko, *et al.*, Preprint, 1996.

Localization Effects in Disordered Kondo Systems

Miranda, E., NHMFL
Dobrosavljevic, V., FSU, Physics/NHMFL

The nature of disorder in heavy fermion compounds, an issue that has been long overlooked in the past, has recently assumed a more fundamental stature after the discovery of certain Kondo alloys that exhibit non-Fermi liquid behavior. In previous work,[1] we have developed a general theory for Kondo disorder that is able to incorporate the strong spatial fluctuations of the local Kondo scale, a feature that seems essential to the description of these systems. Under certain conditions, which can be precisely formulated, this theory has been shown to lead to non-Fermi liquid behavior. In this novel Griffiths phase, the f-spins are never completely quenched at any finite temperature even though no magnetic instability is required. This theory has been put to test in the case of the alloy $UCu_{5-x}Pd_x$ and has been shown to be consistent with several measured properties: static and dynamic magnetic susceptibility, specific heat, resistivity, NMR and optical conductivity.[2] While it is still unclear whether this mechanism is responsible for the anomalous behavior of the other known Kondo alloys, it is not unwarranted to assume that disorder is a relevant piece of the puzzle.

The importance of spatial fluctuations in the conduction electron density of states, however, was left pending in our previous calculation scheme, which treated the conduction electrons "on the average," at the CPA (coherent potential approximation) level. Since it enters the definition of the local Kondo scale in an exponential fashion, it is important to incorporate the full fluctuation range of the conduction electron density of states. It is possible to extend the mean-field theory used previously to include both localization and interaction effects.[3] We are embarking on an analysis of the effects of incorporating the full statistics of these fluctuations on the self-consistent distribution of Kondo scales of general disordered f-electron systems.

References:

1 Miranda, E., *et al.*, to appear in Phys. Rev. Lett.; Miranda, E., *et al.*, J. Phys.: Cond. Matter, **8**, 9871 (1996).

2 Andraka, B., *et al.*, Phys. Rev. B, **47**, 3208 (1993); Bernal, O.O., *et al.*, Phys. Rev. Lett., **75**, 2023 (1995); Aronson, M.C., *et al.*, Phys. Rev. Lett., **75**, 725 (1995); Degiorgi, L., *et al.*, J. Phys.: Cond. Matter, **8**, 9901 (1996).

3 Dobrosavljevic, V., *et al.*, cond-mat/9611100.

Magnetism in CePtPb

Movshovich, R., LANL
Lawrence, J.M., Univ. of California-Irvine, Physics
Hundley, M.F., LANL
Neumeier, J., LANL
Thompson, J.D., LANL
Lacerda, A., NHMFL/LANL
Fisk, Z., NHMFL/FSU, Physics

CePbPt forms into an Fe_2P hexagonal structure and orders antiferromagnetically at $T_N = 0.9$ K. Above T_N the magnetic susceptibility is highly anisotropic, with strong ferromagnetic fluctuations in the basal plane developing below T ~ 13 K. The anisotropy ratios estimated to reach 65 at the phase-transition temperature. The low temperature magnetization is also anisotropic, M_{ab} saturating to $0.92\mu_B$ / Ce atom, where M_c is five times smaller.[1] Resistivity and heat capacity measurements at ambient pressure and AC susceptibility measurements at hydrostatic pressure to 17 kbar were performed at temperatures down to 50 mK.

Three facts suggest that the magnetic order might coexist with heavy-fermion behavior: Heat capacity data below the transition show a linear-in-temperature contribution $\gamma \sim 300$ mJ/mole K^2; below T_N the resistivity remains Fermi-liquid-like, and magnetic entropy is generated very slowly with temperature, reaching the value of Rln(2) by T ~ 7 K. On the other hand the long temperature tail of the heat capacity data correlates with the onset of ferromagnetic fluctuations below

T = 15 K. Also, contrary to the behavior of many Ce-based heavy-fermion materials, T_N increases with pressure at an average rate of approximately 16 mK / kbar, which suggests that CePtPb sits in the small J limit of the Doniach phase diagram, where heavy-fermion effects would be negligible. We would then attribute the long high-temperature tail of the heat capacity data entirely to ferromagnetic fluctuations that persist well above T_N.

Reference:

1 Movshovich, R., *et al.*, Phys. Rev. B **53**, 5465 (1996).

Linear and Nonlinear Magnetic Susceptibility of $U_{1-x}Th_xBe_{13}$

Schmiedeshoff, G.M., Occidental College, Physics
Torikachvili, M.S., San Diego State Univ., Physics
Lacerda, A., NHMFL/Los Alamos
Buford, C.M., North Carolina A&T State University, Physics
Smith, J.L., LANL

Isothermal measurements of the DC magnetization of $U_{1-x}Th_xBe_{13}$ have been made at 2.5 K using a vibrating sample magnetometer. We studied both single crystal (x = 0 and 0.03) and polycrystal samples (with x ranging from 0 to 1). We fit the data to the form $M(H) = \chi_0 + \chi_1 H + (1/3)\chi_3 H^3$ to extract the linear (χ_1) and nonlinear (χ_3) contributions to the susceptibility. Magnitudes of χ_1 and χ_3 at 2.5 K were consistent with earlier evaluations by Ramirez[1] and Aliev[2] who studied $\chi_3(T)$ of pure and thoriated UBe_{13} respectively.

Ramirez and Aliev found different temperature dependencies for χ_3 suggesting dipolar and quadrupolar excitations respectively. Our results for χ_3, which span the thorium concentration range between these earlier studies, showed no thorium dependence within experimental error. While we may have fortuitously chosen a temperature at which the data of the other two groups agreed, it may also be that similar temperature dependencies for pure and thoriated UBe_{13} are expected. Subsequent measurements will address this issue.

Our results for the thorium concentration dependence of χ_1 extend the earlier results of Kim[3] who studied the range from x = 0 to x = 0.9 and found no thorium concentration dependence to χ_1. Our data for x > 0.9 were corrected for the contribution of the Th ions by suitably scaling pure $ThBe_{13}$ data. While this correction did not affect our x = 0.9 data we found that, by x = 0.99, χ_1 had increased by 30% over its x = 0 value. These results suggest that cooperative effects are important in the susceptibility of UBe_{13}. Since we were not able to identify a single ion limit (which would appear as a leveling off of χ_1 with increasing thorium concentration) we are not yet able to estimate what fraction of the susceptibility is due to single-ion effects. These results will appear elsewhere.[4]

References:

1 Ramirez, A.P., *et al.*, Phys. Rev. Lett., **73**, 3018 (1994).

2 Aliev, F.G., *et al.*, Physica B, **223** & **224**, 475 (1996).

3 Kim, J.S., *et al.*, Phys. Rev. B, **41**, 11073 (1990).

4 Schmiedeshoff, G.M., *et al.*, Proceedings of SCES-96, to appear in Physica B.

Giant Magnetoresistance in $ThBe_{13}$

Schmiedeshoff, G.M., Occidental College, Physics
Torikachvili, M.S., San Diego State Univ., Physics
Lacerda, A., NHMFL/LANL
Smith, J.L., LANL

We have observed a giant magnetoresistance (MR) in $ThBe_{13}$. Isothermal measurements of the transverse MR on a polycrystal sample show a quasilinear magnetic field dependence that reaches about 500% at 2 K and 18 T. There is no indication of the MR saturating with increasing field. The magnitude of the MR is temperature independent up to about 20 K and is still robust at higher temperatures (about 150% at 100 K and 18 T).

Doping $ThBe_{13}$ with about 2% U reduces the MR to about 150% at 2 K and 18 T; a similar reduction in magnitude is observed using single crystals of $ThBe_{13}$, which are grown from an Al flux and therefore contain Al impurities.

The temperature and field dependencies of the MR of the pure polycrystal scale very well on a Kohler plot, a result that suggests that the giant MR may be due to the presence of very small effective mass carriers. We have observed a qualitatively similar giant MR in other MBe_{13} compounds (M = Y, Pr, and Ce so far), a full description of our results will appear elsewhere.

On the Magnetization of UBe_{13} Below 1 K

Schmiedeshoff, G.M., Occidental College, Physics
Stewart, G.R., UF, Physics

The goal of this experiment is to measure the temperature dependence of the DC magnetization of UBe_{13} at temperatures below 1 K and in magnetic fields large enough to suppress the superconducting state.[1] A T^2 dependence of M would be consistent with a Fermi liquid ground state and a $T^{1/2}$ dependence is predicted for the non-Fermi liquid state of Cox's Quadrupolar Kondo model.[2]

Our single crystal sample was oriented with its [100] direction parallel to the 10 T magnetic field. We used the cantilever magnetometer, dilution refrigerator, and 20 T magnet at the NHMFL (Tallahassee) for these measurements, which were made from 40 mK to about 1.2 K. We attempted to isolate the magnetic force (which is proportional to M) acting on the sample since it is independent of sample shape effects to first order[3] and since there is an unusual magnetic torque associated with UBe_{13} in high fields[4] which make interpretation difficult. To isolate the magnetic force, the sample was first measured with the magnetometer positioned at the center of the magnet (where only the torque acts) and then a few cm away from the center (where both force and torque act). The difference between these two data sets should yield the magnetic force. An estimated ±5° uncertainty in sample orientation between the two positions was not expected to affect this procedure if the magnetic response of UBe_{13} were isotropic.

We find that both the torque and force have a clear T^2 temperature dependence. Fitting the data to a $1-(T/T_0)^2$ functional form yields 2.5 K or 3.2 K for the value of T_0 associated with the force or torque respectively.[1] This similarity suggests that our error in sample orientation was too large to permit a clean isolation of the magnetic force; we are therefore unable to identify the ground state of UBe_{13} as either Fermi liquid or non-Fermi liquid at this time. The clear presence of a force contribution to the data, however, indicates that the goal of this experiment is achievable by using a gradient coil (which allows the sample to remain in a fixed position) rather than the natural gradient of the main solenoid.

The torque's sensitivity to sample orientation is a clear indication of the presence of magnetic anisotropy for this material such as might be caused by magnetic ordering along an easy axis of the sample (for example). The T^2 dependence of the torque that we observe may reflect a spin-fluctuation origin to this phenomenon. Further work is required to address these issues.

References:

1 Schmiedeshoff, G.M., Czech. J. Phys., **46**, 2061 (1996).

2 McElfresh, M., *et al.*, Phys. Rev. B, **48**, 10395 (1993).

3 Schmiedeshoff, G.M., Philos. Mag. B, **66**, 711 (1992).

4 Schmiedeshoff, G.M., *et al.*, Phys. Rev B, **48**, 16417 (1993).

The Irreversibility Curve of UBe_{13}

Schmiedeshoff, G.M., Occidental College, Physics
Stewart, G.R., UF, Physics

We have measured the irreversibility curves of both single crystal (with H parallel to [100]) and

polycrystal samples of UBe_{13} using the silicon cantilever magnetometer, toploading dilution refrigerator, and 20 T superconducting magnet at the NHMFL (Tallahassee). The irreversibility curve is defined as the point at which the magnitude of the magnetic hysteresis disappears with either increasing field at fixed temperature or increasing temperature at fixed field. Earlier measurements have shown that these measurements in polycrystal samples closely follow the mean field $H_{c2}(T)$ as determined resistively.[1] Both of our samples were fabricated from very high purity starting materials in a manner described elsewhere.[2] Resistive measurements of $H_{c2}(T)$ of both polycrystal[2] and single crystal[3] samples from the same source have appeared elsewhere. The single crystal measurements have resolved a long standing discrepancy on the qualitative shape of $H_{c2}(T)$ between single crystal and polycrystal samples.

The irreversibility curve of our polycrystal sample exhibits the steep initial slope and low temperature positive curvature observed in earlier irreversibility curve measurements and in the recent single crystal $H_{c2}(T)$ mentioned above. The irreversibility curve of our single crystal sample shows a lower T_{irr} of about 890 mK (about 100 mK below that of the polycrystal) and a steep initial slope. The low temperature behavior, however, shows no positive curvature and (comparing to the data of Reference 3) is about 5 T below $H_{c2}(T)$ even at 30 mK. This latter observation is quite surprising since one expects the irreversibility curve to coincide with $H_{c2}(T)$ as $T \rightarrow 0$.[4] Our coldest two data points suggest that an upturn below 40 mK may be occurring. If it exists the upturn may be associated with a transition from 3 to 2 dimensional vortex melting,[4] although the observation of such behavior in such a low temperature, isotropic superconductor would be surprising. On the other hand, if the irreversibility curve does not meet $H_{c2}(0)$ then a zero temperature vortex liquid state exists in UBe_{13} over a wide field range. Further work is necessary to resolve these issues.

References:

1 Schmiedeshoff, G.M., *et al.*, Phys. Rev. B, **38**, 2934 (1988).

2 Kim, J.S., *et al.*, Phys. Rev. B, **44**, 6921 (1991).

3 Thomas, F., *et al.*, JLTP, **102**, 117 (1996).

4 Tinkham, M., *Introduction to Superconductivity*, 2nd ed., p. 316, (McGraw-Hill, New York, 1996); and references therein.

Spin Compensation and the Exhaustion Principle in the 1D Kondo Chain: Implications for Heavy Fermions

Schrieffer, J.R., NHMFL/FSU Physics
Kim, J., Univ. of North Dakota, Physics

To gain insight into the mechanism by which compensation of localized spins occurs in a dense Kondo system, we have studied the 1D Kondo chain using bosonization techniques. The key question is whether Nozieres' exhaustion principle, which assumes that a fraction T_K/T_F of the itinerant electrons compensate all of the localized spins by a wandering set of Kondo-like resonances, is valid. Our studies suggest that a very different mechanism is at work, namely, that the conduction electrons provide an effective retarded coupling between the localized spins that frustrates the spin system, leading to self compensation of the localized spin system. Using the Mandelstam bosonization method, we find a spin gap in the excitation spectrum in agreement with other authors.

High Field Magnetization Study of $Ce_3Bi_4Pt_3$

Thompson, J.D., LANL
Modler, R., LANL
Moshopoulou, E., LANL
Canfield, P.C., Iowa State University/Ames Laboratory
Fisk, Z., NHMFL/FSU, Physics

Quasi-elastic neutron scattering experiments[1] on the Kondo insulator $Ce_3Bi_4Pt_3$ clearly show the existence of a gap (of order 13meV) in the spin-

excitation spectrum at low temperatures that accompanies a gap in the charge-excitation spectrum, as determined by transport measurements. A Kramers-Kronig analysis of the neutron data reproduces the static susceptibility quantitatively, especially the well-defined maximum in χ near 80 K. Therefore, by measuring the field-dependent magnetization, it should be possible to deduce the field dependence of the spin gap. We have measured the temperature-dependent susceptibility of $Ce_3Bi_4Pt_3$ crystals in a SQUID magnetometer to 5 T, in a vibrating sample magnetometer to 18 T and isothermal magnetization in fields to 50 T at several temperatures between 4 and 150 K, the latter two being performed at the NHMFL–Los Alamos. Except for a slight ($\leq 5\%$) difference in magnitude of M/H over most of the temperature range $5\ K \leq T \leq 300K$, the SQUID and VSM data show no field dependence of the spin gap. Preliminary analysis of the pulsed-field magnetization data also are consistent with a lack of field dependence of the spin gap. Assuming g = 1, however, a 50 T field corresponds to about 3 meV, i.e. about 22% of the maximum spin gap. It is possible that a complete analysis of the magnetization data will show partial quenching of the spin gap, but this remains to be seen. In any event, these results are clearly different from the field dependence of the charge gap where fields of order 50-60 T appear to be sufficient to induce metallic behavior.[2]

References:

1 Severing, A., *et al.*, Phys. Rev. B, **44**, 6832 (1991).

2 Boebinger, G.S., *et al.*, in *Proceedings of Physical Phenomena at High Magnetic Fields-II*, eds. Z. Fisk, *et al.*, p. 170, (World Scientific, Singapore, 1996).

Heavy Quasiparticles in the Anderson Lattice Model

Tsutsui, K., Nagoya Univ., Applied Physics, Nagoya, Japan
Ohta, Y., Chiba Univ., Applied Physics, Chiba, Japan
Eder, R., Groningen Univ., Applied Physics, Groningen, The Netherlands
Maekawa, S., Nagoya Univ., Applied Physics, Nagoya, Japan
Dagotto, E., FSU, Physics/NHMFL
Riera, J., Rosario Univ., Physics, Rosario, Argentina

An exact-diagonalization technique on small clusters is used to study the dynamics of the one-dimensional symmetric Anderson lattice model.[1] Our calculated excitation spectra reproduce key features expected for an infinite Kondo lattice such as nearly localized low-energy spin excitations and extended regions of "heavy-quasiparticle" bands. We show that, in contrast to the hybridization picture, low-energy spin excitations of the nearly-localized f-electron system play a key role in the formation of an almost dispersionless low-energy band of heavy quasiparticles.

Reference:

1 Tsutsui, K., *et al.*, J. Phys. Rev. Lett., **76**, 279 (1996).

High Field Ultrasonic Measurements in the Heavy Electron Material UPt_3

Ulrich, V., Univ. of Virginia, Physics
Shivaram, B.S., Univ. of Virginia, Physics
Hinks, D.G., Argonne National Labs.

We have performed high resolution measurements of the longitudinal sound velocity in a single crystal of the heavy electron material UPt_3 in magnetic fields up to 30 tesla with the field oriented both along the c-axis and the a-axis of the hexagonal crystal. For the latter orientation we find a pronounced dip in the sound velocity centered at 20 tesla. This dip is not present for the perpendicular orientation. The magnitude of this dip strengthens

gradually as the temperature is lowered from 10 K with no apparent discontinuities observed near 5 K, which is the temperature where the antiferromagnetic order sets in. The magnitude of this dip, however, is consistent with the "metamagnetic" transition established already through magnetization measurements (see research report by Dorsey, *et al.*, 1996 NHMFL Annual Report, on magnetization measurements in UPt_3).

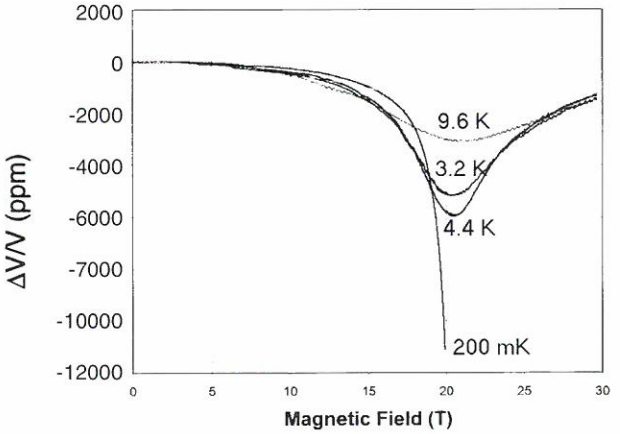

Figure 1. Dip in the longitudinal sound velocity at the metamagnetic transition in UPt_3.

We also have extended the measurements of the sound velocity to temperatures as low as 60 mK in a maximum field of 20 tesla. Although we cannot cross the metamagnetic transition, we have discovered for the first time quantum oscillations in the velocity of sound (Figure 2). The fermi surface of UPt_3 has been studied before, but this is the first demonstration of the oscillations being present in *ultrasound* experiments. It will be extremely exciting to follow these oscillations at ultralow temperatures to even higher fields. Issues such as the nature of the electronic interactions above and below the metamagnetic transition can be addressed this way.

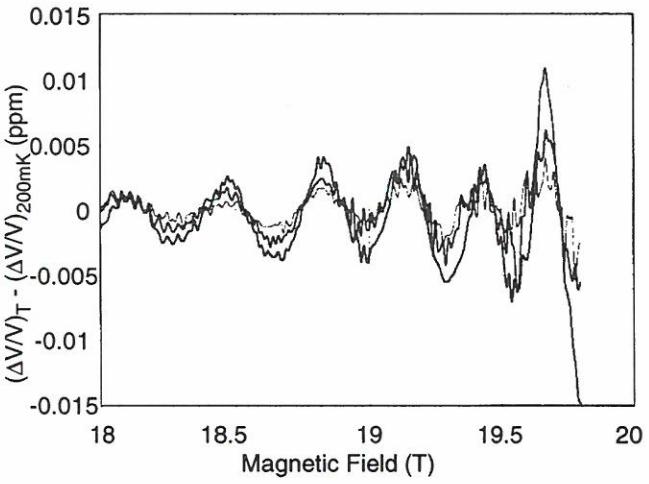

Figure 2. Quantum oscillations in the longitudinal sound velocity in UPt_3.

Reference:

1 Ulrich, V., *et al.*, submitted to Phys. Rev. B, Dec. 1996.

Magnetoresistance and Magnetization in Anomalous Pr Compounds

Yatskar, A., Univ. of California-Riverside, Physics, and NHMFL
Canfield, P.C., Iowa State Univ./Ames Laboratory
Beyermann, W.P., Univ. of California-Riverside, Physics
Lacerda, A., NHMFL/LANL

In many lanthanide-intermetallic compounds, the conduction electrons hybridize with the localized f electrons, and this many-body interaction modifies the material's thermodynamic and transport properties at low temperatures. When a Pr^{3+} ion is at a site of cubic symmetry, the crystal-electric-field (CEF) splits the ground state multiplet into a series of levels that includes a non-magnetic, non-Kramers doublet (Γ_3). The non-Kramers doublet has a quadrupolar rather then a magnetic moment, and if this level is lowest in energy, the many-body interaction associated with this level is fundamentally different from that for the conventional Kondo effect. Recently, a very large linear contribution was observed in the specific heat of $PrInAg_2$ below ~ 0.5 K, which has a Γ_3 ground state.[1] Indications of correlated-electron behavior also exist in several other Pr compounds such as $PrMg_3$ and $Pr_{1-x}La_xPb_3$.

An applied magnetic field will certainly effect the correlated properties differently if the many-body interaction does not involve the electron spin. We have measured the electrical resistance of $PrInAg_2$ as a function of temperature (1.9 - 100 K) and magnetic field (0 - 18 T). The transverse

magnetoresistance is positive up to 18 T, and it increases to ~ 18% as the temperature is decreased to 1.9 K. The magnetization was measured up to 18 T from T = 10 K to 2 K. A non linear component is observed, possibly reflecting the CEF levels. Similar behavior was also observed in $PrMg_3$ and $Pr_{1-x}La_xPb_3$. Measurements at lower temperatures where the correlated ground state develops are planned.

Reference:

1 Yatskar, A., *et al.*, Phys. Rev. Lett., **77**, 3637 (1996).

SCIENCE RESEARCH REPORTS

Molecular Conductors

The Dirac Series: Molecular Conductors in 800 T Fields. I. Overview and Instrumentation

Brooks, J.S., FSU, Physics/NHMFL
Engel, L., FSU, Physics/NHMFL
Qualls, J.S., FSU Physics/NHMFL
Clark, R., UNSW Group, Sydney
Tatsenko, O., Sarov Group, Russia
Tokumoto, M., Electrotechnical Labs., Tsukuba, Japan
Anzai, H., Himeji Institute of Technology, Japan
Fowler, M., LANL
Solem, J., LANL
Rickel, D.G., NHMFL/LANL
Goettee, J.D., NHMFL/LANL
Campbell, L.J., NHMFL/LANL

In magnetic fields of order 600 T, certain quasi-two dimensional organic metals such as (BEDT-TTF)$_2$NH$_4$Hg(SCN)$_4$ reach the extreme quantum limit. In this situation, the magnetic energy is comparable to the electronic energy, and the opportunity exists to realize new physical situations. These are (1) many-body interactions may become important at magnetic fields beyond the final Landau level, as in the 2D electron gas in semiconductor heterostructures; (2) a finite (about 20%) of the flux quantum can be introduced into the unit cell area, opening the opportunity to observe Hoffstadter-type spectra; and (3) the magnetic energy becomes comparable to the Zeeman band, and even cohesive (coulomb) energies, thereby completely changing the nature of the electronic structure at the Fermi level, and perhaps even the structure of the unit cell. It is the characteristically low energy scale of these materials (~ 200 meV), their large unit cells, and their unusual properties as extremely high quality single crystal metals that allow these possibilities.

Materials of the form (BEDT-TTF)$_2$NH$_4$Hg(SCN)$_4$ are advantageous for another important reason in the high magnetic field environment. They are less conducting than

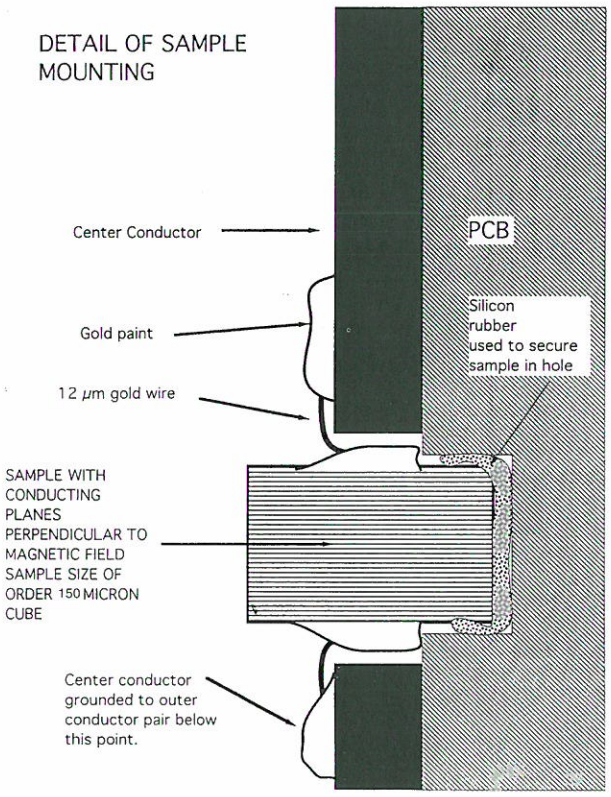

Figure 1. Sample configuration used in Dirac Series 800 T experiments.

conventional metals, hence there is less heating in transient magnetic fields. But equally important is the ability to apply current and measure voltage along the least conducting direction of a single crystal, parallel to the magnetic field, with only a two-terminal connection, and yet derive from the magnetoresistance (which is huge in this direction) the important properties of the Fermi surface behavior. The sample configuration used in the Dirac Series 800 T experiments is shown in Figure 1.

The sample holder is placed in a special disposable pumped helium cryostat that is positioned in an MC-1 type explosive flux compression magnet. The magnetic field varies from about 100 to 800 T in a micro second. To measure resistances on this scale, we have used simple DC-biased circuits (see Figure 2a) where the current is reduced as the sample resistance rises. A fast buffer amplifier drives the signal through coaxial cables to 2 ns resolution scopes 30 m away in a bunker. An alternative AC arrangement is shown in Figure 2b. Here an rf signal at 750 MHz is passed through the sample, rectified, and again driven with a buffer amplifier. The circuit is analogous to amplitude modulation detection. The performance of each method is given in Report II.

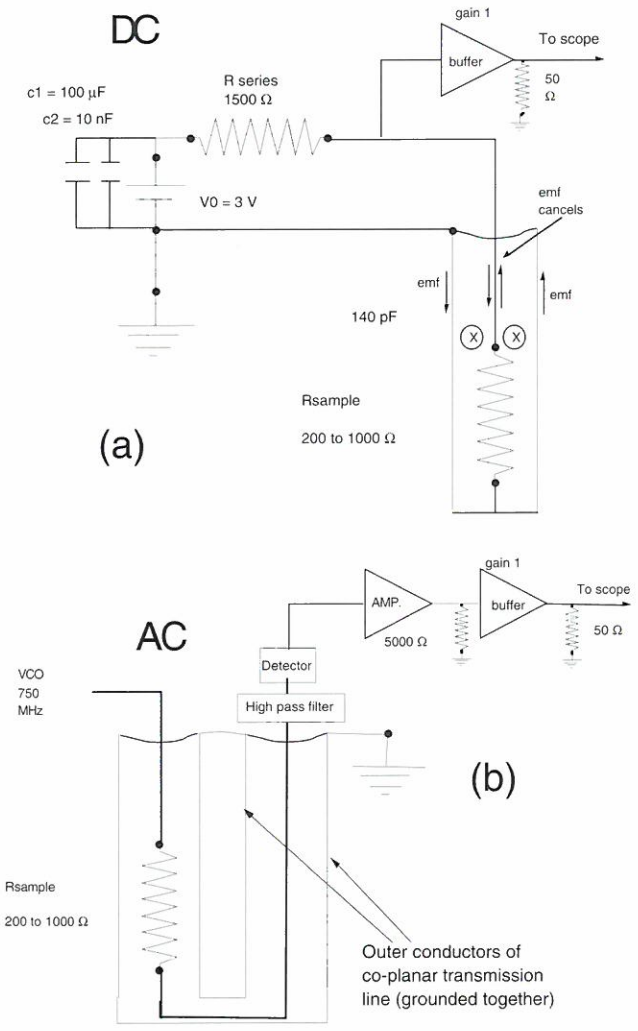

Figure 2. DC and AC electronics used in Dirac series experiments.

The Dirac Series: Molecular Conductors in 800 T Fields. II. Pre-Tests to 60 T

Brooks, J.S., FSU, Physics/NHMFL
Engel, L., FSU, Physics/NHMFL
Qualls, J.S., FSU, Physics/NHMFL
Clark, R., UNSW Group, Sydney
Tatsenko, O., Sarov Group, Russia
Tokumoto, M., Electrotechnical Labs., Tsukuba, Japan
Anzai, H., Himeji Institute of Technology, Japan
Fowler, M., LANL
Solem, J., LANL
Rickel, D.G., NHMFL/LANL
Goettee, J.D., NHMFL/LANL
Campbell, L.J., NHMFL/LANL

Prior to attempting transport measurements in destructive 800 T flux compression MC-1 series magnets, we carried out extensive pre-tests of the sample configuration and electronics described in the previous section. These studies were accomplished in the 50 and 60 T pulsed field magnet systems at the NHMFL-LANL Pulsed Magnet Laboratory. The dewar and electronics were those used latter in the 800 T experiments.

The pretests were very useful, not only in fine tuning the measurements, but in providing new information about certain materials. One example is for $(BEDT\text{-}TTF)_2NH_4Hg(SCN)_4$, as is shown in Figure 1. Here we have utilized both DC and AC methods (as described in Part I.), which we see give comparable results. One can see the rapid increase in magnetoresistance followed by the quantum

oscillation behavior. (Only the 13th Landau level is reached at 50 T.) A new feature, previously only observed in this material at high pressure, is a slow background oscillation of much lower frequency. The origin of this new feature, which was observed in all samples of this material studied in the pre-test measurements, is not yet understood, but may have to do with current density and/or the higher temperature (1.7 K) of this set of measurements.

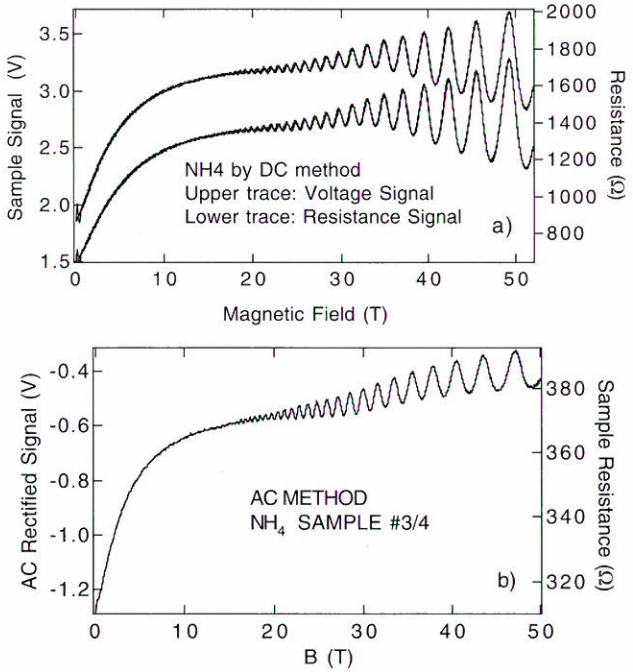

Figure 1. DC and AC signals from NH_4 samples at 1.7 K in a pulsed field magnet.

Equally important in Figure 1 is the fact that *no subtraction of the background induced emf from the pulsed field is performed.* This is due to the extremely small sample and the careful method used to reduce the open loops normally associated with resistance measurements. Hence the rapid field-up and slower field-down traces lie upon each other. This is unprecedented for pulsed field transport measurements.

Another example of new information was in a comparable study of the material $(TMTSF)_2ClO_4$, as shown in Figure 2. Normally this material must be carefully annealed at 24 K to fully establish the metallic state where the ClO_4 anions order, thereby doubling the unit cell in the b-axis direction. Conversely, in the dis-ordered state, which can be achieved by quenching the sample, the material may only partially order. Here the un-ordered Fermi surface will be very similar to that of the isostructural $(TMTSF)_2PF_6$ in which a spin density wave (SDW) ground state forms at low temperatures, and in which a quantum oscillation of about 220 T in frequency is observed. In the pre-test measurements the samples had to be cooled very rapidly (quenched in a few minutes) due to the nature of the dewar, and the $(TMTSF)_2ClO_4$ samples were therefore disordered. We show the magnetoresistance of these materials for three different temperatures to 60 T (see Figure 2). There are several features of note. First is that the resistance rises rapidly above a threshold field. This is due to a magnetic field induced spin density wave transition in the ordered part (domains) of the material. Following this are quantum oscillations of about 25O tesla, also a result of the SDW phase. However, in the high field regime a new, slow oscillation is observed at about 190 T. This oscillation is close to that of $(TMTSF)_2PF_6$, and the oscillation amplitude has a non-monotonic dependence on temperature, as it does in $(TMTSF)_2PF_6$. We believe that this is the first observation of quantum oscillations coming from the non-doubled unit cell of the $(TMTSF)_2ClO_4$ compound.

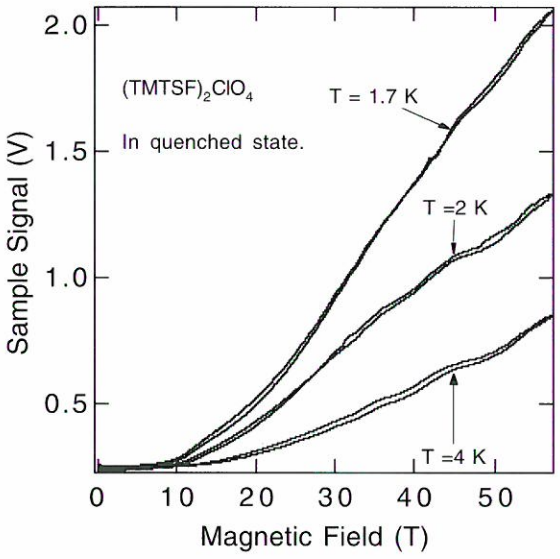

Figure 2. Magnetoresistance of $(TMTSF)_2ClO_4$ at different temperatures to 60 T.

The Dirac Series: Molecular Conductors in 800 T Fields. III. 800 T Transport Measurements

Brooks, J.S., FSU, Physics/NHMFL
Engel, L., FSU, Physics/NHMFL
Qualls, J.S., FSU, Physics/NHMFL
Clark, R., UNSW Group, Sydney
Tatsenko, O., Sarov Group, Russia
Tokumoto, M., Electrotechnical Labs., Tsukuba, Japan
Anzai, H., Himeji Institute of Technology, Japan
Fowler, M., LANL
Solem, J., LANL
Rickel, D.G., NHMFL/LANL
Goettee, J.D., NHMFL/LANL
Campbell, L.J., NHMFL/LANL

The final measurements were performed in three sets of runs in the MC-1 flux compression generators, using the electronics described in Part I. We focused on the material (BEDT-TTF)$_2$NH$_4$Hg(SCN)$_4$. The results of a representative run are shown in Figure 1. Generally, the sample resistance appears finite in many cases throughout the duration of the shot, that the sample voltage stays below the compliance voltage, and that during the seed field period, the magnetoresistance follows that seen in the pulsed field measurements (up to about 18 T).

In Figure 1a we can compare the zero field and seed field signals and note that the resistance in the seed field is higher. Hence the magnetoresistance due to the seed field is evident. There is also very high noise when the capacitor bank fires, but this attenuates reasonably quickly. Further indications of new noise appear at later times. In Figure 1b, we show the simulation and the raw signal vs. magnetic field. The high frequency and higher amplitude oscillations are clearly noise, but it is possible that the background signal, which has a much lower frequency variation of the order of the simulation and which stays below the compliance voltage of the bias circuit, may be partially attributable to the presence of sample's magnetoresistance and Shubnikov de Haas (SdH) oscillation behavior.

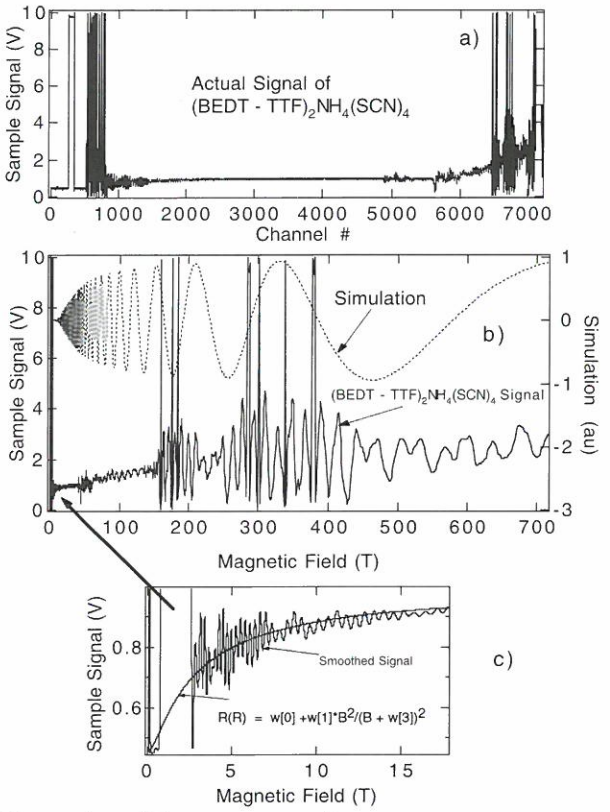

Figure 1. Measurements of (BEDT-TTF)$_2$NH$_4$Hg(SCN)$_4$ to 800 T.

Hence Figure 1 really defines the state of the problem. First the initial EMI when the bank fires is detrimental. Sometimes it may destroy the sample and/or its leads, or may cause the sample to warm significantly. Nevertheless, the observation of magnetoresistance in the seed field tells us that the sample has survived this first trauma. (This behavior is detailed in Figure 1c). Secondly, although 50 ohm termination helps the signal-to-noise, further reduction of the background noise is needed before one can determine with certainly the high field resistance and/or the magneto-oscillatory behavior. The nature of the noise when the second and third segments of the MC1 cascade become active, and whether or not it can be attenuated, is not known at this stage. The cancellation of the dB/dt induced emf seems to be quite good. One can see, however, that the average value of the signal does increase monotonically when the generator fires, and then levels off above about 300 T. Some of the monotonic increase could be due to some form of induced emf, but there is no direct comparison that can be made between the signal and the dB/dt wave form.

Uniaxial Stress Studies of Molecular Conductors: I. Overview and α - (BEDT-TTF)$_2$RbHg(SCN)$_4$

Brooks, J.S., FSU, Physics/NHMFL
Harris, K., FSU, Physics/NHMFL
Qualls, J.S., FSU, Physics/NHMFL
Fisk, Z., FSU, Physics/NHMFL
Sarrao, J.L., FSU Physics/NHMFL
Perenboom, J.A.A.P., Univ. of Nijmegen, The Netherlands, Physics
van Bentum, J., Univ. of Nijmegen, The Netherlands, Physics
Uji, S., NRIM, Tsukuba, Japan
Tokumoto, M., Electrotechnical Labs., Tsukuba, Japan
Kinoshita, N., Electrotechnical Labs., Tsukuba, Japan
Kinoshita, T., Electrotechnical Labs., Tsukuba, Japan
Tanaka, Y., Electrotechnical Labs., Tsukuba, Japan
Takasaki, S., Himeji Inst. of Tech., Japan
Yamada, J., Himeji Inst. of Tech., Japan
Anzai, H., Himeji Inst. of Tech., Japan

Highly anisotropic conducting materials have a number of possible ground state configurations such as superconducting magnetic, metallic, or insulating character. To better understand the mechanisms that determine the various ground states, it is useful to know the relative importance of the parameters that result from the anisotropy, such as lattice constant and electronic bandwidth effects. We have carried out a new initiative to investigate the effects of uniaxial stress on the electronic structure of quasi-one dimensional conductors and have extended similar studies on several quasi-two dimensional molecular conductors.

The general method involves the application of compressional stress vertically on a sample by a gas piston arrangement. The experiments are carried out to low temperatures (0.5 K) and in high magnetic fields (30 T). Single crystals of the materials of interest are first encapsulated in an epoxy medium with flat, parallel boundaries. This ensures that even highly irregular, extremely delicate samples can survive to stresses of up to 10 kbar, whereas under normal conditions even a tweezers can destroy the materials. High magnetic fields play a crucial role in the studies since all of the materials exhibit quantum oscillation behavior (Shubnikov de Haas or SdH oscillations), which reveal details of the electronic structure through their frequency and amplitudes (effective mass).

α-(BEDT-TTF)$_2$RbHg(SCN)$_4$. This material is in the iso-structural class of α-(BEDT-TTF)$_2$MHg(SCN)$_4$ organic conductors where M = K, Rb, Tl, or NH_4. Only for M = NH_4 is the material a superconductor, whereas the others form an anomalous low temperature density wave ground state below 8 to 12 K. We have demonstrated previously that uniaxial stress perpendicular to the conducting molecular layers induces superconductivity for M = K and enhances the transition temperature for M = NH_4. We recently have extended the investigation for M = Rb and have observed an effect similar to that seen for M = K, as is shown in Figure 1. Here we see the onset of superconducting critical field behavior

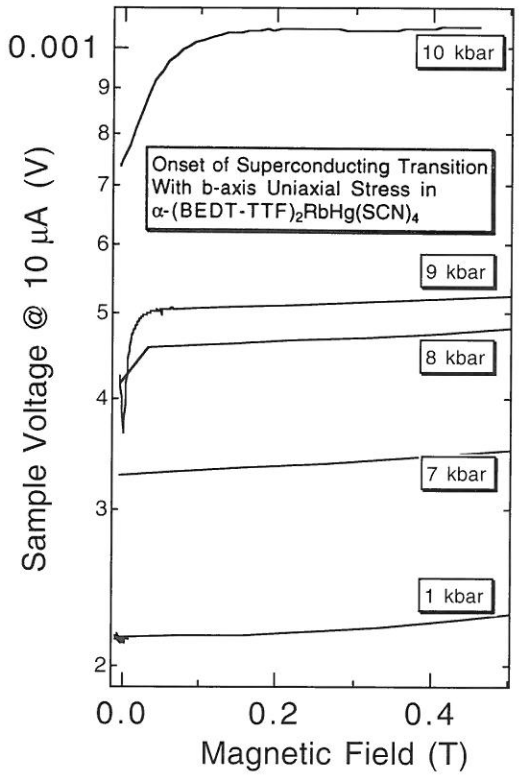

Figure 1. Low field magnetoresistance of RbHg sample at 1.3 K vs. uniaxial stress.

above a critical pressure of about 7 kbar. This corresponds to the destruction of the density wave state at slightly lower pressures. The increase with stress in the normal state magnetoresistance is not yet understood, and is under further investigation.

Uniaxial Stress Studies of Molecular Conductors: II. η - Mo_4O_{11}

Brooks, J.S., FSU, Physics/NHMFL
Harris, K., FSU, Physics/NHMFL
Qualls, J.S., FSU, Physics/NHMFL
Fisk, Z., FSU, Physics/NHMFL
Sarrao, J.L., FSU, Physics/NHMFL
Perenboom, J.A.A.P., Univ. of Nijmegen, The Netherlands, Physics
van Bentum, J., Univ. of Nijmegen, The Netherlands, Physics
Uji, S., NRIM, Tsukuba, Japan
Tokumoto, M., Electrotechnical Labs., Tsukuba, Japan
Kinoshita, N., Electrotechnical Labs., Tsukuba, Japan
Kinoshita, T., Electrotechnical Labs., Tsukuba, Japan
Tanaka, Y., Electrotechnical Labs., Tsukuba, Japan
Takasaki, S., Himeji Institute of Technology, Japan
Yamada, J., Himeji Institute of Technology, Japan
Anzai, H., Himeji Institute of Technology, Japan

η - Mo_4O_{11}. This material undergoes two charge density wave transitions upon cooling to below 30 K, thereby leaving only very small electron and hole pockets at low temperatures. Hence by 20 T, the material reached the quantum limit where the magnetic energy surpasses the electronic (Fermi level) energy. In Figure 1, we show the systematic variation of the magnetoresistance with increasing uniaxial stress along the least conducting direction in the material. We find three important changes induced by stress: (1) The background resistance systematically decreases with stress, most likely as a result of the suppression of the charge density wave gap. (2) The quantum oscillation frequency increases (e.g. peak position), which is an indication that the Fermi energy is increasing with stress. (3) The onset of the metal-insulator transition increases in field with stress, in agreement with our model that describes the M-I behavior in the context of the onset of the quantum limit.

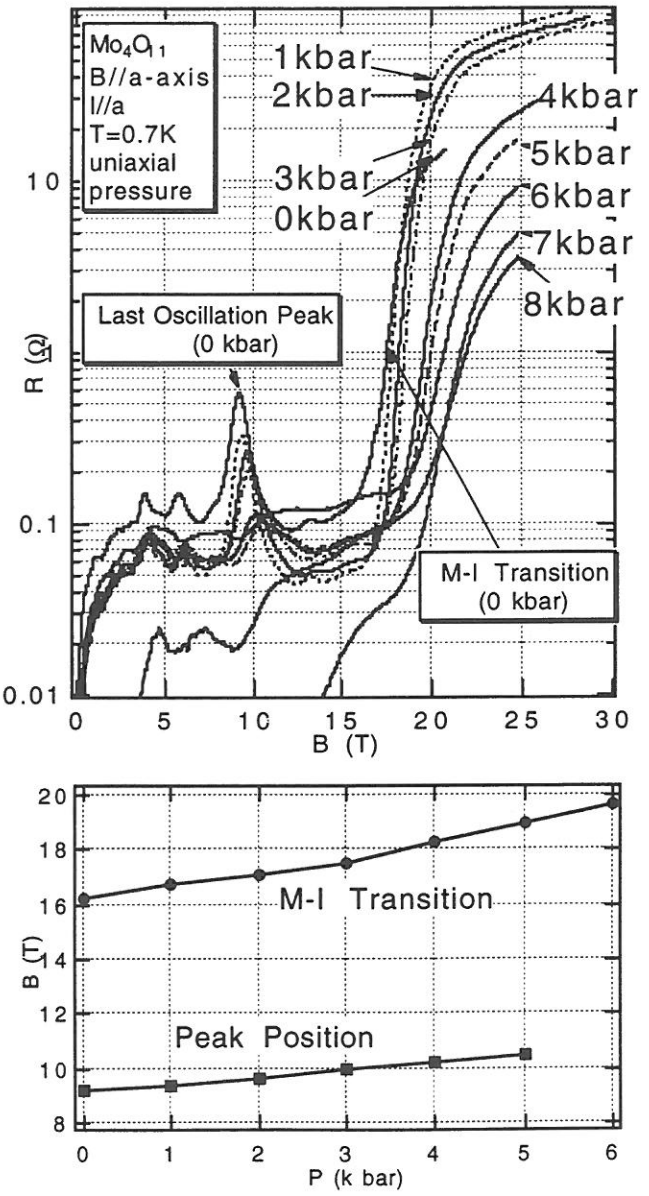

Figure 1. Upper panel: Magnetoresistance of η-Mo_4O_{11} for different values of uniaxial stress at 0.7 K. Lower panel: Stress dependence of peak and M-I transition.

Uniaxial Stress Studies of Molecular Conductors: III. $(TMTSF)_2PF_6$

Brooks, J.S., FSU, Physics/NHMFL
Harris, K., FSU, Physics/NHMFL
Qualls, J.S., FSU, Physics/NHMFL
Fisk, Z., FSU, Physics/NHMFL
Sarrao, J.L., FSU, Physics/NHMFL
Perenboom, J.A.A.P., Univ. of Nijmegen, The Netherlands, Physics
van Bentum, J., Univ. of Nijmegen, The Netherlands, Physics
Uji, S., NRIM, Tsukuba, Japan
Tokumoto, M., Electrotechnical Labs., Tsukuba, Japan
Kinoshita, N., Electrotechnical Labs., Tsukuba, Japan
Kinoshita, T., Electrotechnical Labs., Tsukuba, Japan
Tanaka, Y., Electrotechnical Labs., Tsukuba, Japan
Takasaki, S., Himeji Institute of Technology, Japan
Yamada, J., Himeji Institute of Technology, Japan
Anzai, H., Himeji Institute of Technology, Japan

$(TMTSF)_2PF_6$ This material has the highest degree of anisotropy. Along the a-axis it is highly conducting, along the b-axis it is less conducting, and along the c-axis it is least conducting. We have carried out uniaxial stress studies along each of the three directions using a new method of stress application (see Figure 1). To study the quantum oscillation behavior, the magnetic field must always be perpendicular to the conducting planes. In a given experiment we can run stress in two directions on two different samples, one with Pz stress and one with Pxy for the b-axis stress. Preliminary results are given for the b-axis configuration in Figure 2. Here we note that the conductivity at low temperatures increases by almost 1000 in some cases, and corresponding to this is an increase in the quantum oscillation frequency. By studying the temperature dependence of the resistance with stress, we have determined that increasing stress uniformly reduces the SDW energy gap, which we predict should reach zero (metallic behavior) by 12 kbar (see Figure 3). Analysis of the relative changes in the conductivity and oscillation frequency indicate that a specific transfer integral (I3) that is used in the tight binding band structure calculations is most influential in the electronic structure, and that b-axis stress my provide the largest changes in electronic structure. More work is underway to determine this point.

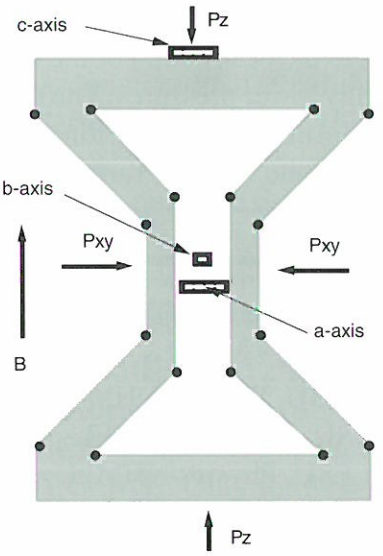

Figure 1. Device for translation of vertical stress to horizontal stress.

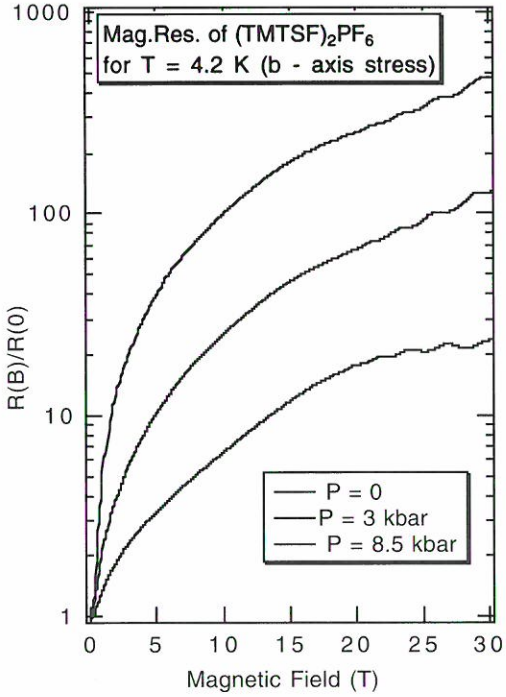

Figure 2. Example of the effects of horizontal (b-axis) stress on $(TMTSF)_2PF_6$ where B//c-axis.

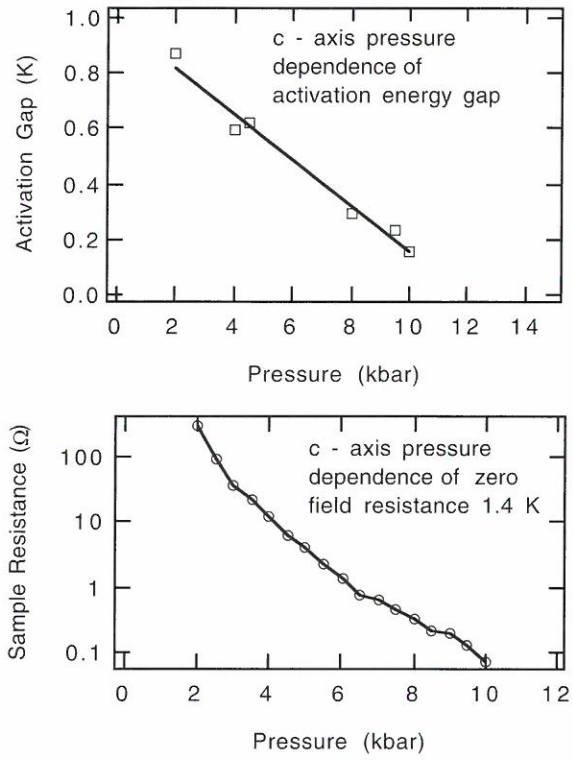

Figure 3. Upper panel: Stress dependence of SDW activation energy. Lower panel: Log plot of 4-decade drop in sample resistance vs. stress.

NMR Investigation of Spin-Density-Wave Dynamics to 1 GHz in $(TMTSF)_2AsF_6$

Clark, W.G., UCLA, Physics
Brown, S.E., UCLA, Physics
Zheng, G.-q., UCLA, Physics and Osaka Univ.
Kuhns, P.L., NHMFL
Moulton, W.G., NHMFL/FSU, Physics

There were two goals for this work: (1) To implement the technological steps needed to carry out condensed matter pulsed NMR up to 1 GHz, and (2) to apply them to study spin-density-wave (SDW) dynamics in organic conductors.

The technology goal was achieved with a 1 GHz pulsed NMR system developed at UCLA and carried to the NHMFL. Its NMR probe includes sample rotation and other novel features. The probe operates over a wide range of frequencies and temperatures in the resistive NMR magnets at NHMFL. It is also compatible with the existing condensed matter NMR spectrometer at the NHMFL. A 300 K spin echo signal of the protons in $(TMTSF)_2AsF_6$ obtained with this system at 1 GHz (23.4 T) is shown in Figure 1. The nulled region is the rf pulse and the large overload immediately afterwards is the FID signal.

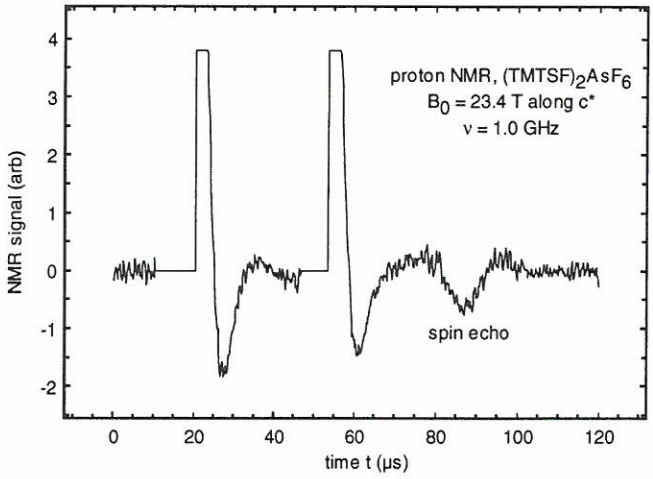

Figure 1. Proton spin echo signal at 1 GHz.

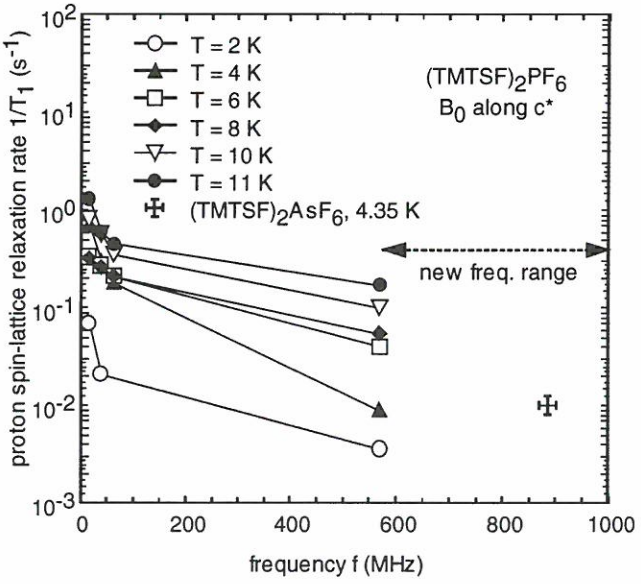

Figure 2. $1/T_1$ vs. frequency.

We also made an initial measurement of the proton spin-lattice relaxation rate ($1/T_1$) in (TMTSF) at 4.35 K and a frequency of 0.85 GHz. The motivation for this kind of measurement in the SDW phase is that it probes the SDW condensate fluctuations[1] at the NMR frequency. Since $1/T_1$ is proportional to the sum over all phason wave vectors of the imaginary part of the SDW condensate dielectric constant at the NMR frequency,[1] one obtains the dissipative part of the electrical response of the pinned SDW condensate.

By going to very high magnetic field, this phenomenon can be studied up to correspondingly high frequencies. Figure 2 shows the point obtained at the NHMFL (cross) along with prior measurements (UCLA, Grenoble) on similar materials. The dotted arrow shows the frequency range that can now be investigated.

A comprehensive analysis of these data will be carried out upon completion of more measurements.

References:

1 Clark, W.G., *et al.*, J. Phys. Paris IV, 235-242 (1993).

2 Brown, S.E., *et al.*, submitted to Phys. Rev. B.

Parallel and Perpendicular Critical Fields in Anisotropic Molecular Superconductors

Coffey, T., Clark Univ., Physics
Ivanov, S.A., Clark Univ., Physics
Agosta, C.C., Clark Univ., Physics
Montgomery, L.K., Indiana Univ., Chemistry
Burgin, T., Indiana Univ., Chemistry
Greenblatt, M., Rutgers Univ., Chemistry

We have measured the critical magnetic fields H_{c2} in the superconductors λ-$(BETS)_2GaCl_4$ and $Li_{0.9}Mo_6O_{17}$ (purple bronze) as a function of temperature. These measurements were done in the dilution refrigerator and 20 T superconducting magnet at NHMFL in Tallahassee. In the case of the BETS material, the applied magnetic field was parallel to the layers and we found the critical field by measuring the rf penetration depth at 26 MHz. The highest critical field we measured was 7.5 T, lower than we expected. Future measurements at higher temperatures will give us the shape of the complete phase diagram. From the shape of the diagram we will be able to determine if there is dimensional crossover, as the superconducting layers decouple, and we will be able to estimate the strength of the electron-phonon coupling parameter $\lambda_{e\text{-}ph}$.

For the purple bronze, the applied field was perpendicular to the conducting layers and we measured both transport and rf penetration depth. We found $H_{c2} = 0.9$ T at 40 mK which changed to only 0.8 T at 500 mK. In the transport data, a more rounded superconducting transition was seen followed by a moderate rise in the resistance as a function of field. At ~13.5 T the resistance reached a peak and began to drop as the field was increased further. This drop in the resistance is most likely associated with the destruction of a charge density wave.

Electron-Electron Interactions in Q1D Conductors

Gor'kov, L.P., NHMFL

The strength of electron-electron interactions in anisotropic organic Q1D materials, such as the Bechgaard salts, remains the actively debated issue. Most of their properties are successfully interpreted in a weak coupling phenomenological "nesting" model, assuming that the conduction electron spectrum consists of the two open Fermi surfaces with approximate congruent features. The point of view that interactions are rather weak, is justified by experimental observation that, first, all phenomena, such as the Spin Density Wave (SDW) transition, take place at temperatures of order of 10 K, while estimated bandwidth is about 0.8eV; and, secondly, that their properties are very sensitive to minor external factors, such as an applied pressure or magnetic field. In reference 1, it is shown that the phenomenological, so-called "standard," model can, in fact, be derived from the one-dimensional (1D) problem of weakly interacting electrons, if three-dimensional effects are taken into account. Expressions for parameters of the standard model in terms of 1D interactions are obtained. It has been found in reference 2 that "nesting" degeneracy of the standard model results in considerable enhancement of some electron-electron relaxation rates in the temperature range of order of characteristic temperature of the SDW instability (usually ~10 K). It is shown in reference 1 that while this effect may be responsible for the experimentally observed deviations from the T^2 behavior of resistivity in the Bechgaard salts and

for their anomalous magnetoresistance in this temperature range, the anomalous behavior of the NMR-relaxation time observed recently, cannot be ascribed to such a phenomenon, urging further experimental studies.

References:

1 Gor'kov, L.P., J. Phys. I, France, **6**, 1 (1996).

2 Gor'kov, L.P., Europhys. Lett., **31**, 46 (1995).

Magnetotransport Phenomena in α-(BEDT-TTF)$_2$KHg(SCN)$_4$ at High Magnetic Field and Low Temperatures

Harrison, N., NHMFL/LANL
Mielke, C.H., NHMFL/LANL
Lacerda, A., NHMFL/LANL
Rickel, D.G., NHMFL/LANL
Honold, M.M., Oxford University, Oxford, U.K., Physics
Singleton, J., Oxford University, Oxford, U.K., Physics
Kurmoo, M., The Royal Institution, London, U.K.
Day, P., The Royal Institution, London, U.K.

Magnetotransport phenomena have been investigated in the charge-transfer salt α-(BEDT-TTF)$_2$KHg(SCN)$_4$ at the extremes of high magnetic field (50 T) and low temperature (40 mK). In the high magnetic field phase at high temperatures the Shubnikov-de Haas oscillations have the conventional form, with pronounced maxima coinciding with the point where the chemical potential is situated in the gap between adjacent Landau levels. At low temperatures, however, a very different picture emerges. Below approximately 2 K, the amplitude of oscillations no longer increases, but instead begins to fall.

The magnetoresistance maxima, which are observed in a number of alpha-phase BEDT-TTF salts, are understood to arise from the vanishing of the longitudinal (inter-plane) group velocity when the chemical potential is located at (or near) the top or bottom of one of the longitudinal minibands.[1] Thus the magnetoresistance is usually observed to increase strongly with decreasing temperature. It is likely that the observed suppression of the magnetoresistance maxima in α-(BEDT-TTF)$_2$KHg(SCN)$_4$ at low temperatures is purely a magnetotransport effect, and is not thermodynamic in origin. Further evidence supporting this conclusion comes from de Haas-van Alphen measurements[2,3] (on the same crystals), which show that the amplitude monotonically increases at low temperatures.

While there is as yet no particular mechanism that can be singled out as the cause of the unusual magnetotransport effect, the most extreme suppression of the magnetoresistance maxima does appear to occur in samples with pronounced eddy current resonance effects.

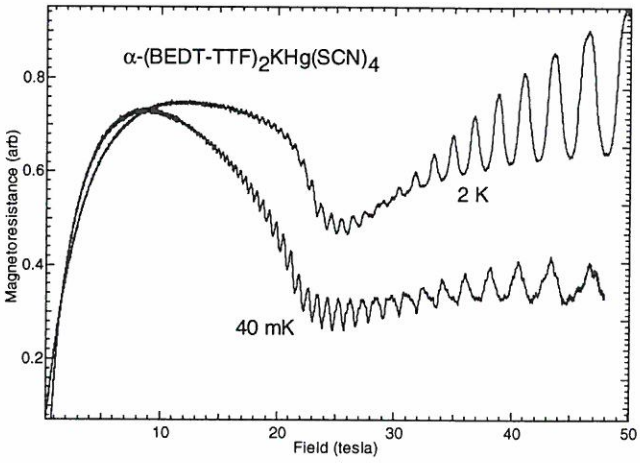

Figure 1. α-(BEDT-TTF)$_2$KHg(SCN)$_4$ measured at 2 K and 40 mK to 50 T.

References:

1 Harrison, N., *et al.*, Phys. Rev. B, **54**, 9977 (1996).

2 Harrison, N., *et al.*, to be published 1997.

3 Harrison, N., *et al.*, Phys. Rev. Lett., **77**, 1576 (1996).

A Semiclassical Description of Cyclotron Resonance in Quasi-Two-Dimensional Organic Conductors: Theory and Experiment

Hill, S., NHMFL

We have examined cyclotron resonance-like behavior in quasi-two-dimensional organic conductors, both from a theoretical perspective, and

from an experimental point of view.[1] We demonstrate how the conductivity in the least dispersive direction (normal to the conducting layers) can dominate the magneto-electrodynamic response of highly anisotropic metals. Consequently, we develop a detailed semiclassical model for the conductivity in this direction, taking into consideration the unique Fermi surface topologies common to these materials. This can result in multiple cyclotron resonance-like features in the conductivity along the least conducting direction, which arise from periodic motion in a plane perpendicular to the applied magnetic field; we refer to these features as "periodic orbit resonances." It is shown that the details of these "periodic orbit resonances" are highly sensitive to the precise shape of the Fermi surface; indeed, both quasi-two-dimensional, and quasi-one-dimensional, Fermi surface sections will contribute to this effect. We also discuss compelling experimental evidence supporting our model, as well as several other consequences of such a semiclassical treatment, for example, magnetoresistance and "periodic orbit resonance" linewidths. The outcome of this work is a clearer understanding of cyclotron resonance-like features observed, recently, in several BEDT-TTF charge transfer salts. In light of our findings, we point out possible complications that can arise in analyzing experimental data. In particular, care should be exercised in experiments on materials possessing both quasi-one- and quasi-two-dimensional Fermi surfaces, bearing in mind that either type of carrier can contribute to the "periodic orbit resonances."

This research was supported by NSF-DMR-95-10427.

Reference:

1 Hill, S., (in press) Phys. Rev. B, **55**, (February 1997).

High-Field Millimeter-Wave Spectroscopy of Low-Dimensional Molecular Metals

Hill, S., NHMFL
Buhler, C., NHMFL/FSU, Physics
Sandhu, P.S., NHMFL and Boston Univ., Physics
Brooks, J.S., NHMFL/FSU, Physics

We have developed unique high-field millimeter-wave spectroscopic techniques that have been used at NHMFL.[1] The main purpose of this effort is to investigate the electrodynamic response of novel conducting materials (mainly low-dimensional metals) in very strong magnetic fields. The use of microwave techniques to probe the electrodynamic properties of metals is not new, however, due to recent interest in conducting systems such as high T_c superconductors, heavy fermion metals, and organic conductors, this experimental field is undergoing a renaissance. The millimeter-wave frequency range is particularly important for studying the electrodynamics of high quality organic conductors because it coincides with the typical electron scattering rates at liquid helium temperatures. Furthermore, the radiation energy ($h\nu$) is comparable to a number of other important energy scales in these materials, for example, superconducting or density-wave energy gaps, or the cyclotron energy in magnetic fields of the order 1 to 100 tesla.

We use a Millimeter-wave Vector Network Analyzer (MVNA) to monitor the reflected/transmitted phase and amplitude of millimeter wave radiation coupled to a resonant cavity containing our samples. The MVNA allows measurements in the frequency range 8 to 350 GHz. Using a cavity perturbation technique, we can evaluate the complex electrodynamic response of our small samples situated in the cavity; both rectangular and cylindrical cavity configurations are used.

Using these techniques, we have observed cyclotron resonance (CR) in the organic conductor $(DMe\text{-}DCNQI)_2Cu$.[1,2] We obtain a large CR mass ($>3m_e$), in agreement with de Haas-van Alphen measurements. We discuss the implications of these results with regards to the role of electron-electron interactions in these, and other, materials. In

addition, we are able to observe magnetic quantum oscillations in the complex surface impedance of a number of other organic conductors, including the superconductor κ-(BEDT-TTF)$_2$Cu(NCS)$_2$.[1] The information obtained from these measurements is extremely rich and is currently attracting considerable theoretical attention. We also have examined the potential of this technique in pulsed magnetic fields where conventional DC magnetoresistance measurements are problematic due to large induced EMFs.

This research was supported by NSF-DMR-95-10427.

References:

1 Hill, S., *et al.,* (to be published) in Proc. Int. Conf. on Millimeter and Submillimeter Waves and Applications III, edited by M. Afsar, pp 296-306 (SPIE, 1996).

2 Hill, S., *et al.,* Phys. Rev. B, **54**, 13536 (1996).

Quantum Limit and Anomalous Field-Induced Insulating Behavior in η-Mo_4O_{11}

Hill, S., NHMFL
Valfells, S., NHMFL and Boston Univ., Physics
Uji, S., NRIM, Tsukuba, Ibaraki 305, Japan
Brooks, J.S., NHMFL/FSU, Physics
Sandhu, P.S., NHMFL and Boston Univ., Physics
Sarrao, J.L., NHMFL
Fisk, Z., NHMFL/FSU, Physics Dept.

The quasi two-dimensional metal η-Mo_4O_{11} undergoes two successive charge-density-wave transitions at 109 K and 30 K, with corresponding changes in the electronic structure. Measurements of the magnetoresistance, Hall effect and magnetization, in magnetic fields of up to 50 tesla (T) and as a function of temperature and pressure, have been performed to determine the ground-state electronic structure.

This work is a continuation of the work reported by Brooks, *et al.*, in the 1995 annual report. Our initial studies identified at least three (possibly up to six) small quasi-two-dimensional Fermi surface pockets, all of which reach the quantum limit by 20 T. Further analysis revealed very low carrier effective masses ($m^* < 0.1m_e$) associated with each of these Fermi surfaces. Above 20 T, a dramatic increase (up to a factor of 10^4 for some samples) in resistance has been observed.

Our recent studies have concentrated on the high field (B > 20 T) properties of η-Mo_4O_{11},[1] using the world record breaking 33.6 T resistive magnet in Tallahassee. We were able to enhance this field in one experiment by using Dysprosium pole pieces,[2] allowing us to achieve a field of 36.1 T (see Figure 1). From this work, we have been able to establish that the high field state in η-Mo_4O_{11} is semiconducting, in contrast to the (semi-) metallic low field state. This crossover from semimetallic to semiconducting behavior is brought about by a "field induced electron and hole band inversion," which results in a clear gap at the Fermi energy. Measurements of this energy gap allow an independent determination of the carrier effective masses that turns out to be in excellent agreement with the values obtained from analysis of the low field (B < 15 T) resistance oscillations. We find that the transport and thermodynamic properties of the field-induced semiconducting state are highly anomalous. In particular, we have investigated the Hall effect and the origin of a new resistance oscillation at high magnetic fields (see Figure 1).

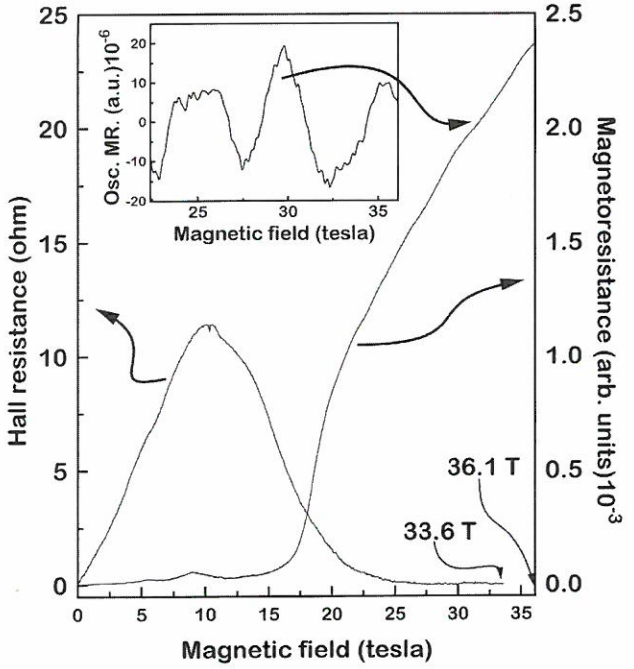

Figure 1. Quantum limit and anomalous field-induced insulating behavior in η-Mo_4O_{11}.

This research was supported by NSF-DMR-95-10427.

References:

1 Hill, S., *et al.*, (in press) Phys. Rev. B, **55,** (January 1997).

2 Developed by V. Stepankin, BI Research, Moscow, Russia.

The Bulk Quantum Hall Effect in Quasi-Two-Dimensional Molecular Metals

Hill, S., NHMFL
Sandhu, P.S., NHMFL and Boston Univ., Physics
Qualls, J.S., NHMFL/FSU, Physics
Brooks, J.S., NHMFL/FSU, Physics
Sarrao, J.L., NHMFL/FSU, Physics
Fisk, Z., NHMFL/FSU, Physics

In the realm of high magnetic fields, there is great interest in what happens when the quantized magnetic energy becomes comparable to the electronic (Fermi) energy—the so-called quantum limit. In a purely two-dimensional system, it is well know that the quantum Hall effect (QHE) is observed under such conditions. In the quasi-one-dimensional Bechgaard salts, a QHE also has been observed. In both of these cases, the ingredients that give rise to the quantized Hall resistance are the same, however, the mechanisms are rather different. Finding other bulk crystalline materials, like the Bechgaard salts, that exhibit a bulk QHE is an exciting prospect. This is particularly so in the light of recent predictions concerning the transport of current at the surface of such conductors—a novel two-dimensional metallic sheath is expected in which localization effects are completely absent.[1] Our recent studies have focused on two rather different systems as possible candidates for a bulk QHE, namely, the quasi-two-dimensional α-(BEDT-TTF)$_2$MHg(NCS)$_4$ salts (M=K, Tl), for which indirect evidence of a QHE has recently been reported,[2] and the inorganic Magnéli phase compound η-Mo_4O_{11}.

Although we have not been able to measure the Hall effect accurately in the α-(BEDT-TTF)$_2$MHg(SCN)$_4$ salts, we find that the high field Shubnikov-de Haas oscillations exhibit a complicated temperature dependence, which is not evident in de Haas-van Alphen measurements on the same samples. These differences have been explained qualitatively in terms of the competition between transport via the bulk and via the surface of the sample—a direct consequence of the bulk QHE.[3]

The semimetallic η-Mo_4O_{11} system undergoes two charge-density-wave transitions on cooling, which nest most of the room temperature Fermi surface. Consequently, measurements of the Hall effect are made much easier due to the low carrier concentration. Figure 1 shows such a measurement at dilution refrigerator temperatures—the development of Hall resistance plateaus can clearly be seen.

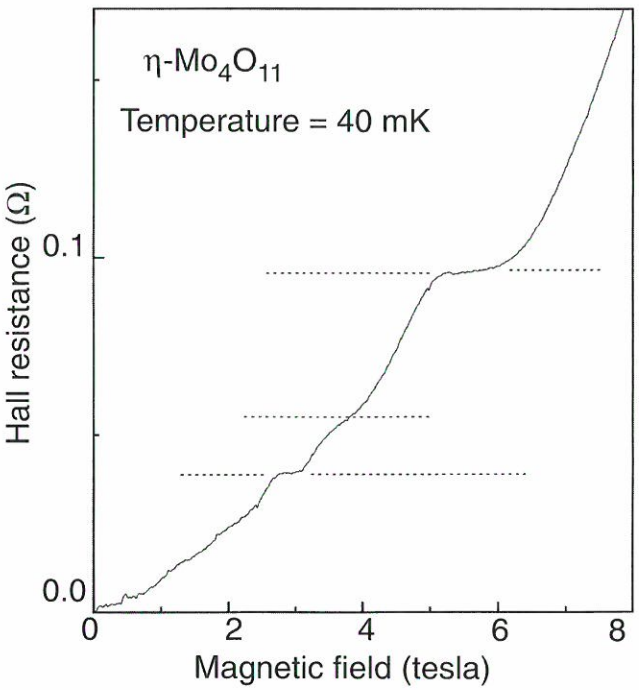

Figure 1. Hall effect in η-Mo_4O_{11}.

This research was supported by NSF-DMR-95-10427.

References:

1 Chalker, *et al.*, Phys. Rev. Lett., **75**, 4496 (1995); Balents, *et al.*, Phys. Rev. Lett. **76**, 2782 (1996).

2 Harrison, *et al.*, Phys. Rev. Lett., **77**, 1576 (1996).

3 Hill, S., *et al.*, in press Phys. Rev. B (Feb. 1997).

Hydrostatic Pressure Studies of the New Organic Conductor α-$(BETS)_2KHg(SCN)_4$

Ivanov, S.A., Clark Univ., Physics
Coffey, T., Clark Univ., Physics
Agosta, C.C., Clark Univ., Physics
Montgomery, L.K., Indiana Univ., Chemistry
Fravel, B.W., Indiana Univ., Chemistry

We performed hydrostatic pressure studies (up to 13.7 kbar) of the new organic metal α-$(BETS)_2KHg(SCN)_4$ at low temperatures (down to 0.5 K) and high magnetic fields (up to 33 tesla). This material is a close relative of $(ET)_2KHg(SCN)_4$, which possesses very interesting electronic properties at low temperatures and has been studied by several groups for some time. In α-$(BETS)_2KHg(SCN)_4$ the inner four sulfur atoms of the ET molecule are replaced with larger selenium atoms.

Our goal is to examine the behavior of the Shubnikov-de Haas oscillations as a function of pressure. A preliminary analysis of the data shows that beats appear in the oscillations when the pressure is applied and that the oscillations persist up to the highest pressures. Analysis of the data will allow us to measure changes in the parameters of the electron system with pressure that we can then compare with theoretical calculations. In an associated experiment we measured the resistance of the samples down to 40 mK and in magnetic fields up to 17 T. Our preliminary analysis of this data show that the samples remain metallic at the lowest temperatures in contrast to the ET salts. These experiments are a continuation of our research directed at the clarification of the strength of electron-electron and electron-phonon interactions, and their influence on the low temperature properties of organic metals.

Fast Oscillations in $(TMTSF)_2X$

Naughton, M.J., SUNY Buffalo, Physics, and NHMFL
Lee, I.J., SUNY Buffalo, Physics
Ulmet, J.P., SNCMP-Toulouse
Fabre, J.M., Univ. of Languedoc, Montpellier, Chemistry

The "fast oscillation" phenomenon in the quasi-one dimensional molecular conductors $(TMTSF)_2X$ was investigated to 30 T, from 0.4 K to 14 K, via magnetoresistance and torque magnetization measurements. In the ambient pressure spin density wave (SDW) state of the X = NO_3, PF_6 and AsF_6 materials, a peak in the transverse magnetoresistances ρ_{xx} (B//c*, I//a) and ρ_{yy} (B//c*, I//b'), and in their oscillatory components, is found at 3 K ± 1 K, with the oscillations vanishing at higher and lower temperatures.[1] No magnetic moment oscillations are detected in PF_6 or AsF_6, while only exceedingly weak oscillations (amplitude $\delta m \sim 10^{-13}$ Am^2) are seen in the NO_3 salt above 25 T. Results of the peculiar T- dependence are shown in Figure 1. The top panel shows background magnetoresistance (bMR) for X = AsF_6 for several values of magnetic field. The bMR can be seen to increase as temperature is lowered, reaching a maximum at a characteristic temperature T* which itself increases with field. Below T*, the bMR falls rapidly toward zero.

The FO amplitudes follow a similar trend, shown in Figure 1(b) for three TMTSF materials. At high T, the data can be reasonably modeled using the Landau formula for conventional quantized orbits, $A(x) \sim x/\sinh(x)$, where $x \sim Tm^*H^{-1}$, m* = effective mass, as shown for X = PF_6 with m* = 1.25. The data dramatically deviate from this line below the same T* as for the bMR, vanishing at low T.

While the cause of this peculiar temperature dependence is presently being debated,[2,3] it appears that a successful explanation should account for the obvious correlation between the FO amplitudes and the bMR, shown more directly in Figure 2.

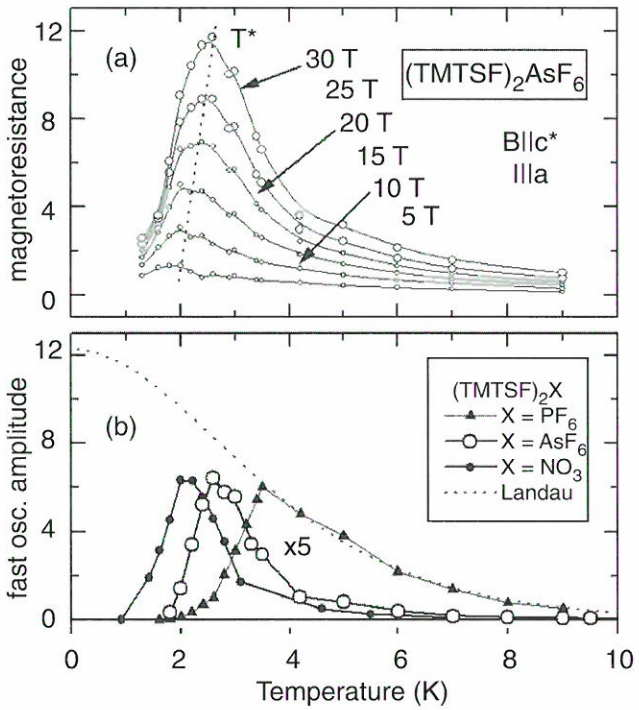

Figure 1. (a) Background magnetoresistance in $(TMTSF)_2AsF_6$, showing the maximum near 2.6K. (b) FO amplitudes for three TMTSF compounds. For PF_6, a Landau-Lifshitz-Kosevich curve is plotted, fit to the high temperature data using an effective mass parameter of 1.25.

The vanishing of the FO at low T may be due to the opening of the SDW gap, reducing the probability for quantum interference orbits,[4] or perhaps to a coexisting CDW-SDW state, or may involved glassy behavior or a new phase transition inside the SDW state. At any rate, theories that rely on anion ordering and subsequent magnetic breakdown between dimerized Fermi surface sheets are clearly *inadequate* for the present systems, as $X = AsF_6$ and PF_6 do not undergo anion ordering.

This work was supported by the NSF, under grant number DMR-9258579.

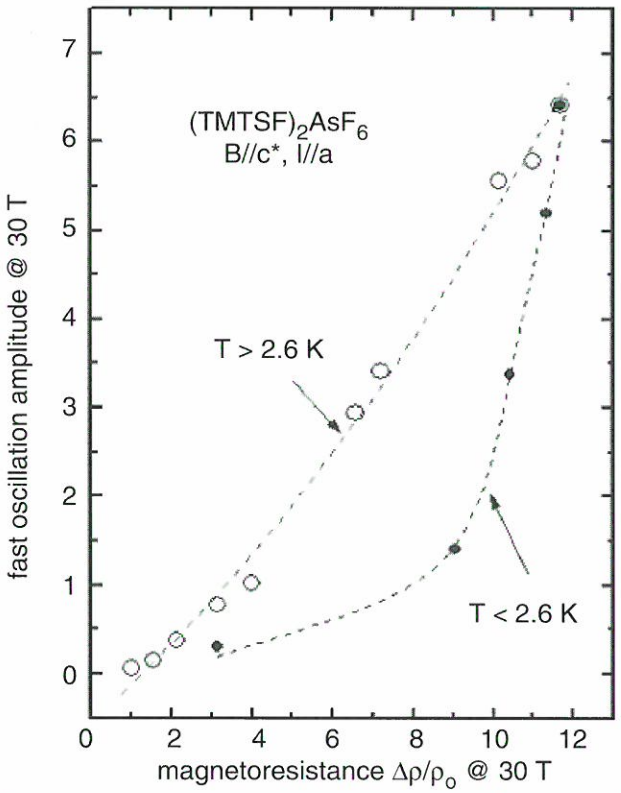

Figure 2. Correlation between FO amplitude and background magnetoresistance in $X = A_{sF6}$.

References:

1 Naughton, M.J., *et al.*, in Proc. Int. Conf. Synthetic Metals, Snowbird, Utah, July 1996; to be published in Synth. Metals.

2 Gor'kov, L.P., *et al.*, Phys. Rev., **B51**, 1362 (1995).

3 Machida, K., *et al.*, Phys. Rev., **B51,** 8946 (1995); **B53**, 5461 (1996).

4 Yan, X., *et al.*, Synth. Metals, **27**, B145, (1988).

Magneto Thermoelectric Power of Synthetic Metals and High T_c Superconductors

Park, Y.W., Seoul National Univ., Physics, Korea
Song, Y.S., Seoul National Univ., Physics, Korea
Choi, E.S., Seoul National Univ., Physics, Korea

We have measured the temperature dependent thermoelectric power (TEP) of doped polyacetylene (PA) under the high magnetic field up to 20 tesla (T). The dopants are I_2, $FeCl_3$, $AuCl_3$ and $NbCl_5$. At H = 20 T, both iodine and metal halide doped PA show an abrupt decrease of 1~2 μV/K in TEP

at T~70 K. In the low temperature region, the $\Delta S(T)=S(T, H=20T)-S(T,H=0T)$ of metal-halide doped PA becomes more negative and the minimum peak of TEP shifts slightly to higher temperature. For the iodine doped PA, the S(T,H=20T) remains quasi-linear as a function of temperature down to 4.2 K. Since no appreciable amount of anisotropy of the stretch oriented PA with respect to the applied magnetic field direction is observed in S(T,H) and ρ(T,H) and furthermore, because of the significant difference of S(T,H) between the iodine doped PA and the metal-halide doped ones, the spin-spin interaction between the conduction electron spin in the metallic PA chain and the localized spin in the metal-halide dopant located nearby the polymer chain could be the prime origin of the observed magneto TEP phenomena.

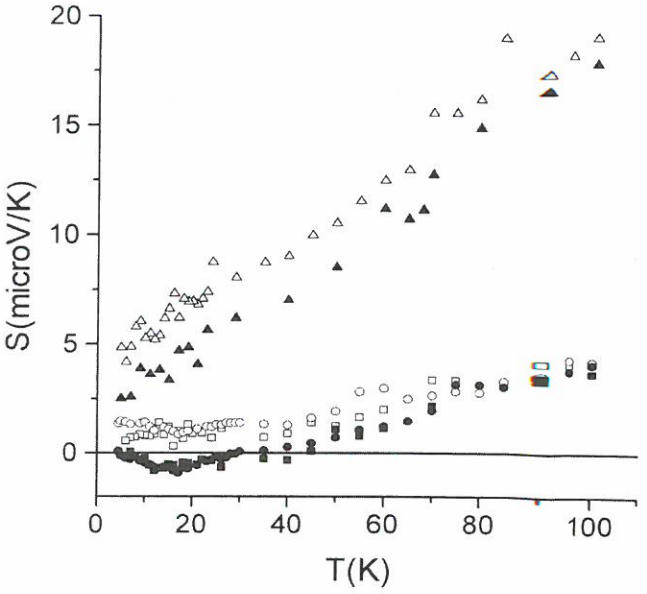

Figure 1. Magneto TEP as a function of temperature, S(T,H=20T) for I_2(▲,σ_{RT}=5495S/cm), $AuCl_3$(●,σ_{RT} = 2599 S/cm) and $FeCl_3$ (■, σ_{RT}=8900S/cm) doped PA. Unfilled symbols are the zero field TEP data, S(T,H=0T) of each sample.

Observation via Magnetization of the Field-Induced Insulator-Metal Transition in the Ferrous Molecular Conductor λ-(BEDT-TSF)$_2$FeCl$_4$

Petrov, D.K., SUNY Buffalo, Physics
Naughton, M.J., SUNY Buffalo, Physics, and NHMFL
Laukhin, V.N., CSIC Barcelona
Kobayashi, H., Institute for Molecular Science, Okazaki
Kobayashi, A., Univ. of Tokyo, Chemistry

The title compound offers an unique opportunity to study interactions between extended π-metal electrons and localized magnetic moments in low dimensional molecular conductors.[1] We have performed magnetization measurements to 30 T and 1.3 K in this "organic Kondo system." It is known that at 8 K the material undergoes a metal-insulator transition. In an applied magnetic field (in any direction with respect to the crystallographic axes), this transition is suppressed,[2] with the metallic state reappearing above 10 T at 1 K. In a similar compound with non-magnetic anions ($GaCl_4$) the system enters a superconducting state below 8 K.

Using silicon cantilever magnetometry, we have studied the isotropic magnetization vs. field in λ-(BETS)$_2$FeCl$_4$ and have found that an observed positive and hysteretic jump in M(H) matches perfectly the insulator-to-metal transition defined from resistive data. We interpret the hysteresis as signifying the first order nature of the transition. Measurements were performed on several needle-like crystals aligned parallel to each other but randomly oriented in the transverse direction and attached with grease to the cantilever. A magnetic field gradient was created by a small axial displacement of the device from the field center of the Bitter magnet. The detected moment had anisotropic and isotropic components, providing force and torque terms. The isotropic force term was then isolated. We were unable to quantify the anisotropic term, due to the lack of precise knowledge of the perpendicular alignment of the multi-single crystal specimen. The magnitude of

the jump in the isotropic magnetic moment is ~10^{-10} Am^2 (10^{-7} emu), or around 10 emu/mole. We show in Figure 1 a portion of a field sweep in the vicinity of the transition, which shows the jump at 1.38 K.

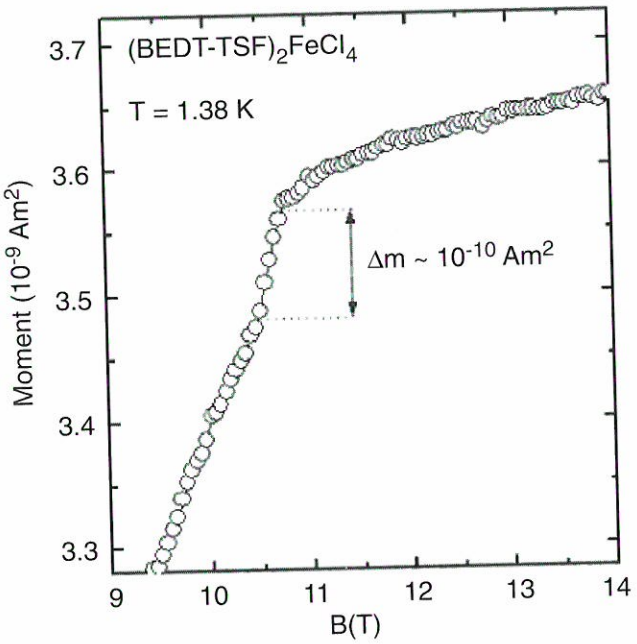

Figure 1. Magnetization of λ-$(BETS)_2FeCl_4$ at 1.38 K, with the jump at 10.6 T signifying the insulator-metal transition.

One possible scenario is that the system exhibits a metamagnetic transition. This is a field-induced transition from an antiferromagnetic ordered state to a ferromagnetic state. In our case, the field-induced transition is accompanied by a several orders of magnitude decrease in the resistance (i.e. back the metal phase). If the transition is metamagnetic, there should exist a second phase boundary in (B,T) space, separating the high temperature nonmagnetic metal from the high field, low temperature ferromagnetic. Such a line is yet to be found. Further studies on individual single crystals throughout the entire phase space 0-33 T, 0.05-20 K should help to clarify this situation. Also, studies on partially substituted (Ga for Fe) are desirable, to reduce antiferromagnetic interactions and thus the transition field.

References:

1 Kobayashi, H., *et al.*, Chem. Lett., 2179 (1993).

2 Goze, F. *et al.*, Europhys. Lett., **28**, 427 (1994).

High-Field Studies of the De Haas-Van Alphen Effect in the Quasi-Two-Dimensional Organic Metals α-$(BEDT\text{-}TTF)_2MHg(SCN)_4$, M=K, NH_4

Sandhu, P.S., NHMFL/FSU, Physics
Qualls, J.S., NHMFL/FSU, Physics
Brooks, J.S., NHMFL/FSU, Physics
Tokumoto, M., ETL, Japan
Kinoshita, N., ETL, Japan
Kinoshita, T., ETL, Japan
Tanaka, Y., ETL, Japan

We have studied the de Haas-van Alphen (dHvA) effect in the quasi-two-dimensional organic metals α-$(BEDT\text{-}TTF)_2MHg(SCN)_4$, M=K, NH_4 at high magnetic fields (B) up to 33 T and temperatures (T) down to 0.4 K. At these high values of B/T, the dHvA oscillations show small but appreciable deviations from the standard Lifshitz-Kosevich theory applicable to systems with a 3D FS. We analyze the field and temperature dependence and lineshape of the dHvA oscillations and compare them with recent theoretical predictions for systems with quasi-two-dimensional (2D) Fermi surfaces (FS). By comparing with model calculations for a system whose FS consists of both 2D (warped cylinder) and 1D (sheets) sections, it is possible to extract some of the band parameters and confirm the low-dimensional character of these organic charge transfer salts.

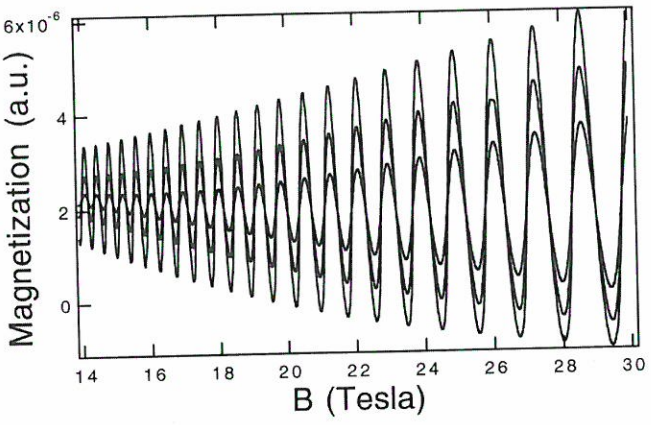

Figure 1. Magnetization of α-$(BEDT\text{-}TTF)_2NH_4Hg(SCN)_4$ at three different temperatures: 0.5, 1.2, and 1.8 K.

The De Haas-Van Alphen Effect in Quasi-Two-Dimensional Organic Metals with Magnetic Breakdown

Sandhu, P.S., NHMFL
Brooks, J.S., NHMFL
Kim, J.H., Univ. of North Dakota, Physics

We present a quantum mechanical model for the de Haas-van Alphen (dHvA) effect in quasi-two-dimensional organic metals such as α-(BEDT-TTF)$_2$KHg(SCN)$_4$ and κ-(BEDT-TTF)$_2$Cu(NCS)$_2$ where magnetic breakdown behavior can occur. We include the realistic band structure for these systems by using a tight-binding Hamiltonian, which has been obtained from previous studies of electronic structure based on the extended Huckel approximation.[1] In this approach, the two Fermi surfaces that are needed to describe the magnetic breakdown behavior arise naturally. We diagonalize the tight-binding Hamiltonian numerically as a function of magnetic field to obtain the field dependent energy spectrum. We then compute the chemical potential and magnetization curves as a function of magnetic field to describe the dHvA spectrum for these materials and discuss a possible origin of the anomalous frequencies that arise as a result of the magnetic breakdown.

References:

1 Campos, C.E., *et al.*, Phys. Rev. B, **53**, 12725 (1996).

2 Sandhu, P.S., *et al.*, (in press) Synthetic Metals, Proceedings of the 13th International Conference on the Science and Technology of Metals, Snowbird, Utah. (1996)

Magnetocaloric Investigation of the High Field Phase Diagram of (TMTSF)$_2$ClO$_4$

Scheven, U.M., Princeton Univ., Physics
Chaikin, P.M., Princeton Univ., Physics
Immer, C.D., NHMFL
Hannahs, S.T., NHMFL

We used AC calorimetry to measure the magnetocaloric effect (change of temperature on adiabatic application of magnetic field) and the specific heat of (TMTSF)$_2$ClO$_4$ from 0 to 30 tesla and 1.5 to 7 K. The idea was to establish the phase diagram that had previously been reported from transport and magnetization measurements. Of particular importance was the controversial discovery of a new phase boundary at 5.5 K and almost independent of field for H > 10 T, and a first order transition line that terminates in a critical point under this phase boundary. Two different cooling rates were used on the sample, to study the effect of an anion ordering transition that controls the low temperature mean free path. Aside from the phase transitions, the magnetocaloric effect also exhibited strong oscillation at the "fast oscillation" frequency. The fast oscillations are usually associated with the magnetic breakdown of the gap formed by the anion ordering transition. It was therefore interesting to see that in the quickly cooled samples the oscillations disappeared (but the phase transitions remained). Quick cooling limits the extent of the anion ordering transition. The main features of the phase diagram were apparent in these calorimetric measurements, proving that they correspond to true phase transitions. The 5.5 K transition and the 1st order line from 1 K 27 T to 3.5 K 20 T were consistent with the data from the field sweeps at different temperatures. A new discovery, however, was that this 1st order phase boundary itself oscillates at the frequency of the fast oscillations, as had been theoretically predicted.

Low Dimensional Metals at High Fields and Low Temperatures

Tessema, G.X., Clemson Univ., Physics
Kuh, J., Clemson Univ., Physics
Mengistu, E.H., Clemson Univ., Physics
Skove, M.J., Clemson Univ., Physics
Mielke, C.H., NHMFL/LANL
Lacerda, A., NHMFL/LANL
Safar, H., Univ. of Illinois at Chicago, Physics

The quasi-one-dimensional compound $Tl_2Mo_6Se_6$ is remarkable among the family $M_2Mo_6X_6$ (M = IA, and IIIA elements, and X = Se, Te) of compounds. In addition to the coexistence of superconductivity and a density-wave instability,

its H_{c2} exhibits a positive curvature below 100 mK range up to 17 T.[1] The material provides an excellent potential for testing theoretical prediction concerning reentrant superconductivity under very high H field.[2] We conducted a series of measurements of the magnetoresistance above 500 mK with the ultimate objective to study the lower temperature behavior of H_{c2} up to 50 T at lower temperatures, < 100 mK.

In general, there are two types of $Tl_2Mo_6Se_6$ samples based on their low temperature R vs. T behavior above T_c. Type-A samples are metallic down to T_c, whereas type-B samples exhibit a slight resistance upturn just above T_c = 6.3 K. In type-B samples, above H_{c2}, we observed two regimes: (1) $H_{c2} < H < 20$ T, (2) and H > 20 T. Such a distinction is not apparent in type-A samples.

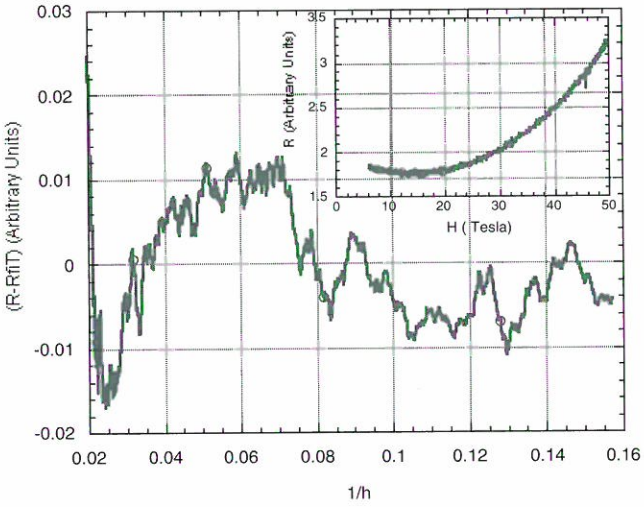

Figure 1. A plot of $\{R(H)-R_m\}$, where R_m results from a polynomial fit to the R vs. H data above 5 T shown in the inset.

In the first regime, the resistance of type-B samples decreases linearly with H. R(H) as well as the magnitude of dR/dH decrease when the current across the sample increases. A quadratic behavior is observed in the second regime. These results confirm previous speculations that a density wave coexists with superconductivity in this material,[1] and that the density wave can be depinned and carry excess current.[1,3] At high currents, when the conductivity of the density wave reaches its maximum conductivity, the negative dR/dH is completely suppressed and the sample behaves like a type-A sample with a monotonic increase in R with H. The negative dR/dH and H induced suppression of R could be due to field induced suppression of spin density wave as in some organic conductors.[4] Also after careful subtraction of a polynomial fit to the background magnetoresistance, we observed very low amplitude oscillations in the resistance of both type of samples. We have indexed the oscillations with the highest amplitude. Figure 2 shows a plot of n vs. 1/H, which gives a frequency of oscillation of the F = 95 T. A similar indexing of the minimum gives 90 T. Assuming a spherical fermi surface, we estimate the low temperature carrier density to be of the order of 3 $x10^{19}/cm^3$. This concentration is smaller than the concentration of $n = 1.7x10^{20}/cm^3$ estimated from the low temperature Hall effect data.[1] Given the fact that we only considered one surface and a spherical approximation, however, this result is not inconsistent with the Hall data.

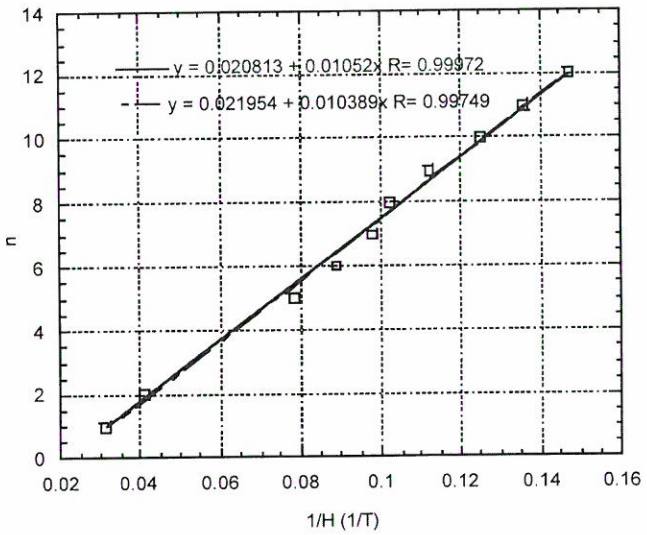

Figure 2. 1/H corresponds to the maxima in R vs. 1/H, n is the corresponding integer.

Partial support for this work has been provided by the NSF, grant No. DMR-9208333.

References:

1 Brusetti, R., *et al*, Phys. Rev. B., **49**, 8931 (1994-I).

2 Rasolt, *et al.*, Rev. of Mod. Physics, **64**, No3, (1992).

3 Tessema, G.X., *et al.*, Phys. Rev. B., **43**, 3434, (1991).

4 McKenzie, R.H, *et al.*, Surface Science, **361/362**, 901 (1996), also Proceedings of 11th International Conference on the Electronic Properties of Two Dimensional Systems.

Anomalous Quantum Oscillation Behavior in the Bechgaard Salts $(TMTSF)_2X$. I. X = PF_6

Uji, S., NRIM, Tsukuba, Japan
Brooks, J.S., FSU, Physics/NHMFL
Chaparala, M.V., NHMFL
Takasaki, S., Himeji Institute of Technology, Japan
Yamada, J., Himeji Institute of Technology, Japan
Anzai, H., Himeji Institute of Technology, Japan

In the quasi-one dimensional organic conductors (TMTSF)2X (where X = ClO_4 or PF_6) anomalous magneto-quantum oscillation behavior is observed, the so-called rapid oscillations or RO. Their origin is unusual in that the underlying Fermi surface for these materials is essentially one dimensional in nature, and at first glance cannot support the kind of periodic (in inverse magnetic field) magnetoresistance (SdH) or magnetization (dHvA) oscillations that are observed.

To better understand the mechanisms that give rise to this behavior, we have undertaken systematic studies of the anisotropic magnetoresistance, Hall, and magnetization (by cantilever) over a broad range of temperature and magnetic field. In particular, we have investigated the correlation between the rapid oscillation (RO) behavior and the spin-density-wave (SDW) formation. In both cases the results are non-trivial in nature due to the complexity of their respective ground states. This is due to several important differences between the two materials that are crucial to our interpretation of the results. In the case of $(TMTSF)_2PF_6$ the SDW forms under ambient conditions below 12 K, whereas for $(TMTSF)_2ClO_4$ (see Part II.) the SDW state is magnetic field induced (FISDW) above a threshold field B(T). Secondly, in the case of $(TMTSF)_2PF_6$, below 12 K, the Fermi surface exists as two imperfectly nested open orbit sheets. See Figure 1. For $(TMTSF)_2ClO_4$, the low temperature metallic/superconducting state results from an anion ordering transition at 24 K, which doubles the unit cell along the b-axis, resulting in four un-nested open orbit sheets. Here it takes a magnetic field along the c-axis to induce nesting above a threshold field.

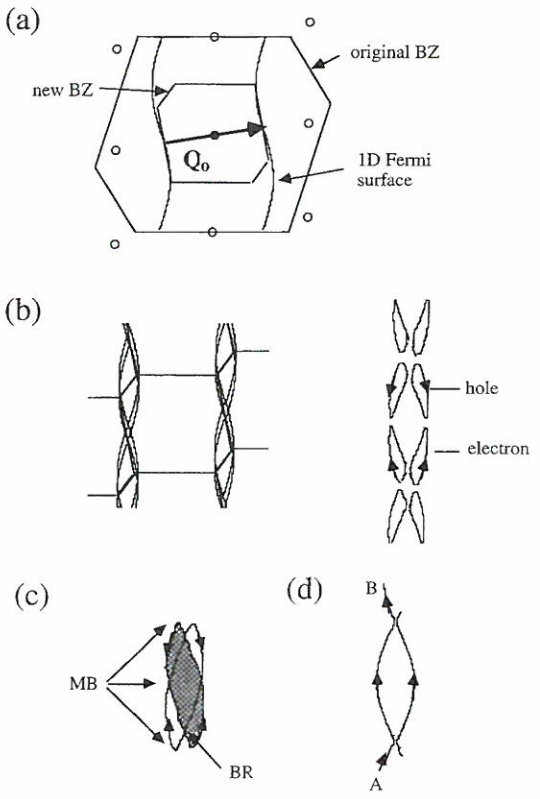

Figure 1. (a) Reconstructed Fermi surface. (b) Electron and hole pockets that result from imperfect nesting. (c) Magnetic breakdown orbits between pockets that lead to RO. (d) Resulting effective closed orbit area.

In the case of $(TMTSF)_2PF_6$ we observe from temperature dependent transport that the material does not become a complete insulator at the lowest temperature studied, that the RO behavior remains, but with a non-monotonic dependence of the amplitude on temperature, and that the transition temperature T_{SDW} increases quadratically with field. Resistance and magnetic torque for $(TMTSF)_2PF_6$ were measured over wide magnetic field and temperature ranges. RO with frequency (~220 T) is observed in the resistance above 15 T for all current directions (a, b, or c-axes), and in Hall resistance (ab-plane) in the SDW phase. The

temperature dependence of the RO amplitude has a sharp peak around 3 K (T_{max}) (see Figure 2), which is associated with a maximum of the normalized magnetoresistance. The magnetic torque shows a jump at the SDW transition temperature (~11.5 K) with decreasing temperature, and then a broad maximum around T_{max} suggesting a sub-phase transition. T_{max} slightly shifts to a high temperature with increasing magnetic field. From these measurements we may conclude that the rapid oscillations result from nearly compensated electron and hole pockets in the imperfectly nested Fermi surface (see Figure 1), but that at the fields where the oscillations are observable, it is the magnetic breakdown between these orbits that gives rise to the observed frequency.

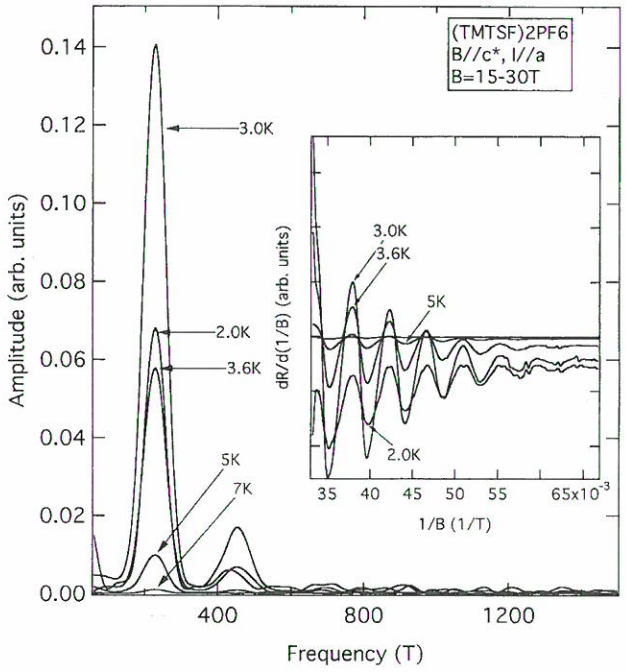

Figure 2. Non monotonic temperature dependence of RO amplitudes from FFT analysis. Inset, oscillatory magnetoresistance vs. 1/B.

Anomalous Quantum Oscillation Behavior in the Bechgaard Salts $(TMTSF)_2X$. II. X = ClO_4

Uji, S., NRIM, Tsukuba, Japan
Brooks, J.S., FSU, Physics/NHMFL
Chaparala, M.V., NHMFL
Takasaki, S., Himeji Institute of Technology, Japan
Yamada, J., Himeji Institute of Technology, Japan
Anzai, H., Himeji Institute of Technology, Japan

For $(TMTSF)_2ClO_4$, the low temperature metallic/superconducting state results from an anion ordering transition at 24 K that doubles the unit cell along the b-axis, resulting in four un-nested open orbit sheets. Here it takes a magnetic field along the c-axis to induce nesting above a threshold field. In $(TMTSF)_2PF_6$ the nesting occurs under ambient conditions below 12 K, and the change in the electronic structure is the nesting of the original open orbit sheets of the Fermi surface.

Unlike $(TMTSF)_2PF_6$, the case of $(TMTSF)_2ClO_4$ is more complex in that there are four open orbits in the Fermi surface at low temperatures. In the metallic state we have recently established that the observed RO behavior is of a Stark interference mechanism. Also at very high (pulsed) fields we find that the oscillations are from MB closed orbit effects. In the field induced spin density wave (FISDW) phase, however, we find from magnetization and transport studies that there are two different kinds of RO oscillations, RO-I and RO-II (see Figure 1) with the following distinctions. RO-I appears when the FISDW state is entered, but the amplitude has a maximum around 2 K, and then vanishes at lower temperatures. RO-II becomes apparent below about 4 K, and its amplitude increases with decreasing temperature. The two RO wave forms are 180 degrees out of phase. We may ascribe the RO-II as a result of MB orbits in the high field limiting SDW phase, as observed in the pulsed field studies. The RO-I oscillations, however, seem specific to a different Fermi surface configuration, and hence it is possible that two SDW phases (nesting configurations) co-

exist. Given that there are four Fermi surface sheets involved, this is not unreasonable. The SDW phase and behavior associated with RO-I follows most closely that of the RO behavior in $(TMTSF)_2PF_6$ discussed above.

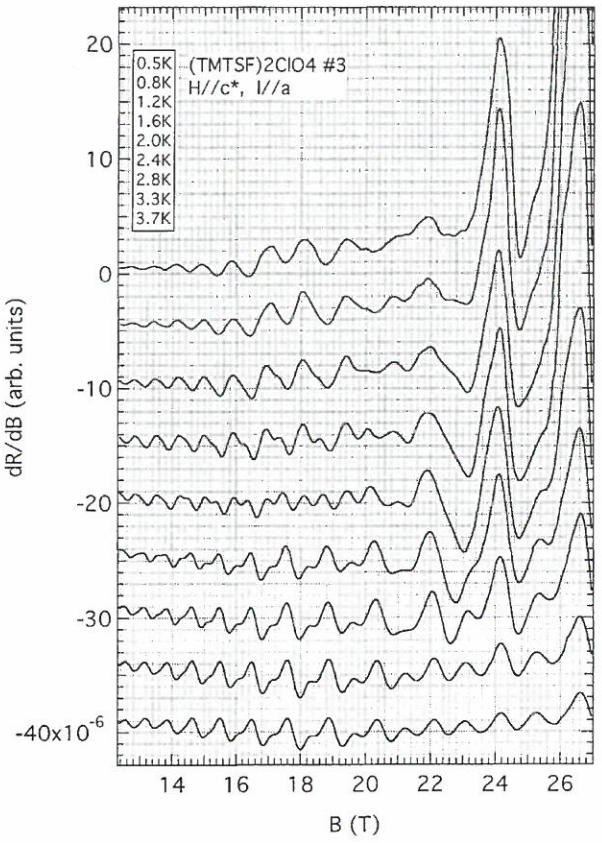

Figure 1. Oscillatory magnetoresistance for different temperatures. Two distinct sets of oscillations with different temperature dependences are observed.

High Field NMR on ^{77}Se in the Spin Density Wave State of $(TMTSF)_2PF_6$

Valfells, S., Boston Univ., Physics
Brooks, J.S., FSU, Physics/NHMFL
Kuhns, P.L., FSU, Physics/NHMFL
Moulton, W.G., FSU, Physics/NHMFL
Takasaki, S., Himeji Institute of Technology, Japan
Yamada, J., Himeji Institute of Technology, Japan
Anzai, H., Himeji Institute of Technology, Japan

In the quasi-one dimensional organic conductor $(TMTSF)_2PF_6$ a spin density wave state (SDW) forms under ambient conditions below 12 K. We observe from temperature dependent transport, and the observation of magneto-quantum oscillation behavior, that the material does not become a complete insulator at the lowest temperature studied. We further note that below about 4 K there are however, features in the transport and quantum oscillation behavior that indicate a second transition, or at least some rearrangement of electronic structure.

The purpose of this study was to investigate, via NMR, the relaxation behavior of the ^{77}Se nucleus, which lies near the center of the TMTSF molecular orbital. This position is most sensitive to the formation of the SDW phase, and to any changes in the behavior of the local moment that result from the antiferromagnetic ground state. Although there have been many proton (^1H) and even ^{77}Se NMR studies of TMTSF-related materials, this was the first very high field study of the SDW ground state of the title material. The NMR coil system used is shown in Figure 1. The experiments were carried out in the NHMFL high homogeneity 24 T magnet with a standard NMR spectrometer.

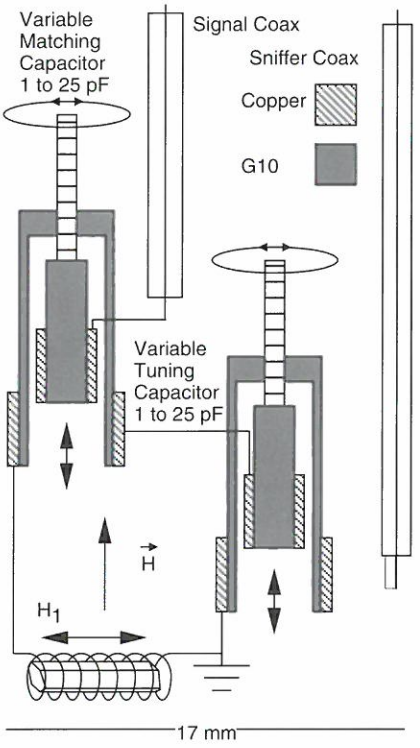

Figure 1. NMR coil system used to investigate the relaxation behavior of ^{77}Se nucleus.

In Figure 2 we show the inverse spin relaxation time over the entire range of the measurements. As the temperature is lowered, we note the following: (1) above 12 K the material is metallic; (2) as the transition temperature is reached, critical behavior is observed in a narrow range of temperature; (3) below 12 K the material again appears metallic, but with a reduced density of states; and (4) at 4 K and below the relaxation rate appears to be activated.

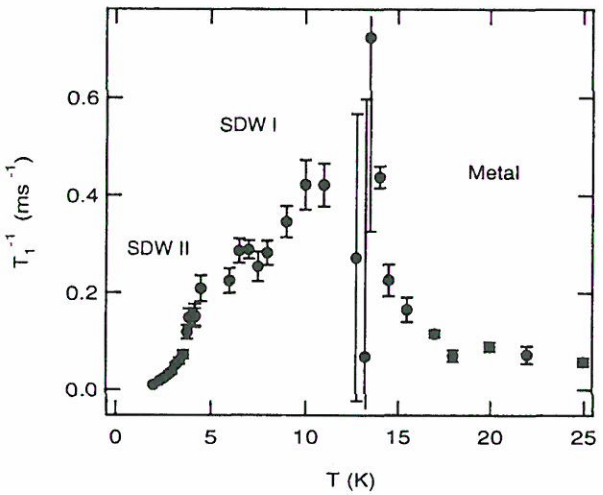

Figure 2. Inverse spin relaxation time over the range of the measurements.

Our interpretation of these results is as follows. The metallic and critical behavior above and near 12 K is as might be expected for a metal to SDW transition. The survival of "Korringa-like" behavior below 12 K, however, where the SDW state has formed, is at first surprising. Two factors come into play. The first is that the SDW gap does not extend over the entire Fermi surface, so that metallic (conduction electron) relaxation still operates. The second is that spin (phason) relaxation, which one might expect in the SDW phase, has the same temperature dependence as the Korringa law. Hence at this point, without doing a detailed frequency dependent study in this temperature regime, we cannot discriminate between the two mechanisms. Finally, below 4 K, the activated nature of the relaxation rate is most likely related to the onset of a more complete SDW gap. A picture where thermally-activated carriers cause relaxation gives reasonable agreement with the data. This picture would further substantiate the notion that conduction, and not phason, mechanisms dominate between 12 K and 4 K.

Semiconductors

Fractional Quantum Hall Effect in High Mobility AlGaAs/GaAs Heterostructures Grown by MOCVD

Du, R.R., Univ. of Utah, Physics
Zudov, M.A., Univ. of Utah, Physics
Simmons, J.A., Sandia National Labs
Chui, H.C., Sandia National Labs
Harff, N.E., Sandia National Labs
Hammons, B.E., Sandia National Labs

Previously, high quality data of the fractional quantum Hall effect (FQHE) was accessible only from the two-dimensional electron system in MBE-grown heterostructures. Sandia National Labs has recently succeeded in MOCVD growth of GaAs-AlGaAs heterostructures exhibiting high resolution FQHE states.[1] The new material has achieved mobilities up to 2×10^6 cm^2/Vs, the highest obtained to date by MOCVD.

Because MOCVD material parameters such as impurity potential profile, defect density, uniformity, and interface quality, are possibly different from MBE, it is worthwhile to examine the magnetotransport behavior in these materials. In particular, we have studied the FQHE states near Landau level filling factor $\nu = 3/2$ in tilted magnetic fields. Measurements were performed in the top-loading Oxford 20 mK/20 T ^{3}He-^{4}He mixture dilution refrigerator at the NHMFL.

In a sample having density 2.8×10^{11}/cm^2, we measured the magnetoresistance R_{xx} around $\nu = 3/2$ in a total magnetic field B_{tot} applied at an angle θ from normal, at 50 mK. Figure 1 shows R_{xx} vs. perpendicular field $B_\perp$ between $\nu = 1$ and $\nu = 2$ for several θ, with the positions of the $\nu=(3p\pm2)/(2p\pm1)$ FQHE states indicated. As θ is increased, the minima associated with these ν disappear and then reappear, as particularly evident for $\nu = 4/3$. Similar oscillatory behavior is observed for 7/5, 8/5, and 11/7; however, 5/3 remains a strong minimum for all θ.[2]

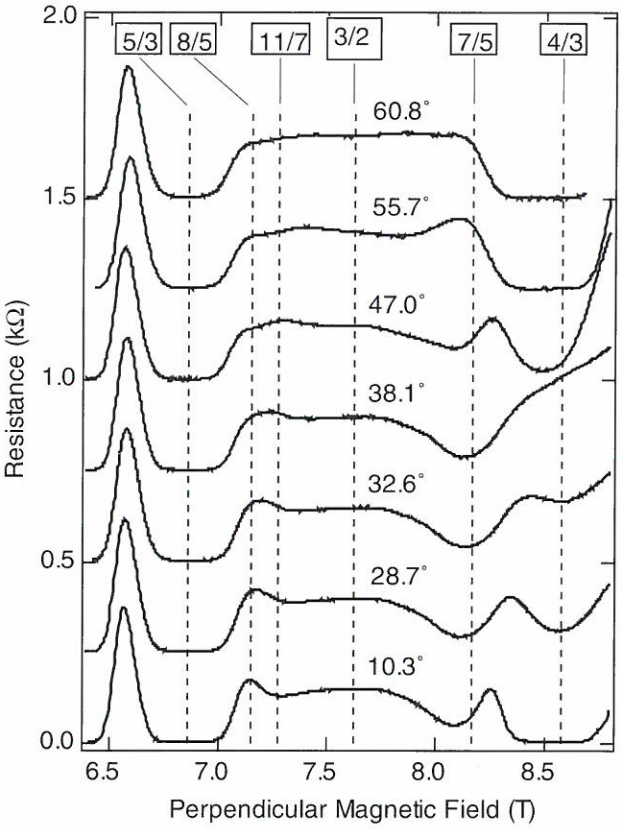

Figure 1. R_{xx} vs. perpendicular magnetic field $\mathbf{B}_\perp$ for several different tilt angles θ.

The data is in agreement with a spin-split composite fermion (CF) model,[3] based on which the complex R_{xx} behavior can be understood as resulting from a sequence of level coincidences as the Zeeman energy is increased by tilted fields. Our results reported here from the high density samples around $\nu = 3/2$ conform to the similar spin-split CF level scheme proposed earlier for low-density MBE samples.

References:

1 Chui, H.C., *et al.*, Appl. Phys. Lett., **68**, 208 (1996).

2 Simmons, J.A., *et al.*, *Proceedings of the 23rd International Conference on the Physics of Semiconductors*, Berlin, 1996, eds. Scheffler, M. and Zimmerman, R., Vol. 3, p. 2511 (World Scientific, Singapore, 1996).

3 Du, R.R., *et al.*, Phys. Rev. Lett., **75**, 3926 (1995).

Magneto-Transport Investigation of $Al_xGa_{1-x}As/In_yGa_{1-y}As$ and $In_xAl_{1-x}As/In_yGa_{1-y}As$ Quantum Wells

Dunford, R.B., City College of CUNY, Physics, and NHMFL

Popovic, D., City College of CUNY, Physics, and NHMFL

Pollak, F.H., Brooklyn College of CUNY, Physics

Wojtowicz, M., TRW, Electronics and Technology Division

Streit, D.C., TRW, Electronics and Technology Division

Considerable research effort is currently being devoted to novel modulation-doped InGaAs-based structures, both for their fundamental physics and for device applications. The $Al_x Ga_{1-x} As/In_y Ga_{1-y}As/GaAs$ structure has been rapidly gaining in importance for a wide range of microwave-related applications. More recently, the $In_xAl_{1-x}As/In_yGa_{1-y}As$ structure has been developed and is expected to be useful for high-speed power devices. Magneto-transport measurements of new materials with a different scale of electron-electron interactions may reveal new phenomena. Additionally, magneto-transport measurements can determine such device parameters as the single particle relaxation time, carrier density and effective mass, which can be used to optimize device performance. We report a study of both $Al_x Ga_{1-x}As/In_yGa_{1-y}As$ and $In_xAl_{1-x}As/In_yGa_{1-y}As$ quantum wells (QWs) using standard low frequency AC transport techniques and perpendicular fields up to 17 T for the temperature ranges 30 mK to 600 mK and 1.8 K to 200 K.

The composition of the high density $Al_{0.2}Ga_{0.8}As/In_{0.2}Ga_{0.8}As/GaAs$ QW has been described elsewhere.[1] The first subband only was occupied and the sample exhibited the integer quantum Hall effect at even integer filling factors $\nu = 4, 6,.., 44$. At 30 mK, the dark sample density was $1.35 \times 10^{12}cm^{-2}$, which increased to $1.76 \times 10^{12}cm^{-2}$ upon illumination with a LED. These data were in reasonable agreement with the value of $(1.9\pm0.2) \times 10^{12}cm^{-2}$ (at 17 K) obtained using a contactless photoreflectance technique.[2]

A typical high density $In_xAl_{1-x}As/In_yGa_{1-y}As$ QW consisted of the following layers: an InP substrate, a 300 nm $In_{0.52}Al_{0.48}As$ layer, a 15 nm $In_{0.65}Ga_{0.35}As$ channel, and a 53 nm $In_{0.52}Al_{0.48}As$ supply layer (δ-doped 3 nm from the interface). The Fourier transform of the longitudinal resistivity reveals that there are at least two occupied subbands with typical carrier densities of 2.3 and 0.8 x $10^{12}cm^{-2}$. The sample density obtained from the Hall resistivity ($3.2 \times 10^{12}cm^{-2}$) is consistent with the sum of the individual subband densities obtained from the longitudinal resistivity (Figure 1). An $In_{0.52}Al_{0.48}As/In_{0.53}Ga_{0.47}As$ device with asymmetric double-sided doping also showed multiple subband occupation. Illumination with an LED had no effect on the device properties. The importance of band nonparabolicity in $In_xAl_{1-x}As/In_yGa_{1-y}As$ quantum wells will be determined by calculating the effective masses of the electrons in each subband.

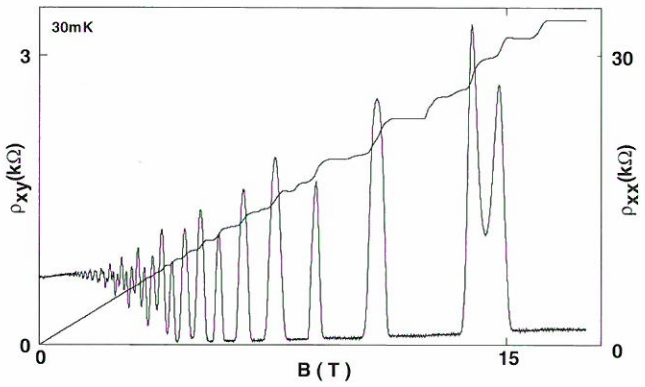

Figure 1. Longitudinal (ρ_{xx}) and Hall (ρ_{xy}) resistivity for an $In_{0.52}Al_{0.48}As$ / $In_{0.65}Ga_{0.35}As$ QW.

This research was supported by a CUNY Collaborative Incentive Grant and PSC-CUNY Research Award Program. The work was performed at NHMFL, which is supported by NSF Cooperative Agreement No. DMR 9527035.

References:

1 Yin, Y., *et al.*, Semicond. Sci. Technol., **8**, 1599 (1993).

2 Gumbs, G., *et al.*, Phys. Rev. B., **48**, 18328 (1993).

Magnetotransport in GaN and Related Alloys

Geerts, W., UF, Materials Science Engineering/ NHMFL
MacKenzie, J.D., UF Materials Science Engineering
Abernathy, C.R., UF, Materials Science Engineering
Pearton, S.J., UF, Material Science Engineering
Schmiedel, T., NHMFL

Variable temperature (1.7 to 400 K) and field (0 to 30 T) Hall measurements were employed to study carrier transport phenomena in p-type GaN(C) and n-type InN and InGaN. All three materials show metallic conduction which in the p-type GaN is due to compensated carbon-related acceptors and in the InN and InGaN due to intrinsic shallow donors. The InGaN shows a negative magnetoresistance over the complete temperature range investigated. From fits to the experimental data we calculated an activation energy of 25 meV for carbon in GaN, which is consistent with recent density functional theory and suggests that under optimized growth conditions carbon may be an effective acceptor dopant in GaN, potentially overcoming the difficulty of the deep ionization energy of the currently used p-dopant, namely Mg. In InGaN there was strong evidence for the presence of two-band conduction. Using the magnetic field dependence of the magnetoresistance and the extrapolated Curie temperature, we obtained the average magnetic moment as 16 μb, which is a similar order of magnitude to that in other semiconductors. For both InN and InGaN the impurity band was found to be merged with the conduction band.

Quantum Properties of Electrons in Spatially Varying Magnetic Fields

Hu, J., NHMFL
Schrieffer, J.R., NHMFL/FSU, Physics

We studied the two dimensional electron gas in spatially varying magnetic fields.

1) The magnetic field has the form $\vec{B} = (0, 0, B_1 x)$

The single-particle electronic structure of two dimensional electron gas in this field corresponds to a quartic oscillator with the effective potential $V(x)$ exhibiting a single minimum and double minimum for positive and negative momentum in y direction respectively. For large negative k_y, the low energy levels occur in pairs, split by weak tunneling between Landau-like states centered on either side of x = 0. For small negative k_y, the tunneling between two wells is not small and gives non trivial energy spectrum of $E_n(k_y)$ which in turn shows an interesting density of states. The conductivities σ_{yy} and σ_{xx} are calculated in the relaxation time approximation with electron spin included. DC conductivities have oscillatory behavior due to the density of states near the $k_y = 0$ region. The non-zero σ_{xx} is due to the electron spin.

2) The magnetic field has the form $\vec{B} = (0, 0, B_o + B_1 \cos(Qx))$.

In the Landau gauge, the effective single particle potential is given by

$$V(x) = \frac{\hbar^2 Q^2}{2m}\left(\frac{k_y}{Q} + \frac{Qx}{(Q\ell_o)^2} + \frac{\sin(Qx)}{(Q\ell_1)^2}\right)^2$$

where $Q = 2\pi/a, \ell_o^2 = \hbar/eB_o$ *and* $\ell_1^2 = \hbar/eB_1$. Energy spectra are calculated numerically exactly for both $B_o = 0$ *and* $B_o \neq 0$ cases. The spectrum forms a magnetic band structure when $B_o = 0$, and the energy of each Landau level is a periodic function of k_y with period a/ℓ_o^2 when $B_o \neq 0$. The optical conductivity $\sigma_{xx}(\omega)$ is calculated as a function of B_o, B_1 *and* Q. The electron spin is considered in the case $B_o \neq 0$.

Evidence for a Spin Transition in the ν=2/5 Fractional Quantum Hall Effect

Kang, W., Univ. of Chicago, Physics
Young, J.B., Univ. of Chicago, Physics
Hannahs, S.T., NHMFL
Palm, E., NHMFL
Campman, K., Univ. of California, Santa Barbara, Elect. and Comp. Eng.
Gossard, A., Univ. of California, Santa Barbara, Elect. and Comp. Eng.

We have studied the effects of hydrostatic pressure on a high-quality, two-dimensional electron system in high magnetic field. Application of large hydrostatic pressure has been shown to decrease the Lande g-factor in semiconductors.[1] Because of its relatively modest g-factor ($g = -0.44$) in GaAs, it may be possible to minimize the magnitude of the g-factor and thereby quench the Zeeman energy, $g\mu_B$, in high magnetic field. We have presently made magnetotransport study of a two-dimensional electron system up to 14 kbar of pressure, up to 20 tesla of magnetic field, and down to 30 millikelvin in temperature.[2]

The ν=2/5 and 3/7 fractional quantum Hall effect are found to gradually collapse and then subsequently reappear with increasing pressure. At pressures slightly above the critical pressure necessary for the collapse, suppression of the ν=2/5 fractional quantum Hall effect may be induced by tilting the sample relative to the external magnetic field. These results imply a transition from a spin-polarized ground state at low pressures to a spin-unpolarized one at high pressures that arises from the application of hydrostatic pressure on the GaAs/GaAlAs heterostructure.

References:

1 Morawicz, N.G., *et al.*, Phys. Rev. B, **41**, 12687 (1990).

2 Kang, W., *et al.*, to be published.

Optical Shubnikov De-Haas Oscillations of a Modulation-Doped $Al_{0.3}Ga_{0.7}As$/GaAs Single Heterojunction

Kim, Y., NHMFL/LANL
Perry, C.H., NHMFL/LANL and Northeastern Univ., Physics
Rickel, D.G., NHMFL/LANL
Lee, K.-S., Electronics and Telecommunications Research Institute, Korea

The carrier concentration of a modulation-doped single heterojunction is sensitive to the external excitation conditions. Excitation energies larger than the band gap cause photo-created electrons from both the valence band and from un-ionized donors to move into the quantum well region. Consequently, the electron density in the quantum well can be changed significantly and can be controlled by the excitation energy power level.

We have measured Shubnikov de-Haas (SdH) oscillations of a modulation-doped single heterojunction with and without illuminating laser light. From the SdH oscillations, we found that in the dark, the sample initially has one occupied subband (E1) with an electron density of 3.4×10^{11}/cm^2. For the optical Shubnikov de-Haas (OSdH) oscillation measurements, we varied the laser power from 0.3μW to 20μW with a 2 ms illumination time. (This time interval is typical of the conditions for a pulsed field magneto-photoluminescence (MPL) experiment.) The electron density in the E1 subband gradually increased with increasing laser power. When the laser power reached 20μW, we fixed the laser power and increased the illumination time. Above 50 ms illumination time, the resistance oscillations showed complicated features as the photo-created electrons occupy the higher energy subband levels. Recently, we reported MPL intensity and energy studies of the same sample.[1] In our interpretation of the spectral data, we had postulated that the 2nd subband was occupied by the photo-created electrons and that the observed MPL intensity and energy oscillations occur when the 1st subband Landau levels cross the Fermi energy. The measured OSdH oscillations confirm the MPL field

dependent studies and our assumption on the occupation of the subband levels.

Reference:

1 Kim, Y., *et al.*, Bull. Am. Phys. Soc., **41**, No. 1, 240 (1996).

Magneto-Luminescence Study of n-Type Modulation Doped ZnSe(Cl)/ZnCdSe Quantum Well Structures

Kioseoglou, G.K., SUNY at Buffalo, Physics
Haetty, J., SUNY at Buffalo, Physics
Chang, H.C., SUNY at Buffalo, Physics
Luo, H., SUNY at Buffalo, Physics
Petrou, A., SUNY at Buffalo, Physics
Schmiedel, T., NHMFL
Hawrylak, P., NRC Ottawa

We have studied band-edge photoluminescence from MBE-grown n-type modulation doped ZnSe(Cl)/ZnCdSe quantum wells in magnetic fields up to 30 tesla (T). The heterostructures contain a dense electron gas (areal densities in the $5x10^{11}$ - $2x10^{12}$ cm^{-2} range) that is confined in the ZnCdSe layers. The electrons originate from chlorine donors in the ZnSe barriers. In undoped structures the PL spectrum is dominated by the sharp e_1h_1 excitonic transition associated with the lowest conduction and valence confinement subbands. The PL spectra of the doped samples on the other hand are broad and featureless and are associated with band-to-band rather that excitonic recombination across the gap. The reason is that the dense electron gas screens the excitons in samples with electron densities in the 10^{11} - 10^{12} cm^{-2} range. When a magnetic field is applied perpendicular to the structure's layers, the undoped samples exhibit a small (3.5 meV in 30 T) diamagnetic shift in the energy of the e_1h_1 exciton. The luminescence band in the doped samples on the other hand breaks into a series of well defined features associated with interband transitions between conduction and valence band Landau levels. A summary plot of the energies of the Landau transitions as a function of magnetic field for a 6.0 nm well with electron areal density $n_A=1.1x10^{12}$ cm^{-2} is shown in Figure 1. The transitions labeled (i), (ii), and (iii) involve electrons in the l = 0, 1, and 3 Landau levels, respectively. The zero field PL spectrum is also shown in Figure 1, using the same energy axis. The horizontal line indicates the energy of the e_1h_1 exciton in an undoped heterostructure of the same well width (6.0 nm). The interband transitions for the doped sample extrapolate at a zero field energy of 2595 meV, which is 19 meV below the e_1h_1 transition. The large red shift is attributed to bandgap renormalization. Feature (iii) disappears at B=12 T, while feature (ii) disappears at B=24 T. These two magnetic field values correspond to filling factors ν=4 and ν=2, respectively. From these values we can directly determine the electron areal density $n_A=(1.1\pm0.1)x10^{12}$ cm^{-2} The deviations of the interband transition energies from linear dependence on B are due to the oscillation of the electron screening with filling factor. This work will appear in the February 15, 1997 issue of Physical Review B.

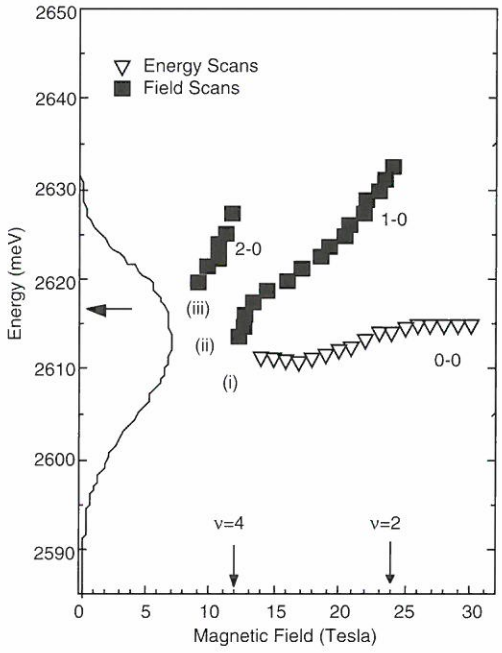

Figure 1. Energies of the interband transitions plotted versus magnetic field for a ZnSe/ZnCdSe/ZnSe heterostructure doped n-type in the ZnSe barriers; well width = 6.0 nm.

Magnetoluminescence Studies of Quantum Wells and Quantum Wires

Ko, H.S., Seoul National Univ., Physics, Korea
Kim, Y.M., Seoul National Univ., Physics, Korea
Kim, Y.S., Seoul National Univ., Physics, Korea
Kim, W.S., Seoul National Univ., Physics, Korea
Leem, Y.A., Seoul National Univ., Physics, Korea
Kim, D.W., Sun Moon Univ., Physics, Korea
Kim, D.S., Seoul National Univ., Physics, Korea
Woo, J.C., Seoul National Univ., Physics, Korea

We have performed magnetoluminescence experiments on the quantum wells (QWs) and quantum wires (QWRs) by using a 20 tesla resistive magnet. The purpose of these study is to determine how the magnetic field affects the excitonic energy structure of QWs and QWRs. Typical magnetoluminescence spectra of a 14 and 25 monolayer single QW (SQW) are shown in Figure 1. From the magnetoluminescence data of SQWs, we found that the diamagnetic shift changes abruptly as the cyclotron diameter becomes comparable to that of 2-dimensional exciton. The formation of QWR is confirmed by magnetoluminescence data.[1] The electron-hole coupling at high magnetic field requires more careful study.

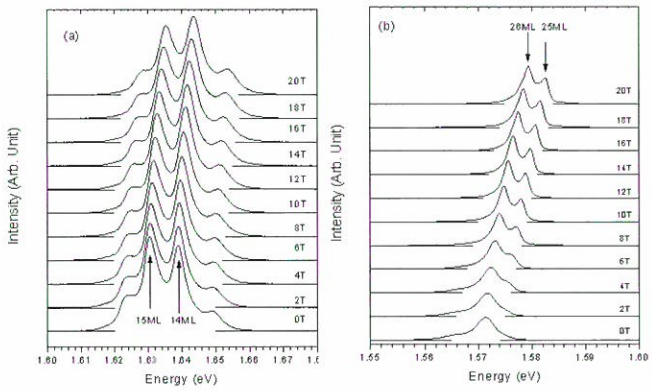

Figure 1. Magnetoluminescence spectra of (a) SQW-1 and (b) SQW-3. Magnetic field was changed from 0 to 20 T.

Reference:

1 Kim, Y.M., *et al.*, J. Korean Phys. Soc., **29**, 482 (1996).

High Field Optically Pumped NMR in GaAs

Kuhns, P.L., NHMFL
Kleinhammes, A., NHMFL
Schmiedel, T., NHMFL
Moulton, W.G., NHMFL
Chabrier, P., UF, Chemistry
Sloan, S., UF, Chemistry
Hughes, E., UF, Chemistry
Bowers, C.R., UF, Chemistry

When nuclear spin order is induced by optical excitation near the band gap of a semiconductor such as GaAs, the effect is referred to as optical pumping. This optical pumping effect occurs not only with circularly polarized light, but also with linear or unpolarized light in a manner analogous to the Overhauser effect originally reported in the microwave saturation of the electron spin resonance transition in metals. We have previously reported measurements of the optical Overhauser effect in semi-insulating GaAs and InP over the magnetic field range of 0 to 24 T, obtained using NHMFL's Bitter magnets. Now we report that the field dependence of the optical Overhauser effect has been quantitatively modelled by a relaxation equation which includes spin diffusion and dark relaxation, and field dependent electron-nuclear cross-relaxation:

$$\frac{d\langle I_z\rangle}{dt} = D\nabla^2\langle I_z\rangle - \frac{1}{T_1^{IS}}\left\{\langle I_z\rangle - \frac{I(I+1)}{S(S+1)}\left(\langle S_z\rangle - S_0\right)\right\} - \frac{\langle I_z\rangle}{T_1^{dark}}$$

Here the cross relaxation rate T_1^{IS} in the random fluctuation model is given by

$$\frac{1}{T_1^{IS}} = \frac{2F^2 a_N^2}{3}\frac{\gamma_e}{\gamma_e^2 + (\omega_I - \omega_S)^2}S(S+1),$$

where $\langle S_z\rangle$ is determined by the optical polarization and $S_0 = -\frac{1}{2}\tanh\left(\frac{\hbar g_e \mu_0 B_0}{2kT}\right)$ is the thermal electron spin polarization. The model used here extends existing theories in several ways: (a) the full magnetic field dependence of S_0 and T_1^{IS} is incorporated, (b) the nuclear spin diffusion term

$D\nabla^2 \langle I_z \rangle$ and "dark" relaxation have been included, and (c) physically meaningful boundary and initial conditions have been employed. These modifications turn out to be essential for the correct interpretation of optical pumping signals. The numerical solutions $\langle I_z \rangle$ (r,t) can be used to derive the total nuclear magnetization by summing over successive shells of atoms centered at the defect origin weighted by the respective number of nuclei in each shell. Simplex fits to the magnetic field yield values for the electron spin correlation time, average hyperfine field, and nuclear spin diffusion constant. The g-factor was fixed to the literature value for conduction electrons. The fitted parameter values are in reasonable agreement with estimates and previous measurements.

In summary, the field dependence of optically pumped NMR in GaAs has been modelled by an equation for scalar relaxation incorporating a spin diffusion term. By extracting the fitted parameters from the macroscopic behavior of the system, the microscopic spatial variation in the vicinity of the donors can be inferred as a function of any other variable, such as the duration of optical irradiation. Similar results in InP also have been obtained and will be reported at a later date.

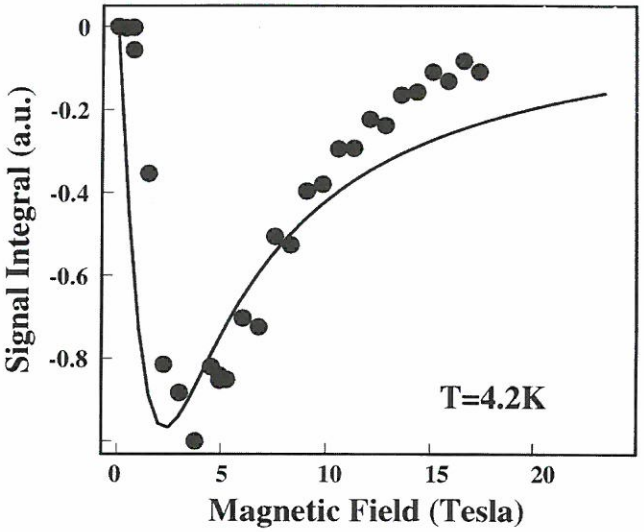

Figure 1. Experimental field dependence of the optically pumped gallium-69 NMR signal obtained at 4.2 K in bulk GaAs using a field cycling technique in the 20 T Grenoble magnet at NHMFL. The solid line indicates the best fit of the model to the data.

High Field Electron Paramagnetic Resonance of Cd(.7)Mn(.3)Se

McCarty, A., NHMFL
Hassan, A., NHMFL
Herbette, S., INSA, Toulouse, France
Martins, G.B., NHMFL
Pardi, L., NHMFL
Furdyna, J.K., Univ. of Notre Dame, Physics
Brunel, L.-C., NHMFL

The compound Cd(.7)Mn(.3)Se is a dilute magnetic semiconductor (DMS) belonging to the $A^{II}_{1-x}Mn_xB^{VI}$ family. A fundamental question in the study of $A^{II}_{1-x}Mn_xB^{VI}$ DMS's is the mechanism of the Mn^{2+} - Mn^{2+} interaction. To address this question we study the Mn^{2+} spin system by high field EPR. The sample was studied at temperatures ranging from 5 K to 295 K at frequencies of 285 and 95 GHz.

We have identified trends in the Lande g factor and the EPR line width with respect to temperature. The Lande g factor and the line width increase with decreasing temperature. The changing line shape is not simply dependent on the spin dynamics, but may signal changes in the local fields.[1] We suspect the resonance to be exchange narrowed.

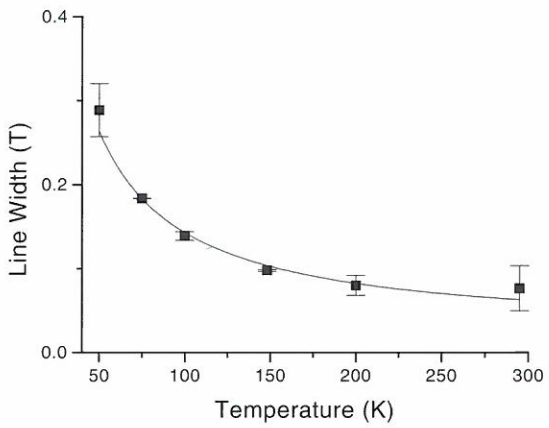

Figure 1. Line width vs. temperature at 285 GHz for Cd(.7)Mn(.3)Se. The fit assumes D-M is the source of the line width broadening.

Larson *et al.* [2] have developed a theoretical picture indicating that the main contributor to the exchange interaction is superexchange. Without inversion symmetry, a perturbation due to spin orbit

coupling within a superexchange mechanism can lead to a term called Dzyaloshinski-Moriya (D-M) interaction, which is an anisotropic exchange term.[3]

The D-M interaction was assumed to be the source of the broadening for the data taken at 95 GHz, and a good fit to the data was obtained at this frequency also.

References:

1 Samarth, N., *et al.*, Phys. Rev. B, **37**, 9227 (1988).

2 Larson, B.E., *et al.*, Solid State Commun., **56**, 347 (1985).

3 Spalek, J., *et al.*, Phys. Rev. B, **33**, 3407 (1986).

Resonant Magnetopolaron Effects with Interface Phonons in GaAs/AlGaAs Quantum Wells

McCombe, B.D., SUNY at Buffalo, Physics
Wang, Y.J., NHMFL
Nickel, H.A., SUNY at Buffalo, Physics
Peeters, F.M., Univ. of Antwerp, Belgium, Physics
Schaff, W.J., Cornell Univ., Electrical Engineering

The goal of this work is to investigate the coupling between electrons and optical phonons in $GaAs/Al_{0.3}Ga_{0.7}As$ multiple-quantum-well (MQW) structures via low temperature far infrared (FIR) magnetospectroscopy, and to determine the strength of the interactions with specific phonon modes, particularly interface phonons. A subsidiary goal is to explore systematically how occupancy of the Landau levels and screening modify the effective strength of the interaction. Only resonance experiments[1] that are sensitive to *specific* phonon modes through the frequency of the resonant interaction can reveal the strength of the interactions directly.

The Brucker FTIR spectrometer was used in conjunction with a light-pipe/bolometer detector system to study the low temperature magnetotransmission spectra of a set of GaAs/$Al_{0.3}Ga_{0.7}As$ MQW samples having well widths between 6 nm and 24 nm in magnetic fields up to 30 T. The samples are doped in the barriers (modulation doped) at sheet densities of 1.5×10^{11} (6 nm, 12 nm and 24 nm well widths), and at 3×10^{11}, 6×10^{11} and 1.2×10^{12} cm^{-2} (at 24 nm well width). The importance of interface phonon modes is predicted to increase with decreasing well width due to increased overlap of the electron and phonon envelope functions along the growth direction; so if the interaction is due to interface modes the narrower well-width samples are expected to evidence larger resonant splittings. The wide range of doping densities for the 24 nm samples permits a systematic study of the effects of screening and Landau-level occupancy on the strength of the interactions for GaAs confined longitudinal-optical (LO) modes (in the vicinity of 295 cm^{-1}) and AlAs-like interface modes (in the vicinity of 373 cm^{-1}).

We have measured the cyclotron resonance (CR) position as a function of magnetic field in the 12 nm MQW sample as the unperturbed transition energy was tuned through resonance with the GaAs confined LO phonons of the wells (at approximately 22 T) and the AlAs-like interface phonons associated with the alloy barriers (at approximately 27.5 T) to compare with the earlier measurements[2] on a 24 nm MQW sample. The earlier measurements provided the first evidence for resonant coupling between electrons and the AlAs-like interface modes in the form of a small avoided-level crossing splitting of the CR in the vicinity of the AlAs-like barrier interface modes (373 cm^{-1}). The minimum splitting between upper and lower branches was about 8 cm^{-1}. Results for the 12 nm sample showed a much larger resonant splitting (about 20 cm^{-1}) as anticipated. Theoretical calculations based on AlAs-like interface modes are in excellent agreement with the experimental measurements for both sample structures.

We also have carried out a preliminary study of the electron density dependence of the resonant interactions in the 24 nm samples. The interaction is definitely decreased at electron densities of 3×10^{11} cm^{-2} and higher. We anticipate that details of the effects of screening and occupancy (Pauli principle effects) on the effective strength of the

interaction will be forthcoming from the analysis of these and additional measurements. These studies should permit a determination of the relative importance of these effects as a function of electron density and Landau level filling-factor.

References:

1 Cheng, J-P., *et al.*, Phys. Rev. B, **48**, 17243, (1993).

2 Wang, Y.J., *et al.*, Int'l. Conf. on the Applications of High Magnetic Fields to Semiconductor Physics, Wuerzburg, Germany (1996).

Spectroscopy of a ZnCdSe/ZnSSe Quantum Well Diode Laser in High Magnetic Fields

Song, Y.-K., Brown Univ., Engineering
Nurmikko, A.V., Brown Univ., Engineering

One of the distinguishing physical features of wide bandgap semiconductors is the strong electron-hole Coulomb interactions that characterize their linear and nonlinear optical response in quasi-2 dimensional (2D) heterostructures. Through the use of optical pump-probe and related techniques at cryogenic temperature, several researchers have shown clearly that bound electron-hole pair states can dominate optical gain and stimulated emission at the n=1 heavy-hole (HH) exciton transition in ZnSe-based quantum wells (QWs).[1] In this experiment, we have investigated the lasing characteristics of ZnCdSe QW diode lasers at room temperature in high magnetic fields, up to 29 tesla (T), which showed spectral behavior consistent with an exciton-like diamagnetic response when compared with the absorption spectrum of the unexcited QW. The results suggest that the electron-hole Coulomb correlations in the many-body system remain crucial under realistic device operating conditions. This conclusion adds direct support to recent spectroscopic studies of optical gain in such diode lasers at room temperature where the impact of the Coulomb interactions was first identified to be an important intrinsic feature in the ZnCdSe QW devices.[2]

We used $Zn_{1-x}Cd_xSe/Zn_{1-x}S_xSe/Zn_{1-x}Mg_xS_ySe_{1-y}$ single quantum well (SQW) separate confinement heterostructure (SCH) diode laser structures grown by molecular-beam epitaxy (MBE) on n-type GaAs substrates. The layering scheme is the same as in the Reference 3, except for the cadmium composition and quantum well thickness that here are nominally $x_{Cd} = 0.40$ and $L_{QW} = 6$ nm, respectively. This choice of quantum well design parameters was made in order to approach the quasi-two dimensional limit, i.e. to enhance the exciton binding energy, which for this concentration range of Cd is estimated to be at least 40meV, based on earlier studies on the ZnCdSe/ZnSSe QW.[4] Index guided laser devices were fabricated with a 5μm wide ridge, formed by a self-aligned technique. The lasers had the following typical characteristics: A threshold current density $J_{th} = 300A/cm^2$, a threshold voltage $V_{th} = 5V$ and an operating wavelength of $\lambda_{lasing} = 541$ nm (2.29eV). The fabricated diode lasers were inserted into a 30 T resistive Bitter magnet at the NHMFL. The devices were operated with 500 ns current pulses at a 2 kHz repetition rate. DC magnetic fields perpendicular to the quantum well plane were applied from B = 0 to 29 T, and series of spectra measured at room-temperature with a spectral resolution of ≈ 0.015 nm. Best results were obtained from those devices that could be operated in a single longitudinal mode. We next show representative results from such a device.

The diode laser was operated above threshold at injection level of I = 18mA. From the measured room temperature electron-hole lifetime under comparable injection,[2] we calculate an e-h pair density of 1.9×10^{12} cm^{-2} in the ZnCdSe single QW. The laser spectrum is shown in Figure 1 in magnetic fields up to 29 T. In Figure 1 we see the mode hopping occurring as discrete jumps between the photon energies of $\hbar\omega = 2.290$eV, $\hbar\omega = 2.291$eV, and $\hbar\omega = 2.292$eV. By carefully comparing the field induced spectral changes in several other multimode devices and knowledge about the optical length of the laser resonator, we verified that the hopping in Figure 1 corresponds to a jump across four or five longitudinal modes. We interpret its

origin to be due most likely to small transverse inhomogeneities in the index guided lasers that impact the spatial gain profile.

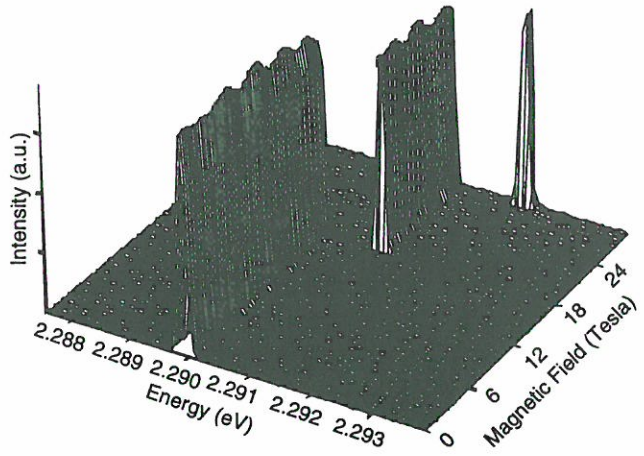

Figure 1. Emission spectra of a single mode ZnCdSe QW diode laser in magnetic fields up to 29 T at room temperature.

We also confirmed that the particular form of mode switching for the device of Figure 1 was reproducible by inducing the hopping with precisely controlled changes in the device temperature from T = 281 to 290 K in zero field. The result from this "temperature tuning" experiment is shown in the inset of Figure 2 where the spectral red shift is indicative of the bandgap shrinkage with temperature. Figure 2 shows the experimental result of the spectral shift of the lasing peak energy, and the theoretical shift for the exciton

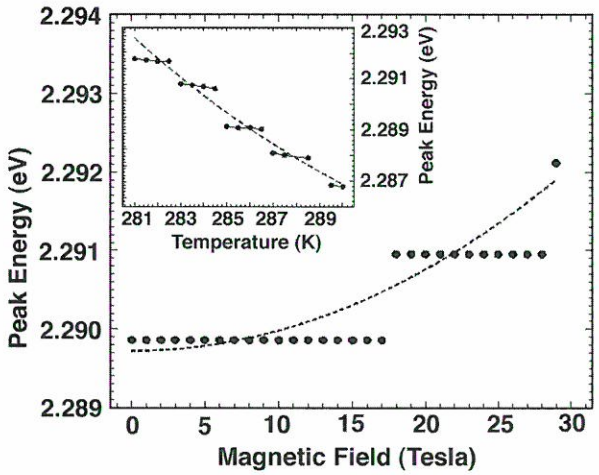

Figure 2. Comparison between measured energy shift (dots) and calculated exciton diamagnetic shift (line) of the diode laser in magnetic fields. The inset shows the emission energy shifts for the same device T = 281 to 290 K in zero field.

ground state in the 2D limit.[5] From the quadratic fit, we extract a diamagnetic shift about 2.35μeV/T^2 for the single mode laser, corresponding to an overall blue shift of 1.95μeV at B = 29 T, in good agreement with the theoretical diamagnetic effect.

In summary, we have presented experimental results for a SQW ZnCdSe diode laser in high magnetic fields that strongly support the physical arguments that the electron-hole Coulomb interaction in the room temperature green-blue laser devices dominates the optical gain and stimulated emission.

References:

1 Ding, J., *et al.*, Phys. Rev. Lett., **69**, 1707 (1992).

2 Ding, J., *et al.*, Phys. Rev. B, **50**, 5787 (1994).

3 Song, Y.-K., *et al.*, Electron. Lett., **32**, 1829 (1996).

4 Pelekanos, N.T., *et al.*, Phys. Rev. B, **45**, 6037 (1992)

5 Akimoto, O., *et al.*, J. Phys. Soc. Jpn., **22**, 181 (1966).

Edge Magnetoplasmons in Quantum Hall Effect

Szabo, T., NHMFL/FSU
Engel, L., NHMFL
Simmons, J.A., Sandia National Laboratories

In a two-dimensional electron system, under the conditions of high magnetic field (B) and low temperature (T) for which the quantum Hall effect can be observed, plasmons confined to the edge of the sample can be produced.[1] These "edge magnetoplasmons" (EMPs) are excitations of the quantum Hall edge states, which have been described as alternating structures of compressible and incompressible strips.[2]

We have constructed and tested an apparatus for observing EMPs over a wide range of frequencies, from 1 to 400 MHz. The apparatus employs probe electrodes positioned to couple capacitively to the sample edges. In a preliminary run in a superconducting magnet, using a sample

of electron density 1.8 x 10^{11} cm^{-2} and mobility 2 x 10^5 cm^2/V-s, EMP resonances were not visible at the comparatively high T ~ 4 K, though the resistance of the sample, $R \sim \rho_{xy}$, was measurable through the probes on the sample edge, allowing a successful characterization of the apparatus. Future work with the measuring system, will focus on EMP's behavior in constrictions and in multilayer samples.

References:

1 See, for example, Zhitenev, N.B., *et al.*, Phys. Rev. B, **49** (11), 7809 (1994).

2 Chklovskii, D.B., *et al.*, Phys. Rev. B, **46**, 4026 (1992).

Pressure Dependence of the Conduction-Band Mass: InGaAs/GaAs Single-Strained Quantum Wells

Tozer, S.W., NHMFL
Schmiedel, T., NHMFL
Jones, E.D., Sandia National Laboratories

We have optically determined the pressure dependence of the conduction-band mass for a 20% indium InGaAs/GaAs 80 nm-wide n-type single-strained-quantum well. The conduction band mass was measured by studying the magnetic field dependencies of the zeroth-order forbidden (low temperature) magnetoluminescence transitions. Hydrostatic pressures (35 kbar maximum) were generated using a helium-filled diamond anvil cell. Analyses of the 4-K magnetoluminescence data indicate that the pressure derivative $\partial \log(m)/\partial P$ for the conduction band mass is about 0.4%/kbar, which is to be compared to the previously reported magneto-transport determination $\partial \log(m)/\partial P = 1\%$/kbar. The pressure dependent magneto-luminescence thus gives accuracies that are about a factor of ten more accurate than the traditional magneto-transport determinations.

Magneto-Transmission Study of Nonparabolicity of the Conduction Band in Heavily n-Doped InGaAsP

Wang, Y.J., NHMFL
Schneider, D., Tech. Univ., Braunschweig, Germany

The compound semiconductor InGaAsP is commonly employed for optoelectronic devices in glass-fiber communication systems. For the design of these devices the accurate value of the effective mass of the material with high electron concentration is very important, in this case strong nonparabolicity effects must be considered. Previously, the effective masses of the system have been measured by Shubnikov-de Haas effect.[1]

The current work has been carried out in several heavily doped InGaAs and InGaAsP samples by Fourier transform mass spectroscopy (FTMS) at 4.2 K and at magnetic fields up to 17.5 T. For the samples with doping concentration higher than $10^{18}cm^{-2}$ (they are all metallic) there is not enough light passing through the sample to do transmission measurements, so both reflectance and transmission FTMS had to be used in our measurements. The results obtained from the optical measurement are consistent with the results obtained from the transport measurements, and the effective mass obtained from different measurements are essentially the same.

Reference:

1 Schneider, D., *et al.*, *Proceedings of Physical Phenomena at High Magnetic Fields-II*, eds. Z. Fisk, *et al.*, p. 105 (World Scientific, Singapore, 1996).

High Hydrostatic Pressure Effects on the Exciton Spin States in CdTe/$Cd_{1-x}Mn_xTe$ Single Quantum Wells

Yokoi, H., National Institute of Materials and Chemical Research, Tsukuba, Japan
Takeyama, S., Himeji Institute of Technology, Dept. of Material Science, Ako-gun, Japan
Kakudate, Y., National Institute of Materials and Chemical Research, Tsukuba, Japan
Fujiwara, S., National Institute of Materials and Chemical Research, Tsukuba, Japan
Schmiedel, T., NHMFL/FSU
Tozer, S.W., NHMFL/FSU
Jones, E.D., Sandia National Laboratories
Wojtowicz, T., Institute of Physics, Polish Academy of Sciences, Warsaw, Poland
Karczewski, G., Institute of Physics, Polish Academy of Sciences, Warsaw, Poland
Kossut, J., Institute of Physics, Polish Academy of Sciences, Warsaw, Poland

The strong exchange interaction between the spins of carriers and those of local magnetic ions in diluted magnetic semiconductors (DMS's) underlies a variety of spin-engineering semiconductor sciences. This interaction is now understood in terms of sp-d hybridization as well as antiferromagnetic spin clusters among the dilute magnetic ions. In order to obtain a systematic knowledge of these interactions, we have investigated hydropressure effects on the exciton spin states in CdTe/$Cd_{1-x}Mn_xTe$ single quantum wells (SQW's). The sample was a CdTe/$Cd_{0.76}Mn_{0.24}Te$ SQW structure, which consisted of 1.3, 1.9, 3.8 nm thick CdTe wells sandwiched by 48.0 nm $Cd_{0.76}Mn_{0.24}Te$ barriers. Pressure up to 2.7 GPa was generated in a diamond-anvil cell. We observed four luminescence signals assigned to band-edge exciton photoluminescences (PL's) from three wells and a barrier, respectively, at low temperatures. The pressure dependence of their peak position was almost linear and became larger in a wider well. These results could be explained by large pressure effect on the exciton binding energy due to the barrier height variation in this high Mn concentration system. Magneto-photoluminescence measurements were conducted at 4.2 K under DC magnetic fields up to 30 T generated by a water cooled resistive magnet. Linear field dependence of the PL peak energies was observed in the higher field region than about 15 T in all layers but the widest well (well A). The observed Zeeman shifts of the PL peaks could be fitted well to a function taking a modified Brillouin function and a linear magnetization term. The sp-d hybridization terms ($N_0(\alpha-\beta)$), antiferromagnetic temperature (T_0), and linear magnetization factor (M_1) for the barrier and the well A were determined at each pressure. The pressure dependence of $N_0(\alpha-\beta)$ in the well A was positive, which agrees very well with theory for the p-d hybridization. That in the barrier, however, was found to be negative. It might suggest the necessity of considering any correction for Mn ions in the second nearest cation site might be necessary. M_1 and T_0 for the barrier decreased and increased, respectively, with increasing the pressure. This tendency reflects enhancement of the antiferromagnetic coupling between Mn ions by the pressure. The pressure dependence of T_0 for the well A was smaller than that for the barrier though it is positive. There is a possibility that the exciton size in the well A is almost the same as the well width.

Magneto-Absorption Study of the Exciton in a CdTe Thin Film

Yokoi, H., National Institute of Materials and Chemical Research, Tsukuba, Japan
Takeyama, S., Himeji Institute of Technology, Dept. of Material Science, Ako-gun, Japan
Kakudate, Y., National Institute of Materials and Chemical Research, Tsukuba, Japan
Kim, Y., NHMFL-Los Alamos
Rickel, D.G., NHMFL-Los Alamos

Absorption study of CdTe has been difficult because all of its available thin single crystals have been grown epitaxially on the substrates, such as GaAs, which are optically opaque at the band-edge region of CdTe. Therefore, high field magneto-absorption study of this material has been almost

impossible despite that it is a very important material both for fundamental interest and for application. We prepared its high quality and stress-free thin single crystals on the (001) surface of mica substrates with the hot-wall epitaxy technique. The thickness of the film was 250 nm. Magneto-absorption measurements were conducted up to 50 T at 4.2 K. A halogen lamp was used as a white light source and a mechanical shutter was employed to illuminate the sample for about 2 ms around the top of pulsed magnetic fields. Transmitted light was analyzed with a spectrometer with a charged coupled device. A blue shift of an exciton peak was observed with increasing magnetic fields. Field dependence of the peak position was described well as parabolic and linear at lower and higher field regions than about 20 T, respectively. The strength of the peak also became much larger with increasing fields above 20 T than below 20 T.

We interpret these results that the diamagnetic shift was observed in the lower field region than 20 T and a Landau-like transition in the higher region than 20 T. Analyzing the diamagnetic shift, we have obtained the exciton reduced mass of $0.096m_0$, which can be compared with the value of $0.073m_0$ reported by Aggarwal, *et al.*, from reflection measurements for the (110) surface of bulk CdTe.[1] If we use a value of 10.3 as the ε, the field value, where the γ is equal to 1, turns out to be 20 T, which is consistent to our result.

Reference:

1 Aggarwal, R.L., *et al.*, Phys. Rev. B, **32**, 5132 (1985).

SCIENCE RESEARCH REPORTS

Magnetism & Magnetic Materials

Ferromagnetic Ordering in hcp ^{3}He

Adams, E.D., UF, Physics
Takano, Y., UF, Physics
Lang, T., UF, Physics
Moyland, P.L., UF, Physics

Solid ^{3}He becomes magnetically ordered at temperatures < 1 mK via exchange interactions made possible because of its large zero point motion. While most of the magnetic properties of the bcc solid are well characterized, there exists little information about the properties of the hcp solid. Theoretical calculations[1] and experimental work[2] indicate that the solid should order ferromagnetically near 20 μK. Because of the large thermal boundary resistance, the ordering temperature can not be reached using indirect cooling.

To achieve such low temperatures, ^{3}He samples may be directly demagnetized as the second stage in a two-stage demagnetization. This method was employed at the University of Tokyo[3] on both bcc and hcp solids. Their results showed that the bcc solid reached both the high-field phase (HFP) and the low-field phase (LFP), implying that the sample was cooled below 28 μK. For their two hcp samples, however, no clear signature of the ordering was observed because of heating of the cell near the end of the demagnetization when their In O-ring became normal.

Using the direct sample demagnetization technique, we carried out pressure measurements for one bcc and two hcp samples. With an improved design of the experimental cell, we have reduced heating near the end of the sample demagnetization and made the first clear observation of the pressure signature of ferromagnetic ordering in hcp solid ^{3}He.[4] The improvements in our cell (which eliminated the heating problem) were a pressure strain gauge constructed without screws or spacer and sealed with epoxy rather than an O-ring.

Pressure measurements were made on one bcc and two hcp samples.[4] Our bcc data are quite similar to those of Okamoto *et al.*[3] with one important difference: We did not observe any pressure decrease, which they observed and attributed to

heating, near the end of the demagnetization. This result showed that the use of epoxy to seal the sample cell significantly reduced heating to the sample and allowed us to make a clear observation of magnetic ordering in the hcp solid.

Our results for two hcp samples with molar volumes of 19.65 cm^3/mole and 19.61 cm^3/mole are shown in Figure 1. These indicate that the pressure of the sample behaves differently depending on the amount of entropy remaining at the end of the pre-cooling. For S/Rln2 = 0.02, achieved with initial temperature and field of 614 μK and 2.485 T, respectively, the hcp sample became magnetically ordered, indicated by a pressure decrease of 10 Pa over the field range from 0.2 T to 0 T.

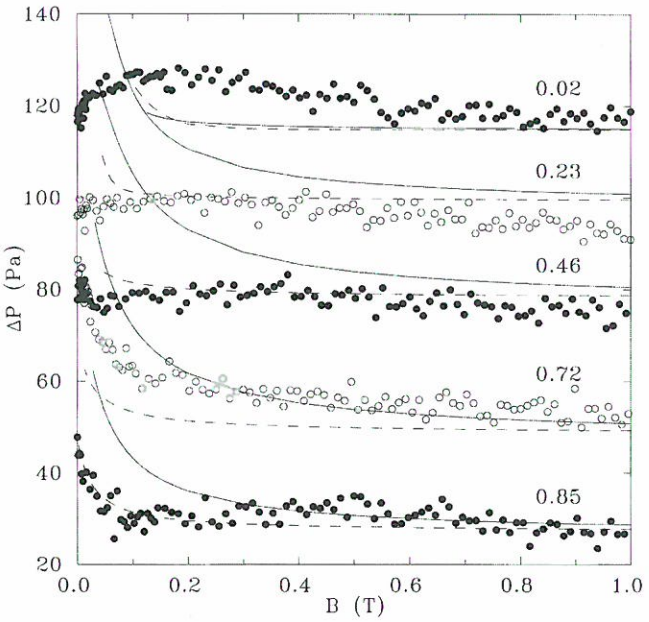

Figure 1. Demagnetization data of hcp samples at different entropies. Solid and dashed lines represent the calculated results from the high-temperature expansion of the multiple exchange and Heisenberg models, respectively.

For S/Rln2 > 0.72, the samples were not expected to reach the ordering temperature T_c, and there was an increase in pressure near zero field. The pressure rise verifies the fact that the observed pressure decrease in low-entropy sample is due to magnetic ordering. We also carried out pressure calculations using the high-temperature expansion of the multiple-exchange[5] and nearest-neighbor Heisenberg[6] Hamiltonians, that are expanded to fourth and tenth order in 1/kT, respectively. As shown in Figure 1, both models yield an increase in pressure at low fields for all entropies S and are in agreement with our high-entropy data. The calculations fail to predict a pressure decrease in an ordered sample because the series expansions are only valid for $T > T_c$. This failure is yet more evidence that the pressure decrease is the ordering signature of the hcp solid.

References:

1 Roger, M., *et al.*, Rev. Mod. Phys., **55**, 1 (1983).

2 See, for example, Yano, H., *et al.*, Phys. Rev. Lett., **65**, 3401 (1990) and references therein.

3 Okamoto, T., *et al.*, Phys. Rev. Lett., **72**, 868 (1994).

4 Lang, T., *et al.*, Phys. Rev. Lett., **77**, 322 (1996).

5 Roger, M., *et al.*, Phys. Rev. B, **35**, 2091 (1987).

6 Rushbrooke, G.S., *et al.*, in *Phase Transition and Critical Phenomena*, Domb, C., *et al.*, editors, p. 245 (Academic Press, London, 1974).

Angular Dependence of Metamagnetic Transitions in $HoNi_2B_2C$

Canfield, P.C., Iowa State Univ./Ames Lab.
Cho, B.K., Iowa State Univ./Ames Lab.
Lacerda, A., NHMFL/LANL

Detailed measurements of M(2K, H, θ), where θ is the angle that the applied field H makes with the [110] axis while remaining perpendicular to the c-axis, reveal three metamagnetic transitions with angular dependencies $H_{C1} = (4.1kG)/\cos(\theta)$, $H_{C2} = (8.4kG)/\cos(\phi)$, and $H_{C3} = (6.6kG)/\sin(\phi)$, where $\phi = \theta - 45$ is the angle from the [100] axis. The high field saturated moment, $M_{sat} = 10\mu_B\cos(\theta)$, is consistent with the local moments being confined to the [110] direction. The locally saturated moments for fields between H_{Ci} (i = 1, 2, 3) also manifest angular dependencies that are consistent with a combination of local moments along the [110] axes. Analysis of these data have allowed for determination of the net distribution of moments in all field ranges.

The result of this research has been accepted for publication in the January 1997 issue of *Physical Review B*.

Strontium and Calcium-Based Ruthenates: Physics of Bad Metals

Cao, G., NHMFL
Crow, J.E., NHMFL
Shepard, M., NHMFL
McCall, S., NHMFL
Bolivar, J., NHMFL
Guertin, R.P., Tufts Univ., Physics, on leave at NHMFL

In spite of extensive research efforts expended on 3d transition metal oxides, spurred by high temperature superconductivity in cuprates and giant magnetoresistance in manganates, surprisingly little is known about the 4d and 5d transition metal oxides. Because of the greater extent of the 4d, 5d shells, the latter are expected to be more metallic, more electronically itinerant, and to bond more covalently with O ions. Among the 4d's and 5d's only Ru-based oxides, ruthenates, appear to show localized-like behavior. The Ru (S=1) compounds display strong manifestations of electron-electron interactions, that affect all magnetic, transport, and low temperature thermodynamic properties. Chemical substitution for the Ru or other cations show the systems border on metal-insulator transitions, a rather poorly understood phenomenon for S>1/2 systems. Several examples of the ruthenates suggest they are "bad" metals, verging and in some cases undergoing metal insulator transitions.

We have undertaken a comprehensive examination of the Ca- and Sr-based ruthenates plus mixtures and derivatives of them. Nearly all fall into the Ruddelsden-Popper (R-P) series: $(Sr,Ca)_{n+1}Ru_nO_{3n+1}$ for n=1 to ∞, where n also signifies the number of Ru-O layers in the structure. Thus R-P systems allow some control of the dimensionality by the choice of n. All are well suited for in-plane (Ru-O) doping and out of plane doping. Our group is the first to fabricate single crystals of all of these systems plus mixed Sr-Ca and doped crystals, for n=1, 2 and ∞, the latter being the familiar ABO_3 perovskite-type structure. The n=1 member has a structure like the La_2CuO_4-based high T_C superconductors. The R-P systems studied show a bewildering array of properties many of which are summarized in Figure 1. Nearly all data in the figure are from our own work.

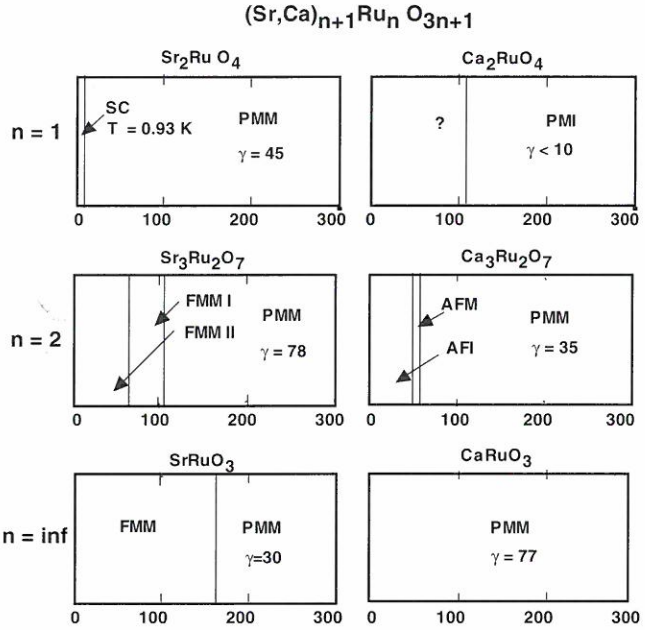

Figure 1. Various properties exhibited by R-P systems under investigation. The abbreviations are PMM = paramagnetic metal, FM = antiferromagnetic metal, AFI = antiferromagnetic insulator, FMM = ferromagnetic metal, PMI = paramagnetic insulator, and SC = superconducting.

We have performed measurements of magnetization (up to 30 T), transport (magnetoresistivity, Hall effect), and heat capacity of $(Sr,Ca)_{n+1}Ru_nO_{3n+}$ and derivative materials, in an effort to understand the basics of the metal-insulator transition, systematics of highly correlated metals, including the influence of dimensionality, the criteria for "bad metals," and the general behavior of the 4d transition metal oxides and their relationship more intensively studied 3d systems. Some of the results suggest device applications for the ruthenates. Collaborative efforts include neutron scattering (NIST and ORNL), infrared spectroscopy (UF), and angular resolved photoemission (Stanford).

Magnetic and Magnetoresistive Properties of Low-Dimensional Multilayers

Childress, J.R., UF, Materials Science Engineering/NHMFL
Sharifi, F., UF, Physics/NHMFL
Geerts, W., UF, Materials Science Engineering/ NHMFL
Caballero, J.A., UF, Materials Science Engineering
Park, Y.D., UF, Materials Science Engineering
Cabbibo, A., UF, Materials Science Engineering
Yang, Y., UF, Materials Science Engineering
Feng, T., UF, Materials Science Engineering
Hudspeth, H.D., UF, Physics
Schultz, T.J., UF, Physics

We have demonstrated the fabrication of low-dimensional magnetic structures by direct sputter deposition through e-beam-fabricated mask openings. This approach can potentially explore dimensionality effects on giant-magnetoresistive (GMR) devices down to 15 nanometer linewidths, without the need for post-deposition processing. The mask structure is integrated on Si substrates using a novel electron-beam fabrication technique (F. Sharifi). The subsequent deposition of films or multilayers in our UHV sputtering system involves a two-step masking scheme where a mm-size collimating mask is first used to reduce the angle of incidence of depositing atoms to within 10° of vertical. This ensures minimal deposition on the side walls of the nano-mask, which would otherwise rapidly block the mask opening to further deposition. Integrated contact areas can be included in the mask fabrication process, which allows *ex-situ* characterization of the magnetotransport properties of the resulting structures as a function of line width.

Initial work has focused on a 2-layer polymer mask structure, which is simpler than a metal mask although restricted to wire widths above 30 nm. The advantage in this case is that the mask structure can be easily lifted off after deposition to directly image the deposited structures. Figure 1 shows an atomic force microscopy image of a 5μmx5μm area onto which a pattern of 250 nm-wide cobalt wire has been deposited. Atomic force microscopy, in particular, allows the imaging of the wire surface roughness that will provide structural clues to understand the magnetotransport behavior in the future. Our work in the near future will focus on understanding the transport and magnetic properties of individual single-component nanowires, before depositing multilayers to investigate size effects in realistic GMR structures.

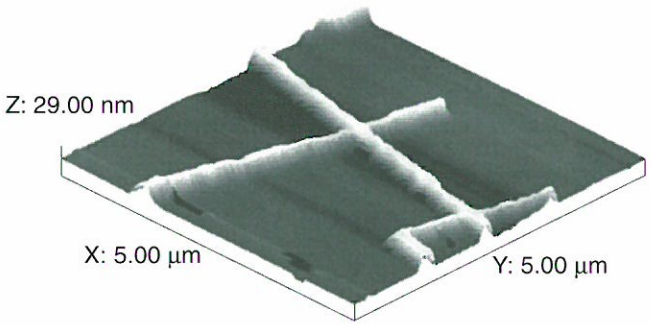

Figure 1. Atomic force microscopy image of a 5μmx5μm area onto which a pattern of 250 nm-wide cobalt wire has been deposited.

The Development of Spin-Polarized Magnetic Layers

Childress, J.R., UF, Materials Science Engineering/NHMFL
Geerts, W., UF, Materials Science Engineering/ NHMFL
Caballero, J.A., UF, Materials Science Engineering/NHMFL
Park, Y.D., UF, Materials Science Engineering
Cabbibo, A., UF, Materials Science Engineering
Yang, Y., UF, Materials Science Engineering
Feng, T., UF, Materials Science Engineering

According to current understanding, significant enhancement of the giant-magnetoresistance (GMR) effect can be obtained by increasing the spin polarization in the magnetic layers. Consequently, the study in this context of half-metallic ferromagnetic materials with 100% spin polarization at the Fermi level, is of particular interest for developing nanoscale magnetic devices with enhanced properties. A number of so-called Heusler alloys, with $C1_b$ crystal structure, are known or predicted to be half-metallic.

Ferromagnetic NiMnSb has the highest Curie temperature (about 750 K) and is therefore ideal for electronic applications using the GMR effect operating at or above room temperature.

Research in 1996 has focused on the fabrication of single films of NiMnSb to investigate the conditions under which a bulk-like structure can be obtained. This has been highly successful, as we have synthesized this alloy in the correct cubic $C1_b$ crystal structure. Depositions of NiMnSb were conducted using our custom-designed sputtering system, with base pressures in the mid-10^{-9} Torr range, argon sputtering gas, and Si wafer and Corning glass 7059 substrates.

We have identified conditions under which high-quality thin films of the potentially half-metallic ferromagnet NiMnSb can be grown by magnetron sputtering using a single composite target. The best structural and magnetic properties are obtained at moderate substrate temperatures (~200 to 300 °C), with low argon pressures (~2.5 mT) and very low RF power (15 W) resulting in low deposition rates (0.025 nm/s), and without post-deposition annealing. Figure 1 illustrates how the film roughness and polycrystalline grain size correlates with the magnetic properties. The 0.5 nm roughness for 3 mT deposition, in particular, would ensure near-ideal interfaces within multilayer structures.

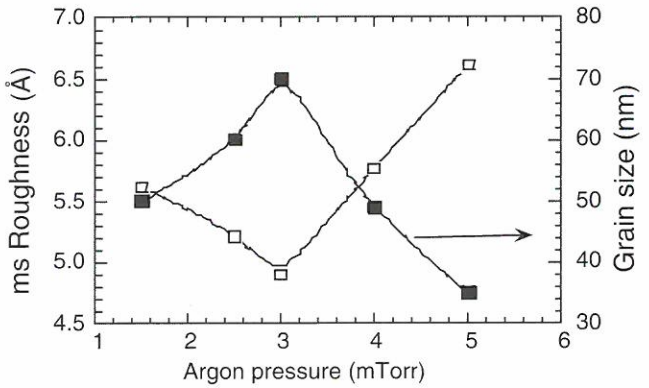

Figure 1. Rms roughness and polycrystalline grain size as a function of sputtering pressure for 20 nm-thick NiMnSb thin films.

The main advantage of this approach is that ultrathin films (10 nm or lower) of NiMnSb can be grown with high crystalline quality and low roughness, which are essential to the application of this material to spin-polarized multilayer magnetic devices. Although NiMnSb is predicted to be half-metallic, this has not conclusively been established experimentally. Magneto-optical measurements on single films have been performed in collaboration with D. Weller at IBM-Almaden, which show that the Kerr rotation spectrum of these films is identical to those observed in bulk ordered alloys. This suggests that they share the same band structure characteristics. Deposition of thin-films at moderate temperatures, in addition, allows the absolute spin-polarization of the conduction electrons to be directly measured from tunneling experiments which are now underway.

Effect of Particle Size on the Colossal Magnetoresistance of $Pr_{1-x}Ba_xMnO_3$

Cohenca, C.H., USP - Brazil, Physics
Jardim, R.F., USP - Brazil, Physics
Torikachvili, M.S., San Diego State Univ., Physics
Lacerda, A., NHMFL/LANL

We have studied the effect of particle size on the electronic transport and general magnetic properties of $Pr_{1-x}Ba_xMnO_3$ for $0 < x < 0.45$. Polycrystalline samples of these compounds have been produced using two different precursors: (1) mixture of the simple oxide Pr_6O_{11} and carbonates $BaCO_3$, and $MnCO_3$, and (2) using sol-gel precursors.[1] These samples were subject to heat treatment in air at 1100C for ~ 60h. Observations of the microstructure and measurements of X-ray diffraction, electrical resistivity, magnetoresistivity, and magnetic susceptibility indicate the important effect that cationic (Ba) distribution has upon the properties of these compounds. Samples prepared by using the sol-gel process are composed of small grains (< 1μm) and do not show any additional phase. Samples prepared with mixture of oxide and carbonates have larger grains, and an additional Ba-rich phase ($BaMn_3$) was observed. We have noticed that their macroscopic properties are strongly sensitive to these differences, e.g, the ferromagnetic

transition temperature of a sol-gel precursor is higher and the magnetotransport properties less sensitive to applied magnetic fields to 18 T.

References:

[1] Jardim, R.F., *et al.*, J. Alloys & Compounds **199**, 105 (1993).

Indications of a Metallic Antiferromagnetic Phase in the Two-Dimensional U-t-t' Model

Duffy, D., NHMFL
Moreo, A., FSU/Physics, NHMFL and MARTECH

We present mean-field and quantum Monte Carlo results that suggest the existence of an itinerant antiferromagnetic ground state in the half-filled U-t-t' model in two dimensions. In particular, working at t'/t=-0.2 we found that antiferromagnetic long range order develops at $U_{c1}/t \approx 2.5$, while a study of the density of states $N(\omega)$ and the response to an external magnetic field indicates that the system becomes insulating at a larger coupling $4<U_{c2}/t<6$.

Preparation and Characterization of $LnNiO_3$ (Ln = Pr, Nd, Sm) and Their Solid Solutions

Escote, M.T., USP - Brazil, Physics
Jardim, R.F., USP - Brazil, Physics
Torikachvili, M.S., San Diego State Univ., Physics
Lacerda, A., NHMFL/LANL

We have prepared polycrystalline samples of $LnNiO_3$ (Ln = Pr, Nd, Sm) and their solid solutions by using three different precursors: (1) mixture of the simple oxides Ln_2O_3 and NiO, (2) via sol-gel precursor, and (3) coprecipitation of hydroxides of Ln^{+3} and Ni^{+3}. These materials were sintered at 750 °C in O_2 environment and under pressures as high as 50 atm. X-ray powder diffraction analysis revealed that samples prepared through methods (2) and (3) are single phase materials. Samples produced through method (1) were found to be a mixture of simple oxides LnO_3 and NiO. Measurements of electrical resistivity as a function of temperature ($\rho(T)$) on $NdNiO_3$ revealed two different regimes: (a) a metallic-like behavior at high temperatures (T > 200 K), and (b) a drastic increase in the magnitude of $\rho(T)$ bellow ~ 200 K. Such a behavior suggests a Metal-Insulator (MI) transition close to 200 K. The application of magnetic fields to 18 T has little effect upon the transport properties of these compounds. This suggests that these compounds, contrary to the MI transition in single oxides (e.g., V_2O_3 and Ti_2O_3) can be understood as a charge transfer gap compounds. We also have tuned the MI transition to around room temperature in $Nd_{1-x}Sm_xNiO_3$.

Broadband High Field AFMR Spectroscopy of Layered Antiferromagnets

Fanucci, G.E., UF, Chemistry
Krzystek, J., NHMFL
Talham, D.R., UF, Chemistry
Brunel, L.-C., NHMFL

Magnetic interactions in layered materials are currently of high interest from a fundamental point of view, partially because of their relationship to layered superconductors. The interest also has been caused by their structural analogy to magnetic thin films since the latter are considered as potential information storage media and as components of multilayered heterostructures, which have lead to unusual phenomena such as giant magnetoresistance.

We have investigated a series of five layered organic/inorganic solid-state manganese phosphonates, which become canted antiferromagnets below the ordering temperature of approximately 14 K: Mn phenyl-, propyl-, pentyl-, and hexylphosphonate as well as their purely inorganic analog, $KMnPO_4$.[1] The experimental method of choice was antiferromagnetic resonance (AFMR). AFMR offers a microscopic view of the magnetic structure in the ordered state leading to determination of exchange interactions, anisotropy fields, spin-flop and critical fields, and canting fields. We have used

the unique broadband capability of the high-field EMR spectrometer in operation at the NHMFL (a 30 to 400 GHz frequency range, and 0 to 15 tesla magnetic field range) to perform a complete normal mode analysis of the compounds under study (Figure 1). Established models for AFMR in canted antiferromagnets have been employed to analyze the data and extract magnetic parameters that can be used to compare the different materials. Structure/property analysis have allowed us to correlate the influence of organic substituents on the magnetic properties of the layered solids.

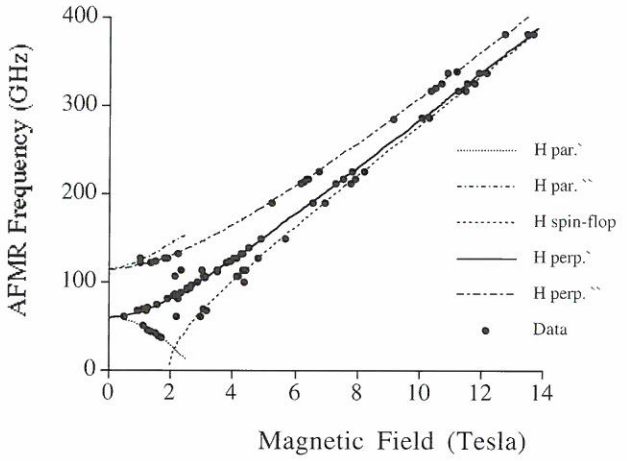

Figure 1. AFMR normal modes in Mn phenylphosphonate at 5 K. Dots are experimental points, lines are simulated using a model following extended Nagamiya-Asida theory.

In the future we are planning to extend the AFMR studies to Langmuir-Blodgett films. These films have been shown to exhibit properties similar to those of Mn phosphonates.[2] Preliminary experiments on Mn phenylphosphonate single crystal have demonstrated the feasibility of the project from the sensitivity criteria.

References:

1 Cao, G., *et al.*, Inorg. Chem., **27**, 2781 (1988).

2 Seip, C.T., *et al.*, Inorg. Chem. **35**, 3479 (1996).

Evidence of a Haldane Gap in an S = 2 Quasi-Linear Chain Antiferromagnet

Granroth, G.E., UF, Physics
Meisel, M.W., UF, Physics
Chaparala, M.V., NHMFL
Jolicoeur, Th., SPT-CEA-Sacaly
Ward, B.H., UF, Chemistry
Talham, D.R., UF, Chemistry

We have reported[1] the first evidence of the presence of the Haldane gap in an S = 2 chain antiferromagnet. We have studied the magnetic properties of $MnCl_3$(bipy), where bipy represents $C_{10}H_8N_2$. The system consists of a quasi-linear chain of Mn^{3+} (S = 2) ions in $MnCl_2$(bipy) units, asymmetrically connected by bridging Cl^- ions. The magnetization data as a function of magnetic field at a temperature of 30 mK are shown in Figure 1. The results clearly indicate the presence of a nonmagnetic state at the lowest fields, and the continuous onset of a magnetic state for fields above a critical field, H_c, which depends on crystal orientation, namely $H_{c\|}$ = 1.2±0.2 T and $H_{c\perp}$ = 1.8±0.2 T. Furthermore, no discontinuities, hysteresis, or other anomalies were observed up to 16 T. These results indicate no evidence for three-

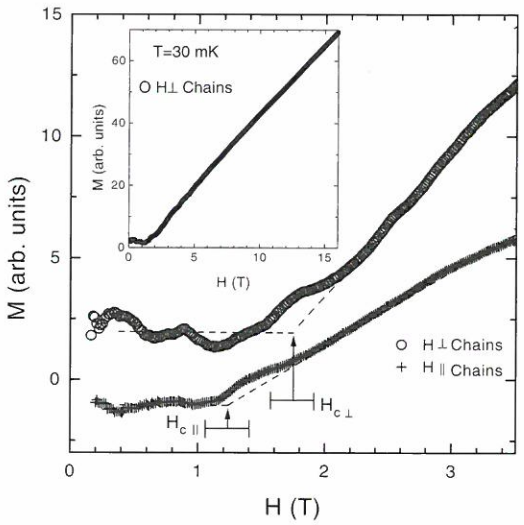

Figure 1. M(H) at 30 mK for the field applied ⊥ (O) and || (+) to the chains of two single crystals with total mass ≈ 200 μg, where both traces are offset vertically from zero for clarity. The arrows identify $H_{c\perp}$ and $H_{c\|}$ with their respective uncertainties. The inset show a more complete view of the H ⊥ chains data.

dimensional long-range magnetic order to 30 mK, where either hysteresis or a spin-flop transition should have been detectable. In addition, the presence of an H_c for both crystal orientations is incompatible with the existence of long-range order or the presence of a gapless phase.[2] Consequently, the spins are either in a Haldane phase or large D/J state, where D is the single-ion anisotropy and J (> 0) is the intrachain nearest-neighbor interaction. The crystal structure suggests, however, that D should be small compared to J.

Therefore we conclude the H_c values are related to a Haldane gap in the presence of a small $D \neq 0$. A finite D value causes the singlet ground state to shift and the excited triplet to split. The application of an external magnetic field causes additional splitting of the triplet states, where the lowest excited level crosses the ground state at H_c. This analysis yields $D/J = 0.010 \pm 0.003$ and, for the $S = 2$ Haldane gap, $\Delta_{S=2}/J = 0.07 \pm 0.02$, which agree well with the numerical work.[2,3] The sign of D, obtained from this analysis, conflicts with the sign predicted by the crystal structure. Both the numerical work and the experimental estimate, however, should include all anisotropies.

References:

1 Granroth, G.E. *et al.,* Phys. Rev. Lett., **77**, 1616 (1996).

2 Schollwöck, U. *et al.*, Europhys. Lett., **30**, 493 (1995).

3 Schollwöck, U. *et al.*, Phys. Rev. Lett., **77**, 2844 (1996); Yamamoto, S., *ibid.*, **77**, 2845 (1996), and references therein.

Frustrated Spin Chains: Spinons and Their Dynamics

Ha, Z.N.C., NHMFL

It is a generally accepted theoretical as well as experimental fact that the elementary excitations of the isotropic S = 1/2 antiferromagnetic (AF) Heisenberg spin chain consist of pairs of unbound S = 1/2 objects called spinons.[1] Their dynamics are not well-understood, however. The goal of this research is to understand this dynamical aspect of spinons in the context of the recently introduced notion of fractional statistics in one-dimensional systems.[2,3]

An ideal system to study the spinon dynamics is the frustrated spin chains (i.e. the AF next nearest neighbor interaction J_2 is turned on). I found that the 1D version of the wavefunction for the $\nu = 1/2$ bosonic FQH (fractional quantum hall) fluid has better than 99% overlap with the true ground state of the finite size (up to 16 sites) frustrated spin system (at $J_2/J_1 \approx 0.16$). This is a strong indication that the semionic description of the spinon excitations is a valid one. I also discovered that when the frustration is increased further the exact numerical ground state begins to have smaller overlap with the variational ground state and larger overlap with the states with higher spinon number. This is an indication that the spinons begin to proliferate as the frustration is increased. Once the spinon density reaches a thermodynamically finite number there is an interesting possibility that the spinons condense to form a next level fluid. Currently, I am examining this possibility.

I mention the following two related projects:

- *Frustrated spin chains in magnetic field*: This system provides a nice framework in which the notion of 1D fractional statistics can be examined in detail for which I found some numerical evidence.
- *General numerical method for large spin systems*: Smart choice of the basis vectors for the spin system combined with the numerical renormalization group technique might provide a new window for accessing large periodic systems where the finite size effects are small. This work is being carried out in collaboration with P. Monthoux.[4]

References:

1 Faddeev, L.D., *et al.*, Phys. Lett., **85**A, 375 (1981); Tennant, D.A., *et al.*, Phys. Rev. Lett., **70**, 4003 (1993).

2 Haldane, F.D.M., Phys. Rev. Lett., **66**, 1529 (1991); in *Proceeding of the 16th Taniguchi Symposium*, Kashikojima (1993).

3 Ha, Z.N.C., Phys. Rev. Lett., **73**, 1574 (1994); *Quantum Many-Body Systems in One Dimension*, World Scientific, Singapore, 1996.

4 Monthoux, P., *et al.*, (in progress).

Critical Behavior of the S=3/2 Antiferromagnetic Heisenberg Chain

Hallberg, K., Max-Planck-Institut fur Physik komplexer Systeme
Wang, X.Q.G., Max-Planck-Institut fur Physik komplexer Systeme
Horsch, P., Max-Planck-Institut fur Festkorperforschung
Moreo, A., FSU/Physics, NHMFL and MARTECH

Using the density-matrix renormalization-group technique we study the long-wavelength properties of the spin S=3/2 nearest-neighbor Heisenberg chain. We obtain an accurate value for the spin velocity v=3.87±.02, in agreement with experiment. Our results show conclusively that the model belongs to the same universality class as the S=1/2 Heisenberg chain, with a conformal central charge c=1 and critical exponent η=1.

Transport in Nanostructured Magnetic Materials

Hershfield, S., UF, Physics
Kroha, H., Univ. of Karlesruhe, Germany, Physics
Schiller, A., UF, Physics
Zhao, H.L., UF, Physics
Hettler, M., UF, Physics
Beck, G., UF, Physics

Our research continues to focus on (1) strongly correlated nanostructured materials and (2) magnetic multilayers and related materials.

In the first area, we succeeded in solving exactly a time dependent nonequilibrium Kondo problem. The model consists of two leads that are coupled via tunneling through a Kondo impurity. The voltage across the leads is time dependent. Our solution allows us to compute all harmonics of the current, the differential conductance, magnetization, and magnetic susceptibility. We find that the resonances for the time dependent Kondo model occur at different characteristic frequencies than for the resonant level model. In some cases we are able to relate the differential conductance and the susceptibility, opening the possibility of doing susceptibility-like measurements on a single impurity using the differential conductance.

In the second area, we have modeled two dimensional charge and spin current flows in magnetic devices such as the spin-transistor. Not surprisingly we find that the current flows are complex and that there are hot spots in the nonequilibrium magnetization. Using the Onsager relations, however, we are able to relate the conductance in the spin-transistor geometry to those in the current perpendicular to plane giant magnetoresistance geometry. This justifies our earlier analytic work on this same problem.

High Field Magnetization of the Spin Fluctuation Compounds UPt_3, $U_{0.1}Pr_{0.9}In_3$, and $U_{1-x}Y_xAl_2$

Kim, J.S., UF, Physics
Haanappel, E., LANL
Mayr, F., Universität Augsburg, Fachbereich Physik
Stewart, G.R., UF/Universität Augsburg, Fachbereich Physik

Measurements on M versus H up to 50 T in pulsed fields are reported for the spin fluctuation compounds UPt_3 (where measurements up to 35 T already exist), $U_{1-x}Y_xAl_2$ and $Pr_{0.9}U_{0.1}In_3$. The known metamagnetic transition at 20 T in UPt_3 is observed; no further transition is observed in UPt_3 up to 50 T. Although the compounds $U_{0.9}Y_{0.1}Al_2$, $U_{0.7}Y_{0.3}Al_2$, and $Pr_{0.9}U_{0.1}In_3$ also show T^3lnT spin fluctuation terms in their specific heat with specific heat γ values spanning the range 190 - 670 mJ/mole

U-K^2, (where UPt_3 has $\gamma = 450$ mJ/mole-K^2), no metamagnetic transitions up to 50 T are observed in these systems. Possible scaling relations between $B_{metamag}$ and various parameters are discussed.

Magnetic Anisotropy and Magnetic Phase Transition in R_2Fe_{17} Compounds, Where R Represents Rare Earth Elements

Kou, X.C., Vienna Univ. of Technology, Austria
Grössinger, R., Vienna Univ. of Technology, Austria
de Boer, F.R., Univ. of Amsterdam, The Netherlands
Wolters, Ch., NHMFL

Until the present time, due to the limited availability of single crystals, the magnetic anisotropy of R_2Fe_{17} intermetallic compounds has not been studied in a systematic way. The main emphasis in the present report is on a systematic study of the magnetic anisotropy and the magnetic phase transitions in R_2Fe_{17} compounds with R = Y, Pr, Nd, Sm, Gd, Tb, Dy, Ho, Er, Tm, or Lu. The studied materials were magnetically-aligned by using the spin-sample-magnetic-alignment (SSMA) technique.[1] The degree of the magnetic alignment has been checked at room temperature by X-ray diffraction. Nearly perfect magnetic alignment was obtained in the [001] direction of the hexagonal (R = Y, Gd, Tb, Dy, Ho, Er, Tm, Lu) or the rhombohedral (R = Pr, Nd, Sm) structure.

Magnetization measurements have been carried out on the magnetically-aligned samples in the temperature range from 4.2 to 200 K in a vibrating sample magnetometer (VSM). External fields up to 29 T were applied either parallel or perpendicular to the alignment direction, i.e. the [001] direction. The observed field-induced phase transitions in the R_2Fe_{17} compounds are first-order magnetization processes (FOMP), which are due to the R-sublattice anisotropy. The crystalline electric field (CEF) acting on the magnetic R^{3+} ions is the origin for the existence of the FOMP transition. From an experimental point of view, the present investigation can be summarized as follows.

1. For the first time, a FOMP has been detected in Pr_2Fe_{17} ($H_{CR}(4.2\ K) = 5.9$ T) in an external field parallel to the [001] direction. Also in Nd_2Fe_{17} ($H_{CR}(4.2\ K) = 11.5$ T) and Er_2Fe_{17} ($H_{CR}(4.2\ K) = 5.5$ T), a FOMP transition was detected. In Tb_2Fe_{17}, ($H_{CR1}(4.2\ K) = 3.7$ T), $H_{CR2}(4.2\ K) = 10.1$ T), two FOMPs were found. The critical FOMP fields H_{CR} obtained at 4.2 K in the present investigation are in good agreement with the measurements on single crystals of Tb_2Fe_{17} [2] and Er_2Fe_{17} [3]. In addition, the onset temperatures of the FOMP transition were found to be around 200 K for Pr_2Fe_{17}, Nd_2Fe_{17}, Tb_2Fe_{17}, and around 100 K for Er_2Fe_{17}.

2. For the first time, the magnetocrystalline anisotropy of Sm_2Fe_{17} has been determined. At 4.2 K, the anisotropy field of Sm_2Fe_{17} is 13 T.

3. For Dy_2Fe_{17}, Ho_2Fe_{17}, and Tm_2Fe_{17}, a cross-over behavior on magnetization has been detected at low temperatures.

References:

1 Kou, X.C., *et al.*, J. Phys.: Condens. Matter, **8**, 1557 (1996).

2 Verhoef, R., *et al.*, J. Magn. Mater. 104-107, 1473 (1992).

3 Sinnema, S., Ph.D. Thesis, University of Amsterdam (1988).

Magnetization of 2D and 1D Quantum Heisenberg Antiferromagnets

Landee, C.P., Clark Univ., Physics
Albrecht, A.S., Clark Univ., Physics
Turnbull, M.M., Clark Univ., Chemistry

We are investigating the properties of several new families of low-dimensional S = 1/2 Heisenberg antiferromagnets with the goal of understanding the influence of quantum effects on the magnetic behavior. These new families have small exchange strengths (2J = 1 – 15 K), a novel feature that permits the examination of a variety of field-dependent properties that cannot be studied in the analogous copper oxide compounds.

One of the new families consists of layers of CuX_4 (X = Cl, Br) distorted tetrahedra packed into C-centered layers and separated by organic cations, 5-MAP or 5-CAP, where 5-MAP = 5-methyl, 2-aminopyridinium and 5-CAP is the chloro analog. The exchange interaction occurs through halide-halide contacts and is approximately five times stronger for the bromides than the chlorides. Preliminary susceptibility studies of $(5\text{-MAP})_2CuBr_4$ and $(5\text{-CAP})_2CuBr_4$ were interpreted using exchange strengths of 3.4 K and 4.3 K, respectively. Molecular field calculations indicate T = 0 K saturation fields of approximately 19 T and 24 T, respectively.

We have begun our high-field studies with low-temperature measurements of the magnetizations of these two compounds (Figure 1), using the NHMFL Vibrating Sample Magnetometer and a 30 T Bitter magnet. The observed saturation fields are in good agreement with the anticipated values. The data are notable for the upward curvature in the M(H) plot, a behavior qualitatively similar to that predicted[1] and observed for the linear-chain quantum Heisenberg antiferromagnet. We know of no corresponding theoretical prediction for the 2D case. Similar behavior has been seen in chloride analogs, $(5\text{-MAP})_2CuCl_4$ and $(5\text{-CAP})_2CuCl_4$, at correspondingly smaller fields.[2] Single crystal magnetization studies of $(5\text{-MAP})_2CuBr_4$ show evidence of slight magnetic anisotropy in this material.

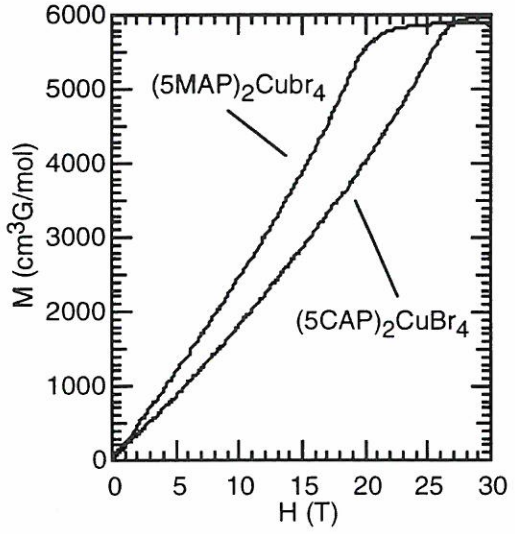

Figure 1. Molar magnetization at T = 1.3 K of $(5\text{-MAP})_2CuBr_4$ and $(5\text{-CAP})_2CuBr_4$.

References:

1 Griffiths, R.B., Phys. Rev., **133**, A768 (1964).

2 Hammar, P.R., *et al.*, J. Appl. Phys., in press (1997).

Phase Diagram of the One Dimensional Kondo Model for Manganese Oxides

Malvezzi, A.L., NHMFL
Yunoki, S., NHMFL
Dagotto, E., FSU, Physics/NHMFL

The Kondo model in one dimension is studied numerically as a model for the manganese oxides. The techniques used are Density Matriz Renormalization Group and Lanczos. For the localized ions, two values of spin are considered, i.e. S = 3/2 and S = 1/2. In order to study the nature of the ground state, quantities like the compressibility and structure factor are calculated for several values of the Hund coupling and electron concentration. If the Hund coupling is large a fully ferromagnetic phase dominates and for moderated values of that coupling a region of phase separation exists.

Rapid Suppression of the Spin Gap in Zn-Doped $CuGeO_3$ and $SrCu_2O_3$

Martins, G.B., NHMFL
Dagotto, E., FSU, Physics/NHMFL
Riera, J., Rosario Univ., Physics, Rosario, Argentina

The influence of non-magnetic impurities on the spectrum and dynamical spin structure factor of a model for $CuGeO_3$ is studied.[1] A simple extension to Zn-doped $SrCu_2O_3$ is also discussed. Using Exact Diagonalization techniques and intuitive arguments we show that Zn-doping introduces states in the Spin-Peierls gap of $CuGeO_3$. This effect can be understood easily in the large dimerization limit where doping by Zn creates "loose" S=1/2 spins, which interact with each other through very weak effective antiferromagnetic couplings. When the

dimerization is small, a similar effect is observed but now with the free S=1/2 spins being the resulting S=1/2 ground state of severed chains with an odd number of sites. Experimental consequences of these results are discussed. It is interesting to observe that the spin correlations along the chains are enhanced by Zn-doping according to the numerical data presented here. As recent numerical calculations have shown, similar arguments apply to ladders with non-magnetic impurities simply replacing the tendency to dimerization in $CuGeO_3$ by the tendency to form spin-singlets along the rungs in $SrCu_2O_3$.

Reference:

1 Martins, G., *et al.*, to appear in Phys. Rev. B.

Stability of Antiferromagnetic Ordering Versus Glassy Transition in $Fe_xZn_{1-x}F_2$

Montenegro, F.C., UFPE–Brazil, Physics
Lima, K.A., UFPE–Brazil, Physics
Torikachvili, M.S., San Diego State Univ., Physics
Lacerda, A., NHMFL/LANL

The tridimensional (d = 3) insulating compound $Fe_xZn_{1-x}F_2$ is used intensively as an experimental realization of a random-field Ising model system (RFIM). Most of the experimental work in this system has been performed at the weak RFIM regime, where antiferromagnetic long range order is stable at low temperature (T) for all concentrations to $x > 0.3$. Due to the large values of the exchange (H_E) and the anisotropic (H_A) fields of this compound, intense external magnetic field is needed in order to evaluate the tridimensional (H, T, x) phase diagram of the strong RFIM state. At the NHMFL–Los Alamos Facility, we have mapped the phase diagram of this compound for x = 0.6, 0.56, and 0.41. By applying the external magnetic field along the easy magnetization axis, we were able to observe an extension of the random-field-induced glassy phase for all measured concentrations. This phase was observed previously only for x = 0.31.[1] A multicritical point also arises for higher values of x, indicating the presence of the above mentioned glassy regime.

Reference:

1 Montenegro, F.C. *et al.*, Phys. Rev. B, **44**, 2155, 2161 (1991).

Electronic Hamiltonian for Transition Metal Oxide Compounds

Müller-Hartmann, E., Institut für Theoretische Physik, Universitat zu Koln, Koln, Germany
Dagotto, E., FSU, Physics/NHMFL

An effective electronic Hamiltonian for transition metal oxide compounds is presented.[1] For Mn-oxides, the Hamiltonian contains spin-2 "spins" and spin-3/2 "holes" as degrees of freedom. The model is constructed from the Kondo-lattice Hamiltonian for mobile e_g electrons and localized t_{2g} spins, in the limit of a large Hund's coupling. The effective electron bond hopping amplitude fluctuates in sign as the total spin of the bond changes. In the large spin limit, the hopping amplitude for electrons aligned with the core ions is complex and a Berry phase is accumulated when these electrons move in loops. The new model is compared with the standard double exchange Hamiltonian. Both have ferromagnetic ground states at finite hole density and low temperatures, but their critical temperatures could be substantially different due to the frustration effects induced by the Berry phase.

Reference:

1 Mueller-Hartmann, E., *et al.*, Phys. Rev. B, **54**, R6819 (1996).

Infrared Study of Magnetoelastic Coupling in the Spin-Peierls System $GeCuO_3$

Musfeldt, J.L., State Univ. of New York-Binghamton, Chemistry
Wang, Y.J., NHMFL
Li, G., SUNY-Binghamton, Chemistry

$GeCuO_3$ is the first inorganic compound found to undergo spin-Peierls transition.[1] Interest is

focused on its magnetic-field/temperature phase diagram, which has remarkable resemblance with that obtained from well-studied organic spin-Peierls materials.[2] In order to investigate the nature of the spin-Peierls transition and the lattice dynamics of the uniform, dimerized, and magnetic phases, we have made infrared reflectance measurements of $GeCuO_3$ as a function of temperature and applied magnetic field. The B_{3u} shearing mode near 300 cm^{-1} was found to be very sensitive to changes in the magnetoelastic coupling that take place with the uniform → dimerized and dimerized → magnetic phase transitions (see Figure 1), indicating this particular elastic motion of the lattice to be involved in the loss of the clear dimerization when applying the magnetic field or increasing the temperature.

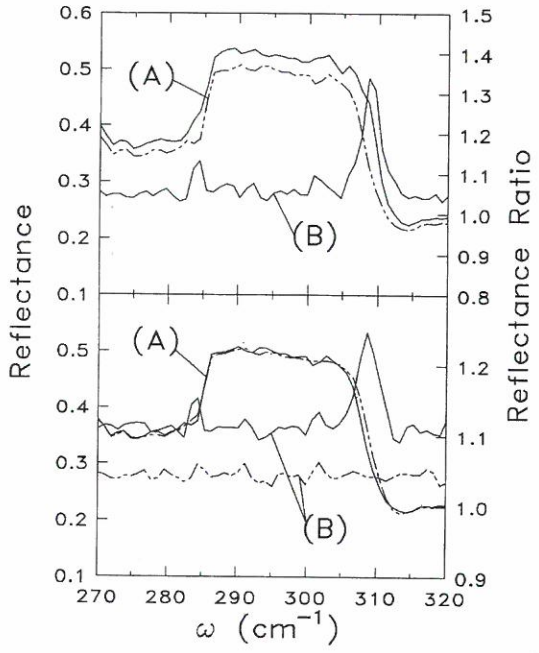

Figure 1. Upper panel: (A): Zero-field reflectance spectra of $GeCuO_3$. Solid line: T = 20K; double-dashed line: T = 5K. (B): Zero-field reflectance ratio for $GeCuO_3$: 20 K/5 K. Lower panel: (A): 5 K reflectance spectra taken at 0, 9 and 17 T. (B): 5 K reflectance ratios of $GeCuO_3$ as a function of applied field. Solid line: 17 T/0 T; double-dashed line: 9 T/0 T.

Application of a magnetic filed causes an unusual structure to develop in the reflectance ratio near 44 cm^{-1}, which moves in a systematic way with the increasing field (see Figure 2). Above the 12.5 T dimerized magnetic phase boundary, only the center feature of the structure remains. The field dependence of the dips in the reflectance ratio display a Zeeman like splitting, suggesting that we are probing the split of the second singlet/triplet gap, which is calculated to be 45 cm^{-1} at zero field[3]. We attribute the disappearance of the reflectance ratio dips to the 12.5 T transition to the magnetic phase.

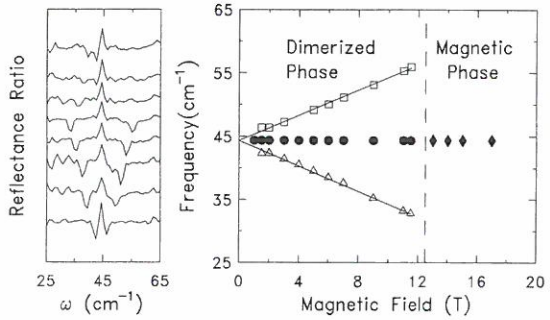

Figure 2. Left panel: reflectance ratios of $GeCuO_3$ at 5K. From bottom to top: 2 T/0 T, 5 T/0 T, 7 T/0 T, 9 T/0 T, 11 T/0 T, 13 T/0 T, 15 T/0 T, and 17 T/0 T. Right panel: frequency vs. magnetic field for the phonon structure shown in the left panel.

References:

1 Hase, M., *et al.*, Phys. Rev. Lett., **70**, 3651 (1994).

2 Bray, J., *et al.*, in *Extended Linear Chain Compounds*, Vol. 3, edited by J.S. Miller (Plenum, New York, 1983).

3 Nishi, M., *et al.*, Phys. Rev. B, **50**, 6508 (1994).

Increase Conductivity in UNiSn with the Application of Magnetic Fields

Ng, H.K., FSU, Martech and Physics
Wang, Y.J., NHMFL
Yuen, T., Temple Univ., Physics
Lin, C.L., Temple Univ., Physics
Love, B., FSU, Physics
Cope, C.J., FSU, Physics

UNiSn is a modified Huesler alloy that undergoes a semiconducting-to-metallic transition at 43 K.[1] Below this temperature it is also in an antiferromagnetic state. For the isostructural compound, ThNiSn, however, no such transition is observed. We examine the nature of the metallic state for UNiSn.

Figure 1 shows the frequency dependent conductivity of UNiSn for different magnetic field strengths. For frequencies above 400 cm^{-1}, the conductivity rises indicating the presence of a semiconducting gap. The value of the gap is consistent with resistivity measurements. With increasing fields, the oscillator strength is reduced, but the value of the gap is unchanged. At lower frequencies, there is a strong field dependence. The conductivity increases with field. The conductivity for frequencies below 100 cm^{-1} is a result of the metallic state of UNiSn. For ThNiSn no field dependence is observed. This implies that the increase in conductivity at low frequencies comes as a result of partial destruction of the antiferromagnetic state by the magnetic field. It can be further concluded that the metallic state of UNiSn is not related to the antiferromagnetic state.

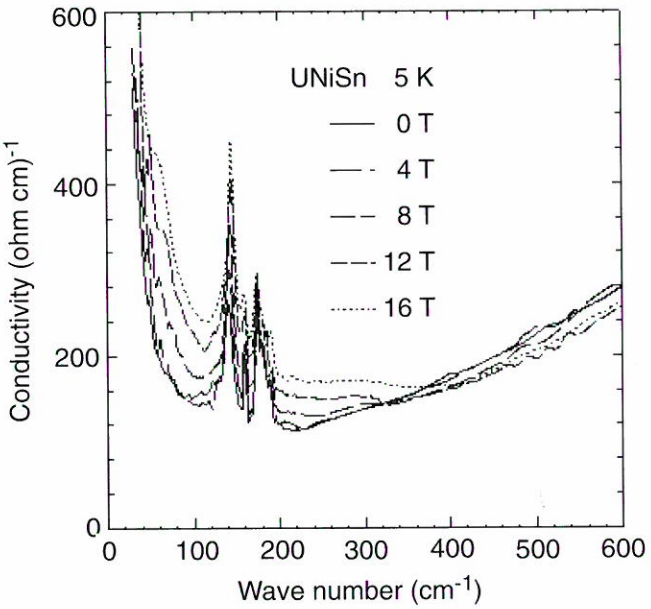

Figure 1. Real part of the conductivity. Note that there is a shift of oscillator strength from above 400 cm^{-1} to lower frequencies as field is increased. This shift results in increased conductivity in the metallic state.

In summary, magnetic field on UNiSn at 5 K does not change the value of the semiconducting gap. The field, however, shifts some of the spectral weight to lower frequencies resulting in higher conductivity in the metallic state. The increase in conductivity may be the result of partial destruction of the antiferromagnetic state by the field. No field dependence is observed for the isostructural compound ThNiSn.

References:

1 Bykovetz, N., *et al.*, J. Appl. Phys, **63** 8, 4127 (1988).

2 Aoki, Y., *et al.*, J. Magn. Mat., **90** & **91**, 496 (1990).

Direct Measurement of Zero Field Splitting in a One-Dimensional Heisenberg Antiferromagnet by High Frequency/High Field EPR Spectroscopy

Pardi, L., NHMFL

Reedijk, J., Univ. of Nijmegen, The Netherlands, Chemistry

Hulsbergen, F.U., Univ. of Nijmegen, The Netherlands, Chemistry

Brunel, L.-C., NHMFL

The study of the magnetism of one-dimensional Ni(II) systems has been pursued recently with the aim to investigate practical realization of one-dimensional Heisenberg antiferromagnets which, according to Haldane conjecture,[1,2] show an energy gap between the ground spin singlet state and the triplet state at the bottom of the excited band. Experimental evidence confirmed the existence of the energy gap.[1,2] The anisotropy term D is in general much smaller than the exchange coupling constant, and for that reason is generally treated as a perturbation of the exchange term, but in the case of divalent nickel it can be as high as 10 cm^{-1}. The possibility to have a direct measurement of D is in this contest very attractive because only indirect measurements exist, namely from the fitting of magnetic susceptibility and magnetization of single crystal sample. EPR spectroscopy is traditionally the appropriate tool to solve this problem. In this context the new high frequency/high field EPR techniques are a valuable tool offering radiation quanta ranging from the lowest limit of 3 to 11 cm^{-1} and higher.

Profiting of the fact that the series of linear chain compound $Ni(ox)L_2$ (where ox = oxalate and L is an imidazole) are prone to doping with Zn(II)

in any Ni/Zn ratio, we decided to study them in the low Nickel concentration range in order to measure the single ion ZFS of the Ni ions. From the spectra at 110, 220, and 330 GHz shown in Figure 1, the ZFS parameter is extracted and the sign of D is determined.

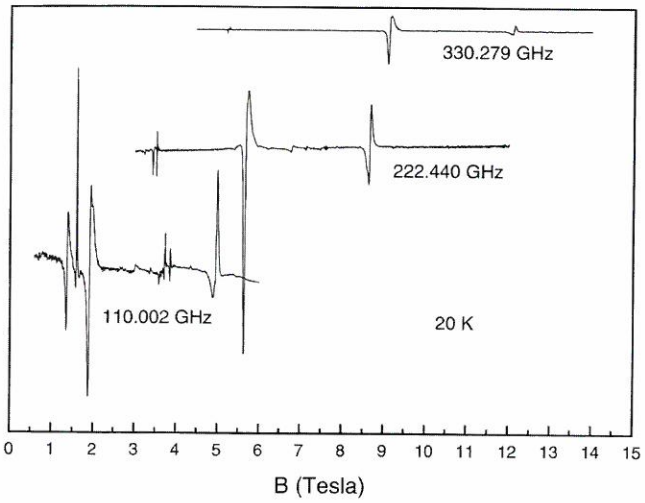

Figure 1. EPR spectra of Ni(ox)L_2 at 110, 220, and 330 GHz.

References:

1 Ajiro, Y., *et al.*, Phys. Rev. B, **51**, 9399 (1995).

2 Brill, T.M., *et al.*, Physica B, **204**, 303 (1995).

Ferrimagnetic Resonance in a Molecular-Based Magnetic Material

Pardi, L., NHMFL
Gatteschi, D., Univ. of Florence, Chemistry
Sessoli, R., Univ. of Florence, Chemistry
Caneschi, A., Univ. of Florence, Chemistry
Brunel, L.-C., NHMFL

The compound $[Mn(F_5benz)_2]_2NITEt$ (F5benz = pentafluorobenzoate, NITEt = 2 - Ethyl - 4,4,5,5 - tetramethyl - 4,5 - dihydro - 1- *H* imidazolyl - 1 - oxy - 3 - oxide) undergoes a magnetic phase transition at ca 20 K.[1] The ordered phase has been described as a ferrimagnet or a weak ferromagnet. High field/high frequency EPR spectra were recorded at the EMR facility of the NHMFL. The sample was in the form of a pellet in order to avoid orientation of the microcrystallites by the (high) magnetic field. The data in Figure 1 show a large temperature dependence of the EPR spectra, with a downfield shift of the perpendicular component and a upfield shift of the parallel component. Other component are also observable at low temperature. Similar results were obtained at higher frequencies. As expected in this kind of soft magnetic materials a broadening of the transition is observed in high magnetic field compared with the low field data.[1] These data can be interpreted in the frame of ferrimagnetic resonance.[2] More experimental work is needed to complete the frequency/magnetic field/ temperature phase diagram.

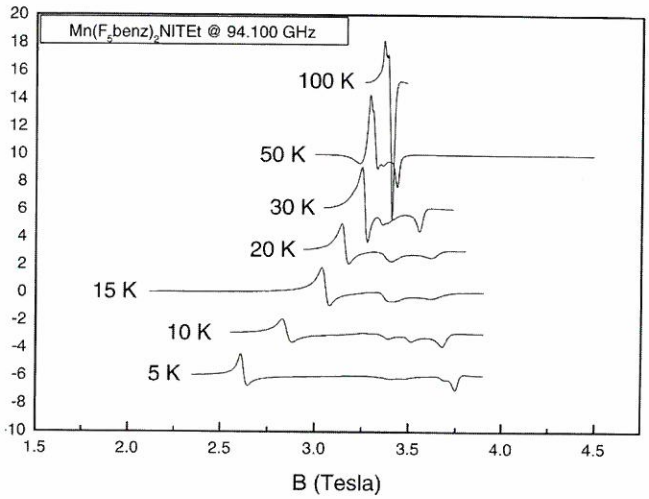

Figure 1. High field/high frequency EPR spectra of $[Mn(F_5benz)_2]_2NITEt$.

References:

1 Caneschi, A., *et al.*, J. Am. Chem. Soc., **111**, 785 (1989).

2 Foner, S. in *Magnetism I,* eds. G.T. Rado, *et al.*, (Academic Press, New York and London 1963).

Hall Effect Measurements on Colossal Magnetoresistive Materials

Salamon, M.B., Univ. of Illinois, Physics
Jaime, M., Univ. of Illinois, Physics
Hardner, H., Univ. of Illinois, Physics
Emin, D., Sandia National Laboratories
Rubenstein, M., Naval Research Laboratory
White, P., Univ. of Illinois, Physics
Lacerda, A., NHMFL/LANL

Once thought to be understood, the magnetoresistivity of materials based on $LaMnO_3$

has been the object of considerable reanalysis. In addition to the double-exchange mechanism proposed by Zener, it has become clear that strong electron-lattice effects are involved, resulting in self-trapping of the carriers above the ferromagnetic transition. The carriers are then small polarons, and exhibit activated conductivity and a thermopower whose characteristic energy is much smaller than the conductivity activation energy. The Hall effect in a small polaron conductor is not temperature independent as in a metal, but rather exhibits an activated Hall mobility with an activation energy one-third that of the electrical conductivity. What is more, when the hopping geometry permits triangular hopping paths, the sign of the Hall effect is always electron-like, even for hole doping.

In this experiment, we studied the Hall effect in laser-deposited films of $(La_{1-x}Gd_x)_{0.67}Ca_{0.33}MnO_3$. Using a high-temperature insert constructed for this purpose (and now part of the equipment complement at the NHMFL), we measured the Hall effect in the 20 T superconducting magnet at temperatures up to 600 K. When x = 0, the transition temperature is T_c = 250 K, and residual "colossal" magnetoresistance effects make it difficult, though not impossible, to extract the Hall coefficient in the small-polaron regime. Doping with Gd to x = 0.25 lowers the transition temperature to 140 K, and permits us to extract the Hall coefficient over a wide temperature range $2\,T_c < T < 4\,T_c$. We found that the Hall effect is electron-like, even though Ca doping should result in hole-like conduction as confirmed by the thermopower. Further, the activation energy for the Hall coefficient is two-thirds that of the electrical conductivity, a result that follows from small polaron theory. The anomalous sign of the Hall effect indicates that triangular hopping loops are possible, although the lattice is orthorhombic. We suggest that the non-collinear Mn-O-Mn bonds permit hopping directly across the face diagonals.

Reference:

1 Jaime, M., *et al.*, accepted for publication, Phys. Rev. Lett.

Anomalous Magnetoluminescence Intensity Changes in $Zn_{1-x}Mn_xSe$ Epilayers at High Magnetic Fields

Schmiedel, T., NHMFL
Lee, S., Univ. of Notre Dame, IN, Physics
Dobrowolska, M., Univ. of Notre Dame, IN, Physics
Furdyna, J.K., Univ. of Notre Dame, IN, Physics

In our high magnetic field studies of ZnMnSe, a representative wide gap II-VI-based diluted magnetic semiconductor (DMS) system, we have previously reported[1] the observation of a giant non-saturating red shift of the photoluminescence (PL) peak, which reflects the value $\langle S_z \rangle$ of the thermally averaged spin of the Mn ions. This shift also shows magnetization steps at a value of the exchange constant of about J = 18 T. We have now turned to the investigation of a second prominent feature of the luminescence spectra, the giant increase of PL intensity with field.

We also have investigated these phenomena in another set of molecular beam epitaxy (MBE) grown samples with the alloys CdMnSe, CdMnTe, and ZnMnTe as well as interrupted ZnMnSe epilayers where the ZnMnSe alloy is interrupted by monolayers of non-magnetic ZnSe. The PL behavior observed in these systems is essentially the same as in ZnMnSe, described above. All measurements were performed at 1.8 or 4.2 K with excitation from an argon laser at 364 nm. In Figure 1, we show a summary plot of the normalized peak intensity versus magnetic field of several ZnMnSe epilayers with different Mn content. Even at moderate fields of about 5 T, the peak intensity of some of the specimen has already increased by a factor of 10. At higher fields, all samples show the dramatic intensity increase regardless of the Mn concentration while a non-magnetic ZnSe epilayer does not.

We describe this behavior by thinking of the emission as consisting of radiative (Rad) and non-radiative (Nrad) recombination. Assuming the number of electrons and holes to be constant, the luminescence will depend on the wavefunction

overlap as well as the balance between Rad and Nrad recombinations. Once we rule out deep levels as electron traps, we concentrate on a scenario where a central role is played by the competition between bound and free exciton recombination. Bound excitons will acquire energy from the magnetic field and eventually be rendered free, enhancing the population of the free excitons, which we expect to act as more radiative centers.

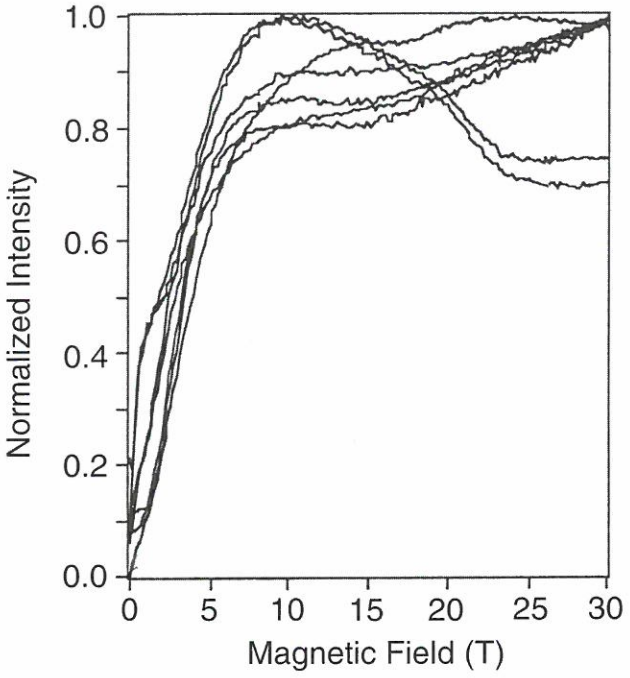

Figure 1. Normalized intensity of ZnMnSe with Mn concentration from 0.6 to 25%.

In a second scenario we consider acceptor and donor bound excitons. It has been shown by Pareek[2] that the red shift of free excitons in DMS alloys is substantially larger than either that of the donor- or the acceptor-bound excitons. Thus, as the field increases, the free exciton can eventually obtain the ground-state status. As the recombination from the free-exciton gradually becomes dominant, it will thus automatically also become increasingly radiative.

References:

1 Schmiedel, T., *et al.*, APS March Meeting, St. Louis, MO, 1996.

2 Pareek, A., Ph.D. Dissertation, Univ. of Notre Dame 1995 (unpublished).

One Particle Spectral Weight of the Three-Dimensional Single-Band Hubbard Model

Ulmke, M., Institut für Theoretische Physik, Aachen, Germany
Scalettar, R.T., UC Davis, Physics
Nazarenko, A., Boston College, Physics
Dagotto, E., FSU, Physics/NHMFL

Dynamic properties of the three-dimensional single-band Hubbard model are studied using Quantum Monte Carlo combined with the maximum entropy technique.[1] At half-filling, there is a clear gap in the density of states and well-defined quasiparticle peaks at the top (bottom) of the lower (upper) Hubbard band. We find an antiferromagnetically-induced weight above the naive Fermi momentum. Upon hole doping, the chemical potential moves to the top of the lower band where a robust peak is observed. Results are compared with spin-density-wave mean-field and self consistent Born approximation results, and also with the infinite dimension Hubbard model, and experimental photoemission for three-dimensional transition-metal oxides.

Reference:

1 Ulmke, M., *et al.*, to appear in Phys. Rev. B.

Phase Diagrams of the One- and Two-Dimensional Kondo Model for Manganites

Yunoki, S., NHMFL
Malvezzi, A.L., NHMFL
Hu, J., NHMFL
Moreo, A., FSU, Physics/NHMFL
Dagotto, E., FSU, Physics/NHMFL

The phase diagrams of the Kondo model for manganese oxides in one- and two-dimensions are studied using numerical techniques. The Monte Carlo method is applied to the 1D system, replacing the S = 3/2 t_{2g} spin by a classical spin, on chains of up to 80 sites. We find that there is a phase separation region at the electron concentrations next to that of the half-filled antiferromagnetic phase.

This phase has not been observed in previous studies. It is also shown that a ferromagnetic phase appears when the holes are doped further. A region of incommensurate spin order is also found. These phases are also observed for the 1D system with spin 3/2 t_{2g} using finite-size cluster studies (Lanczos and density matrix renormalization group methods). The phase diagram of the 2D system with classical spins is also discussed.

SCIENCE RESEARCH REPORTS

Other Condensed Matter

High Field Magnetotransport Measurements in EuB_6

Aronson, M.C., Univ. of Michigan, Physics
Cooley, J.C., Univ. of Michigan, Physics
Lacerda, A., NHMFL–LANL
Sarrao, J.L., NHMFL
Fisk, Z., NHMFL/FSU, Physics

We have measured resistivity and transverse magnetoresistance on a single crystalline sample of EuB_6 in magnetic fields to 18 T and temperature range 3 K < T < 100 K. The ferromagnetic transition (T_c) determined by resistivity vs. temperature measurements at constant fields varies from 10 K to 25 K at zero and 4 T, respectively. T_c is completely suppressed at 8 T. For $T > T_c$ a positive magnetoresistance is observed with slight indications of SdH oscillations at low temperatures. At high temperatures, $T > T_c$, a negative magnetoresistance is observed reaching -20% at 100 K (at 18 T). The effect of high applied magnetic field on the transport properties below T_c and the possibility of field induced metal-insulator transition is under investigation.

Spin-Lattice Relaxation of ^{87}Rb in the Charge-Density Wave State of $Rb_{0.3}MoO_3$

Brown, S.E., UCLA, Physics
Clark, W.G., UCLA, Physics
Zheng, G.-q., UCLA, Physics, and Osaka Univ.
Tanaka, K., UCLA, Physics
Kuhns, P.L., NHMFL
Moulton, W.G., NHMFL/FSU, Physics

$Rb_{0.3}MoO_3$ and its potassium analog are stoichiometric compounds with strongly anisotropic conductivity tensors. In both cases, a continuous metal-insulator transition is observed near 180 K indicating the onset of charge-density wave (CDW) order. The order parameter is known to be incommensurate with the lattice, and the observed non-ohmic conductivity below the transition is associated with the sliding of the density wave.

^{87}Rb NMR has been shown to be a valuable probe of both the static and dynamic properties of the CDW. The coupling is through the nuclear quadrupole moment and the modulation of the electric field gradient. Of relevance for this work is the observation of an enhanced spin-lattice relaxation rate ($1/T_1$) below the transition; it has many features consistent with relaxation by phase fluctuations of the CDW.[1] The fluctuation spectrum is expected to be frequency-dependent.[1,2] By sampling $1/T_1$ at different fields (and thus different Larmor frequencies), we can reconstruct the fluctuation spectrum and compare to charge-transport measurements.

In Figure 1, we show a spectrum for the (-1/2,1/2) central transition with external field B_0 = 21.1 T (f_N = 275.94 MHz) obtained at the NHMFL. There are two lines, because there are two unique sites with different second-order quadrupolar shifts. The crystal orientation is such that some CDW broadening is just barely evident for the lower-frequency line. Two distinct values of $1/T_1$ can be measured because the features are well-separated. Measurements for the more prominent feature in the spectrum were carried out at 80 K and 21.1 T for several crystal orientations, all in a plane perpendicular to the high-conductivity axis (along which the CDW slides). We found $1/T_1 \sim 1.3\ s^{-1}$ in all cases. The smaller of the two features exhibited an angular dependence of T_1 which was generally longer. More complete analysis will proceed in conjunction with studies at lower fields.

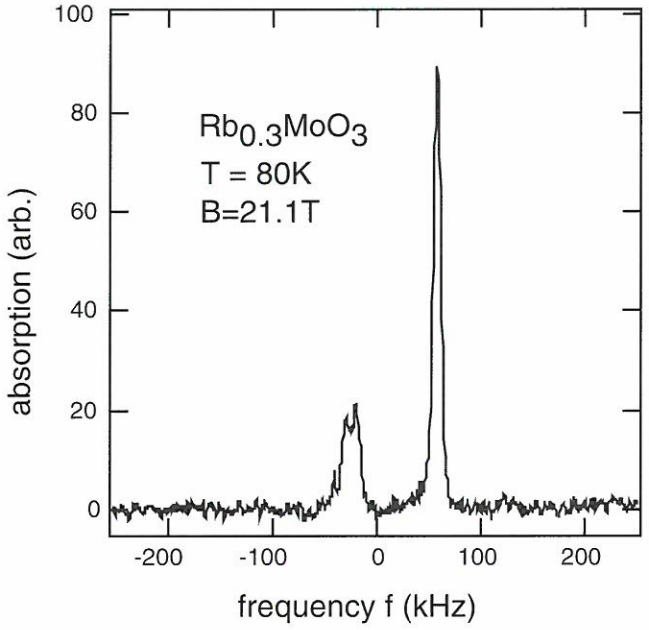

Figure 1. Spectrum for ^{87}Rb central transition in $Rb_{0.3}MoO_3$ at 80 K and B_0 = 21.1 T.

References:

1 Berthier, C., in *Nuclear spectroscopy on charge-density wave systems*, Butz, T., editor, p. 205 (Kluwer, Dordrecht, 1992).

2 Brown, S.E., *et al.,* (submitted to Phys. Rev. B).

High Field EPR Spectroscopy of Low-Dimensional Magnetic Systems: The Role of Exchange Effects and g-Strain in Determining Spectral Resolution

Dalal, N.S., FSU, Chemistry/NHMFL
Cage, B., FSU, Chemistry
Hassan, A., FSU, Chemistry/NHMFL
Pardi, L., NHMFL
Krzystek, J., NHMFL
Brunel, L.-C., NHMFL

The objective of this investigation was to evaluate the role of electron spin exchange and g-strain processes in the overall resolution of EPR spectra of undiluted S=1/2 paramagnetic systems. The major impetus for this undertaking derived from the fact that while earlier work had demonstrated the utility of high magnetic fields in enhancing the g-factor resolution, these studies had focused on dilute paramagnetic samples (millimolar spin concentrations), where exchange effects are minimal or non-existent. For undiluted systems, such as those that undergo magnetic ordering, exchange effects play a dominant role in determining their spectral linewidths, and these systems need to be examined systematically as a function of applied magnetic fields and exchange parameters.

Our studies utilized Cr(V) ($3d^1$, S=1/2) systems that had been earlier investigated by low-field EPR, magnetic susceptibility, and group-theoretical techniques.[1] The compounds investigated were the Cr(V)-peroxychromates of the various alkali metals (Li, Na, K, Rb, Cs, and their mixed crystals). The EPR measurements were carried out at various frequencies ranging from 9.5 GHz to 375 GHz, with the corresponding resonance fields varied from 0.3 to 14 tesla (T). Figure 1 shows some typical spectra for one of the samples, Na_3CrO_8. The three spectra presented here were obtained at the applied fields of 0.34 T, 3.95 T and 13.6 T, as marked. It is evident that the spectral resolution improved with the strength of the applied field, thereby demonstrating that at least for the S=1/2 systems, the EPR resolution improves at high magnetic fields, for the Zeeman strengths up to 14 T. Prior to this work,[2] it

was a normal practice that to obtain a high resolution EPR spectrum of a paramagnetic system, one must dilute it by doping it into a diamagnetic host, but with the possible change in the crystal field environment. This study demonstrates that high field EPR enables one to obtain the same information, at least on the Zeeman interaction, without the need to change the chemical environment.

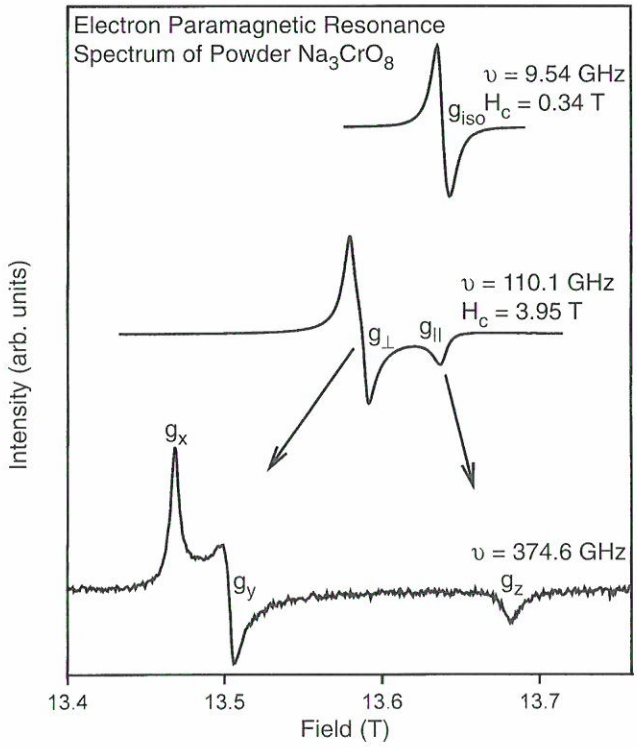

Figure 1. Comparison of the EPR spectra of Na_3CrO_8 powder at 9.54 GHz / 0.34 T (top), 110.1 GHz / 3.95 T (middle) and 374.6 GHz / 13.6 T (bottom). Notice how the singlet in the 0.3 T spectrum splits into a well resolved triplet at 13.6 T, implying a substantial enhancement in spectral resolution as a function of the applied field.

References:

1 Dalal, N.S., *et al.*, J. Chem. Phys., **74**, 1916 (1981).

2 Cage, B., *et al.*, J. Magn. Reson. (in Press), Feb. (1997).

Mean Field Theory of the Mott-Anderson Transition

Dobrosavljevic, V., NHMFL
Kotliar, G., Rutgers Univ., Physics

The nature of the metal-insulator transition is a fundamental problem in condensed matter science. There are two basic mechanisms that cause electron localization. Mott demonstrated that electron-electron interactions, can produce a metal insulator transition (MIT) even in a clean system. Anderson discovered that disorder, i.e. strong spatial fluctuations in the potential due to impurities, can drive a metal insulator transition in a system of non interacting electrons.

Despite many years of intense effort, many basic questions about the metal-insulator transition remain essentially unanswered. In particular, it proved very difficult to incorporate the effects of strong electronic correlations, such as the formation of local magnetic moments, in a comprehensive theory of the MIT. This is a serious shortcoming, since it is well established experimentally that the metallic state close to the MIT is characterized by a divergent magnetic susceptibility and linear specific heat coefficient.

Very recently, a new approach[1] to the strong correlation problem has been developed and successfully applied to systems in the vicinity of the Mott transition. The approach has furthermore been extended to disordered systems[2] and used to investigate phenomena such as disorder-induced local moment formation. If formulated in its strict large-coordination limit, however, the theory misses strong spatial fluctuations, and thus cannot incorporate Anderson localization effects.

The goal of the present study is to present a theory[3] that can describe both the Mott and the Anderson route to localization, and therefore address the interplay of these effects. We follow an approach very similar to the well known Thouless-Anderson-Palmer (TAP) formulation of the mean field theory of spin glasses. Specifically, we treat the correlation aspects of the problem in a dynamical mean-field theory fashion, but allow

3 Barber, B.P., *et al.*, Phys. Rev. Lett. **69,** 3839 (1992).

4 Hiller, R., *et al.*, Phys. Rev. Lett. **69** , 1182 (1992).

5 Barber, B.P., *et al.*, Phys. Rev. Lett. **74,** 5276 (1995).

6 Chou, T., *et al.*, Phys. Rev. Lett. **76**, 1549 (1996).

7 Young, J.B., *et al.*, Phys. Rev. Lett. **77**, 4816 (1996)

A New 2D Quantum Rotor Glass

Kim, K., UF, Physics
Sullivan, N.S., UF, Physics/NHMFL

NMR studies in moderately high magnetic field (~ 7 T) of films of hydrogen physisorbed on carefully prepared hexagonal BN surfaces have revealed new orientationally ordered structures for registered $\sqrt{3}\times\sqrt{3}$ submonolayer film as well as for incommensurate full monolayer coverages. In view of the small number of spins in the films, high magnetic field NMR studies are important in order to obtain useful signal-to-noise ratios.

The ortho-H_2 molecules behave as quantum rotors with angular momentum J = 1 and at low temperatures the molecules adopt orientations to minimize their anisotropic (principally electrostatic quadrupole-quadrupole) interactions. The interactions with the substrate also have an anisotropic component, and as a result of the competitions between the two types of interactions, there is a rich variety of ordered structures that can result (theoretically) depending on the relative strength of the interactions. Furthermore, the intermolecular interactions are highly frustrated as the underlying lattice symmetry is incompatible with the symmetry properties of this interaction. As a result of frustration, it is expected that a small amount of disorder will suffice to suppress long-range periodic ordering and result in a spin-1 tensorial glass-ordering at low temperatures.

NMR studies are ideal for studying the ordering of diatomic molecules as the quadrupolar order parameters can be determined directly from the line shapes. For a unique order parameter (e.g. ferro-orientational ordering) the line shapes are similar to the familiar Pake doublet line shapes, and for the glass state they become characteristic "helmet" shaped absorption lines. Quadrupolar glasses have been observed for 3D samples, but experiments for 2D ortho-para mixtures have not been carried out previously. The changes from one ordered structure to another can be identified from sharp changes in the NMR line shapes, and the different phases also give very different forms for the NMR lines: narrow Gaussian for the disordered phase ($\bar{\sigma}\cong 0$, $\langle\sigma^2\rangle^{1/2}\cong 0.2$), long-range herringbone phase ($\bar{\sigma}\cong 0.85$, $\langle\sigma^2\rangle^{1/2}\cong 0.85$), spin-1 glass ($\bar{\sigma}\cong 0.5$, $\langle\sigma^2\rangle^{1/2}\cong 0.5$). There are two different possibilities for periodic ordering: herringbone (HB) and pinwheel (PW) ordering, and the NMR experiments alone cannot distinguish between these structures. The theoretical predictions of the conditions for the formation of theses phases are, however, very clear, and we identify the low concentration low temperature long range ordered structure as a herringbone orientational ordering. The phase diagrams for the commensurate $\sqrt{3}\times\sqrt{3}$ submonolayer coverage, and the incommensurate full monolayer coverage is shown in Figures 1 and 2, respectively.

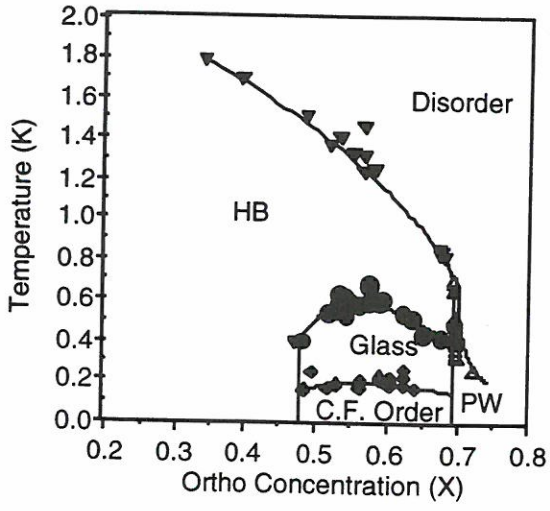

Figure 1. Phase diagram for commensurate $\sqrt{3}\times\sqrt{3}$ submonolayer coverage of H_2 on BN.

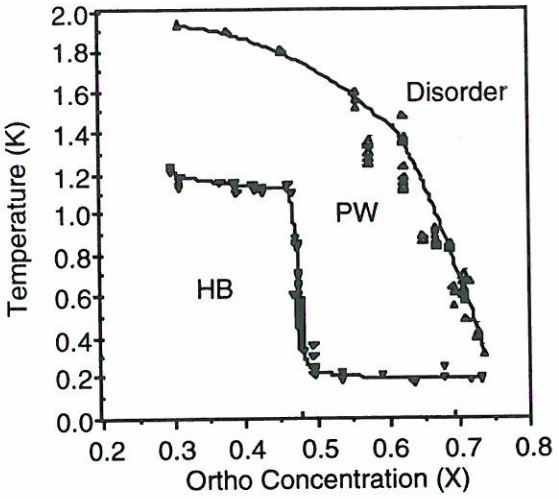

Figure 2. Phase diagram for an incommensurate full monolayer coverage of H_2 on BN.

Photoluminescence Studies of Modulation Doped Coupled Double Quantum Wells in Pulsed Magnetic Fields

Kim, Y., NHMFL/LANL
Perry, C.H., NHMFL/LANL and Northeastern Univ., Physics
Rickel, D.G., NHMFL/LANL
Simmons, J.A., Sandia National Laboratories
Jones, E.D., Sandia National Laboratories
Klem, J.F., Sandia National Laboratories

Strongly coupled double quantum well (QW) structures have been receiving increasing attention as new phenomena arise due to the combined effect of tunneling and electron-electron interactions. We have studied the temperature dependence of the magneto-photoluminescence (MPL) spectra in pulsed magnetic fields up to 65 tesla (T) for three different n-type modulation doped GaAs/AlGaAs coupled double quantum wells.[1]

These samples typically have well widths of 13-15 nm, barriers of 2.5-3.5 nm, and carrier concentrations in the 10^{11}-10^{12} cm^{-2} range. They have been subjected to magnetic fields parallel and perpendicular to the growth direction. For in-plane magnetic fields, large deviation in the cyclotron mass have been observed near the energy gap formed from an anticrossing of the two QW dispersion curves.[2]

The MPL spectra show distinct Landau transitions for B//z with abrupt changes in slopes at the intersection of the Landau fans associated with symmetric and antisymmetric intersubband states. At low fields below 5 T, the spectral peaks show forbidden Landau level transitions and 0-0 Landau level transition is missing. At high fields above 5 T, however, the lowest transition smoothly approaches to 0-0 Landau level. The spectra observed in in-plane B fields display magneto-excitonic behavior. At higher fields beyond 30-40 T the lowest transition clearly subdivided into two peaks. We have attributed these peaks to spin splitting. The partial energy gap discovered in conductance measurements in in-plane fields was not conclusively observed using photo-luminescence spectroscopy, although anomalies in the energy dependence of the lowest level with magnetic field were evident at similar field values.

References:

1 Kim, Y., *et al.*, in *Proceedings of the 23rd International Conference on the Physics of Semiconductors* (Berlin, Aug. 1996), ed. Zimmerman, World Scientific, Singapore, **3**, 1859 (1996).

2 Simmons, J.A., *et al.*, Phys. Rev. B, **51**, 1156 (1995).

Magneto-Optical Investigations of Neutral and Charged Excitons in a Periodic GaAs/(Al,Ga)As Quantum Wells

Lee, K.-S., Electronics and Telecommunications Research Institute, Korea
Kim, Y., NHMFL/LANL

We have observed the neutral and the charged excitons from photoluminescence investigations of a periodic GaAs/(Al,Ga)As quantum wells(QW). The sample used in this work consists of four 32, 21, 14, and 9 nm GaAs wells separated by 15 nm (Al,Ga)As barriers, and a 60 nm GaAs cap. The 4.2 K photoluminescence spectrum clearly shows peaks associated with the neutral and charged excitons localized in each well. This result is understood by that the tunneling probability of an

electron from a narrow well to a wide well is higher than that of a hole and that the imbalance of charges is resulted in each well. Therefore, we associate the lower line of the doublet peaks from a 32 nm QW as the negatively charged exciton (X^-) and the similar peaks from other QWs as the positively charged exciton (X^+). Magnetoluminescence investigations of the neutral and the charged excitons were performed in DC fields to 18 tesla (T). The Zeeman splitting of X^- singlet state is rather smaller than that of the neutral exciton. The binding energy of a trion, defined by the energy difference between the 1s neutral exciton and X^- without taking into account the Zeeman splitting, increases from 1.1 meV to 1.8 meV for magnetic fields from 0 to 6 T, but are saturated at 1.8 meV for $B > 6$ T.

Work at the NHMFL is supported through the NSF Cooperative Agreement #DMR 95-27035, the State of Florida, and the U.S. Department of Energy. K-S. Lee has been partly supported by the Ministry of Information and Communications, Korea.

Analysis of Electrophoretic Transport of Macromolecules by Pulsed Field Gradient Nuclear Magnetic Resonance

Locke, B.R., FAMU-FSU Chemical Engineering
Moerland, T.S., FSU, Biology
Kinsey, S., FSU, Biology
Penke, B., FAMU-FSU Chemical Engineering
McFadden, L., FSU, Biology
Gibbs, S.J., NHMFL/FAMU-FSU Chemical Engineering

The overall objective of the work in this project is to apply pulsed field gradient NMR spectroscopy (PFGNMR) to the analysis of electrophoretic and diffusive transport of biological molecules in solutions of polymers, in gels and in gel-like media. This project is supported by NASA through grant UGS95-0041. The work performed during the last year has focused on measurement of water self diffusion in gels and polymer solutions, comparing these results with other measurements from the literature and with theoretical models developed in the literature. These measurements, coupled with other NMR measurements of pore size distributions in these same gels, have been used to test theoretical models developed in the literature for diffusion in polymer gels. NMR spectra were acquired using a pulse sequence using incorporated bipolar gradients and a longitudinal eddy current delay (BPP-LED). Samples in capillary tubes were placed in a microsolenoid radio frequency transceiver coil (2.2 mm ID), which was tuned to a 1H resonant frequency of 600 MHz.

The major findings for the water self-diffusion in polyacrylamide gels found to date include the following. (1) There were no effects of diffusion time, the time for the NMR experiment, for water self-diffusion in solutions or gels during the course of experiments with times ranging from 10 to 900 ms. This result is expected, however it is in contrast to one published study from the literature. (2) The diffusion coefficients for gels and solutions were observed to decrease monotonically with increasing polymer concentration as would be expected by diffusion theory in matrices of rigid obstructions. (3) The diffusion coefficients in the gel showed no effect of the gel cross-linking. This result was somewhat surprising in light of reported work using light scattering, which shows that the pore size distribution in polyacrylamide gels is markedly influenced by the extent of crosslinking. Our results have been fully verified using multiple sample tests with various gel preparations and NMR runs. It may be that for water in these gels the nature of the pore size distribution plays a small role in determining the self-diffusion coefficient. Further work with larger probes and various crosslink concentration will be carried out. There is very limited information on the effect of crosslink concentration on macromolecular diffusion in these gels in the literature. (4) The diffusion coefficients for water at 5% total acrylamide were the same in crosslinked gels, in uncrosslinked polymers, and in solutions of monomers. This is a new and interesting result that shows that the low acrylamide concentration gels behave in manner very similar to polymer solutions.

Rapid Suppression of the Spin Gap in Zn-Doped $CuGeO_3$ and $SrCu_2O_3$

Martins, G.B., NHMFL
Hassan, A., NHMFL
Pardi, L., NHMFL
Brunel, L.-C., NHMFL
Riera, J., Instituto de Física Rosario, Argentina
Dagotto, E., NHMFL

The influence of nonmagnetic impurities on the spectrum and dynamical spin structure factor of a model for $CuGeO_3$ is studied. A simple extension to Zn-doped $SrCu_2O_3$ is also discussed. Using exact diagonalization techniques and intuitive arguments we show that Zn doping introduces states in the spin-Peierls gap of $CuGeO_3$. This effect can be understood easily in the large dimerization limit where doping by Zn creates "loose" S=1/2 spins, which interact with each other through very weak effective antiferromagnetic couplings. When the dimerization is small, a similar effect is observed but now with the free S = 1/2 spins being the resulting S = 1/2 ground state of severed chains with an odd number of sites. Experimental consequences of these results are discussed. It is interesting to observe that the spin correlations along the chains are enhanced by Zn doping according to the numerical data presented here. As recent numerical calculations have shown,[1] similar arguments apply to ladders with nonmagnetic impurities simply replacing the tendency to dimerization in $CuGeO_3$ by the tendency to form spin singlets along the rungs in $SrCu_2O_3$.

Reference:

1 Montome, Y., *et al.*, preprint.

Block Spin Approach to Electron Correlations

Monthoux, P., FSU, Physics/NHMFL
Manousakis, E., FSU, Physics

After Wilson[1] successfully applied the renormalization group program to the Kondo problem, there were numerous attempts to use the renormalization group formalism, such as the real-space Kadanoff "block-spin" transformation, to the quantum many-body problem and in particular to lattice Hamiltonians.

In the simplest of the real-space schemes, one only kept a few of the low energy states in each block and either completely neglected the high energy states or calculated their contribution to second order in the block-block interaction. The blocks then were grouped into super-blocks and the lowest energy states of the super-blocks were retained and so on.

Unfortunately, because of the small energy difference between the highest state retained and the lowest state to be integrated out, the problem is non-perturbative and also non-local, since the block-block interaction treated to high orders of perturbation theory generates long ranged effective Hamiltonians.

A block spin basis is, however, a good starting point to expand the ground state wavefunction of a finite system, provided the basis is chosen variationally. To obtain a set of many-block configuration which is optimal to describe ground state correlations, given the relatively small number of basis states that can be handled in practice, we use partitioning and state selection techniques developed in the context of Quantum Chemistry by K.G. Wilson[2] and the Ohio State University group. This approach allows one to recover 99.9% of the correlation energy with only 5 X 10^{-5}% of the Hilbert space for a 40-site Heisenberg spin chain,[3] a problem that is totally out of the reach of exact diagonalization techniques. The spin-spin correlations at the largest distance are within 1% of the "exact" results (obtained from Quantum Monte Carlo methods). We plan to extend the approach to higher dimensions.

References:

1 Wilson, K.G., Rev. Mod. Phys., **47**, 773 (1975).

2 Wentzel, W., *et al.*, Phys. Rev. Lett., **69**, 800 (1992); Steiner, M.M., *et al.*, Chem. Phys. Lett., **231**, 263 (1994).

3 Monthoux, P., *et al.*, in preparation.

Fermi Surface Parameters in Highly Correlated Systems

Vuillemin, J.J., Univ. of Arizona, Physics
Goodrich, R.G., Louisiana State Univ., Physics
Hall, D., Louisiana State Univ., Physics
Chaparala, M.V., Univ. of Virginia, Physics

High-field de Haas-van Alphen (dHvA) measurements were made in the exchange-enhanced metal palladium at temperatures between 2.0 and 0.5 K. The dHvA oscillations were observed in the field of a 30 T resistive magnet at the National High Magnetic Field Laboratory (NHMFL) in Tallahassee. Previous studies in palladium do not include steady fields this high. The present data yield new information about Zeeman splitting in the Landau levels. This knowledge is useful for understanding exchange and correlation effects in metals.

The dHvA oscillations were detected using field modulation and cantilever force magnetometry. Analysis focused on the oscillation due to the small hole pocket in the Fermi surface centered at the L point in the Brillouin zone (see Figure 1). With the field near [100], the corresponding dHvA frequency was found to be 224 T in agreement with previous work. Near the highest field, the tenth Landau level passes through the Fermi energy and the dHvA amplitude grows at an anomalous rate.

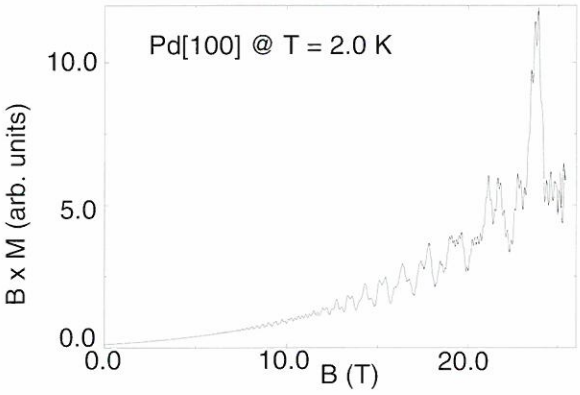

Figure 1. Magnetometer signal versus the field B.

The harmonic content in the oscillations contains new information about spin splitting in the Landau levels. The ratio of harmonic amplitudes permit the first measurement of Zeeman splitting for the small L-pocket of holes in the Fermi surface. The spin splitting is amenable to theoretical analysis including exchange and correlation effects.[1] The present experimental information should contribute to a better understanding of the properties of exchange-enhanced metals. Further experiments are planned at different field orientations to obtain the anisotropy in the Zeeman splitting.

Reference:

1 Hjelm, A., J. of Mag. Mat., **104-107**, 727 (1992).

Magnetic Resonance Techniques

NMR Techniques Development

Boulat, B., NHMFL
Epstein, D.M., Mitoxix Inc.
Rance, M., Univ. of Cincinnati, College of Medicine
Desvaux, H., NHMFL and CEA (France)

Three main projects were conducted and finalized during the period covered by this report:

1. Numerical analysis of the synchronous nutation experiment applied to determine the off-rate constant of the folate molecule in a biomolecular complex comprised of the enzyme dihydrofolate reductase (DHFR) and the ligand folate. *E. Coli* DHFR is composed of 159 amino acids and has a molecular weight of 18 Kdalton. It has been characterized in exquisite structural and dynamic details[1,2] and has proven to be an attractive target for rational drug design.

Using double radio frequency irradiation the modified synchronous nutation method[3] allows to isolate a pair of non-equivalent nuclear spins with respect to cross-relaxation and slow exchange with further nuclear spins. The two irradiated spins can exchange magnetization, due to some nuclear Overhauser effect or underlying chemical exchange process. In analyzing the outputs of this experiment it is not necessary to take into account the effect of spin diffusion. The numerical analysis can thus be performed using a spin system containing a very small number of spins (three in the present case). The NMR experiments were performed at The Scripps Research Institute, La Jolla, California. The numerical analysis was performed using a program whose underlying mathematical formalism was described earlier.[4] The program was run on the SGI Power Challenge located at the NHMFL. Participants to the project: B. Boulat, D.M. Epstein, and M. Rance.

2. Implementation at the Varian 17 T (720 MHz proton frequency) high resolution NMR spectrometer located at the NHMFL, of an NMR experiment designed by H. Desvaux, to measure homonuclear dipole-dipole cross-correlations. The measurement of dipole-dipole cross-correlations allows the determination of the angle subtending two internuclear vectors joining three different nuclei. The experimental scheme developed by H. Desvaux, utilizes a two-dimensional approach that correlates triple-quantum coherences with the single quantum coherences that are obtained from them via dipole-dipole cross-correlations. The experimental procedure enables the recording of in-phase signals in both dimensions. This feature allows a safe quantitative analysis of the experimental outputs. The experiments were conducted on the decapeptide cyclosporin. Participants to the project: B. Boulat and H. Desvaux.

3. Design and implementation of new NMR experiments aimed at recording the creation of multispin order by semi-selective irradiation of a single spin multiplet. Results were obtained for both homo- and hetero-nuclear spin systems. In the homonuclear case the method was applied to assign the resonances of nuclear spins in carbohydrates, in which this task if often difficult to perform due to poor spectral dispersion. The experimental scheme was implemented at the Bruker 7.05 T (300.13 MHz proton frequency) and at the Varian 11.77 T (500.13 MHz proton frequency), both located at the NHMFL. Participant to the project: B. Boulat.

References:

1 Bystroff, *et al.*, Biochemistry, **30**, 3263 (1990).

2 Falzone, *et al.*, J. Biomol. NMR, **4**, 349 (1994).

3 Boulat, B., *et al.*, JMR, **A120**, 223 (1996).

4 Boulat, B., *et al.*, Mol. Phys., **83**, 1021 (1994).

Simple, Distortion-Free Homonuclear Spectra of Proteins and Nucleic Acids in Water Using Excitation Sculpting

Callihan, D., FSU, Chemistry
West, J., Walt Disney Memorial Cancer Center
Kumar, S., Walt Disney Memorial Cancer Center
Schweitzer, B.I., Walt Disney Memorial Cancer Center and Univ. of Central Florida, Chemistry
Logan, T.M., NHMFL/FSU, Chemistry

We have modified standard two dimensional homonuclear experiments used in the assignment and structure determination of peptides, carbohydrates, and nucleic acids to improve solvent suppression. NMR spectra of these compounds must be collected in aqueous solution, often in the presence of ^1H_2O, and suppressing the intense solvent signal generates significant problems with dynamic range, baseline and phase distortion, and signal loss through saturation transfer. Improved solvent suppression and phase/baseline behavior are obtained by incorporating the excitation sculpting building block, developed by Shaka and co-workers, at the end of standard TOCSY and NOESY experiments, as shown in Figure 1.

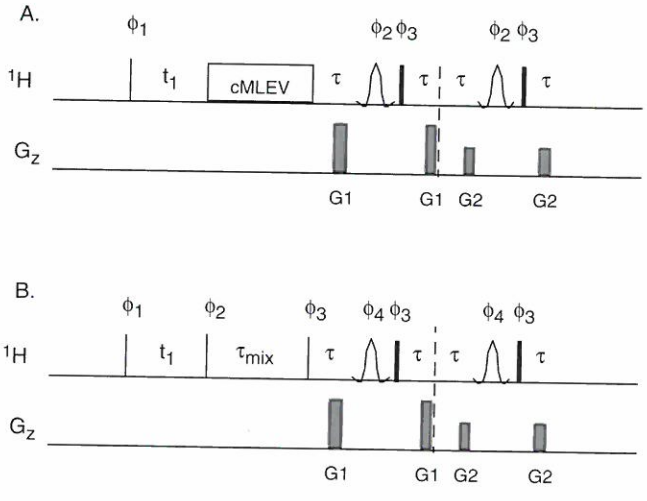

Figure 1. Pulse sequences for TOCSY (A) and NOESY (B) experiments using excitation sculpting solvent suppression.

The excitation sculpting building block uses a double spin echo into the end of the pulse sequence. Solvent suppression is effected by selective rotation of the solvent resonance coupled with dephasing by pulse-field gradient pulses symmetrically placed about the spin echo 180° pulse. The key to the solvent suppression is the use of two spin echoes with vastly different gradient pulse amplitudes. The degree of suppression is excellent as shown in Figure 2.

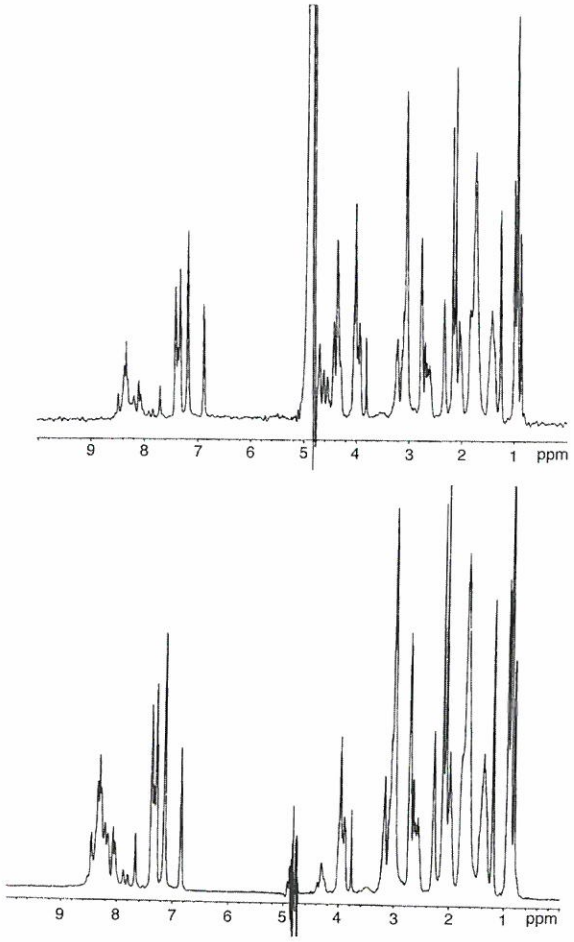

Figure 2. Comparison of presaturation (top) and excitation sculpting for solvent suppression. The sample is a 17 residue peptide.

This method is general and easily implemented in other homonuclear two dimensional pulse sequences to provide improved solvent suppression (Callihan and Logan, unpublished).

Field Stabilization and ^2H NMR Spectroscopy in a 24.6 T Resistive Magnet

Cross, T.A., NHMFL/FSU, Chemistry, and
Institute of Molecular Biophysics
Cotten, M., NHMFL/FSU, Chemistry
Soghomonian, V., NHMFL/FSU
Rosanske, R., FSU, Chemistry

High magnetic fields offer unique conditions and challenges for conducting NMR spectroscopy. Literature abounds on the advantages and disadvantages of high magnetic fields for NMR spectroscopy. In the 24 T magnet system we demonstrate two advantages of high B_0 fields for solid state deuterium spectra: (1) reduction of tau values in quadrupole echo sequences that allows for the detection of spins possessing short relaxation times, and (2) enhanced sensitivity.

The characteristics of the raw magnetic field of the 24 T magnet are dominated by temporal instability and spatial inhomogeneity. The temporal instability is dictated by the temperature of the inlet cooling water and by power supply ripple. To compensate for the temporal instability, a field/frequency lock unit and a flux stabilizer have been installed. This arrangement provides a stable magnetic field allowing for extensive signal averaging. The spatial homogeneity of the magnet yields, for a 2 mm spherical sample of D_2O, a 1.7 ppm linewidth at half height.

Within the present spatial and temporal restrictions, a number of deuterium powder pattern spectra and spectra of uniformly-oriented samples have been recorded. These preliminary experiments reveal short quadrupole echo delays (15 μs) that will allow for the detection of signals unobtainable at lower field strengths where echo delays are longer due to the frequency dependence of acoustic ringing. This advantage is exploited for samples in liquid crystalline media where sensitivity is often compromised by efficient T_{2e} relaxation that occurs during the echo delays. Figure 1 demonstrates the spectra of d_4 alanine obtained on the 24 T resistive magnet system. The observed quadrupolar splitting in Figure 1B is consistent with the $\nu_{||}$ shoulders of the powder pattern, thereby demonstrating that the global motional axis of this molecule is parallel to the magnetic field direction.

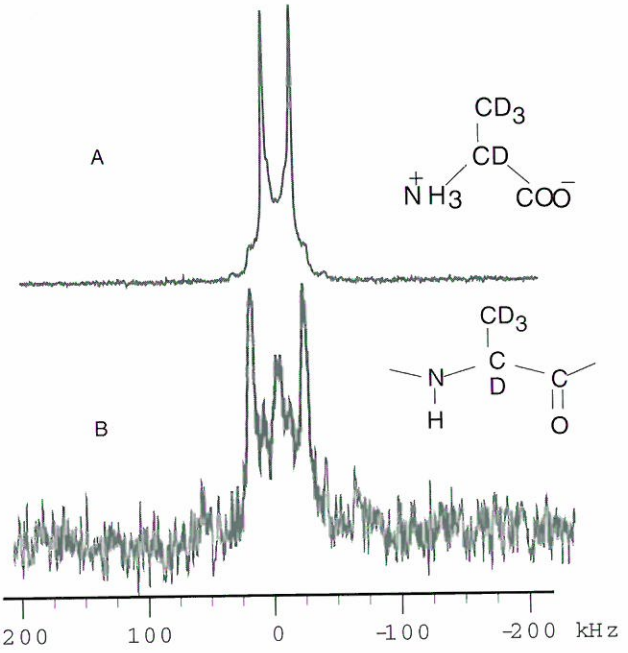

Figure 1. ^2H spectra at 158 MHz of (A) 2 mg of d_4-alanine obtained in 8 acquisitions, and (B) oriented samples of d_4-alanine labeled gramicidin (0.6 mg of d_4-alanine) in hydrated lipid bilayers obtained in 2k acquisitions. This latter sample was contained in a sample chamber 6 x 7 x 8 mm.

Frequency-Modulated Cross-Polarization for Fast Magic Angle Spinning NMR at High Fields: Relaxing the Hartmann-Hahn Condition

Fu, R., NHMFL
Pelupessy, P., NHMFL
Bodenhausen, G., NHMFL/FSU, Chemistry

CPMAS[1,2] has become a routine technique in high resolution solid state NMR. If the spinning speed is comparable to, or larger than, the homogeneous linewidth of the abundant I spins, the efficiency of cross-polarization is a direct function of the mismatch $\Delta = \omega_{1I} - \omega_{1S}$, where ω_{1I} and ω_{1S} are the spin-locking RF amplitudes of the I spins and the dilute S spins, respectively. The Hartmann-Hahn matching condition[3] is broken up

into a series of sidebands at $\Delta=n\omega_r$, where ω_r is the spinning frequency and n an integer. The width of these sidebands is very narrow, and the matching condition tends to be very sensitive to RF inhomogeneities. Thus at high spinning speeds CP becomes critically dependent on the precise calibration of the RF fields. These problems tend to be exacerbated at high static magnetic fields, in part because the magnitudes of the chemical shift anisotropies make it necessary to use very fast spinning to attenuate spinning sidebands, and in part because the dispersion of the isotropic chemical shifts can be large so that one must fulfill the matching condition over a wide range of offsets with respect to the RF carrier.

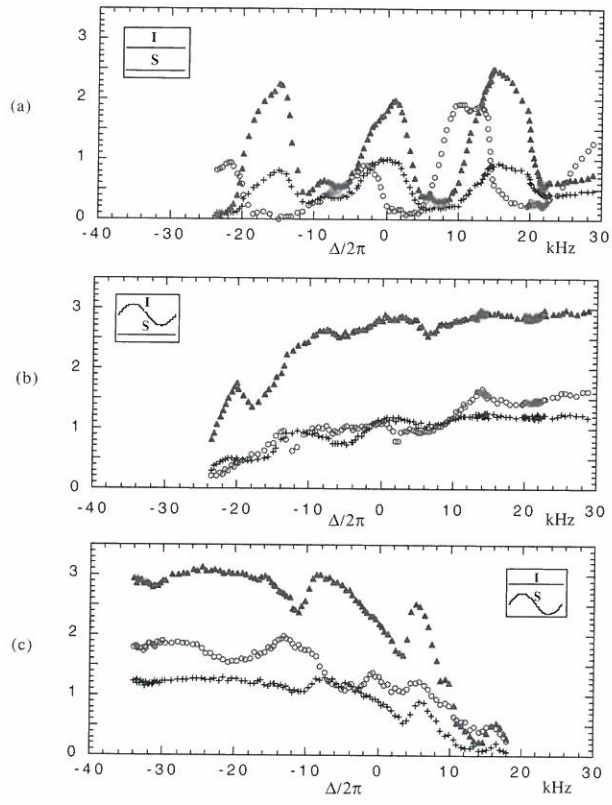

Figure 1. Polarized intensities of three ^{13}C resonances, i.e. COO (o), CH (+) and CH_3 (▲), of DL-alanine spinning at 15 kHz recorded as a function of mismatch $\Delta = \omega_{1S} - \omega_{1I}$ ("matching profiles"). The contact time τ_{CP} was 5 ms in all cases. The modulation parameters used were: $\omega_\Delta/2\pi$ = 85 kHz, $\omega_m/2\pi = 1/\tau_{CP}$ = 200 Hz (a) Conventional CW spin-locking of both spins, with a fixed amplitude $\omega_{1I}/2\pi$ = 42 kHz. (b) The I spin-lock pulse was modulated, with a fixed amplitude $\omega_{1I}/2\pi$ = 42 kHz. (c) The S spin-lock pulse was modulated, with a fixed amplitude $\omega_{1S}/2\pi$ = 42 kHz. All intensities were normalized to the CH signal obtained with Δ = 0 and the conventional scheme (a). A Bruker DMX 600 WB spectrometer was employed.

We have proposed two novel CP schemes that make it possible to achieve an efficient transfer of polarization from I spins to S spins under high-speed MAS. These techniques are useful for systems with large chemical shift anisotropies at high fields. The frequency of one of the RF carriers is modulated sinusoidally during spin-locking, i.e. $\Delta\omega^{I,S}_{\rm mod}(t) = \omega^{I,S}_{\Delta} \sin \omega^{I,S}_{m} t$, while the RF amplitude is kept constant. It is shown by experiment that frequency modulation greatly attenuates the critical character of the Hartmann-Hahn matching condition, and allows one to obtain uniform excitation over a wide range of offsets. Figure 1 shows the CP matching profiles.

References:

1 Andrew, E.R., *et al.*, Nature, **182**, 1659 (1958).

2 Lowe, I.J., Phys. Rev. Lett., **2**, 285 (1959).

3 Hartmann, S.R., *et al.*, Phys. Rev., **128**, 2042-2053 (1962).

Magnetic Resonance Imaging of Foams

Gibbs, S.J., NHMFL/FAMU-FSU Chemical Engineering

Glazier, J.A., Univ. of Notre Dame, Physics

Prause, B.A., Univ. of Notre Dame, Physics

We have investigated the suitability of the 600 MHz microimaging facility to image the structure of polyurethane foams and to study the coarsening of liquid foams. The NHMFL 14 tesla facility combines a high primary magnetic field with strong (96 G/cm) field gradients, to give high polarization density and spatial resolution.

Polyurethane foam consists of a polymer network, in which the cell faces are open. The foam was immersed in $CuSO_4$ doped water in which T_1 was reduced to 100 ms. A 3d spin -echo sequence was used to image the water inside the cells, with an isotropic voxel resolution below 100 μm^3. The

static foam allowed relatively long TR (350 ms) and TE (25 ms), with integration time up to 16 hours for 256^3 real data points. T_1 was slightly short for the permissible repetition time. The method succeeded in extracting not only Plateau borders, but also connecting vertices, which will aid in topological analyses.

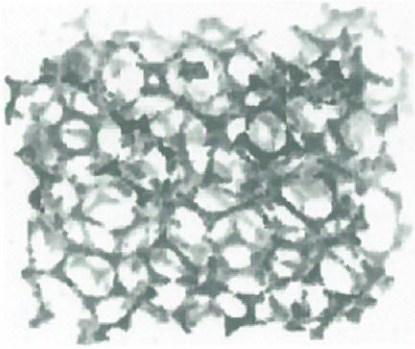

Figure 1. Polyurethane foam. Voxel size 50 μm^3. Acquisition time: 14 hours

The experiment to image liquid protein foams was largely successful. We used a 3d spin-echo sequence to image the fluid contained in the walls. $CuSO_4$ and $DyCl_3$ were added to enhance relaxation and make the sample magnetically homogeneous. We found strong dependence of the signal intensity and linewidth on wall thickness. Altering the surfactant content of the liquid reduced linewidth from > 1500 Hz to 800 Hz. Difficulties with the gradient system, a lack of water cooling, and a broken temperature sensor, precluded running the machine at high duty cycles, which would be optimal for imaging an evolving system with short relaxation times. T_2 was below 2 ms and T_1 about 90 ms, so that the fastest sustainable TE of 2.7 ms and TR of 300 ms were too long to achieve optimal S/N.

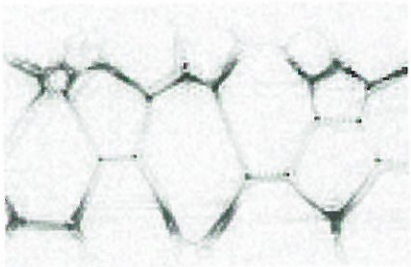

Figure 2. Liquid protein foam. Voxel size 86 μm^3. Acquisition time: 2:44 hours

Anticipated improvements in the 600 MHz facility, chiefly in the data handling systems, will allow time series measurements for liquid foams. The images are fully adequate in spatial and time resolution for our purpose of topological reconstruction, and are superior in resolution and S/N to images obtained previously at lower fields.

Observations of Diffusive Diffraction in a Cylindrical Pore by Pulsed Field Gradient NMR

Gibbs, S.J., NHMFL/FAMU-FSU Chemical Engineering

Pulsed field gradient (PFG) NMR observations of spatial restrictions to diffusion have great potential for aiding spatial structure determination in a wide variety of porous media. Some practical examples of current interest include the noninvasive determination of nerve fiber orientation and size, characterization of pore sizes and permeability in oil-bearing rock formations, and structure and transport property determination in packed beds and other porous media of use in chemical reaction engineering and separation processes.

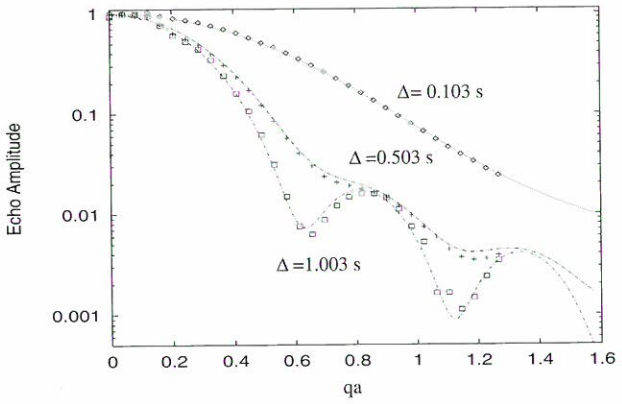

Figure 1. Experimental data (points) and prediction of theory for restricted diffusion (lines) for pulsed gradients applied orthogonal to the axis of a water-filled 100 μm i.d. capillary for three different diffusion times. For longer diffusion times the water molecules explore more of the pore space by diffusion. Data obtained with proton NMR at 600 MHz.

Recently, Callaghan has published exact, analytical expressions for the echo attenuation in planar, cylindrical, and spherical pores valid for conditions of short gradient pulses and possible wall or surface induced relaxation.[1] Work during 1996 has demonstrated a favorable comparison of experimental PFG NMR data obtained at 600 MHz for a 100 micron diameter, water-filled capillary and the analytical treatment. Experimental verification of the positions of diffractive minima in the PFG NMR data for restricted diffusion in a cylindrical geometry has been obtained. Detailed consideration of predictions of the theory suggest caution in the interpretation of PFG data from fluids enclosed in mm-sized containers using theory developed for unrestricted diffusion.

Reference:

1 Callaghan, P.T., J. Magn. Reson. A, **113**, 53 (1995).

Determination of Scalar Coupling Constants by Multiplet Analysis in Selective NMR Correlation Spectroscopy

Jeannerat, D., NHMFL
Bodenhausen, G., NHMFL/FSU, Chemistry

A recursive procedure is presented allowing the separation of overlapping multiplets in two-dimensional correlation spectra by exploiting the fact that each constituent multiplet has a center of symmetry.[1] Figure 1 shows an example taken from a soft-COSY experiment. The method can also be used for the contraction of E-COSY type multiplets by removing splittings due to passive coupling partners.

Two-dimensional convolution of complementary multiplets obtained by selective correlation spectroscopy (soft-COSY) and by selectively inverted soft correlation spectroscopy (SIS-COSY) allows one to determine the magnitude and relative signs of passive scalar coupling constants with great accuracy.[2]

Homonuclear proton-proton coupling constants can be determined accurately by recording selective

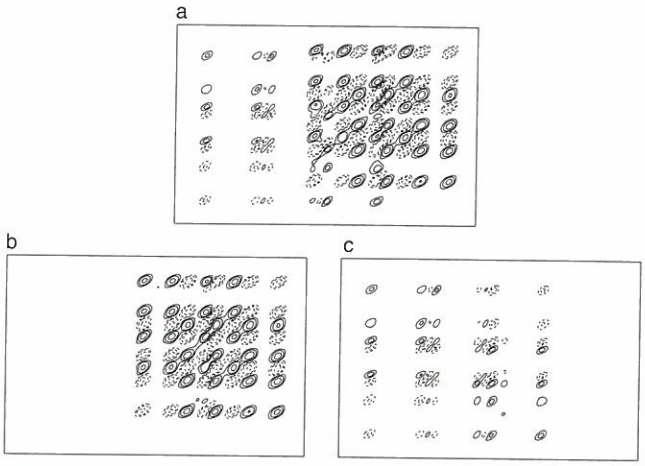

Figure 1. (a) Overlapping crosspeak multiplets resulting from coherence transfer from X^{trans} to A^{trans} and from X^{cis} to A^{cis} in a 3:1 mixture of *trans*- and *cis*-2-phenylcyclopropanecarboxylic acid ethyl ester, recorded with the soft-COSY method. (b,c) multiplets obtained after separation with two recursive cycles.

two-dimensional correlation spectra and by analyzing the resulting multiplets by two-dimensional convolution and deconvolution methods.[3] These methods were evaluated by attempting to determine the complete set of homonuclear couplings in Paclitaxel (Taxol). Convolution methods[4] have been applied successfully to ten pairs of complementary multiplets recorded by selective correlation spectroscopy (soft-COSY) and pure in-phase correlation spectroscopy (PICSY). These pairs of multiplets gave reliable measurements of ten active couplings. In some cases, satisfactory PICSY spectra could not be obtained, so that the complementary information of soft-COSY and PICSY could not be exploited. Furthermore, couplings involving two strongly-coupled diastereotopic protons could not be determined in a satisfactory manner. Additional problems arose due to partial overlap of the chemical shifts of two other protons. Deconvolution has been applied successfully to all fourteen soft-COSY multiplets, yielding fourteen estimates of active couplings and thirty-eight estimates of passive splittings. One example is given in Figure 2. The accuracy of these different estimates must be weighed with the complexity of the methods used. This work may help to assess the perspectives of completely

automated computer-supported analysis of two-dimensional spectra.

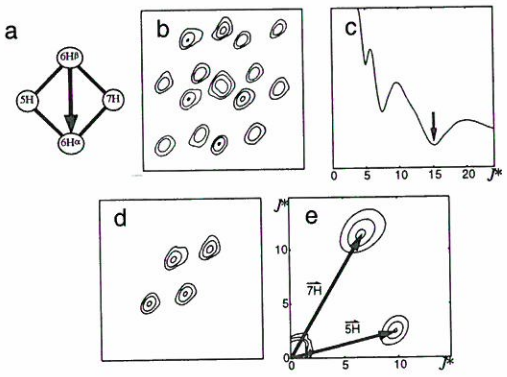

Figure 2. Shows the stepwise simplification of the soft-COSY multiplet due to magnetization transfer from $6H^{\beta}$ to $6H^{\alpha}$ in Paclitaxel (Taxol). Deconvolution with respect of the active coupling constant gives the global magnitude function shown in Figure 6c, which clearly indicates that $J(6H^{\alpha}, 6H^{\beta})$ = 15.20 Hz. Deconvolution with respect of the passive couplings gives the two-dimensional global magnitude function of Figure 6e. One of the two minima, which corresponds to the coupling to the passive spin 5H, has the coordinates J(5H, $6H^{\beta}$) = +2.40 Hz and J(5H, $6H^{\alpha}$)= +9.70 Hz.

References:

1 Jeannerat, D., *et al.*, J. of Magn. Res, Ser A **119**, 139-144 (1996).

2 Jeannerat, D., *et al.*, J. of Magn. Res, Ser A **118**, 126-131 (1996).

3 Peng, C., *et al.*, Magn. Res. in Chem, in print, (1996).

4 Jeannerat, D., *et al.*, J. of Magn. Res, Ser A **117**, 123-127 (1995).

DPPH As a Standard for High Frequency EPR Spectroscopy

Krzystek, J., NHMFL
Sienkiewicz, A., Polish Academy of Sciences
Pardi, L., NHMFL
Brunel, L.-C., NHMFL

The growing popularity of high field EPR spectroscopy has brought attention back to the problem of a suitable standard for calibrating the magnetic field and determining the g-factor of the spin species under study. This problem is of even more importance in high field than in conventional EPR since (1) there are no commercial gaussmeters available to measure the field above a few tesla, and (2) the settability of superconducting magnets operating at high fields leaves some margin for error that can be significant in high resolution EPR spectroscopy.

One of the most widely used standards in conventional EPR is 2,2-Diphenyl-1-picrylhydrazyl (DPPH). Its room temperature EPR spectrum in polycrystalline form at X-band consists of a single narrow (0.15 mT) line appearing at g = 2.0036 ± 0.0002.[1] The high frequency EPR spectra obtained so far in several different laboratories on the other hand were much broader (up to 4.8 mT at 249 GHz) and structured.[2] This disqualified DPPH as a convenient standard for field calibration.

In order to clarify the issue and determine the properties of DPPH at high frequencies and fields, we obtained EPR spectra of solid and dissolved DPPH samples using the high field, broadband spectrometer at the NHMFL in a 109 to 465 GHz frequency range. A single exchange-narrowed line with no apparent structure was observed for polycrystalline samples within the whole range (Figure 1). The solution spectra revealed a broader spectrum with a characteristic quintet due to the partly resolved hyperfine ^{14}N structure. The overall shape and width of the high field signals are similar to the well known results obtained from conventional experiments, which leads us to a conclusion that DPPH can be used as a standard for high frequency/field EPR, at least for measurements up to 17 tesla (0.5 THz).

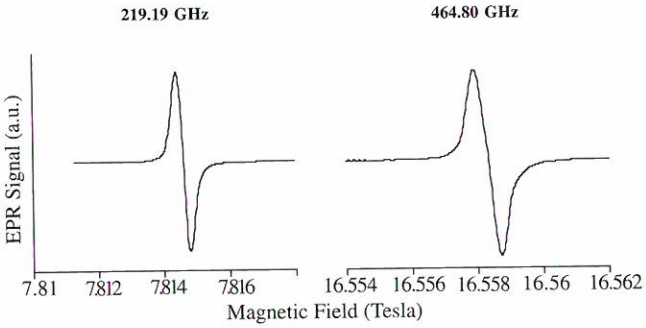

Figure 1. Room temperature EPR spectra of polycrystalline DPPH at two different Larmor frequencies.

References:

1 Al'tshuler, S.A., *et al.*, "Electron Paramagnetic Resonance", ed. C.P. Poole, Jr., (Academic Press, New York, 1964).

2 Lynch, W.B., *et al.*, Rev. Sci. Instrum., **59**, 1345 (1988).

Advantages of High Magnetic Field for Fourier Transform Ion Cyclotron Resonance Mass Spectrometry

Marshall, A.G., NHMFL/FSU, Chemistry
Guan, S., NHMFL/FSU, Chemistry

It is well known that mass resolving power in Fourier transform ion cyclotron resonance mass spectrometry (FT-ICR MS) can increase linearly with increasing applied magnetic field induction, B. We recently pointed out that *eight* other FT-ICR primary performance parameters theoretically also increase linearly (quadrupolar axialization efficiency, data acquisition speed), quadratically (upper mass limit, maximum ion kinetic energy, maximum number of trapped ions, maximum ion trapping duration, two-dimensional FT-ICR mass resolving power), or inverse-quadratically (peak coalescence tendency) with increasing B.[1] These dependencies are illustrated graphically in Figure 1. 7 T is the highest field for FT-ICR MS elsewhere; 9.4 T is NHMFL's superconductive high-resolution magnet, and 25 T is NHMFL's resistive magnet (spatial/temporal inhomogeneity, 1 ppm) now under construction. The origin of (and conditions for) the magnetic field dependence of each of these parameters are presented and discussed in Reference 1. These fundamental advantages lead to corollary improvement in other FT-ICR performance parameters: e.g., signal-to-noise ratio, dynamic range, mass accuracy, ion remeasurement efficiency, and mass selectivity for MS/MS. Finally, we note that these various advantages may be exploited in combination, so as to produce even higher enhancement in a particular parameter: e.g., signal-to-noise ratio can improve by more than a factor of B^2 if mass resolving power is fixed at the same value as at lower magnetic field.

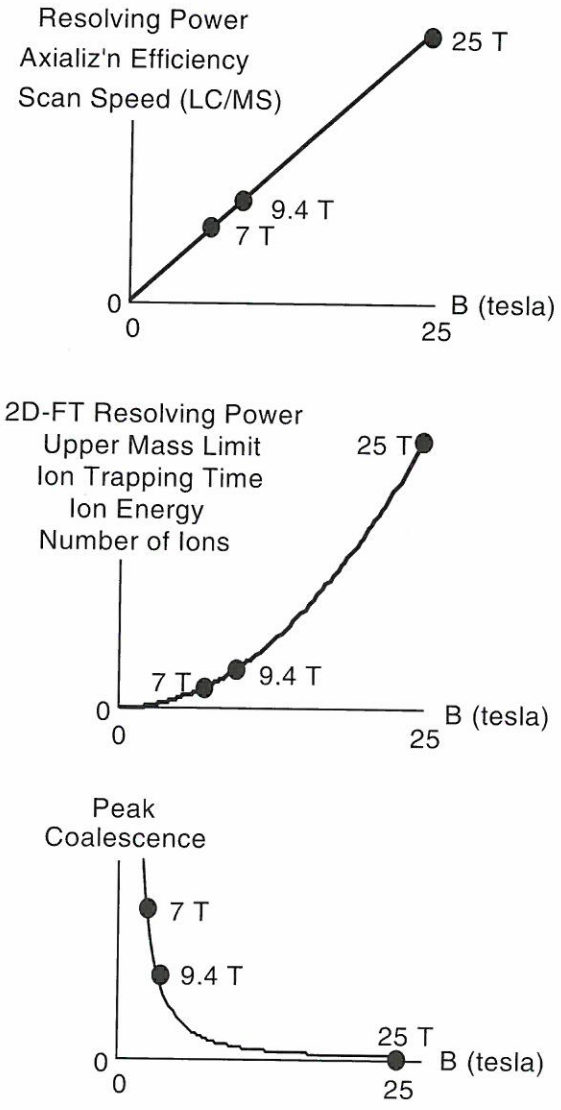

Figure 1. Magnetic field dependence of various FT-ICR performance parameters.

Reference:

1 Marshall, A.G., *et al.*, Rapid Commun. Mass Spectrom., **10**, 1819 (1996).

Electrospray Ionization Fourier Transform Ion Cyclotron Resonance Mass Spectrometry at 9.4 Tesla

Marshall, A.G., NHMFL/FSU, Chemistry
Senko, M.W., NHMFL
Hendrickson, C.L., NHMFL
Pasa-Tolic, L., NHMFL
Marto, J.A., FSU, Chemistry
White, F.M., FSU, Chemistry
Guan, S., NHMFL/FSU, Chemistry

In 1996, we produced the first results from a new electrospray ionization Fourier transform ion cyclotron resonance mass spectrometer operated at a magnetic field of 9.4 T (*i.e.*, ≥ 2.4 T higher than for any prior FT-ICR instrument). The 9.4 T instrument (see Figure 1) provides substantially improved performance for large molecules (≥ 50% increase in mass resolving power) and complex mixtures (≥ 100% increase in dynamic range) compared to lower-field (≤ 6 T) instruments.[1]

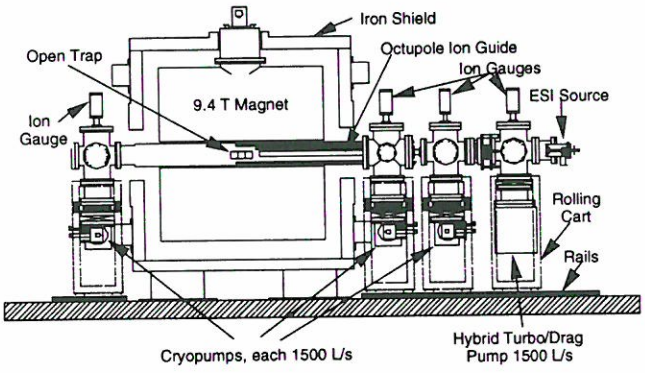

Figure 1. Schematic of 9.4 T FT-ICR mass spectrometer at NHMFL in Tallahassee.

The higher magnetic field makes possible larger trapped ion population without introduction of significant space-charge effects such as spectral peak shift and/or distortion, and coalescence of closely-spaced resonances. For bovine ubiquitin (8.6 kDa) we observe accurate relative isotopic abundances at a signal-to-noise ratio greater than 1000:1, whereas a complete nozzle-skimmer dissociation ESI FT-ICR mass spectrum for bovine carbonic anhydrase (29 kDa) is achieved from a single scan with a signal-to-noise ratio more than 250:1. Finally, we are able to obtain world-record mass resolving power, m/Δm > 200,000, routinely for porcine serum albumin (67 kDa), as shown in Figure 2.

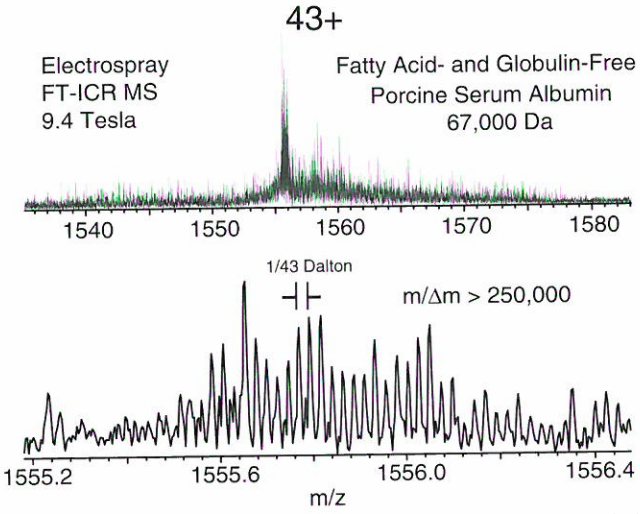

Figure 2. Electrospray FT-ICR mass spectroscopy at 9.4 T of fatty acid- and globulin-free porcine serum albumin.

Reference:

1 Senko, M.W., *et al.*, Rapid Commun. Mass Spectrom., **10**, 1824 (1996).

Fourier Transform Ion Cyclotron Resonance Mass Spectrometry in a 20 Tesla Resistive Magnet

Marshall, A.G., NHMFL/FSU, Chemistry
Hendrickson, C.L., NHMFL
Guan, S., NHMFL/FSU, Chemistry
Drader, J.J., Univ. of Texas at Austin, Chemistry
Laude, D.A., Univ. of Texas at Austin, Chemistry

Here we present Fourier transform ion cyclotron resonance (FT-ICR) mass spectra at a magnetic field of 20 tesla: more than twice the highest field yet used for FT-ICR.[1] Our instrument is based on a resistive magnet installed at NHMFL. The magnet has a 50 mm diameter bore and spatial inhomogeneity of ~1000 ppm over 1 cm diameter spherical volume. However, FT-ICR mass resolving power far in excess of magnet homogeneity is achieved routinely for ions produced by either electron ionization (EI) or matrix assisted laser desorption/ionization (MALDI). For example,

Figure 1 shows a MALDI mass spectrum of $(M+H)^+$ quasimolecular ions of the peptide, human luteinizing hormone-releasing hormone (monoisotopic molecular weight, 1181.6 Da), at mass resolving power, $m/\Delta m > 10{,}000$; and Figure 2 shows an EI mass spectrum of molecular ions of the platinum cluster compound, $Pt_4(PF_3)_8$ (average molecular weight, 1484 Da), at mass resolving power, $m/\Delta m \approx 20{,}000$. Much better FT-ICR MS performance is predicted for future NHMFL resistive magnets of higher spatial and temporal homogeneity.

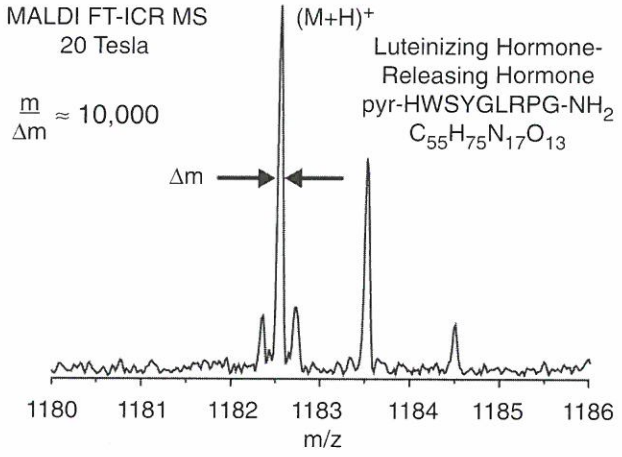

Figure 1. MALDI mass spectrum of $(M+H)^+$ quasimolecular ions of the peptide, human luteinizing hormone-releasing hormone (monoisotopic molecular weight, 1181.6 Da), at mass resolving power, $m/\Delta m > 10{,}000$.

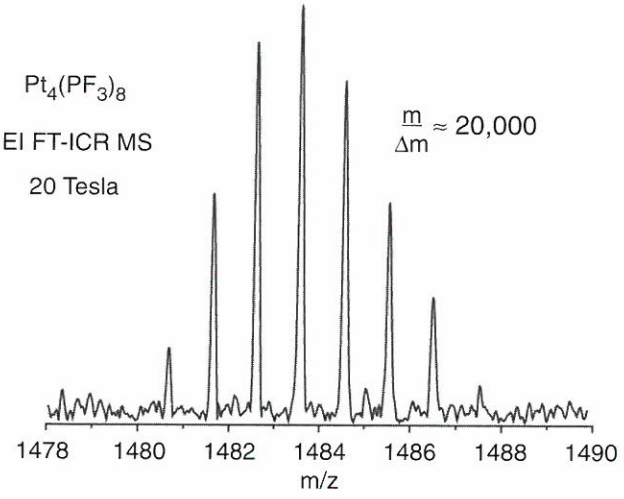

Figure 2. Electron ionization mass spectrum of molecular ions of the platinum cluster compound, $Pt_4(PF_3)_8$ (average molecular weight, 1484 Da), at mass resolving power, $m/\Delta m \approx 20{,}000$.

Reference:

1 Hendrickson, C.L., *et al.*, Rapid Commun. Mass Spectrom., **10**, 1829 (1996).

Multiple-Quantum ^{131}Xe NMR Spectroscopy As a Probe for Gas/Solid Interfaces

Meersmann, T., NHMFL
Smith, S.A., NHMFL
Bodenhausen, G., NHMFL/FSU, Chemistry

We report on multiple-quantum filtered (MQF) experiments using ^{131}Xe ($I = 3/2$) that can serve as a probe for the interface between gaseous xenon with solid surfaces. While physisorbed on a surface, the xenon is typically not observable with spectroscopy due to severe signal broadening. However, the detected multiple-quantum filtered (MQF) xenon-131 signal in the gas-phase strongly depends on the physisorbed surface xenon behavior through exchange. Two fundamentally different effects, relaxation and coherent evolution, can give rise to observable signals in these kind of experiments. Relaxation can lead to third rank (octupolar) order in spin $I = 3/2$ systems and depends on the ratio between the surface area and gas volume as well as on the dwell time of the xenon on the surface. In principle, this makes xenon MQF relaxation experiments analogous to measurements performed on $I > 1/2$ nuclei (e.g. alkali metal cations) bound to biological macromolecules.[1] Such measurements have been given a great deal of attention in the past ten years in both the NMR and MRI communities. Coherent evolution under the quadrupolar coupling of surface xenon depends strongly on the orientation of the surface angle with respect to the magnetic field. This can cause splittings in the ^{131}Xe gas phase signals in glass cells, as previously observed in optical pumping experiments.[2,3] Our experimental results have been theoretically validated using the GAMMA simulation platform. We anticipate that such experiments, in combination with simulations, will provide valuable information about surface-xenon interactions, surface-gas phase ratios, and surface geometry.

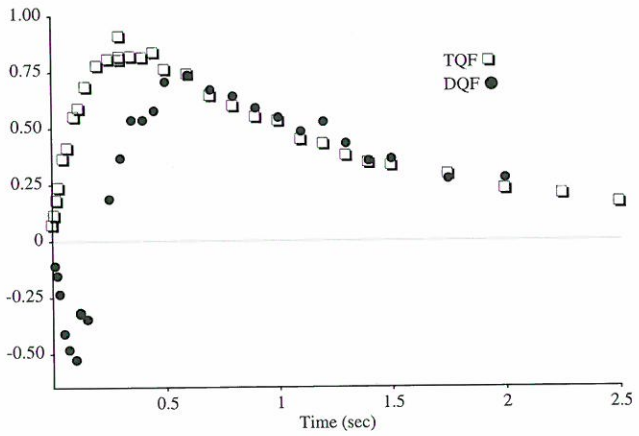

Figure 1. Intensity curves from triple-quantum filtered (squares) and double-quantum filtered (circles) xenon-131 NMR. The xenon gas is in the vicinity of glass capillaries, which were aligned with the magnetic field. The signals are detected from gas phase xenon but are strongly influenced by interactions with the surface of the solid host structure. Both coherent and relaxation processes contribute to the signals, thus providing detailed information about the host structure.

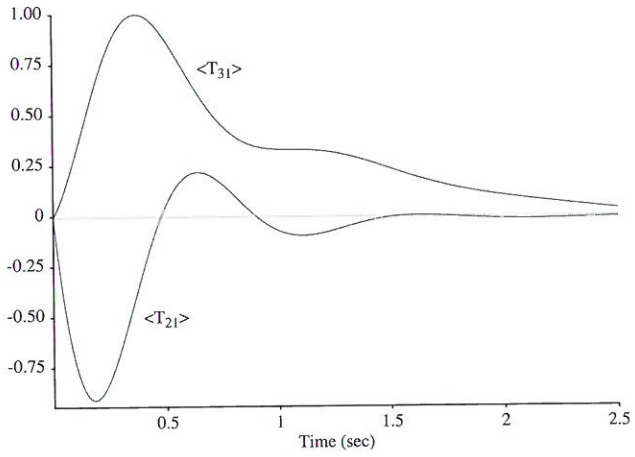

Figure 2. A GAMMA simulation of second rank ($<T_{21}>$) and third rank ($<T_{31}>$) single quantum coherence evolution in ^{131}Xe gas that is exchanging with physisorbed xenon. It is striking that these curves generally follow the experimental MQF spectra of Figure 1, given that they dramatically change when any of the input parameters—surface quadrupolar interaction, gas/surface exchange rate, applied field strength, gas/surface population ratio—are altered. We expect to fit the curves more precisely through minimization procedures.

References:

1 Jaccard, G., *et al.*, J. Phys. Chem., **100**, 6923 (1994).

2 Wu, Z., *et al.*, Phys. Rev. Lett., **59**, 1480 (1987).

3 Butscher, R., *et al.*, J. Phys. Chem., **100**, 6923 (1994).

Relaxation-Induced Oscillations of Spin-Echo Envelopes

Meersmann, T., NHMFL
Bodenhausen, G., NHMFL/FSU, Chemistry

In scalar-coupled spin systems, where in-phase and antiphase coherences have different life-times, the envelopes of spin echoes may feature modulations that are induced by relaxation. These modulations are most pronounced when the couplings that lead to the interconversion of in-phase and antiphase coherences are too small to provide an effective mechanism for averaging. The modulations occur even if the scalar coupling term is formally eliminated from the average Hamiltonian that describes the evolution between the initial excitation and the time of the echo. The frequency of the relaxation-induced oscillations is one-half of the scalar coupling constant, whereas the modulation depth is determined by the ratio of the difference between the relaxation rates of the in-phase and antiphase coherences to the scalar coupling.

Results and consequences:

- Relaxation curves obtained from a selective spin echo experiment may show *relaxation-induced oscillations*.
- These oscillations depend on the difference between $T_2^{in-phase}$ and $T_2^{antiphase}$.
- They may have a severe influence on the outcome of homonuclear and heteronuclear selective spin echo experiments if *remote couplings* are present.
- The influence will be increased due to the effect of field inhomogeneities during the acquisition.

- If information about spectral densities is desired, selective (low power) spin echo experiments will often be the better choice for measurement of transverse relaxation. Cross relaxation and cross correlation, however, might have to be taken into account.
- Selective spin echo experiments can give information about very small couplings.
- Decoupling of *remote coupling* partners during the acquisition can result in improved lineshapes.

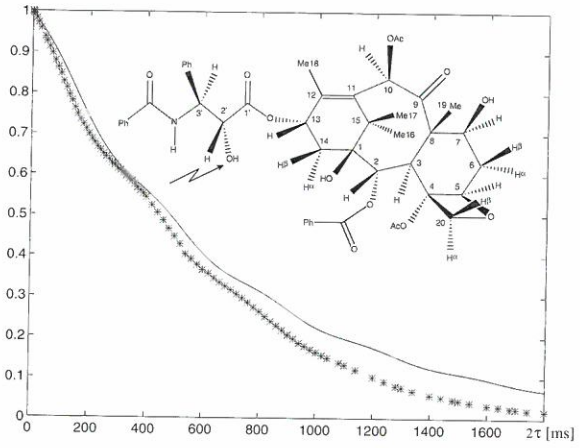

Figure 1. Oscillating decays observed with a selective spin echo sequence. The stars represent the echo amplitudes of the 2'OH-proton in Taxol (see arrow on molecular structure) when its magnetization is refocused with a single selective Q^3 Gaussian cascade. The modulations are due to the interplay between the scalar coupling J(2'OH, 2'H) = 5.4 Hz and the difference between the life-time $T_2^{in-phase}$ of the in-phase magnetization and $T_2^{antiphase}$ of the antiphase coherence. The solid line is the result of calculations using life-times and couplings determined by independent experiments.

Relaxation Effects of Spin 1/2 Nuclei Coupled to Quadrupolar Spins Subjected to RF Irradiation: Applications to Macromolecular NMR

Murali, N., NHMFL
Smith, S.A., NHMFL

Recent developments in high-resolution multi-nuclear multi-dimensional NMR methods for the determination of macromolecular structure involve extensive use of selective, semi-selective or uniform ^{13}C, ^{15}N, and ^{2}H labeling of the macromolecule. Such labeled spin systems often contain fragments with a spin 1/2 and spin 1 directly bonded to each other such as ^{13}C-^{2}H, ^{13}C-^{14}N, ^{15}N-^{2}H, and ^{1}H-^{14}N. All of these spin pairs have a J-coupling interaction between them. However, the spin-spin splitting is partially or totally "washed out" by the rapid quadrupolar relaxation of the spin nucleus.[1] In addition, there is usually some residual line broadening in the observed spectrum of the spin 1/2 nucleus.[1] Because one motivation behind isotope editing is to enhance resolution, and thereby facilitate structure determination in macro-molecules of larger size, strategies have been used to minimize these line broadening through use of radio frequency (rf) irradiation in the vicinity of the spin 1 resonance. Alternatively, and in contrast to NMR in lower fields, experiments in high magnetic fields can produce resolved transitions in these systems due to relaxation induced dynamic frequency shifts. These shifts contain both structure and dynamics information and can be invaluable to NMR investigations of macromolecules.

We have undertaken a study of the lineshape variations in the multiplet structure of a spin 1/2 nucleus I (^{13}C or ^{15}N) scalar-coupled to several quadrupolar spins, such as deuterium (^{2}H, designated by the symbol S). Both one-dimensional and heteronuclear multi-dimensional NMR experiments that incorporate ^{2}H decoupling are underway using the Varian Unity Plus 720 NMR spectrometer at NHMFL. Preliminary results obtained using a per-deuterated glycerol solution (Figure 1) clearly shows the effects of dynamic frequency shifts as the temperature of the solution

is varied to change the viscosity to mimic spins in a wide range of motional regimes. The GAMMA[2] simulation platform was used to generate analogous spectra by varying theoretical rotational correlation times (Figure 2).

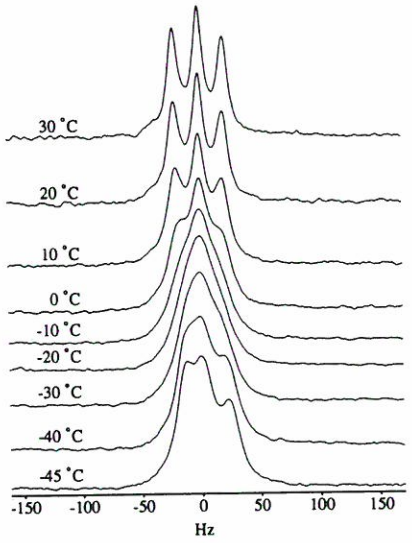

Figure 1. Methyne ^{13}C spectra of glycerol recorded using the 720 MHz Varian Unity Plus spectrometer. 600 ul of the sample contained about 10% DMSO-d6, 10% D20, and 0.5 mM sugar to prevent glycerol from freezing.

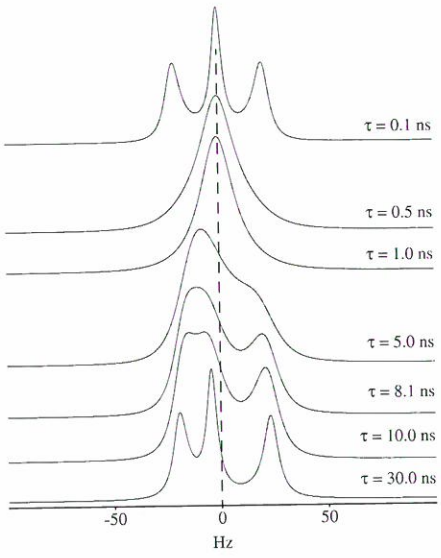

Figure 2. GAMMA simulations of ^{13}C spectra in ^{13}CD for different rotational correlation times assuming spherical top rotational dynamics using appropriate dipolar and quadrupolar couplings.

A triply labeled (^{2}H-^{15}N-^{13}C) FK506 binding protein FKBP is currently being used to understand the performance of the optimized decoupling techniques in the heteronuclear multi-dimensional NMR experiments.

References:

1 Murali, N., *et al.*, J. Magn. Reson., Ser. A **118**, 202, (1996).

2 Smith, S.A., *et al.*, J. Magn. Reson., Ser. A **106**, 75, (1994).

Orbital Magnetism and NMR Shifts of Ortho-Hydrogen in High Magnetic Fields

Sullivan, N.S., UF, Physics/NHMFL

Measurements of NMR line shapes of very dilute samples of ortho-hydrogen (1.1%) in a crystal of para-hydrogen also containing HD impurities (1.5%) have revealed an unusual shift of the center of the ortho-hydrogen line shape relative to the HD line shape.[1] The shift has been studied up to an applied field of 7 T and has a strong field and temperature dependence (Figure 1). The ortho-hydrogen molecules are quantum rotors in the orbital angular momentum state J=1. In zero applied field, the ortho-hydrogen molecules experience a crystal field, $V_c = V_0 (3 J_z^2 - J^2)$, that creates an energy gap between the states $| J_z = 0 >$ and $| J_z = \pm 1 >$. The sign of V_0 is not known and experiments that can determine the magnitude

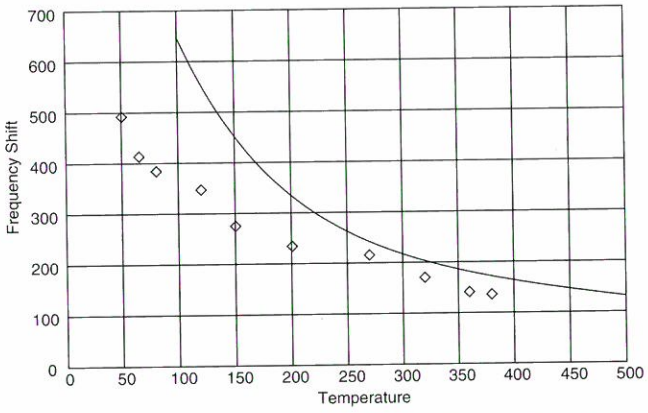

Figure 1. Temperature dependence of shift of ortho-H_2 NMR lines at 7 T. Symbols: experimental data. Solid line: theoretical prediction.

differ widely in their values.[2] We have been able to relate the shift to the establishment of a finite orbital magnetism for the ortho-hydrogen molecules, and show how measurements at higher magnetic fields can establish the sign of V_0, unambiguously.

The small but finite orbital magnetic moment of ortho-hydrogen, $\mu_J = 0.88291\ \mu_N$, leads to a detectable lifting of the degeneracy of the $J_Z = \pm 1$ levels in a high applied magnetic field H_0. This leads to a finite orbital magnetism given by:

$$\langle J_z \rangle = \frac{2e^{-3\beta V_o}\sinh\left(\beta\mu_J H_o \cos\theta_z\right)}{1+2e^{-3\beta V_o}\cosh\left(\beta\mu_J H_o \cos\theta_z\right)}$$

where θ_Z is the orientation of H_0 with respect to the crystal symmetry axis, and $\beta = 1/k_B T$. As a result of the non-vanishing $\langle J_Z \rangle$, the spin orbit interaction, $H_{SO} = A\,\vec{I} \bullet \vec{J}$ between the nuclear spins and the orbital electronic charge, leads to a perturbation of the nuclear spin Zeeman levels equivalent to an effective internal magnetic field, $H_{eff} = A\langle J_z \rangle \cos\theta_Z$. This leads to a shift of the NMR lines for the J = 1 hydrogen molecules given by:

$$\Delta\upsilon = -\frac{2}{3}h^{-1}A\left(1-\frac{3V_o}{k_B T}\right)m_J H_o \cos^2\theta_z$$

The observed shifts are compared with this theoretical prediction in Figure 1 for a crystal field $V_0 = 2.8$mk. The agreement is only qualitative.

The magnitude and sign of V_0 can be determined unambiguously by observing the rotational magnetic fields using a UHF absorption spectrometer. For an observation frequency ω_J, the allowed absorptions occur at $H_1 = (\hbar\omega_J - 3V_o)\mu_J \sim 5$T and $H_2 = (\hbar\omega_J + 3V_o)\mu_J \sim 20$ T (for $\omega_J \cong 250$ MHz). The amplitudes of the absorption are NOT equal and are given by:

$$\frac{I_1}{I_2} = \frac{1+2e^{-3\beta V_o}\cosh\left[\beta\left(6V_o+\mu_J H_1\right)\right]}{1+2e^{-3\beta V_o}\cosh\left(\beta\mu_J H_1\right)}$$

and the sign of V_0 can be easily determined for measurements at T ~ mk.

This work is funded by the National Science Foundation, DMR-9623536.

References:

1 Washburn, S., *et al.*, J. Low Temp. Phys., **45**, 167 (1985).

2 Zhou, D., *et al.*, Phys. Rev. Lett, **62**, 1528 (1989).

3 Van Kranedonk, J., *Solid Hydrogen* , (Plenum Press, New York, 1983).

Chapter 2

MAGNET SCIENCE & TECHNOLOGY REPORTS

Overview

For the Magnet Science and Technology (MS&T) group, the year 1996 was a year of transition from the first five years of building the laboratory to a more steady, high level of ongoing activities. It also was an extremely successful and productive year.

Fifty-five papers were published (a total of 270 since 1992), and another forty-four papers and ten patent applications were submitted. Innovative code development, detailed magnet analysis, the establishment of unique test and characterization facilities, material developments, and several world records contributed to the gratifying fact that MS&T is considered worldwide as the most competent authority in many areas of magnet science, especially in high field technology. As a result, more than ten national and international cooperations have been established. Most noteworthy are the purchase of a complete resistive 30 T magnet including housing by the Japanese National Research Institute of Metals, the contract with the Indian Institute for Plasma Research to participate in studies and magnet design of a fusion reactor, and the cooperation with LANL/DoE on the design and construction of another world-first: a 10 ms, 100 T pulsed magnet system.

Figure 1. Scanning electron micrograph of Bi-doped Hg-1223 superconductor showing good grain growth and texturing.

The 100 T magnet will utilize the latest progress in magnet design optimization, material technologies, and reinforcement techniques developed at the lab. The greater experimental (24 mm diameter) and magnet volume requires considerable energy resources that will be supplied by the 600 MJ, 560 MW generator/rectifier system and a 2.4 MJ capacitor bank. Operational in 1998, this unique magnet will open completely new science opportunities, as it offers up to 10,000 times longer pulse duration in a non-destructive mode and at much lower dB/dt than existing devices.

As major projects are brought to conclusion, we try to establish new ones in order to maintain in-house staff and accumulated competence. This approach allows us to widen the variety of our activities and to fulfill our charge to be the pre-eminent U.S. center for magnet science and technology. New activities will involve development and tests of HTS current leads,

characterization of large conductors (4 T in 2 m diameter) and of wires under compressive stress, and magnetic separation. We also want to focus on the use of magnetic fields for industrial applications. A workshop was held—*High Magnetic Fields: Industry, Materials and Technology*—that underlined the strong connections and promising future interactions between these four spheres of interest.

Each of MS&T's eight programs experienced significant progress during 1996, and the highlights are presented here. Following this, the program leaders describe the activities in greater detail and introduce the groups' research reports.

Large Superconducting Magnet Systems: The NHMFL Hybrid Magnet. Continuous, steady progress characterizes this ambitious project since the NHMFL became the sole responsible party in March, 1996. The two inner superconducting coils have been heat treated (Nb_3Sn) and are being impregnated. The outer (NbTi) pancakes are being insulated. It is hoped that the superconducting part can be tested this fall, and that we can demonstrate the superiority of the cable-in-conduit conductor concept for hybrid magnets. The success of the resistive insert depends on the quality of the material (CuAg) that has to be used. Preliminary tests have not been satisfactory because of the strong anisotropy in its mechanical strength. A 35 T resistive magnet is being built to prove a newly developed concept that then will be applied to the hybrid insert.

High Field Magnetic Resonance Magnet Systems: The 900 MHz NMR Magnet. This magnet will set a new record for adiabatically stabilized superconducting NMR magnets with a stored energy of 40 MJ. The engineering design has been completed. The Nb_3Sn conductor has been ordered and takes full advantage of recent progress in large cross-section conductors with high current densities. This magnet, designed and built in cooperation with IGC, incorporates many new features and developments, such as co-impregnated reinforcement, a new tough low-viscosity epoxy, and a new concept of shim coils.

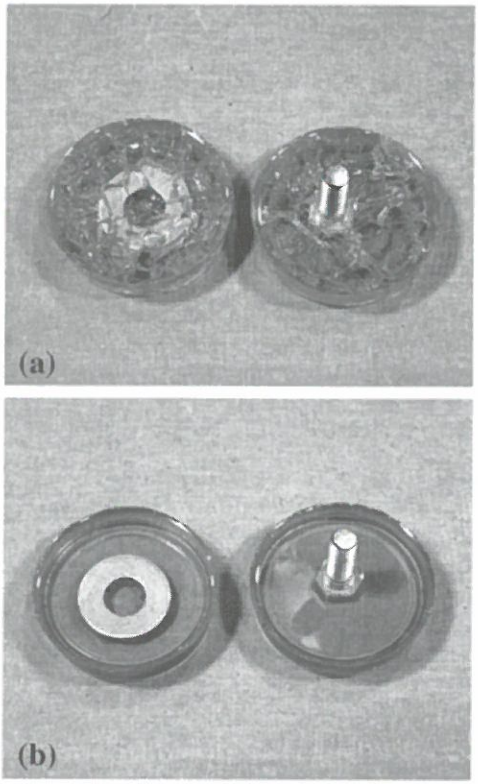

Figure 2. Qualitative evaluation of thermal shock resistance: (a) anhydride-cured resin after one cycle in liquid nitrogen, and (b) amine-cured resin after 25 cycles.

Resistive Magnets. The available magnets cover the field range from 20 T in 50 mm to 33 T in 32 mm. Longevity is outstanding: over 1800 hours and still running! It demonstrates the unique superiority of the Florida-Bitter design at these extreme levels of 12 W/mm^3 power density and 750 MPa stress. A 20 T, 20 cm, 20 MW magnet is being built in cooperation with Grenoble and nearing completion. This magnet will be used as background field, predominantly for tests of other LTS and HTS high field coils. A resistive NMR magnet (25 T, 1 ppm) is being designed and will explore the limits of what can be achieved in resistive NMR magnet technology.

Pulse Magnets. The consistently high quality of our pulse magnets has generated a high international demand. With the help of a larger number of test coils, conductor and reinforcement evaluations were performed, our understanding of the physics of pulse magnets—especially operation under plastic deformation—improved, and the results of our

computer codes verified. The potential of structured reinforcement is being investigated. All these developments merge in the combined efforts necessary to build the 100 T system successfully.

High Temperature Superconductor Technology. The HgBaCaCuO material synthesis had a remarkable breakthrough as a significant degree of texturing can now be achieved. A new technique in BSCCO-2212 powder-in-tube wire manufacturing showed the first promising results. It consists of a continuous process where the wire is reacted, then insulated and wound into a coil, and then sintered for final performance. An HTS shim coil to improve the homogeneity of LTS magnets has been developed and is being tested. The laboratory now possesses the technology to build reproducibly BSCCO-2212 double pancakes in the wind-and-react method at 85% of short sample current. They generate 0.2 T in a background field of 17 T. The next step will involve larger coils to generate insert fields of several teslas, which will require considerable lengths of conductor. The final goal is the construction of superconducting high field magnets in high resolution NMR quality at fields of 25 T. Intermediate steps will be low and medium resolution systems with resistive outserts or inserts.

Cryogenics. The work on the 1.8 K 900 MHz cryostat has begun. Special attention is devoted to safe operation, low losses, and vibration level. Other activities involve component development and optimization. The cryostat of the hybrid magnet has been tested twice up to now, and improvements are in progress. Preparations for installation of the superconducting magnets are being made. Heat and mass transfer in superfluid helium, especially of two phase flow, is of great importance in many cryogenic devices and is therefore a focus of our activities.

High Strength Conductors. The development of conductors with high conductivity and high strength is of crucial importance for magnet technology. The systems under investigation are *in situ* microcomposites, CuAg, CuNb, CuNbAg, CuCrAg, and Cu-Al_2O_3-Nb as they show, at high deformation ratios, mechanical strength well above the rule of mixtures. The relationship between processing (such as casting, heat treatments, deformation, shear), the resulting microstructure (lamellae thickness and spacing), and the wire properties (electrical resistivity, magnetoresistance, strength) was studied and revealed several promising results.

Materials Development and Characterization. The physical properties of the advanced materials needed for the construction of our state-of-the-art magnet systems are characterized and measured extensively. Unique facilities have been established and are listed in the program overview. New facilities are being added as our programs continue to develop. This includes a test facility for large conductors, as used in SMES, fusion or large detector magnets, a device to measure critical current density reduction under compressive forces, and a test stand for HTS current leads.

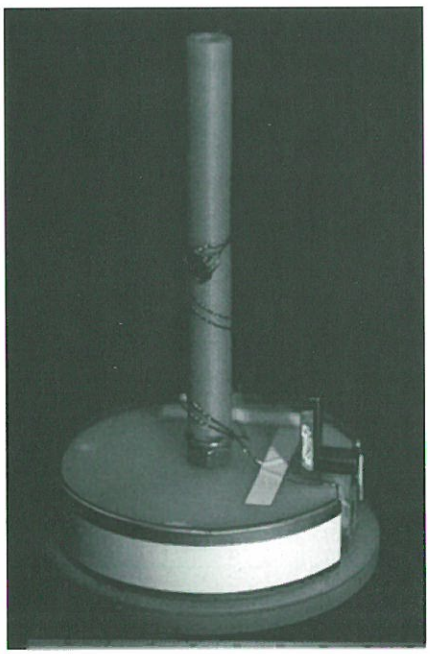

Figure 3. Lorentz force hoop stress device. The stress is determined by the hoop stress, the strain is measured via the change in capacitance between sample and cylindrical capacitor electrode.

Large Superconducting Magnet Systems

Status of the 45 T Hybrid Magnet System

J.R. Miller

There has been continuous, steady progress this year on the 45 T Hybrid Magnet System, which has been designed to be a versatile, reliable, user-friendly magnet system capable of providing at least 45 T steady field to researchers in a 32 mm clear bore. The name *Hybrid* derives from the fact that both resistive and superconducting-magnet technologies are combined in this system to achieve this world-record level of field. The system also has been designed with capability for future upgrades up to 50 T using higher-power resistive inserts that may be developed. Most major subsystems have been delivered and are undergoing operational tests, while the large superconducting magnets are well into the manufacturing stages.

The 45 T objective will be achieved using a resistive insert magnet capable of producing 31 T while positioned inside the 616 mm warm bore of a superconducting outsert that adds 14 T to the field. The challenge for the outsert design is to accommodate the potential for sudden shut down, or even failure, of the insert—certainly without damage, but in most cases, without upset to the normal operation of the outsert. This requirement has led to a superconducting outsert design capable of over 15 T on axis (nearly 17 T maximum field at the windings) when operated alone.

Consistent with the NHMFL's mission, the Hybrid incorporates technology that significantly advances the state of the art for large, high field magnet systems. The superconducting outsert actually comprises three solenoids, all using cable-in-conduit-conductor (CICC) technology, two with Nb_3Sn superconductors and one with NbTi. It will be capable of highly stable operation with nearly 120 MJ stored energy and winding-pack current densities in the range of 40 to 50 A/mm^2. The resistive insert will use higher power (24 MW) than any previous steady-state resistive magnet, and new high-strength conductors, to achieve contributed field significantly greater than the stand-alone field available from a resistive magnet anywhere else in the world.

A typical CICC for the superconducting outsert is pictured schematically in Figure 1. Wire for the Hybrid conductors was manufactured by Oxford Superconducting Technologies (NbTi) and Teledyne Wah Chang (Nb_3Sn), cable was produced by New England Electric Wire, and jacketing was done on a special tube mill assembled for us as a collaboration of Intermagnetics General Corporation and Gibson Tube. The IGC/Gibson tube mill (shown schematically in Figure 2) was used to produce more than 10 km of jacketed conductor (dummy and real) during development and production runs for the Hybrid.

Figure 1.
A typical CICC (cable-in-conduit-conductor).

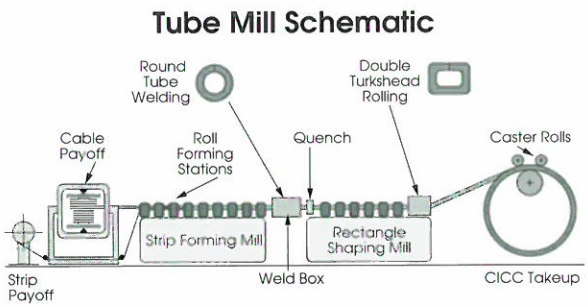

Figure 2. The IGC/Gibson tube mill

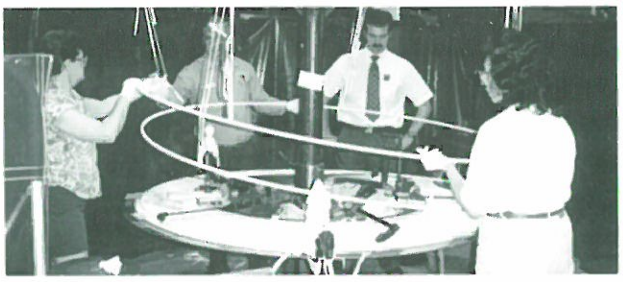

Figure 5. The NbTi coils, a pancake-style winding, are now at Everson Electric for insulation and VPI.

The two Nb_3Sn coils that were wound for us by IGC have been delivered to the NHMFL (Figures 3 and 4) for heat-treatment and vacuum/pressure impregnation (VPI). The NbTi coils, a pancake-style winding formerly the responsibility of Francis Bitter Magnet Laboratory (FBML), are now at Everson Electric for insulation and VPI (Figure 5). When Everson is finished with their part, the pancakes will be delivered to the NHMFL for terminating, stacking, joining, and assembly with the two Nb_3Sn coils.

Major subsystems for the Hybrid that have already been delivered to the NHMFL include the outsert power supply, all components of the protection circuit, a pair of refrigerator/liquefiers, the outsert cryostat, and much of the instrumentation and controls system. These have been installed and put through a variety of performance tests representative of their operation as a combined system. Figure 6 shows the magnet vessel, which will house the superconducting outsert, being checked for fit to the outsert cryostat. Figure 7 shows the site as it will appear to researchers who will use the facility for experiments in the highest steady fields available anywhere in the world.

Presently, we project all manufacturing processes to be complete on the two Nb_3Sn coils in late January or early February, 1997. The completion of coil C, which is an assembly of 29 separate pancake coils, is projected for late May, 1997. The outsert will be assembled and ready for test in August, 1997. The resistive insert (originally the purview of FBML) is presently being designed from scratch by the NHMFL team. The complete outsert system is projected to be operational in October, 1997. Principal NHMFL contributors are listed in Table 1.

Figure 3.
The A Nb_3Sn coil.

Figure 4.
The B Nb_3Sn coil.

Figure 6.
The magnet vessel.

Figure 7.
The site as it will appear to researchers who will use the facility.

Table 1. NHMFL contributors to the 45 T Hybrid Magnet.

Contributors	Areas of Responsibility
M. Bird S. Bole Y. Eyssa B. Gao	Resistive Insert
M. Haslow O. Hill J. Kenney S. Kenney G. Miller T. Painter R. Walsh L. Windham	Superconducting Outsert
K. Bartholomew S. Van Sciver S. Welton	Outsert Cryogenics
H. Gill S. Hannahs P. Murphy	Power/Protection/ Instrumentation
W. Walker T. Shewan V. Danart	Utilities/Site

Quench Initiation and Propagation Study (QUIPS) for Large scale Superconducting Magnets

Amemiya, N., NHMFL and Yokohama National Univ., Japan, Engineering
Hill, O.L., NHMFL
Miller, J.R., NHMFL
Kenney, J., NHMFL

Large scale superconducting magnets such as subcoils of the 45 T Hybrid are often wound with cable in conduit conductor (CICC). The quench initiation and propagation of CICC involve complicated processes, and understanding of them is essential to designing reliable large scale superconducting magnets and to protecting them.

A series of quench initiation and propagation study (QUIPS) is underway to accumulate the experimental data for a database on the quench and stability properties of CICC. In QUIPS II, to simulate the quench initiation and propagation processes of high field magnets made with Nb_3Sn superconductor, a small coil producing a relatively low magnetic field, almost 0 T, was wound with a NbTi superconductor. Actually, this coil was designed for a scale-down test of the subcoil A of the 45 T Hybrid whose magnetic field is 17 T. The critical temperature of Nb_3Sn at 17 T is almost same as that of NbTi at 0 T. Therefore, if the critical current density of the NbTi superconductor at 0 T agrees with that of the Nb_3Sn superconductor at 17 T, the quench initiation and propagation processes of the subcoil A can be simulated with the QUIPS II coil. Since the critical current density of usual NbTi superconductors is too high, a heat treatment was done to degrade the critical current density to the suitable level.

Table 1. Specifications of QUIPS II.

Superconductor	
Material	NbTi
Number of strand	3
Length	80 m
Coil	
Layer	2
Turn / layer	144
Inner layer ID	99 mm
Outer layer OD	112 mm
Coil height	550 mm

Table 2. Propagation velocity in QUIPS II.

Coil current	Propagation velocity
400 A	160 m / sec
230 A	40 m / sec

The specifications of the QUIPS II coil are listed in Table 1. Quench tests of the QUIPS II coil were made with a resistive heater. The normal zone propagation was studied with voltage taps. Figure 1 shows the temporal evolution of the normal voltages across the whole coil and the section L8, where the transport current before quench is 230 A. The distance between the heater and the section L8 is about 80 m. The estimated propagation velocities are listed in Table 2.

The fast quench propagation that was observed is favorable from the view point of the coil protection. Further investigation with larger QUIPS III coil is scheduled to get more data including the current transfer characteristics between strands during the quench initiation process.

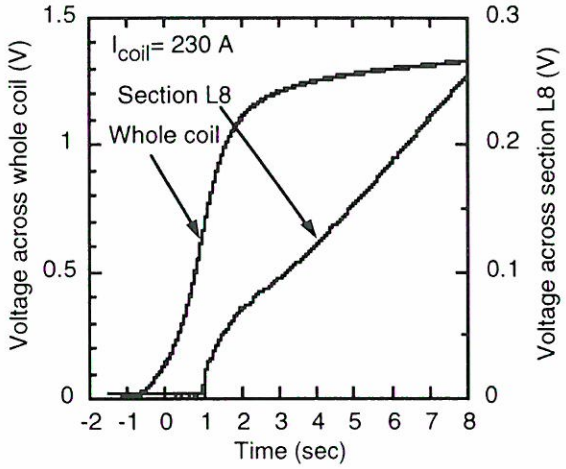

Figure 1. Temporal evolution of normal voltage, where distance between heater and section L8 is 80 m.

The Degradation of Critical Current for a NbTi Conductor Used in a Quench Initiation and Propagation Study for the 45 T Hybrid

Hill, O.L., NHMFL
Miller, J.R., NHMFL
Weijers, H.W., NHMFL

Efforts have been undertaken to experimentally model the 45 T Hybrid's high field stability and quench propagation characteristics using low field apparatus. This is in part based on the realization that the low field critical temperature of NbTi is comparable to that of Nb_3Sn at high field.[1]

One model cable-in-conduit coil design and its associated processes are discussed. This QUIPS II coil, carrying a NbTi-Cu stabilized triplex inside a tubular stainless steel sheath, required heat treatment for the purposes of degrading the critical current density. Despite the difficulties of processing, satisfactory progress has been made, yielding useful quench results at a significantly lower helium expense than that of a full scale model.[2]

I_c degradation was directly related to two primary factors: the dwell temperature and dwell time. Although reason was found for the cooling rate to have, potentially, a first order effect, such an event was not conclusive from the series of heat treatments and coiled-sample I_c measurements performed at the NHMFL.

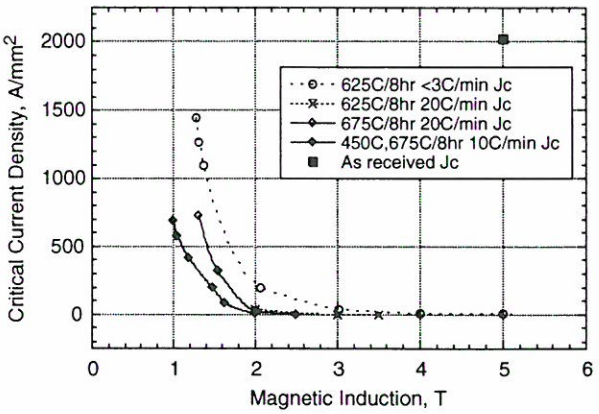

Figure 1. The effect of heat treatment on the field dependence of critical current density for NbTi. The processed conductors have been spoiled significantly.

Although it is likely that higher dwell temperatures and times would have reduced the J_c even more, 700 °C was the determined limit for the sake of other coil components. Longer dwell times also would have obliged greater degradation, yet it was noticed on a previous series of tests that most degradation occurred within 8 hours at temperature.

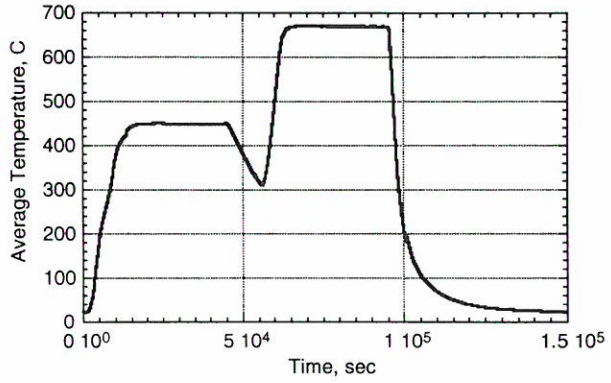

Figure 2. The heat treatment of QUIPS II NbTi coil. The glass fiber insulation inside the winding pack was desized at 450 °C/8 hrs in air. After purging the retort with argon the coil was stepped up to 670 °C/8 hrs for sufficient degradation, then force-flow cooled.

Sensitivity to final cooling rate is implicit in the works of C. Baker[3] and J. Sutton[4], which identify the formation of α Ti precipitates in a NbTi alloy with higher J_c and a β Ti prevalence in lower J_c alloys[1].

Heat treating the NbTi-Cu composite conductor had three noticeable effects in addition to J_c degradation[1]: increases in residual resistivity ratio, decreases in Cu fraction, and major increases in brittleness.

References:

1 Hill, O.L., *et al.*, in Proceedings for 1996 Applied Superconductivity Conference.

2 Amemiya, N., *et al.*, NHMFL 1996 Annual Report (1996).

3 Baker, C., *et al.*, Philosophical Magazine, **19**, 1223 (1969).

4 Sutton, J., *et al.*, Physics Letters, **21**, 601 (1966).

Test and Analysis of Joints for High-Current Superconducting Magnets

Miller, J.R., NHMFL
Miller, G.E., NHMFL
Kenney, W.J., NHMFL
Eyssa, Y.M., NHMFL

The quality of the joints and terminations for the superconducting coils of the 45 T Hybrid, which must carry 10 kA during normal operation, is a critical issue because the heating in these joints must be absorbed at 1.8 K. Resistances of ~ 10^{-10} ohms are desirable. Once these joints are installed, they cannot easily be reworked or repaired. Therefore, it is extremely important that the process for completing the joints be extremely reliable and repeatable. Joints of the type planned for the Hybrid, which basically comprise a lap joint between identical terminations, have been measured previously in fields up to 10 T to confirm feasibility of the design, and recently a series of tests was completed showing that the process yielded joints of repeatably high quality.

A simple apparatus was constructed to test a set of four joints simultaneously at currents up to 10 kA. Of a set, two of the joints were of the shaking-hands type and two were of the praying-hands type. Noise and drift in the voltage measured across each joint was a few μV, making a 10^{-10}-ohm joint just beyond our resolution by voltage measurement alone. In our test of the second set of four joints, the voltages across all joints were less than a few μV at 10 kA. For two of these joints, one a praying-hands type and one a shaking-hands, we used an array of three Hall probes to infer the relative uniformity of the transverse resistivity between legs of the joint, and in the case of the praying-hands joint, to accurately deduce the absolute resistance. In each case the Hall probes were equally spaced along the joint length, centered in the plane dividing the two terminals of the joint (but outside the joint), and oriented with the wide face of the probe perpendicular to that plane.

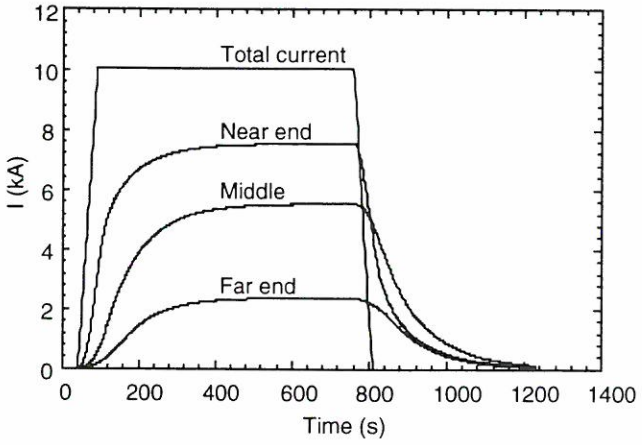

Figure 1. Current distribution vs. time in a high-quality praying-hands joint.

The Hall probe position and orientation allowed the current in each leg of the joint to be measured at that position. In the case of the praying-hands joint, which has a distributed inductance that is both significant and easily calculable, the distributed transverse resistance can be deduced from the time constant for achieving an equilibrium current distribution following a step change in total current. Figure 1 shows the observed current distribution vs. time in a praying-hands joint. The transverse resistance corresponding to these observations is approximately 2 x 10^{-10} ohm.

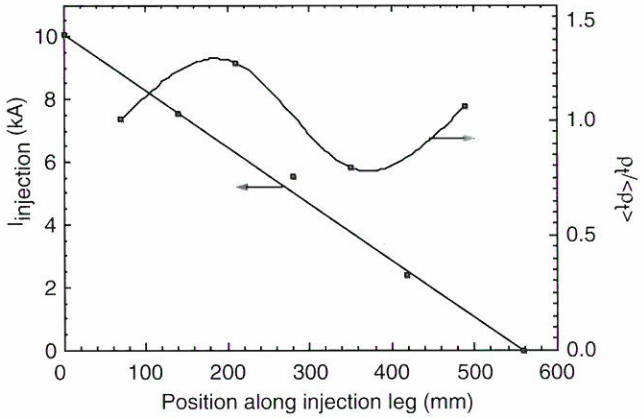

Figure 2. Equilibrium distribution of current along a high-quality, praying-hands joint and the deduced variation of relative transverse resistivity in that joint.

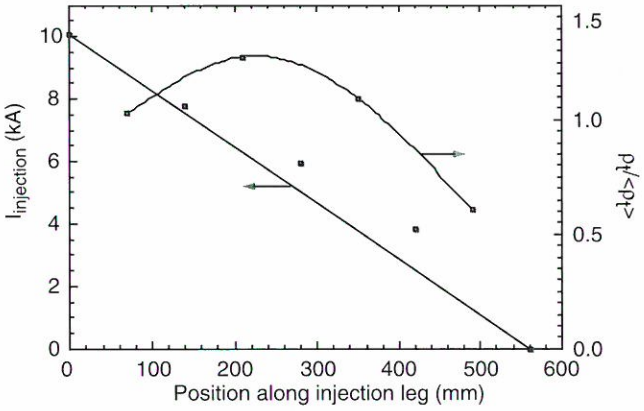

Figure 3. Equilibrium distribution of current along a high-quality, shaking-hands joint and the deduced variation of relative transverse resistivity in that joint.

For either type joint, the local value of transverse resistivity relative to the overall can be deduced from the local derivative of current vs. displacement along one leg of the joint. Figures 2 and 3 show the measured current distributions for two joints, a praying-hands and a shaking-hands joint, respectively. The measurements are compared to the ideal straight-line distributions, and the deduced relative variation of transverse resistivity is also plotted. We regard the observed variations as small and representative essentially of the highest quality obtainable with the present joint design.

MAGNET SCIENCE & TECHNOLOGY REPORTS

High Field Magnetic Resonance Magnet Systems

Program Overview

W.D. Markiewicz

Introduction

A number of advanced magnet systems are central to the future of the science and user programs at the National High Magnetic Field Laboratory (NHMFL). In the area of magnetic resonance, these magnets will provide high resolution nuclear magnetic resonance (NMR) at greater than 1 GHz, magnetic imaging research at 12 tesla (T), and ion cyclotron resonance (ICR) at 15 T. All of these systems represent an extension of the application of superconducting magnet technology. The ongoing activity in magnetic resonance magnets within Magnet Science and Technology seeks to address these instrument magnet requirements through a program of technology and magnet development. The program activity is directed specifically at the longer term objective of a 25 T high resolution NMR system. A significant challenge on the way to 25 T is the major, outer portion of the magnet based on conventional metallic superconductors. While advanced superconductors suitable for a high field inner coil are in development, the technology of the major, outer magnet is being addressed through the design and construction of a wide bore 900 MHz magnet. In support of this design, there is ongoing within MST, a wide ranging program of technology development that is applicable to the 12 T imaging magnet and the 15 T ICR magnet as well.

The difficulty of a high field superconducting magnet may be summarized by the magnitude of the magnetic stored energy. Figure 1 shows for high field NMR magnets, in schematic and graphical form, the growth in stored energy and magnet size with increasing proton resonance frequency. This extension of size and stored energy beyond existing magnets is coupled to increasing cost. In order to decrease the risk of unreliable performance, new developments in several aspects of the technology are required. This technology is presently being developed for application in the wide bore 900 MHz magnet.

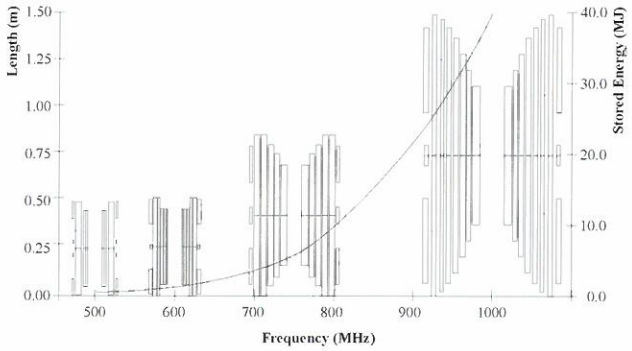

Figure 1. Size and stored energy of high resolution NMR Magnets versus proton resonance frequency.

900 MHz Magnet

An Engineering Design has now been generated for the 900 MHz magnet. In many of the features, this magnet can be seen to incorporate the concepts and configuration of lower field magnets. There are important aspects of the design that have emerged in a new direction and represent the advances in the technology. Recent improvements in Nb_3Sn conductor properties, motivated by the requirements of high field NMR, have lead to the availability of larger conductors with high current density at the highest fields. Further improvements in conductor properties are expected over time, which will help reduce the size of these magnets. The high stress in the windings of the 900 MHz magnet will be contained by stainless steel external reinforcement. While external reinforcement is common on smaller coils, issues of mechanical and electrical performance of the reinforcement on a magnet like the 900 MHz take on great importance for the magnet performance, and the reinforcement must be designed with all the care of the superconducting windings. The increase in stored energy, in addition to providing an indication of the degree of difficulty of the magnet, represents a significant issue for the quench protection of the magnet. An active protection system has been selected with the objective of providing the greatest degree of control of the critical elements of the system. The result is that the current density of the windings are maintained at high level even though there is a large stored energy to dissipate.

Technology Development

The design of the 900 MHz magnet has produced dramatic examples of the relationship between technology development activity and the implementation of the results of that activity in improved design. The NHMFL has created computer software that provides a more detailed and comprehensive understanding of the conditions in a coil during a quench than has been available in the past. The software was written initially as an example of an improved calculation method, based on the controlling physical processes, independent of scaling factors for specific conductors. In the application of the software to the design of the 900 MHz magnet, because of the comprehensive nature of the results, unexpected thermal stress effects were found that if not accommodated in the design could have lead to compromised performance. The NHMFL software revealed the problem. The software was also instrumental in performing the calculations for the design of the solution to the problem. In a similar fashion, the formulation of new tough epoxy has lead to improved designs of components like lead transitions that resolve long-standing issues.

Program Status

The Engineering Design for the 900 MHz magnet addresses issues of field, uniformity, protection and stress, and conductor design. Magnet configuration and dimensions have been generated, and the long lead Nb_3Sn conductor has been ordered. The magnet is a major construction project. Fabrication concepts and component layout activities are in progress in preparation for the production of detailed drawings. Technology development activities continue with the fabrication of test specimens, model coils, and test coils.

Computation of Nb_3Sn Component Properties from Mechanical Testing of Superconductor with and without Copper Stabilizer at 4.2 K

Dixon, I.R., NHMFL
Markiewicz, W.D., NHMFL

Stress-strain measurements on Nb_3Sn wires, manufactured by Vacuumschmelze, are performed at 4.2 K. The tensile tests are performed on a machine designed for testing at cryogenic temperatures at NHMFL. The copper, originally 41% area fraction, is stripped to produce a wire that consists of only the tantalum barrier, bronze, and superconducting filaments. The wires are tested in the standard and etched state to determine the initial influence copper has on the primary modulus, to obtain mechanical property data on the Nb_3Sn filaments, and to learn more about the condition of plastic deformation in the copper and bronze regions.

The wire is designated as V50 for the standard 41% Cu conductor and V50e for the etched conductor. Table 1 contains the fractions of each constituent. The sample length is six inches. Two samples of each type were tested. The dimensions of the standard conductor are 1.11 mm x 1.73 mm with an area of 1.835 mm^2. The dimensions of the etched conductor are 0.81 mm x 1.43 mm with an area of 1.066 mm^2.

Table 1. Constituent fractions of Nb_3Sn samples.

Type	f_{Cu}	$f_{Barrier}$	f_{CuSn}	f_{Nb3Sn}
V50	0.410	0.070	0.390	0.130
V50e	0.000	0.119	0.661	0.220

Stress-strain curves of each conductor type are shown in Figures 1 and 2. Tabulated results include the primary (elastic), secondary (elastic-plastic), and secant moduli. The secant modulus is the stress-strain ratio to 0.3% strain. Table 2 contains the moduli of wire sample.

Table 2. Test results of Nb_3Sn wires at 4.2 K.

Sample	Copper	E_1 (GPa)	E_2 (GPa)	E_S (GPa)
V50-1	41%	80.5	32.7	42.6
V50-2	41%	81.0	30.2	43.5
V50e-1	Etched	104.0	53.3	68.6
V50e-2	Etched	108.8	51.0	67.0

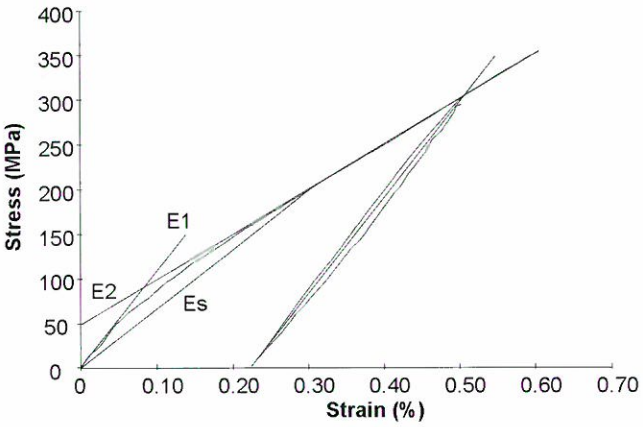

Figure 1. Stress-strain curve of VAC Nb_3Sn at 4.2 K, sample V50-1.

From the rule of mixtures and the above results, the modulus of bronze may be computed, assuming the Nb_3Sn filaments and tantalum barrier remain elastic. The modulus of Nb_3Sn filaments is 110 GPa and the modulus of tantalum is 186 GPa. Thus from the etched conductors the effective bronze primary and secondary moduli are computed to be 90.9 and 8.84 GPa.

These values may be used in predictions of the stress-strain characteristics of Nb_3Sn conductors

for a variety of compositions. The mechanical characteristics of the conductors are essential aspects of the mechanical design of high field magnets.

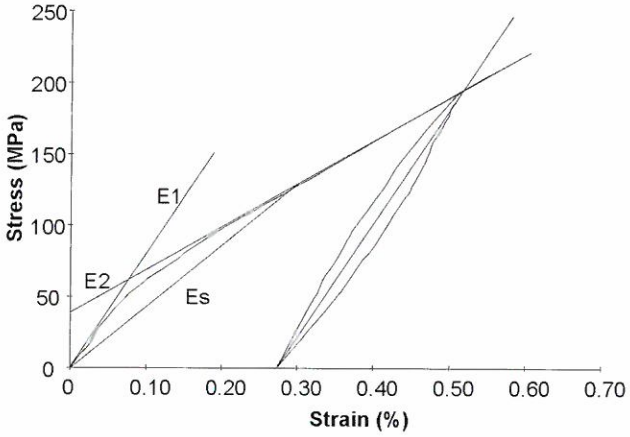

Figure 2. Stress-strain curve of VAC Nb_3Sn at 4.2 K, sample V50e-1, stabilizer removed.

Critical Current Measurements of Nb_3Sn Superconductors for the 900 MHz NMR Magnet

Dixon, I.R., NHMFL
Markiewicz, W.D., NHMFL

The critical currents of three types of Nb_3Sn superconductors, produced by Vacuumschmelze, are measured for application in the 900 MHz NMR magnet. Tests are performed in background fields up to 20 T and at 4.2 K.

Two test samples of each conductor type are measured. The conductor characteristics are listed in Table 1. Conductor type V105 is comparable in size to the conductor in the first Nb_3Sn coil of the 900 MHz NMR Magnet. Conductor V106 is essentially the same conductor as V105 but has been drawn down to a smaller size. Conductor V107 is applicable to the fifth Nb_3Sn coil.

The heat treat schedule for all samples was 200 hrs at 670 °C. The atmosphere during each temperature stage was stagnant argon and during temperature ramps the retort was evacuated. After reaction, the samples are removed from their heat treat fixtures and dip soldered onto the base of a high current sample holder. The sample spans over a Ti-6Al-4V shunt, which is chosen because of thermal contraction similarities.

Table 1. Nb_3Sn superconductor characteristics.

NHMFL ID	Dimension (mm)	Aw (mm^2)	Asc (mm^2)	f_{Cu}	f_B
V105	1.97 x 3.17	6.24	4.31	0.25	0.06
V106	1.51 x 3.17	4.79	3.30	0.25	0.06
V107	1.1 x 1.73	1.90	1.01	0.41	0.06

The samples were tested in the resistive magnet user facility at NHMFL. A magnet with a 50 mm bore was used to produce a background field up to 20 T. A 0.1 μV/cm sensitivity above the baseline voltage was followed in determining the critical currents.

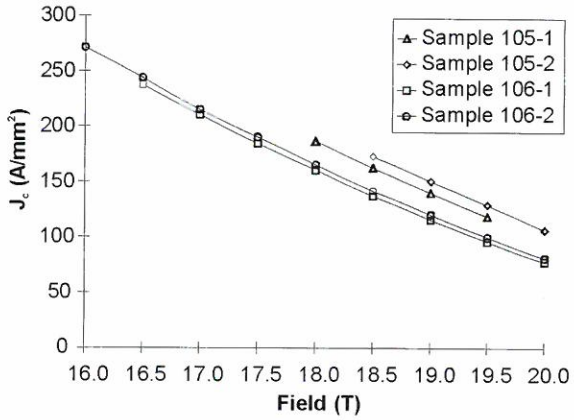

Figure 1. Critical current densities of Nb_3Sn superconductors #105 and #106 at 4.2 K.

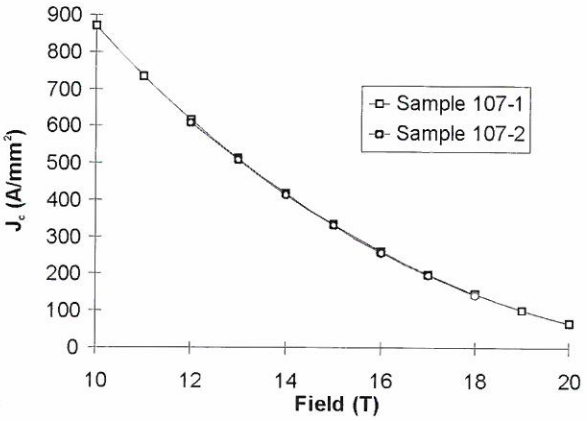

Figure 2. Critical current densities of Nb_3Sn superconductor #107 at 4.2 K.

The critical current density in the superconductor region is shown in Figures 1 and 2. The critical current density of conductor V105 is 107 A/mm^2 at 20 T and 4.2 K, a relatively high value that contributes to the feasibility of high field magnets. The current density for conductors V106 is significantly less at 80 A/mm^2, showing a detrimental effect of additional area reduction. The conductor V107 is typical of performance in the mid-field range.

Data on critical currents is combined with analytical expressions to predict current densities at 1.8 K and high strain as required for magnet design.

Finite Element Analysis of Coil Forms for NbTi Coils of the 900 MHz NMR Magnet

Dixon, I.R., NHMFL
Markiewicz, W.D., NHMFL

The present concept for the construction of the NbTi coils of the 900 MHz NMR magnet includes the use of an aluminum coil form. The fabrication process consists of winding conductor, epoxy impregnation, and overwinding with steel reinforcement. Clearance constraints require the coil form to be limited in thickness.

An option for the manufacture of the bore tube includes the use of a relatively thick tube for coil fabrication followed by a machining operation to remove some of the tube thickness. A finite element analysis is performed at NHMFL to study the response of the coil form to winding loads and to review the option of machining the inner radius of the form.

In the analysis, twenty layers of 1 mm high NbTi wire and fourteen layers of 1 mm high steel wire are applied to an aluminum coil form. The analysis uses axisymmetric finite elements for the structural model. Contact elements are used to model the coil to coil form interface. The coil dimensions are nominal values representing the largest two NbTi coils of the 900 MHz NMR magnet. The inner and outer radii of the NbTi windings are 0.28 m and 0.30 m respectively. The reinforcement is assumed to be perfectly bonded to the windings and has an outer radius of 0.314 m. The properties of the NbTi and steel composites are listed in Table 1.

Table 1. Mechanical properties of NbTi coil and steel reinforcement at room temperature.

Property	NbTi	Steel
E_{11} (GPa)	85.52	187.5
E_{22} (GPa)	26.76	123.9
E_{33} (GPa)	42.15	136.6
G_{23} (GPa)	5.4	32.6
ν_{23}	0.129	0.188

The analysis represents a boring operation on a 29 mm coil form as it is cut down to 4 mm thick in 2.5 mm increments. Initially it proceeds by winding NbTi and reinforcement around an aluminum former at 34.5 MPa and 69.0 MPa. The analysis then starts to remove layers of material from the inner radius by reducing the stiffness of the finite elements along the machined layer to near zero and then solving for equilibrium. This is repeated for each layer. It continues by removing the elements at a prescribed layer thickness until the coil form reaches 4 mm of thickness.

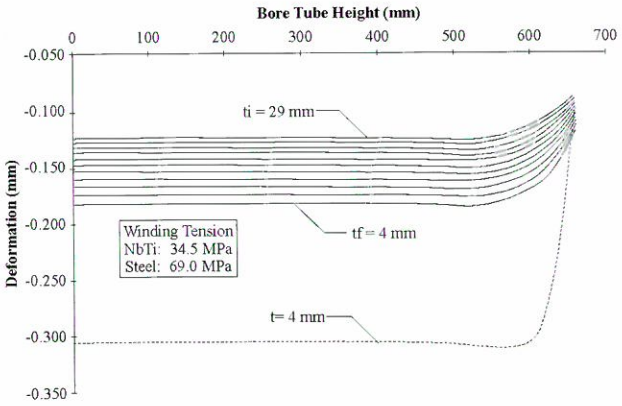

Figure 1. Deformation from winding tensions of a 29 mm thick coil form with material removed in 2.5 mm increments and a 4 mm thick coil form.

Although the displacement increases by approximately 50% as the form is cut from 29 mm to 4 mm, it does not reach the magnitude of a coil form that is initially 4 mm thick. These results are

compared together in Figure 1. In the figure, the deformation of the coil form after each machining pass is plotted. The final deformation of the machined coil is -0.183 mm, which is 0.122 mm less than the deformation of a coil form that is originally 4 mm thick.

The pressures from the winding tensions cause the initial radial deformations. After the epoxy impregnation the coil stiffness increases and thus is able to support more of the winding stresses. Therefore the final deformation of a coil form is dependent on its initial thickness.

Persistent Joint Development

Swenson, C.A., NHMFL
Markiewicz, W.D., NHMFL

The 900 MHz magnet design consists of a series of ten nested Nb_3Sn and NbTi solenoid coils. The magnet requires persistent superconducting joints between and within these coils. The field decay requirements for high resolution NMR limit the allowable joint resistance to the order of 10^{-11} Ω. Figure 1 presents the field decay vs. circuit resistance.

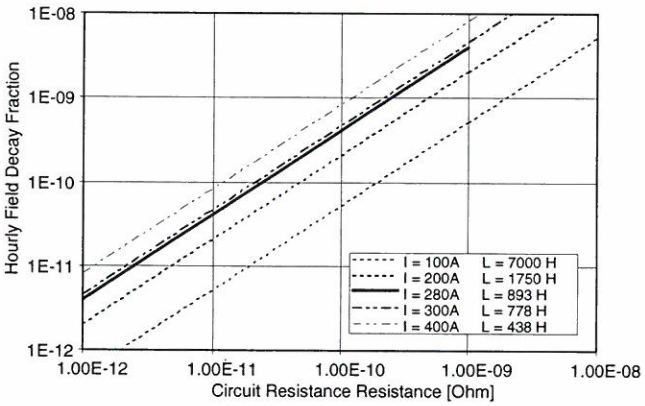

Figure 1. Hourly decay fraction vs. circuit resistance for 35 MJ designs.

In the engineering design, a fractional hourly decay rate of $1x10^{-9}$ would imply a total circuit resistance of $\cong 2.5x10^{-10}$ Ω. The circuit resistance represents a sum of all joints in the circuit.

Joint development for the 900 MHz magnet encompasses the following persistent joint configurations:

Nb_3Sn-Nb_3Sn	Joints within Nb_3Sn coils
Nb_3Sn-NbTi-Nb_3Sn	Joints between Nb_3Sn coils
NbTi-Nb_3Sn	Nb_3Sn and NbTi coils
NbTi-NbTi	Joints within NbTi coils
NbTi-NbTi	Joints between NbTi coils

Phase I Progress

We have completed a phase one study on Nb_3Sn joint technology. The study emphasized development of powder metallurgy techniques for Nb_3Sn joints. We have fabricated Nb_3Sn-Nb_3Sn joints using powder metallurgy. Our powder processing methods produce tough, mechanically-stable sintered Nb_3Sn blocks that are superconducting. Figure 2 presents an example of testing data from a Nb_3Sn joint. The joint geometry was a 6.2 x 32 mm long block. The effective block thickness containing the Nb_3Sn joint was 3 mm.

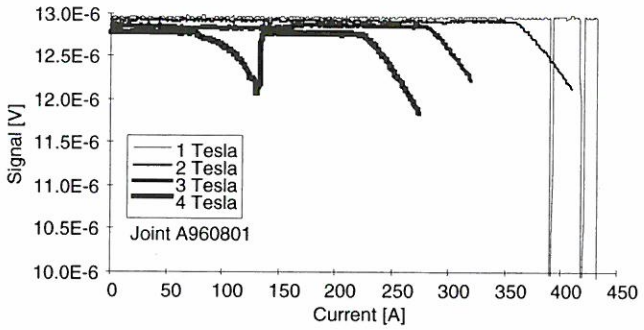

Figure 2. Voltage traces for Nb_3Sn-Nb_3Sn powder metallurgy joints.

The voltage trace at 4 T has an inductive signal in the 100 to 150 A range. This is due to a current path redistribution in the joint block. Signal levels return to baseline values when the current ramp rate is zeroed.

Conclusion

The current process will produce Nb_3Sn joints that transition above 350 A in a 2 T magnetic field. Measurements indicate that the present level of technology would allow a 2 T magnetic joint background field for magnet construction.

Development will focus on hybrid joints between Nb_3Sn and NbTi conductors.

Quench Heater Development

Swenson, C.A., NHMFL
Markiewicz, W.D., NHMFL

Quench heaters are encapsulated within the epoxy and glass on the coil circumference. The mechanical integrity of the epoxy and glass in the neighborhood of the heater is critical. The interface is subject to large temperature gradients and mechanical stress during operation of the protection system. Characterization of this interface allows the reliable design of heater networks on large epoxy impregnated coils. We have fabricated models demonstrating heater interfaces with and without over-banding. We characterize the interface using a damage threshold concept in the context of cyclic life testing on the interface.

The central fabrication technology for these coils is vacuum epoxy impregnation. A heater is a thin stainless steel strip located axially on the outside of the coil. Quench heaters are on the outside of the superconducting coils in the interface region between the over-banding and the coil. There is a single layer of glass cloth between the heater and the outermost layer of the superconducting coils. Two to three layers of inter-layer cloth are wrapped over the heaters prior to impregnation. The interface is this layered region filled with glass and epoxy between the heaters and coil. Figure 1 presents a representation of this geometry.

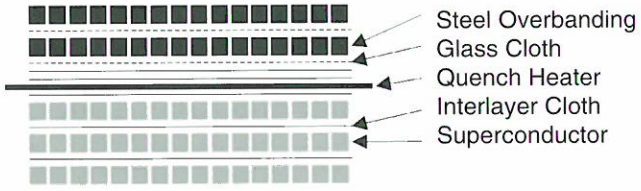

Figure 1. Axial cross-section of quench heater interface for 900 MHz magnet.

During heater operation this interface region is subject to large thermal gradients that can cause damage to the surrounding glass epoxy layer. Damage to this mechanical interface can degrade magnet performance. The objective of power testing was to establish the durability of the epoxy heater interface. Figure 2 presents a logical schematic of the experiment. This investigation has measured the damage threshold associated with this geometry when operated at 4.2 K in liquid helium.

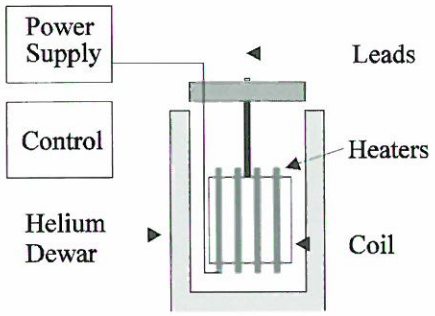

Figure 2. Logical schematic for quench heaters during power testing.

No heater interface damage was observed after 100 cycles at 5 and 10 W/cm^2. Cracking and delamination of epoxy was observed after 10 pulses at a heat flux of 30 W/cm^2. The 10 cycle damage threshold occurs when the maximum element temperature is between 100 and 120 K.

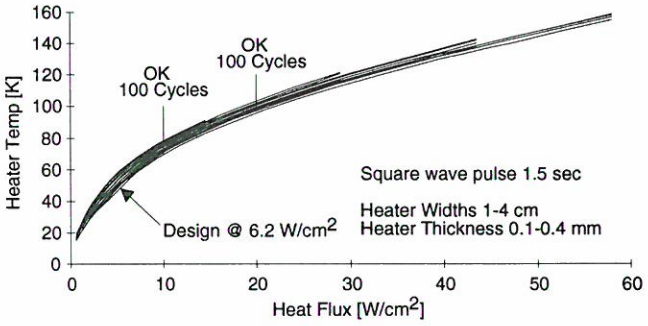

Figure 3. Damage thresholds measured for epoxy-quench heater interface on 900 MHz design. (T_0 = 4.2 K)

Sizing Removal from Glass Fiber

Swenson, C.A., NHMFL
Markiewicz, W.D., NHMFL

Glass fiber textiles are fabricated using a starch and oil lubricant to prevent fiber fracture during the weaving operation. The residual lubricant remaining on these fabrics is called a sizing or finish. The starch and oil finish is usually called a greige finish.

The starch and oil sizing that is present on the inter-layer cloth and conductor insulation is a

problem for Nb_3Sn coil construction. During the heat treatment the sizing decomposes forming carbon and carbonaceous residues that interfere with impregnation and bonding of epoxy to the glass and conductor. The carbonaceous residues are also prone to migration and will contaminate the entire coil assembly. Therefore, it is desirable to remove the starch and oil from the fabrics prior to heat treatment.

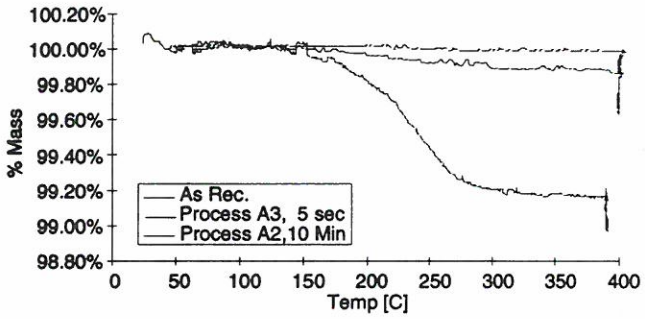

Figure 1. TGA plots of in-line cleaned conductor in comparison with dip cleaned materials.

Glass fiber can be either heat cleaned using an oxidation burn-off method in air or chemically cleaned using detergents or solvents. Roughly 1% of the mass of braid and 1 to 2 % of the mass of glass cloth can be attributed to the sizing.

The sizing that is present on conductor insulation is the primary problem for Nb_3Sn coil construction. Our development activities are directed at understanding the most efficient method to remove the sizing. Heat cleaning is unsuitable for copper jacketed conductor. Our experience is that the copper jacket is susceptible to irreversible oxidation damage at temperatures where sizing removal is effective.

We have developed an in-line chemical cleaning process that takes about 5 to 10 seconds. The process is a wash rinse sequence. We have validated this processing approach using data based upon thermogravimetric analysis. Approximately 90 to 95% of the sizing can be removed using this method. Figure 1 presents an example TGA plot illustrating the relative effectiveness of two sizing removal methods. The final process will be adjusted to clean the specified S-glass conductor braid.

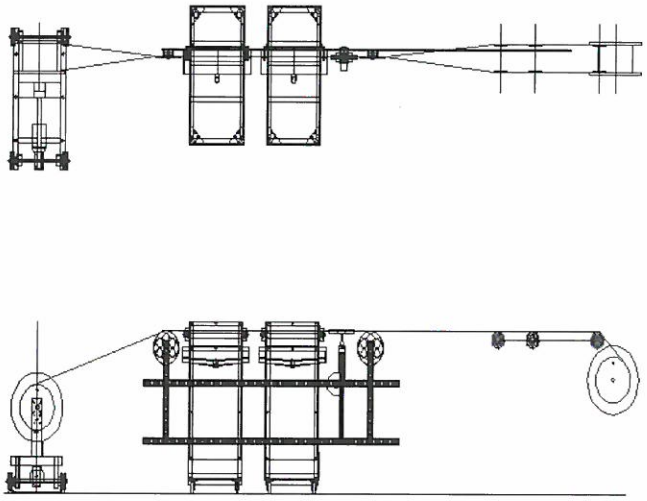

Figure 2. Engineering layout for sizing removal wire cleaning line.

Conclusion

The in-line cleaning method has been being implemented using an in-line process with wash and rinse tanks. The line is being designed to clean conductor at 10 meters per min. Figure 2 illustrates the line engineering concept. There are ten defined stations. Each station performs a critical operation for the line function. The line is now in assembly.

Thermal Contraction Measurement Results for Nb_3Sn Composites

Swenson, C.A., NHMFL
Markiewicz, W.D., NHMFL

Strain gauges were mounted on four Nb_3Sn composite samples. Two samples were made with a 0.35 copper fraction Nb_3Sn wire, and two samples were made with a 0.6 copper fraction Nb_3Sn wire. There were a total of four gauges for each principal axis of the composite. Reference sample materials were 304:SS and Al 6061-T6. The 304:SS reference material replaced the invar 36 because the observed scatter in gauge resistance was smaller with the steel than the invar. The differential strain was measured at 77 and 4 K. The gauge signals from steel and aluminum were used as reference materials to estimate the gauge factors and the thermal contraction along each composite axis. Three thermal cycles were performed to determine

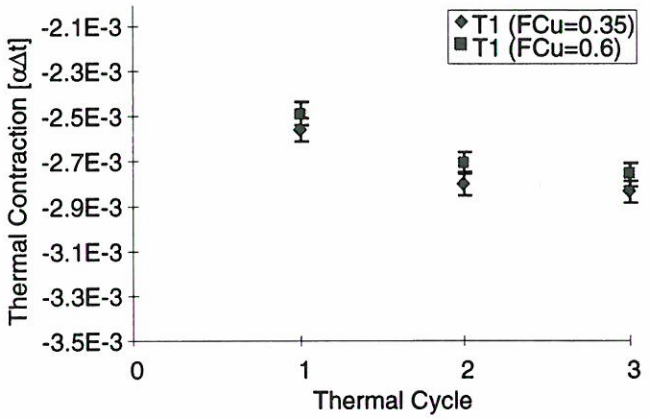

Figure 1. Comparison of thermal contraction between high and low copper fraction Nb_3Sn winding composites at 4.2 K. (T_1 orientation)

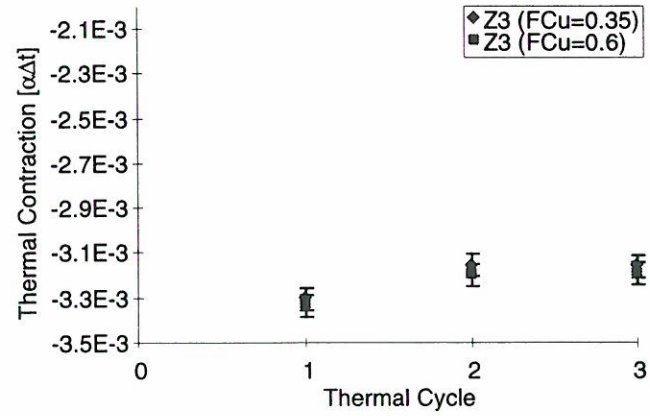

Figure 2. Comparison of thermal contraction between high and low copper fraction Nb_3Sn winding composites at 4.2 K. (R_2 orientation)

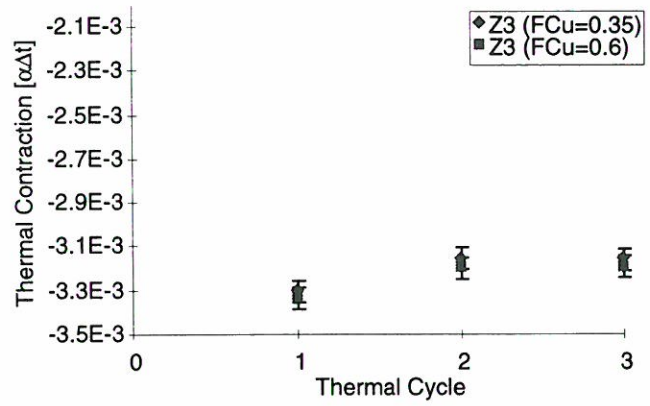

Figure 3. Comparison of thermal contraction between high and low copper fraction Nb_3Sn winding composites at 4.2 K. (Z_3 orientation)

repeatability, data scatter, and any cyclic trends. Data scatter was consistent with estimated error. Cyclic trends were present in the data. This could possibly be attributed to strain relief in the Nb_3Sn conductor filaments as the bronze and copper yield during cool-down.

Figures 1-3 present cyclic data for the T_1, R_2 and Z_3 composite orientations. Copper fraction influences the thermal contraction in the R_2 direction. This also may be caused by a difference in the copper yielding in each conductor.

Conclusion

Model winding composites have been manufactured to be representative of epoxy impregnated NbTi and Nb_3Sn coils. The modeling activity has provided a mechanism to understand composite properties and refine coil processing issues.

Thermal Contraction Measurements on NbTi Winding Composite

Swenson, C.A., NHMFL
Markiewicz, W.D., NHMFL

Accurate knowledge of winding composite thermal contraction properties is critical to the design of large epoxy impregnated Nb_3Sn and NbTi coils. Measurement of thermal contraction properties allows the reliable design prediction of cold coil dimensions, the state of the coil form interface resulting mechanical stresses from cool-down, and the correct locations of coils in an assembly. NbTi and Nb_3Sn epoxy glass winding composites have been built to precisely model the materials, packing factors, and processing steps consistent with coil fabrication. Figure 1 presents a representative cross section of a model winding composite. Thermal contraction properties are measured using a strain gauge measurement technique where gauge signals are compared to known reference samples. Composites are inherently anisotropic. Gauges are placed on each sample to measure the thermal contraction along each principal axis of the composite.

Measurement Results for NbTi Composites

Strain gauges were mounted on two NbTi composite samples. There were a total of four gauges for each principal axis of the composite. Reference sample materials were invar 36, and Al 6061-T6. The differential strain was measured at 77 and 4 K. The gauge signals from invar and aluminum were used as reference materials to estimate the gauge factors and the thermal contraction along each composite axis. Three thermal cycles were performed to determine repeatability, data scatter, and any cyclic trends. Data scatter was consistent with estimated error. No cyclic trends were present in the data.

A comparison between measured and analytical thermal contractions is presented in Table 1. Figure 2 presents a graphical summary of the measured data. The analytical results are computed by first using laminate theory to determine the effective orthotropic properties of the glass and epoxy regions. The average composite properties are then computed by applying a law of mixtures approach to the individual glass-epoxy and conductor properties. The results agree very well with a maximum difference of 4%.

Table 1. Data summary for NbTi composite.

Temp [K]	T_1 $\alpha\Delta t$	R_2 $\alpha\Delta t$	Z_3 $\alpha\Delta t$
77	-2.71E-3	-3.65E-3	-3.23E-3
4.2	-2.94E-3	-4.03E-3	-3.55E-3
Theory @4.2K	-3.06E-3	-4.07E-3	-3.68E-3
% Difference	4%	1%	3.6%

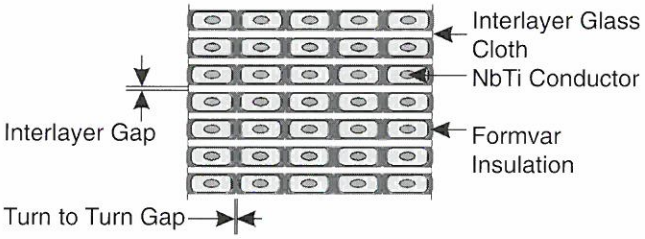

Figure 1. Cross-section of a NbTi winding composite.

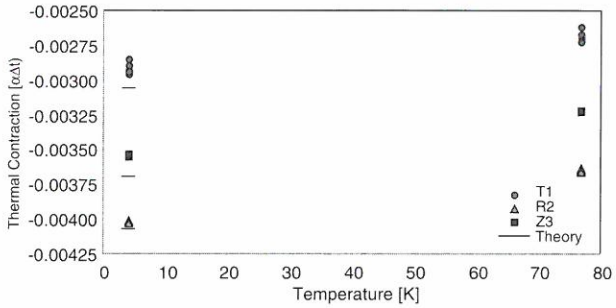

Figure 2. Thermal contraction of NbTi winding composite at 77 and 4.2 K. Orientation: T_1 is the tangential, R_2 is radial, and Z_3 is axial.

MAGNET SCIENCE & TECHNOLOGY REPORTS

Resistive Magnets

Program Overview

M.D. Bird and Y.M. Eyssa

Mission

The Resistive Magnet Program is responsible for the design, construction, and maintenance of all the high field DC resistive magnets at the National High Magnetic Field Laboratory (NHMFL). These magnets typically provide fields above 20 T in room temperature bores greater than 32 mm while consuming greater than 8 MW of power. All magnets constructed to date have used perforated copper alloy sheets (Bitter and Florida-Bitter magnet technology).

Recent Accomplishments

On February 5, 1996, the world's first 33 T resistive magnet was successfully tested to a peak on-axis field of 33.1 T in a 32 mm bore at the NHMFL. Later that evening, Dysprosium pole pieces built by Stepankin, *et al.*, were installed in the bore of the magnet concentrating the field to 36.3 T. On February 29, 1996, the magnet was restacked to better match the power supplies and attained a peak on axis field of 33.6 T without flux concentrators. The magnet is now available routinely to users at 33.1 T. As of February 11, 1997, this new magnet had been operated for 433 hours consuming 1234 MW hours of energy. The 33 T magnet uses the same outer coil as our earlier 27 T, 30 T, and 24.5 T high homogeneity magnets. The middle coil is of a new design using the Florida-Bitter technology developed at the NHMFL and is capable of carrying more current and generating a higher field than the earlier Bitter design. The innermost coil also uses the Florida-Bitter technology and consists of two subcoils in parallel electrically. These subcoils are too slender to allow tierods and share a common clamping system making them the first poly-Bitter coils at the NHMFL. In addition, this magnet uses new, non-circular tierods to reduce the peak stress, current density, and temperature associated with round tierod holes. Table 1 presents the resistive magnets operational at the NHMFL as of February 11, 1997, and the amount of time that the various coils (A, B, and C labeled from the inside out) have been operated.

Future Plans

NSF Core Grant

In July, 1997, we will deliver another poly-Bitter magnet, this one providing 20 T in a 200 mm bore. The magnet is presently in the construction phase and is being built in collaboration with the High Magnetic Field Laboratory of Grenoble, France. Stamping tooling for the inner two coils has been accepted, and the outer two coils were finished in November, 1996. The housing was pressure tested in December. We hope to upgrade this magnet to 40 T in a 50 mm bore using 40 MW of power at some future time.

The 33 T magnet has been redesigned to provide 33 T while consuming only 17 MW of power compared with the 19.2 MW of the existing 33 T magnet. This new 33 T design has been developed to further push the limits of Florida-Bitter magnet technology and determine the final design parameters of the hybrid insert.

We are nearing completion of a test stand in which we will be able to operate coils one at a time and develop a better understanding of energy and momentum transfer in resistive magnet cooling water flows. This information will be used in selecting final design parameters for the NHMFL hybrid insert.

We have nearly completed coil design for the hybrid insert and have developed concepts generating fields up to 45 T using 24 MW and 50 T using 32 MW.

Table 1. Resistive magnets available at the NHMFL February 11, 1997.

Cell No.	Field (T)	Bore (mm)	Power (MW)	Homogeneity (ppm /10 mm)	Runtime (hrs) A	B	C
3	20.4	50	8.0	750	546	2064	
5	20.4	50	8.0	750	941	941	
7	24.5	32	13.1	30	1471	333	2238
8	30.1	32	16.0	1500	1376	1376	1376
9	30.1	32	16.0	1500	1763	1763	1763
12	33.1	32	19.2	600	433	478	478

In addition, we are in the final stages of coil design for a new magnet to provide 29 T in a 52 mm bore to replace the aging 20 T, 50 mm bore magnets. This new magnet should be finished in the second quarter of 1998. Shortly thereafter we will construct wire wound coils to be installed in this magnet to provide 29 T in a 32 mm bore with field modulation and field gradient.

We have begun design studies for a split pair (radial access) magnet. It appears that 30 T in a 32 mm bore with a 32 mm radial bore should be feasible.

Outside Grants

In August, 1995, we received a grant from NASA to build a 0.16 T, 186 mm bore magnet for growing crystals on the space station. This magnet is in the assembly phase and should be finished in April, 1997.

In July, 1996, we received a contract to build a 30 T Florida-Bitter magnet for the National Research Institute for Metals in Tsukuba, Japan. This magnet is in the fabrication phase and will be installed at the NRIM in September, 1997.

In June, 1996, we received a grant from the Keck Foundation to build a 25 T, 52 mm bore magnet with inhomogeneity less than 1 ppm over a 10 mm diameter spherical volume. This magnet is in the detailed design phase and should be installed and operational at the NHMFL in December, 1997.

Design of a Resistive Insert for the 45 T Hybrid Magnet

Bird, M.D., NHMFL
Eyssa, Y.M., NHMFL
Gao, B.-J., NHMFL

A preliminary coil design for the 45 T Hybrid insert has been completed and is presented in Table 1. The superconducting outsert of this magnet system should provide 14 T in a 616 mm warm bore. The resistive insert should provide greater than or equal to 31 T in a 32 mm bore to bring the total to 45 T.

Table 1. Design parameters of NHMFL 45 T Hybrid magnet resistive insert.

Coil label	A1	A2	B	C	D
Inner radius (mm)	19	32.7	70.5	124.2	181.7
Outer radius (mm)	32	68.5	121.2	178.7	255
Coil height (mm)	237.7	406.7	509.3	510.6	563.4
Field (T)	4.8	7.1	33.4	25.9	19.9
Material	Cu-Ag	Cu-Ag	Cu-Be	Cu-Be	Cu-Zr
Max. stress (MPa)	584	606	602	551	402
Jmax (A/mm^2)	556	310	198	147	104
Heat flux (W/mm^2)	4.0	2.5	1.9	2.0	1.5
P density (W/mm^3)	7.6	2.4	1.0	0.59	0.24
Hyd. diameter (mm)	1.3	1.4	1.5	1.9	1.9
Hole numbers	40	168	336	300	360
Pressure drop (bars)	28	28	28	28	28
Flow rate (l/s)	9	18	38	64	71
Velocity (m/s)	16	14	13	15	14
Ave. temp (C)	49	47	45	42	41
Max temp (C)	72	72	70	62	60
No. of turns	42	46	46	40	50
No. of disks/turn	8	12	16	15	15
No. of tie rods	0	12	16	15	60
Disk thick. (mm)	0.62	0.62	0.62	0.73	0.71
Insulator thick. (mm)	0.15	0.15	0.15	0.15	0.15

This magnet is of the Florida-Bitter type using elongated cooling holes in a staggered grid to reduce stress concentrations and radial force transmission.[1] This magnet is conceptually very similar to the existing 33 T magnet at the NHMFL.[2] Like the 33 T magnet, the two innermost coils, A1 and A2, are electrically in parallel and will be made of Cu-Ag sheet. The B coil will be made of Cu-Be or Cu-Ag depending on the availability and cost of Cu-Ag. The C and D coils will be made of Cu-Be and Cu-Zr respectively.

In the past few years the Florida-Bitter magnet technology has been developed to provide higher fields more reliably. Consequently, the requirement to make 45 T that was set approximately five years ago seems a little outdated. Presently we are considering the possibility of attaining as much as 50 T with this magnet design. Before finalizing the design and operating current for this magnet, we will conduct a series of development activities to verify our understanding of high field DC resistive magnet design. To begin with, we have redesigned our 33 T magnet to provide the same field as the

present design with substantially less power consumption.[3] This redesigned magnet will operate at stresses and power densities higher than any attained to date. Furthermore, we are building a test stand in which individual coils can be operated to better understand the heat transfer coefficients and friction factors associated with these new magnet geometries. Finally, we are developing computational methods to accurately model three dimensional turbulence in very rough channels to further our understanding of the heat and momentum transfer occurring in Florida-Bitter magnets.[4]

References:

1 Bird, M.D., *et al.*, IEEE Trans. on Magn., **32**, No. 4, 2444-2449 (July 1996).

2 Bird, M.D., *et al.*, IEEE Trans. on Magn., **32**, No. 4, 2542-2545 (July 1996).

3 Bird, M.D., *et al.*, NHMFL 1996 Annual Report (1997).

4 Prestemon, S., NHMFL 1996 Annual Report (1997).

Recent Developments in High Field Resistive Magnet Design

Bird, M.D., NHMFL
Eyssa, Y.M., NHMFL
Gao, B.-J., NHMFL

Traditionally when high field Bitter magnets have been built, copper alloy disks with round holes have been stamped and stacked between heavy brass endplates. This process has been successful in providing fields up to about 24 T at other facilities and up to 27 T here at the NHMFL. Attaining higher fields requires higher current densities that result in stresses, power densities, and heat fluxes that cannot be supported by traditional Bitter magnets. To overcome these obstacles, the Grenoble High Magnetic Field Laboratory introduced polyhelix magnets and the Francis Bitter National Magnet Laboratory developed monohelices.

Here at the NHMFL we feel that an axially-cooled Bitter magnet provides the most efficient cooling system of the various types of high field resistive magnets and is the cheapest and fastest to construct. To improve upon it we developed the Florida-Bitter magnet,[1] which is substantially stronger than a traditional Bitter magnet but still has the efficient cooling system. The first of these magnets attained 30.1 T in a 32 mm bore.

Our next step was to develop a poly-Florida-Bitter magnet, which reduces stresses even further and allows more efficient use of current and power than a Florida-Bitter magnet. This magnet attained 33.1 T in a 32 mm bore[2] making it comparable or superior to all other DC magnets, including hybrids. We then undertook an experiment to see how far we could push the poly-Florida-Bitter magnet technology. We attained 33.6 T before acoustic noise induced us to disassemble the magnet. Upon disassembly it was seen that the end turns (top and bottom) of the innermost coil had moved as well as individual conductors and insulators in these end turns had broken.

These coils do not employ axial current density grading so the current densities at the ends of the coils are the same as those at the midplanes. The magnetic field, however, is greater at the midplane than at the ends. Consequently, the nominal Lorentz forces and stresses are highest at the midplane of the coil and one might expect the coil to fail at the midplane. In the endplates, however, the current density is rather low (3 to 4 A/mm^2) and is in the axial direction, while in the active disks the current density is very high (400 to 600 A/mm^2) and is in the hoop direction. Furthermore, the transition from the low current density region to the high current density region occurs over about 160 mm^3. In addition, in the same region that the current is making the transition from low density to high density, the cooling water is making a transition from flow through round channels to flow through obround channels. Consequently, at the start of the active part of the coil the cooling water flow may not be fully developed and the heat transfer may not be as high as in most of the magnet. These sharp transitions probably introduced stress concentrations and hot spots that resulted in the shifting and failure of disks in the end turns. Finally, the coloration of the disks upon disassembly

suggests that the clamping of the disks by the structure was not uniform.

Before re-assembling the magnet the final time, several changes were made to the clamping structure to provide more uniform clamping and the end turns of the coil were built with lower current density to provide for a transition from low to high current density over approximately 1500 mm^3. This final assembly has been most successful operating very reliably up to 33.1 T for 433 hours as of February 11, 1997, using Cu-Be alloy conductors.

We previously reported difficulties in making good Florida-Bitter disks from Cu-Ag alloy sheet due to inhomogeneous material and the different oxidation potentials of Cu and Ag.[3] Since that time, we have improved the quality of the Cu-Ag sheet and have improved our etching process such that we can now consistently fabricate good disks from this material. The result of this development work is the set of Cu-Ag Florida-Bitter disks that is now ready for the 30 T magnet for NRIM.

We have now redesigned our 33 T magnet using the improved transition, clamping, sheet, and etching. The new magnet is under construction and should provide the same field as the present version but use only 89% as much power.

References:

1 Bird, M.D., *et al.*, IEEE Trans. on Magn., **32**, No. 4, 2444-2449 (July 1996).

2 Bird, M.D., *et al.*, IEEE Trans. on Magn., **32**, No. 4, 2542-2545 (July 1996).

3 Bird, M.D., *et al.*, NHMFL 1995 Annual Report, 99-100 (1996).

A 30 T Split Pulse Water Cooled Magnet Concept for Neutron Scattering Experiment Study: Material Characterization and Design Options

Eyssa, Y.M., NHMFL
Bird, M.D., NHMFL
Schneider-Muntau, H.-J., NHMFL
Walsh, R.P., NHMFL
Pernambuco-Wise, P., NHMFL
Boeing, H., LANL
Robinson, R., LANL

The Manuel Lujan Jr. Neutron Scattering Center at LANL has need of an engineering design study for a split-pair, pulse magnet that would provide a 25 to 30 T field in a 30 to 50 mm bore, 10 mm split gap magnet for 3 ms at a repetition rate of 2 Hz.

Single stack, capacitor driven, water cooled Bitter magnets of this type providing a 16 and 18 T have been constructed in Japan. Because of the pulsed nature, the current in a single stack Bitter magnet flows only on the inner surface in a radial thickness equal to the skin depth, which is about 3 to 6 mm for 1 to 3 ms half sine wave pulses. The rest of the disk provides mechanical support for the current carrying region. Cooling holes have to be located close to the energy dissipation region to remove the energy dissipated in the time between pulses. The advantage of this concept is that it has low stored energy. The disadvantage is the large energy density needed to be removed. Another disadvantage is that the maximum stress is limited by the copper alloy used in Bitter disks.

The use of a multi-layer single coil winding made out of a conductor that is smaller than 3 mm in width and is supported by a cylindrical external reinforcement can remove some of the difficulties and will generate fields up to 25 T. The advantages of this design are: (1) the current carrying region is spread beyond the skin depth limitation, and (2) the non-current carrying portion of the disks is replaced by higher modulus material to reduce the stresses. Generation of higher fields would require internal reinforcement to reduce the stresses.

In trying to go beyond the Japanese experience, we chose the maximum field of 30 T, and it soon became clear that we needed a geometry that allows the current density to spread radially (with internal reinforcement between layers) larger than the skin depth, which is the limit in the Japanese Bitter plates design. We came up with a winding design that uses small conductor to minimize the eddy current heating and mechanical stresses to an acceptable value. Figure 1 shows a preliminary design concept. It is a water cooled split-pair magnet with internal reinforcement that can be constructed in different ways: (1) internally cooled conductor winding, (2) axially cooled wound magnet, (3) axially cooled multi-Bitter stacks or poly-helices. The winding is divided into three zones, each of which has its reinforcement. In this design we tried to minimize the internal reinforcement as much as possible with a stress constraint of 500 MPa in conductor and 700 MPa in reinforcement. The 25 T version has lower stresses.

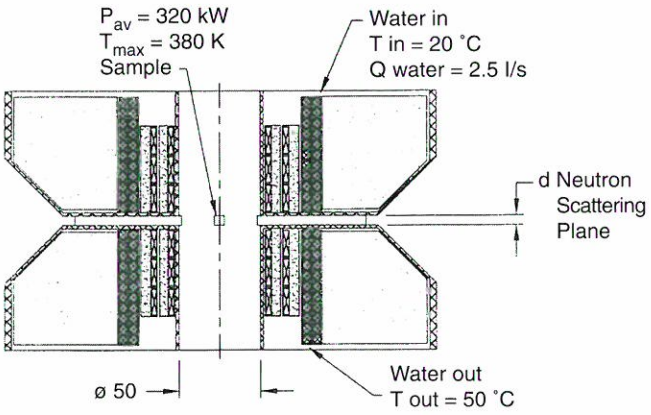

Figure 1. Schematic diagram of a multi-layer split pair pulse magnet for neutron diffraction experiment.

The neutron scattering magnet is required to have a lifetime of 10^7 full power cycles. The preliminary calculation for the 30 T design shows conductor stresses of about 500 MPa and reinforcement stresses of 700 to 900 MPa. It would require a strong copper alloy such as CuAg to support such stress level for so many cycles. We need to characterize the fatigue limit of high strength alloys such as CuAg at an operating temperature of 330 to 340 K and up to 10^7 cycles. To reduce the conductor stresses, we have considered using high modulus (200 GPa) reinforcements at stress level of about 650 to 700 MPa. We will consider special steel alloys or fiber reinforced composites that meet the required fatigue values. We have started a one tear testing program to characterize different conductor, insulation, and reinforcement materials that are needed for this project. The fatigue test results of potential conductors will allow us to optimize the design by using minimum internal reinforcements to meet the conductor fatigue life. It will allow us to quantify the trade off between safe operating stresses and the increase in power requirement due internal reinforcements.

Magnetic Field Modulation Coil Test

Fortune, N.A., Smith College, Physics

I acquired data on the amplitude and frequency dependence of the magnetic field generated by a modulation coil wrapped around a NHMFL 32 mm bore magnet dewar. This data was taken to evaluate the feasibility of modulated field measurements of specific heat and magnetothermal effect using the 30 tesla class resistive magnets, which do not have built-in modulation coils.

My estimate for the peak modulating field at the center of the modulation coil is 250 G +/- 50 G rms, corresponding to a peak field of 5 V. This amplitude field is possible over the frequency range 1 Hz to 100 Hz. The field falls off as the square of the inverse distance from field center. At 9 mm out of center, I measured 160 G; at 14 mm out, I measured 63 G.

These calculations use the supplied calibration for the Hall probe at 300 K of 87.1 mV/tesla for a DC current bias to the Hall probe of 100 mA. The measured Hall voltage at 13.6 tesla and 2.2 K using a 1 mA DC bias was 83.7 mV/tesla.

The available frequency range depended on the amplifier. 250 G at field center was possible from 1 Hz to 100 Hz using a Kepco amplifier and from 20 Hz to 50 Hz using a (non-impedence matched)

audio amplifier. For comparison, roughly 90 G rms is available at 10 Hz and 27 tesla by directly modulating the current supplied to the main resistive magnet. Ideally, a modulation field equal to at least 1% of the applied "DC" magnetic field—3000 G at 30 T—would be available over the frequency range 10 mHz to 100 Hz (and minimally, over the frequency range 100 mHz to 10 Hz).

There were detectable shielding and eddy current heating effects at 50 Hz and above. I found the amplitude of the modulation field to be 67% lower at 500 Hz than at 50 Hz for the same voltage across the modulation coil. The shielding is attributed to the dewar and cryostat tails. Eddy current heating was also observed: the temperature of samples immersed in liquid He remained at 2.5 K between 1 Hz and 44 Hz, but rose to 2.6 K at 55 Hz, 3.5 K at 88 Hz and to over 4 K at 110 Hz. The magnitude of this effect will vary with choice of probe and sample.

Contact Resistance As a Function of Surface Finish Between Cu-Ag Bitter Disks

Hascicek, Y.S., NHMFL
Boutemy, B., NHMFL
Dur, O.*, NHMFL
Löffelbein, W., NHMFL
O'Reilly, J., NHMFL
Bird, M.D., NHMFL
Eyssa, Y.M., NHMFL

Contact resistance can be an important resistive factor in the design of a resistive magnet when the magnet consists of large number of these contacts as is the case in Bitter magnets. This assumes that the resistivity of the conductor is isotropic. If a lamellar composite structure is present, then the interface resistance also should be taken into consideration. To quantify the effect of contact resistance we have undertaken a systematic study of contact resistance as a function of surface finish between the Florida Bitter Disks made of Cu-Ag.

A series of Bitter disk pairs were ground and polished down to 600, 800, 1200 grade, 6, 3, 1 μm surface finishes. They were then stacked (Figure 1) to create a well defined contact area, and the resistance of the contact under varying pressure was measured. A computer-controlled, four-wire DC pulse technique was used to collect the I-V data, and the contact resistance was determined from the slope of I-V plot. The measurements were done at room temperature, and the I-V data were all linear.

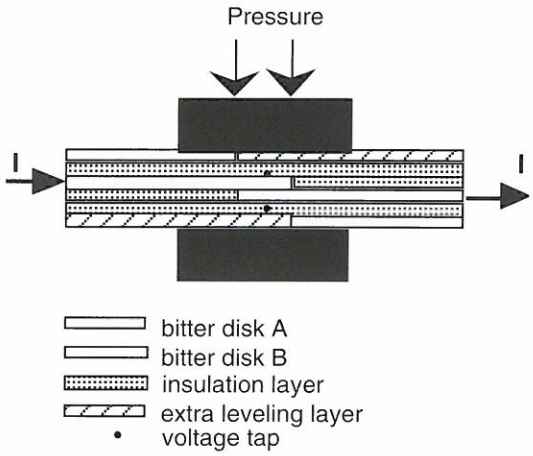

Figure 1. Experimental set-up.

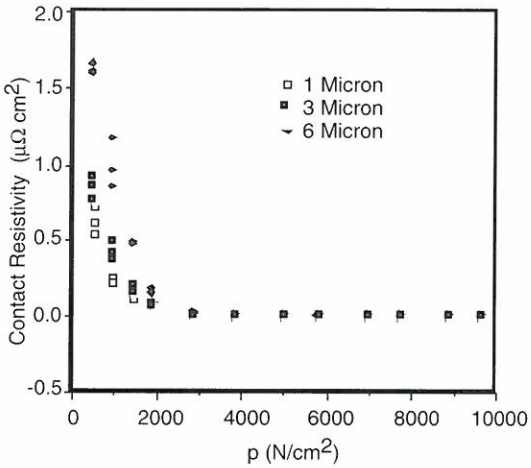

Figure 2. Contact resistivity as a function of pressure for the surface finishes as marked.

Figure 2 shows the contact resistivity as a function of contact pressure for varying surface finishes as marked. As seen in the figure, beyond certain pressure, surface finish does not really affect the contact resistivity, but below that pressure, surface finish can be altered. Below 2000 N/cm^2 we see that as the surface finish gets finer, contact resistivity decreases. This decrease becomes more pronounced as the pressure decreases.

* On leave from Dept. of Physics, Marmara University, Istanbul, Turkey.

Code Development for the Simulation of Flows in Complex Geometry

Prestemon, S., NHMFL/FAMU-FSU College of Engineering

A code for the numerical simulation of the flow in cooling channels in resistive magnets is being developed. Due to the complex geometry of the channels, multi-domain methods are required. The high Reynolds numbers of the flows requires high accuracy methods. We have therefore chosen to implement the spectral element method.

The spectral element method is based on the decomposition of the global domain into many quadrilateral elements. The elements are then mapped via a simple one-to-one transformation onto the interval $[1,1]^d$. On each mapped element we define a tensor product grid of Gauss-Lobatto-Legendre points. Any function can then be approximated on this grid through the use of Lagrange interpolating polynomials.

In order to simplify the grid generation, we use the preprocessor of Ansys to generate the elements and define node lists corresponding to the type of boundary conditions that will be imposed on element faces. The resulting data files are then read into the spectral element code and the full spectral element model is generated automatically.

The spectral element approach is based on a variational form of the original partial differential equation. The resulting integrals are calculated using Gauss-Lobatto quadrature. Due to the tensor product nature of the method, very high accuracy can be obtained without a correspondingly high number of numerical operations.

We illustrate the power of the method on the 2D Poisson equation $\nabla^2 T = f$ in Figures 1 and 2.

Figure 1 shows a 20 element discretization of a 2D channel domain, with each element admitting a polynomial of degree 10 in each direction. Isotherms of temperatures (T) are shown for a forcing term f defined such that $T = \exp(\sin(6\pi x)+\sin(6\pi y))$. The maximum error in this case was $\approx 10^{-4}$.

Improved accuracy is typically obtained by increasing the polynomial order of the method rather than increasing the number of elements, as is done in the case of finite elements. An example of the improvement that can be obtained is shown in Figure 2. The figure is a plot of error norms as a function of the polynomial order.

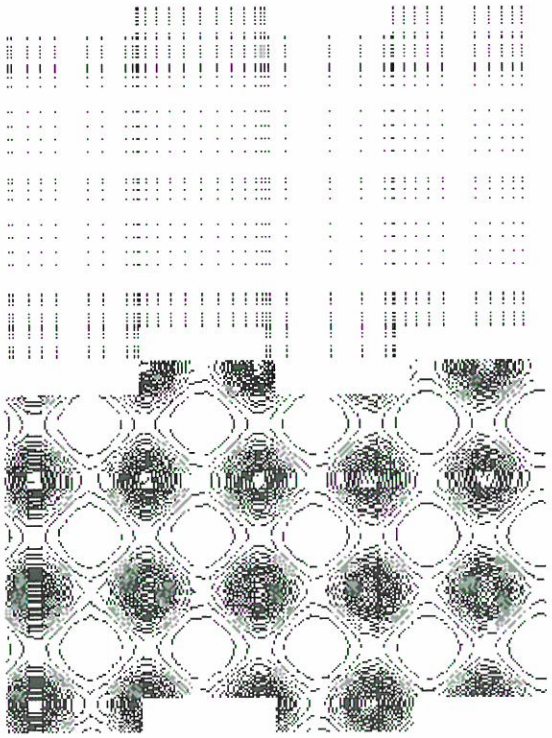

Figure 1. Grid (top) and isolines of temperature (bottom).

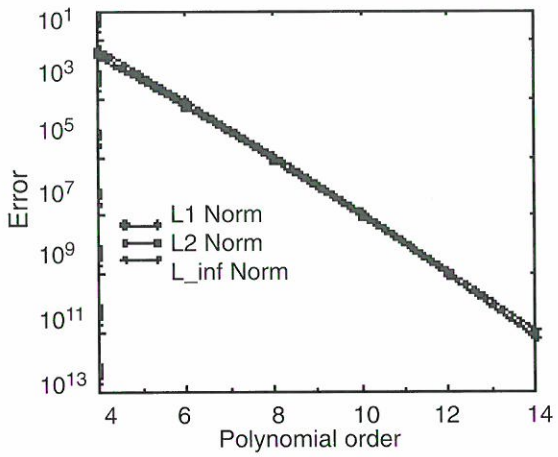

Figure 2. Error norms showing convergence to the analytic solution.

Note that the error decays exponentially rather than algebraically, as is the case with finite difference or finite element schemes. The high accuracy of spectral methods is important for high Reynolds number fluid dynamics problems, where

numerous instability mechanisms exist that need to be correctly resolved during the simulation.

Using the spectral element method, we can maintain the high accuracy of spectral methods on complex geometries. Together with large-eddy simulation techniques, we will be able to analyze the complex flow in the cooling channels of resistive magnets.

MAGNET SCIENCE & TECHNOLOGY REPORTS
Pulse Magnets

Program Overview

P. Pernambuco-Wise

The Pulse Magnet Group in Tallahassee set a new record for the number of magnets produced in a twelve-month period—over thirty. In addition to the coils intended to sustain the user facility, much effort has been focused on the building and testing of small experimental magnets used to evaluate new conductor and reinforcement materials. These coils form the basis of knowledge for future designs with an aim to providing ever increasing capabilities for the users of the NHMFL Pulsed Field Facility at Los Alamos National Laboratory. In the last year, the Tallahassee group has focused principally on steel and composite reinforcement and combinations of these, impacting as they will, on the final design of the DoE/NHMFL 100 T magnet.

In addition to these activities, there has been a substantial increase in outside requests for coils of all descriptions. For example:

- Subsequent to a successful test of a 50 T magnet by NHMFL staff at the University of New South Wales, the National Pulse Magnet Laboratory of Australia has asked to purchase a regular supply of new coils citing the reliability, performance, and quality control of the Tallahassee magnets as major considerations.
- A more ambitious series of coils is being undertaken at the request of the University of Wisconsin. The Pegasus project is a small, quasi-spherical, high β Tokamak device that requires a pulsed central solenoid for energizing the confined plasma. This coil will be approximately 1.5 m long with a bore of 60 mm and generating a field of 14 T. Two such coils are to be built with a third planned at 20 T.

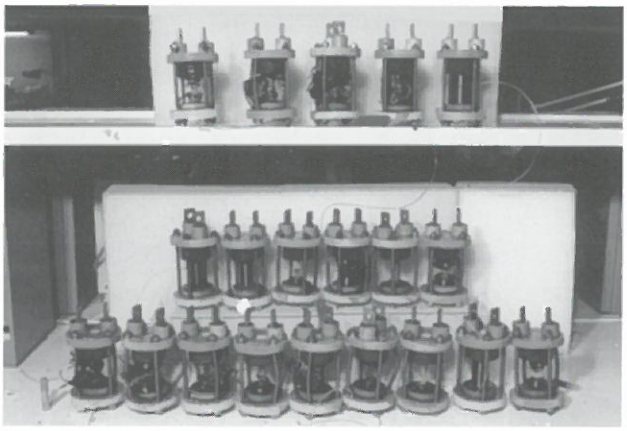

Figure 1. Two layer soft copper test magnets with varying reinforcement schemes after failure.

- The NHMFL has been approached by Sandia National Laboratory to provide coils for the pinching of an electron beam in an X-ray production facility. The initial magnets will be modifications of standard designs with an evaluation paper to be produced on a much more ambitious 80 to 100 mm bore, 40 T solenoid.

- Other requests have come from such varied places as Tyndall Air Force Base in Florida (a coil for pyrotechnic investigations) and laboratories in Vienna, Austria (magnetic materials).

The 100 T Optimization Analysis: Part I – Choice of Outsert Initial Temperature

Eyssa, Y.M., NHMFL
Pernambuco-Wise, P., NHMFL
Schneider-Muntau, H.-J., NHMFL

The 100 T pulse magnet will consist of a 50 T, 200 to 220 mm bore outsert powered by a generator and a 50 T, 24 mm bore insert powered by a capacitor bank. In this report we examine how the initial temperature at the pulse start affects the maximum obtainable field from the outsert, given the constraint on maximum stresses and strains in the winding and reinforcements and the limited number of power supply modules available.

In this analysis we have used the following assumptions for the outsert: (1) Five mechanically independent coils. The first four are made of copper/stainless steel (CuSS) conductor reinforced by stainless steel (SS) or Nitronic Shell followed by a carbon fiber shell. The last coil is hard copper reinforced only by SS or Nitronic shell. (2) One power supply (PS), 4 kV/20 kA is energizing coils 1 and 2. Another one is energizing coil 3. Two PS's energize coil 4. Three PS's energize coil 5. Field vs. time is shown in Figure 1. (3) Winding bore is 200 mm. (4) Eddy current and magnetoresistance heating are included. (5) Geometry is kept constant for all 3 cases (30, 68 and 77 K starting temperature). (6) Stresses are calculated using no return field from the inside circuits.

As shown in Table 1, there is a gain of about 2 T from reducing the starting temperature from 77 to 68 K and about 5 T by going to 30 K. The advantage of lower temperature is lower starting resistance and stronger material properties.

A1-68 K Cooling Requirements

The enthalpy difference of copper (66 to 77 K) is 2.5 J/g or 22.3E06 J/m^3. Steel is about 1.4 j/gm

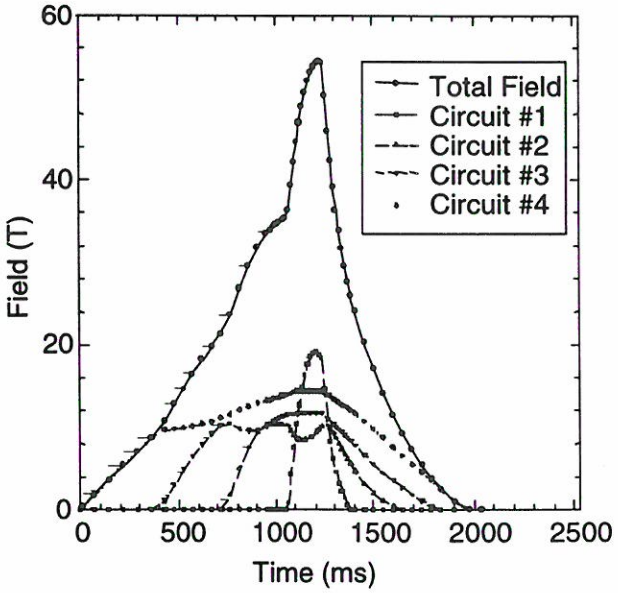

Figure 1. Outsert fields from a 68 K starting temperature, CuSS, 5 coils, 4 circuits coil arrangement.

Table 1. Summary of effect of initial temperature choice.

T_i (K)	B_{max} (T)	I^2Rdt (MJ)	$T(B_{max})$ (K)	T_f (K)	% strain	σ_{cond} (MPa)	σ_{shel1} (MPa)	σ_{shel2} (MPa)
77	52.8	153	171-198	212-237	1.1	1033	1100	2400
68	54.7	144	149-183	209-225	1.4	1045	1150	2800
30	57.5	109	95-169	146-180	1.8	1073	1180	3500

(11.0E6 J/m^3). Assuming the copper volume is about 0.30 m^3, the steel volume is 0.2 m^3 and the nitrogen heat of vaporization is 200 kJ/liter (0.85 g/cm^3), there is a need to pump about 45 liters of nitrogen.

A2-30 K Cooling Requirements

The enthalpy difference of copper (30 to 77 K) is 5.2 J/g or 46.4E06 J/m^3. Steel is about 2.8 J/g (22.0E6 J/m^3). Assuming the copper volume is about 0.33 m^3, the steel volume is 0.2 m^3 and the cool down process from 77 to 30 K is an hour, there is a need to remove an average 5000 W of heat between 77 and 30 K.

Conclusion

The lower the starting temperature is, the higher the field that can be obtained using fixed number of power modules. It appears that a 68 K starting temperature is not hard to obtain by pumping on liquid nitrogen.

The 100 T Optimization Analysis: Part II – Choice of Reinforcement

Eyssa, Y.M., NHMFL
Pernambuco-Wise, P., NHMFL
Schneider-Muntau, H.-J., NHMFL

The 100 T pulse magnet will consist of a 50 T, 200 to 220 mm bore outsert powered by a generator and a 50 T, 24 mm bore insert powered by a capacitor bank. In this report we examine the effect of reinforcement materials on the maximum field.

Analytical and numerical modeling points out the advantage of combining carbon fibers and steel as reinforcement, compared to a pure steel cylinder with modest mechanical properties such as Nitronic 40 (UTS = 1.5 GPa). A 10 to 20 mm carbon fiber shell (Fiber UTS = 5 GPa) would be considered a thin shell with relatively uniform stress distribution. A peak hoop stress of 3 GPa and filling factor of 0.6 results in an average stress ≈ 1.5 to 1.6 GPa compared to 1.1 to 1.2 GPa for Nitronic cylinder. Results from model coils testing by P. Wise show that thin carbon fiber shells perform as expected from analytical modeling.

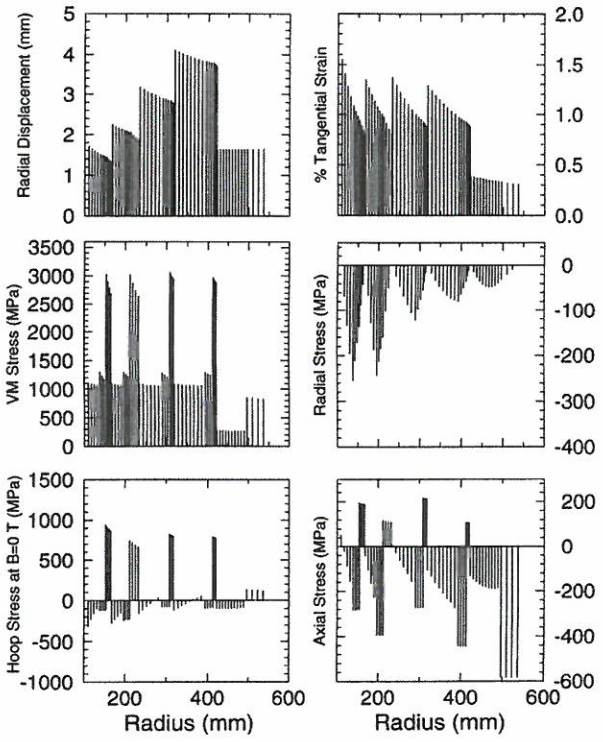

Figure 1. Stresses and strain distribution in a 50 T outsert.

Table 1. Performance of a steel shell (Nitronic) and a hybrid steel/carbon fiber under similar magnetic loads.

	σvm (MPa)	u (mm)
All Nitronic Shell (36 mm thick)	1294	2.219
Hybrid (Nitronic/C.F.) Shell (20+16 mm thick)	1226/ 2815	1.766/ 2.065
Hybrid (Nitronic/C.F.) Shell (20+12 mm thick)	1287/ 2815	2.173/ 2.065

Table 1 shows the maximum stress in a 36 mm thick Nitronic shell subjected to a 213 MPa radial pressure along with a hybrid Nitronic/carbon fiber shell (20 + 16 mm). Then we show that the same load can be supported for the same strain by 32 mm hybrid shell (20+12 mm). Figure 1 shows the stress distribution in a hybrid Nitronic/carbon fiber reinforcement for an outsert design.

The 100 T Optimization Analysis: Part III – Choice of Conductor

Eyssa, Y.M., NHMFL
Pernambuco-Wise, P., NHMFL
Schneider-Muntau, H.-J., NHMFL

The 100 T pulse magnet will consist of a 50 T, 200-220 mm bore outsert powered by a generator and a 50 T, 24 mm bore insert powered by a capacitor bank. In this report we examine the effect of conductor materials on the maximum field.

For this analysis, we have assumed a 220 mm bore, 68 K outsert design. The conductors used here are CuSS(40% steel), CuAg, CuNb, and AL-60 Glidcop. The properties of each conductor are listed in Table 1, along with the maximum obtainable field, energy requirements, conductor, and reinforcements volume. As shown, CuSS has a slight edge over CuNb and CuAg and 2 T over AL-60.

Table 1. Summary of analysis as function of conductor choice.

	B (T)	E (MJ)	I^2Rdt (MJ)	Cond (m^3)	Shell 1 (m^3)	Shell 2 (m^3)	YTS (MPa)	UTS (MPa)	% IACS	RR
CuSS	53.38	179	111	0.312	0.218	0.052	900	1100	60	7.5
CuNb	53.22	199	125	0.330	0.208	0.043	950	1150	70	4.3
CuAg	53.03	199	125	0.335	0.209	0.043	950	1150	80	3.3
AL-60	51.58	189	119	0.336	0.216	0.093	600	700	80	4.0

Conclusion

As shown in Table 1, CuSS has a slight edge over CuNb and CuAg and 2T over AL-60. So it seems there is no clear advantage between CuSS, CuAg, and CuNb based on the assumptions we made above.

The 100 T Optimization Analysis: Part IV – Choice of Outsert Bore

Eyssa, Y.M., NHMFL
Pernambuco-Wise, P., NHMFL
Schneider-Muntau, H.-J., NHMFL

The 100 T pulse magnet will consist of a 50 T, 200 to 220 mm bore outsert powered by a generator and a 50 T, 24 mm bore insert powered by a capacitor bank. In this report we examine the effect of trade off between outsert bore and insert outer diameter on total insert and outsert combined field.

In this analysis we have assumed a CuSS conductor, at 68 K for the outsert, and calculated the maximum outsert field for different bores fixing the power supply in each case. Table 1 lists the maximum obtainable field as function of outsert bore. As shown the field drops with the bore, but we expect to gain the difference from a larger insert. In Figure 1, we show a combined insert/outsert analysis that shows that the total field has a broad maximum for 240 to 300 bore outsert.

The insert used is eight mechanically independent coils. The first four have CuSS (40% SS) conductor reinforced by 0.5 mm glass fiber and followed by carbon fiber shell. The last four coils are similar except they are 30% SS. One capacitor bank is used to power all coils except for the 260 mm bore outsert, where we examine the use of two capacitor banks vs. one capacitor bank.

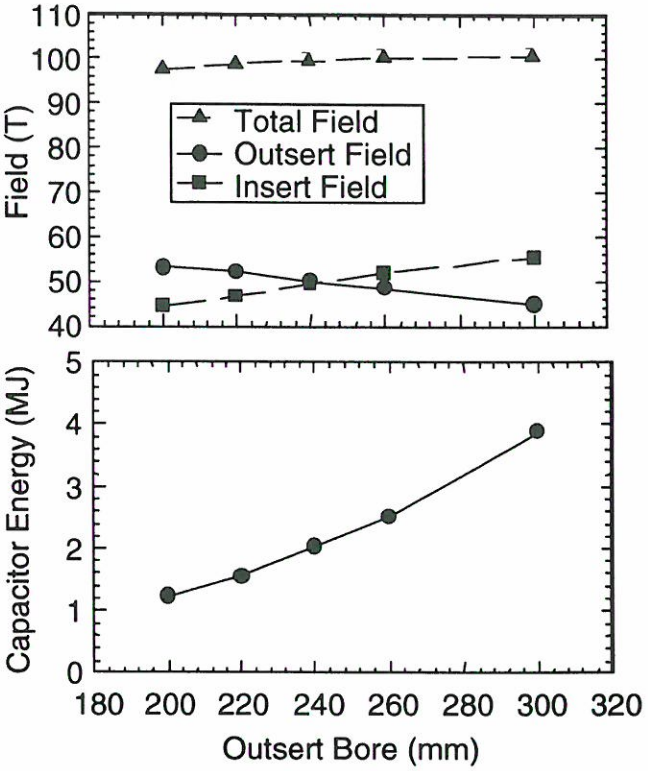

Figure 1. Total insert and outsert field and energy requirements for the insert.

Conclusion

The analysis shown in Figure 1 indicates that there is slight advantage for larger outsert bore (260 to 300 mm bore).

Table 1. Outsert field as function of bore diameter.

Bore (mm)	OD (mm)	B (T)	E (MJ)	I^2Rdt (MJ)	Cond (m^3)	Shell 1 (m^3)	Shell 2 (m^3)	T_{max} (K)	T_{min} (K)
200	1052	54.58	181	112	0.304	0.213	0.052	263	166
220	1068	53.38	179	111	0.312	0.218	0.052	250	160
240	1088	51.22	181	113	0.318	0.222	0.054	253	163
260	1108	49.55	182	110	0.337	0.230	0.045	225	150
300	1139	46.24	198	119	0.364	0.294	0.051	240	149

Design of a 75 T, 10 mm Bore Test Magnet

Pernambuco-Wise, P., NHMFL
Gao, B.-J., NHMFL
Eyssa, Y.M., NHMFL
Lesch, B., NHMFL
Tozer, S.W., NHMFL

The continuing goal of the NHMFL to provide ever higher fields for users of its pulse facility has

prompted the development of a magnet designed to achieve at least 75 T at destruction, with a regular operational field of 70 T+. In keeping with the current philosophy of the pulse magnet group, the initial coil is designed specifically for testing of materials and thus is somewhat smaller (a 10 mm bore as opposed to the usual 15 mm bore) than a standard user magnet. Optimization for the lowest possible stress configuration has been performed by computer and hand, using both analytic thermo-mechanical and finite element codes.

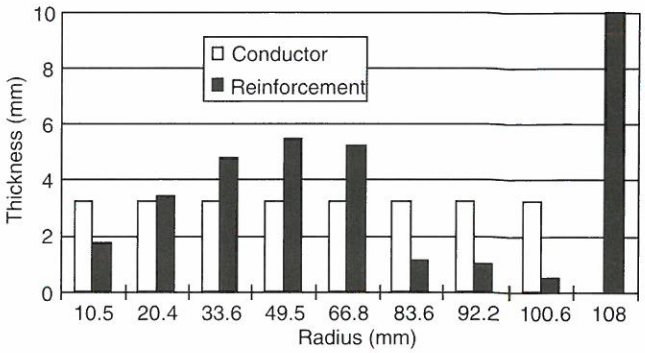

Figure 1. Build of the 75 T, 10 mm bore magnet.

The conductor for this test coil will be a length of 3x4 mm CuNb provided for evaluation by the Bochvar Institute of Moscow. Insulation will be by double wrapped 0.05 mm Kapton tape wound in house. Internal reinforcement is a significant problem in this coil. The limited elongation of CuNb combined with the extremely high stresses generated by the field necessitate the use of high strength carbon fiber. The electrical conductivity of carbon at 77 K together with the ability of individual filaments to penetrate pinholes in insulation have caused the failure of carbon reinforced magnets wound by other groups. Additional precautions to prevent electrical failure have to be made. These will include buffering the carbon with thin layers of S2 glass and Kapton and wet winding the magnet to prevent migration of filaments during construction. Figures 1 and 2 show the magnet build and stresses respectively.

Some additional design modifications have been introduced with the wish to concurrently test a new concept in high pressure cells. The magnet bore will be sealed in order to act as the outer vacuum jacket of a pumped He^4 cryostat. A plastic (celazole) diamond anvil or sapphire ball cell will be used to perform electrical and optical transport measurements on an organic conductor at 1.6 K.

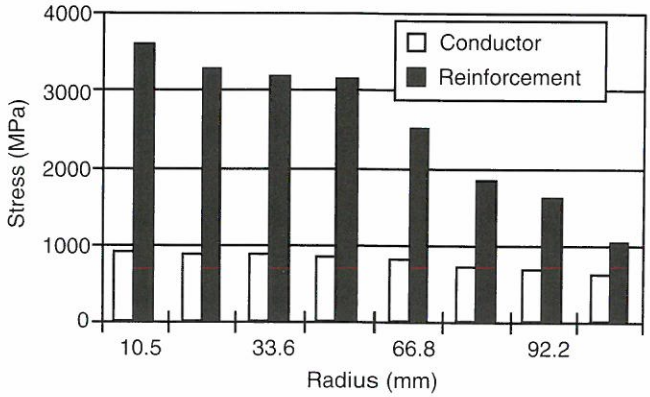

Figure 2. Von Mises stress in 75 T magnet.

Effects of Elastic Moduli Anisotropy on Fiber Composite Reinforcement Shell Performance

Pernambuco-Wise, P., NHMFL
Eyssa, Y.M., NHMFL

As stated in the related report, *Results of Test Magnet Evaluation of Fiber Composite Reinforcement Shells*, the results of a series of test magnets have indicated that fiber composites used as reinforcement shells for pulse magnets have properties that do not scale as expected as the thickness is increased. Calculations have shown that while the ultimate tensile strength (UTS) of the fiber is important in knowing the final strength of the composite, of even greater importance are the tangential and radial elastic moduli E_t and E_r respectively. While E_t can be ascertained from a rule of mixtures (ROM) approach using the moduli of the fiber and matrix material, E_r must be estimated from Halpin-Tsai or similar engineering equations. The effect of the anisotropy of the elastic moduli E_t/E_r can be dramatic as shown in Figure 1.

While the average stress across the cylinder may be well within the UTS of the fiber (taking into account the filling factor of the composite), the stress generated at the inner surface may exceed

it due to the poor stress transmission characteristics of the material. This will lead to fiber breakage at the inner surface, crack propagation, and catastrophic magnet failure. Analysis of this sort has allowed a much more accurate determination of the properties of composite shells used in pulse magnet construction. When compared with test magnet results, it has revealed that while the carbon fibers used in the composites perform at a good fraction of their theoretical maximum, the radial moduli given by the Halpin-Tsai formulation is optimistic and would result in misleading predictions when used in the magnet design calculations. Figure 2 shows the maximum field results of a series of test magnets and the predictions based upon a more realistic estimate of the UTS and anisotropy of the elastic moduli.

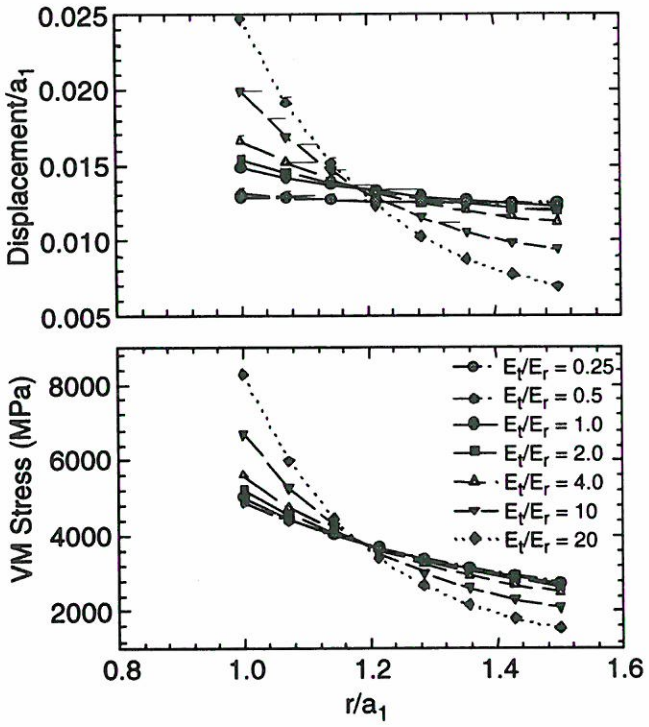

Figure 1. The radial displacement and Von Mises stress across the width of a carbon fiber composite cylinder when a pressure of 1020 MPa is applied to the inner surface. a_1 is the diameter of the cylinder.

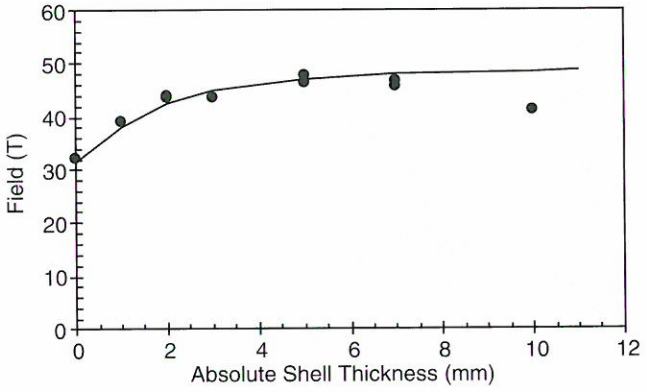

Figure 2. Points show the maximum fields obtained from test magnets when reinforced with composite fiber shells of the stated thickness. Broken line indicates the predicted values.

Results of Test Magnet Evaluation of Fiber Composite Reinforcement Shells

Pernambuco-Wise, P., NHMFL
Lesch, B., NHMFL
Eyssa, Y.M., NHMFL

In a series of small experimental coils tested in late 1995, it was observed that in magnets with thick outer fiber composite reinforcements, fields at failure were lower than predicted due to premature shell failure. Microscopic examination of the shells suggested crack formation and propagation because of tensile stress in the axial direction, perpendicular to the fibers. A series of twenty test magnets were built, with an aim to examining the shell behavior. All of the magnet windings were identical: two-layer, soft copper wire with 0.5 mm S2 glass insulation. The constructions varied only in the thickness of outer shell and in some cases the material or method of constructing the reinforcement layer. The failure fields can be seen in Figure 1.

It can be seen that there is little if any increase in the maximum attainable field for simple hoop direction fiber shell thickness greater than about 3 mm, and indeed after this plateau effect, the fields appear to decrease. For coils reinforced with both axial and hoop fiber (an effort to decrease the axial strain), the fields are lower than those reinforced with hoop fiber alone. This is due to the lowering

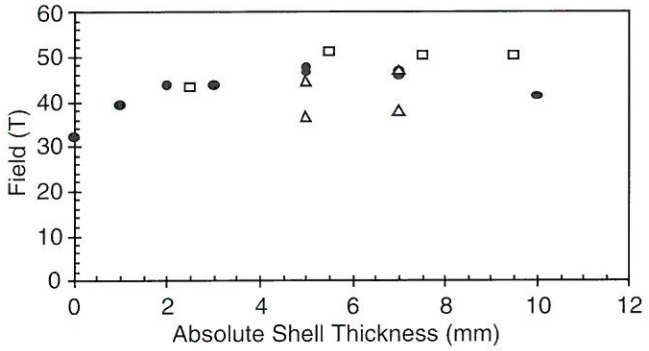

Figure 1. Maximum fields reached by test magnets. Circles show magnets with solid, hoop-reinforcement-only, carbon composite shells. Squares show steel-reinforced magnets, and triangles are magnets reinforced with both hoop and axial carbon fibers.

of hoop filling factor caused by the introduction of the axial fibers. Indeed, the lower triangle points are those coils with more axial reinforcement, indicating that the negative effects of increased axial fibers far outweigh any positive gains. Of the coils reinforced with A286 steel, one has a 2.5 mm shell without additional material and the remaining three had varying thickness of fiber outweigh any positive gains. Of the coils reinforced with A286 steel, one has a 2.5 mm shell without additional materials and the remaining three has varying thickness of fiber overwrap. The results indicate that steel alone provides approximately the same reinforcement capability as an equal thickness of fiber but that fiber plus steel is more efficient than fiber alone—a factor that is of some importance for situations where volume is a limitation in the design.

The results of these test magnets were most instructive and impact heavily on future magnet designs where composites will be used. In particular the reinforcement scheme for the Department of Energy/NHMFL 100 T magnet is still being debated, pushing as it does the edges of available materials technology. A follow-up of this test series concentrating on various alloys of steel is being planned in cooperation with the design team at LANL.

The 100 T Magnet: Insert Coil Design

Pernambuco-Wise, P., NHMFL
Eyssa, Y.M., NHMFL

The design of the 100 T insert coil is strongly dependent on materials and thus as new products become available, the design continues to evolve. At present the most satisfactory projected performance has been obtained by using CuSS in conjunction with intermediate modulus carbon fiber composite. The magnet build is shown in Table 1.

Table 1. Construction of 100 T insert coil.

Layer	Wire	Height mm	Reinforcement mm
1	3.2x6.2 mm CuSS (40%)	142	2.5 mm IM8 Carbon
2	3.2x6.2 mm CuSS (40%)	142	3.5 mm IM8 Carbon
3	3.2x6.2 mm CuSS (40%)	142	4.7 mm IM8 Carbon
4	3.2x6.2 mm CuSS (40%)	142	5.5 mm IM8 Carbon
5	2.6x6.0 mm CuSS (50%)	298	7.8 mm IM8 Carbon
6	2.6x6.0 mm CuSS (50%)	298	8.7 mm IM8 Carbon
7	2.6x6.0 mm CuSS (50%)	298	9.7 mm IM8 Carbon
8	2.6x6.0 mm CuSS (50%)	298	10.4 mm IM8 Carbon

The coil is intended to produce a field of 48 T in a background field of 53 T, thus providing a total field of 100 T+ in a 24 mm bore. The risetime of the insert field would be approximately 7.5 ms. The specifications call for a repetition rate of 1 pulse per hour and a lifetime of the insert of 100 shots at 100 T. The coil would be precooled to 77 K with liquid nitrogen and reach a final average temperature of 377 K.

The stresses generated within the insert, while significantly reduced by using an outsert/insert design strategy, are still extremely high (see Figure 1). At present there are no known conductors that

can be used that will not be stressed well into their plastic regime, thus the lifetime of a particular coil is limited by fatigue. To ensure that a premature stress failure will not cause damage to the outsert coil, a cylindrical steel blast containment shell will be fitted around the outer diameter of the insert coil.

Investigations into increasing the efficiency of composite shells are ongoing as are cooperations in developing higher strength and lower conductivity wires. It is likely that these will have significant impact on the 100 T design.

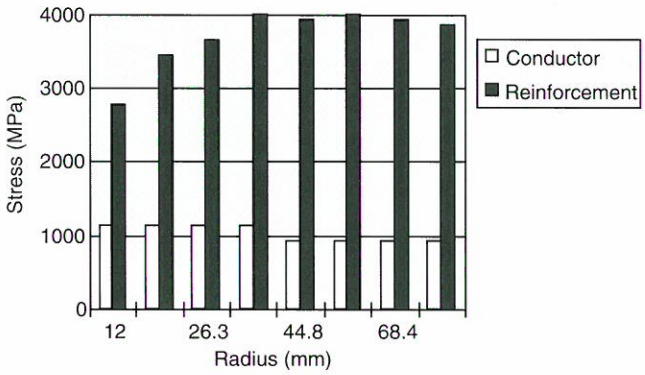

Figure 1. Von Mises stress in 48 T insert in 53 T background field.

Magnetoresistance of CuAg Wire

Rickel, D.G., NHMFL/LANL
Campbell, L.J., NHMFL/LANL

CuAg wire is the preferred conductor for constructing the high strength solenoids for the 100 T magnet project. This wire has suitable mechanical properties for the task and the electrical zero magnetic field conductivity is adequate. To determine resistivity increase in the wire due to imposed magnetic field on the conductor, we measured the magnetoresistance of a CuAg wire at liquid nitrogen temperature up to 60 T.

The wire (Cu - 24%wt Ag) was first annealed at 450 C before drawing and had a final diameter of 0.23 mm. The wire (23 cm long) was bifilar wound onto a 5 mm diameter cylindrical core in preparation for the measurement.

The measurements were made in the 60 T pulsed magnet at the NHMFL-Los Alamos Facility at fields up to 60 T. Both AC and DC resistance measurements were recorded and are shown in Figure 1. Since the sample resistance was very low (103 milliohms) the DC waveform is noisy. The prominent oscillatory behavior on the DC measurement is due to sample motion during the pulse. Both measurements give the same high field magnetoresistance ratio (R(60T) / R(0)) of 1.28.

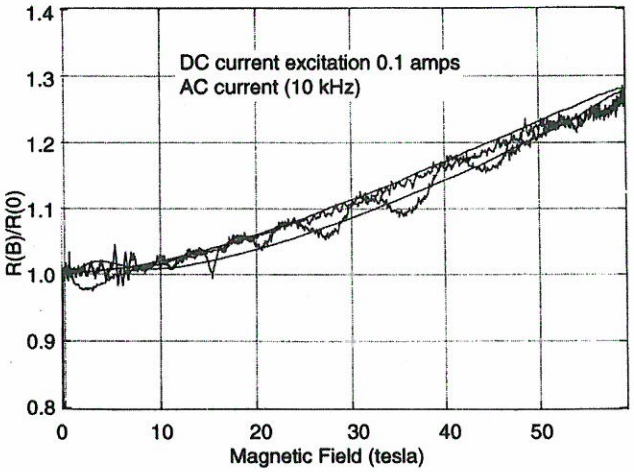

Figure 1. Magnetoresistance of copper silver wire sample.

40 T Long Pulse Magnet

Rickel, D.G., NHMFL/LANL
Pernambuco-Wise, P., NHMFL/LANL
Campbell, L.J., NHMFL/LANL

Preparation

The 40 T magnet has a large inductance and hence requires a relatively high energy to drive it to full field. In order to accommodate the magnet, the capacitor bank at the NHMFL/Los Alamos facility was upgraded to 1.6 MJ (33 mF @ 10 kV). This upgrade enabled us to pulse the magnet at full field while keeping the maximum charge voltage at 8.3 kV. To limit the maximum bank current in the event of a low impedance breakdown of the magnet, a 140 microhenry inductor was inserted in series with the test magnet.

Cool Down

We carefully measured the DC resistance of the magnet during the cool down cycle. We used a precision current source and a digital multimeter to record the necessary data. Figure 1 shows the results of the cool down from room temperature to liquid nitrogen temperature and the resistances recorded after the magnet was pulsed at various energies. We followed the cool down after many of the pulses and found that the subsequent cool down faithfully followed the initial cool down. This curve therefore allows one to predict the cool down interval required after a magnet pulse of a given energy.

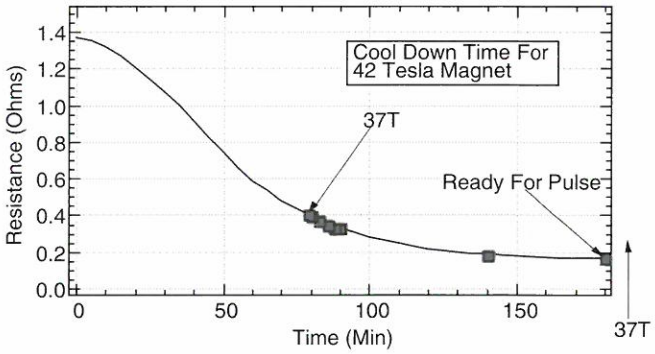

Figure 1. Cool down time for 42 T magnet.

Inspection of the figure reveals that it is likely possible to reduce the cool down time between magnet pulses by choosing an endpoint for the cooling at a temperature slightly higher than that of liquid nitrogen.

Current Versus Magnetic Field

Each magnet pulse was accompanied by a current and magnetic field measurement. The current was measured by a 0.0002553 ohm resistor connected to a 2440 Tektronix digital oscilloscope. The maximum voltage of each magnet pulse was measured to 1% accuracy by the scope and converted to a peak current. The magnetic field was measured by carefully wound pickup coils. The coil used for the final 10 measurements was 24 turns of 0.004" copper wire wound on a G10 form 0.003" in diameter. The shrinkage of the coil form due to cooling to 77 K was measured at 0.5% and applied as a correction factor to the coil loop area. Figure 2 shows the current data plotted as a function of field. The value of B/I is 10.2 tesla/kA.

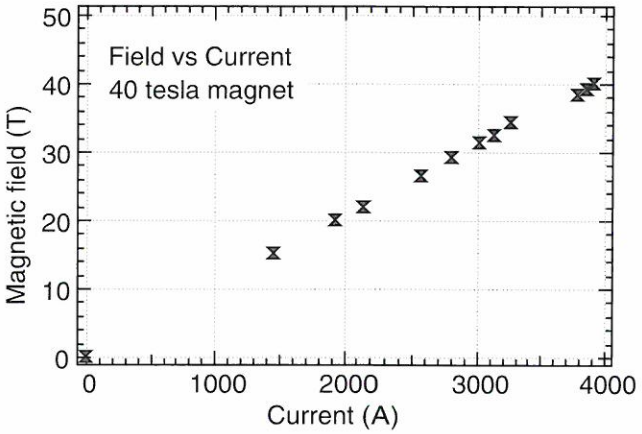

Figure 2. Field vs. current in 40 T magnet.

Magnetic Field Waveform

The observed waveform at the peak magnet field of 40 T is shown in Figure 3. The bank charge voltage was 8.2 kV with 33 mF capacitance for a peak energy of 1.1 MJ.

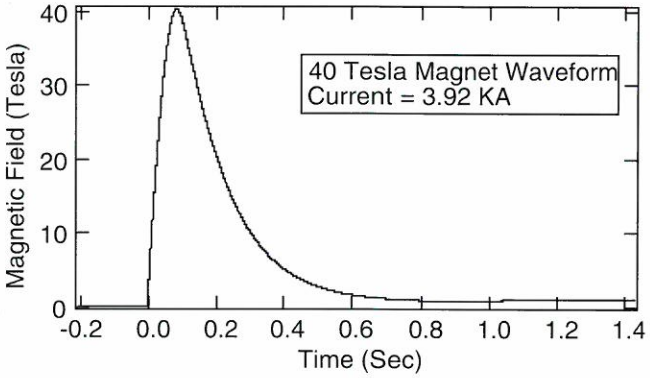

Figure 3. Waveform at peak magnetic field of 40 T magnet.

The rise time was 70 ms and the field decays from the peak value of 40.1 T to baseline over a period of 800 ms. At this field value, the magnet cool down time for the next pulse was 1 1/2 hours.

High Temperature Superconductor Technology

Program Overview

Y. S. Hascicek, J. Schwartz, and S.W. Van Sciver

The High Temperature Superconductor (HTS) Technology Program is developing the technology of high field (B > 20 T) superconducting magnets. Within this program, there are three main research and development activities: HTS material and conductor development; characterization of these materials for magnet applications; and superconducting coil technology. Over the last year, each of these subareas has made significant progress.

HTS material and conductor development has two major thrust areas: Ag/BSCCO 2212 conductor development and HgBaCaCuO material synthesis, the latter project being primarily supported by a separate grant from the National Science Foundation. A new development over the last year involves the React-Wind-Sinter (RWS) processing technique for powder-in-tube Ag/Bi2212 conductor. This technique allows for the eventual continuous processing of conductor into coil form. To date, we have achieved critical current densities near those obtained using batch process heat treatment techniques. The HgBaCaCuO studies are focused on synthesis approaches that reduce the peak sintering temperature to allow the use of Ag-alloy substrates. In the past year a two-step process was developed that results in 133 K T_c with a peak sintering temperature well below 800 °C.

HTS characterization efforts have focused on new methods of measuring composite conductor properties. This work includes studies of J_c (B,T) on short samples; measurements of $J_c(\varepsilon)$ by several methods including *in-situ* stress application using a Lorentz force technique; studies of the mechanical properties for composite Bi2212 conductors; and measurements of the thermal and electrical conductivity of Ag alloys for conductors up to 30 T. To support this work, a compact automated multi-sample probe together with drivers are being developed for fast J_c screening of short HTS samples. This work has focused on both in-house-produced conductors and conductors supplied by our industrial collaborators. Most conductors studied are produced by the powder-in-tube technique, but we are also studying surface-coated conductors.

Coil technology is essentially divided into two areas: coil fabrication and testing and analysis of magnet systems. In the former area, we report recent results on a set of mini pancake coils containing typically ten meters of conductor and developments in high temperature cryoinsulation for the wind-and-react coil technology. Over the last year, we have established a technique for production of double pancakes and wound, reacted, and characterized about ten such coils. These coils are prototypes for the 1-T class insert coils for operation in a 20 T background field. Also, an HTS shim coil, which comprises three pairs of pancakes with varying splits, has been designed and built. The shim coil is to achieve few ppm homogeneity in 5 mm DSV (the current homogeneity is 150 ppm) in the 20 T Oxford superconducting magnet. The homogeneity will be determined by NMR measurements. In addition to the coil development, we have performed a variety of analytical investigations of HTS magnet systems. These include studies of force-reduced coil configurations and two investigations into the thermal stability of HTS tape conductors.

An Optimized Toroidal Superconducting Magnet Using a Force-Reduced Winding Scheme

Amm, B.C., NHMFL/FAMU-FSU CoE
Schwartz, J., NHMFL/FAMU-FSU CoE

There are two limiting factors to the operation of superconducting magnets. The first requirement is that the current density be below the critical current density J_c, which is an intrinsic property of all superconductors. The second limitation is the Lorentz forces generated, which necessitate large amounts of structural mass to support the magnet and can lead to mechanical failure of the superconductor.

A new magnet winding geometry specific to superconducting magnets that addresses the J_c and Lorentz force limitations has been devised. Fortunately, both limitations can be addressed by the same solution—a force-free magnet with parallel electric and magnetic fields. The goal of this work is (1) to create a computer model of the new winding scheme; (2) to produce a methodology, including creation or assemblage of all necessary components, for analyzing the computer model; (3) to analyze the results; and (4) to compare them to a similar analysis performed on conventional geometries.

Unfortunately, the Virial theorem sets a limit for any force-free solution applied to a physical device. In light of the Virial theorem, the force-reduced magnet concept was introduced, and a promising force-free solution, the modified square toroid (MST) based on a force-free solution proposed by Furth, *et al.*, was selected.

The MST design parameters and optimization were based upon a superconducting magnetic energy storage device application, and two optimal MST designs were generated. One design was optimized solely for maximum stored energy. The second was additionally optimized for minimum stray field and is shown in Figure 1. Both magnets used identical material properties and structural boundary conditions.

A conventional D-shaped toroid (CDST) was selected as the model for comparison. The advantages of the MST over a CDST are greater geometric freedom and higher magnetically stored energy. The MST can be arrayed in a far greater range of aspect ratios than the CDST, and it can achieve higher magnetically stored energy values for a given stress-limit. The disadvantages of the MST compared to a CDST are its greater geometric complexity and its larger stray field. The presence of a poloidal field component in the MST yields a larger stray field than the CDST.

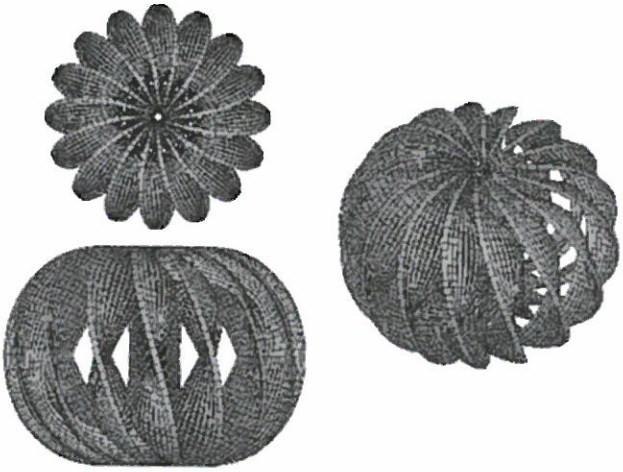

Figure 1. Three-dimensional renditions of the modified square torus.

React-Wind-Sinter Technique for $Bi_2Sr_2CaCu_2O_x$ High T_c Coils

Boutemy, S., NHMFL
Kessler, J., NHMFL
Miller, V., NHMFL
Remley, T., NHMFL/FAMU-FSU CoE
Schwartz, J., NHMFL/FAMU-FSU CoE

Heat treating high temperature superconducting $Bi_2Sr_2CaCu_2O_x$ (Bi2212) magnets so that their properties are comparable to those of short sample of conductor is an important challenge. The large thermal mass of magnets makes it virtually impossible to reach the temperature accuracy and uniformity needed to react Bi2212 with the conventional heat-treatment techniques. For that reason, a new technique is being developed at the NHMFL: the react-wind-sinter (RWS) technique.

Long lengths of powder-in-tube conductor are reacted by pulling the tape continuously through a static temperature profile in a controlled atmosphere. The precursor is partial-melted and slowly cooled to form large grains. The tape is then insulated, wound into the desired coil shape, and sintered at constant temperature. This repairs the cracks and achieves high phase purity and grain alignment. The whole process emulates the conventional partial-melt heat treatment of Bi2212 conductor and is shown in Figure 1.

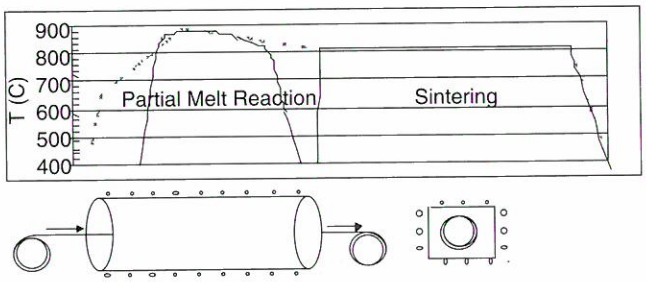

Figure 1. Comparison of heat-treatment schedule between the conventional partial-melt process and the RWS process.

This approach has many advantages including (1) the temperature of the tape during the partial-melt is more accurately controlled than for the wind-and-react method; (2) the length of conductor is unlimited and the process is homogeneous; (3) the profile of the furnace is simple as the sintering is separate from the partial-melting; and (4) the final sintering repairs damage from bending and does not require as precise a temperature distribution.

The RWS approach has been studied on medium lengths of conductor. The profile of a three-zone furnace was optimized to match as closely as possible with the conventional heat treatment, using a pulling speed of 15 cm/h. The process speed could be increased significantly by using a longer furnace. Pulling several conductors in parallel would also increase the output.

Conductors on the order of 30 cm in length were reacted using several peak temperatures. The samples, monocore and multifilamentary Ag1.2at.%Mg clad Bi2212 tapes, were either react-sintered (RS) or taken through the entire RWS process using a 26 mm diameter former. Although the sheath material of the monocore samples cracked during the RWS sinter due to excessive bending strain, the problem could be avoided by (1) reducing the Mg content in the sheath, (2) using a larger diameter former, or (3) using multifilamentary conductor.

On straight samples, the J_c values reached 60 kA/cm^2 on the monocore tapes and 87 kA/cm^2 on the multifilamentary tapes. Such results rival the ones obtained with the conventional heat-treatment on short samples. As the RWS process is independent of the amount of conductor, the same values are expected on magnets, which would represent a big step forward in high temperature superconductor magnet development.

J_c and *In-Situ* Lorentz Force Straining of HTS Conductors Up to 30 Tesla

Hascicek, Y.S., NHMFL
Dur, O.*, NHMFL
Van Sciver, S.W., NHMFL/FAMU-FSU CoE

We have used *in-situ* Lorenz force straining[1] (ILFS) to determine stress dependence of J_c of HTS conductors. The conductors were actually pulled to failure *in-situ*. First, the critical current density of multifilamentary and monofilament Bi-2212/Ag tape conductors were measured as a function of applied magnetic field under increasing and decreasing field values up to 30 T. The Lorentz force was compressive during these measurements. Once the expected hysteresis in $J_c(H)$ is obtained the polarity of the sample current was changed and the HTS sample was progressively stressed by the Lorentz force.

Since the sample had circular geometry the stress was hoop stress as it would be in the coil turns. I-V data was collected during the straining sample current pulse. The whole experiment is at 4.2 K, and there is no grip or handling problem.

There seems to be a critical stress for a given sample geometry below which no degradation in J_c was observed even after cyclic loading below the critical stress. There are reports in the literature that cyclic loading, below the critical strain of HTS

conductors, was causing degradation in J_c.[2] Once the critical stress value is reached there is a precipitous drop in the J_c value. This is very similar to what was observed in the J_c versus bend strain experiments.[3] Figure 1 shows I_c versus hoop stress for a multifilamentary Bi-2212/Ag tape conductor. Note that the critical stress is about 45 MPa. I_c decreases and becomes zero at about 90 MPa. This particular conductor was actually strained to failure at about 120 MPa.

Figure 2 shows I-V curves at various hoop stress (JBr) levels as marked. Note that the resistive baseline increases as the hoop stress increases above the critical stress. SEM micrographs taken from the longitudinal sections of Bi-2212/Ag tape samples (after ILFS experiment) showed small cracks at the outer filaments. The increasing number of these cracks must constitute the increasing resistive baseline in the I-V curves in Figure 2. As expected, SEM fragtography shows ductile and brittle failure in the Ag matrix and the Bi-2212 filaments respectively.

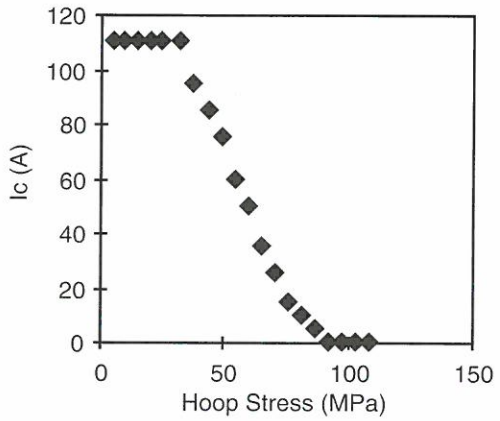

Figure 1. J_c versus hoop stress obtained by ILFS at 30 T and 4.2 K.

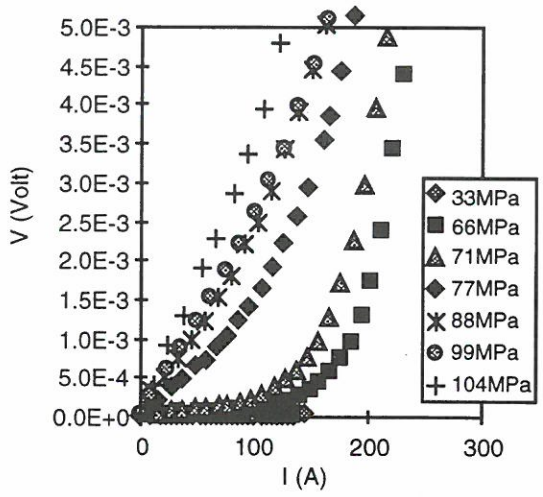

Figure 2. I-V curves at various hoop stress (JBr) levels as marked at 30 T and 4.2 K. Note that the resistive baseline increases as the hoop stress increases above the critical stress.

References:

1 Hascicek, Y.S., *et al.*, NHMFL 1995 Annual Report, 145 (1996).

2 ten Haken, B., *et al.*, 14th Int'l. Mag. Tech. Conf., Tampere, Finland, June 11-16, 1995.

3 Hascicek, Y.S., *et al.*, *Processing of Long Length of Superconductors,* eds. Balachandran, *et al.*, p. 262 (TMS Pub., 1993).

* On leave from Dept. of Physics, Marmara University, Istanbul, Turkey.

A Novel Lorentz-Force Tensile Stress-Strain and Critical Current Density Fatigue Apparatus

Hilton, D.K., NHMFL
Weijers, H.W., NHMFL
Hascicek, Y.S., NHMFL
Van Sciver, S.W., NHMFL/FAMU-FSU CoE
Schwartz, J., NHMFL/FAMU-FSU CoE

A new apparatus that utilizes the circumferential stress induced by the current carried in a tape conductor of circular geometry in an externally-applied, uniform, magnetic field has been developed. The stress of the conductor sample is determined by the current density, magnetic field, and radius of the conductor. The strain so induced in the sample is measured by a novel capacitive technique. The disk on which the conductor sample is wound consists in part of a fixed, circular, copper ring plate, and a single layer of polyimide tape for electrical insulation between the copper ring plate and the tape conductor, forming a capacitor system. The strain is determined by the change in capacitance of this system as the radius of the conductor changes. The capacitance is in turn determined by the frequency shift of a Hartley LC

oscillator in the laboratory, with the capacitor system being remotely in parallel with a fixed solenoid inductor to form the LC circuit.

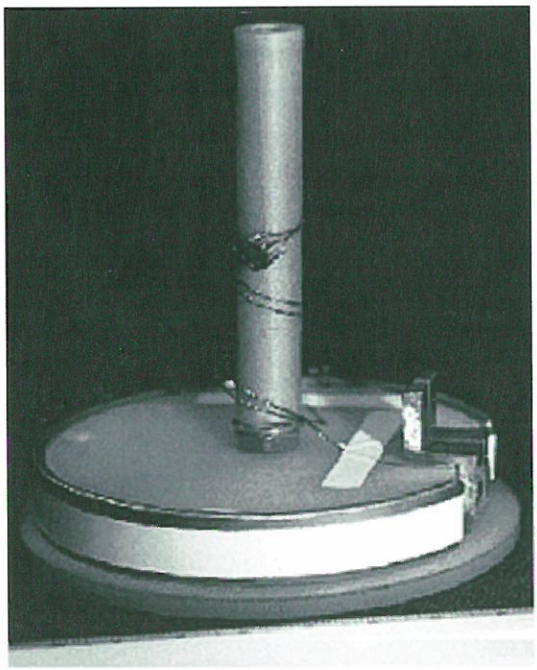

Figure 1. LHe temperature tensile stress-strain device.

With this new apparatus, shown in Figure 1, several interesting experiments become possible, since the conductor is in a nearly identical configuration to that of a magnet application. Specifically, a circle of HTS tape is tested in saturated LHe (T = 4.2 K) in the applied magnetic field of a 9 T, 100 mm bore superconducting solenoidal magnet. From this, the tensile stress-strain behavior of the conductor can be estimated. By cycle ramping the sample current, its critical current density fatigue behavior, as well as its mechanical fatigue behavior can be determined. A prototype version of the apparatus already has been built at the NHMFL, and tested with silver and silver alloy tape conductors. The results for an annealed pure silver tape are shown in Figure 2, as an example. Testing of the critical current density fatigue of HTS tapes is underway, with results forthcoming. The immediate interest of the group with these experiments is to determine the degree of degradation of the critical current density with respect to the number of ramping cycles, because this will have a direct impact on the in-service life of the HTS conductors.

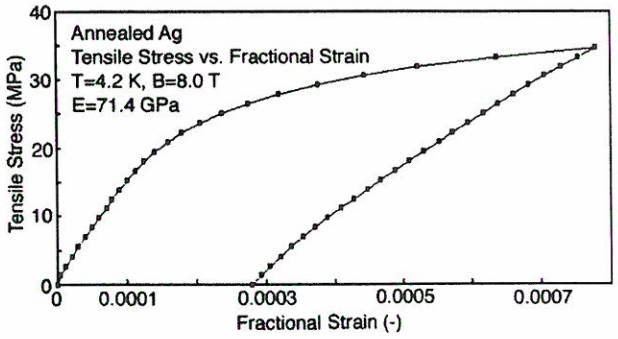

Figure 2. Stress vs. strain for anneal Ag.

Magneto-Thermal Conductivity of $Bi_2Sr_2CaCu_2O_x$ Superconductors

Nakamae, S., NHMFL/FSU, Physics
Schwartz, J., NHMFL/FAMU-FSU CoE

The investigation of the thermal conductivity (κ) of $Bi_2Sr_2CaCu_2O_x$ superconductors continues. The thermal conductivity, κ, of type-II oxide superconductors reflects the scattering processes between the charge carriers, phonons, and vortices. The change in κ in the presence of applied magnetic field is believed mainly due to their unique vortex movements. Thus, the study of magneto-thermal conductivity can provide important information about the vortex dynamics.

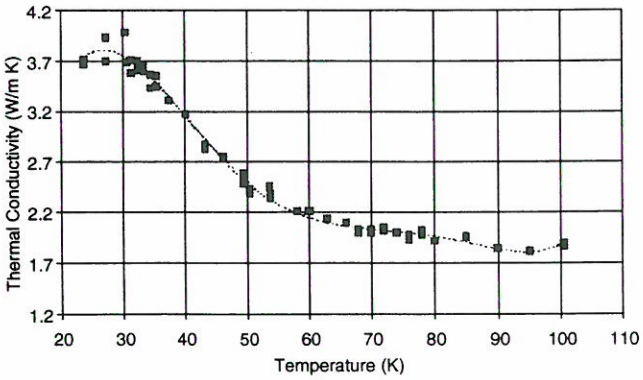

Figure 1. κ vs. temperature in zero field.

κ of a well-aligned $Bi_2Sr_2CaCu_2O_x$ sample has been measured with and without the presence of the external magnetic field. The field, supplied by the NHMFL 20 T resistive magnet, was applied both parallel and perpendicular to the *c*-axis of the

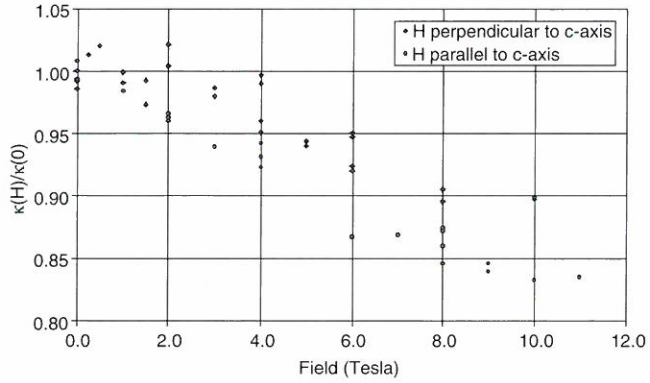

Figure 2. κ vs. field at 50 K.

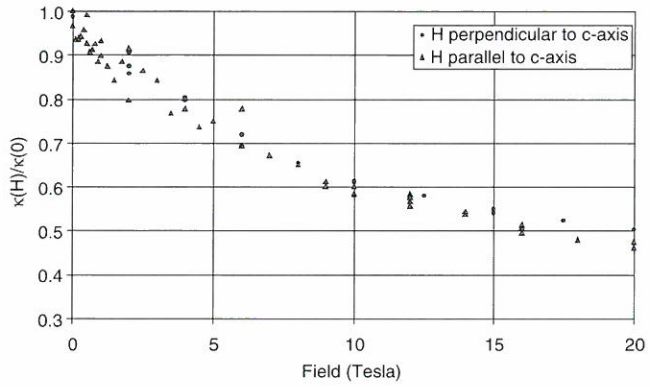

Figure 3. κ vs. field at 30 K.

sample. It has been found that the thermal conductivity reaches its maximum value at T 30 K and $H = 0$ T (Figure 1). κ decreases as the applied field strength increases. The change in κ (H,T) is larger when the field is applied parallel to the c-axis of the sample at higher temperature range (Figure 2) where the electronic contribution is considered to be the dominant factor. At lower temperatures, where the phonons are considered to be the dominant contributors to κ, the magnetic field direction does not have a recognizable effect on the κ (H,T) behavior (Figure 3).

Flux Pinning Enhancement in $Bi_2Sr_2CaCu_2O_x$ by Nanosize MgO Additions

Schwartz, J., NHMFL/FAMU-FSU CoE
Wei, W., NHMFL/FAMU-FSU CoE
Goretta, K.C., Argonne National Laboratory
Balachandran, U., Argonne National Laboratory
Bhargava, A., Univ. of Queensland, UNIQUEST

Weak flux pinning remains the most serious limitation for the practical applications of $Bi_2Sr_2CaCu_2O_x$ (2212) at elevated temperatures. Investigations have shown that flux pinning can be improved by introducing various types of defects into the superconductor. In particular, nanosize-second phase particle additions trapped within the 2212 grains are effective flux pinning sites. In this research, nanosize MgO particles were introduced into the 2212 powder. Ag-sheathed tapes were then made from the doped powders by the powder-in-tube (PIT) method. The objectives of this research include investigating the phase evolution process, optimizing the heat treatment, and exploring the effects of nanophase doping on the electrical magnetic behavior.

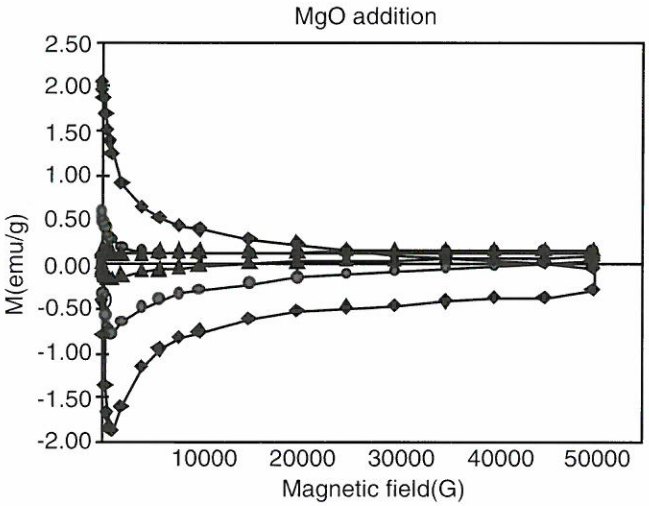

Figure 1. Magnetization hysteresis loops of the MgO doped samples: ◆ 4(2212):1 (MgO); ● 8(2212):1 (MgO); ▲ undoped.

Commercial superconducting powder with composition of $Bi_{2.1}Sr_{1.7}Ca_{1.2}Cu_{2.0}O_x$ made by Superconducting Components Inc. (SCI) was used in the experiments. Nanosize MgO powder with size less than 20 μm was prepared at the University of Queensland using a co-precipitation method. The superconducting powder and nanosize particles in varying ratios were mixed by the vibratory mill. Conventional powder-in-tube method was used to make the Ag-sheathed tapes.

Scanning electron microscopy (SEM) and energy dispersive spectroscopy (EDS) were used to identify the phases present in the samples. SQUID magnetometer measurements were used to measure the T_c and magnetization hysteresis. The

NHMFL 33 T VSM was used for magnetic hysteresis measurements. Magnetic J_c (J_{cm}) was derived from a hysteresis loop using the Bean critical state model. Shown in Figure 1 is the magnetic moment per gram versus field at 10 K for the MgO doped and undoped samples. The samples used were in powder form, which was made by grinding the sintered pellet into powder of about 1mm. Thus we exclude grain boundary effects and conclude that the J_C for the 4:1 MgO doped sample was about 10 times higher than the doped one.

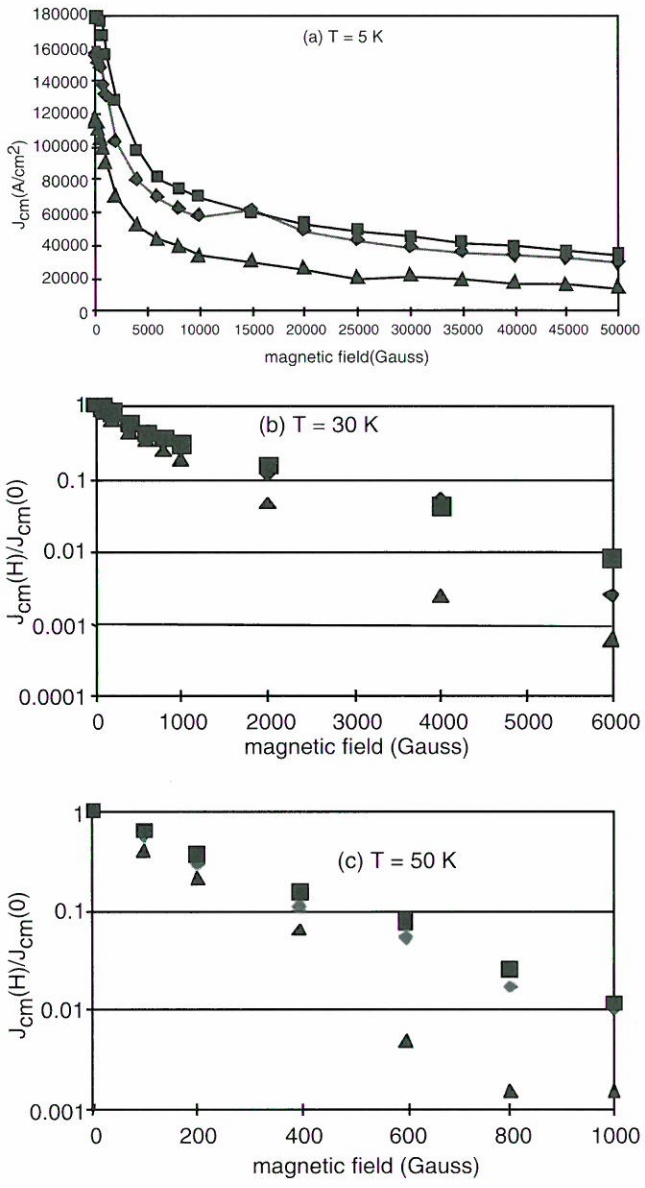

Figure 2. Magnetic J_c at different temperatures: ▲ undoped; ◆ 8 (2212):1 (MgO); ■ 4 (2212):1 (MgO).

Shown in Figure 2 are the normalized J_cs at 5, 30, and 50 K for the MgO doped and undoped samples derived from the magnetization hysteresis using the Bean model. At 5 K, all samples showed similar magnetic field dependence. At higher temperatures, however, J_{cm} of the MgO-doped samples is significantly less sensitive to magnetic fields. For example, at 30 K, the ratio of J_c (4000G)/ J_c(0) of the doped samples is more than one order of magnitude higher than that of the undoped sample. MgO doped PIT tapes showed I_c of 45A (corresponding J_c of about 50,000 A/cm^2). This was achieved by applying peak heat treatment temperature 10 to 20 °C higher than that used for pure 2212 tapes. Increased irreversible fields and magnetic J_c was observed by our high field VSM measurement at temperatures ranging from 5 to 27 K. MgO particles in fully processed tapes were detected by SEM investigation. Their sizes ranged from 0.1 μm to 40 μm. Particles smaller than the resolution of SEM were detected by EDS and further observations are ongoing.

Improved flux pinning by MgO doping was observed in powders and tapes. The cause of the flux pinning in the MgO doped tapes is not yet clear. Future investigations will focus on detailed microstructural studies for understanding possible reasons for the flux pinning enhancement.

Mechanical Properties and Strain Effects in $Bi_2Sr_2CaCu_2O_x$/AgMg Composite Conductors

Schwartz, J., NHMFL/FAMU-FSU CoE
Amm, B.C., NHMFL/FAMU-FSU CoE
Garmestani, H., Martech/FAMU-FSU CoE

The development of powder-in-tube $Bi_2Sr_2CaCu_2O_x$ technology has progressed such that high critical current density (J_c) conductors are produced by many researchers. Prototype systems are being tested to demonstrate engineering feasibility. An important issue that remains, however, is the effect of mechanical strain. While it is evident that large strains induce irreversible damage, applications may be limited by fatigue at low strain values due to crack propagation. In the case of composite ceramic superconductors, there

is the added complexity of the effect of these forces on superconducting properties. The local peak strain within the superconductor filaments may limit the coil properties. Recent work suggests that BSCCO tape properties degrade with cycling at low strain. Such fatigue behavior may limit other applications and relate to the fundamental J_c limit as well.

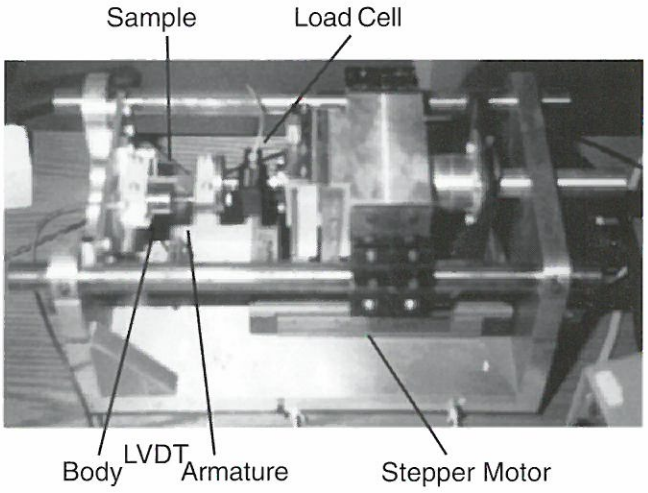

Figure 1. Room temperature testing device.

Due to the small size of the typical BSCCO/AgX superconducting tape, standard testing machines (hydraulic and pneumatic MTS types) are unusable. The loads required to fail such tapes does not usually exceed 200 N (45 lb_f). Also, the tape geometry (width to height ratios on the order of 20 or more) necessitates special gripping techniques. Smaller and more sensitive instrumentation is required to perform mechanical testing. In order to meet these requirements a new device has been developed specifically for such small scale testing at room temperature. The tester, shown in Figure 1, employs a stepper motor and conventional transducers for force and extension measurement.

The first room temperature tests conducted were simple stress-strain tests to failure on all samples. This was used as a confirmation of the expected values for the metals and to give a feel for the behavior of the BSCCO/AgMg. The first material tested was well-characterized Cu for benchmarking purposes. Once the results of the tester were confirmed to be accurate, the relevant materials were tested. The sheath materials of annealed Ag

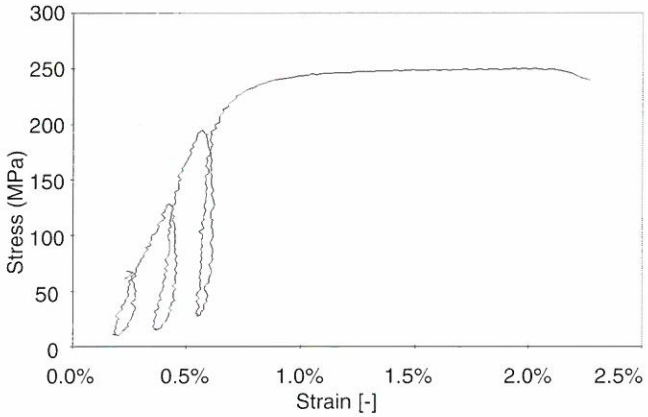

Figure 2. Stress vs. strain for BSCCO/AgMg monocore superconducting tape.

tape and oxidized Ag1.2at%Mg tape were tested. Having detailed information of the sheath material's mechanical behavior allows extrapolation of the bulk superconductor behavior from the composite wire behavior. Monocore powder-in-tube (PIT) AgMg/BSCCO tapes also have been tested. A sample stress-strain curve for the superconducting tape is shown in Figure 2.

The room temperature testing device has been found to be effective for mechanical testing. The device allows fatigue studies over the entire σ-ε range. Future tests will fatigue the superconducting material to determine its cyclic behavior.

Powder-in-Tube $Bi_2Sr_2CaCu_2O_x$ Conductor Development

Schwartz, J., NHMFL/FAMU-FSU CoE
Miller, V., NHMFL
Boutemy, S., NHMFL
Kessler, J., NHMFL

The goal of the high temperature superconductor development program is to make high magnetic field insert coils. For that reason, the research focuses on $Bi_2Sr_2CaCu_2O_x$ (Bi2212) exclusively as its performance at 4.2 K in high field is unequaled. Also, due to the large Lorentz forces present in high field magnets, the sheath of our powder-in-tube (PIT) conductor is dispersion-hardened by the addition of 1.2at.% Mg in the silver. Several stages of the conductor processing are under investigation to improve conductor performance.

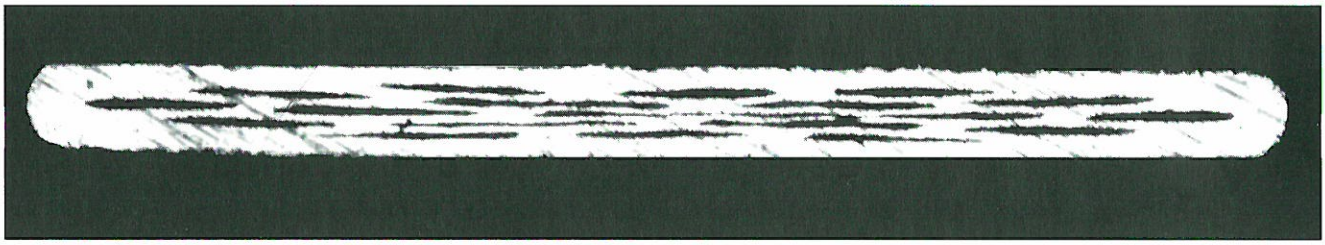

Figure 1. Transverse cross-section of an AgMg 19 filament multifilamentary tape.

The packing of the AgMg tube with the superconducting powder is an important step in the PIT process. As impurities in the powder, such as carbon and moisture, cause bubbling in the final tape and destroy its performance, we have developed a powder handling procedure that prevents such contamination. The powder is first annealed in flowing oxygen to remove carbon and other impurities. It is then transferred into a glovebox where it is packed into the tube. The entire assembly is then annealed in vacuum to purge the tube of gasses. During the first steps of the mechanical deformation, the wire is kept under vacuum until the sheath is sealed. This procedure has significantly reduced bubbling in samples of a few meters in length.

Another way to prevent bubbling is to apply an external pressure that balances the internal pressure and keeps the sheath from bubbling. A furnace insert has been constructed that regulates the pressure during the heat-treatment and withstands pressures up to 10 bars at 900 °C. Processing at 5 bars total pressure eliminated bubbles in conductors that previously showed serious bubbling problems.

To reduce sausaging in long lengths of conductors and to eliminate filament bridging in multifilamentary tapes, we are optimizing our mechanical deformation process. During each drawing step, the properties of the matrix change due to work-hardening. If the matrix becomes too hard compared with the powder, sausaging or breaking of the conductor occurs. The drawing schedule was therefore optimized, integrating number of intermediate annealings to release the work hardening of the matrix. After drawing the wire to a small diameter, it is rolled into a tape. At present, the influence of the roller size on conductor uniformity is being investigated. Large rollers have a broad contact region with the tape. Since no lubricant is being used during rolling, there is no slipping at the tape roller interface. As a result, the longitudinal flow of material is limited. The superconducting powder tends to flow laterally somewhat but primarily it densifies. By using smaller rollers, we expect to improve the longitudinal flow of powder and thus to reduce the longitudinal density inhomogeneity that causes sausaging. Smaller rollers have been installed on the rolling mill and preliminary studies have begun. Finally, the variation of the powder density is also being studied throughout the processing of the conductor. As a result, the influence of different starting packing densities can be predicted and the final filling factor can be estimated.

Stability of High Temperature Superconducting Conductors

Schwartz, J., NHMFL/FAMU-FSU CoE
Burkhardt, E.E., NHMFL/Univ. of Illinois at Urbana, Nuclear Engineering

The stability of superconducting magnets subjected to external thermal disturbances or flux jumps depends on the interplay between the electromagnetic and thermal characteristics of the system. As stability can limit the performance of a superconducting magnet, the stabilities of NbTi and Nb_3Sn conductors have been well studied. Here, we analyze the stability of $Ag/Bi_2Sr_2Ca_2Cu_3O_x$ (Ag/BSCCO) superconducting tape conductors (shown in Figure 1) using the finite element method (FEM) by solving the heat conduction equation at each time step.

FEM consists of dividing a section of the tape into small elements and analyzing each element separately. As a result, each element can be

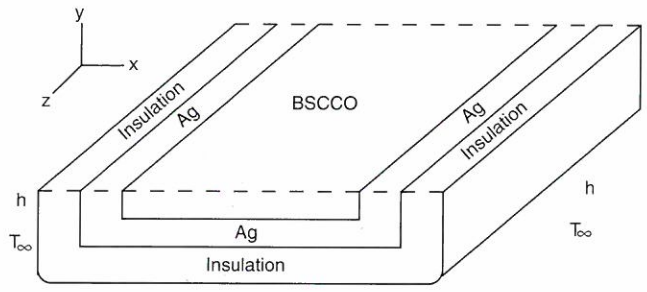

Figure 1. One-half cross-section of a Ag/BSCCO superconducting composite tape.

considered homogeneous, which allows the analyses of a variety of geometries readily. This numerical analysis is used as a result of the temperature dependence of the material properties of both the superconductor and the stabilizer. Both two- and three-dimensional codes have been written. To illustrate the FEM approach, the stability of a composite tape with a 2.5:1 Ag/BSCCO ratio is determined. The current propagates in the z-direction and anisotropy of the BSCCO occurs in the y-direction relative to the x- and z-directions. Starting with the tape at steady-state with a current I_{op} operating in a magnetic field B, a heat pulse is introduced to drive the tape normal locally. The external disturbance must be large enough to create a substantial electric field, which will contribute to heating ($Q = E \bullet J$).

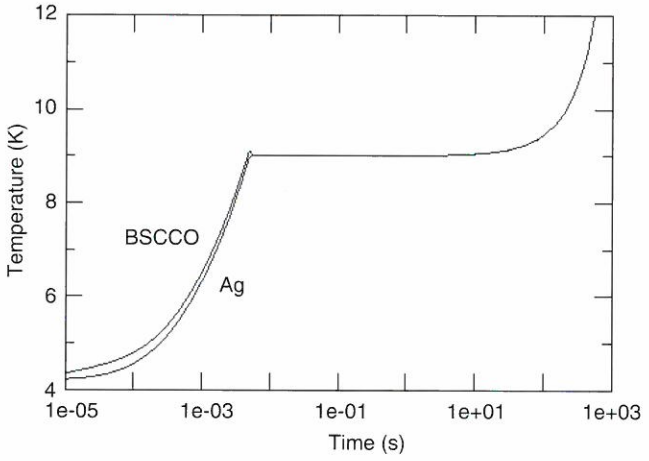

Figure 2. Temperature vs. time for a uniform 5 ms source for a conductor operating at 4.2 K, 0 T, I_{op}/I_c=0.9.

The tape is considered unstable when the temperature rises such that E_f does not vanish and the tape does not return to the initial state. If a pulse source is used, only the $E \bullet J$ source term remains after the pulse. If a constant heat source is applied, however, both that and the $E \bullet J$ source term exist. The critical current density is found for each field at the operating temperature, with the operating current set to a fraction of I_c. A pulsed source is then applied, which causes the temperature of the tape to rise locally. If the pulse is sufficiently large, I_c decreases to a value such that the amount of heat generated is sufficient for the tape to not return to a stable state, *i.e.* the temperature continues to rise. The magnitude of the pulse required to cause the tape to become critically unstable is determined and the values at various fields ranging from 0 to 20 T are calculated. Figure 2 shows a typical plot of the temperature vs. time for a slightly unstable case at 4.2 K, 0 T, with an infinitely long uniform 5 ms source in the BSCCO (*i.e.* no variation in the z-direction). At lower times, the bottom curve is the temperature of a point in the Ag and the top curve is the center of the BSCCO. After the pulse finishes, the temperature in any given x-y plane is nearly uniform across the tape.

Issues that are considered include variation of parameters (*e.g.* the geometry/cross-section of the tape, the fraction of superconductor, the operating current, etc.), addition of insulation and convective cooling, anisotropy of the Ag in a magnetic field, inhomogeneity of the Ag, the current density distribution in the BSCCO, and current diffusion from the BSCCO into the Ag. This ongoing effort will model conductors used in coils built and tested by the NHMFL and industry.

Synthesis of $HgBa_2Ca_{n-1}Cu_nO_x$ High Temperature Superconductors

Schwartz, J., NHMFL/FAMU-FSU CoE
Wolters, Ch., NHMFL
Pamidi, S., NHMFL
Amm, K., NHMFL/FSU, Physics
Knoll, D.C., NHMFL/FAMU-FSU CoE

The $HgBa_2Ca_{n-1}Cu_nO_x$ superconductors have set a record of 135 K for the superconducting transition temperature (T_c) and irreversibility fields of up to 12 T at 77 K. Thus, they are strong

candidates for applications at liquid nitrogen temperature. The main technique for the synthesis of bulk $HgBa_2Ca_{n-1}Cu_nO_x$ superconductors is encapsulating and post-annealing. Small amounts of precursor powder are encapsulated in evacuated quartz tubes and reacted with Hg vapor by annealing between 650 and 950 °C. This technique involves numerous critical parameters such as carbon content of the precursor, heating rate, annealing conditions, and Hg vapor pressure.

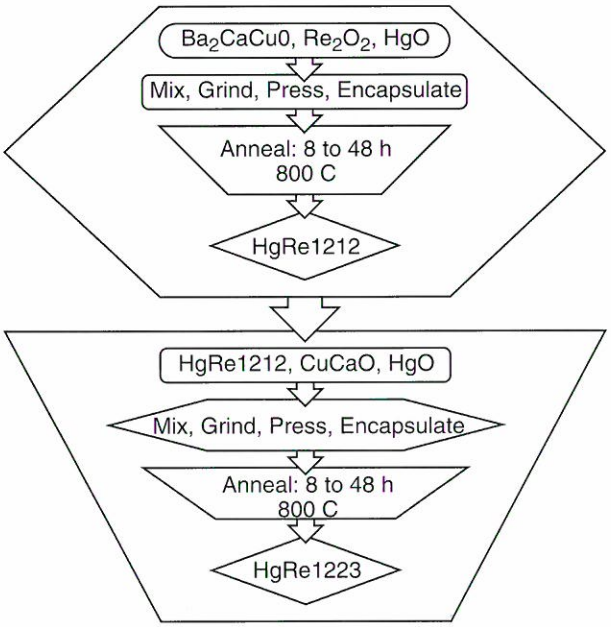

Figure 1. Preparation of (Hg,Re)1223 by the two-step method. In the first step bulk HgRe1212 superconductor is prepared from commercial precursors. In the second step CaO, CuO, and HgO are added to finely ground (Hg,Re)1212 and annealed to form (Hg,Re)1223.

$(Hg,Re)Ba_2Ca_1Cu_2O_y$ and $(Hg,Re)Ba_2Ca_2Cu_3O_y$ superconductors were prepared with high phase purity starting from carbonates, nitrates, and commercially available precursors with optimal annealing temperatures between 900 °C and 950 °C for the $(Hg,Re)Ba_2Ca_2Cu_3O_y$ phase and below 850 °C for the $(Hg,Re)Ba_2Ca_1Cu_2O_y$ phase. The addition of Re was found to have beneficial effects on the phase formation and chemical stability of the superconducting phase, especially regarding its sensitivity to H_2O and CO_2. Systematic investigations of samples quenched from various stages of the annealing procedure indicated that the $(Hg,Re)Ba_2Ca_2Cu_3O_y$ phase forms via the $(Hg,Re)Ba_2Ca_1Cu_2O_y$ phase. Based on these results a new two-step method has been developed to synthesize $(Hg,Re)Ba_2Ca_2Cu_3O_y$ with lower annealing temperatures as compared to conventional methods. This approach uses a precursor containing the $(Hg,Re)Ba_2CaCu_2O_y$ phase, see Figure 1 (patent pending). In the first step, high phase purity $(Hg,Re)Ba_2CaCu_2O_y$ superconductors are prepared from commercially available $Ba_2CaCu_2O_x$ precursors, HgO, and Re_2O_7. In the second step, the finely ground $(Hg,Re)Ba_2CaCu_2O_y$ is mixed with Ca-Cu-O and HgO. This precursor mix is encapsulated in evacuated quartz tubes and annealed for 8 to 48 h between 750°C and 850 °C. The resulting samples have $(Hg,Re)Ba_2Ca_2Cu_3O_y$ as a majority phase and exhibit a critical temperature of 133 K.

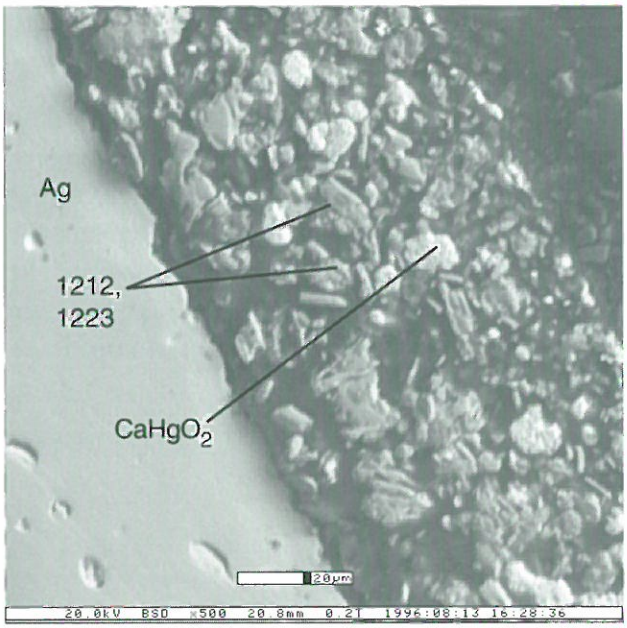

Figure 2. SEM micrograph of the polished cross-section of a (Hg,Re)1223/AgHg sample (AgHg on the left). The large gray blocks near the AgHg interface as well as the thin, needle-like grains are (Hg,Re)1223 and (Hg,Re)1212. The large, bright white circular regions are $CaHgO_2$, while the smaller, round gray regions are Ba-Cu-O phases. Much of the powder layer is filled with dark gray porosity.

The large-scale application of any high-temperature superconductor will require a metallic sheath to satisfy the mechanical and thermal requirements of superconducting magnets. Thus, an important step in the development of a high

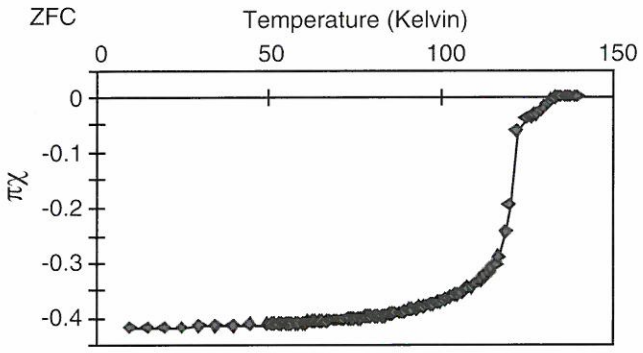

Figure 3. Magnetic susceptibility plotted vs. temperature for a (Hg,Re)1223/AgHg sample. The second step in the transition at 120 K is probably indicative of an underdoped (Hg,Re)1212 phase.

temperature superconductor is to study the properties of the superconductor in contact with a metallic interface. Due to the highly corrosive atmosphere necessary for the synthesis of, $Hg_{0.9}Re_{0.1}Ba_2Ca_2Cu_30_y$, the selection of a suitable metal substrate is critical. In this study, we attempt to synthesize $Hg_{0.9}Re_{0.1}Ba_2Ca_2Cu_30_y$ samples on Ag, AgHg, Au, AgPd, and Pt substrates. The samples were prepared via the two-step method. $(Hg,Re)Ba_2CaCu_2O_y$, Ca-Cu-O, and HgO precursor powders were suspended in a dry methanol solution. This mixture was then dropped and centrifuge coated onto the metal substrates. The samples were encapsulated in quartz and annealed. Microstructural analysis of phase growth and grain alignment at the superconductor/metal interface were carried out on multiple length scales via x-ray diffraction, scanning electron microscopy (SEM), and x-ray microanalysis indicated the presence of the $Hg_{0.9}Re_{0.1}Ba_2Ca_2Cu_30_y$ phase. Figure 2 shows a SEM micrograph of the metal/superconductor interface and Figure 3 shows the magnetic susceptibility plotted versus temperature.

One of the problems with HBCCO superconductors is their high sensitivity to atmospheric moisture and carbon dioxide. All the processes such as mixing and grinding were carried out under inert atmosphere in glove boxes. The synthesized superconducting materials are also susceptible to degradation with time. Both of these problems were solved by partially substituting Re for Hg. The exact role of the Re substitution is not understood. We are planning a systematic investigation on the role of composition (stoichiometry) and substitutions on the formation and stability of Hg1212 and Hg1223. We also plan to investigate the role of precursors in grain growth and possible formation of some liquid during synthesis by partial melting.

This research is supported by the National Science Foundation, DMR-9526231.

Fabrication and Characterization of HTS Joints in Bi-2212/Ag Conductors

Shoaff, P.V., Jr., NHMFL
Hascicek, Y.S., NHMFL
Schwartz, J., NHMFL/FAMU-FSU CoE
Van Sciver, S.W., NHMFL/FAMU-FSU CoE

Several joint prototypes were investigated in the first phase of this program with the wrap joint determined to have the highest probability of success for our desired application. The wrap joint is basically a butt joint that has its superconducting properties enhanced with various types of BSCCO fill material and reinforced by an outer wrapping of silver tape. First, the two free ends of the stock conductor pieces to be joined are placed end to end. The tape legs are cut to 2.5 cm lengths and the end faces are positioned as close together as possible and held in place with a custom-made clamping device. Next, the region of convergence is wrapped with BSCCO fill material and then silver tape and pressed and reacted.

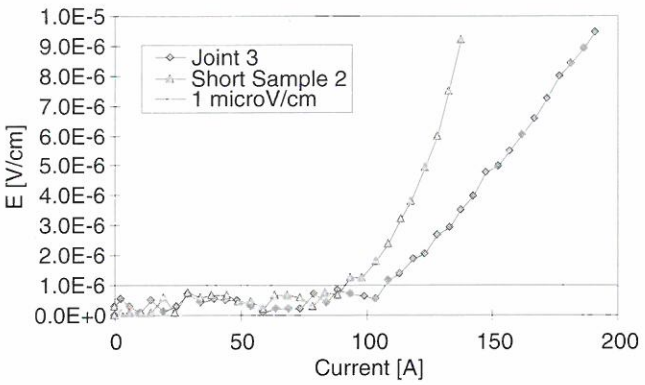

Figure 1. A comparison of the E vs. I curves for a monocore joint and an equivalent short sample. Note that the I_c of the joint is greater than that of the short sample.

A comparison of the electric field vs. current curves for one joint and a straight sample are seen in Figure 1. An additional finishing step was added to the wrap joint process for the multifilamentary conductors. This finishing procedure increases the surface area of conductor core exposed to the junction and provides a square mating surface for the butt joint created by the conductor leg ends. Figure 2 compares the E-I plots of a joint and straight multifilament conductor. Once again, this figure illustrates how the wrap joint technique, this time applied to multifilamentary conductor, outperforms the 245 A critical current of the short sample.

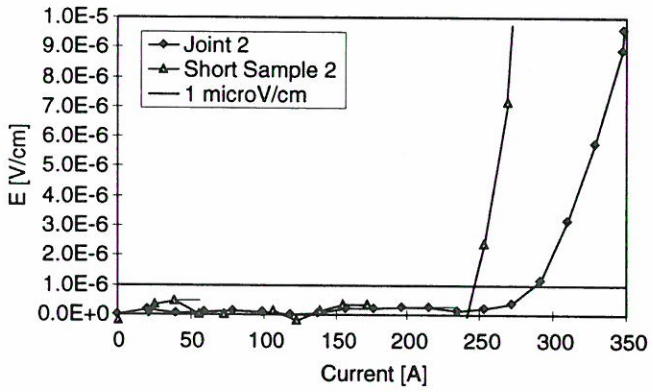

Figure 2. A comparison of the E vs. I curves for a multifilament joint and an equivalent short sample.

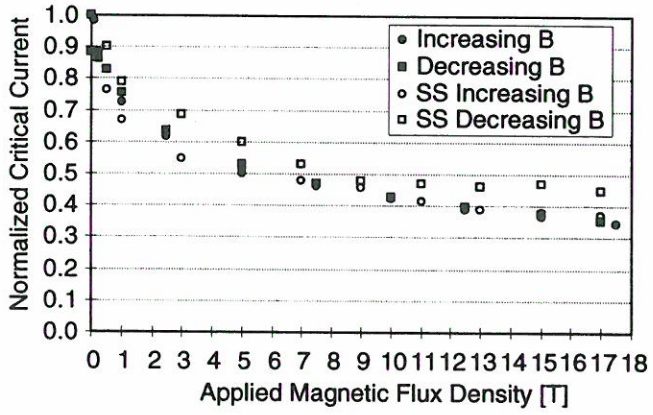

Figure 3. A plot of the normalized critical currents vs. applied magnetic flux density for a multifilament joint and a short sample.

Figure 3 is a plot of the normalized I_c values for a joint and a short sample of multifilament conductor from the same tape batch at different applied fields. This study shows that the wrap joints appear to have critical currents that are constrained by the bulk conductor and not by some intrinsic property of the wrap joint technique.

HTS Coil Development Using Bi-2212 Conductor

Weijers, H.W., NHMFL
Godfrey, M., NHMFL
Hascicek, Y.S., NHMFL
Van Sciver, S.W., NHMFL/FAMU-FSU CoE
Hazelton, D., Intermagnetics General Corp.
Cowey, L., Oxford Superconducting Technology

The development of HTS insert coil technology using powder-in-tube (PIT) Bi-2212 conductor and utilizing the wind-and-react (W&R) approach has continued, resulting in a number of fully impregnated double pancake units that are stackable for coils. Additionally, work has started to develop react-and-wind (R&W) technology using surface coated conductor. The following sections will discuss both approaches and the obtained results in more detail.

Wind and React. To date, we have focused our research on pancake magnets. A total of twenty-five double pancake and twenty-three single pancake coils have been built. Most of the double pancakes are for 1 T Class coils, the single pancakes are typically intended to test lengths of a few meters of conductor to support in-house conductor development. One double pancake and five single pancakes have been built as part of the development of a NMR shim coil.

In many cases the conductor showed either pinhole leaks or bloating, or both, making a systematic study of coil technology difficult. The mechanical effects of bloating on the shape of the coil can be eliminated by applying an overbanding during the heat treatment. The pinhole problem is more serious. For insulated conductor, the

insulation acts as a wick and complicated reactions take place in the core material that leaks out. This causes shorts and often limits the performance of coils to less then 20% of the uninsulated short sample performance. Therefore, only a much smaller number of coils had no shorts and had critical currents of more than 50% of the short sample value. Among the successful coils were three coils that carried over 100 A/mm^2 in the conductor, which is about 50% of the critical current of the best short samples from that conductor batch. Two double pancakes were made that performed at 85% of the best short sample values. This indicates that it is possible to heat treat small coils and obtain properties close to the short sample performance. Both coils have a remarkably high n-value, n = 17 when using the common 1 μV/cm criterion. These n-values increase when using stricter criteria and are over 30 for currents just above the measurable onset of the transition. This is a highly desirable property for NMR magnets especially if persistent mode operation is considered. These coils are fully epoxy impregnated, stackable, and have withstood thermal cycling and operation in a 17 T background field without degradation of properties. The in-field behavior is typical with a decrease of I_c to 41% of the self field value and a narrow hysteresis loop. The absolute value of the critical current of the coils, however, was untypically low with I_c = 57 A. This limited the engineering current density to about 90 A/mm^2.

React and Wind (R&W). R&W coil technology allows the use of different materials for insulation and structural elements such as Kapton and G-10, which are common materials in cryogenic engineering. Since there is no heat treatment that can be performed after winding to cure defects, the effect of bend strain on J_c must be considered. Experiments on short samples indicate a critical bend strain of about 0.2%, above which critical current degradation occurs for the type of surface coated conductor used. Three coils with an inner diameter of 52 mm have been built to date. The critical currents of these coils were consistent with the short sample bending strain measurements. This validates the use of short sample measurements to predict the minimum radius necessary to avoid bending strain degradation of the critical current in coil. The obtained engineering current densities in the conductor (110-140 A/mm^2 at 4.2 K and self field) are comparable to the two best W&R coils so far.

The conductor used for these coils was either manufactured in-house or made available by Intermagnetics General Corp. (IGC) or OxfordSuperconducting Technologies as part of co-operative magnet development program. Conductors continue to improve on average. Currently conductor is available in long lengths with demonstrated current densities up to 450A/mm^2 in lengths up to at least 1 meter. A coil that has a self-field overall current density of 75% of that value has the current density required by the benchmark design of the final 5 T NMR insert magnet.

Intrinsic Stability of High T_c Superconducting Tapes Including the Effect of Anisotropic J_c

Xiao, L.Y., NHMFL
Van Sciver, S.W., NHMFL/FAMU-FSU CoE

In the tape-wound magnets, the field distribution may not be homogeneous, and probably is tilted with respect to the wide surface of the tape. In such a situation, the external field will induce equivalently two screening currents corresponding respectively to the parallel component ($B_{//}$, i.e. B_z) and perpendicular component ($B_\perp$, i.e. B_x); Figure 1 shows the detail. Due to the 2D layered structure of the HTS tape, these two screening currents behave differently in the value and sensitivity to the external field.[1,2] If a thermal disturbance is applied to a HTS tape, both of the screening currents will degrade and further heat generation will occur. Therefore, the intrinsic stability HTS tapes will be different from that of low T_c tapes due to the anisotropic J_c.

In order to analyze the intrinsic stability of this case, we develop a 2D critical state model to describe the anisotropic J_c effect. When a HTS tape

is exposed to an external field tilted to the wide surface of the tape at an angle θ, the screening currents can be expressed as follows:

$$J_{c\parallel} = \frac{\alpha_{\parallel}}{B\cos\theta + B_{0\parallel}} + \beta_{\parallel} \quad (1a)$$

$$J_{c\perp} = \frac{\alpha_{\perp}}{B\sin\theta + B_{0\perp}} + \beta_{\perp} \quad (1b)$$

$\alpha_{\perp}$, $\beta_{\perp}$, $B_{0\perp}$; $\alpha_{//}$, $\beta_{//}$, $B_{0//}$ are constants for a specified case. On the other hand, when the external field is parallel to the wide surface, the critical transport current J_{ct} is field-independent due to the intrinsic pinning.[3] When external field is intersected with the wide surface, $J_{ct}(B)$ can be also expressed as (1b).

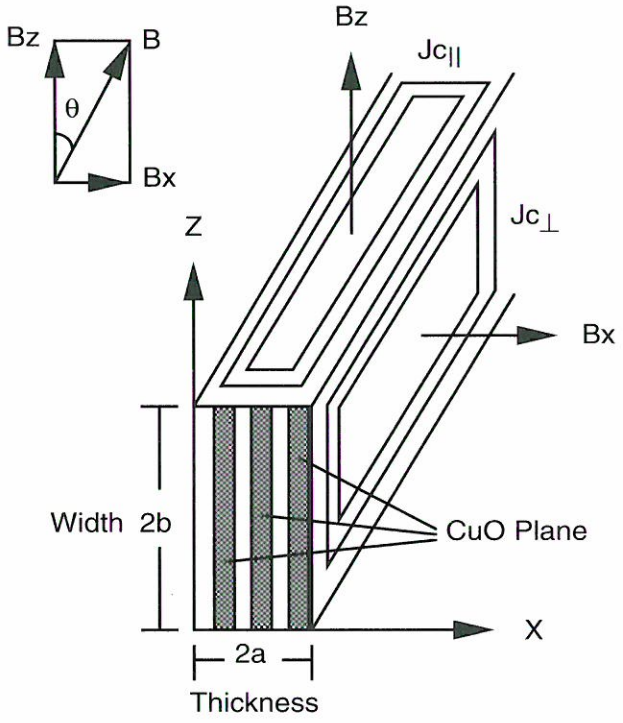

Figure 1. Schematic figure for the external field and screening currents in a layered superconducting tape.

By this 2D critical state model, intrinsic stability was analyzed. The simulations of the adiabatic stability of a BSSCO tape at 4.2 K and 20 T is shown in Figure 2.

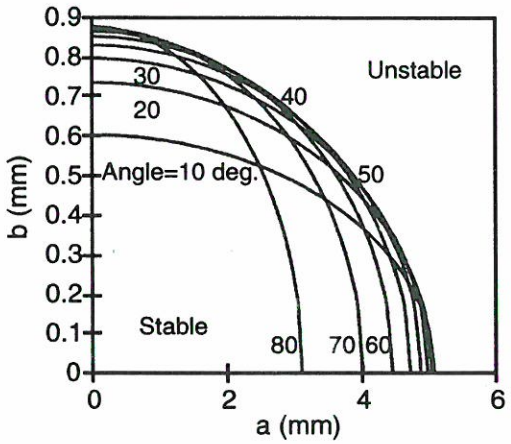

Figure 2. A 2D restraint for the half-width and half-thickness of a superconducting tape at different field orientation. where: $\alpha_{\perp}=1.5\times10^{9}$ A(T/m^2, $\beta_{\perp}=6.0\times10^{8}$ A/m^2, $B_{0\perp}=0.5$ T; $\alpha_{//}=3.5\times10^{8}$ A·T/m^2, $\beta_{//}=1.0\times10^{8}$ A/m^2, $B_{0//}=0.35$ T.

References:

1 Blatter, G., *et al.*, Rev. Mod. Phys., **66**(4), 1125 (1994).

2 Feinberg, D., Physica C, **194**, 126 (1992).

3 Tachiki, M., *et al.*, Cryogenics, **32**, 923 (1992).

Cryogenics

Program Overview

S.W. Van Sciver

The Cryogenics Program serves two principal purposes at the National High Magnetic Field Laboratory. First, we engineer the systems that supply cooling to the large superconducting magnets. An example of such a system is the cryostat for the 45 T Hybrid magnet, which has been tested and is now ready for installation of the superconducting outsert magnet. We are also working actively on the 900 MHz NMR project by supplying the design of the cryostat for that magnet system. To go along with those support activities, we conduct component development research in an effort to better understand how to design and operate these kinds of facilities. For example, we recently completed an analysis of He II heat exchanger such as is incorporated in the 45 T Hybrid and compared the results to the actual performance of the system. A short report on this project is enclosed. We also have analyzed continuous cooling of thermal support structures for large magnets and are comparing this analysis to experiment. Proper understanding of component performance is critical to the optimization of cryogenic system design.

In addition to the cryogenic work that supports the in-house magnet development programs, we also carry out research and development in connection with other cryogenic applications. The main activity within this other work involves heat and mass transfer in superfluid helium, or He II. This activity is mostly supported by the Department of Energy, Division of High Energy Physics. For example, we have initiated a He II/vapor two phase heat transfer and flow study and completed a preliminary experiment (see research report that follows). Model calculations support this work. In another activity, we have conducted a study of high Reynolds number liquid helium fluid dynamic drag on bluff bodies. This work, supported by the Navy Department, evaluated and demonstrated the feasibility of large scale hydrodynamic experimentation in a liquid helium system. Two research reports present the results, including one concerning a method for a drag measurement using a superconducting magnetic balance system.

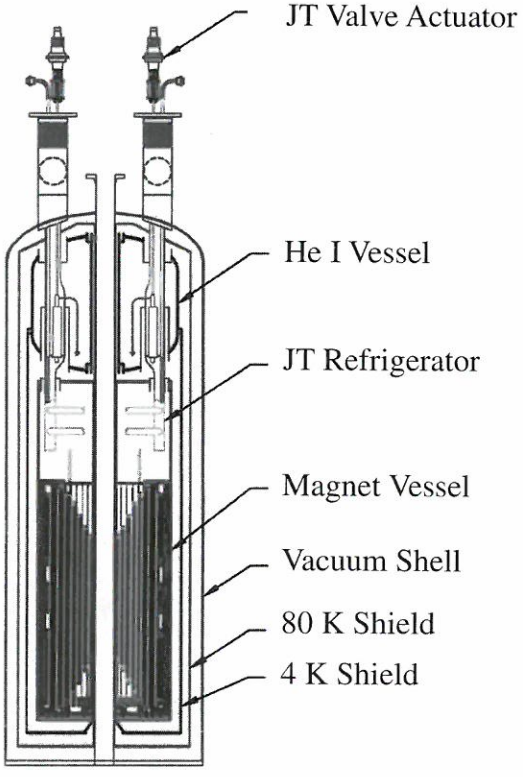

Figure 1. 900 MHz NMR cryostat.

Magnetoresistance of CERNOX™ Temperature Sensors, 1.5 K to 300 K

Brandt, B.L., NHMFL
Liu, D.W., FSU/Physics Dept.

The increasing use of higher field magnets for laboratory research has increased the need for temperature sensors that give accurate, repeatable measurements in magnetic fields ≥20 T. An ideal sensor would be independent of magnetic field. The next best alternative would have field dependence that is small and correctable by a method that is independent of the manufacturing process. Considerable research aimed at developing sensors has been done and several commercially available sensors have been characterized. Carbon-glass sensors were found by previous work to be the most generally applicable to the temperature range from 1.5 to 320 K in magnetic fields up to 20 T.[1]

Sputtered zirconium nitride films were demonstrated to be useful temperature sensors by Yotsuya, Yoshitake, *et al.*[2] and have been developed into a commercially available product by Lake Shore Cryotronics, Inc. Our previous work has shown the CERNOX™ sensors to have significantly less magnetoresistive error than carbon-glass sensors.

We continued our study of the behavior of CERNOX™ zirconium oxy-nitride film sensors from Lake Shore Cryotronics in magnetic fields up to 20 T at temperatures between 1.5 and 320 K. We added to the study more sensors with different specific sensitivities and from different production batches to find out whether or not it is possible to generate a correction procedure that can be applied to a new, off-the-shelf sensor. We also determined that two of the original batches of sensors were improperly made and rejected those sensors from the overall study. We measured a variety of sensor models and decided that only those designated as models CX-1030 and CX-1050 should be included in a table of magnetic field corrections because other models were too different from the mean. Finally, we gathered more data comparing the magnetoresistance effects with the plane of the sensor oriented parallel or perpendicular to the magnetic field. More data on orientation dependence are needed to get a clear comparison.

References:

1 Sample, H.H., *et al.*, Rev. Sci. Instrum., **53**, 1129 (1982).

2 Yotsuya, T., *et al.*, Appl. Phys. Lett., **51**, 235 (1987).

Heat and Mass Transfer in Two-Phase Helium II

Panek, J., NHMFL/FAMU-FSU CoE
Huang, X., NHMFL
Van Sciver, S.W., NHMFL/FAMU-FSU CoE

A new cooling scheme using two-phase vapor/He II has been proposed for the next generation of high-energy physics particle accelerators. The objective is to absorb the heat generated at 1.9 K in the magnets with minimum temperature rise by utilizing the latent heat of liquid He II. Such a cooling scheme will use two-phase flow and heat transfer in saturated He II over the whole range of vapor qualities. Unfortunately, despite preliminary experimental tests demonstrating the feasibility of such a cooling scheme, not enough is known about the basic heat transport mechanisms in two-phase He II. To better understand this system, we have conducted an analytical and experimental study on the heat and mass transfer between two saturated He II baths. The configuration consists of two vessels partially filled with He II and connected by two cross-tubes, one in the liquid space and one in

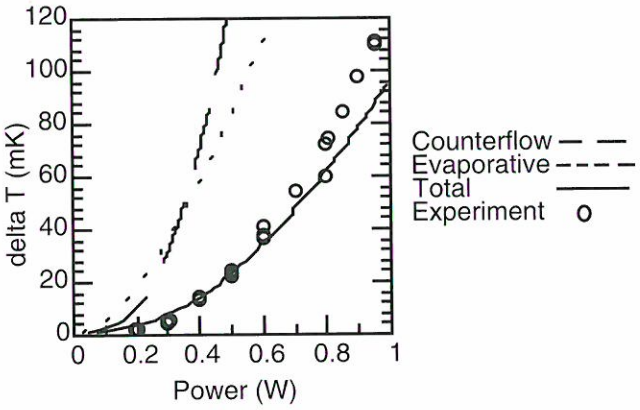

Figure 1. Total heat transfer rate.

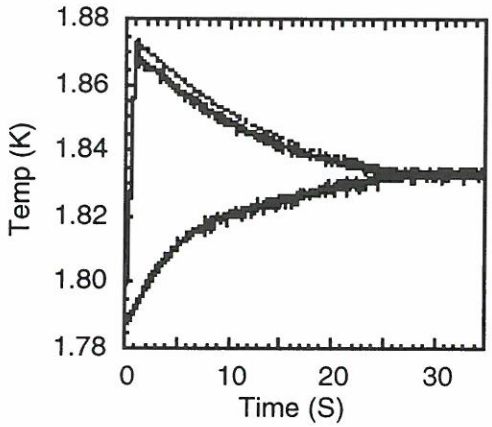

Figure 2. Transient temperature difference following 30 J pulse.

the vapor space. This geometry decouples the counterflow heat transfer in the liquid from the mass transfer in the vapor and enables us to quantify the two transport processes separately.

Results have been obtained[1] for a vapor tube ID of 1.3 mm and a liquid tube of ID 5.0 mm. Steady state values of temperature rise vs. heat input are shown in Figure 1. The results show that the evaporative vapor flow mechanism is the dominant one under these conditions. This is true in spite of the large cross-sectional area difference in the vapor and liquid cross tubes. The numerical model is able to accurately predict the behavior.

Transient experiments also have been performed, as shown in Figure 2. A 30 W heat pulse is applied for 1.0 s to one bath, and temperature rises of both sides are recorded. The initial helium level is 36.0 cm and the initial bath temperature is 1.79 K. Results from the numerical model are plotted with good agreement with the observed temperature traces. These results show that considerable time is required for the heat transfer mechanisms to restore a steady state condition after a disturbance. Times of 15 to 30 seconds are required, depending on initial liquid level and energy supplied.

In the following year we plan to modify the double bath experiment to replace the bottom liquid tube with a slot channel containing both liquid and vapor. Further work on a numerical model for this geometry is also required.

This work is supported by the Department of Energy, High Energy Physics Division.

Reference:

1 Huang, X., *et al.*, *Heat and Mass Transfer between Two Saturated He II Baths*, Proceedings of the ICEC 16.

Low Temperature Cryostat for Experiments in Megagauss Fields

Rickel, D.G., NHMFL/LANL
Goettee, J.D., LANL/DX

We describe the construction and performance of a cryostat built from inexpensive nonconducting materials. The following criteria for the dewar had to be met. The dewar volume had to hold a vacuum leading to the requirement that the inner dewar walls be sufficiently strong to resist buckling. This same requirement obviously applies to the outer walls of the dewar. The dewar inner tail I.D. needed to be 6 mm with an outer tail O.D. of 8 mm. An ultimate temperature of 1.8 K was desired.

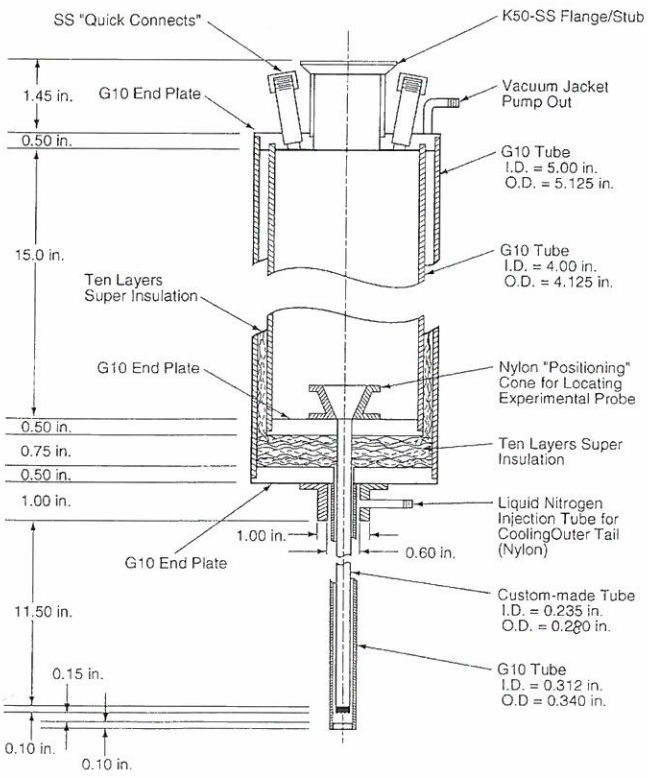

Figure 1. MC-1 helium dewar.

As can be seen from the drawing in Figure 1, the dewar has a single vacuum jacket, therefore, radiation heat flow is going to be the dominate heating mechanism of the liquid helium. Ten layers of super insulation (1 mil aluminized mylar) was loosely wrapped inside the vacuum jacket of the main body of the dewar. Also, the same number of layers were installed in the stepdown region between the tails and the main dewar body. Reduction of heat flow in the tail region is achieved by directing a flow of liquid nitrogen along the outer surface of the dewar tail, as can be seen from the drawing a chimney is placed on the bottom of the dewar body. This enables injection of liquid nitrogen that then is constrained to flow along the dewar tail.

Except for one piece, all of the cylindrical wall materials were made from G10 tubing. The tubing was not intended for vacuum applications and needed some treatment to fill in the pores. All the tubing surfaces were painted with 1250 Stycast™, the excess resin wiped off and the resin allowed to cure before assembly. Wall thicknesses were adequate to avoid collapse of the tubes under vacuum.

The inner tail was custom made because tubing sizes to meet the dimensional and strength requirements were not available. One mil kapton film was used to fabricate the inner tail. The film was coated with a thin layer of Stycast™ 2850 FT (an alumina loaded epoxy) and wrapped around a 6 mm diameter glass tube for a total of five layers. The resulting tube was then oven cured at 150 °C. The thickness of the tube wall ranged between 0.3 and 0.4 mm.

Assembly of the dewar was straight forward. All of the tubes were epoxied into grooves in the circular endplates with Stycast™ 1250. The inner tube of the tail had a spacer glued to the endcap for locating the tube on axis with the outer tube. The inner tube also had a 0.009" nylon monofilament fishing line wrapped around the outer periphery to prevent contact with the outer tube of the tail. The pitch was 3 cm/rotation. A KF-50 stub was attached to the upper plate of the dewar to serve as a pump out port and the attachment flange for the instrumentation probe. Two stainless steel stubs with compression rings also were attached to the top plate for liquid helium filling and level measurement. The dimensions of all the dewar elements are included in Figure 1.

The helium leak rate of the dewars at room temperature was less than 1 x 10^{-8} atm/cm^{3}sec. With long exposure to helium, however, there was a steady state diffusion rate at room temperature that was on the order of 5 x 10^{-7} atm/cm^{3}sec. This diffusion is considerably lower at liquid helium temperature but could not be reliably measured.

After a second helium fill we were able to pump the liquid helium down to 8 millitorr after approximately 20 minutes. In this configuration we had approximately 1 hour and 45 minutes of hold time from the end of the second filling. This corresponded to a temperature of 1.7 K.

Observed Pressure Distribution and Drag on a Sphere in Flowing Helium I and Helium II

Smith, M.R., NHMFL
Van Sciver, S.W., NHMFL/FAMU-FSU CoE

To initiate an effort in high Reynolds number liquid helium flow studies and demonstrate some of the relevant technology, we have designed, constructed, and operated an apparatus for

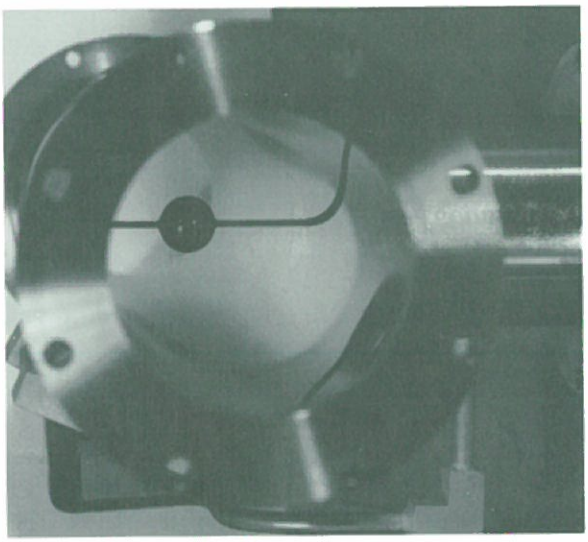

Figure 1. 10 mm sphere mounted within the test section.

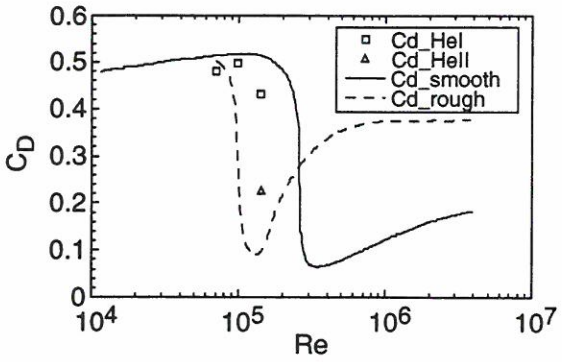

Figure 2. Coefficient of drag in the neighborhood of the drag crisis.

measuring the pressure distribution around a 10 mm sphere (see Figure 1) as a function of Reynolds number (mass flow rate) in both He I and He II. Our goal in this work is to first demonstrate the measurement of the drag coefficient using liquid helium, with the intent to improve on previous measurements. A further purpose is to study the boundary layer development in He I and He II, comparing our findings to classical results. Thus, we are attempting to address the degree to which He II behaves as a classical fluid for the purpose of dynamic similarity studies. Specifically, the pressure distribution and separation point will yield important clues about boundary layer development and the dynamics of the flow field. A secondary aspect of this work is to develop a concept for a larger and higher Reynolds number liquid helium flow facility.[1]

The drag coefficients, calculated by integrating the pressure over the surface of the sphere, are plotted as a function of Reynolds number in Figure 2. The solid line shows published results for a smooth sphere, while the dashed line shows the effect a surface roughness ε=0.015 mm would have on shifting the drag crisis to lower Reynolds numbers.[2] Data taken thus far suggest a drag crisis for He I/He II in this region, consistent with classical fluid mechanics. Future work will be directed toward expanding the data for He II to lower and higher Reynolds number in hope of establishing a drag crisis and corresponding behavior between He I and He II.

The preliminary work reported herein was supported by the Naval Undersea Warfare Center in Newport, RI.

References:

1 Van Sciver, *et al.*, *Realization of a 10^7 Reynolds Number Helium Flow Facility*, to be published by Springer-Verlag.

2 Munson, B.R., *et al.*, *Fundamentals of Fluid Mechanics*, 2nd Ed., John Wiley and Sons, 1990.

Superconducting Magnetic Suspension System for Liquid Helium Flow Experiments

Smith, M.R., NHMFL
Eyssa, Y.M., NHMFL
Van Sciver, S.W., NHMFL/FAMU-FSU CoE

We performed the magnetic and dynamic analysis for a superconducting Magnetic Suspension and Balance System (MSBS) to support and measure the drag on a sphere in a liquid helium flow field. We considered the case of a sphere supported within an existing liquid helium flow facility at the National High Magnetic Field Laboratory (NHMFL). A Reynolds number of $3x10^5$ may be readily achieved on a sphere of diameter d = 9.525 mm (0.375 in). The corresponding drag is approximately $2.15x10^{-4}$ N. A superconducting sphere, acting as a perfect diamagnet (below the bulk critical field), is inherently stable within the support field. This eliminates the need for an active control system. To minimize the weight, and thus the support field to which the sphere is exposed, we envisioned a quartz or glass sphere coated with a thin niobium film. Niobium was chosen for its high bulk critical field. The weight of such a sphere is approximately 0.01 N, though a heavier sphere of solid niobium may be required if the bulk critical field cannot be achieved with a thin film.

Support is accomplished by means of two independent magnet assemblies operated in persistent mode. The drag and support fields are orthogonal, so that sensitive drag measurements

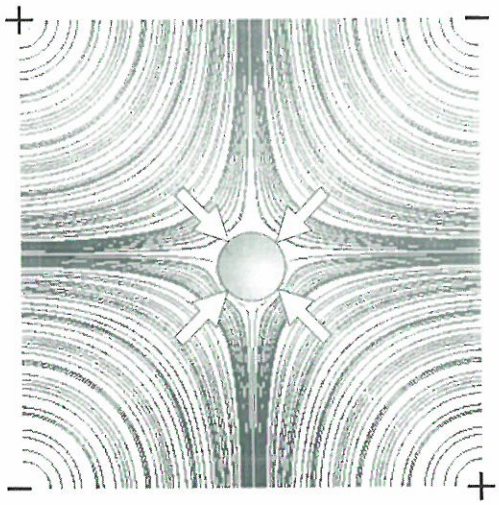

Figure 1. Field lines in a quadrapole support system. Arrows indicate regions of highest field intensity.

may be made with minimal interference from the support coils. These support coils are each of a counter wound racetrack configuration, designed to produce a quadrapole field (Figure 1). The drag coil assembly comprises sets of Helmholtz coils, tuned to provide a particular B and dB/dz. In the passive magnetic drag measurement scheme that we considered, the sphere is allowed to deflect slightly under applied drag. This results in a change in the magnetic flux distribution, detected by the superconducting sensing coils, which in turn induces a current flow in a closed superconducting loop to which the sensing coils are attached. The current flow creates a field in the secondary, or measuring coil, which may be measured by a hall probe (see Figure 2). Such a system will reliably resolve drag forces as small as 4.3 μN.

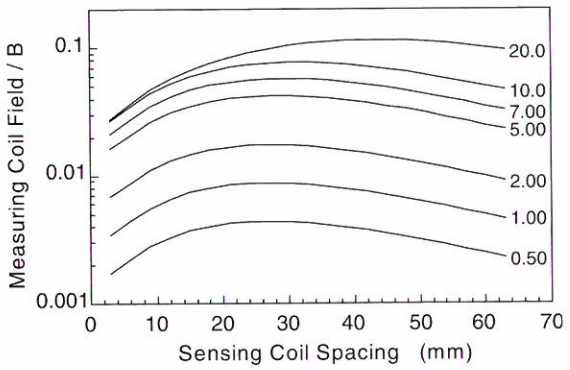

Figure 2. Induced field in the measuring coil vs. sensing coil spacing, for different allowed sphere deflections, δ.

Analysis and Characterization of Saturated Bath He II Heat Exchangers

Van Sciver, S.W., NHMFL/FSU-FAMU CoE
Welton, S.J., NHMFL

Saturated bath heat exchangers similar to those used in the 45 T Hybrid Cryogenic System were analyzed. Analytic and numerical solutions to the appropriate heat equation were obtained, and the governing equations for critical design parameters were developed.

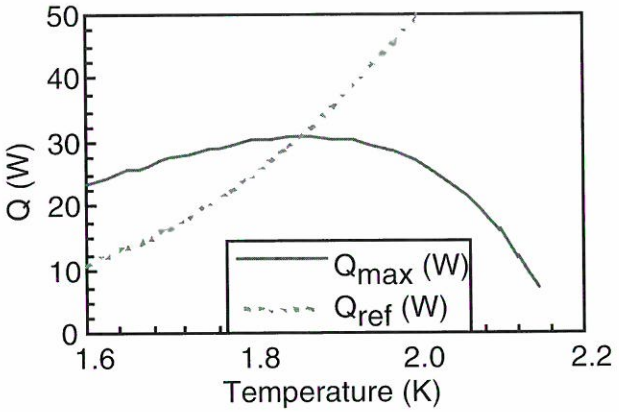

Figure 1. Q_{max} and Q_{ref} vs. temperature.

The critical design parameters for saturated bath He II heat exchangers are cooled surface area and LHe cross section. The cooled surface area should be maximized to reduce the temperature difference (due to Kapitza resistance) across the wall of the heat exchanger. The He cross section determines the maximum cooling capacity (Q_{max}) of the heat exchanger. If Q_{max} is exceeded, boiling will occur and affect the heat exchanger efficiency. The refrigeration capacity (Q_{ref}) of the system is a function of vacuum pumping capacity. Figure 1 shows Q_{max} and Q_{ref} as functions of temperature for the 45 T Hybrid geometry. Normal operation should be where $Q_{ref} < Q_{max}$.

The temperature profile in the saturated He II bath can be determined by solving the non-linear turbulent counterflow equation for He II with a surface heat transfer condition.[1,2] This equation can be solved analytically for constant properties.[3] To include the temperature dependence of the

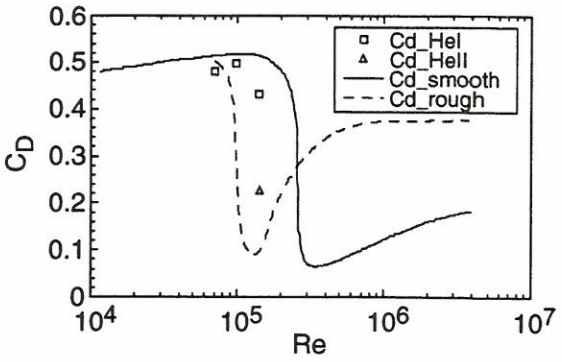

Figure 2. Coefficient of drag in the neighborhood of the drag crisis.

measuring the pressure distribution around a 10 mm sphere (see Figure 1) as a function of Reynolds number (mass flow rate) in both He I and He II. Our goal in this work is to first demonstrate the measurement of the drag coefficient using liquid helium, with the intent to improve on previous measurements. A further purpose is to study the boundary layer development in He I and He II, comparing our findings to classical results. Thus, we are attempting to address the degree to which He II behaves as a classical fluid for the purpose of dynamic similarity studies. Specifically, the pressure distribution and separation point will yield important clues about boundary layer development and the dynamics of the flow field. A secondary aspect of this work is to develop a concept for a larger and higher Reynolds number liquid helium flow facility.[1]

The drag coefficients, calculated by integrating the pressure over the surface of the sphere, are plotted as a function of Reynolds number in Figure 2. The solid line shows published results for a smooth sphere, while the dashed line shows the effect a surface roughness ε=0.015 mm would have on shifting the drag crisis to lower Reynolds numbers.[2] Data taken thus far suggest a drag crisis for He I/He II in this region, consistent with classical fluid mechanics. Future work will be directed toward expanding the data for He II to lower and higher Reynolds number in hope of establishing a drag crisis and corresponding behavior between He I and He II.

The preliminary work reported herein was supported by the Naval Undersea Warfare Center in Newport, RI.

References:

1 Van Sciver, *et al.*, *Realization of a 10^7 Reynolds Number Helium Flow Facility*, to be published by Springer-Verlag.

2 Munson, B.R., *et al.*, *Fundamentals of Fluid Mechanics*, 2nd Ed., John Wiley and Sons, 1990.

Superconducting Magnetic Suspension System for Liquid Helium Flow Experiments

Smith, M.R., NHMFL
Eyssa, Y.M., NHMFL
Van Sciver, S.W., NHMFL/FAMU-FSU CoE

We performed the magnetic and dynamic analysis for a superconducting Magnetic Suspension and Balance System (MSBS) to support and measure the drag on a sphere in a liquid helium flow field. We considered the case of a sphere supported within an existing liquid helium flow facility at the National High Magnetic Field Laboratory (NHMFL). A Reynolds number of $3x10^5$ may be readily achieved on a sphere of diameter d = 9.525 mm (0.375 in). The corresponding drag is approximately $2.15x10^{-4}$ N. A superconducting sphere, acting as a perfect diamagnet (below the bulk critical field), is inherently stable within the support field. This eliminates the need for an active control system. To minimize the weight, and thus the support field to which the sphere is exposed, we envisioned a quartz or glass sphere coated with a thin niobium film. Niobium was chosen for its high bulk critical field. The weight of such a sphere is approximately 0.01 N, though a heavier sphere of solid niobium may be required if the bulk critical field cannot be achieved with a thin film.

Support is accomplished by means of two independent magnet assemblies operated in persistent mode. The drag and support fields are orthogonal, so that sensitive drag measurements

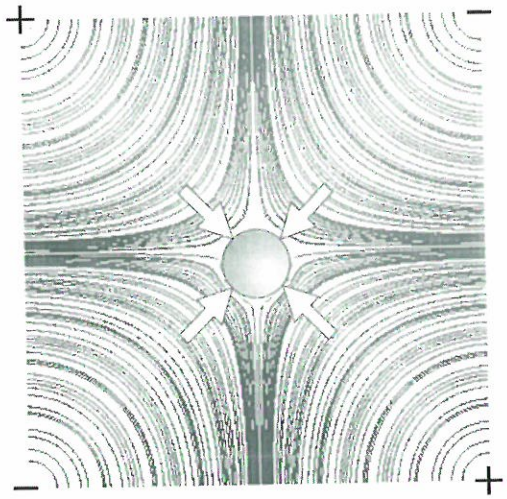

Figure 1. Field lines in a quadrapole support system. Arrows indicate regions of highest field intensity.

may be made with minimal interference from the support coils. These support coils are each of a counter wound racetrack configuration, designed to produce a quadrapole field (Figure 1). The drag coil assembly comprises sets of Helmholtz coils, tuned to provide a particular B and dB/dz. In the passive magnetic drag measurement scheme that we considered, the sphere is allowed to deflect slightly under applied drag. This results in a change in the magnetic flux distribution, detected by the superconducting sensing coils, which in turn induces a current flow in a closed superconducting loop to which the sensing coils are attached. The current flow creates a field in the secondary, or measuring coil, which may be measured by a hall probe (see Figure 2). Such a system will reliably resolve drag forces as small as 4.3 μN.

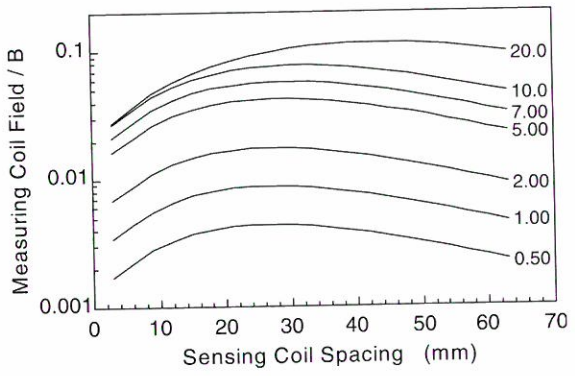

Figure 2. Induced field in the measuring coil vs. sensing coil spacing, for different allowed sphere deflections, δ.

Analysis and Characterization of Saturated Bath He II Heat Exchangers

Van Sciver, S.W., NHMFL/FSU-FAMU CoE
Welton, S.J., NHMFL

Saturated bath heat exchangers similar to those used in the 45 T Hybrid Cryogenic System were analyzed. Analytic and numerical solutions to the appropriate heat equation were obtained, and the governing equations for critical design parameters were developed.

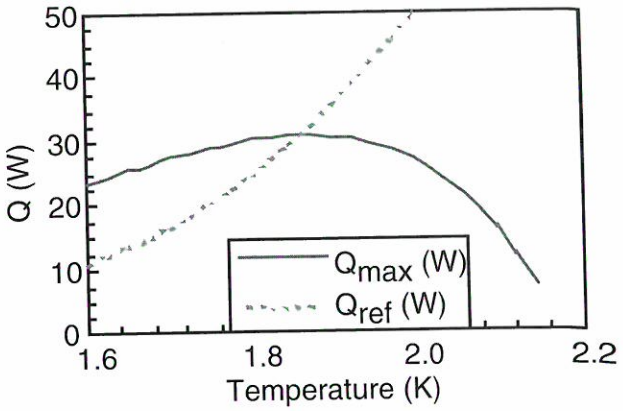

Figure 1. Q_{max} and Q_{ref} vs. temperature.

The critical design parameters for saturated bath He II heat exchangers are cooled surface area and LHe cross section. The cooled surface area should be maximized to reduce the temperature difference (due to Kapitza resistance) across the wall of the heat exchanger. The He cross section determines the maximum cooling capacity (Q_{max}) of the heat exchanger. If Q_{max} is exceeded, boiling will occur and affect the heat exchanger efficiency. The refrigeration capacity (Q_{ref}) of the system is a function of vacuum pumping capacity. Figure 1 shows Q_{max} and Q_{ref} as functions of temperature for the 45 T Hybrid geometry. Normal operation should be where $Q_{ref} < Q_{max}$.

The temperature profile in the saturated He II bath can be determined by solving the non-linear turbulent counterflow equation for He II with a surface heat transfer condition.[1,2] This equation can be solved analytically for constant properties.[3] To include the temperature dependence of the

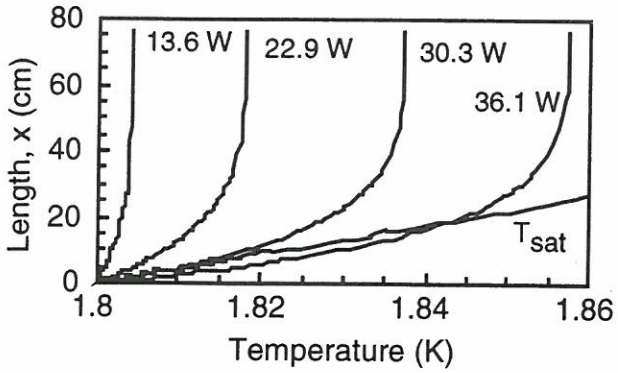

Figure 2. Temperature profile in the saturated bath heat exchanger for various heat loads.

variables; and for complex geometries; however, numerical methods must be used.

Figure 2 shows some numerical results for various refrigeration loads for the 45 T Hybrid heat exchangers. At the highest heat load, the boiling condition has occurred as the fluid temperature has exceeded the local saturation temperature in the heat exchanger.

A paper on this work was presented at the 16th International Cryogenic Engineering Conference in Japan.

References:

1 Shajii, A., *et al.*, Adv. Cryo. Engn., **35**, 1165-1172 (1990).

2 Huang, Y., *et al.*, Cryogenics, **36**, 535-545 (1996).

3 Van Sciver, S.W., ASME Journal of Heat Transfer.

MAGNET SCIENCE & TECHNOLOGY REPORTS

High Strength Conductors

Program Overview

F. Heringhaus

There are many applications that require materials that combine high mechanical strength with good electrical and thermal conductivity. High field magnet technology, in particular, has a need for high strength conductors for both non-destructive pulse magnets and resistive magnets. High electrical conductivity minimizes Joule heating and, together with high strength, allows for higher current densities and thus higher magnetic fields.

Our activities have focused on two major directions: reinforcement of the Cu matrix with precipitates or dispersoids, and *in situ* deformation processing of Cu with a secondary ductile phase. As for the *in situ* composites, much attention has been given to the development of Cu-20%Nb and hypereutectic Ag-Cu (see Figure 1). Preliminary investigations have been carried out in order to narrow the set of parameters leading to optimized properties. The current emphasis is to develop a detailed understanding of the underlying physical and metallurgical fundamentals that are crucial for future achievements: (1) the relationship between the processing (melting, casting, powder-processing, heat treatment, deformation, etc.) and resulting microstructure, and (2) the correlation of microstructure and properties.

More recent initiatives aim also for a combination of both major directions. The goal is to strengthen

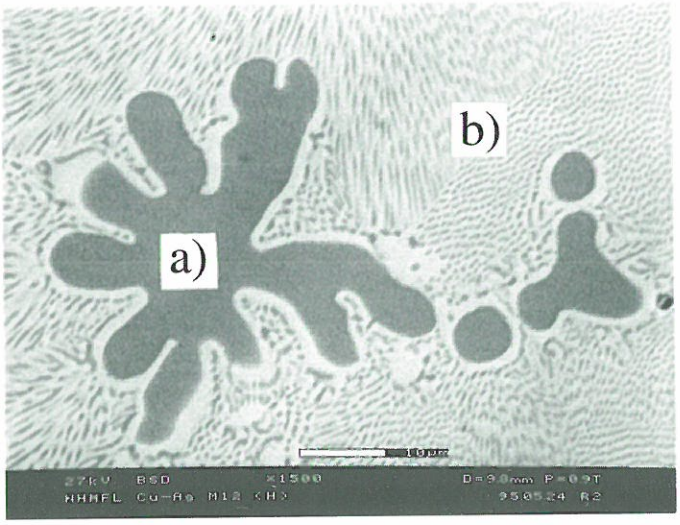

Figure 1. Microstructure of hypereutectic Ag-Cu, as-cast. The two phases are primary α_{Cu} (a) and eutectic Ag-Cu (b). Their volumetric ratio in the microstructure depends not only on the composition but also on solidification condition and subsequent heat treatment. The eutectic can occur as plate-like lamellae or in rod form.

Figure 2. Pulse magnet after failure. It occurred due to mechanical overstressing of the conductor and the reinforcement caused by excessively high Lorentz forces.

the matrix of an *in situ* composite. Besides the hope for further gain in strength and conductivity combinations, the typically lower content of high-melting refractory metal will simplify industrial processibility. The materials currently under investigation are Cu-Ag-Nb, Cu-Ag-Cr, and Cu-Al_2O_3-Nb.

Part of our activities are devoted to processing, including directional solidification of eutectic and near-eutectic compositions in the Ag-Cu system, the equal channel angular extrusion (ECAE), and investigations comparing properties of rotary swaged and wire-drawn composites.

Furthermore, investigations on the anisotropy of both mechanical and physical properties have been carried out. Isotropy of properties plays a very important rule in Bitter magnets. For pulse magnets, detailed knowledge of the anisotropy is required in order to optimize the design. Studies of the anisotropy of high strength conductors are also of strong scientific interest and lead to appropriate models that help to develop a new understanding of mechanical and physical transport properties in multi-phase metallic materials.

High Strength–High Conductivity Composites

Embury, J.D., McMaster Univ., Hamilton, Ontario, Canada
Hill, M., LANL, Center for Materials Science
Zhou, R., LANL, Center for Materials Science
Wood, J.T., Cymat Aluminum Crop., Mississauga, Ontario, Canada

Basic Sciences Issues

A broad range of experimental methods including mechanical testing, x-ray texture analysis, neutron diffraction, and transmission electron microscopy have been used to follow the evolution of the fine scale microstructure in Cu-Nb and Cu-Ag *in situ* composites during wire drawing.

The salient features of this study are as follows. Drawn *in situ* composites contain complex short wavelength internal stresses that influence both the yielding behavior and the dimensional stability of the final drawn wire.

As wire drawing proceeds, the structure becomes so fine in scale that the dominant mode of energy storage is the creation of interphase interfaces in which dislocations are incorporated. The detailed structure of these interfaces has been studied using high resolution electron microscopy.

The cross section of the particles of the embedded phase, e.g. Nb in Cu, remains remarkably uniform during drawing, which is indicative that at high stress levels the plastic deformation becomes very uniform, i.e., the spacing of slip events is at most a few lattice spacings. These observations have been confirmed by careful AFM/STM observations at Los Alamos.

At the finest scale microstructures achieved by drawing, the resistivity is controlled by interface scattering rather than scattering by individual line defects. Comparison of models and experimental data for this process has been performed using vapor deposited layer structures produced by Dr. M. Nastasi's group at Los Alamos.

Design and Fabrication of High Strength High Conductivity Wires

In drawn *in situ* composites both the strength and the conductivity are controlled by the scale of the structure; thus, the influence of various fabrication routes on the final properties of the drawn wire composites can be explained in diagrammatic form.

Selection charts have been developed based on the design constraints of minimizing ohmic heating and resisting the Lorentz forces generated in the coil. Using the selection charts, the merits of various materials are compared. The effects of processing techniques on the material properties and, therefore, the performance of the magnet design are illustrated in the use of selection charts. This leads finally to a discussion of development vectors for composite winding materials. These development vectors can be applied to conventional drawing of composites such as Cu-Ag or Cu-Nb or to combinations of rapid-solidification and drawing or to the development of macroscopic composites based on "jelly roll" layers structure or co-axial wires.

Shear Processing of Bulk Cu-Nb and Cu-Ag

Hartwig, K.T., Texas A&M Univ., Mechanical Engineering

A new method for the fabrication of *in situ* composites is under investigation. It is found that intensive simple shear, performed repeatedly, transforms ductile second phase particles in a ductile matrix into aligned filaments. Processing is performed by multi-step equal channel angular extrusion (ECAE). Results of experiments on Cu-Nb and Cu-Ag alloys demonstrate the ability of this method to fabricate filamentary composites from cast bulk products with no change in the workpiece cross-section.[1,2]

Preliminary investigations included arc cast Cu-18Nb and induction melted Cu-25Ag alloys. Deformation was accomplished at room temperature with tooling that adds an equivalent strain of 1.16 per extrusion. Billets of both materials were extruded 25 times, which lead to an effective

phase deformation strain of 4.5. Specimens of both materials were rolled after extrusion to further refine the structure.

Table 1. Effect of ECAE on mechanical properties of Cu-18Nb.

# of ECAE Passes N	UTS (MPa)	YS (MPa)	AR (%)	EL (%)	Equiv. Red. on Nb λ_R	Equiv. Strain Intens. ε_i
(a) 0	255	102	70	40	0	0.0
(b) 8	468	405	65	35	16	3.3
(c) 16	510	465	50	25	32	4.0
(d) 24	557	496	30	15	48	4.5

Results are shown in the accompanying tables. ECAE processing is shown to produce similar levels of strength in Cu-Nb and Cu-Ag alloys as can be achieved by conventional rolling and wire drawing operations up to true strains of at least 4.5. This result is encouraging for producing further gains in strength by ECAE processing to higher levels of phase distortion strains.

Table 2. Effect of ECAE and intermediate annealing on properties of Cu-25Ag.

Processing	UTS (MPa)	EL (%)	AR (%)	El. Resist. (%IACS)
N=12 (interm. anneals at N=1,2,5)	875	11	50	76
N=12 (interm. anneals at N=1,2,5) + post extrusion annealing + rolling to area red.				
65%	655	22	55	-
86%	870	17	39	-
92%	985	14	30	69
N=25 (interm. anneals at N=1,2,5,10,15,20)	710	20	50	82

The greatest practical benefit of applying ECAE processing to bulk *in-situ* composites may be best realized by combining it with conventional rolling, drawing, or extrusion. Under these circumstances and by processing material first by ECAE, the diameter of an original ingot or billet necessary to develop a high level of strength in a large cross section product may be reduced substantially.

References:

1 Summers, T.S.E., *et al.*, Adv. Cryo. Eng., **42**, 1996, in press.

2 Segal, V.M., *et al.*, J. Mat. Sci. and Eng. A., in press.

Dissolution and Precipitation Studies of the System Ag-Cu

Heringhaus, F., NHMFL and Institut für Metallkunde und Metallphysik (IMM), RWTH Aachen, Germany
Leffers, R., IMM, RWTH Aachen, Germany
Döker, E., IMM, RWTH Aachen, Germany
Raabe, D., IMM, RWTH Aachen, Germany

Optimized precipitation hardening is one of the most effective ways to increase the strength of materials. The advantage over dispersion strengthening is the very fine distribution of the precipitates throughout the matrix. In order to achieve maximum strength increase, it has to be ensured that a supersaturated state of the matrix is attained prior to the precipitation treatment. For optimization of the primary phase strength, dissolution and precipitation studies have been carried out on both sides of the Ag-Cu system on alloys containing the maximally soluble amount.[1]

It is difficult to reach the maximum solubility of both Ag in Cu and Cu in Ag. In addition to that, the values of the respective solubility limits have been found to vary to a non-negligible extend from author to author. The dissolution of the as-cast state, commonly found to partially show eutectic components (Figure 1), can be tracked by various experimental methods, including optical

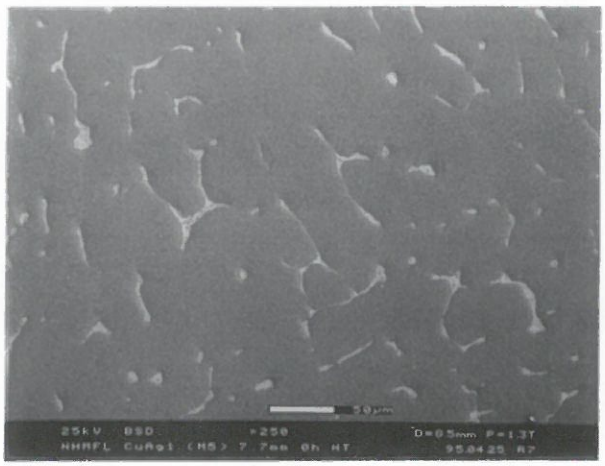

Figure 1. SEM micrograph, as-cast Cu-maxAg, comprising of primary Cu (dark) and eutectic (light) due to non-equilibrium solidification.

microscopy and X-ray diffraction. Figure 2 depicts this by means of quantitative image analysis of metallographic cross-sections and the change of the lattice parameter of the matrix determined from the shift of the Bragg reflexes.

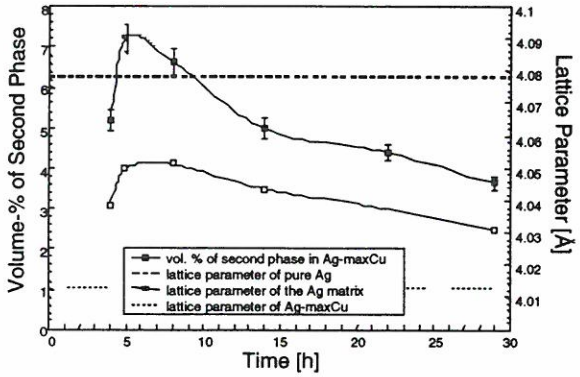

Figure 2. Dissolution of the second phase (Cu) in Ag-maxCu.

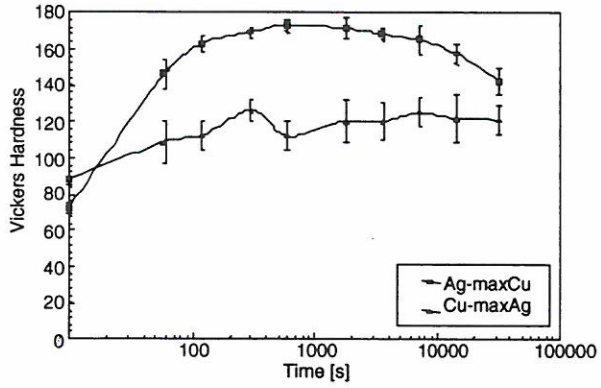

Figure 3. Precipitation hardening of Cu-maxAg and Ag-maxCu.

While deformation prior to the first precipitation heat treatment leads to an increase in nucleation density and thus increases its effectiveness, heat treatments later in the deformation process are predominantly used to regain ductility through spheriodization, recrystallization, and discontinuous precipitation.[2] In order to optimize the processing, further investigations on the initial deformation and its influence on the precipitation process have to be carried out. When comparing the Cu-rich and the Ag-rich side of the system with respect to their precipitation potential, a strong difference becomes apparent (Figure 3), likely to be due to the much higher atomic solubility limit in Ag-maxCu.

References:

1 Massalski, T.B., Binary Alloy Phase Diagrams (2).

2 Hong, S.I., *et al.*, Acta Met., **43** (9), 3313 (1995).

Electrical Resistivity and Magnetoresistance of Eutectic Ag-Cu

Heringhaus, F., NHMFL and Institut für Metallkunde und Metallphysik (IMM), RWTH Aachen, Germany
Leffers, R., IMM, RWTH Aachen, Germany
Gottstein, G., IMM, RWTH Aachen, Germany
Schneider-Muntau, H.-J., NHMFL

As part of the optimization program for Ag-Cu composites, the electrical resistivity and the magnetoresistance of eutectic Ag-Cu were investigated. The results are discussed with respect to the deformation-induced changes in the microstructure, for example, refinement of the average lamellae thickness and strong increase of internal interface density.

The anomalous change of the electrical resistivity with decreasing lamellae thickness due to the size effect can be simulated by a modification of Sondheimer's approach for thin wires and films[1] (Figure 1). A somewhat surprising result was found with respect to the temperature dependence of the electrical resistivity. While the low temperature

behavior was found to exhibit no noticeable anomaly, the linear regime of ρ vs. T reveals a deformation dependence of the temperature coefficient α. (Figure 2). This can be understood in terms of a difference in the phonon dispersion in interface layers and the increase in the density of internal interfaces with ongoing deformation. The field dependence of the electrical resistivity, the magnetoresistance, was investigated in transverse and longitudinal field up to 27 tesla by use of a steady-state field Bitter magnet.

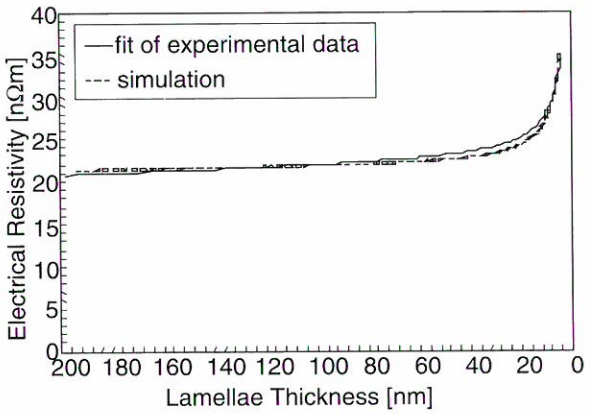

Figure 1. Electrical resistivity of eutectic Ag-Cu.

At 273 K and 27 T the magnetoresistance was found to be in the order of 1%. With decreasing temperature and increase in electron mean free path, a strong deformation dependence occurs, leading to a reduction of the magnetoresistance at 4.2 K and 27 T from over 40% in the as-cast state to less than 3% for a total deformation of η=8 (Figure 3).

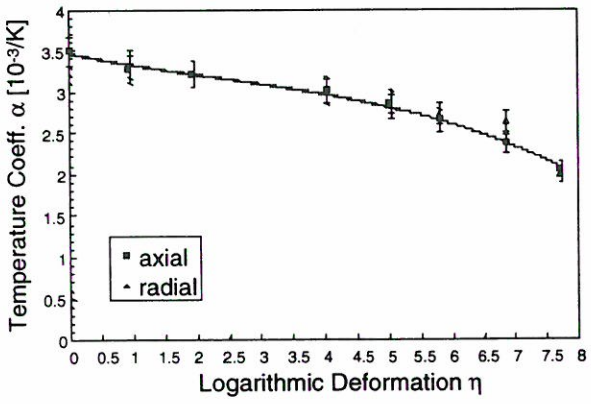

Figure 2. Temperature coefficient parallel (axial) and perpendicular (radial) to wire axis.

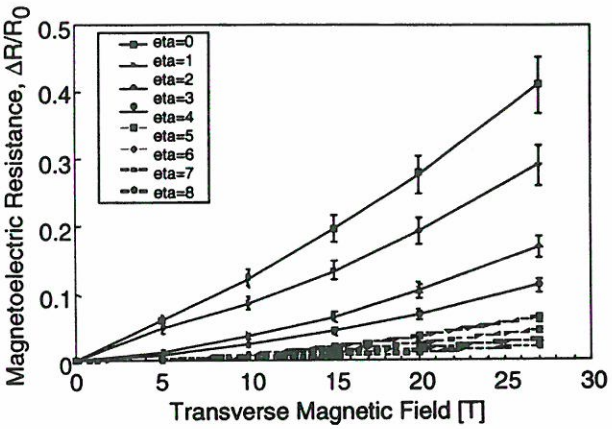

Figure 3. Magnetoresistance of eutectic Ag-Cu in a transverse field.

As has been reported by Fickett,[2] Copper alloys with low residual resistivity ratio (RRR) show deviations from Kohler's rule.[3] This also holds for eutectic Ag-Cu composites with an increasing deviation with increase in total wire deformation.

References:

1 Sondheimer, E.H., Adv. in Phys., **1**(1), 1 (1952).

2 Fickett, F.R., IEEE Magnetics, **3**, 228 (1983).

3 Kohler, M., Ann. der Physik, **32**(5), 211 (1938).

Optimum Microstructure for Strength and Conductivity Combinations

Heringhaus, F., NHMFL and Institut für Metallkunde und Metallphysik (IMM), RWTH Aachen, Germany

Gottstein, G., IMM, RWTH Aachen, Germany

Schneider-Muntau, H.-J., NHMFL

As is apparent from their nature, there is a trade-off between mechanical strength and electrical conductivity. Detailed knowledge of the microstructural implications on the considered properties enables the determination of the optimum microstructure for a well defined property profile. This is demonstrated on heavily deformed, lamellar eutectic Ag-Cu, the microstructure of which has been determined by quantitative transmission electron microscopy.

The example given in Figure 1 observes the microstructure-property relation regarding the rule of mixture (ROM). Both electrical resistivity and UTS increase with decreasing lamellae thickness. By normalizing both to their respective ROM value for the eutectic composition, their ratio reveals a maximum. Up to the maximum (thicker lamellae) the further gain in strength is higher than the increase in resistivity, after the maximum (thinner lamellae) the increase in resistivity is stronger than the gain in strength.

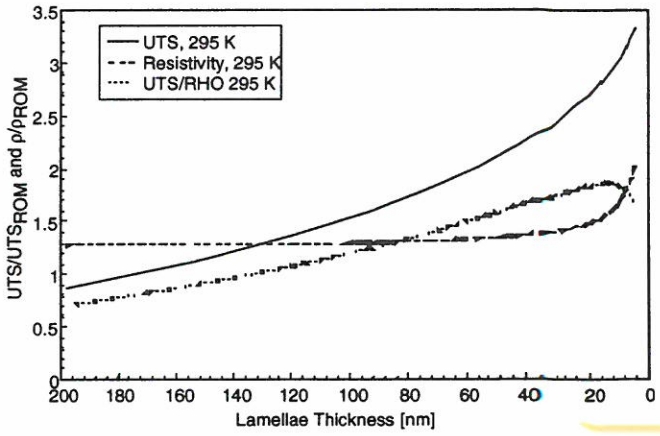

Figure 1. Normalized UTS and resistivity and their ratio vs. lamellae thickness.

When observing the properties at different temperatures, a shift of the maximum to higher lamellae thicknesses with decreasing temperature becomes apparent. This reflects the much stronger temperature-microstructure interrelation of the electrical conductivity compared to the mechanical strength of Ag-Cu.

The scheme described can be enhanced to cover multiple properties including respective "importance factors" and interrelations between two or more of the regarded properties. At long last explicit knowledge on the influences of each processing step on the microstructure development is required to achieve the determined optimum microstructure.

Rotary-Swaging Versus Wire Drawing

Heringhaus, F., NHMFL and Institut für Metallkunde und Metallphysik (IMM), RWTH Aachen, Germany
Summers, T.S.E., NHMFL

The aim of this study is to uncover differences in microstructure and properties of swaged and drawn composite wires. Three Cu-7.9wt.%Ag composites of same origin and equal initial microstructure were (a) wire drawn to ε=93%, (b) rotary-swaged to ε=93%, and (c) rotary-swaged (approximately 74%) followed by wire drawing (another 74%) to ε=93%. The yield strength of the drawn wire was found to be 12.5% higher than the yield strength of the swaged wire, however, the observed difference decreases to 6.6% with respect to the ultimate tensile strength. Inversely the electrical conductivity was 86% IACS for the swaged and only 84% IACS for the drawn wire. Further differences were found in the work-hardening rate, uniform elongation, hardness profile, microstructural appearance of the phases, and texture development. The processing route (c) tends to result in properties very close to the ones found for the solely drawn wire.

Ternary High-Strength Cu-Based *In Situ* Metal Matrix Composites

Raabe, D., Institut für Metallkunde und Metallphysik (IMM), RWTH Aachen, Germany
Reinartz, C., IMM, RWTH Aachen, Germany
Mattissen, D., IMM, RWTH Aachen, Germany

Cu and most high melting body centered cubic (bcc) transition metals have negligible mutual solubility by practical means. Fiber or ribbon reinforced *in situ* metal matrix composites (MMCs) can thus be processed by large degrees of deformation, for example, by cold rolling or wire drawing of cast ingots. These Cu-bcc alloys are of considerable interest since after heavy deformation very high tensile strength combined with good electrical conductivity can be achieved.

Furthermore, fundamental aspects such as the origin of the extreme strength attract much attention.

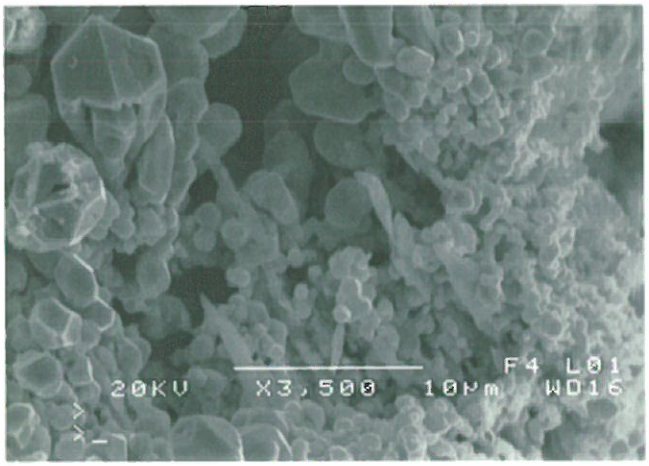

Figure 1. SEM micrograph of Nb extracted from an as-cast Cu-Nb-Ag composite.

In the last year, substantial efforts were made to investigate and optimize alloys based on the binary systems of Cu with Nb (bcc) or Cr (bcc). Additional investigations addressed *in situ* MMCs that are based on the eutectic system of Cu and Ag (fcc). While in the first case the fibers are formed by the elongated body centered cubic phase (Nb, Cr), in the second case Ag precipitations were used to increase the matrix strength and/or to form additional fibers after wire drawing or rolling.

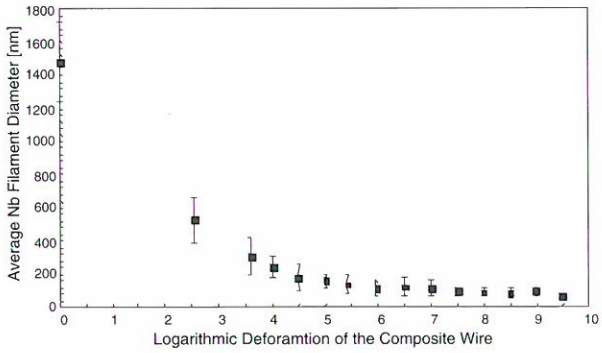

Figure 2. Average filament diameter of the Nb phase as a function of the logarithmic deformation.

The present project focuses on the experimental investigation and theoretical prediction of the properties of the ternary systems Cu - 4wt.%Nb - 8.2wt.Ag and Cu - 10wt.%Cr - (1-7)wt.%Ag. Figure 1 shows the typical as-cast structure of the Nb phase, as revealed after selectively etching the Cu matrix. With ongoing deformation, the Nb deforms into thin filaments. This development has been investigated by quantitative microscopy (Figure 2) and will be used for a correlation of properties and microstructure development.

Tensile Strength and Electrical Conductivity of Directionally-Solidified Near-Eutectic Cu-Ag Alloys After Deformation Processing

Sohn, K.Y., UF, Materials Science and Engineering
Kaufman, M., UF, Materials Science and Engineering

The microstructure-property (mechanical and electrical) relationships in directionally-solidified (DS) near-eutectic Cu-Ag alloys after mechanical processing are reported. As will be shown, the properties vary with (a) variations in the solidification conditions and (b) deformation level.

The interlamellar spacing (λ) of the as-cast near-eutectic (Cu-58at%Ag, DS 58) alloys (Figure 1) produced by coupled growth[1] at different solidification rates are shown in Table 1. Clearly, higher withdrawal speeds result in smaller λ of the eutectic as expected.

The effects of λ on the strength of the DS 58 alloys after deformation to various draw ratios, η (where $\eta=\ln(A_o/A)$), are shown in Figure 2a. The

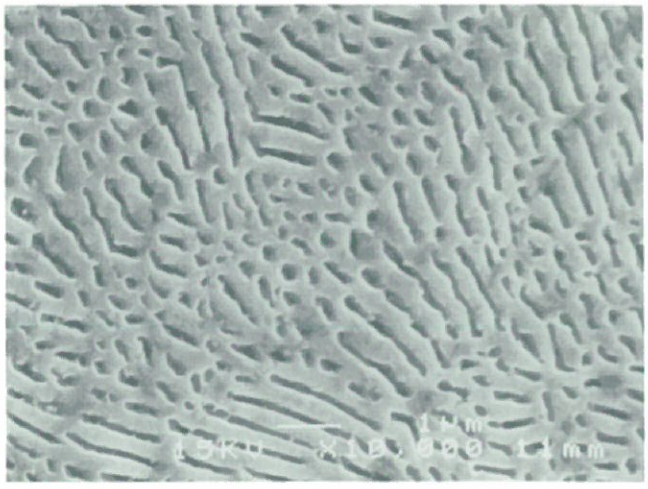

Figure 1. SEM micrograph of as-solidified DS 58 grown at 55 µm/s (transverse section).

conventionally solidified (CS) Cu-58at% Ag (CS 58) ingot has about three times smaller λ compared to the DS ingot of the same composition solidified at a withdrawal speed of 55 μm/sec and a strength of about 200 MPa higher than that of the DS alloy at the same η value. The strain hardening rate appears to be a little higher for the DS alloy with large λ.

Table 1. Interlamellar spacings (λ) of as-cast alloys for different withdrawal speed.

Specimen ID as-cast	Withdrawal speed (μm/sec)	Average interlamellar spacing (nm)
DS 58	12	780~1020
	55	400~450
CS 58	-	140~200

The CS 58 alloy with the much finer λ, shows much lower conductivity than the DS 58 alloy at the same draw ratio. Although there are only two data points (draw ratios), the electrical conductivity of the alloy appears to be more sensitive to draw ratio in the CS 58 alloy. This is because of its higher initial interfacial area and smaller λ. Therefore, the smaller the initial interlamellar spacing, the higher the sensitivity of conductivity on the draw ratio.

The effect of withdrawal speed (interlamellar spacing) on the strength-conductivity (SC) values is given in Figure 2b. As is evident, the slope of the SC curves for the DS 58 alloy grown at v=12 μm/s is about 25% higher than that for the DS 58 alloy grown at v=55 μm/s. Therefore, it is clear that the larger λ tends to have higher SC slopes. These results indicate that, at higher deformation levels, the conductivity decrease due to the smaller λ (higher interfacial area) is higher than the strength increase due to the same. This is presumably related to a minor increase in strain hardening rate for the alloy with large λ combined with the fact that the λ gets closer to the mean free path of free electrons[2] in both phases at the higher deformation levels. At lower deformation levels, however, the relative conductivity decrease due to interphase interfaces is not as effective as the relative strength increase by the interfaces because the interlamellar spacing

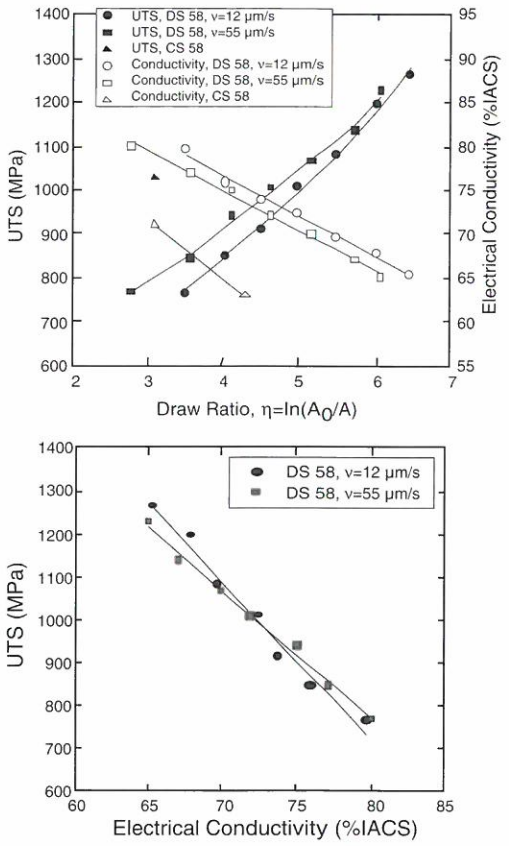

Figure 2. Tensile strength and electrical conductivity of DS Cu-58Ag alloys.

is much larger than the mean free path of electrons in both phases. Also, the influence of the interfacial area on reducing the maximum dislocation density is not as effective. Therefore, the alloy with smaller interlamellar spacings can have higher relative strengths in this case. In summary, the alloys with larger initial interlamellar spacings provide better combinations of strength and conductivity at the higher deformation levels. On the contrary, alloys with smaller interlamellar spacings provide a better combination of properties at the lower deformation levels. Overall however, a eutectic alloy with large interlamellar spacing is preferred because of the lower sensitivity of conductivity to lamellar spacing.

References:

1 Kurz, W., *et al.*, International Metals Review, **24**, 177-204 (1979).

2 Frommeyer, G., *et al.*, Physica Status Solidi (a), **27**, 99-105 (1975).

Characterization and Strength Optimization of a Copper-Al_2O_3-Nb Composite

Walsh, R.P., NHMFL
Pernambuco-Wise, P., NHMFL
Troxel, J.D., SCM Metal Products, Research Triangle, NC
Schneider-Muntau, H.-J., NHMFL

A commercially available composite, Cu-Al_2O_3-Nb (GlidCop Al-15+Nb1000), is being studied to explore its strength limitations. The advanced composite combines two traditional strengthening mechanisms (dispersion and filament strengthening) to produce a high strength/high conductivity copper based material. Preliminary tensile test results (Figure 1) from an 85% cold drawn condition indicate that strengths higher than predicted by simple modeling can be achieved.

A quantity of material (supplied by SCM Corp.) will be thermo-mechanically processed in a sequential procedure. The materials properties will be characterized at key steps. Typically the as-extruded product can be cold-reduced to some limit (around 90% area reduction) whereupon a heat treatment must be performed to allow further reduction. The role of cold reduction and intermediate heat treatments will be thoroughly investigated to produce an optimum strength material.

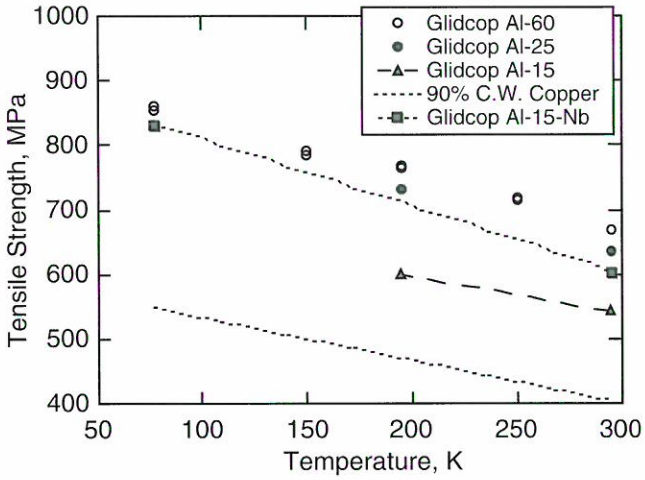

Figure 1. Tensile strength vs. temperature for dispersion strengthened copper alloys, 90% C.W., commercially pure copper, and Cu-Al O_3-Nb.

MAGNET SCIENCE & TECHNOLOGY REPORTS
Materials Development & Characterization

Program Overview

R.P. Walsh

The Materials Development and Characterization Group (MD&C) investigates the physical and mechanical properties of advanced materials used in magnet design and cryogenic applications. The group supports internal magnet design teams by generating engineering design data and conducts basic applied research for the improvement of magnet materials. The unique facilities of the MD&C enable detailed characterization of advanced structural materials, electrical conductors, and commercial materials. In addition, the MD&C provides testing and analysis services to industrial and academic researchers with interest in cryogenic or magnet materials.

There are several cryogenic materials research projects ongoing in the MD&C group. These research projects include mechanical and electrical testing of advanced superconducting wires; an international cooperative program (VAMAS) to standardize low temperature test methods and analyses; testing of structural fiber-reinforced composite insulations; and investigations of current transport characteristics of cable-in-conduit conductors.

Figure 1. Photographs of the Large Scale Critical Current Test Facility.

Investigations of resistive magnet materials include measurements of the mechanical and electrical properties of high-strength, high-conductivity copper alloys, such as CuNb, CuAg, CuBe for steady state magnets; and mechanical tests of high strength fiber-reinforced composite insulation systems and tests of composite conductors, such as Cu-stainless steel wires for pulsed magnet applications.

In addition, a great number of routine characterization of magnet materials has been performed for the different projects within Magnet Science and Technology and for industrial researchers.

A description of the facilities is given in Tables 1 through 4.

Table 1. Magnets and power supplies of the NHMFL's Materials Development and Characterization Group.

System	Specifications	Comments
Small bore split solenoid	50 mm bore, 13 T, 20 x 25 mm radial.	Field increase by addition of Fe or Ho pole pieces.
Wide bore split solenoid	150 mm bore, 12 T, 30 x 70 mm fixed gap	14 T with Ho inserts.
Power Supplies	0-200 A, 10-4 current ripple 0-1 kA, 10-5 current ripple 0-80 kA, 10-5 current ripple	10 kA leads available, 80 kA for conductor testing with installation of larger VCL's.

Table 2. Mechanical/electrical test facilities.

System	Specifications	Comments
Structural Materials Test System	500 N to 100 kN Force. Digital test control. Temperatures - 1.8 K through 400 K.	ASTM and prototype test procedures. Tension, compression, fatigue fracture toughness, shear, torsion, etc. Variable temperature cryostat.
Small Scale Critical Current Measurement System	500 N to 500 kN Force. Digital test control. Temperatures- 4 K , 77 K, and 295 K.	Superconducting wire strain tests in 13 T field. Structural tests of components or large scale materials.
Large Scale Critical Current Measurement System	500 N to 250 kN Force. Digital test control. Temperatures- 4 K, 77 K, and 295 K.	Large scale superconductors and components in magnetic fields. Large scale materials or components. Field to 14 T.
High Force Materials Test System	2.5 MN max. Force. Digital test control. Temperatures- 77 K and 295 K.	Testing of structural or magnet components, 77 K, 295 K. (DOT SITE)

Table 3. Superconductor test capabilities.

System	Specifications	Comments
J_c vs. B	Extensive capabilities within MD&C and users facility.	Fields to 20 T, temperatures from 0.5-300 K.
J_c vs. B, strain (wire)	Field to 13 T, 45 mm between voltage taps, current to 1 kA, force to 4 kN.	Fields to 20 T, temperatures from 0.5 K-300 K.
J_c vs. B, strain (conductors)	Fields to 14 T, 140 mm between voltage taps, current to 10 kA, force to 250 kN.	Uniaxial tension and fatigue in field, suitable for CICC or cabled conductors simultaneous mechanical properties.

Table 4. Microanalysis facility.

System	Specifications	Comments
Environmental Scanning Electron Microscope	40 Å resolution by secondary imaging Pressures to 50 Torr. Variable gaseous environments Magnification 50 - 600,000x Up to 30 KeV.	Hydrated, oily, and non-conductive samples examined without modification or preparation. Elemental analysis Na and higher PGT EDS System (mapping and quantitative). Back-scatter electron mode. Back-scatter Kikuichi strain orientation images.

Magnetoresistivity of Silver and Silver Alloys As Sheath Material for HTS Conductors

Dur, O.*, NHMFL
Hascicek, Y.S., NHMFL

Silver and silver alloys are the most commonly used sheath material in powder-in-tube (PIT) processed high temperature superconductors (HTS), particularly $Bi_2Sr_2Ca_1Cu_2O_x$ (Bi-2212) and $Bi_2Sr_2Ca_2Cu_3O_x$ (Bi-2223).[1] The application of such composite conductors includes high field superconducting magnets. The stability of the HTS conductors is strongly related to the electrical resistivity of the sheath material during the operation. Therefore, it is important that the resistivity and magnetoresistivity of the sheath materials is measured accurately in wide temperature and magnetic field ranges in order to predict the stability and quench behavior. Here we report the resistivity of silver, silver magnesium, and silver aluminum tapes up to 17.5 T, 30 T in the temperature range between 1.5 K and 300 K.

The silver tape sample used in this experiment was a commercial tape with purity of 99.99%. Ag-1.2 at % Mg (Ag-Mg) tape samples were made via mechanical reduction from Ag-Mg tube samples, which are used for HTS conductor development at the NHMFL.[2] Ag-0.1 at % Al (Ag-Al) tape was supplied by IGC. All of these samples received the same heat treatment used for the partial melt texturing of Bi-2212/Ag tape conductors in a ceramic crucible within a tube furnace containing an oxygen atmosphere.

Figure 1 shows the resistivity versus temperature curves of Ag, AgMg[3] and Ag-Al at zero field, together with those of Iwasa, *et al.*,[4] and Nakamae, *et al.*[5] As can be seen from the curves in Figure 1, a small amount of Mg and Al doping increases the residual resistivity considerably. This could be due to the remnant Mg and Al in the silver lattice after the heat treatment.

Figure 2 shows the Kohler plots for Ag, Ag-Mg, and AgAl. Kohler plots of Ag, Ag-Al, and Ag-Mg show the same behavior, except AgAl and AgMg fall at lower range than Ag.

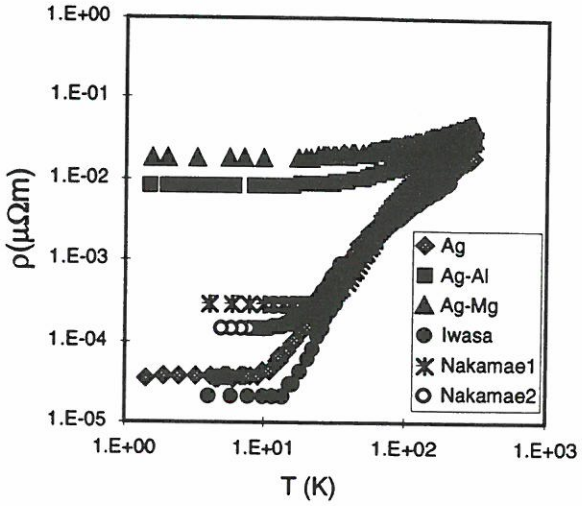

Figure 1. Resistivity versus temperature in zero field for Ag, Ag-Mg, and Ag-Al tapes together with those already published.

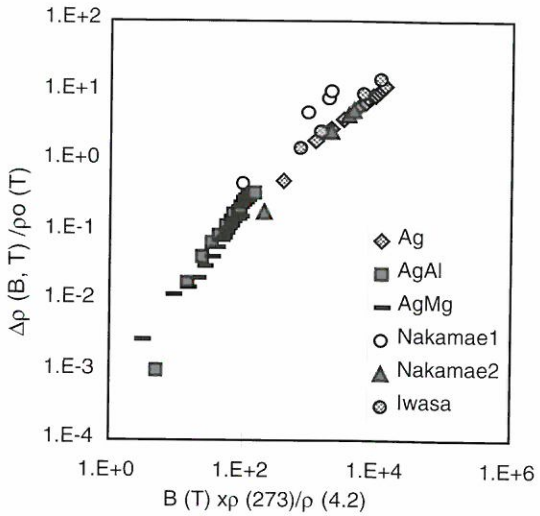

Figure 2. Kohler plot for Ag and Ag-Mg and Ag-Al tapes together with those already published.

References:

1 Heine, K., *et al.*, Applied Physics Letters, **55**, 2441-2443 (1989).

2 Kessler, J., *et al.*, Superconducting Science and Technology (to be submitted).

3 Dur, O., *et al.*, IEEE Transactions on Applied Superconductivity (submitted 1996).

4 Iwasa, Y., *et al.*, Cryogenics, **33**, No. 8, 837 (1993).

5 Nakamae, S., *et al.*, Cryogenics, **36**, No 5, 395 (1996).

* On leave from Dept. of Physics, Marmara University, Istanbul, Turkey

Lorentz Force Simulation Tests on a Full-Scale Prototype Model Coil of the 45 T Hybrid Magnet

Walsh, R.P., NHMFL
Miller, J.R., NHMFL
Miller, G.E., NHMFL

The 45 T Hybrid Magnet employs cable-in-conduit conductor design with glass fiber-reinforced epoxy insulation for its superconducting coils. The steel conduit acts as the main structural component to resist large Lorentz forces, but the insulation is constrained to endure similar strain. The integrity of the insulation must be assured over the lifetime of the magnet during which it will experience approximately 1000 charge/discharge cycles.

A scale-model coil (about 1 m diameter) provides a prototype sample for the mechanical and electrical tests of the insulation. By side-loading the coil in proving-ring fashion (Figure 1), we impose strain equivalent to the operating strain. The coil is fatigue tested for 100 cycles at 295 K and 1000 cycles at 77 K. The electrical integrity of the coil is tested before and after mechanical testing using a transformer technique.

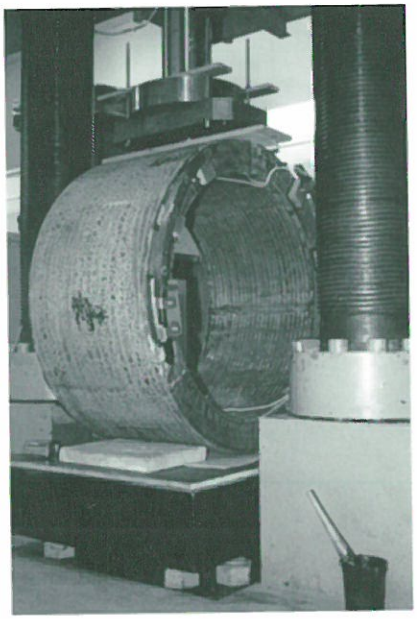

Figure 1. Photograph of model coil test sample in place for room temperature fatigue cycling. Test conducted in Boulder, Colorado, on 5 MN test machine (courtesy of NIST).

The effective modulus of the coil changes significantly during the initial load cycle, Figure 2. This is due to the debonding of the composite insulation from the steel conduit and is desirable since it reduces the overall stress in the insulation. The structural performance of the insulation is acceptable since the effective modulus reaches a minimum after a few cycles without subsequent degradation. The electrical performance was verified and also found to surpass specifications.

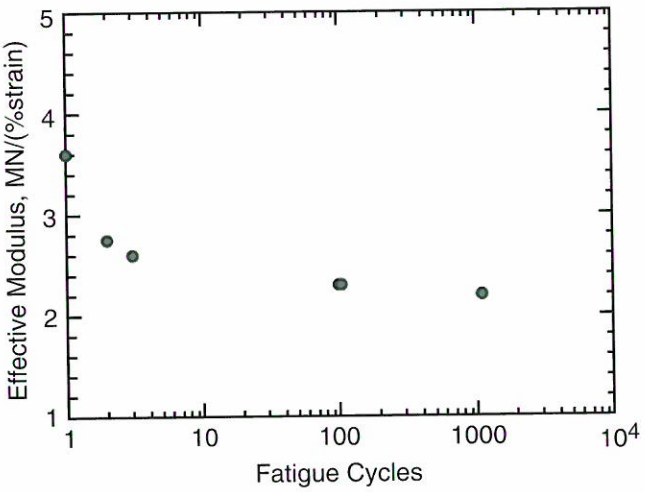

Figure 2. Graph of effective coil modulus vs. number of cycles, T = 77 K.

The Effect of Thermal and Operating Strain on Transport Current of Large Cabled Superconductors

Walsh, R.P., NHMFL
Summers, L.T., NHMFL
Miller, J.R., NHMFL

The NHMFL large-scale critical-current test facility[1] has been used to test model conductors representative of the Nb_3Sn cable-in-conduit conductors (CICCs) used for the two innermost superconducting coils (coils A and B) in the 45 T Hybrid. For conductors fitting its radial-access port, this facility is capable of the simultaneous application of transverse magnetic field to 14 T and longitudinal mechanical load to 250 kN.

The critical current of Nb_3Sn conductors is sensitive to strain as well as field and temperature. Their operating strain state in a magnet depends

not only on the mechanical loading of the windings but also on the thermal history from reaction temperature (625 C in the case of the Hybrid) to the operating temperature (1.8 K). Hybrid model conductors were tested in this facility for two reasons: first, to provide the developmental basis for selecting the appropriate heat-treatment steps for the coils, and then, to confirm that the heat treatment was successful (by testing witness samples processed along with the coil).

The test conductors were good models for those in the Hybrid magnet in all important aspects: i.e., conductor, helium, and steel fractions. Commercially fabricated cables were selected from the production lots for coils A and B, but they were jacketed at NHMFL with round, stainless-steel tubing rather than the production rectangular jacket. (This was done for several reasons specific to the test and in-house fabrication capabilities.) An important aspect of the test-sample design is the requirement to anchor the cable ends securely within the conduit, assuring constant relative strain between it and wires in the cable during all phases of processing and test.

Initially, the critical current was measured at 14 T, 4.2 K, and zero applied strain (zero applied force) by ramping current through the specimen until voltage marking the onset of resistance was observed. The voltage taps on the sample had a separation of 100 mm and were centered on the region of highest field applied to the sample. The sensitivity to onset of resistance was about 1 μV. Then, the specimen was strained incrementally and the onset of voltage with increasing current was recorded at each level of applied jacket strain. The test sequence was repeated until the peak in critical current vs. strain was surpassed and sufficient data was taken to characterize the conductor fully.

Tests on individual, identically processed wires allow a separate determination of the critical parameters of the superconductor, so that fits to the tests of the CICC model conductors could be used to determine their initial state of strain and the relation between jacket strain and wire strain (Figure 1). The knowledge gained from the combination of single-wire and model-conductor tests allows a high-confidence projection of the critical current for such conductors at the expected operating conditions in the Hybrid magnet.

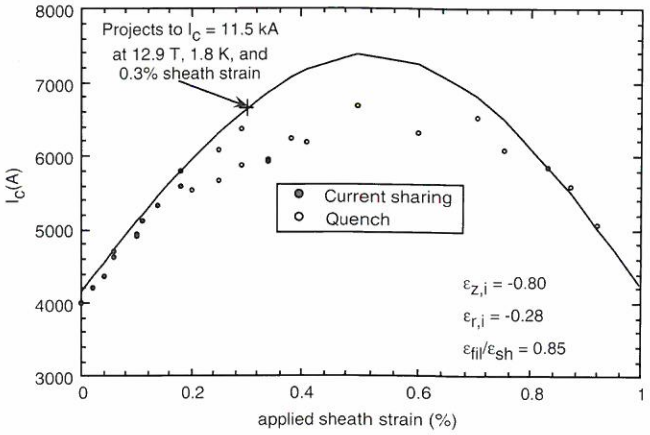

Figure 1. Critical current vs. applied sheath (or jacket) strain in a model of the CICC for coil B of the 45 T Hybrid.

Reference:

1 Summers, L.T., *et al.*, IEEE Trans. on Appl. Superconductivity, **5**, No. 2, 1896 (1995).

The 4 K Tensile and Fracture Toughness Properties of a Modified 316LN Conduit Alloy

Walsh, R.P., NHMFL
Summers, L.T., NHMFL
Miller, J.R., NHMFL

Large superconducting magnets often employ cable-in-conduit conductors (CICC). When the CICC concept is employed for Nb_3Sn superconductors, the conduit is subjected to the Nb_3Sn reaction heat treatment. In this type of heat treatment, austenitic alloys are susceptible to a loss of fracture toughness.[1-5] The wire selected for the 45 T Hybrid Magnet is given an abbreviated heat treatment; 21 h/210 °C + 5 h/340 °C + 70 h/625 °C. Previous investigations austenitic steel sensitization have concentrated on the higher temperatures and longer times.

Table 1. Composition of the stainless steels in weight percent, the balance is iron.

Steel	C	N	Mn	Si	P	S	Cr	Ni	Mo	Nb+Ta
316L	0.012	0.05	1.2	0.43	0.021	0.004	16.44	10.29	2.1	—
316LN	0.010	0.21	1.53	0.26	0.011	0.005	16.91	13.75	2.32	0.11

A commercial heat of AISI 316L is investigated to address preproduction process variables of the 45 T Hybrid conduit. The second alloy is the modified AISI 316 LN conduit alloy produced to NHMFL specifications for the Hybrid Magnet. The alloy compositions are shown in Table 1. Test results are shown in Table 2.

Table 2. The mechanical properties test results.

Alloy	Material Condition	Yield Strength (MPa)	Tensile Strength (MPa)	Elongation (%)	Fracture Toughness ($MPa*m^{0.5}$)
316L	Annealed	485	860	37	260
	Ann + aged H.T. 1	460	845	35	232
	20% CW	1006	1734	35	117
	20% CW + H.T. 1	843	1722	35	111
316LN Mod.	20% CW	1284	1648	28	159
	20% CW + H.T. 1	1326	1677	31	133
	20% CW + H.T. 2	1202	1586	26	90

H.T. 1 = 340 °C for 48 h + 625 °C for 70 h in Argon
H.T. 2 = 700 °C for 100 h in Argon

The high 4 K yield strength of the 316LN alloy is the result of its high nitrogen content. For the 316L alloy, the effect of cold work is nicely shown with a twofold change in both tensile and fracture properties. The results are plotted in Figure 1 along with the NIST trend line for comparison. The 316 L alloy falls slightly below the trend line while the modified 316 LN has excellent properties that are above the trend line. The excellent properties are attributed to the strict specifications of the alloy.

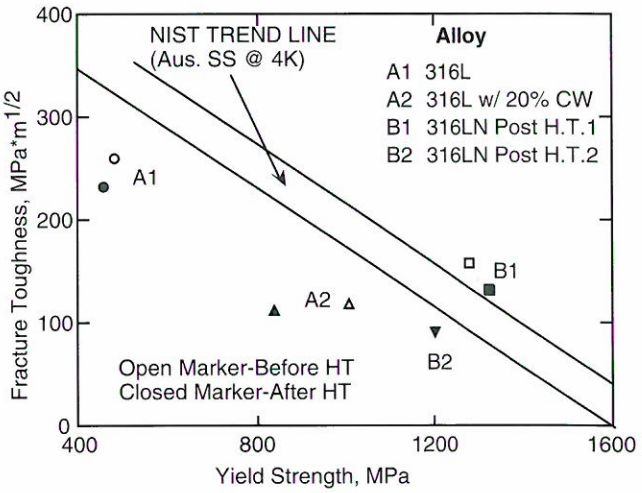

Figure 1. The 4 K yield strength vs. fracture toughness of the alloys studied plotted along with the NIST trend line for austenitic steels.

Reaction heat treatment # 1 for the NHMFL 45 T Hybrid magnet does not have a marked influence on the cryogenic fracture toughness of these 316 alloys. The more severe heat treatment (#2), of 700 °C for 100 hours, significantly degrades the fracture toughness of the 316LN alloy. The mechanism for the toughness reduction has not been fully studied but is at least partially attributed to increased intergranular brittle fracture, caused by precipitate formation at the grain boundaries.

References:

1 Nohara, K., *et al., Aus. Steels at Low Temperatures*, Plenum Press, 117 (1983).

2 Reed, R.P., *et al.*, Adv. Cryo. Eng., **38**, 45 (1992).

3 Shimada, M., *et al.*, Adv. Cryo. Eng., **34**, 131 (1988).

4 Muster, W.J., *et al.*, Cryogenics, **30**, 799 (1990).

5 Kübler, J., *et al.*, Adv. Cryo. Eng., **38**, 191 (1992).

PART TWO

Facilities, Programs, Outreach, & Publications

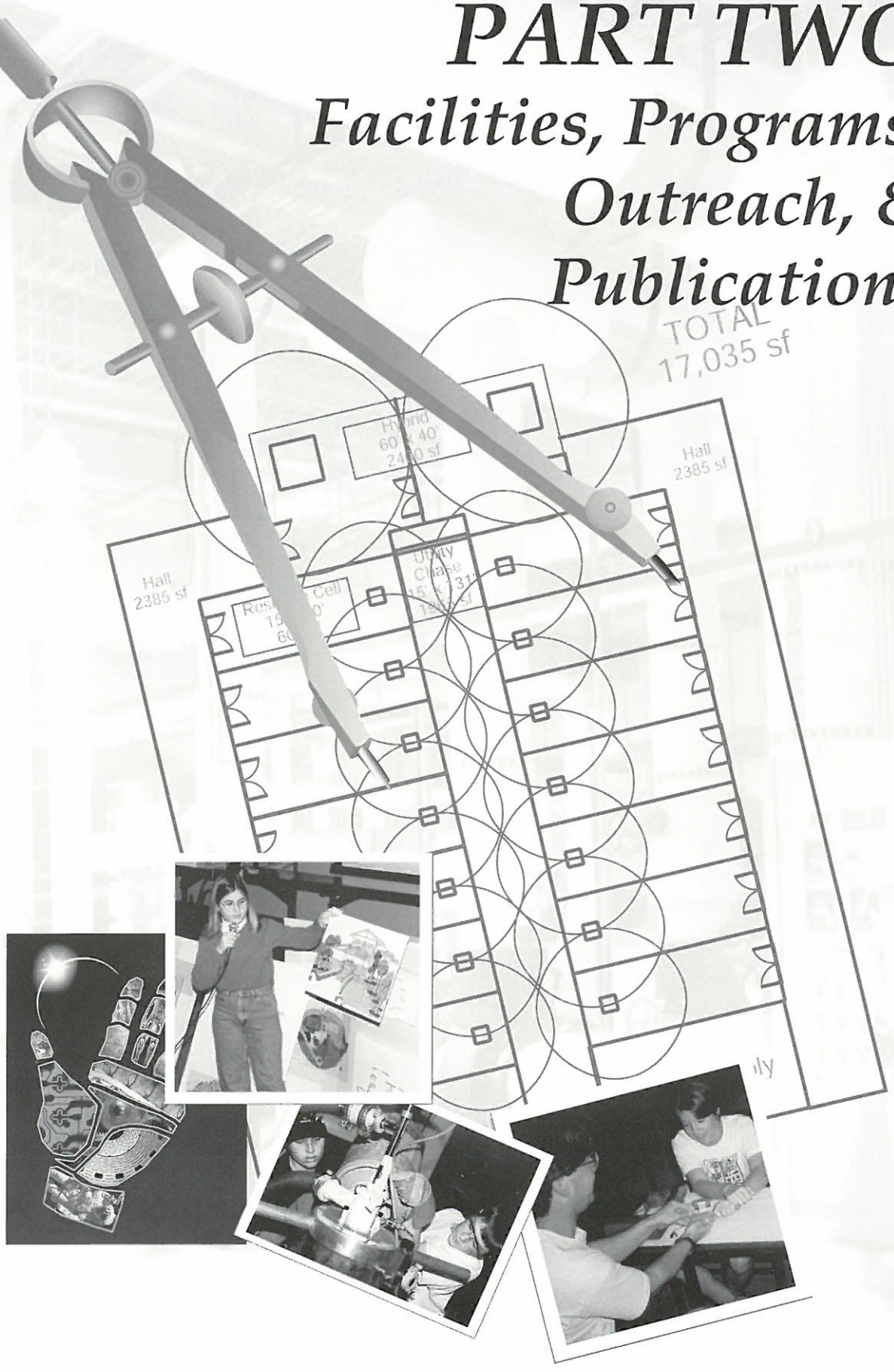

USER FACILITIES & PROGRAMS

The various user programs of the NHMFL continued to expand during 1996. New magnets and instrumentation were added and new users appeared. Listed below are a few highlights of the new support offered users during 1996, followed by some program-by-program details.

- In February 1996, the General Purpose DC Field Facility in Tallahassee installed a 33 T, 32 mm bore magnet. It was used the same day to examine the Fermi surface of a low-dimensional organic conductor and has continued to run routinely throughout the year.
- The 24.5 T, 32 mm bore, higher homogeneity magnet continued to be used for NMR studies of high T_c superconductors, quantum wells, and other condensed matter systems. This magnet also was used to better understand and eliminate the sources of field fluctuations with the aim of producing a magnet system for all kinds of magnetic resonance research at the 1 ppm level of inhomogeneity and instability.
- The number of pulsed magnet stations that can accommodate concurrent experiments has been increased to four, and the amount of equipment available has also increased.
- The newest pulsed magnet produces 42 T in 24 mm over a long pulse length of 500 ms.

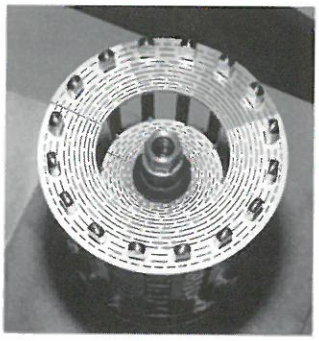

Figure 1.

The inner two coils of the 33 T 32 mm bore resistive magnet.

- Multiple units of high demand instrumentation were purchased or built for users of the DC and Pulsed Field Facilities, thereby increasing the number of samples that could be studied per magnet hour. NHMFL staff responded to user requests for new sample holders to support interesting new techniques. Experience with operating major equipment led to improvements that increased reliability, user friendliness, and/or performance.
- Wide-line NMR in a resistive magnet was improved by development of a new low temperature cryostat insert and sample probe.
- The Ultra-High B/T Facility in Gainesville put its dilution refrigerator into operation and built and installed many small parts that will allow immediate use of the facility as soon as the high field magnet is delivered.

Each of the groups that make up the Center for Interdisciplinary Magnetic Resonance (CIMAR) continued the development and use of magnet-based instruments originally brought on-line in 1995.

- Sixteen research groups have used the EMR facility since it was first made available in November 1995.
- A new 400 MHz, 89 mm bore, high sensitivity spectrometer was delivered and is available

to users. Varian and Conductus have designated the NHMFL a beta test site for a new, jointly developed, two-channel spectrometer that uses a detector made of high T_c superconducting material.

- The new 3 T, 80 cm bore, whole-body system for MRI and MRI/Spectroscopy that was installed last fall has already given exquisite head images and angiograms of unrivaled resolution during its testing and development phase.
- The world's highest-field, highest performance FT-ICR mass spectrometer (9.4 T superconductive) was completed.

General Purpose DC Field Facilities—Tallahassee

The DC Field Facilities of the NHMFL offer users from a wide range of disciplines a variety of superconducting and resistive magnet systems for their research. Details are shown in Table 1.

Table 1. General purpose DC magnets available in Tallahassee in December, 1996.

Field (T), Bore (mm)	First Use	No. in Use	Supported Research
Superconducting			
20, 52	3/93	2	Magneto-optics, ultra-violet through far infrared; Magnetization; Specific heat; Transport; Temperatures from 20 mK to 300 K; Pressure from ambient to 13 GPa.
15, 45	7/95	1	
14, 150	7/95	1	Split coil magnet with 30 X 70 radial access. Stress testing of materials, especially superconducting cable.
Resistive			
20, 50	3/94	2	Same as superconducting except the available temperature range is from 0.5 K to 600 K, and the possible experiments include low resolution magnetic resonance.
30, 32	3/95	2	
33, 32	2/96	1	
24.5, 32[1]	7/95	1	

[1] *Increased homogeneity (10 ppm over 2 mm DSV) magnet for magnetic resonance experiments.*

Instruments for Users of the Continuous Field General Purpose Magnets

Considerable effort went into improving the array of available instruments and experimental techniques based on our increasing experience meeting users' needs. Multiple copies of popular instruments increase the amount of data that can be taken per magnet hour. This makes more efficient use of researchers' time and NHMFL resources.

- A single axis rotator has been built for use in the 32 mm bore magnets. It accommodates diamond anvil cells capable of reaching at least 6 GPa or other samples able to fit into an 8.9 mm diameter hole. Its temperature range is 0.5 K to 350 K.

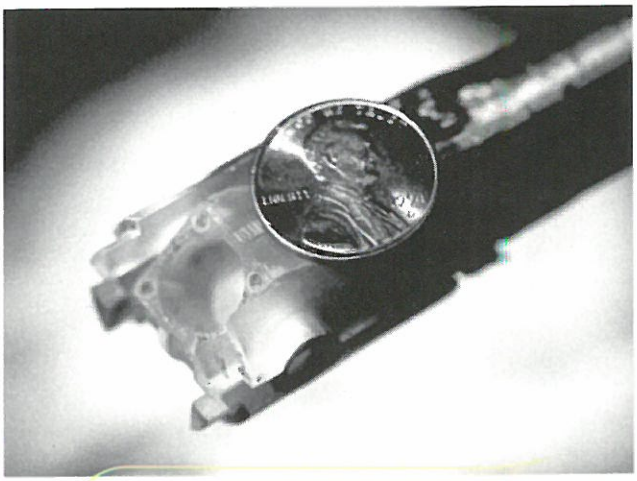

Figure 2. A single axis rotator has been built for use in the 32 mm bore magnets.

The two 20 T superconducting magnets were moved to their own low-noise hall away from the resistive magnets and their power supply. The move included the following improvements:

- Significantly lower vibration levels, reduced ambient acoustic noise, and cleaner electrical power.
- All user instrumentation, lab benches, etc. are located on a mezzanine at the same level as the tops of the magnet cryostats. No more climbing ladders or working on scaffolding.
- A low friction rotator was designed and built for the dilution refrigerator. It uses highly polished sapphire bearings and causes no detectable heating even when quickly rotated through large angles at 20 mK.

Magneto-Optics

In 22 of the available 43 weeks of magnet time, visible and near infrared optics users did photoluminescence, reflectance, optically detected cyclotron resonance, photoluminescence excitation, Faraday rotation, and Voigt geometry (k vector perpendicular to B) measurements.

- We exchanged one of our argon lasers for a 25 W laser with deep UV option in order to improve the range and the output of the Ti:S laser as well as to provide deeper UV lines for UV photoluminescence measurements of GaN gap exciton spectra.
- A new germanium detector expands our infrared detection range to 1.7 μm with ultra high sensitivity.
- A new software program controls the Ti:S laser in order to take photoluminescence excitation spectra.

Infrared (IR) magneto-spectroscopy is a sensitive probe of various physical phenomena, and has been applied with great success to study many microscopic interactions such as single particle gap features, lattice dynamics, charge density wave transitions, electron-phonon coupling, and superconductivity. Since many of the aforementioned processes are either magnetic field dependent or are in competition with various magnetic ground states, IR magneto-spectroscopy is definitely a necessary technique for the study of exotic materials.

- A reflectance probe for the small bore magnets was developed last year, so that we now have probes for transmission and reflectance measurements in fields to 33 T. The sample temperature can be controlled over the range from 2 K to 50 K (reflectance) or 100 K (transmission).

Magnetization

- A vibrating sample magnetometer was purchased and put into operation for samples that are too large or have moments that are too large for the cantilever force magnetometer. It will cover temperatures from 0.5 K to 350 K and its noise level is less than 10^{-3} emu.
- Cantilever force magnetometry is still the method of choice for temperatures below 1 K, for small moments, and special experiments.

NMR Spectrometers for High Field, Low to Medium Resolution Experiments

NMR is a very valuable tool for examining a broad range of condensed matter systems. The facilities developed at the NHMFL provide a unique opportunity to extend measurements to 30 T, at temperatures from 1.5 to 300 K. The range of parameter space that is accessible is therefore greatly expanded. The 24.5 T magnet with 5 ppm 1 mm DSV installed in August 1995 has been used for studies of highly correlated electron systems, cuprates, organic low dimensional electron systems, optically pumped NMR in semiconductors, chalcogenide arsenide glasses, and high temperature superconductors. Nineteen nuclear species have been studied. New probes and inserts developed over the past year have greatly simplified and improved temperature stability and control at all fields.

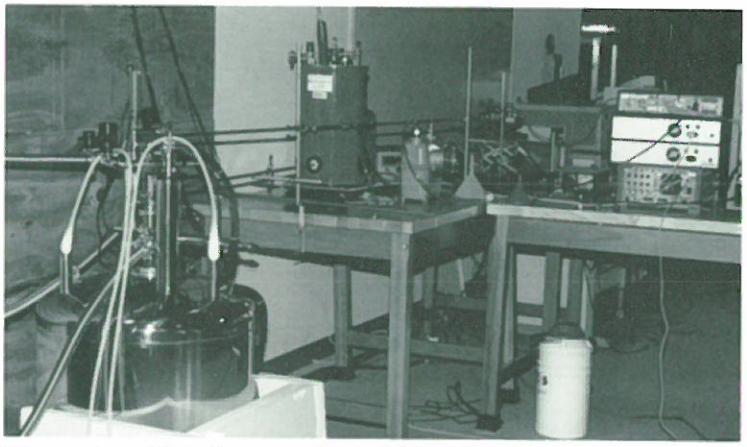

Figure 3. High frequency/high field EMR spectrometer (15/17 T) at the NHMFL in Tallahassee. This instrument became fully operational in 1996.

- A new insert designed in collaboration with W. P. Halperin (Northwestern University), and built under his direction at NWU, has solved the He "bubble" problem encountered above 17 T. This insert displaces the bubble using a slight He over pressure, allowing good temperature control from 1.5 to 77 K at all fields. The capacitors and all elements of the tuned circuit in the probe, except the sample coil, have been placed in vacuum. This has considerably reduced RF breakdown problems.
- A 15 T at 4.2 K, 17 T at 2.2 K, superconducting magnet, 1 ppm homogeneity, has been ordered for condensed matter NMR research, and as a staging magnet for NMR experiments in the medium homogeneity resistive magnet.
- A newly purchased Tecmag dual frequency spectrometer with RF leveling, dedicated to NMR in the resistive magnets, covers the frequency range 10 to 300 MHz. The dual frequency feature allows interleaving data from a standard and the nucleus being studied, greatly enhancing the accuracy of Knight shift data, or interleaving two different nuclei in the sample under study, effectively doubling the data acquisition rate.
- Recently, with a probe built by W. G. Clark (University of California, Los Angeles), proton NMR experiments on $(TMTSF)_2PF_6$ at 952 MHz were carried out. This is a record for standard NMR in a magnetic field and shows that higher frequencies can be reached easily with the same probe.

High Pressure Research

- A new plastic diamond anvil cell makes possible transport and optical measurements to high pressures in pulsed magnetic fields without eddy current heating of the sample. The cell has been used to 1.2 GPa at a temperature of 2 K.
- Brush Wellman, in a loose collaboration with NHMFL and Meigan Aronson of the University of Michigan, has developed a magnetically clean BeCu:Co alloy that Stan Tozer has used to make small diamond anvil cells for magnetization work using a SQUID magnetometer. This cell has been successfully used to measure the magnetization of ferrite colloids at 6.7 GPa.

Pulsed Field Facility—Los Alamos

The Pulsed Field Facility of the NHMFL located at Los Alamos National Laboratory in New Mexico offers researchers a variety of pulsed magnet systems, two superconducting magnets, and unique flux compression capabilities. Details are shown in Table 2.

Table 2. General purpose magnets available in Los Alamos in December, 1996.

Field (T), Bore (mm)	First Use	Pulse, rise/duration (ms)	Supported Research
Pulsed, General Purpose			
50, 24	12/92	6/30	Magneto-optics, ultra-violet through far infrared; Magnetization; Mechanical properties; Thermal expansion; Specific heat; Transport; Temperatures from 25 mK to 550 K; Pressure from ambient to 3 GPa; NMR in highest fields - low resolution.
63, 15	3/93	7/35	
45, 24[1]	2/95	9/60	
42, 24	3/96	10/500	
Superconducting			
20, 52	12/92		Same as pulsed fields.
9, 32	11/95		Magneto-optics, ultraviolet to near infrared.
Flux Compression			100 T to 1,000 T available through LANL programs.

[1] *Higher homogeneity*

Magnet and Instrumentation Update

A number of user enhancements were made in the pulsed field facilities.

20 T Superconducting Magnet

- A cell for heat capacity measurements on milligram samples from 4 K to 30 K was built and successfully tested. Also, a special high temperature probe was constructed for Hall and magnetoresistance measurements from 4 K to 600 K.
- Brought on-line were new software applications in the area of data acquisition and control that automate measurements of resistance and magnetization *vs.* temperature and magnetic field.

Capacitively Driven Magnets

- The number of pulsed magnet stations that can accommodate concurrent experiments was increased to four. Dedicated gas handling systems were built for two stations and the addition of mobile pumping stations and additional cryostats increased the efficiency of operations.
- A new magnet was installed that produces 42 T in 24 mm over a long pulse length of 500 ms.
- Experiments with the dilution refrigerator (attached to a 50 T magnet) were made more user friendly by designing a standard sample holder that can be mailed to users for prior sample mounting.

- A 94 GHz microwave spectrometer was built for reflectance and transmission phase sensitive measurements of complex conductivities.
- The standard 50 T and 60 T pulsed magnets are now offered at higher fields—up to 55 T and 65 T respectively—for those users willing to risk somewhat shorter magnet life. Also, noise levels were significantly reduced by employing better measurement techniques.
- Some of the new software applications mentioned above for the 20 T superconducting magnet were also installed for pulsed magnet measurements.

Flux Compression

- Flux compression experiments up to 1,000 T are possible at Los Alamos in cooperation with other laboratory programs. The most recent series, code-named "Dirac," began in April and concluded in July 1996. NHMFL is the liaison between outside users and the explosive flux compression capabilities at Los Alamos. In effect, NHMFL, through Los Alamos, becomes perhaps the only magnet lab in the world offering general user access to this technique for producing ultra high fields.
- A "disposable" plastic He-4 cryostat was designed that can maintain a temperature of 1.8 K for almost two hours. Several were built and successfully used for the Dirac series.

Figure 4. Bob Clark, Director of the National Pulsed Magnet Laboratory of Australia, carefully lowering the He-4 cryostat into the armed 1,000 T MC-1 flux compression generator during the Dirac series at Los Alamos.

Optics

- A femto/picosecond rapid scanning autocorrelator was acquired along with electronics for time resolved spectroscopy.

60 T Quasi-Continuous Magnet

- Cryostats, including a dilution refrigerator, have been ordered for this magnet, the first of its kind in the United States, that is now undergoing final assembly.
- Three of the five AC to DC power converters that will power this magnet were commissioned. These converters, rated at 80 MVA each, already constitute the world's highest power source for any magnet that can be sustained for two seconds and, by themselves, will allow 45 T to be achieved. The remaining converters will be installed in the spring of 1997 and will permit full operation at 60 T.

User Environment

The Pulsed Field Facility operates its user program within the general guidelines established by the NHMFL Executive Committee and in a manner tailored to the specific characteristics of pulsed field experiments. In particular, the heightened safety requirements attending pulsed field experiments, arising from the intrinsic high voltage and the non-negligible probability of magnet failure, dictate that experiments be reviewed for safe operation within the magnet and

that users be assigned an NHMFL contact who guides and assists them in following local laboratory procedures, setting up the experiment, pulsing the magnet, and acquiring data. Even for experiments with the 20 T superconducting magnet, the NHMFL contact is needed to ensure the safe operation of the magnet and the associated instrumentation and equipment. The role of the NHMFL contact is described in *NHMFL Reports*, Summer, 1995.

Proposals are reviewed for feasibility (including safety) and scientific merit by NHMFL staff, and a date for the experiment is scheduled based on mutual convenience and existing commitments. In those cases where greater than average resources are requested, or where there is an implied impact on other experiments, further review of the proposal outside NHMFL may be required to help establish priorities. Usually, this is not necessary, and we are able to schedule accepted proposals within four to six weeks, or even sooner if an opening appears due to cancellation.

A new Web site, *http://www.mst.lanl.gov/nhmfl/welcome.html*, was established to give pulsed field users access to magnet and cryostat dimensions and characteristics, as well as to procedures and hints for requesting and performing pulsed field experiments.

The staff that contributes to user support includes three postdoctorals, a low temperature scientist, the operations manager, two mechanical technicians, a secretary, and the Director of User Programs.

Ultra-High B/T Facility—Gainesville

A special annex facility for studies of materials at ultra-high values of the ratio of magnetic field to temperature (B/T) is being developed as a collaborative effort between the NHMFL and the Microkelvin Laboratory at the University of Florida. Fields up to 20 T and temperatures down to 500 μK provide a B/T ratio of 4×10^4 T/K, the highest available anywhere. Users will be able to study new phenomena that require the establishment of high spin polarization or high magnetization.

Accomplishments in 1996 include:

- The magnet dewar and dilution refrigerator were tested, and the design temperature of less than 10 mK was achieved.
- The $PrNi_5$ demagnetization stage was built and installed on the dilution refrigerator along with the necessary superconducting heat switch.
- The helium-3 melting pressure thermometer and the Pt nuclear resonance thermometer were built and installed ready for use.
- A cold finger extension from the demagnetization stage into the high field region was built.
- A cell with heat exchanger and leads for immersing samples in liquid ^{3}He has been constructed.

The high field magnet system has not yet been delivered because of failure of the wire in one of the Nb_3Sn coils. In order to correct this problem, new wire must be obtained and the coil replaced. In the meantime, the magnet without this coil, which produces 15/17 T, will be delivered in late February 1997. As soon as testing occurs, the facility will be open to external users. Installation of the new insert coil to reach 18/20 T is expected in late 1997. This magnet is the first with such a high field that Cryomagnetics has attempted and is an example of NHMFL work with U. S. industry to enhance its capabilities.

Center for Interdisciplinary Magnetic Resonance (CIMAR)

The magnetic resonance program spans all three institutions of the NHMFL. The primary facilities for nuclear magnetic resonance (NMR), electron magnetic resonance (EMR, including electron paramagnetic resonance (EPR) and electron cyclotron resonance), and ion cyclotron resonance (ICR) are housed in Tallahassee. The primary site for magnetic resonance imaging and *in vivo* spectroscopy (MRI/S) is at the University of Florida, but there are NMR spectrometers at UF and MRI instruments in Tallahassee. A detailed list of NMR and MRI/S facilities is shown in Table 3, and the list of ICR spectrometers is shown in Table 4.

Table 3. Instrumentation for NMR and MRI/S available in Tallahassee and Gainesville in December, 1996.

Frequency (MHz)	Field (T), Bore (mm)	Homogeneity (ppb)	Supported Research
850*	18/20, 31	100	Solid-state NMR.
720*	16.9, 50	1	Solution-state NMR, test bed for powered mode and 2.2 K operation aimed at ≥21 T system development.
600*	14, 89	1	Solid-state NMR, diffusion studies, *in vivo* spectroscopy, and micro-imaging.
600**	14, 50	1	Solution-state NMR, NMR microscopy.
500*	11.75, 50	1	Solution-state NMR.
500**	11.75, 50	1	Solution- and solid-state NMR.
300*	7, 89	1	Developing new solid-state methods, including magic angle spinning techniques.
300*	7, 50	1	Developing new solution-state methods.
200**	4.7, 330	100	MRI and MRI/S of animals.
125**	3, 800	100	Whole body MRI and MRI/S.

* Tallahassee ** Gainesville

NMR Program

NMR systems that were put into operation in 1995 continue to be improved and used for research, and efforts to attract highly qualified staff are ongoing. Research and development has concentrated on a wide range of areas.

- The Magnex Scientific 20 T superconducting magnet has made field at 2.2 K. The drift rate was too great for the planned NMR experiments, however, so the field has been lowered to 19.6 T where the drift rate appears to be well below the 0.1 ppm/h specification. The current homogeneity over a 1 cm diameter spherical volume is approximately 1 ppm without room temperature shim controls.
- The NHMFL has been designated a beta test site for a new kind of NMR detector that has been developed jointly by Varian and Conductus. They have loaned the NHMFL a complete 400 MHz, 89 mm bore, two channel spectrometer and magnet. The detector is made with high T_c material and has about five times the sensitivity of prior detectors.

NMR Imaging and *In Vivo* Spectroscopy

The major events in MRI/Spectroscopy in the past year were the acquisition of the 3 T whole body magnet at the UF Brain Institute/VA Hospital and the funding of the 12 T, 400 mm warm bore MRI magnet system. The 3 T system came on-line in late 1996. Rare or unique features of this system will produce images with spatial resolution of ≤250 microns/pixel and provide for 10 image/second acquisition rates, compared to the 1 to 3 image/second available on most other whole body systems. The use of high fields combined with high speeds should provide better head and spinal cord image quality. The 12 T, 400 mm system was funded by the Department of Defense through the UF Brain Institute. It will be designed and built by an NHMFL–private sector partnership.

Electron Magnetic Resonance Spectroscopy

High resolution EMR (0.01 mT) began in November, 1995 with the installation of a 15/17 T, 61 mm superconducting magnet specially designed for EMR experiments up to 450 GHz, including EPR X-band measurements to 9 GHz. Research by in-house and visiting users has proceeded along with development of instruments. The scientific projects are drawn from physics (high T_c superconductors); chemistry (molecular magnetism); and biology (photosynthesis and proteins).

Fourier Transform Ion Cyclotron Resonance Mass Spectrocopy

During 1996, the FSU ICR group's main activity was the design, construction, and assembly of new instruments. As new techniques and experiments are developed on the NHMFL instruments, those methods will be implemented on external user instruments in the NSF National High-Field FT-ICR Mass Spectrometry Facility.

- Design and construction of a 9.4 T FT-ICR mass spectrometer with home-built electrospray source and dual octupole ion guides were completed early in 1996. It represents the world's highest field (and highest performance) FT-ICR mass spectrometer, and is available to external users. It offers improvements in dynamic range (factor of 10) and mass resolving power at high mass (factor of 2) compared to the best prior instrument anywhere. Mass

Table 4. Ion cyclotron resonance spectrometers available in December, 1996.

Field (T), Bore (mm)	Supported Research
9.4, 220	Electrosprayed multiply-charged biomolecular ions of high molecular weight
7, 150	MALDI-generated singly-charged ions of peptides and polymers; and analysis and reaction chemistry of elemental ions generated by r.f. glow-discharge.
6, 150	Test bed for an inside-the-bore electrospray ion source being developed and constructed by Prof. Laude's group at University of Texas
3, 150	Excitation and detection of fluorescence from mass-selected trapped ions
3, 150	Routine ICR applications and tests to see whether higher-field performance is needed for a particular sample

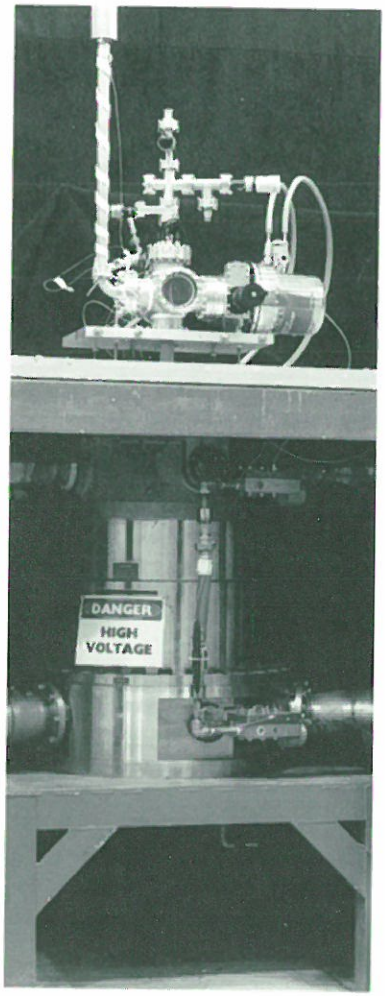

Figure 4. A 20 T resistive-magnet FT-ICR mass spectrometer producing the world's highest-field FT-ICR mass spectra.

resolving power of 150,000 for a protein of 112,000 dalton molecular weight was achieved, and hundreds of combinatorial peptides can be detected simultaneously in a mixture.

- The ICR and NMR groups at NHMFL combined to produce the first mass spectrum of a ^{13}C, ^{15}N isotopically doubly-depleted protein. Just as ^{13}C, ^{15}N *enrichment* simplifies and improves S/N ratio for NMR spectra of proteins and nucleic acids, ^{13}C, ^{15}N *depletion* compresses the isotopic distribution and improves S/N for mass spectrometry.
- A 20 T resistive-magnet FT-ICR mass spectrometer with a home-built (MALDI) fiber-optic source was built. This small-bore system produced the world's highest-field (by a factor of more than 2) FT-ICR mass spectra, at a mass resolving power more than 10 times higher than the spatial homogeneity of the magnet itself.
- $1,500,000 was granted by the State of Florida to develop a 15 T, 110 mm warm bore magnet system. Proposals have been sought from companies wishing to join with the NHMFL in a partnership to design and build this system.

The NHMFL Tallahassee site ICR capabilities derive from the magnets listed in Table 4. All have 10 ppm inhomogeneity. Additional superconducting magnet-based FT-ICR instruments at UF serve as development sites for other applications (e.g., DC glow-discharge ion source, inside-the-bore electrospray ion source).

Geochemistry

The geochemistry facility specializes in the precise and accurate determination of trace elements in both natural and synthetic materials, as well as high precision measurement of the natural variation in isotopic composition of elements. Such variations exist due to the accumulation of radiogenic nuclei in materials as well as to mass fractionation that occurs during physical, geochemical, and biochemical processes. In addition, they provide natural tracers of the sources and pathways of elements in nature. These natural tracers are providing us tools to increase understanding of processes operating in the deep interior of the Earth, in its crust, and oceans and atmosphere. Radioactive and radiogenic nuclei permit the tracing of these processes over time scale from years to billions of years.

- During the year, construction of the trace metals clean lab was completed and a third type of mass spectrometer was purchased. This is the Finnigan Mat ELEMENT, an ICPMS sector instrument. It is equipped with a laser ablation system that will permit *in situ* trace element and isotopic analyses on spot sizes down to 1μm. 1996 was the first full year of research activity in the NHMFL's isotope geochemistry program. Some accomplishments are outlined below.

- Partition coefficients for a group of key elements (U, Th, Nb, Hf, Y, Zr, Ce, Nd, Sm, Er, Yb, Lu) between clinopyroxenes, orthopyroxenes, garnets, and melt over a range of temperatures (1570 °C to 1375 °C), pressures (2.8 to 1.0 GPa), and melt compositions have been determined. These are presenting new insights on the conditions under which primary mid-ocean-ridge basalts (MORB) are formed and the reasons for observed ^{230}Th excesses in MORB.

- Soils are now recognized as an important and easily accessible inventory for carbon and CO_2, and they must be considered significant factors in developing greenhouse models for global, long term, climatic prediction. Analyses have been conducted of the soil CO_2 flux of paired natural and disturbed soils and of the C and ^{14}C content of organic matter in both pre- and post-bomb samples of these soils, in order to understand better the effects of land use on C cycling rates and CO_2 fluxes.

- Isotopic and concentration analyses of Hf in seawater indicate that approximately 50% of the Hf inventory in the oceans is derived from hydrothermal activity, and that the residence time of Hf in the oceans is on the order of several thousand years. Hf isotopic analyses of deep sea sediments can serve as a new indicator of hydrothermal activity, with an age resolution higher than any currently available. In the future, Hf isotopes could become a significant geochemical prospecting tool, as we begin to mine the ocean floors.

- The isotopic composition of Pb in rainwater collected over south Florida is providing information regarding the sources of heavy metal contamination that has reached a serious level in fish and wildlife of the Everglades. By secondary ionization mass spectrometry, we have obtained what we believe to be the most precise determination ever made of mercury isotope ratios and have begun a search for natural variations that might provide clues to Hg sources and pathways in the environment.

- Stored within defects and the electronic structure of α–quartz is information regarding its radiation, thermal, and light exposure history. Research has been directed on learning how to retrieve and decode this information. Thermal treatment of quartz can disturb the natural equilibrium between competing hole centers, to the extent that ESR analyses can provide good estimates of the concentration of oxygen vacancies. We have studied the dosimetric properties of quarts and the thermal stability of oxygen vacancies on a geologic timescale.

Figure 5. Construction of Geochemistry's trace metals clean lab was completed in 1996.

Chapter 4

IN-HOUSE RESEARCH PROGRAM

In-House Research Program Goals

The National Science Foundation charged the National High Magnetic Field Laboratory (NHMFL) with developing an in-house research program that:

- Utilizes the NHMFL facilities to carry out high quality research at the forefront of science and engineering, and
- Advances the NHMFL facilities and their scientific and technical capabilities.

To this end, the NHMFL envisions an in-house research program that not only guides and stimulates magnet and facility development, but additionally provides intellectual leadership for experimental and theoretical research in magnetic materials and phenomena. The NHMFL In-House Research Program (IHRP) seeks to achieve these objectives through funded research projects of normally one to two years in duration in the following categories.

- Small, seeded collaborations between internal and/or external investigators that utilize their complementary expertise.
- Bold but risky efforts that hold significant potential to extend the range and type of experiments.
- Initial seed support for new faculty and research staff, targeted to magnet laboratory enhancements.

The IHRP strongly encourages collaboration across host-institutional boundaries and between internal and external investigators in academia, national laboratories, and industry, as well as interaction between theory and experiment. Projects are also encouraged to drive new or unique research, i.e., serve as seed money to develop initial data leading to external funding of a larger program. In accord with NSF policies, the NHMFL cannot fund clinical studies.

Proposal Solicitation & Review

The IHRP will solicit proposals at least once yearly. Faculty and staff of the three host institutions (FSU, UF and LANL) may submit proposals in response to this solicitation. Scientists and engineers from outside organizations may be named as active collaborators on proposals in collaboration with on-site faculty and staff. As a complement to this solicitation, LANL staff are encouraged to pursue funding opportunities provided through the LANL with University of California faculty. Funding will be provided only for research taking place at NHMFL facilities. Proposals submitted by young researchers, i.e., researchers within seven years of the most advanced degree, will be given a higher funding priority. The IHRP will adhere strictly to the guidelines stated in the NSF Cooperative Agreement DMR-9527035.

The four primary review criteria of the IHRP are:

1. **Research performance competence**. This criterion relates to the capability of the investigator(s), the technical soundness of the proposed research, and the adequacy of the institutional resources available.

2. **Intrinsic merit of the research**. This criterion is used to assess the likelihood that the research will lead to new discoveries or fundamental advances in the fields of high-magnetic-field science or engineering, or have substantial impact on progress in those fields.

3. **Utility or relevance of the research to the NHMFL mission**. This criterion is used to assess the likelihood that the research can contribute to the achievement of the NHMFL In-House Research Program objectives, and thereby serve as the basis for driving, enhancing or improving the NHMFL user facilities, capabilities, or expertise.

4. **Effect on the infrastructure of high-magnetic field science and engineering**. This criterion relates to the potential of the proposed research to contribute to better understanding or improvement of the quality, distribution or effectiveness of the nation's high-magnetic-field scientific and engineering research, education, and manpower base.

Funded projects must be of the highest quality and will be reviewed using a three-part review process. These review steps are as follows:

1. **Initial review by the NHMFL Research Program Committee**. As determined by the Director of the In-House Research Programs, the members of this internal review committee may be augmented by additional investigators in order to ensure fairness and/or adequate representation of various research disciplines. Proposals deemed to hold the highest merit will then pass on to the second review step.

2. **Subsequent review by an external review panel**. The members of this review panel will be chosen by the Director of the In-House Research Programs in consultation with the Research Program Committee. The external reviewers evaluate the proposals based on the goals and criteria stated in the solicitation.

3. **Final determination of project funding by the NHMFL Chief Scientist**. The NHMFL Chief Scientist, J. Robert Schrieffer, will make the final funding decisions based on the internal and external review reports.

The present membership of the NHMFL Research Program Committee is: James Brooks, Zachary Fisk, Lev Gor'kov, Alan Marshall, Stephan von Molnár, and Stan Tozer (FSU); John Graybeal, Kevin Ingersent, and Thomas Mareci (UF); Alan Bishop, Chris Hammel, and Joe Thompson (LANL).

Funded projects will be periodically reviewed and continuation of funding will depend on adequate performance. The principal investigator(s) (PIs) of funded projects must file a progress report to the NHMFL Director of the In-House Research Programs every six months for the duration of funding. A final report also must be provided at the end of the funded period.

Detailed grievance procedures have been established for the review process, and have been approved by the NSF. In accord with NSF policy, individuals may grieve the handling of their proposal but not the content of the reviewer reports. Grievances are to be handled by the NHMFL Director and Executive Committee.

In-House Research Program Budget

The NHMFL has budgeted the funds for the in-house research program for 1996 through 2000 (see Table 1). These numbers include the full loading of benefits and institutional indirect costs.

Table 1. Five-year funding for NHMFL In-House Research Program.

Year	Research Budget (includes indirect cost loading)	% of NHMFL budget
1996	1,120,000	6.4
1997	1,530,000	8.7
1998	1,700,000	9.7
1999	1,870,000	10.7
2000	1,870,000	10.7

1996 Solicitation – Proposals Received

The first NHMFL IHRP solicitation was released on May 10, 1996, immediately following verbal approval from the National Science Foundation. A total of 67 proposals were received by the proposal submission deadline of August 16, 1996. The proposals span a very significant intellectual breadth, consistent with the intentions of the NHMFL. Their approximate breakdown by research discipline and/or technique is shown in Table 2.

Table 2. Proposals received for the NHMFL In-House Research Program for 1996.

Research Area or Technique	Research Subarea	# of Proposals (per Subarea)
Magnetic resonance	System & hardware development	11
(non-physics)	Biochemistry	4
30 proposals	Solid-state chemistry	4
NMR - 11	Biology	4
EMR/ENDOR - 7	Chemistry	4
MRI - 6	Geochemistry	1
ICR - 6	Biomedicine	1
	Hydrodynamics	1
Condensed matter physics	Heterostructures/Quantum Hall effect	8
27 proposals	Oxides	7
	Theory	4
	Heavy Fermions	3
	Quasi-1D systems	2
	General magnetism	2
	Quantum fluids	1
Materials Science & Engineering	Materials science & processing	5
10 proposals	Applied superconductivity	4
	Biology	1

1996 Solicitation – Internal Review Results

An internal review of the submitted proposals was performed by the NHMFL Research Program Committee (RPC), in conjunction with internal researchers as deemed appropriate by the committee chairman. Reviewer selection was based on the following criteria.

- Reviewers must be highly qualified in the proposal's stated research area.
- Reviewers must not have a conflict of interest or close association with proposal PI or collaborators.
- RPC members must abstain from involvement on their own proposals.

Reviewer identities were held strictly confidential. The total number of internal reviewer reports received totaled 125, an average of 1.9 reports per proposal. For the internal review decisions, "program managers" were designated in the areas of physics, magnetic resonance (non-physics), and materials/engineering. These program managers were responsible for making the final internal review decisions based on the reviews received.

Of the 67 proposals received, the committee recommended that 38 proposals be sent out for external review. The remaining 29 proposals were returned to their respective PIs together with a copy of the referee reports. A breakdown of the internal review results is shown in Table 3.

Table 3. Internal review results of NHMFL In-House Research Program proposals.

Research Area	# Proposals Submitted	# Proceeding to External Review	Pass %
Magnetic Resonance	30	17	57%
Condensed Matter Physics	27	15	56%
Materials Science & Engineering	10	6	60%
TOTAL	**67**	**38**	**57%**

1996 Solicitation – Status of the External Review Results & Final Funding Decisions

A detailed external peer review was performed on those proposals that passed the internal review. This review was performed by mail, with members of the external peer review panel being chosen by the IHRP Director in consultation with the NHMFL Chief Scientist and members of the Research Program Committee. When a conflict of interest arose involving the IHRP Director, reviewer selection was performed by the NHMFL Chief Scientist. Reviewer selection was based on the following criteria:

- Highly distinguished reviewers, leaders in their respective fields, and
- Absence of conflict of interest or close association with proposal PI or collaborators.

External reviewer identities were held strictly confidential. Again, two reviews were sought for each proposal. Each reviewer received a copy of the proposal, a description of the IHRP goals and

criteria, plus a reviewer rating form. In all, 64 reviews were received from 27 reviewers. This yields an average of 1.7 reviews per proposal, and 2.4 reports per reviewer.

Final funding decisions were determined by the NHMFL Chief Scientist (J. Robert Schrieffer), based on the external peer review reports. The funded projects are listed in Table 4 by the lead principal investigator, and abstracts of the projects follow the table.

1997 IHRP Solicitation

The second IHRP proposal solicitation was released in late January 1997, with a proposal deadline of April 7, 1997.

Table 4. Approved NHMFL In-House Research Program projects.

Lead PI	NHMFL Institution	Project Title	Project Duration	Year 1 Award
Brooks, James	FSU (Physics)	*Experimental & Theoretical Aspects of Quasi-3D Quantum Hall Systems*	2 years	$43,140
Brunel, Louis-Claude	FSU (CIMAR)	*Development of a High Frequency Short-Pulse Gyrotron for Pulsed EPR*	1 year	$79,491
Dagotto, Elbio	FSU (Physics)	*Study of Spin Gapped Quasi-1D Compounds Using ESR Techniques & Numerical Simulations*	2 years	$68,396
Dalal, Naresh	FSU (Chemistry)	*High-Resolution Solid-State NMR Techniques & Applications to Materials Science*	2 years	$75,186
Fisk, Zachary	FSU (Physics)	*Doped Hole Physics In Single-Layer Perovskites*	2 years	$64,546
Gibbs, Stephen	FSU (Physics)	*Applications of MR Velocimetry to Flow in Media & Fiber/Composite Manufacturing*	2 years	$70,082
Moulton, William	FSU (Physics)	*NMR Studies Of Superconducting and Magnetic Cuprates & Low Dimensional Electron Systems at High Magnetic Fields*	2 years	$36,205
Douglas, Elliot	UF (Matls Sci.)	*Materials Processing in Magnetic Fields: High-Strength Polymers*	2 years	$55,132
Eyler, John	UF (Chemistry)	*Novel Syntheses & Fourier Transform Mass Spectrometric Analyses of Combinatorial Libraries*	2 years	$65,848
Mareci, Thomas	UF (Biochem)	*High Field, High Frequency RF Coils for NMR Spectroscopy and Microscopy of Small Samples*	1 year	$51,487
Talham, Daniel	UF (Chemistry)	*Comparing Magnetic Langmuir-Blodgett Films to Their Isostructural Solid-State Analogs Using Antiferromagnetic Resonance*	2 years	$54,130
Tanner, David	UF (Physics)	*High-Field Optical Studies of Highly Correlated Metals*	2 years	$66,611
Hammel, P. Chris	LANL (MST-10)	*Very High Magnetic Field NMR Studies of the Cuprate Spin Gap*	2 years	$75,054
Movshovich, Roman	LANL (MST-10)	*Heat Capacity Measurement in the NHMFL 60 Tesla Quasi-Continuous Magnet*	2 years	$62,985
Rickel, Dwight	LANL (DX-6)	*Time-Resolved Photoluminescence Studies of Semiconductor Heterostructures in Ultra-High Magnetic Fields*	2 years	$84,084 *(est.)*

"Experimental & Theoretical Aspects of Quasi-3D Quantum Hall Systems" - James Brooks, FSU ($86,185 over 2 years)

This project will investigate both experimentally and theoretically the low temperature, high magnetic field transport properties of quasi-3D electronic materials. The regime of physical interest to us is where the individual layer of two dimensional electron gas (2DEG) exhibits the quantum Hall effect (QHE) in isolation, a large number of layers are coupled, and the tunneling strength between the layers may be varied. We propose to carry out systematic temperature and magnetic field dependent transport measurements on GaAs/GaA1As superlattice structures of variable layer number, interlayer coupling, and carrier concentration where the integer QHE reaches the quantum limit by 30 tesla. We further propose to vary the interlayer coupling of individual samples over significant ranges by uniaxial stress. The proposed work will bring together the expertise of three principals, J. Brooks (Exp-FSU), Z. Wang (Theory-Boston College), and J. Simmons (Materials-Sandia Laboratory), and three collaborators, R. G. Clark, B. Kane, and A. Dzurak at University of New South Wales, Sydney, Australia. The project will provide on completion a uniaxial stress probe for general use at the NHMFL.

"Development of a High Frequency Short-Pulse Gyrotron for Pulsed EPR" - Louis-Claude Brunel, FSU ($79,491 for 1 year)

The project's goal is to determine the feasibility of a gyrotron as a source for a short pulse, high frequency Electron Paramagnetic Resonance (EPR) spectrometer. It is driven by the need to perform EPR measurements at higher magnetic fields and with shorter pulses (to observe over wider bandwidths). The program will include the design of a gyrotron producing radiation in multiple frequencies between 150 GHz and 600 GHz, with power levels of about 1 kW. The pulse width will be between 1 Ns and 10 Ns. The capacity to produce a train of at least 3 pulses, with spacing varying from 1 Ns to 20 Ns will be included. The development of such a gyrotron is extremely relevant to the NHMFL In-House Research Program objectives. This project is being carried out in collaboration with scientists from three universities and two private companies. The EPR spectrometer we envision to build will be unique in the world and will be eventually installed as a new user facility at the NHMFL.

"Study of Spin Gapped Quasi-One-Dimensional Compounds Using ESR Techniques and Numerical Simulations" - Elbio Dagotto, FSU ($138,061 over 2 years)

Research on recently synthesized quasi-one-dimensional inorganic compounds that have a spin gap in their spectrum is proposed. These materials include $CuGeO_3$ with spin Peierls behavior, as well as $Y_{2-x}Ca_xBaNiO_5$, $(VO)_2P_2O_7$, $SrCu_2O_3$ and others where their spin gap is induced by purely quantum mechanical (QM) effects. It is expected that this proposal, which includes experimentalists and theorists from FSU, UF and abroad, will foster greater understanding of the characteristics of magnetic excitations in these systems and their behavior in the presence of large magnetic fields. The influence of Zn-doping on these spin-gapped compounds will also be studied. End-chain state in Haldane systems will be investigated. The project utilizes the high field facilities to explore the field dependence of QM ground states and enhances the electron spin resonance (ESR) facilities at the NHMFL. Expertise to interpret the ESR spectra of many-body systems will be achieved through the

analysis of QM models for the compounds under study. The phase diagram with and without intense magnetic fields and Zn impurities will be calculated using a variety of numerical techniques. The PI and collaborators have common interests and complementary expertise in the subject of this project.

"High-Resolution Solid-State NMR Techniques & Applications to Materials Science" - Naresh Dalal, FSU ($111,030 over 2 years)

It has been reported for NMR spectroscopy and imaging of solid, nonrubbery organics, that higher Zeeman fields B_0 may not substantially improve (and may even degrade) resolution. If true, this would deter future development of high field NMR of solids. This proposal addresses several questions in this regard. We will develop new experimental and theoretical methodologies for enhancing the resolution of NMR as applied to anisotropic solids (liquid crystals, single crystals, and powders), especially at high B_0. The nuclei that will be selected, including protons, ^{13}C and ^{31}P, and quadrupolar nuclei with half-integer spins such as ^{17}O, ^{39}K, and ^{85}Rb, should provide complementary information on the role of different sites in cooperative phenomena. Proton NMR studies are important because obtaining high resolution NMR spectra of protons is a key challenge of solid state NMR. The chief cause of broadening is strong dipole-dipole interaction between the (usually abundant) protons. An attractive approach is to dilute the protons by partial deuteration, so that the homonuclear interactions between protons are weakened, while the heteronuclear dipolar interactions can be removed by deuterium decoupling. For this purpose, we will extend the scope of our PAD and CHIRP-95 decoupling techniques. Our preliminary results indicate that the resolution enhancement obtained in this manner improves at higher fields. For quadrupolar nuclei with half-integer spins, the signal from the central transition is to first order independent of the quadrupolar interaction and thus best studied at high fields where the sensitivity is most favorable. However, even at very high fields, the signal is broadened by the second-order quadrupolar interaction. Recently a novel multi-quantum (MQ) technique has been introduced whose only significant investment is a high-speed spinning probe. We will develop new pulse sequences to efficiently excite MQ coherences and to separate the isotrophic chemical shifts from the second-order quadrupolar shifts. Methods for obtaining high-resolution spectra will be extended to variable-temperature solid-state NMR measurements and NMR applications to materials science, in particular to structural and dynamics studies of solids in the vicinity of co-operative phase transitions. We expect that these investigations will lead to significant improvements in high resolution NMR techniques in solids, and in turn, point to the benefits of employing high fields.

"Doped Hole Physics in Single-Layer Perovskite" - Zachary Fisk, FSU ($130,641 over 2 years)

Sr- and Li-doped La_2NiO_4 will be studied using optical transmission and reflection measurements, NMR, and EPR, utilizing the high magnetic fields available at the NHMFL. The study will compare the physical changes resulting from out-of-plane doping with those due to in-plane hole doping in La_2NiO_4, as well as with the companion La_2CuO_4 systems. The rapid evolution of magnetic and electronic properties with doping is important both to the high-T_c superconductivity problem and the much more general understanding of oxide materials. The reduced scale of J in the nickelates makes measurements in high magnetic fields an important extra dimension in the study of the layered perovskites. The team investigators are Z. Fisk and J. Sarrao (FSU), J.M. Graybeal (UF), P.C. Hammel (LANL), and S.B. Oseroff (SDSU).

"Applications of MR Velocimetry to Flow in Media & Fiber/Composite Manufacturing" - Stephen Gibbs, FSU ($141,543 over 2 years)

This project will investigate and model fluid behaviors at the interface or boundary layer between a channel flow (bulk liquid) and a flow through a porous media. Many investigations show that the boundary layers of a porous material block dominate the mass and energy exchange with the environment. Numerous models describing the flow profiles at the boundary layers have been proposed, however a reliable measurement has not been found to validate them. Flow in porous media is important in a wide variety of disciplines and applications, although the specific emphasis of this project will emphasize fiber composite manufacturing applications.

Traditional flow measurement techniques (x-ray, optical, ultrasound, hot wire, dye,...) have important limitations. Hence high-field NMR imaging, with its ability to penetrate dielectric materials and its fine spatial resolution, represents a unique technique for this task. In this project, NMR flow imaging will be used to measure velocity fields in a simple model geometry, a tube with a concentric ring made of a fiber preform, thus making an annular space with a permeable inner core and an impermeable outer wall. In this way a Poiseuille flow with and without possible slip boundary conditions at the interface can be easily generated. The relationship between the velocity at the interface and the porous material characteristics such as permeability, porosity, pore size, anisotropy, and related orientation of the porous medium and the flow field will be determined. Based on our results, current models to describe the slip boundary will be tested and a simplified model will be developed. In addition, in-house facilities and capabilities for NMR flow imaging and study of flow through porous media will be developed.

"NMR Studies of Superconducting and Magnetic Cuprates and Low Dimensional Electron Systems at High Magnetic Fields" - William G. Moulton, FSU ($73,045 over 2 years)

This project will investigate the fundamental nature of the correlations (spin and charge, and the interplay between magnetism and superconductivity) in highly correlated electron systems and low dimensional magnetic systems in high magnetic fields. The systems proposed for study include ^{157}Tb NMR in Tb doped $YBa_2Cu_3O_7$. This will help to understand the important questions of why, unlike Ce or Pr that also have mixed-valent substituting for the RE, Tb doping does not decrease T_c. ^{17}O NMR studies of the flux melting transition at high fields in $YBa_2Cu_3O_7$ will carry these investigations to fields where other microprobes become ineffective. Studies in previously little understood field induced spin density waves in low dimensional organic conductors by ^{77}Se NMR will also be carried out. Experiments will be performed in the "Florida Bitter" magnet with homogeneity of 5 ppm/mm DSV at 25 T, a unique facility for high-field NMR that became operational in September 1995. This work will be carried out in collaboration with W. P. Halperin (Northwestern University), James Brooks (NHMFL, W. G. Clark (UCLA) and J. E. Crow (NHMFL).

"Materials Processing in Magnetic Fields: High-Strength Polymers" - Elliot Douglas, UF ($112,819 over 2 years)

High magnetic fields hold great promise for materials processing, leading to new materials that cannot be obtained by other techniques. In particular, orientation of liquid crystalline polymers using high magnetic fields holds tremendous potential for creating high strength materials without the use of fillers or complex fabrication techniques. It is well known that

magnetic fields can orient crystalline polymers, and a few studies have examined the physical properties of magnetically processed polymers which indicate that substantial improvements in properties are achievable. All studies to date, however, have resulted in uniaxially aligned materials, with properties perpendicular to the field direction that are inferior to those in the parallel direction. For practical applications, a way must be found to create reinforcement in multiple directions. To create multidimensional reinforcement using high magnetic fields, we will utilize a novel approach using blends of an unreacted liquid crystalline thermoset (LCT) and a B-staged (partially reacted) LCT. The reinforcement approach is a two-step process. In the first step, a flow field is used to orient the B-staged resin. In the second, a magnetic field is applied perpendicular to the flow direction. Since the orientation kinetics for the B-staged resin are significantly slower than for the unreacted resin, the unreacted thermoset will be oriented perpendicular to the orientation of the B-staged resin. Complete reaction of both resins then locks in the biaxial orientation induced by this process. As a number of variables can affect this process, this study will systematically examine the effects of the extent of B-staging, the mixing process, the magnetic field strength, and the processing time in field. Scattering, thermal expansion measurements and mechanical property measurements will be used to characterize the orientation process. Successful demonstration of this technique will provide new opportunities for the use of high magnetic fields in materials processing.

"Novel Syntheses and Fourier Transform Mass Spectrometric Analyses of Combinatorial Libraries" - John Eyler, UF - $134,523 over 2 years

A collaborative research project that combines novel syntheses of combinatorial libraries with mass spectrometric analyses utilizing high field magnets at the NHMFL is proposed. Successful completion of the proposed research will demonstrate new methods for synthesizing combinatorial libraries and identify promising "lead" compounds for interaction with HIV reverse transcriptase, which participates in the first stages of the infection that causes AIDS, and different varieties of SH2-domains, which are involved in intracellular signal transduction pathways and, therefore, of crucial interest to cancer research. Of equal importance will be the establishment of high field Fourier transform ion cyclotron resonance (FTICR) mass spectrometry as the analytical method of choice for assessing the degeneracy and diversity of newly-synthesized combinatorial libraries, as well as for identifying the masses and structures of favored "lead" compounds from these libraries that bind preferentially to receptors of biochemical and pharmaceutical interest.

In addition to conventional bead-bound library syntheses of small peptide libraries to aid in the implementation of FTICR analysis methods, Receptor Assisted Combinatorial Synthesis (RACS) will be developed and exploited to produce complete libraries of compounds for screening. Both the high mass resolution of the extremely high field FTICR mass spectrometers at the NHMFL, and the ability to carry out collisionally-activated dissociation, photo-dissociation, and selective ion/molecule reactions to determine ion structure will be exploited and further refined when characterizing the combinatorial libraries and identifying lead compounds.

The proposed experiments will demonstrate the applicability of NHMFL instrumentation and techniques to the solution of an entirely new class of problems for an entirely new clientele (e.g., biochemists and pharmaceutical chemists), which differs significantly from users currently making the most use of the NHMFL facility (physicists and chemists). In addition, compounds that may

be quite important in AIDS and cancer research should be identified from "lead" compounds produced by RACS synthesis of combinatorial libraries. The project Co-PI is Steve Benner (UF).

"High Field, High Frequency RF Coils for NMR Spectroscopy and Microscopy of Small Samples" - Thomas Mareci, UF ($51,487 over 1 year)

The overall goal of this project is to construct and optimize a range of small diameter (0.15 to 1.5 mm) volume radio-frequency (RF) coils for NMR spectroscopy and microscopy at 300, 500, 600, 720, 850 and 1000 MHz (magnetic fields of 7 to 25 T) in order to maximize the available signal-to-noise ratio (SNR) of higher resolution studies (both spectral and spatial) on small samples. Theoretical and practical design considerations will be explored, in particular the SNR, susceptibility effects, and the limitations imposed at high frequencies as the self resonant frequency of the coils is reached. The impact of tuning some of the coils to multiple frequencies will also be explored. The final objective will be to make a range of general purpose robust coils available to outside users of the NHMFL, and to provide the resources and expertise to construct dedicated submillimeter coils for specialized applications.

"Comparing Magnetic Langmuir-Blodgett Films to Their Isostructural Solid-State Analogs Using Antiferromagnetic Resonance" - Daniel Talham, UF ($108,949 over 2 years)

This project will use antiferromagnetic resonance (AFMR) to investigate the ordered state of the first known examples of magnetic Langmuir-Blodgett (LB) films. As part of the investigation, a series of isostructural powder and single crystal solid-state analogs of the LB films will also be studied, in order to compare the magnetic behavior in the solids to that of the two-dimensional LB films. Magnetic interactions in layered materials are currently of high interest from a fundamental point of view, partially because of their relationship to layered superconductors. Magnetic thin films are also of interest as potential information storage media and as components of multilayered heterostructures, which have lead to unusual phenomena such as giant magnetoresistance. The chemistry group at UF has recently developed LB films of manganese octadecylphosphonate and demonstrated that these films undergo a transition to long-range magnetic order at 13.5 K, exhibiting a spontaneous magnetization characteristic of a canted antiferromagnet. These results are the first demonstration of cooperative ordering phenomena in LB films. The LB films are isostructural with a series of layered organic/inorganic solid-state manganese phosphonantes, which are also canted antiferromagnets. The project will use AFMR to investigate three solid-state manganese salts—the phenylphosphonate, $Mn(O_3PC_6H_5)$-H_2O; the propylphosphonate, $Mn(O_3PC_3H_7)$-H_2O; and the purely inorganic analog, $KMnPO_4$-H_2O—in addition to two LB film materials, manganese octadecylphosphonate and manganese octadecoxyphenylphosphonate, which are the corresponding LB analogs of the manganese propylphosphonate and phenyl-phosphonate solids, respectively. Since the LB films are single layer analogs of the solid-state manganese phosphonates, they offer a unique opportunity to explore the ordered state of a truly two-dimensional magnetic lattice and to compare the behavior to the isostructural solids. The proposed project is a collaborative effort between the solid-state chemistry group at UF and the high-field EPR group at the NHMFL.

"High Field Optical Studies of Highly Correlated Metals" - David Tanner, UF ($141,634 over 2 years)

Infrared measurements on a variety of highly correlated metals will be carried out at the NHMFL. The materials to be studied include

cuprate superconductors, cuprate antiferromagnetic insulators, organic conductors, and heavy-Fermion metals. In addition, an improved detector cryostat would be constructed, allowing transmission and reflection studies in fields up to 30 T and at temperatures between 4 and 300 K.

"Very High Magnetic Field NMR Studies of the Cuprate Spin Gap" - P. Chris Hammel, LANL ($151,997 over 2 years)

Experimental tests of various theories of the origin of the spin gap in the high T_c cuprates shall be carried out using NOR studies performed in very high magnetic fields. Both the static uniform susceptibility and the dynamical spin susceptibility of underdoped cuprates are strongly suppressed with increasing temperature as shown by reductions of the Knight shift and $(T_1T)^{-1}$. ARPES measurements have shown that electronic excitations near the Fermi surface are also gapped in underdoped cuprates. Commonly referred to as the "spin-gap," this phenomena has been the subject of a great deal of study, both experimental and theoretical. It is now clear that the spin gap is a dominant feature of the normal state of the underdoped cuprates, and a full understanding of these materials is contingent upon a knowledge of the microscopic origin of the spin gap. It is further likely that the physics leading to the spin gap plays a crucial role in the mechanism responsible for superconductivity. Obtaining an improved understanding of this phenomenon is thus a matter of central importance.

There will be three specific objectives in the proposed work. First, we hope to determine whether the spin gap temperature scale is most closely related to the superconducting T_c or tied to a normal state energy scale. Second, we seek to determine if a spin gap exists in the single layer compounds such as $La_{2-x}Sr_xCuO_4$ independent of superconductivity. Third, we seek to clarify the relationship between the normal state transport and the AF spin fluctuations. This project will exploit the 24 T resistive NMR magnet at the NHMFL and will improve development of an NMR probe appropriate to performing NMR in that magnet, software for measuring the nuclear spin relaxation rates, and technique development in general.

"Heat Capacity Measurements in NHMFL 60 Tesla Quasi-Continuous Magnet" - Roman Movshovich, LANL ($127,860 over 2 years)

This project is centered on developing heat capacity measurements in the NHMFL 60 T quasi-continuous magnet and using this capability to study several correlated electron systems. Two compounds to be investigated are high temperature superconductor $La_{2-x}Sr_xCuO_4$ and Kondo insulator $Ce_3Bi_4Pt_3$, both of which have shown interesting behavior in resistivity in the pulsed fields of up to 60 tesla. The project will contribute to general understanding of the high temperature superconductors and Kondo insulators. It will also result in the heat capacity measurements in pulsed magnetic fields. There is great potential for this new and powerful tool in investigating a wide variety of systems such as high T_c superconductors, Kondo insulators, and various other f-electron systems, organics, metamagnetics, and many others. Successful completion of this project will serve as a basis for advancing NHMFL facilities and introduction of heat capacity in pulsed magnetic field as a tool available for NHMFL users.

"Time-Resolved Photoluminescence Studies of Semiconductor Heterostructures in Ultra-High Magnetic Fields" - Dwight Rickel, LANL ($169,962 (est.) over 2 years)

The intent of this project is to install a gatable photon counting system to study time-resolved magnetophotoluminescence from semiconductor heterostructures. The facility will be incorporated

into the current laser-spectroscopy lab previously established in pulsed and DC magnetic fields at LANL by the principal investigators and co-workers. The instrumentation development and its implementation is planned to coincide closely with the introduction of the 60 T quasi-continuous magnet due to come on-line in the near future and to be a proven asset when the 100 T project is complete.

The research component has the potential for providing significant information of the optical properties of newly developed and higher quality electronic materials. Attention will be focused on studies of electron-electron interactions in confined semiconductor heterostructures subjected to intense magnetic fields. Specifically, the photoluminescence decay dynamics (lifetimes) of interband Landau transitions and magneto-excitons will be examined. Collaborative programs with others have been established to probe many novel magnetic properties associated with correlated electron interactions. It is anticipated that when the time-resolved instrumentation is operational, it will encourage more potential users of the NHMFL spectroscopic facilities.

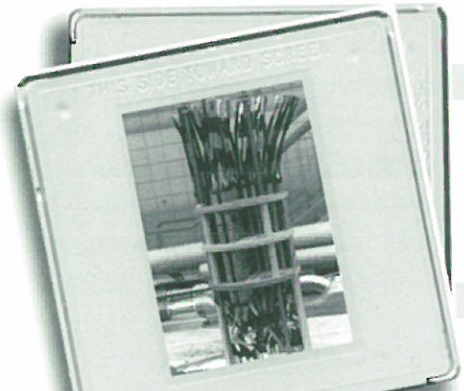

Chapter 5

COLLABORATIONS

This section of the Annual Report describes the industrial collaborations, inter-agency and inter-institutional activities, and international cooperations of the laboratory during 1996.

Industrial Collaborations

The NHMFL continues to expand its affiliations with private industry and to pursue new development opportunities in materials and magnet technology areas as an important component of its NSF mission. Partnerships with the private sector broaden the expertise and talent pool of the NHMFL to assist in magnet and magnet development issues that are critical to advancing these technologies. The leadership of the laboratory is devoting more time and resources to encouraging economic development opportunities in this region of Florida, which has been a vacuum for such high-tech activities in the past. By targeting several industrial partnerships that could benefit from being in closer proximity to the laboratory to more effectively utilize its resources, the NHMFL hopes to relocate a coterie of firms that will expand our responsiveness to users through mutual development opportunities. EURUS Technologies, Inc.®, a high-tech company specializing in taking emerging technologies to the marketplace, has recently announced the relocation of its headquarters to the same research park that is home to the NHMFL.

The NHMFL also hosted a joint international conference with the Japanese National Research Institute of Metals on *High Magnetic Fields: Industry, Materials, and Technology.* Over 100 leading experts explored the applications of medium and high strength magnetic fields on a broad array of current and future industrial processes. The proceedings of the workshop have been edited by Hans Schneider-Muntau of the NHMFL and are being published by World Scientific Company.

Brush Wellman, Cleveland, Ohio

Interactions between Brush Wellman, a copper and alloy firm, and the NHMFL's high pressure diamond anvil group have resulted in new magnet and instrument development activities. The company, Dr. Stan Tozer from the NHMFL, and Prof. Meigan Aronson of the University of Michigan have recently developed and produced a magnetically cleaner form of BeCu. They have found that the new material has a higher conductivity than previously available alloys. The company is also supplying this new alloy in the form of BeCu-clad wire for the NHMFL's pulsed magnet development program.

Cryomagnetics, Inc., Oak Ridge, Tennessee

The NHMFL and Cryomagnetics, Inc. are collaborating to develop a 18-20 T superconducting magnet system for the NHMFL's Ultra-High B/T facility at the University of Florida. The collaboration includes a sharing of magnet design, development, and testing information, along with specific projects focused on joint and impregnation areas.

Deepstar, Houston, Texas

Fourteen oil companies have formed a research and development consortium, Deepstar, to study problems confronting the industry. The NHMFL was approached by Deepstar to organize a research team from the laboratory that has resulted in a grant to the University of Florida to explore magnetic field effects on multi-phase petroleum systems. The NHMFL is also interacting with a subsidiary oil consortium, Deeplook, on technology development opportunities to enhance and identify petroleum in existing U.S. oil fields using magnetic resonance techniques.

Dow Chemical Co., Freeport, Texas

The CRADA with the NHMFL's Pulsed Field Facility at Los Alamos and Dow Chemical continues to mature. This collaborative research focuses on the study of polymer and liquid crystal processing in high magnetic fields. A special furnace has been constructed for polymer processing at temperatures up to 200 °C in a 20 T superconducting magnet system. Measurements being conducted at the DC facilities in Tallahassee at higher fields have confirmed the important impact of high magnetic fields on the synthesis of a new class of strong materials.

DuPont Central Research & Development Experimental Station, Wilmington, Delaware

DuPont, in collaboration with the ICR program at the NHMFL, is concentrating on characterizing the size and shape of isolated gas-phase polymer ions. This experiment is the gas-phase analog of hydrodynamic determinations of frictional coefficients of macromolecules in solution.

EURUS Technologies, Inc., East Hampton, New York

The NHMFL and EURUS Technologies initiated a co-development and testing program for high temperature superconducting (HTS) current leads. The program measures the mechanical, electrical, and thermal properties of a new class of current leads under varying cryogenic conditions. It will culminate in the production of the world's first commercially available 10,000-amp-class, encapsulated, HTS leads, which may be adapted for use in NHMFL and other magnet systems, such as the 45 T Hybrid. The NHMFL will provide EURUS with space at the facility for these joint development activities.

Everson Electric, Allentown, Pennsylvania

Everson Electric and the NHMFL have been working together to develop the insulation and impregnation technology for the 33 double pancakes that will be used to fabricate coil C of the 45 T Hybrid magnet. These double pancakes are cable-in-conduit conductors made from NbTi superconductors. The implementation of the jointly developed insulation and impregnation procedures will be the first time that such procedures have been brought to the production level, which signifies another example of successful technology transfer from government laboratories to U.S. industry.

Handy & Harman, Fairfield, Connecticut

This collaboration focuses on the development of high-strength, high-conductivity wires, and plates for high-field resistive magnets. Advanced processing methods will be tested in consultation with materials scientists from McMaster University who are also closely associated with the NHMFL.

Intermagnetics General Corporation (IGC), Latham, New York

Collaborations on the design of the 45 T Hybrid magnet already have resulted in unique and new manufacturing capabilities for the United States. IGC in cooperation with Gibson Tube developed a manufacturing process to produce world-record lengths of high quality superconducting cable-in-conduit conductors. Presently, IGC is working together with NHMFL to implement the jointly developed impregnation procedures, which is one of the final steps before the Nb_3Sn coils are completed. This collaboration has increased U.S. competitiveness in large magnet systems, e.g., magnet systems responding to the need for the fusion program and superconducting magnetic energy storage devices.

Physical Sciences Inc., Andover, Massachusetts

The development of high frequency pulse electron magnetic resonance (EMR) is one of the greatest challenges in magnetic resonance. This development is hindered mainly by the lack of high frequency sources. The EMR group of the NHMFL recently initiated a collaboration with Physical Sciences Inc. to develop a pulsed gyrotron at high frequency (150 up to 600 GHz) with a very good time resolution in the nanosecond range.

Supercon, Shrewsbury, Massachusetts

The NHMFL and Supercon have established a cooperative program to further develop Cu-stainless steel (CuSS) wire for pulsed magnets. Supercon uses CuSS as electrical feed-through for some glass containers and has made several short lengths of very high strength wire for evaluation.

Varian Associates, Palo Alto, California

The NHMFL and its Center of Interdisciplinary Magnetic Resonance (CIMAR) is a beta test site for a new high temperature superconducting (HTS) probe for NMR spectrometers. The prototype HTS probe is on loan to the laboratory and is the result of a joint

venture between Varian Associates and Conductus Inc. HTS probes are expected to open a wide range of novel applications in solution-state NMR, as the sensitivity, which has been a major source of concern since NMR was discovered fifty-one years ago, increases dramatically. The HTS probe utilizes radio-frequency coils made from the high temperature superconductor YBCO.

Inter-agency & Inter-institutional Activities

These significant collaborations have always played an integral part in the development of the laboratory's unique instrumentation and user facilities. The outstanding and critical human resources that have been recruited to the NHMFL's inter-disciplinary programs also contribute to the success of these endeavors. These collaborations continue to flourish and grow as all faculty and staff are encouraged to pursue new avenues for cooperation and expansion in order to enhance the facilities at the NHMFL.

Department of Defense

The DoD has provided partial support for the development of the new University of Florida Brain Institute (UFBI) including an additional $5 M this year for the development and fabrication of the 12 T, 40 cm bore magnetic resonance imaging (MRI) magnet. This magnet system will be the centerpiece of the NHMFL's MRI/Spectroscopy (MRI/S) facility to be housed at the UFBI. The user facility will be in a new 200,000 sq. ft. building and will provide a variety of MRI/S instruments in support of bio-medical research.

Department of Energy

The Department of Energy and the NSF have established a cooperative program with the Los Alamos National Laboratory and the NHMFL to design and develop the world's first 100 T, 24 mm bore, non-destructive magnet system to be housed at the NHMFL Pulsed Field Facility. Los Alamos has the lead responsibility for the design of the outsert magnet and overall integration of the magnet design and installation. The NHMFL has the lead for the insert magnet design and construction and for providing the 560 MW power supplies.

Department of the Navy & Westinghouse, Pittsburgh, Pennsylvania

The NHMFL will be the test site for the superconducting magnetic energy storage (SMES) device developed by Westinghouse for the Navy. Westinghouse and the Navy are interested in using the laboratory because of its unique testing facilities and its personnel expertise in building large-scale magnet systems, such as the 45 T Hybrid system. The large SMES magnet was developed and built by Westinghouse and is in the process of being shipped to Tallahassee. Upon completion of the testing, Westinghouse will leave behind their magnet-related equipment for use by the NHMFL as a large coil and conductor test facility.

National Aeronautics and Space Administration

NASA and the NHMFL are collaborating on a 0.15 T, 3 KW, 190 mm bore shielded, water-cooled Bitter magnet for crystal growth in zero gravity. The NHMFL has designed and built the unique magnet system that will fly on future shuttle mission flights.

Northeastern University

The electron magnetic resonance (EMR) user facility at the NHMFL represents the culmination of recent worldwide efforts to push EMR beyond its traditional operating range at centimeter wavelengths to the millimeter and submillimeter wavelength region of the electromagnetic spectrum. This thrust has vastly increased the potential of EMR but requires technology significantly different from conventional EMR technology, which remains to be fully optimized. The EMR group of the laboratory and colleagues at Northeastern University recently initiated a collaboration to extend quasioptical methods, developed at millimeter wavelength, and to apply them in the submillimeter range. This research effort will enhance the potential of the EMR facility tremendously.

Sandia National Laboratories, Albuquerque, New Mexico

The NHMFL has been asked by Sandia National Laboratories to provide a series of four coils for a high intensity X-ray radiography experiment. The initial magnets will be modifications of the standard NHMFL designs with an evaluation of a more ambitious 80 to 100 mm bore, 40 T solenoid.

U.S. National Science Foundation—Science & Technology Center for Superconductivity, Illinois

The NHMFL is coupled with the NSF Superconductivity Center through the work of user W.P. Halperin and NHMFL collaborators who are performing very high field NMR experiments on high T_c materials. The ^{17}O NMR lineshape has been used to monitor the vortex phase diagram at fields up to 24 T, which are much higher than any previous studies. The results have shown surprising and unpredicted high field behavior that has important implications in applications of high temperature superconductors.

University of California Directed Research and Development Program

This program sponsored by the University of California State University of System allows opportunities for California system faculty, postdocs, and graduate students to conduct experiments at the NHMFL's unique Pulsed Field Facility at Los Alamos. Campus faculty who have research interests that can be advanced by high fields were invited to submit individual proposals. Seven individual faculty proposals were funded in 1996 at $50,000, and the program is being funded in 1997 at $110,000.

University of Wisconsin, Madison, Wisconsin

The NHMFL's Pulsed Magnet Group is collaborating with the Pegasus toroidal experiment on the design and construction of a pulsed central solenoid for a mini-tokamak device for energizing the confined plasma. Two coils will be approximately 1.5 m long with a bore of 60 mm and generating a field of 14 T; a third planned coil will be at 20 T.

International Cooperation

Collaborations with international organizations have benefited the laboratory in many areas in a relatively short amount of time. The NHMFL senses that international cooperation needs to remain an integral part of facilities development and scientific exchanges. A brief summary of the cooperative programs and areas of cooperation are summarized below.

A.A. Bochvar Institute, Moscow, Russia

The collaborations between the Bochvar Institute and the NHMFL to develop, produce, and deliver advanced high strength, high conductivity wire for use in high field pulsed magnets have been very beneficial for both organizations. A new activity to develop CuSS (stainless steel clad cooper) has resulted in a purchase order from the NHMFL for initial test lengths of this advanced conductor for possible use in the 100 T insert coil. The NHMFL and the Bochvar Institute also have established a complementary cooperative program in further development of low and high temperature superconductors for high field applications. The NHMFL will help focus this collaboration on specific conductor configurations critical to the NHMFL project goals and use the laboratory facilities to test and characterize material produced by the Bochvar Institute.

All Russian Institute of Experimental Physics, Arzamas-16

Scientific exchanges between the Russian Institute, LANL, and NHMFL culminated in a series of broad-based experiments in the 1000 T regime known as the *Dirac Series*. With the cooperation of the Los Alamos Dynamic Experimentation Division and scientists at Arzamas-16, almost a dozen flux compression generators capable of producing these ultra-high fields allowed a team of international scientists to explore solid-state physics in new regimes. These collaborations will continue with at least three series of experiments at LANL in 1997.

CNRS/MPIF High Field Magnet Laboratory, Grenoble, France

This multi-year cooperation addresses the development of resistive magnets and housings with particular emphasis on magnets for 24 MW power supplies. The two laboratories have established a joint development project and are building 20 T, 200 mm bore magnets with minor variations for their respective facilities. The fabrication of parts is a collaborative effort with each of the laboratories making half of the parts and shipping them to each other. Each laboratory will assemble their magnet, and the system for the Tallahassee laboratory is expected to be commissioned in late summer 1997.

European Community 100 T Pulsed Magnet Joint Development Committee

The NHMFL and representatives of the European Community met twice this year and established an international committee to oversee the joint program to explore avenues for cooperation, sharing data, and testing for the development of non-destructive 100 T pulsed magnet systems. The international committee will generally provide a forum for establishing cooperation in magnet research and development for the participating countries. The committee selected N. Miura, Institute for Solid State Physics, University of Tokyo, as the chair. The committee also agreed to meet at least once a year in conjunction with a major international magnet conference. The committee will meet next in August 1997 at the Fifth International Symposium in Research at High Magnetic Fields in Sidney, Australia.

High Magnetic Field Laboratory, Institute of Plasma Physics, Academia Sinica, Hefei, China

The NHMFL and the high field magnet laboratory at Hefei continue to collaborate under a 1995 Memorandum of Understanding that enhances the scientific and engineering capabilities at both facilities. Specifically, collaborations are focused on the design of resistive and hybrid magnets, development of new high power density and high stress level Bitter plate geometries, and the development of a 45 T, 2 second flat top, quasi-continuous, water cooled magnet for the Hefei laboratory.

Institute of Low Temperature Physics & Engineering, National Academy of Sciences, Ukraine

Collaborations are continuing between the Institute's group working on the low temperature properties of cryocrystals and the thermodynamic measurements and the University of Florida scientists using NMR to study the microscopic dynamics.

National Pulse Magnet Laboratory, University of New South Wales, Sidney, Australia

The NHMFL is producing a class of 50 T pulsed magnets for this Australian laboratory. The National Pulse Magnet Laboratory is interested in purchasing a regular supply of the newly developed pulsed magnets, citing the reliable and predictable performance and quality control of the NHMFL magnets at the Pulsed Field Facility.

National Research Institute for Metals (NRIM), Tsukuba, Japan

The NHMFL and NRIM have entered into a cooperative program for the Florida laboratory to build a 30 T resistive magnet as the first such class of magnets for the Japanese facility. Collaborative activities continue to proceed on developing higher strength and higher conductivity plates and wire for our resistive and pulsed field magnet programs. NRIM has funded an extensive visitors program to the benefit of both laboratories.

Royal Holloway College, University of London

Researchers at the University of Florida are collaborating with the Royal Holloway College's Millikelvin Laboratory on two-dimensional quantum nuclear magnets. The English scientists are planning cooperative experiments at the NHMFL's new high B/T facilities at the University of Florida.

University of Manchester, England

Researchers from England will use the NHMFL's ion cyclotron resonance facilities to determine the mechanism of fragmentation and rearrangement reactions of peptides.

University of Queensland, Australia

The two groups have been collaborating on the use of nanoscale particle inclusions into high temperature superconducting tapes. A research team at Queensland are experts in the synthesis of such particles who have produced extremely high-quality, ultrafine MgO powder. NHMFL scientists have incorporated their MgO powder into BSCCO tapes and have demonstrated significantly improved superconducting properties.

EDUCATION PROGRAMS

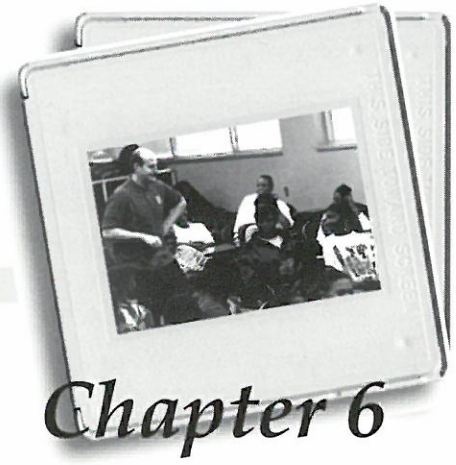

Chapter 6

Students in the State of Florida and throughout the United States lag far behind international standards for literacy in science and mathematics. This shortfall has ominous implications for the technology-based global economy of the 21st century, and it demands solutions that integrate state, federal, business, school, and institutional resources [1996 National Academy of Sciences, National Science Education Standards, 227-230, (1996)]. The NHMFL—a model federal-state partnership with well-established links to industry and academia—is in a position to stimulate public awareness and interest of science and mathematics by utilizing its unique strengths—world-class research facilities and human resources (i.e., leading scientists and engineers)—to develop educational programs for students at all academic levels. As an institutional citizen of the local community, state, and nation, the NHMFL strives to be an active contributor to enhancing science education, especially for underrepresented populations.

K-12 Programs

The NHMFL has instituted a myriad of K-12 educational programs and activities that foster scientifically literate citizens for the 21st century by actively engaging students, parents, and teachers.

Figure 1. Nearly 10,000 visitors explored the Tallahassee facilities to learn about the laboratory and to enhance their understanding of science.

Educational Tour Program

Our educational tour program has continued to grow and expand under the direction of a science educator, Sam Spiegel, who joined the laboratory in 1996 to refine and extend our K-12 education programs. The educational tour program targets two main audiences: K-12 students and teachers, and the general public. Our educational tours include a lecture with demonstrations, an overview providing a general grounding in the science and technology of the NHMFL, and a guided tour of the facilities. In 1996 *approximately 3955 K-12 students*, and *5939 members of the general public toured the laboratory*. For comparison, in 1995 we toured slightly over 700 students.

Open House

The 3rd Annual Open House held on October 12 attracted a record number of visitors—1,570; over 800 of these guests were first-time visitors to the NHMFL. During the Open House, interactive displays, demonstrations, hands-on activities, special information packages, and a large percentage of the NHMFL faculty and staff were available to orient members of the regional community to the work and mission of the NHMFL. The strongest criticism we received for the event was that there wasn't enough time to explore all the interesting facets of the laboratory in one day!

Figure 2. Students, parents, and teachers gather around the "cryo-brew" to learn about the sweeter side of science during our 3rd Annual Open House. Ice cream samples were enjoyed by all.

Outreach Program

A newly created aspect of our K-12 efforts is the outreach program. This program brings the science and resources of the laboratory to schools, allowing us to extend the NHMFL's educational involvement with young people. Through a series of presentations and workshops, such as "What Does a Scientist Do?"; "Magnets—What's the Attraction?"; and "What's a Matter—Molecules, Resistance, and Superconductivity", the NHMFL has *challenged over 3,142 young students* in 1996 to "look, think, ask, and solve" as they explore the magnetic world around them through science.

Middle School Mentorship Program

Our middle school mentorship program had a second consecutive successful year. For a whole semester, *twenty-four local students* spent one morning each week at the laboratory working with a scientist-mentor on a project. Their results were given at a poster presentation session that received extensive publicity in the community. The impact of this program on the students is as impressive as the students' projects. As one parent stated, "My daughter entered the program hesitantly, but after the first week she was so enthralled that she is now considering a career in computers or science. Thank you!" The students' projects included building a heat pump system, conducting NMR experiments, and developing instructional computer programs for elementary students.

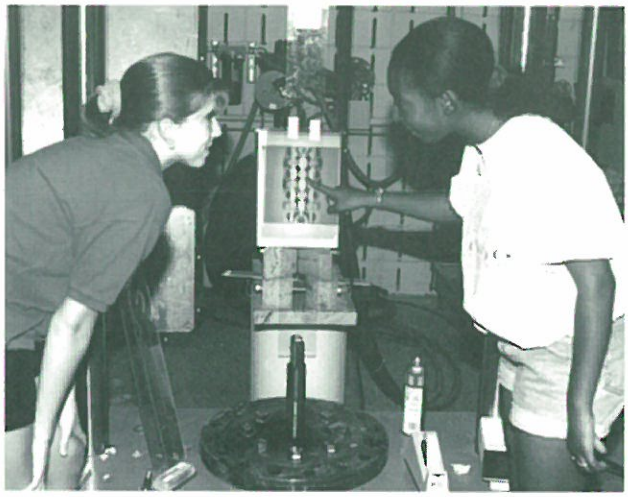

Figure 3. Mariah Jensen and Kendra Lewis, middle school students participating in our mentorship program, examine the results of their research.

Externships for High School Students

A parallel program providing externships for local high school students gave *thirty-five students* the opportunity to work alongside scientists in their laboratories after school for a semester to earn credit. The students spent a minimum of 300 hours at the laboratory during their externship. One of our goals is to encourage young women and

minorities to pursue advanced science and mathematics studies, thereby stimulating parallel career options. In this program, over 70% of these students were female and approximately 50% represented minorities. Several of these students continue to work at the laboratory with their mentors.

NHMFL Ambassador Program

In Fall, 1996, the first meeting of the NHMFL Ambassador Program was held. The NHMFL Ambassadors serve as liaisons between area school communities and the laboratory. Each school in the surrounding three counties has been invited to join this program, and we currently have about 75% of the schools participating. Specifically, the ambassadors serve in an advisory role to the NHMFL K-12 Education Programs, helping us to identify and define ways that we can work together to promote the teaching and learning of science and mathematics. They are also important contact persons who disseminate information to the school communities. The NHMFL Ambassadors meet twice each year (in the Fall and Spring) to discuss needs and strategies for promoting science and mathematics education.

Teacher In-Service Initiatives

Teacher in-service initiatives offer the NHMFL important avenues through which the laboratory may address a critical need in teacher education. NHMFL staff have been conducting workshops with teachers on the improvement of science, mathematics, and technology education. Teachers have received training at the lab, at schools, and at conferences such as the Florida Educational Technology Conference.

STAR TREE Program

In the summer of 1996, the NHMFL initiated the STAR TREE program (Science Teachers and Researchers Translating Research Experiences into Educational Materials). Nine master middle school science teachers came to the NHMFL and worked alongside NHMFL scientists, educators, and staff. In a few short months, they produced a comprehensive program of prototype middle school materials that guides educators and students to a greater understanding of science and mathematics through the study of magnetism and related concepts. These prototypes include:

- twenty-five hands-on, issue-based student activities;
- a video program;
- a website (*http://k12.magnet.fsu.edu/*);
- a 100-page teacher resource manual; and
- a computer program.

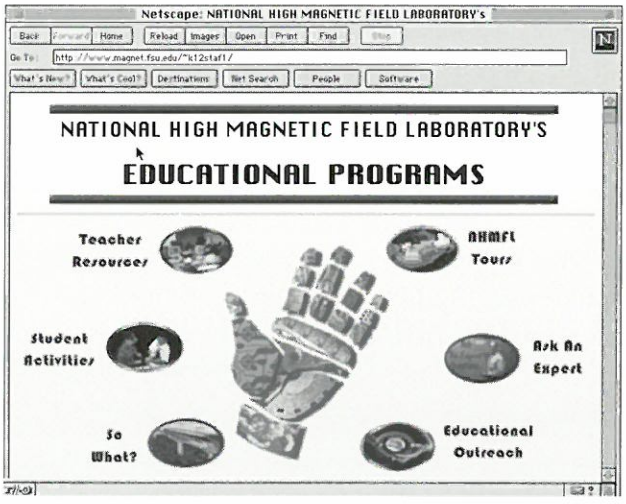

Figure 4. Our K-12 website provides links and resources for teachers, parents, and students of all ages and from around the globe.

These products are presently being field tested, and we are seeking additional funding from the Florida Department of Education to complete product development and to implement a training protocol that integrates this curricula into middle schools across Florida. We anticipate their widespread use in the state and hope to expand the initiative nationwide.

"Ask an Expert" on the Web

One new aspect to our web site is the *Ask an Expert* link. This allows students of all ages from around the world to ask questions of the scientists and experts at the NHMFL. Since its posting in September 1996, we have received requests from as far west as California and Washington State, through the midwest states, up to New England, and from numerous local schools. Requests have come from students at all age levels from several six year olds through a few geriatrics. There seems to be a lot of interest lately about projects evolving around the effect of magnetic fields on plants.

Interactive Curriculum Products

The laboratory is also developing interactive curriculum products that utilize a variety of delivery formats. One example is a virtual tour of the NHMFL, which will be available through our web site, in a CD-ROM version, and possibly in a video-based version. These products will allow students to explore the magnet laboratory and its resources and to investigate a variety of related scientific concepts and careers. We are in the process of developing strategies to incorporate a component that will allow students to actually run a magnet and gather and analyze data through these resources.

Educational Resource Laboratory

In conjunction with the State of Florida we have developed a new teacher/student Educational Resource Laboratory. The state-of-the-art laboratory houses multimedia development equipment, manipulative development equipment, curriculum materials, and instructional resources. It is intended for use by educators, students, and NHMFL personnel, and already it has become a popular instructional and development resource for regional schools. During open hours, teachers can come to the Laboratory to develop a new interactive multimedia program; to desktop publish student

Figure 5. Our curriculum development projects received significant attention from the education community and local media groups. Lloyd Graham, a local middle school student who helped in the development of our prototype products, is discussing the development process with a local television news reporter.

materials; to create quicktime movies and video clips; to preview a variety of curriculum products such as those produced by other classroom teachers, Tom Snyder Productions, and Optical Data. Additionally, teachers can schedule classes for small groups of teachers or students to learn about the development or integration of multimedia into their classroom. Some of the projects developed in the laboratory include the following:

- Students and teachers from local "critical needs" elementary schools have created tutorial programs for other students at their schools.

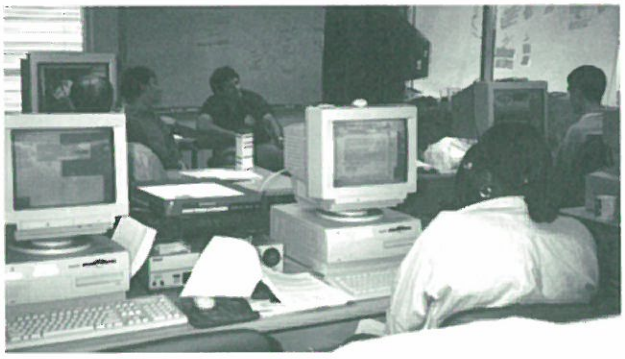

Figure 6. Teachers using the Educational Resource Laboratory have developed new resources for their classes while learning new strategies and skills to enhance the teaching and learning of science.

- Local high school students are using the laboratory to develop an instructional program for middle schools students about preventing, diagnosing, and treating skin cancer.

Education Partnerships and Community Support

The NHMFL has begun to develop partnerships with a variety of agencies and groups interested in enhancing science and mathematics education. For example, we have developed partnerships with the Tampa Museum of Science and Industry, Odyssey Science Museum of Tallahassee, and the Orlando Science Center to design and develop interactive traveling and permanent exhibits.

Additionally, members of the NHMFL have contributed countless hours of community support through services such as judging science fairs, serving on education boards and committees, mentoring students through Big Brother and Sister organizations, October Fix with the Tallahassee Housing Foundation, Rotary Summer Camp for special needs children, and so forth.

Nearly every member of the NHMFL faculty and staff participates in some way in the NHMFL's K-12 education efforts. The K-12 Education Program is continuously evolving, as new ideas and opportunities to promote science and mathematics arise. We are striving to develop the program as a collaborative effort by integrating the expertise, facilities, and strengths of various interested parties.

Undergraduate Programs

Minority/Women Summer Research Internship Program

For the fourth consecutive year, the NHMFL sponsored its Minority/Women Summer Research Internship Program. Applications for the 1996 program increased by 270% and came from twenty-seven states, the U.S. Virgin Islands, Washington, DC, and Puerto Rico. Sixteen undergraduate students accepted offers and participated in the program at one of the three consortium sites. Of these students, ten were women and six were men, which is a marked change from 1995, when only one in ten was a woman. One of the interns worked with a condensed matter experimentalist, James Brooks, and is listed as a second author on a paper to be published in "Application of High Magnetic Fields in Semiconductor Physics" (World Press, 1997).

Figure 7. Our Minority/Women Summer Research Internship Program has seen a significant increase in the number of women applicants and participants.

NSF Alliances for Minority Participation Student Research Conference

The NHMFL and Florida A&M University co-hosted the Fourth Annual NSF Alliances for Minority Participation (AMP) Student Research Conference during the summer of 1996. Over 150 college students from throughout the United States and Puerto Rico, along with AMP project directors and NSF officials, attended the three-day conference in Tallahassee. The

students' research posters and presentations were judged by local faculty; distinguished lectures were given by Nobel Laureate Dr. Robert Schrieffer and former astronaut and professor Dr. Norm Thagard; and an afternoon was spent at the NHMFL learning about magnet-related research and technology and touring the laboratory.

NSF National Chautauqua Short Course

The NHMFL offered a new course for college science teachers as part of the NSF's National Chautauqua Short Course Program. Entitled "Magnetic Fields in Science and Technology," the presentations to twenty-one educators focused on the generation of magnetic fields, the application of magnet technology, and various magnetic resonance techniques. A follow-on to this course will be offered in July 1997.

Vocational Programs

This year cooperative programs were reactivated with two regional vocational and technical schools. Students from Lively Vo-Tech worked in the electrical program, and we have arranged with Thomas Technical Institute to have vocational students work in Facilities (using AutoCad engineering software) and in Electronics Instrumentation. The cooperative program with Thomas Tech should serve to reinvigorate our vocational programs next year.

SEMINARS, WORKSHOPS & CONFERENCES

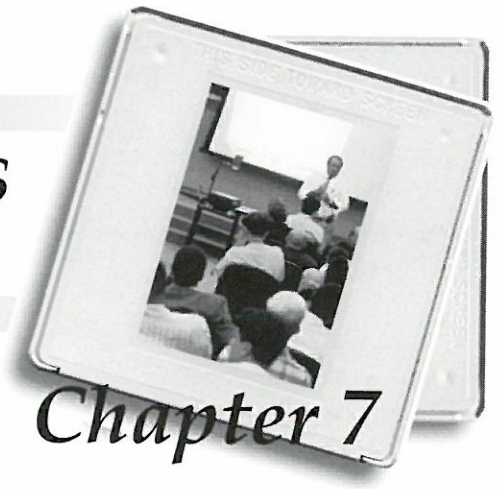

Chapter 7

Seminars

The seminars, workshops, and conferences listed in this section were held at the NHMFL in Tallahassee, unless otherwise noted. Recurring affiliations are abbreviated as follows: Magnet Science and Technology Group—MS&T; Center for Interdisciplinary Magnetic Resonance—CIMAR; Condensed Matter/Theory Group—CM/T.

January 2, 1996
Doug Scalapino
University of California
Cu - O Ladders

January 8, 1996
Hans Schneider-Muntau
NHMFL/MS&T
Program and Goals, The Next Five Years

January 9, 1996
Erwin Mueller-Hartmann
University zu Koln - Germany
Ferromagnetism in Hubbard Models

January 9, 1996
John Weisend
DESY
Cryogenics for TESLA & the TESLA Test Facility

January 9, 1996
Scott A. Smith
NHMFL/CIMAR
Relaxation in GAMMA

January 9, 1996
Frank Wilczek
Institute for Advanced Study
Possible Ordering for Mott Insulators

January 11, 1996
Scott A. Smith
NHMFL/CIMAR
Relaxation in GAMMA

January 11, 1996
Michael Gross
Washington University
Applications of Tandem Mass Spectrometry: Metal Ion-Peptide Interactions and Carcinogenesis Mechanisms

January 12, 1996
S. Lance Cooper
University of Illinois
Unconventional Charge Dynamics in Kondo Insulators and C-Axis $YBA_2Cu_3O_{6+x}$

January 18, 1996
Benoit Boulat
NHMFL/CIMAR
Application of Floquet Formalism in NMR

January 18, 1996
Albert Migliori
Los Alamos National Laboratory
Magnetically Enhanced Thermoelectric Cooling

January 18, 1996
Helmut Schwarz
University of Berlin
Probing Enzyme-Related Oxygenations by Gas-Phase Experiments

January 22, 1996
John Austin
Sun Micro
Sun Technology Transfer Day

January 23, 1996
Riqiang Fu
NHMFL/CIMAR
Averaging of Second Order Quadrupolar Interaction

January 23, 1996
Joao Paulo Leal
Lisbon, Portugal
Gas-Phase Lanthanide Ion-Molecule Chemistry

January 25, 1996
Joel B. Thompson
Eckerd College
The Role of Synechococcus in the Precipitation and Fractionation of Carbonate Minerals in Aquatic Whiting Events and Microbialites

January 26, 1996
James W. Allen
University of Michigan
Fermi Liquids and Non Fermi Liquids - The View from Photoemission

January 26, 1996
Bennett B. Goldberg
Boston University
Characterization of Materials and Devices by Near Field Optical Scanning Microscopy

January 29, 1996
Iain Dixon
NHMFL/MS&T
Stress Analysis of Superconducting Coils Using Finite Elements

January 29, 1996
Denis Markiewicz
NHMFL/MS&T
Field Uniformity in Solenoid Magnets: Garrett Formulation

January 30, 1996
Benoit Boulat
NHMFL/CIMAR
Algebraic Formulation of the Product Operator Formalism in the Numerical Simulation of the Dynamic Behavior of Multispin Systems

January 30, 1996
Yoshiaki Tanaka
Tsukuba Magnet Laboratories
Bi2223 Tapes Prepared with AgCu Alloy Sheaths

February 6, 1996
Geoffrey Bodenhausen, *et al.*
NHMFL/CIMAR
Impressions of European NMR

February 7, 1996
Jamil Tahir-Kheli
California Institute of Technology
Inter Band Theory of Superconductors: Resolution of Observed S and D-Wave Tunneling with Isotropic S-Wave Pairing

February 8, 1996
Carolyn Ruppel
Georgia Institute of Technology
The Siberian Proto-Atlantic(?): Passive Rifting in the Baikal Rift Zone

February 12, 1996
Christian Wolters
NHMFL/MS&T
Synthesis of Hg Based High Temperature Superconductors

February 12, 1996
Krishna Iyengar
NHMFL/MS&T
Cooling of Cryogenic Supports

February 16, 1996
Subir Sachdev
Yale University
Finite Temperature Crossovers Near Quantum Critical Points: Application to Ferromagnets

February 16, 1996
Martin Rohrer
Free University of Berlin
EPR and ENDOR at 95 GHz: Anisotropic Hyperfine Structure and Spin Relaxation of Organic Radicals

February 19, 1996
Robert Walsh and Leonard Summers
NHMFL/MS&T
316LN: An Old Steel Gets a New Life

February 20, 1996
Philippe Pelupessy
NHMFL/CIMAR
ESR Spectroscopy

February 22, 1996
Scott Hannahs
NHMFL
Bibliographic Databases - Inspect and Biosys Introduction

February 22, 1996
Marc Hirschmann
University of North Carolina
Role of Pyroxenite in Basalt Petrogenesis

February 23, 1996
H.A. Mook
Oak Ridge National Laboratory
Neutron Scattering from High-Temperature Superconductors

February 26, 1996
Kathleen Amm
NHMFL/MS&T
Growth of Bulk Hg-Ba-Ca-Cu-O on Metallic Surfaces

February 27, 1996
Donald Hirsh
Washington University, St. Louis
Solid State NMR

March 1, 1996
Gene Bickers
University of Southern California
Self-Consistent Diagrammatic Calculations for Models of Correlated Electrons

March 4, 1996
Luguang Yan
Member of the Chinese Academy of Sciences
Recent Progress of Applied Superconductivity in China

March 5, 1996
Donghui Wu
The University Of North Carolina at Chapel Hill
Pulsed Field Gradient NMR and Its Applications

March 8, 1996
Gabriel Aeppli
NEC Research Institute, Inc.
Very Short and Very Long Magnetic Coherence Lengths in a High-T_c Superconductor

March 9, 1996
Major General Robert Dickman
U.S. Department of Defense
U.S. Space Program Overview

March 11, 1996
Mohammad Reza Vaghar
NHMFL/MS&T
Closed Form Solutions for Elastoplastic Behavior of Superconducting Coils

March 11, 1996
Paul Pernambuco-Wise
NHMFL/MS&T
Fiber Composites in Pulse Magnet Construction

March 12, 1996
Philippe Pelupessy
NHMFL/CIMAR
The Use of Trajectories for Describing Electron Spin Echo Experiments

March 13, 1996
M.-H. Whangbo
North Carolina State University
Structural and Electronic Instabilities of Transition Metal Oxide and Chalcogenide Metals

March 18, 1996
Maxwell Godfrey
NHMFL/MS&T
Insulation for HTS Conductors

March 25, 1996
Yusuf S. Hascicek
NHMFL/MS&T
Innovative Approaches to HTS Magnet Technology: In-Situ Lorentz Force Straining of HTS Conductors Up to 30 Tesla

March 25, 1996
Soren Prestemon
NHMFL/MS&T
A Spectral Method for Flows with Two Inhomogeneous Directions

March 25, 1996
Karen Hallberg
Max-Planck Institute for Physics of Complex Systems
Density Matrix Algorithm for the Calculation of Dynamical Properties of Low Dimensional Systems

March 26, 1996
E.W. Randall
Queen Mary and Westfield College, London, UK
NMR Imaging in Stray Fields: From Basics to the Latest Results

March 26, 1996
Kay Mehr
Materials Engineering Department
Texture Analysis of Superplastically Biaxially Deformed Aluminum Lithium (80%) Alloy

March 28, 1996
Ago Samoson
Uppsala University, Estonian Academy of Science, Estonia
Experimental Results Obtained at NHMFL Using DOR Techniques

March 28, 1996
Jennifer A. Lewis
University of Illinois at Urbana-Champaign and NSF Science and Technology Center for Superconductivity
Magnetic Field/Liquid Assisted Texturing (MFLAT) of $YBa_2Cu_3O_{7-x}$ Thick Films

April 1, 1996
Sylvain Boutemy
NHMFL/MS&T
Optimization of BiSCCO 2212 Heat Treatment for Coils

April 1, 1996
Earle Burkhardt
NHMFL/MS&T
Stability of Ag/BSCCO Superconducting Tapes Using the Finite Element Method

April 2, 1996
Geoffrey Bodenhausen, *et al.*
NHMFL/CIMAR
ENC Reminiscences I

April 4, 1996
Naotuki Amemiya
Yokohama University
Current Re-Distribution in Multi-Strand Superconducting Cable

April 4, 1996
Geoffrey Bodenhausen, *et al.*
NHMFL/CIMAR
ENC Reminiscences II

April 8, 1996
John Miller
NHMFL/MS&T
Critical Components for the 45-T Hybrid I. Requirements & Specifications

April 8, 1996
G.E. Miller and W.J. Kenney
NHMFL/MS&T
Critical Components for the 45-T Hybrid II. Development & Test

April 9, 1996
Geoffrey Bodenhausen, *et al.*
NHMFL/CIMAR
ENC Reminiscences III

April 10, 1996
Soren Grabowski
Freie Universitat Berlin
Short Range Order in the Cuprates: Normal and Superconducting State

April 12, 1996
Werner Hanke
University of Wurzburg
Quantum-Monte-Carlo Simulations of High–T_c Superconductors

April 12, 1996
Kiyoshi Inoue
NRIM
High Field Magnet Materials in Development at NRIM: Nb_3Al and CuCr

April 15, 1996
Frank Heringhaus
NHMFL/MS&T
Dissection of the Electrical Conductivity of High-Strength Composites

April 15, 1996
Xiaodong Huang
NHMFL/MS&T
Dynamic Study of Heat and Mass Transfer in Vapor/Superfluid Helium

April 16, 1996
Johannes Huth
NHMFL/CIMAR
Spectral Editing and Strong Coupling Effects in Selective Correlation Spectroscopy

April 17, 1996
Yung Woo Park
Seoul National University
Thermoelectric Power of High–T_c Superconductors

April 22, 1996
Branko Berkes
Magnet Consulting Services
SENTRON Hall Probes for Scientific and Research Institutions

April 23, 1996
Guy D. Gilliland
Emory University
Type-II Nanostructures: Excitons and Interfaces

April 23, 1996
Isabella Felli
NHMFL/CIMAR
The NMR Solution Structure of a Paramagnetic Protein

April 24, 1996
Vinay Ambegaokar
Cornell University
Superconductivity in Small Grains: Effect of Number Parity

April 26, 1996
M.R. Beasley
Stanford University
Vortices in Two-Dimensional Superconductors - Lessons Learned, Lessons Unlearned, and Lessons Yet to be Learned

April 29, 1996
Tom Painter and Vince Toplosky
NHMFL/MS&T
45 T Hybrid Outsert Coil Assembly: Components and Procedures

April 30, 1996
Timothy M. Logan
NHMFL/Florida State University
NMR Characterization of Unfolded Proteins

May 3, 1996
Aleksander Wittlin
Max-Planck Institute für Festkörperforschung
Far-Infrared Magneto-optical Properties of $La_{1-x}Sr_xCu0_4$

May 3, 1996
Qimiao Si
Rice University
Non-Fermi Liquids in a Lattice of Anderson Impurities

May 7, 1996
Naresh Dalal
Florida State University
Proton Glasses and Their Characterization by EPR Spectroscopy I

May 10, 1996
James Jorgensen
Argonne National Laboratory
Structural Optimization of Transition Temperature and Flux Pinning in High–T_c *Superconductors*

May 13, 1996
Chandra Varma
AT&T Bell Laboratories
Properties of a General Model of Copper Oxides

May 13, 1996
Justin Schwartz
NHMFL/MS&T/FAMU-FSU CoE
Status and Directions in High–T_c *Superconductivity*

May 13, 1996
Saco Nakamae
NHMFL/MS&T
Magnetothermal Conductivity of Bi2212 Bulk Superconductor

May 14, 1996
Yoshi Fukumoto
Kobe Steel
Detailed Voltage - Current Characteristics of Bi2212 and Bi2223/Ag Tapes

May 14, 1996
Naresh Dalal
Florida State University
Proton Glasses and Their Characterization by EPR Spectroscopy II

May 16, 1996
Gang Cao
NHMFL
The Physics of Bad Metals: The Study of Ruthenates

May 16, 1996
William White
Cornell University
Chemical Geodynamics

May 17, 1996
Sang-Soo Oh
Korean Electrotechnology Research Institute
Research Activities on Applied Superconductivity at the Korean Electrotechnology Research Institute

May 17, 1996
Ian Affleck
University of British Columbia
The Kondo Screening Cloud

May 20, 1996
Huub Weijers
NHMFL/MS&T
HTS Coil Development in the Delta B Program

May 20, 1996
Karen Harris
NHMFL/MS&T/MARTECH
Orientation Imaging Microscopy in the ESEM

May 21, 1996
Sven Rogge
Bell Labs
Evidence for the Importance of Interactions Between Active Defects in Glasses

May 24, 1996
Naomichi Hatano
Harvard University
Localization in Non-Hermitian Quantum Mechanics and Flux-Line Depinning in Superconductors

May 31, 1996
Matt Brenneman
NHMFL/CIMAR
Characterization of Secondary Structure Using Solid State NMR

May 31, 1996
George Martins
NHMFL/CIMAR
ESR of Gd^{3+} and Er^{3+} in $Pr_{2-x}Ce_xCuO_4$

June 3, 1996
Yang Ren Sun
NHMFL/MS&T
Anisotropy Studies on Aligned $HgBa_2CaCu_2O_{6+x}$ Powder

June 3, 1996
Wangshui Wei
NHMFL/MS&T
Nanosize Particle Addition to the $Bi_2Sr_2CaCu_2Ox$ Superconductor

June 4, 1996
Geoffrey Bodenhausen, *et al.*
NHMFL/CIMAR
Reminiscences of the European ENC

June 8, 1996
Karen A. Veverka
Mayo Foundation
Inhibition of Aldehyde Dehydrogenase by Disulfiram and Metabolites

June 10, 1996
Rainer Meinke
Advanced Magnet Laboratory
Helical Dipole Magnets Using Advanced Manufacturing Technology

June 11, 1996
Jack Troxell
SCM Products
Glidcop Nb Composites

June 13, 1996
Anatoly Frenkel
New Mexico Highlands University
HTS Materials and Devices Studied by Ultrafast Optical Spectroscopies

June 17, 1996
Robert B. Moore
McGill University
Quadrupole High-Pressure Ion Guide for ESI FT-ICR MS

June 18, 1996
Michael Salib
SUNY at Buffalo
What is Optically Detected Resonance (ODR)?: A New Look at Hydrogenic Complexes and Other Excitations in Quasi-Two-Dimensional Systems

June 20, 1996
Geoffrey Bodenhausen, *et al.*
NHMFL/CIMAR
NMR

June 21, 1996
Ziqiang Wang
Boston University
Hubbard Model, Spin Chains, and the Quantum Hall Effect

June 24, 1996
Loc Vu-Quoc
University of Florida
Analysis of Advanced Multilayer Capacitors

June 27, 1996
Benoit Boulat
NHMFL/CIMAR
Dynamic Origin of Geometric Dephasing in NMR/NQR

July 1, 1996
Pierre Mutzenhardt
NHMFL/CIMAR
Radiofrequency Gradient Pulses in NMR: "What Can We Do with a Single Turn Coil?"

July 1, 1996
Scott Bole
NHMFL/MS&T
Structural Design of a 33 Tesla Magnet

July 1, 1996
Mark Bird
NHMFL/MS&T
Development of Florida Bitter Magnets at the NHMFL

July 8, 1996
Scott Marshall
NHMFL/MS&T
An Overview of the NHMFL 900 MHz Nb_3Sn Coil Fabrication Process

July 8, 1996
Chuck Swenson
NHMFL/MS&T
Development Issues for 900 MHz Nb_3Sn Coils

July 11, 1996
Jose Riera
Universidad Nacional de Rosario, Argentina
A Heisenberg Model for the Spin-Peierls System $CuGeO_3$

July 15, 1996
David Hilton
NHMFL/MS&T
Circumferential Tensile Stress-Strain Characterization of Silver and Silver Alloys with Applications to HTS Tapes

July 15, 1996
John Panek
NHMFL/MS&T
Heat and Mass Transfer in Two-Phase Helium II

July 18, 1996
Riqiang Fu
NHMFL/CIMAR
Frequency Modulation Techniques in Rotating Solids

July 19, 1996
Bruce Robinson
University of Washington
Sequence Dependent Dynamics of Duplex DNA As Seen by EPR

July 22, 1996
Warren Henry
Howard University
High Magnetic Field Research, 1948 - 1970

July 29, 1996
Steve W. Van Sciver
NHMFL/MS&T/FAMU-FSU CoE
Realization of a 10^7 Reynolds Number Helium Flow Facility

August 6, 1996
Riqiang Fu and Philip Pelupessy
NHMFL/CIMAR
Reminiscences of the 38th Rocky Mountains Conference NMR Symposium

August 12, 1996
Li-Ye Xiao
NHMFL/MS&T
Intrinsic Stability of High T_c Superconducting Tapes Including the Effect of Anisotropic J_c

August 12, 1996
Phillip Shoaff
NHMFL/MS&T
A Further Investigation of the Characterization and Development of HTS Joints in BSCCO 2212/Ag Composites

August 12, 1996
David Peyrade
NHMFL/MS&T
Critical Current Density Measurements on High–T_c Superconductors

August 12, 1996
Sabine Astie
The Institute of National Applied Science in Toulouse, France
Quench Simulation Magnetic and Thermal Diffusion in Coupled Solenoidal Magnet System

August 13, 1996
Bailin Hao
Institute of Theoretical Physics, Chinese Academy of Sciences
Counting the Number of Periodic Orbits in Chaotic Systems

August 19, 1996
Oscar Hill
NHMFL/MS&T
The Status of Experimental Quench Initiation and Propagation Studies at the NHMFL

August 19, 1996
Neil Bednar
NHMFL/MS&T
An Overview of Materials Characterization at NHMFL

August 20, 1996
Riqiang Fu
NHMFL/CIMAR
Frequency-Modulated Cross Polarization for Fast Magic Angle Spinning NMR at High Fields

August 30, 1996
Herman Cho
Pacific Northwest Laboratories
Solid State NMR Spectroscopy at the Environmental Molecular Sciences Laboratory

September 1, 1996
Yasuhide Naito
University of Manchester, England
Mechanisms for Collisionally Activated Cleavage of Gas-Phase Peptides

September 1, 1996
Bruce Reinhold
Boston University
Mass Spectrometric Determination of Oligosaccharide Sequence and Linkages

September 3, 1996
Ülker Onbasli
University of Marmara, Istanbul, Turkey
Investigations on the Aging Effect of Mercury Cuprate Superconductors with T_c of About 138 K

September 4, 1996
Masanori Arata
NHMFL/MS&T
Maglev Train R&D Status

September 6, 1996
Damien Jeannerat
NHMFL/CIMAR
Deconvolution in DQF-COSY Spectrum: Effect of Strong-Coupling Between Hetero Nuclei in 1H DQF-COSY Experiments

September 9, 1996
Bruce Amm
NHMFL/MS&T
Mechanical Properties of BSCCO/AgX Composite Superconductors

September 9, 1996
Christian Wolters
NHMFL/MS&T
Hg-Superconductors and Marble Cake

September 9, 1996
Andrzej Sienkiewicz
Institute of Physics, Polish Academy of Sciences, Warsaw, and SUNY at Albany
Novel Sensitive Microwave Resonant Structures and Their Applications in Biophysics and Biochemistry

September 10, 1996
Brian Cutting
NHMFL/CIMAR
Topics on QUIET-BIRD-NOESY Using Eggenberger's Notation

September 13, 1996
Geoffrey Bodenhausen, *et al.*
NHMFL/CIMAR
Review of Two Years of NMR at the NHMFL

September 13, 1996
Steven Blackband
University of Florida
Cryoprotectant Permeation Into Zebrafish Embryos Using Chemical Shift Selective MR Microscopy

September 13, 1996
Alexander Balatsky
Los Alamos National Laboratory
Impurity States in s- and d-Wave Superconductors

September 17, 1996
Peter Hirschfeld
University of Florida
Transport in the Superconducting State of Cuprates

September 19, 1996
Pierre Mutzenhardt
Nancy, France
1. Clean Editing and Relaxation Effects in QUIET-BIRD-NOESY Experiments
2. Refocalization in Single and Double Pulse Gradient Echo Experiments

September 20, 1996
Yuri Kagan
Kurchatov Institute - Moscow
Kinetics of the Bose Condensate Formation in Interacting Gases

September 23, 1996
Wangshui Wei
NHMFL/MS&T
Preparation and Properties of the Nanosize TiO_2 and MgO Doped $Bi_2Sr_2CaCu_2O_X$

September 23, 1996
Bob Walsh
NHMFL/MS&T
Lorentz Force Simulation Tests on Hybrid Dummy A Coil

September 24, 1996
Parmeswar Hari
University of Utah
High Field NMR Studies of Arsenic Compounds

September 26, 1996
Frank Wong
MIT/DoE
An Overview of the ITER Magnet Design and R&D

September 27, 1996
Kevin Bedell
Boston College
A Local Fermi Liquid in a High Magnetic Field

September 30, 1996
Friedrich Haug
CERN
Cryogenics at CERN: An Overview on Current and Future Applications

October 1, 1996
Girsh Blumberg
NSF Science and Technology Center for Superconductivity and University of Illinois at Urbana-Champaign
Electronic Raman Scattering in Cuprate Insulators and Doped Superconductors

October 1, 1996
Sasha Gerber
Tel Aviv University
Magnetoresistance of Granular Ferromagnets

October 2, 1996
Serguei Brazovskii
L.D. Landau Institute for Theoretical Physics
Vortex Dynamics and Melting in Layered Superconductors: Theory Versus NMR Experiments (in Organic and High-T_c Materials)

October 7, 1996
Paul Pernambuco-Wise
NHMFL/MS&T
Composites Reinforcement Schemes for Pulse Magnets

October 7, 1996
Reza Vaghar
NHMFL/MS&T
Three-Dimensional Axisymmetric Stress Analysis of High Field Solenoid Magnets

October 8, 1996
Marc Teng
CERN
Superconducting Magnet Systems for the Large Hadron Collider

October 9, 1996
Leonid Burlachkov
Bar-Ilan University, Israel
Plastic Creep of Vortices in High Temperature Superconductors

October 14, 1996
Keith Bartholomew
NHMFL/MS&T
A Cryocooler for Thermal Shield Cooling

October 14, 1996
Scott Welton
NHMFL/MS&T
Analysis of He II Heat Exchangers and More Hybrid Stuff

October 22, 1996
K. Tachikawa
Tokai University
Recent Developments of Superconductors

October 23, 1996
Jun Xu
BIO-RAD Sadtler Division
Computer-Assisted Structure Elucidation from 2D NMR By Means of Molecular Diversity Analysis and Fuzzy Graph Theory

October 25, 1996
Zachary Ha
NHMFL/CM/T
One-Dimensional Quantum Ether: Elementary Excitations and Beyond

October 28, 1996
Guenter Gottstein
Institute of Physical Metallurgy and Metal Physics, Aachen, Germany
Microtexture: A Novel Tool in Microstructure Research

October 28, 1996
L.S. Shvindlerman
Institute of Solid State Physics, Russian Academy of Sciences
Grain Boundary Migration

October 28, 1996
Remy Jost
High Magnetic Field Laboratory, Grenoble, France
I. Magnetic Field Lowering of Photodissociation Threshold of the NO_2 Molecule
II. Stability, Shielding, Homogeneity and Temperature Effects in the Homogeneous M5 Grenoble Bitter Coil

November 1, 1996
John Tranquada
Brookhaven National Laboratory
Charge Stripes and Antiferromagnetism in Copper Oxide Superconductors

November 4, 1996
Uschi Steigenberger
ISIS Facilities, Rutherford Appleton Lab
Non-Equilibrium States in Ferroelectrics: Time-Resolved Neutron Scattering Studies

November 4, 1996
Terry Miller
Ohio State University
Spectroscopy and Dynamics of the Methoxy Family of Chemical Intermediates

November 7, 1996
Vladimir N. Stepankin
General Physics Institute, Moscow, Russia
New Ideas for High-Magnetic Field Poles and Boosters, Including Field Gradient Generators for Faraday Effect and Torque Magnetometry, and New Alloys Usable at More Temperatures

November 8, 1996
David Ceperley
University of Illinois
Superfluidity of Molecular Hydrogen?

November 12, 1996
Jim Norris
NHMFL/CIMAR
Exploring Electron Transfer Chemistry in Integral Membrane EPR

November 13, 1996
Lisa Cowey
Oxford Instruments
HTS Conductor and Magnet Development at Oxford Superconducting Technology

November 15, 1996
Ching-Jen Chen
FAMU-FSU College of Engineering
Development of Biomagnetic Fluid Dynamics

November 16, 1996
Diethard Bohme
York University
Gas-Phase Chemistry of Singly and Multiply-Charged C_{60} Cations

November 18, 1996
Vasken Hagopian
Florida State University
Large Hadron Collider Project at CERN

November 18, 1996
Joachim Schoenes
Institute für Halbleiterphysik und Optik, Technische Universität
Giant 90 Degree Kerr Rotation and Superstructure Effect in CeSb

November 19, 1996
Uma Srinivasan
Max-Planck Institute
Directional Magnetic Susceptibility and Specific Heat Studies on $Y_{1-x}Pr_xBa_2Cu_3O_{7-\delta}$ Single Crystals

November 19, 1996
Robert Palmer
Brookhaven National Laboratory
Magnets for a Muon Collider

November 20, 1996
Ken Ghiron
University of Illinois
Magnetic Thermometry in the Aseptic Processing of Food

November 20, 1996
Tiruppattur V. Ramakrishnan
Indian Institute of Science
Microscopic Approach for Vortex Masses and Magnus Force in a Superconductor

November 21, 1996
Michel Aïn
Laboratoire Léon Brillouin (CEA-CNRS) CE - Saclay FRANCE
Double Gap in the Spin-Peierls Compound $CuGeO_3$

November 22, 1996
Daniel Dessau
University of Colorado
Electronic Structure Measurements of "Colossal" Magnetoresistive Oxides

November 25, 1996
Paul Pernambuco-Wise
NHMFL/MS&T
Composite Materials and Pulse Magnets Revisited

November 25, 1996
Xuanchao Kou
University of Vienna
Magnetic Phase Transition in Rare Earth/ Transition Metal Intermetallic Compounds

December 5, 1996
Jack Crow
NHMFL
FSU Physics Colloquium Series - "Science and Technology at the Extremes of Magnetic Fields"

December 5, 1996
Richard Caprioli
University of Houston
Direct High Sensitivity Analysis of Sı from Biological Tissues with Micro-I MALDI Mass Spectrometry Using Microsampling Techniques

December 6, 1996
Steven G. Louie
University of California, Berkeley
Structures and Properties of Carbon Boron-Nitride Nanotubes

December 9, 1996
Ibrahim H. Mutlu
NATO, Turkey
Flux Pinning Mechanism and Flame Melt Growth Method for YBCO

December 10, 1996
Shimon Reich
Weizmann Institute in Israel
Giant Mass Anisotropy and High Cri Current in Hg-1223 Superconductin

December 12, 1996
A.K. Majumdar
Indian Institute of Technology, Kanp
Resistivity Minima in Bulk Disordere

December 13, 1996
Dragana Popovic
NHMFL/CM/T
Mesoscopic Behavior Near a Two-Di Metal-Insulator Transition

December 16, 1996
Frank Heringhaus
NHMFL/MS&T
Precipitation and Dispersion Strengti Copper

7, 1996
ıan
versity
ck-Body IR Photodissociation of FT-ICR MS

8, 1996
Parrell
of Wisconsin - Madison
rocessing and the Connectivity, g, and Critical Current Density in CCO-2223 Tapes

s and Conferences

3-March 1, 1996
ıd NRIM
al Workshop on High Magnetic ıstry, Materials and Technology

1996
er
of Groningen
echt
Paul Sabatier, France
aas
h
n Numerical Techniques Applied to perconducting Materials

, 1996
HMFL
auqua Program
ields in Science and Technology

96
HMFL
tional workshop for teachers
g in UF's *Teacher Research Update* (TRUE) program and teachers
g in NHMFL's *Science Teachers chers Translating Research s into Educational Materials* (STAR

July 8-13, 1996
ODYSSEY Science Center of Tallahassee
Star Lab Workshop

July 22, 1996
NSF, FAMU, and NHMFL
Fourth Annual NSF Alliances for Minority Participation (AMP) Student Research Conference

October 24-25, 1996
UF and NHMFL, at Gainesville
Properties of Molecules in Strong Magnetic Fields (≥100 T): A Workshop

November 15, 1996
FSU President's Office and *Tallahassee Democrat*
Economic Development Workshop
Regional Economic Development and the Role of the University

PUBLICATIONS, PRESENTATIONS & RELATED ACTIVITIES

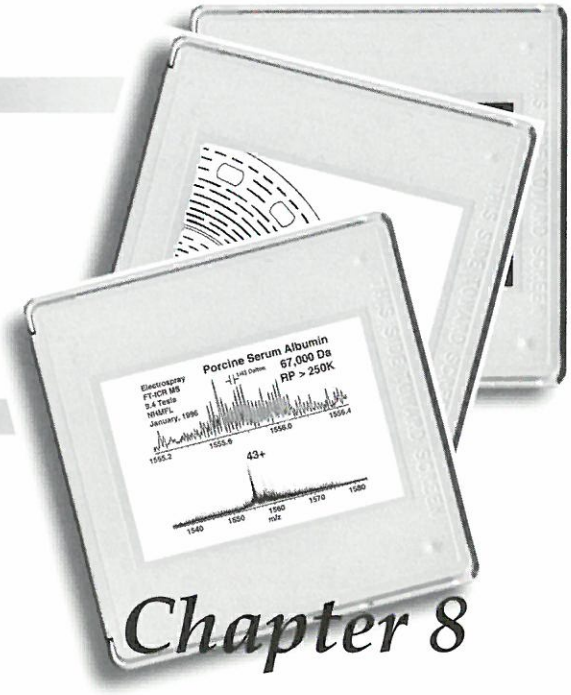

Chapter 8

Peer-Reviewed Publications

This section includes refereed publications and peer-reviewed conference proceedings.

Alvarenga, A.D.; Rao, D.; Sanjuro, J.A.; Granado, E.; Torriani, I.; Rettori, C.; Oseroff, S.B.; Sarrao, J.L. and Fisk, Z., *Raman Scattering and Weak Ferromagnetism in Eu_2CuO_4*, Physica B, **223 & 224**, 522 (1996).

Alvarenga, A.D.; Rao, D.; Sanjuro, J.A.; Granado, E.; Torriani, I.; Rettori, C.; Oseroff, S.B.; Sarrao, J.L. and Fisk, Z., *Raman Scattering and Weak Ferromagnetism Studies in Eu_2CuO_4*, Phys. Rev. B, **53**, 837 (1996).

Arumugam, S.; Pascal, S.; North, C.L.; Hu, W.; Lee, K.-C.; Cotten, M.; Ketchem, R.R.; Xu, F.; Brenneman, M.; Kovacs, F.; Tian, F.; Wang, A.; Huo, S. and Cross, T.A., *Conformational Trapping in a Membrane Environment: A Regulatory Mechanism for Protein Activity?*, Proc. Natl. Acad. Sci. U.S.A., **93**, 5872-5876 (1996).

Baudouy, B.J.P.; Bartholomew, K. and Van Sciver, S.W., *New Calorimetric AC Loss Measurement Technique Involving Superfluid Helium*, Advances in Cryogenic Engineering, **41A**, 397-404 (1996).

Baudouy, B.J.P.; Juster, F.-P.; Meuris, C.; Vieillard, L. and Francois, M.X., *Steady-State Heat Transfer in He II Through Porous Superconducting Cable Insulation*, Advances in Cryogenic Engineering, **41A**, 289-296 (1996).

Bird, M.D.; Bole, S.; Eyssa, Y.M.; Gao, B.J. and Schneider-Muntau, H.-J., *Design of a Poly-Bitter Magnet at the NHMFL*, IEEE Transactions on Magnetics, **32**, 4, 2542-2545 (1996).

Bird, M.D.; Bole, S.; Eyssa, Y.M.; Gao, B.J. and Schneider-Muntau, H.-J., *Resistive Magnets at the National High Magnetic Field Laboratory: Design and Operation, 27 to 33 T*, Physica B, **216**, 193-195 (1996).

Bird, M.D.; Bole, S.; Eyssa, Y.M.; Gao, B.J. and Schneider-Muntau, H.-J., *The World's First 27 T and 30 T Resistive Magnets*, IEEE Transactions on Magnetics, **32**, 4, 2444-2449 (1996).

Boebinger, G.S.; Passner, A.; Canfield, P.C. and Fisk, Z., "Intrinsic Metallic Behavior Above 50 Tesla in a Kondo Insulator," in *Physical Phenomena at High Magnetic Fields II*, eds. Fisk, Z.; Gor'kov, L.; Meltzer, D. and Schrieffer, R. (World Scientific, Singapore, 1996), p. 170.

Boettcher, E.J.; Ihas, G.G.; Reghu, M. and Heeger, A.J., *Oscillations in Resistivity of an Organic Polymer at Low Temperatures,* Czechoslovak Journal of Physics, **46**, 2605-2606 (1996).

Bonesteel, N.E., "Pairing Instability of a Double Layer Composite Fermion Metal," in *Physical Phenomena at High Magnetic Fields II*, eds. Fisk, Z.; Gor'kov, L.; Meltzer, D. and Schrieffer, R. (World Scientific, Singapore, 1996), pp. 85-90.

Bonesteel, N.E.; McDonald, I.A. and Nayak, C., *Gauge Fields and Pairing in Double-Layer Composite Fermion Metals*, Phys Rev Lett, **77**, 3009-3013 (1996).

Bonito-Oliva, A.; Baudouy, B.J.P.; Miller, J.R. and Van Sciver, S.W., *AC Losses in Superconducting Nb_3Sn and NbTi CIC Conductors*, IEEE Transactions on Magnetics, **32**, 4, 2834 (1996).

Bonito-Oliva, A.; Kenney, S.J.; Schneider-Muntau, H.-J. and Summers, L.T., *The Potential for SAGBO Cracking in a Nb_3Sn Wind-and-React Solenoid Using a CICC with Incoloy 908 Jacket and Glass Fabric Insulation*, IEEE Transactions on Magnetics, **32**, 4, 2495 (1996).

Boulat, B. and Rance, M., *Selective Transfer of Magnetization by Incoherent Processes in Nuclear Magnetic Resonance Spectroscopy*, J. Magn. Res. B, **110**, 288-297 (1996).

Boulat, B.; Najfeld, I. and Rance M., *A Theoretical Analysis of the Synchronous Nutation Experiment*, J. Magn. Res. A, **120**, 223-230 (1996).

Bowers, M.T.; Marshall, A.G. and McLafferty, F.W., *Mass Spectrometry: Recent Advances and Future Directions*, J. Phys. Chem., **100**, 2897-2910 (1996).

Brooks, J.S.; Clark, R.G.; McKenzie, R.H.; Newbury, R.; Starrett, R.P.; Skougarevsky, A.V.; Tokumoto, M.; Takasaki, S.; Yamada, J.; Anzai, H. and Uji, S., *Magneto-Oscillations in the High Magnetic Field State of $(TMTSF)_2CIO_4$*, Phys. Rev. B., **53** 14406 (1996).

Brooks, J.S.; Clark, R.G.; Starrett, R.P.; Newbury, R.; McKenzie, R.H.; Skougarevsky, A.V.; Tokumoto, M.; Kinoshita, N.; Kinoshita, T.; Tanaka, Y.; Anzai, H.; Takasaki, S.; Yamada, J.; Kartsovnik, M.V.; Shegolev, A.I.; Athas, G.J. and Sandhu, P.S., *Applications of Pulsed Magnetic Fields and Low Temperatures to Low-Dimensional (organic) Conductor Physics*, Physica B, **216**, 380 (1996).

Brooks, J.S.; Uji, S.; Aoki, H.; Kato, R.; Sawa, H.; Clark, R.G.; McKenzie, R.H.; Athas, G.J.; Sandhu, P.S.; Valfells, S.; Campos, C.E.; Perenboom, J.A.A.P.; van Bentum, J.; Tokumoto, M.; Kinoshita, N.; Kinoshita, T.; Tanaka, Y.; Anzai, H.; Fisk, Z. and Sarrao, J.L., "Molecular Conductors: the Mesopotamia of Low-Dimensional Physics," in *Physical Phenomena at High Magnetic Fields II*, eds. Fisk, Z.; Gor'kov, L.; Meltzer, D. and Schrieffer, R. (World Scientific, Singapore, 1996), p. 249.

Brunel, L.-C., *Recent Developments in High Frequency CW ESR*, Applications in Chemistry and Biophysics, Appl. Mag. Res., **11**/3-4, 417 (1996).

Bucher, B.; Schlesinger, Z.; Mandrus, D.; Fisk, Z.; Sarrao, J.L.; DiTusa, J.F.; Oglesby, C.; Aeppli, G. and Bucher, E., *Charge Dynamics of Ce-Based Compounds: Connection Between the Mixed Valent and Kondo-Insulator States*, Phys. Rev. B, **53**, 2948 (1996).

Butera, A.; Tovar, M.; Oseroff, S.B.; Rettori, C.; Maley, C. and Fisk, Z., *Coupling of CuO_2 Planes in $Eu_{2-x}Y_xCuO_4$ Single Crystals*, Czech. Journal of Physics, **46** Suppl. S5, 2697-2698 (1996).

Campbell, L.J.; Boenig, H.J.; Parkin, D.M.; Rickel, D.G.; Schillig, J.B. and Sims, J.R., *The NHMFL Long Pulse Magnet System-60 to 100T*, Physica B, **216**, 218-220 (1996).

Campbell, L.J.; Boenig, H.J.; Rickel, D.G.; Schillig, J.B.; Sims, J.R. and Schneider-Muntau, H.-J., *Status of the NHMFL 60 Tesla Quasi-Continuous Magnet, IEEE Transactions on Magnetics*, **32**, 4, 2454 (1996).

Campos, C.E.; Sandhu, P.S.; Brooks, J.S. and Ziman, T., *Extended Huckel Tight-Binding Study of the Effect of Pressure and Uniaxial Stress on the Electronic Structure of α(BEDT-TTF)^{2}KHg(SCN)^4 and κ(BEDT-TTF)^{2}Cu(NCS)^2*, Phys. Rev. B, **53**, 12725 (1996).

Cao, G.; Bolivar, J. and Crow, J.E., *A Simultaneous Polarization and Magnetization Ordering in Some Insulating Cuprates*, J. Superconductivity, **8**, 607 (1996).

Cao, G.; McCall, S.; Bolivar, J.; Shepard, M.; Freibert, F. and Crow, J.E., *Itinerant-to-Localized Electron Transition in Peroviskites $CaRu_{1-x}Sn_xO_3$ and $SrRu_{1-x}Pb_xO_3$*, Phys. Rev. B, **54**, 15144 (1996).

Cao, G.; McCall, S.; Freibert, F.; Shepard, M.; Crow, J.E. and Andraka, B., *Transport and Thermodynamic Studies of $Y_{1-x}Tb_xBa_2Cu_3O_7$*, J. Superconductivity, **8**, 669 (1996).

Cao, G.; McCall, S.; Freibert, F.; Shepard, M.; Henning, P. and Crow, J.E., *Anomalous Low Dimensional System: Study of Magnetism and Electrical Conductivity in $Na_2Ru_4O_9$*, J. Appl. Phys., **79**, 4567 (1996).

Cao, G.; McCall, S.; Shepard, M. and Crow, J.E., *Observation of An Anomalous Quasi-One-Dimensional Behavior in $Na_2Ru_4O_9$ Single Crystals*, Phys. Rev. B, **53**, 12215 (1996).

Comisarow, M.B. and Marshall, A.G., *The Early Development of Fourier Transform Ion Cyclotron Resonance (FT-ICR) Spectroscopy*, J. Mass Spectrom., **31**, 581-585 (1996).

Continentino, M.A.; Fernandes, J.C.; Guimaraes, R.B.; Boechat, B.; Borges, H.A.; Valarelli, J.V.; Haanappel, E.G.; Silva, P.R. and Lacerda, A., *Strongly Disordered Heisenberg Spin-1 Chains: Vanadium Warwickites*, Phil. Mag. B, **73**, 601-609 (1996).

Corsépius, S.; Lenkewitz, M.; Scheidt, E.-W. and Stewart, G.R., *Substitution Experiments in $U_3Cu_3Sn_4$ and $U_3Au_3Sn_4$*, J. of Alloys and Compounds, **235**, 192-196 (1996).

Cox, A.W.; Garmestani, H.; Markiewicz, W.D. and Dixon, I.R., *Power Series Stress Analysis of Solenoid Magnets*, IEEE Transactions on Magnetics, **32**, 4, 3012 (1996).

Crow, J.E.; Parkin, D.M. and Sullivan, N.S., *The United States National High Magnetic Field Laboratory: Facilities, Science and Technology*, Physica B Cond. Mtr., **216** (3/4), 146 (1996).

Dagotto, E. and Rice, T.M., *Surprises on the Way From 1D to 2D Quantum Magnets: The Novel Ladder Materials*, Science, **271**, 618 (1996).

Dagotto, E.; Riera, J.A.; Sandvik, A., and Moreo, A., *Spin Dynamics of Hole Doped $Y_{2-x}Ca_xBa$ Ni O_5*, Phys. Rev. Lett., **76**, 1731-1734 (1996).

Devernoe, A.L.; Ciancetta, G.; King, M.; Parish, M.; Painter, T.A. and Miller, J.R., *Tension Layer Winding of a Cable-in-Conduit Conductor*, IEEE Transactions on Magnetics, **32**, 4, 2499 (1996).

Dixon, I.R.; Walsh, R.P.; Markiewicz, W.D. and Swenson, C.A., *Mechanical Properties of Epoxy Impregnated Superconducting Solenoids*, IEEE Transactions on Magnetics, **32**, 4, 2917 (1996).

Du, R.R.; Yeh, A.S.; Störmer, H.L.; Tsui, D.C.; Pfeiffer, L.N. and West, K.W., *Composite Fermions around Landau Level Filing Factor $\upsilon = 3/2$*, Surf. Sci, **360/361**, 26 (1996).

Duffy, D. and Moreo, A., *Influence of Next-Nearest-Neighbor Electron Hopping on the Static and Dynamical Properties of the 2D Hubbard Model*, Phys. Rev. B, **52**, 15607-15616 (1995).

Duffy, D., and Moreo, A., "Influence of Next-Nearest Neighbor Electron Hopping on the Magnetic Properties of the 2D Hubbard Model," in *Physical Phenomena at High Magnetic Fields II*, eds. Fisk, Z.; Gor'kov, L.; Meltzer, D. and Schrieffer, R. (World Scientific, Singapore, 1996), pp. 493-498.

Eyssa, Y.M. and Pernambuco-Wise, P., *Design and Modeling of Coupled Pulsed Magnets,* IEEE Transactions on Magnetics, **32**, 4, 2522 (1996).

Eyssa, Y.M.; Bird, M.D.; Gao, B.J. and Schneider-Muntau, H.-J., *Design and Analysis of a 25 T Resistive NMR Magnet*, IEEE Transactions on Magnetics, **32**, 4, 2546-2549 (1996).

Eyssa, Y.M.; Markiewicz, W.D. and Pernambuco-Wise, P., *Plastic Stress Analysis of Resistive and Pulsed Magnets*, IEEE Transactions on Magnetics, **32**, 4, 2526 (1996).

Eyssa, Y.M.; Pernambuco-Wise, P.; Schneider-Muntau, H.-J.; Van Cleemput, M. and Jones, H., *Comparative Analysis of Micro-Composite and Macro-Composite Conductors for Pulsed Magnets*, IEEE Transactions on Magnetics, **32**, 4, 2462 (1996).

Fisk, Z. and Sarrao, J.L., "Kondo Insulators," in *Physical Phenomena at High Magnetic Fields II*, eds. Fisk, Z.; Gor'kov, L.; Meltzer, D. and Schrieffer, R. (World Scientific, Singapore, 1996), p. 139.

Fisk, Z.; Sarrao, J.L. and Thompson, J.D., *Heavy Fermions*, Current Opinion in Solid State and Materials Science, **1**, 42 (1996).

Fisk, Z.; Sarrao, J.L.; Cooper, S.L.; Nyhus, P.; Boebinger, G.S.; Passner, A. and Canfield, P.C., *Kondo Insulators*, Physica B, **223 & 224**, 409 (1996).

Fontes, M.B.; Bud'ko, S.L.; Continentino, M.A.; El-Massalami, M.; Sampaio, L.C.; Guimaraes, A.P.; Baggio-Saitovitch, E.; Hundley, M.F. and Lacerda, A., *Physical Properties of the* $Ce(Ru_{1-x}Fe_x)_2Ge_2$ *Compounds*, Phys. Rev. B, **53**, 11678-11684 (1996).

Freibert, F.; Cao, G.; Crow, J.E.; Shepard, M. and McCall, S., *Upper Critical Field and Irreversibility in the (H,T) Plane for* $Y_{1-x}(Pr,Tb)_xBa_2Cu_3O_7$ *and* $YBa_2(Cu_{1-x}Zn_x)_3O_7$ *Thin Films and Single Crystals*, J. Superconductivity, **8**, 619 (1996).

Freibert, F.; Cao, G.; McCall, S.; Shepard, M. and Crow, J.E., "Magneto-Resistivity and Magnetic Phase Boundaries in Selectively Doped $YBa_2Cu_3O_7$," in *Physical Phenomena at High Magnetic Fields II*, eds. Fisk, Z.; Gor'kov, L.; Meltzer, D. and Schrieffer, R. (World Scientific, Singapore, 1996), p. 499.

Freibert, F.; Cao, G.; McCall, S.; Shepard, M. and Crow, J.E., *Effect of Pr, Tb and Zn Doping into* $YBa_2Cu_3O_7$ *on Magnetoresistivity and Magnetic Phase Boundaries*, J. Appl. Phys., **79**, 5876 (1996).

Fu, R. and Bodenhausen, G., *Evaluation of Adiabatic Frequency-Modulated Schemes for Broadband Decoupling in Isotropic Liquids*, J. Magn. Reson. **A119**, 129-133 (1996).

Fu, R.; Ermakov, V. and Bodenhausen, G., *Divergent Double Chirp Pulses for Refocusing Quadrupolar Interactions*, Solid State Nucl. Magn. Reson., **7**, 1-10 (1996).

Gambarelli, S.; Jaouen, D.; Rassat, A.; Brunel, L.-C. and Chachaty, C., *High-Field Electron Spin Resonance Study of a Nitroxide Biradical, 1,4-bis(4', 4'-dimethyloxazolidin-N-oxyl) cyclohexane*, J. Phys. Chem., **100**, 9605 (1996).

Gao, B.J.; Bird, M.D.; Bole, S.; Eyssa, Y.M. and Schneider-Muntau, H.-J., *Design of a 20 T, 200 mm Bore Resistive Magnet*, IEEE Transactions on Magnetics, **32**, 4, 2562-2565 (1996).

Gao, B.J.; Chen, J.L.; Yuan, S.L.; Yuan, W.F.; Wang, F.T.; Ding, L.R.; Liu, X. N.; Liu, Z.M.; Huang, Z.; Chen, Z.Y. and Wang, S., *Development and Research in High Magnetic Fields at ASIPP*, Physica B, **216**, 166-170 (1996).

Gao, B.J.; Schneider-Muntau, H.-J.; Eyssa, Y.M. and Bird, M.D., *A New Concept in Bitter Disk Design,* IEEE Transactions on Magnetics, **32**, 4, 2503-2506 (1996).

Geerts, W.; MacKenzie, J.D.; Abernathy, C.R.; Pearton, S.J. and Schmiedel, T., *Electrical Transport in p-GaN, n-InN and n-InGaN*, Solid State Electronics, **39** no.9, 1289-1294 (1996).

Genio, E.B.; Xu, J.W.; Sullivan, N.S. and Ihas, G.G., *Nuclear Spin Coupling of ^{3}He to Metallic Sb at Low Temperatures*, Czech J. Phys. **46**, S1, 219-220 (1996).

Gloos, K.; Kim, J.S. and Stewart, G.R., *Transition from Diffusive to Thermal Transport Through Metallic Point Contacts Between the Heavy-Fermion Superconductor UBe_{13} and Tungsten,* J. Low Temperature Physics, **102**, 325-334 (1996).

Godfrey, L.V.; White, W.M., and Salters, V.J.M., *Dissolved Zirconium and Hafnium Distributions across a Shelf Break in the Northeastern Atlantic Ocean*, Geochim. et Cosmochim. Acta, **60**, 3995-4006 (1996).

Godfrey, M.I.; Weijers, H.W. and Hascicek, Y.S., *Coaxial Probe for Transport J_c Characterization of Superconductors*, Cryogenics, **36**, 1, 57 (1996).

Gonzalez-Buxton, C. and Ingersent, K., *Stabilization of Local Moments in Gapless Fermi Systems*, Phys. Rev. B, **54**, 15614 (1996).

Gor'kov, L.P., "Non-Fermi Liquid Behavior of Kinetic Characteristics in Quasi-One-Dimensional Organic Conductors," in *From High-Temperature Superconductivity to Microminiature Refrigeration,* eds. Blas Cabrera, *et al.* (Plenum Press, NY, 1996), p. 263.

Gor'kov, L.P., "Precursor Effects and Anomalous Magnetoresistance in the Bechgaard Salts," in *Physical Phenomena at High Magnetic Fields II*, eds. Fisk, Z.; Gor'kov, L.; Meltzer, D. and Schrieffer, R. (World Scientific, Singapore, 1996), p. 315.

Gor'kov, L.P., *et al.*, "Thermodynamics of Alloys with Magnetic Impurities," in *Physical Phenomena at High Magnetic Fields II*, eds. Fisk, Z.; Gor'kov, L.; Meltzer, D. and Schrieffer, R. (World Scientific, Singapore, 1996), p. 197.

Gor'kov, L.P., *et al.*, *Interplay Between the Kondo Effect and the RKKY Interaction in the Two-Impurity Model*, Phyl. Mag. B, **74**, 447 (1996).

Gor'kov, L.P., *Phase Transitions in Mixed Valence Systems*, Physica B, **223 & 224**, 245 (1996).

Gor'kov, L.P., *Quasi-One-Dimensional Organic Metals: Theory and Experiment*, J. Phys. I, France 6, 1 (1996).

Gorbunov, M.B.; Bottura, L.; Miller, J.R. and Van Sciver, S.W., *Finite Element Code for Quench and Stability Analysis of Superconducting Magnets Cooled by the He II*, Advances in Cryogenic Engineering, **41**, 335 (1996).

Goretta, K.C.; Routbort, J.L.; Thayer, R.L.; Carroll, J.P.; Wolfenstine, J.; Kessler, J. and Schwartz, J., *Deformation of Ag/1.2 at.% Mg*, Physica C, **265**, 201-206 (1996).

Granroth, G.E.; Meisel, M.W.; Chaparala, M.; Jolicoeur, Th.; Ward, B.H. and Talham, D.R., *Experimental Evidence of a Haldane Gap in an $S = 2$ Quasi-Linear Chain Antiferromagnet*, Phys. Rev. Lett., **77**, 1616-1619 (1996).

Guan, S. and Marshall, A.G., *A Mass- and Velocity-Broadband Ion Deflector for Off-Axis Ion Injection into a Cyclotron Resonance Ion Trap*, Rev. Sci. Instrum., **67**, 423-427 (1996).

Guan, S. and Marshall, A.G., *Stacked-Ring Electrostatic Ion Guide*, J. Amer. Soc. Mass Spectrom., **7**, 101-106 (1996).

Guan, S. and Marshall, A.G., *Stereoscopic Views of Three-Dimensional Ion Trajectories in Ion Cyclotron Resonance and Quadrupole Ion Traps*, Rapid Comm. Mass Spectrom., **10**, 1833-1838 (1996).

Guan, S. and Marshall, A.G., *Stored Waveform Inverse Fourier Transform (SWIFT) Ion Excitation in Trapped-Ion Mass Spectrometry: Theory and Applications*, Int. J. Mass Spectrom. Ion Proc., **137/138**, 5-37 (1996).

Guan, S.; Huang, Y.; Xin, T. and Marshall, A.G., *Determination of Ion Magnetron Radius Distribution in Fourier Transform Ion Cyclotron Resonance Mass Spectrometry*, Rapid Comm. Mass Spectrom., **10**, 1855-1859 (1996).

Guan, S.; Marshall, A.G. and Scheppele, S.E., *Resolution and Chemical Formula Identification of Aromatic Hydrocarbons and Aromatic Compounds Containing Sulfur, Nitrogen, and/or Oxygen in Crude Oil Distillates*, Anal. Chem., **68**, 46-71 (1996).

Guha, E.; Scheidt, E.-W. and Stewart, G.R., *$U_2Pt_{15}Si_7$: Competition Between Magnetism and the Formation of a Heavy Fermion Ground State,* Phys. Rev. B, **53**, 6477-6481 (1996).

Haas, S.; Moreo, A. and Dagotto, E., "Shadow Bands in the Cuprates," in *Physical Phenomena at High Magnetic Fields II*, eds. Fisk, Z.; Gor'kov, L.; Meltzer, D. and Schrieffer, R. (World Scientific, Singapore, 1996), pp. 506-517.

Hallberg, K.; Wang, X.Q.G.; Horsch, P. and Moreo, A., *Critical Behavior of the S=3/2 Antiferromagnetic Heisenberg Chain*, Phys. Rev. Lett., **76**, 4955-4958 (1996).

Hamida, J.A.; Genio, E.B. and Sullivan, N.S., *A New Orientational Glass in Low Concentration N_2-Ar Solid Mixtures*, Czech J. Phys., **46**, S1, 513-514 (1996).

Hamida, J.A.; Genio, E.B. and Sullivan, N.S., *NMR Studies of the Orientational Ordering in Dilute Solid N_2-Ar Mixtures*, J. Low Temp. Phys., **103**, 49-70 (1996).

Hascicek, Y.S.; Pernambuco-Wise, P.; Mignosi, C. and Schneider-Muntau, H.-J., *Microstructure of Wound Conductors for High Field Pulse Magnets, IEEE Transactions on Magnetics*, **32**, 4, 2530 (1996).

Havela, L.; Schecvsky, V.; Nakotte, H.; Lacerda, A. and Bruck, E., *Low Temperature Behavior of Electrical Resistivity in UTX Compounds*, Czechoslovak Journal of Physics, **46**, 2043-2044 (1996).

Havela, L.; Schecvsky, V.; Prokes, K.; Nakotte, H.; Fujii, H. and Lacerda, A., *Giant Magnetoresistance in Uranium Compounds*, Physica B, **223&224**, 245-247 (1996).

Hayden, S.M.; Aeppli, G.; Mook, H.A.; Perring, T.G.; Mason, T.E.; Cheong, S.W. and Fisk, Z., *Comparison of the High-Frequency Magnetic Fluctuations in Insulating and Superconducting $La_{2-x}Sr_xCuO_4$*, Phys. Rev. Lett., **76**, 1344-1347 (1996).

Hendrickson, C.L.; Drader, J.J.; Laude, D.A.; Guan, S. and Marshall, A.G., *Fourier Transform Ion Cyclotron Resonance Mass Spectrometry in a 20 Tesla Resistive Magnet*, Rapid Comm. Mass Spectrom., **10**, 1829-1832 (1996).

Henning, P.; Cao, G.; Crow, J.E.; Putikka, W.O. and Hirschfeld, P.J., *Thermal Conductivity of High T_c Systems*, J. Superconductivity, **8**, 453 (1996).

Heringhaus, F.; Eyssa, Y.M.; Pernambuco-Wise, P.; Bird, M.D.; Gottstein, G. and Schneider-Muntau, H.-J., *Werkstoffanforderungen in der Hochmagnetfeld-technologie*, Metall, **50**, 272-279, Jahrgang, Nr. (1996).

Hill, S.; Boonman, M.; Uji, S.; Perenboom, J.A.A.P.; Wittlin, A.; Brooks, J.S.; Kato, R.; Sawa, H. and Aonuma, S., "Cyclotron Resonance Studies of the Molecular Conductor $(DMe\text{-}DCNQI)_2Cu$," in *Physical Phenomena at High Magnetic Fields II*, eds. Fisk, Z.; Gor'kov, L.; Meltzer, D. and Schrieffer, R. (World Scientific, Singapore, 1996), p. 322.

Hill, S.; Sandhu, P.S.; Boonman, M.; Perenboom, J.A.A.J.; Wittlin, A.; Uji, S.; Brooks, J.S.; Kato, R.; Sawa, H. and Aonuma, S., *Magnetoelectrodynamics of a Three-Dimensional Organic Conductor: Observation of Cyclotron Resonance in* $d_2[1,1;0]$-$(DMe\text{-}DCNQI)_2Cu$, Phys. Rev. B, **54**, 13536 (1996).

Hu, J.; Dagotto, E. and MacDonald, A.H., "Interlayer Coherence in Double-Layer Quantum Dots," in *Physical Phenomena at High Magnetic Fields II*, eds. Fisk, Z.; Gor'kov, L.; Meltzer, D. and Schrieffer, R. (World Scientific, Singapore, 1996), pp. 368-373.

Hu, J.; Dagotto, E. and MacDonald, A.H., *Spontaneous Coherence and Collective Modes in Double-Layer Quantum Dot Systems*, Phys. Rev. B, **52**, 1286-1289 (1996).

Huang, X. and Van Sciver, S.W., *The Performance of a Venturi Flowmeter in Two-Phase Helium Flow*, Cryogenics, **36**, 303 (1996).

Huang, Y. and Van Sciver, S.W., *Forced Flow He II Heat Exchangers*, Cryogenics, **36**, 535 (1996).

Huang, Y. and Van Sciver, S.W., *Heat Transfer from Aluminum Surfaces to Pool Boiling He I*, Advances in Cryogenic Engineering, **41**, 211 (1996).

Huang, Y.; Guan, S.; Kim, H.S. and Marshall, A.G., *Ion Transport Through a Strong Magnetic Field Gradient by rf-Only Octupole Ion Guides,* Int. J. Mass Spectrom. Ion Proc., **152**, 121-133 (1996).

Huang, Y.; Guan, S. and Marshall, A.G., "Ion Transport Through a Strong Magnetic Field Gradient by RF-Only Octupole Ion Guide," in *Physical Phenomena at High Magnetic Fields – II*, eds. Fisk, Z.; Gor'kov, L.; Meltzer, D. and Schrieffer, R., (World Scientific Publishing Co., Singapore, 1996), pp. 642-647.

Huth, J.; Fu, R. and Bodenhausen, G., *Curious Consequences of Strong Coupling in NMR Experiments Involving Selective Pulses*, J. Magn. Reson., **A123**, 87-94 (1996).

Ingersent, K., "The Kondo Effect in a System with a Singular Density of States," in *Physical Phenomena at High Magnetic Fields II*, eds. Fisk, Z.; Gor'kov, L.; Meltzer, D. and Schrieffer, R. (World Scientific, Singapore, 1996), p. 179.

Ingersent, K., *Behavior of Magnetic Impurities in Gapless Fermi Systems*, Phys. Rev. B, **54**, 11936 (1996).

Iyengar, K. and Van Sciver, S.W., *A Continuously Cooled Mechanical Support For Cryogenic Equipment*, Advances in Cryogenic Engineering, **41**, 1913 (1996)

Jackson, G.S.; Guan, S. and Marshall, A.G., "Universal ICR Ion Trap: Segmented and Optimized for Excitation, Detection, and Trapping," in *Physical Phenomena at High Magnetic Fields – II*, eds. Fisk, Z.; Gor'kov, L.; Meltzer, D. and Schrieffer, R., (World Scientific Publishing Co., Singapore, 1996), pp. 649-654. .

Janossy, A.; Brunel, L.-C. and Cooper, J.R., Gd^{3+} *ESR Determination of the Local Spin Susceptibility in* $Gd{:}YBa_2Cu_3O_y$ *High Temperature Superconductors*, Phys. Rev. B, **54**, 10, 186 (1996).

Jin, D.S.; Carter, S.A.; Rosenbaum, T.F.; Kim, J.S. and Stewart, G.R., *H-T Phase Diagrams of the Double Transition in Thoriated UBe_{13}*, Phys. Rev. B., **53**, 8549-8552 (1996).

Jones, H. and Van Cleemput, M., *The Fabrication and Characterization of High Strength Copper/Stainless Steel Conductors for Pulsed Magnets*, IEEE Transactions on Magnetics, **32**, 4, 2466 (1996).

Kebede, A.; Aronson, M.C.; Buford, C.M.; Canfield, P.C.; Cho, J-H.; Coles, B.R.; Cooley, J.C.; Coulter, J.Y.; Fisk, Z.; Goettee, J.D.; Hults, W.L.; Lacerda, A.; McLendon, T.D.; Tiwari, T.D. and Smith, J.L., *Studies of the Correlated Electron System SmB_6*, Physica B, **223&224**, 256-258 (1996).

Ketchem, R.R.; Lee, K.-C.; Huo, S. and Cross, T.A., *Macromolecular Structural Elucidation through Solid State NMR-Derived Orientational Constraints*, J. Biomol. NMR, **8**, 1-14 (1996).

Kim, K.; Bodart, J.R. and Sullivan, N.S., *Reliable Low Temperature NMR Cell for Reduced Geometry Studies*, Cryogenics, **36**, 311-312 (1996).

Kim, K.; Bodart, J.R. and Sullivan, N.S., *High Sensitivity Continuous Wave NMR Spectrometer for Low Temperatures and Ultra-High Frequencies*, J. Mag. Res., **A118**, 28-31 (1996).

Kim, K.; Bodart, J.R. and Sullivan, N.S., *Orientational Ordering in Thick Films of Molecular Hydrogen*, Czech J. Phys., **46**, S1, 515-516 (1996).

Kim, Y.M.; Kim, W.S.; Kim, Y.S.; Ko, H.S.; Kim, D.H.; Bae, J.H.; Woo, J.C. and Schmiedel, T., *Quantum Wire Superlattices Grown by Migration Enhanced Epitaxy and Analyzed by Photoluminescence Excitation and Magnetoluminescence Spectroscopy*, J. Korean Phys. Soc., **29**, 482 (1996).

Kleinhammes, A.; Kuhns, P.L.; Moulton, W.G.; Meyer, D.; Sarrao, J.; Fisk, Z. and Sullivan, N.S., "^{7}Li NMR in $La_2Cu_{1-x}Li_xO_4$ to 27 Tesla," in *Physical Phenomena at High Magnetic Fields II*, eds. Fisk, Z.; Gor'kov, L.; Meltzer, D. and Schrieffer, R. (World Scientific, Singapore, 1996), pp. 531-536.

Kuhns, P.L.; Kleinhammes, A.; Schmiedel, T.; Moulton, W.G.; Hughes, E.; Sloan, S.M. and Bowers, C.R., *Optically Pumped NMR In Semiconductors: Theory And Experiment Revisited*, 28th Congress Ampere on Magnetic Resonance and Related Phenomena, Extended Abstracts, eds. Smith, M.E. and Strange, J.H., (1996) pp. 67-68.

Kumar, N.; Reisberg, L. and Zindler, A., *A Major and Trace Element and Sr, Nd, and Os Isotopic Study of a Thick Pyroxenite Layer from the Beni Bousera Ultramafic Complex of N. Morocco,* Geochim. Cosmochim. Acta, **60**, 1429-1444 (1996).

Lacerda, A.; Goettee, J.D.; Schmiedeshoff, G.M.; Kebede, A. and Smith, J.L., *The Energy Gap of SmB_6 at Low Temperatures and in High Magnetic Fields*, Czechoslovak Journal of Physics, **46**, 1991-1992 (1996).

Lacerda, A.; Yatskar, A.; Schmiedeshoff, G.M.; Beyermann, W.P. and Canfield, P.C., *High-Field Low-Temperature Magnetoresistance of Single Crystalline Heavy Fermion $YbNi_2B_2C$*, Phil. Mag. B, **74**, 641-645 (1996).

Lang, T.; Moyland, P.L.; Sergatskov, D.A.; Adams, E.D. and Takano, Y., *Observation of Ferromagnetic Ordering in hcp ^3He*, Phys. Rev. Lett., **77**, 322-325 (1996).

Langlois, D.A.; Smith, M.E.; Benicewicz, B.C.; Hjelm, R.P. and Douglas, E.P., "Properties of Liquid Crystal Thermosets and Their Nanocomposites," in *Applications of High Temperature Polymers* (CRC Press, Boca Raton, 1996), pp. 79-96.

Lawrence, J.M.; Graf, T.; Hundley, M.F.; Mandrus, D.; Thompson, J.D.; Lacerda, A.; Torikachvili, M.S.; Sarrao, J.L. and Fisk, Z., *Kondo Hole Behavior in $Ce_{0.97}La_{0.03}Pd_3$*, Phys. Rev. B, **53**, 12559-12562 (1996).

Lawrence, J.M.; Kwei, G.H.; Sarrao, J.L.; Fisk, Z.; Mandrus, D. and Thompson, J.D., *Structure and Disorder in $YbInCu_4$*, Phys. Rev. B, **54**, 6011 (1996).

Le, L.P.; Heffner, R.H.; MacLaughlin, D.E.; Kojima, K.; Luke, G.M.; Nachumi, B.; Uemura, Y.J.; Sarrao, J.L. and Fisk, Z., *Magnetic Behavior in Li-Doped La_2CuO_4*, Phys. Rev. B, **54**, 9538 (1996).

Lenkewitz, M.; Corsépius, S.; Scheidt, E.-W. and Stewart, G.R., *Investigations of the Transitions in UPd_3*, Journal of Alloys and Compounds, **232**, 67-70 (1996).

Li, G.-Z.; Vining, B.A.; Guan, S. and Marshall, A.G., *Laser-Induced Fluorescence of Ba^+ Ions Trapped and Mass-Selected in a Fourier Transform Ion Cyclotron Resonance Mass Spectrometer*, Rapid Comm. Mass Spectrom., **10**, 1850-1854 (1996).

Li, G.-Z.; Musfeldt, J.L.; Wang, Y.J.; Jandl, S.; Poirier, M.; Revcolevschi, A. and Dhalenne, G., *Optical Observation of the Interplay Between Magnetic and Elastic Energy in a Spin-Peierls System*, Phys. Rev. B (Rapid Comm.), **54**, 1(1996).

Li, G.-Z.; Guan, S. and Marshall, A.G., "Optically Detected Electron Spin Resonance of Trapped, Mass-Selected Gas Phase Molecular Ions," in *Physical Phenomena at High Magnetic Fields – II*, eds. Fisk, Z.; Gor'kov, L.; Meltzer, D. and Schrieffer, R., (World Scientific Publishing Co., Singapore, 1996), pp. 656-661.

Liu, H.L.; Zibold, A.; Tanner, D.B.; Li, M.Y.; Wu, M.K. and Wang, Y.J., "Far-Infrared Studies of $YBa_2Cu_3O_{7-\delta}$ Films in High Magnetic Fields," in *Physical Phenomena at High Magnetic Fields II*, eds. Fisk, Z.; Gor'kov, L.; Meltzer, D. and Schrieffer, R. (World Scientific, Singapore, 1996), pp. 594-600.

Maekawa, R.; Smith, M.R. and Van Sciver, S.W., *Thermal Hydraulic Characteristics of a Prototype CEA Cable-in-Conduit Conductor*, Advances in Cryogenic Engineering, **41**, 529 (1996).

Mani, R.G., and von Klitzing, K., *Fractional Quantum Hall Effects as an Example of Fractal Geometry in Nature*, Zeitschrift Phys. B, **100**, 635-642 (1996).

Markiewicz, W.D.; Bonney, L.A.; Dixon, I.R., Swenson, C.A. and Schneider-Muntau, H.-J., *Technology of 1 GHz NMR Superconducting Magnets*, Physica B, **216**, 200-202 (1996).

Markiewicz, W.D.; Dixon, I.R.; Eyssa, Y.M.; Schwartz, J.; Swenson, C.A.; Van Sciver, S.W. and Schneider-Muntau, H.-J., *25 T High Resolution NMR Magnet Program and Technology,* IEEE Transactions on Magnetics, **32**, 4, 2586-2589 (1996).

Marshall, A.G. and Guan, S., *Advantages of High Magnetic Field for Fourier Transform Ion Cyclotron Resonance Mass Spectrometry*, Rapid Comm. Mass Spectrom., **10**, 1819-1823 (1996).

Marshall, A.G., "Fourier Transform Ion Cyclotron Resonance Mass Spectrometry," in *Physical Phenomena at High Magnetic Fields II*, eds. Fisk, Z.; Gor'kov, L.; Meltzer, D. and Schrieffer, R. (World Scientific, Singapore, 1996), pp. 626-638.

Marshall, A.G., "Ion Cyclotron Resonance Mass Spectrometry: A Brief History," in *Encyclopedia of Nuclear Magnetic Resonance*, Vol. 1, eds. Grant, D.M. and Harris, R.K. (Wiley, London, 1996), pp. 486-489.

Marshall, A.G., *Ion Cyclotron Resonance and Nuclear Magnetic Resonance Spectroscopies: Magnetic Partners for Elucidation of Molecular Structure and Reactivity*, Acc. Chem. Res., **29**, 307-316 (1996).

Martins, G.B.; Rao, D.; Barberis, G.E.; Rettori, C.; Duro, R.J.; Sarrao, J.L.; Fisk, Z.; Oseroff, S.B. and Thompson, J.D., *Electron Spin Resonance of Er^{3+} in YBiPt*, Physica B, **223 & 224**, 396 (1996).

McKenzie, R.H.; Athas, G.J.; .Brooks, J.S.; Clark, R.G.; Dzurak, A.S.; Newbury, R.; Starrett, R.P.; Skougarevsky, A.V.; Tokumoto, M.; Kinoshita, N.; Kinoshita, T. and Tanaka, Y., *Magnetoresistance and Magnetic Breakdown in the Quasi-Two-Dimensional Conductors $(BEDT\text{-}TTF)_2MH_g(SCN)_4[M=K,Rb,Tl]$*, Phys. Rev. B (Rapid Comm.), **54**, R8289 (1996).

McKenzie, R.H.; Brooks, J.S.; Clark, R.G.; Newbury, R.; Starrett, R.P.; Skougarevsky, A.V.; Lewis, R.A.; Takasaki, S.; Yamada, J.; Anzai, H.; Tanaka, Y.; Kinoshita, T.; Kinoshita, N.; Tokumoto, M. and Kushch, N.D., *Magneto-Oscillations and Field-Induced Phase Transitions in Organic Conductors*, Surf. Sci., **362**, 901 (1996).

Melik-Alaverdian, V. and Bonesteel, N.E., "Landau Level Mixing and the Energy Gap in the Fractional Quantum Hall Effect," in *Physical Phenomena at High Magnetic Fields II*, eds. Fisk, Z.; Gor'kov, L.; Meltzer, D. and Schrieffer, R. (World Scientific, Singapore, 1996), pp. 79-84.

Miller, J.R.; Bird, M.D.; Brandt, B.; Painter, T.A.; Schneider-Muntau, H.-J.; Walker, W. and Welton, S.J., *Progress on the NHMFL 45 T Hybrid Magnet System*, IEEE Transactions on Magnetics, **32**, 4 (1996).

Miller, J.R.; Van Sciver, S.W. and Schneider-Muntau, H.-J., *An Overview and Status of the NHMFL 45-T Hybrid Project*, Journal of the Cryogenic Society of Japan, Cryogenics Engineering, **31**, 5, 2 (1996).

Miranda, E., "Mixed Valence and Small Moment Magnetism," in *Physical Phenomena at High Magnetic Fields II*, eds. Fisk, Z.; Gor'kov, L.; Meltzer, D. and Schrieffer, R. (World Scientific, Singapore, 1996), pp. 227-232.

Miranda, E., *Mixed Valence and Small Moment Magnetism*, Phys. Lett. A, **217**, 176-180 (1996).

Miranda, E.; Dobrosavljevic, V. and Kotliar, G., *Kondo Disorder: A Possible Route Towards Non-Fermi Liquid Behavior*, J. Phys.: Cond. Matter, **8**, 9871-9900 (1996).

Monthoux, P. and Manousakis, E., *Low-Lying Excitation Spectrum of Quantum Many-Body Systems*, Phys. Rev. B, **54**, 15101 (1996).

Movshovich, R.; Graf, T.; Mandrus, D.; Thompson, J.D.; Smith, J.L. and Fisk, Z., *Superconductivity in Heavy-Fermion $CeRh_2Si_2$*, Phys. Rev. B, **53**, 8241-8244 (1996).

Movshovich, R.; Hundley, M.F.; Neumeir, J.; Thompson, J.D.; Lawrence, J.M.; Lacerda, A. and Fisk, Z., *Magnetism in Heavy-Fermion CePtPb*, Phys. Rev. B, **53**, 5465-5471 (1996).

Movshovich, R.; Lawrence, J.M.; Hundley, M.F.; Neumeier J.; Thompson, J.D.; Lacerda, A. and Fisk, Z., *Magnetism in CePtPb*, Phys. Rev. B, **53**, 5465-5471 (1996).

Moyland, P.L.; Lang, T.; Adams, E.D.; Stewart, G.R. and Takano, Y., *Nuclear Antiferromagnetic Ordering in $PrBe_{13}$*, Czech. J. Phys, **46**, S1-2199 (1996).

Mueller-Hartmann, E. and Dagotto, E., *Electronic Hamiltonian for Transition Metal Oxide Compounds*, Phys. Rev. B, **54**, R6819 (1996).

Musfeldt, J.L.; Wang, Y.J.; Poirier, M.; Jandl, S.; Revcolevschi, A. and Dhalenne, G., *An Infrared Investigation of the Broken Symmetry Ground State in $GeCuO_3$*, Phys. Rev. B, **54**, 469 (1996).

Nakamae, S. and Schwartz, J., *Magnetoresistivity of Ag Tape Co-Processed with $Bi_{1.4}Pb_{0.6}Sr_2Ca_2Cu_3O_x$ Superconductor*, Cryogenics. **36**, 5, 395-397 (1996).

Nawrocki, J.P.; Wigger, M.; Watson, C.H.; Hayes, T.M.; Senko, M.W.; Benner, S.A. and Eyler, J.R., *Analysis of Combinatorial Libraries Using Electrospray Fourier Transform Ion Cyclotron Resonance Mass Spectrometry*, Rapid Comm. Mass Spectrom., **14**, 1860-1864 (1996).

Nazarenko, A. and Dagotto, E., *A Possible Phononic Mechanism for d-Wave Superconductivity in the Presence of Short-Range AF Correlations*, Phys. Rev. B, **53**, R2987 (1996).

Nazarenko, A.; Haas, S.; Moreo, A. and Dagotto, E., "Low-Hole Doping Regime of the t - j Model: Possible Microscopic Scenario for Cuprates," in *Physical Phenomena at High Magnetic Fields II*, eds. Fisk, Z.; Gor'kov, L.; Meltzer, D. and Schrieffer, R. (World Scientific, Singapore, 1996), pp. 555-560.

Nazarenko, A.; Moreo, A.; Riera, J.A. and Dagotto, E., *d_{x2-y2} Superconductivity in a Model of Correlated Fermions*, Phys. Rev B (Rapid Comm.), **54**, R768 (1996).

Panek, J.; Huang, X. and Van Sciver, S.W., *Localized Heat Transfer to Vertical Forced Flow Two-Phase Helium*, Advances in Cryogenic Engineering, **41A**, 173-177 (1996).

Paschen, S.; Felder, E.; Chernikov, M.A.; Ott, H.R.; Fisk, Z. and Sarrao, J.L., *Electrical Transport, Magnetic, and Thermal Properties of FeSi*, Czech. Journal of Physics, **46** Suppl. S4, 1997 (1996).

Pernambuco-Wise, P.; Gilmore, P.; Lesch, B.; Eyssa, Y.M. and Schneider-Muntau, H.-J., *Systematic Failure Testing of Internally Reinforced Magnets*, IEEE Transactions on Magnetics, **32**, 4, 2458 (1996).

Popova, M.N.; Klimin, S.A.; Golubchik, S.A.; Cao, G. and Crow, J.E., *Spectroscopic Detection of Magnetic Phase Transition in $BaPrO_3$*, Phys. Lett., **A211**, 242 (1996).

Prestemon, S.; Gilmore, P.; Gao, B.J. and Bird, M.D., *Design Optimization of Multi-Coil Resistive Magnets*, IEEE Transactions on Magnetics, **32**, 4, 2550-2553 (1996).

Rettori, C.; Oseroff, S.B.; Rao, D.; Valdivia, J.A.; Barberis, G.E.; Martins, G.B.; Sarrao, J.L.; Fisk, Z. and Tovar, M., *ESR of Gd^{3+} in Magnetically Ordered Eu_2CuO_4*, Phys. Rev. B, **54**, 1123 (1996).

Rosenbaum, J.M.; Zindler, A. and Robenston, J.L., *Mantle Fluids: Evidence from Fluid Inclusions,* Geochim. Cosmochim. Acta, **60**, 3229-3252 (1996).

Salters, V.J.M., *The Generation of Mid-Ocean-Ridge-Basalts from the Hf and Nd Isotope Perspective,* Earth and Planet. Sci. Lett., **141**, 109-123 (1996).

Samoilov, A.V.; Yeh, N.-C., and Tsuei, C.C., *High-Field Magnetoresistance in Amorphous Superconducting Thin Films of Mo_3Si and Nb_3Ge,* Czech. J. Phys., **46,** Suppl. 2, 761 (1996).

Sandhu, P.S.; Athas, G.J.; Brooks, J.S.; Haanappel, E.G.; Goettee, J.D.; Rickel, D.G.; Tokumoto, M.; Kinoshita, N.; Kinoshita, T. and Tanaka, Y., *High Field Shubnikov de Haas Studies of the Organic Superconductor $(BEDT\text{-}TTF)_2NH_4H_g(SCN)_4$*, Surf. Science, **361-362**, 913 (1996).

Sarrao, J.L.; Benton, C.L.; Fisk, Z.; Lawrence, J.M.; Mandrus, D. and Thompson, J.D., *$YbIn_{1-x}Ag_xCu_4$: Crossover from First-Order Valence Transition to Heavy Fermion Behavior*, Physica B, **223 & 224**, 366 (1996).

Sarrao, J.L.; Cassady, L.S.; Fisk, Z.; Mandrus, D. and Thompson, J.D., "Lithium Doping in $La_{2-y}Sr_yCuO_4$," in *Physical Phenomena at High Magnetic Fields II*, eds. Fisk, Z.; Gor'kov, L.; Meltzer, D. and Schrieffer, R. (World Scientific, Singapore, 1996), p. 585.

Sarrao, J.L.; Immer, C.D.; Benton, C.L.; Fisk, Z.; Lawrence, J.M.; Mandrus, D. and Thompson, J.D., *Evolution from First-Order Valence Transition to Heavy Fermion Behavior in* $YbIn_{1-x}Ag_xCu_4$, Phys. Rev. B, **54**, 12207 (1996).

Sarrao, J.L.; Young, D.P.; Fisk, Z.; Moshopoulou, E.G.; Thompson, J.D.; Chakoumakos, B.C. and Nagler, S.E., *Structural, Magnetic, and Transport Properties of* $La_2Cu_{1-x}Li_xO_4$, Phys. Rev. B, **54**, 12014 (1996).

Schiller, A. and Hershfield, S.P., *Solution of an AC Kondo Model*, Phys. Rev. Lett., **77**, 1821-1824 (1996).

Schmiedeshoff, G.M.; Lacerda, A.; Fisk, Z. and Smith, J.L., *The Electrical Resistivity of* UBe_{13} *in High Magnetic Fields*, Phys. Rev. B, **54**, 7401-7405 (1996).

Schrieffer, J.R. and Kampf, A.P., "ARPES: Novel Effects in the Energy and Momentum Distributions of Nearly Antiferromagnetic Metals," in *Physical Phenomena at High Magnetic Fields II*, eds. Fisk, Z.; Gor'kov, L.; Meltzer, D. and Schrieffer, R. (World Scientific, Singapore, 1996), p. 607.

Schwartz, J.; Wolters, Ch.; Amm, K.M. and Sun, Y.R., *HgBaCaCuO Superconductors: Processing, Properties and Potential*, Physica B, **216**, 261-265 (1996).

Senko, M.W.; Canterbury, J.D.; Guan, S. and Marshall, A.G., *A High-Performance Modular Data System for FT-ICR Mass Spectrometry*, Rapid Comm. Mass Spectrom., **10**, 1839-1844 (1996).

Senko, M.W.; Hendrickson, C.L.; Pasa-Tolic, L.; Marto, J.A.; White, F.M.; Guan, S. and Marshall, A.G., *Electrospray Ionization Fourier Transform Ion Cyclotron Resonance Mass Spectrometry at 9.4 Tesla*, Rapid Comm. Mass Spectrom., **10**, 1824-1828 (1996).

Shepard, M.; Cao, G.; McCall, S.; Freibert, F. and Crow, J.E., *Magnetic and Transport Properties of Na Doped* $SrRuO_3$ *and* $CaRuO_3$, J. Appl. Phys. **79**, 4821 (1996).

Shoaff, P.V., Jr.; Schwartz, J.; Van Sciver, S.W. and Weijers, H.W., *HTS Coil and Joint Development for a 5T NMR Insert Coil*, Advances in Cryogenic Engineering, **41**, 413 (1996).

Sievers, K.; Scheidt, E.-W. and Stewart, G.R., UPt_3 *in* $AuCu_3$ *Structure*, Phys. Rev. B, **53**, 699-702 (1996).

Simmons, J.A.; Du, R.R.; Zudov, M.A.; Chui, H.C.; Harff, N.E. and Hammons, B.E., "Composite Fermions in 2 x 10^6 cm^2/Vs Mobility AlGaAs/GaAs Heterostructures Grown by MOCVD," in *Proceedings of the 23rd International Conf. on the Physics of Semiconductors*, Berlin, 1996, eds. Scheffler, M. and Zimmerman, R., (World Scientific, Singapore, 1996), Vol. 3, p. 2511.

Solouki, T.; Pasa-Tolic, L.; Jackson, G.S.; Guan, S. and Marshall, A.G., *High-Resolution Multistage MS,* MS^2*, and* MS^3 *Matrix-Assisted Laser Desorption/Ionization FT-ICR Mass Spectra of Peptides from a Single Laser Shot*, Anal. Chem., **68**, 3718-3725 (1996).

Sullivan, N.S., "NMR Studies of Quantum Solids at High Magnetic Fields and Low Temperatures," in *Physical Phenomena at High Magnetic Fields II*, eds. Fisk, Z.; Gor'kov, L.; Meltzer, D. and Schrieffer, R. (World Scientific, Singapore, 1996), pp. 617-625.

Sun, Y.R. and Schwartz, J., *Anisotropy Studies on Aligned* $HgBa_2CaCu_2O_{6+\delta}$ *Powder-Confirmation of the Collective Pinning Theory for Anisotropic Materials*, Physical Review B, **53**, 9, 5830 (1996).

Swenson, C.A.; Eyssa, Y.M. and Markiewicz, W.D., *Quench Protection Heater Design for Superconducting Solenoids*, IEEE Transactions on Magnetics, **32**, 4, 2659 (1996).

Thomas, F.; Wand, B.; Luehmann, T.; Gegenwart, P.; Stewart, G.R.; Steglich, F.; Brison, J.P.; Buzdin, A.; Glémot, L. and Flouquet, F., *Upper Critical Field and the Possibility of FFLO State in UBe_{13}*, J. Low Temp. Phys., **102**, 117-132 (1996).

Tian, F.; Lee, K.-C.; Hu, W. and Cross, T.A., *Monovalent Cation Transport: Lack of Structural Deformation Upon Cation Binding*, Biochemistry, **35**, 11959-11966 (1996).

Tsutsui, K.; Ohta, Y.; Eder, R.; Maekawa, S.; Dagotto, E. and Riera, J.A., *Heavy Quasiparticles in the Anderson Lattice Model*, Phys. Rev. Lett., **76**, 279 (1996).

Trinkl, W.; Corsépius, S. and Stewart, G.R., *New Clues for Understanding the Magnetic Behavior of UPt_3*, J. Alloys and Compounds, **240**, 96-100 (1996).

Trinkl, W.; Corsépius, S. and Stewart, G.R., *Transition from Magnetic Ordering to Kondo—Behavior in $Ce_{3-x}La_xAl_{11}$*, J. Alloys and Compounds, **239**, 46-49 (1996).

Trinkl, W.; Corsepius, S.; Guha, E. and Stewart, G.R., *Spin Glass Behavior in Doped and Pure UPt_3—A Possible Key*, Europhysics Letters, **35**, 207-213 (1996).

Trinkl, W.; Weilnhammer, U.; Corsepius, S.; Schreiner, T.; Scheidt, E.-W. and Stewart, G.R., *Non-Fermi-Liquid Behavior Over Two Decades of Temperature in Doped UPt_3*, Phys. Rev. B, **54**, 1163-1168 (1996).

Uji, S.; Brooks, J.S.; Chaparala, M.; Seger, L.; Szabo, T.; Tokumoto, M.; Kinoshita, N.; Kinoshita, T.; Tanaka, Y. and Anzai, H., *Wave Shape of De Haas-Van Alphen Oscillations and Effective Mass in the Two-Dimensional Organic Conductor α-$(BEDT\text{-}TTF)_2KH_g(SCN)_4$*, Solid State Comm., **100**, 825 (1996).

Uji, S.; Terashima, T.; Aoki, H.; Brooks, J.S.; Tokumoto, M.; Kinoshita, N.; Tanaka, Y. and Anzai, H., *Fermi Surface Studies in the Two Dimensional Organic Conductors $(BEDT\text{-}TTF)_2MH_g(SCN)_4$ $(M=Tl,K,Rb,NH_4)$*, Phys. Rev. B, **54**, 9332 (1996).

Uji, S.; Terashima, T.; Aoki, H.; Brooks, J.S.; Tokumoto, M.; Takasaki, S.; Yamada, Y. and Anzai, A., *Rapid Oscillations in the Organic Conductor $(TMTSF)_2ClO_4$*, Phys. Rev. B., **53**, 14399 (1996).

Uwatoko, Y.; Ishii, T.; Oomi, G.; Takahasi, H.; Mori, N.; Thompson, J.D.; Sarrao, J.L.; Mandrus, D. and Fisk, Z., *Pressure Collapse of Kondo Gap in Kondo Compound CeRhSb*, J. Phys. Soc. Jpn., **65**, 27 (1996).

Vaghar, M.R.; Garmestani, H. and Markiewicz, W.D., *Elastoplastic Stress Analysis of Nb_3Sn Superconducting Magnet*, Journal of Applied Physics, **80**, 4, 2490-2500 (1996).

Valfells, S.; Brooks, J.S.; Uji, S.; Goettee, J.D.; Athas, G.J.; Klepper, S.J.; Sandhu, P.S.; Sarrao, J.L. and Fisk, Z., "Magnetoresistance of η—Mo_4O_{11} in High Magnetic Fields and at Low Temperatures," in *Physical Phenomena at High Magnetic Fields II*, eds. Fisk, Z.; Gor'kov, L.; Meltzer, D. and Schrieffer, R. (World Scientific, Singapore, 1996), p. 352.

Van Cleemput, M.; Jones, H.; van der Burgt, M.; Barrau, J.R.; Lee, J.A.; Eyssa, Y.M. and Schneider-Muntau, H.-J., *Copper/Stainless Steel Conductor for High Field Pulsed Magnets*, Physica B, **216**, 226-229 (1996).

Van Sciver, S.W.; Welton, S.J.; Bartholomew, K. and Miller, J.R., *Cryogenic System for the 45 T Hybrid Superconducting Magnet*, Teion Kogaku (Japanese Journal of Cryogenic Engineering), **31**, 2 (1996).

Van Sciver, S.W.; Welton, S.J.; Bartholomew, K.; Gorbunov, M.B.; and Miller, J.R., *et al*, *Design, Development, and Testing of the Cryogenic System for the 45-T Hybrid Magnet*, Advances in Cryogenic Engineering, **41B**, 1273-1282 (1996).

Wang, Y.; Amundson, R.G. and Trumbore, S., *Radiocarbon Dating of Soil Organic Matter*, Quaternary Research, **45**, 282-288 (1996).

Wang, Y.; McDonald, E.; Amundson, R.G.; McFadden, L. and Chadwick, O., *An Isotopic Study of Soils in Chronological Sequences of Alluvial Deposits, Providence Mountains, California,* Geological Society of America Bulletin, **108**, 379-391 (1996).

Wang, Y.J.; Kaplan, R.; Ng, H.K.; Doverspike, K.; Gaskill, D.K.; Ikedo, T.; Akasaki, I. and Amono, H., *Magneto-Optical Studies of GaN and GaN/$Al_xGa_{1-x}N$: Donor Zeeman Spectroscopy and Two Dimensional Electron Gas Cyclotron Resonance*, J. of Appl. Phys., **79**, 8007 (1996).

Welton, S.J.; Van Sciver, S.W.; Bartholomew, K.; Gorbunov, M.B.; McIntosh, G.E.; Bon Mardion, G. and Viargues, F., *Design, Development and Testing of the JT Refrigerators for the 45-T Hybrid Magnet*, Advances in Cryogenic Engineering, **41B**, 1283-1289 (1996).

White, F.M.; Marto, J.A. and Marshall, A.G., *An External Source 7 Tesla FT-ICR Mass Spectrometer with Electrostatic Ion Guide*, Rapid Comm. Mass Spectrom., **10**, 1845-1849 (1996).

Wolters, Ch.; Amm, K.M.; Sun, Y.R. and Schwartz, J., *Synthesis of (Hg, Re) $Ba_2Ca_{n-1}Cu_nO_y$ Superconductors*, Physica C, **267**, 164-172 (1996).

Wood, J.T. and Embury, J.D., *Plasticity and Fracture of In-Situ Composites*, Fatigue & Fract. of Eng. Mat. Structures, **18**, 747-753 (1995).

Wood, J.T.; Griffin, A.L.; Embury, J.D.; Zhou, R.; Nastasi, M. and Veron, M., *The Influence of Microstructural Scale on the Combination of Strength in Electrical Resistivity in Cu Based Composites*, J. Mech. Phy. Solids, **44**, 737-750 (1996).

Xu, F.; Wang, A.; Vaughn, J.B. Jr. and Cross, T.A., *A Catalytic Role for Protic Solvents in Conformational Interconversion*, J. Am. Chem. Soc., **118**, 9176-9177 (1996).

Yoshinari, Y.; Hammel, P.C.; Martindale, J.A.; Thompson, J.D.; Sarrao, J.L. and Fisk, Z., *Magnetic Excitations of the Doped-Hole State in Diamagnetic $La_2Cu_{0.5}Li_{0.5}O_4$*, Phys. Rev. Lett., **77**, 2069 (1996).

Yuen, T.; Seyedahmadian, M.; Salomon, R.E.; Myer, G.H. and Cao, G., *Magnetic Properties of a High T_c Superconductivity Related System $Y_{1-x}Pr_xBa_2Fe_3O_8$*, J. Appl. Phys., **79**, 6001 (1996).

Zou, H. and Zindler, A., *Constraints on the Degree of Dynamic Partial Melting and Source Composition Using Concentration Ratios in Magmas*, Geochim. Cosmochim. Acta, **60**, 711-717 (1996).

Presentations and Posters

This section includes invited and contributed talks and papers at conferences; papers in conference proceedings that were not peer-reviewed; abstracts; and presentations at universities and public forums.

Amm, K.M.; Wolters, Ch.; Knoll, D.C.; Peterson, S.C. and Schwartz, J., *Growth of $Hg_{0.9}Re_{0.1}Ba_2Ca_2Cu_3O_{8+x}$ on a Metallic Substrate,* Applied Superconductivity Conf., Pittsburgh, PA, August 25-30, 1996.

Bird, M.D., *Experience with Cu-Ag Sheet in Resistive Magnets at the NHMFL*, Intl. Workshop on High Magnetic Fields: Industry, Materials and Technology, Tallahassee, FL, February 28-March 1, 1996.

Bird, M.D., *The Development of Florida-Bitter Magnets at the National High Magnetic Field Laboratory*, National Superconducting Cyclotron Laboratory, Michigan State Univ., East Lansing, MI, May 1996; Applied Superconductivity Center, Univ. of Wisconsin, Madison, WI, 1996.

Bodart, J.R.; Masterton, A.; Moulton, W.G.; Kuhns, P.L.; Garcia, B.M.; Pilla, S. and Sullivan, N.S., *The Effect of High Magnetic Fields on JFET Device Performance*, Bull. Am. Phys. Soc., **41**, 303 (1996).

Bonesteel, N.E. and Melik-Alaverdian, V., *d-Wave Pairing in a Double-Layer Composite Fermion Metal,* APS March Meeting, St. Louis, MO, March 18-22, 1996.

Bonesteel, N.E., *Composite Fermions and Gauge Fields in the Quantum Hall Effect,* SCRI, Tallahassee, FL, May 15, 1996; FAMU Physics Dept., Tallahassee, FL, September 11, 1996.

Bonesteel, N.E., *Introduction to Solid State Physics*, NSF Chautauqua Course, NHMFL, Tallahassee, FL, June 14, 1996.

Bonesteel, N.E., *Monte Carlo Studies of Composite Fermion Wave Functions*, The Electron Quantum Liquid in Systems of Reduced Dimensions Conf., Trieste, Italy, July 5, 1996.

Bonesteel, N.E., *Pairing and Gauge Fields in Composite Fermion Metals*, New Developments in the Quantum Hall Effect Conf., Minneapolis, MN, May 3, 1996.

Boulat, B.; Epstein, D.M. and Rance, M., *Application of the Synchronous Nutation Method to a Complex of Molecules in Slow Dynamic Equilibrium*, 37th Experimental Nuclear Magnetic Resonance Conf., Asilomar, CA, March, 1996.

Boutemy, S.; Kessler, J. and Schwartz, J., *React-Wind-and-Sinter Technique for $Bi_2Sr_2CaCu_2O_8$ High T_c Coils*, Applied Superconductivity Conf., Pittsburgh, PA, August 25-30, 1996.

Bowers, C.R.; Kuhns, P.L.; Kleinhammes, A.; Schmiedel, T.; Sloan, S.M.; Chabrier, P. and Moulton, W.G., *NMR Detected Optical Dynamic Nuclear Polarization Studies of 69Ga in GaAs and 115In in InP*, Bulletin of the Amer. Phys. Soc., **41** (1) 591 (1996).

Brunel, L.-C., *High Field/High Frequency Electron Magnetic Resonance*, Institute of Molecular Biology, FSU, September, 1996.

Brunel, L.-C., *Modern Developments in High Field/High Frequency Electron Magnetic Resonance,* XVIIth Intl. Conf. on Magnetic Resonance in Biological Systems, Keystone, CO, August, 1996; Workshop on Millimeter Wave Spectroscopy of Solids, Univ. of California at Los Angeles, CA, March, 1996.

Brunel, L.-C., *Recent Progress in High Field/High Frequency Electron Magnetic Resonance*, 28th Southeastern Magnetic Resonance Conf., Tuscaloosa, AL, October 10-12, 1996.

Brunel, L.-C., *The Electron Magnetic Resonance Program at the NHMFL*, Univ. of Florida, April 11, 1996.

Burkhardt, E.E. and Schwartz, J., *Three-Dimensional Numerical Analysis of the Stability of $Ag/Bi_2Sr_2Ca_2Cu_3O_x$ Tape Conductors*, Applied Superconductivity Conf., Pittsburgh, PA, August 25-30, 1996.

Burkhardt, E.E. and Schwartz, J., *Two-Dimensional Finite Element Analysis of the Stability of Ag/BSCCO Tapes*, Advances in Cryogenic Engineering 41; Cryogenic Engineering Conf., 1996.

Cage, B.; Hassan, A.K.; Pardi, L.; Krzystek, J.; Brunel, L.-C. and Dalal, N., *Beating the Exchange Broadening with High Field EPR Spectroscopy*, 28th Southeastern Magnetic Resonance Conf., Tuscaloosa, AL, October 10-12, 1996.

Cassady, L.S.; Sarrao, J.L.; Fisk, Z. and Lochner, E., *Lithium Doping in $La_{2-x}Sr_xCu_{1-y}Li_yO_4$*, APS March Meeting, St. Louis, MO, March 18-22, 1996.

Cooper, W.T.; Fievre, A.; Solouki, T. and Marshall, A.G., *Characterization of Aquatic Humic Substances. Part 2. FT-ICR Mass Spectrometry*, Geochemistry Talk #3, 212th Amer. Chem. Soc. Natl. Meeting, Orlando, FL, August, 1996.

Crawford, M.K.; Harlow, R.L.; McCarron, E.M.; Tozer, S.W.; Huang, Q.; Cox, D.E. and Zhu, Q., "Structural Phase Transitions and Superconductivity in Lanthanum Copper Oxides," in *Proceedings of NATO Advanced Study Institute Materials Aspects of High T_c Superconductivity: 10 Years After the Discovery*, Delphi, Greece, August 19-31, 1996.

Cross, T.A., *The Unique Advantages of NMR Spectroscopy,* Tokyo Univ. of Agriculture & Technology, Tokyo, Japan, November, 1996.

Cross, T.A., *Trytophan, the Unique Amino Acid of Membrane Proteins: A Perspective from Gramicidin and Solid State NMR*, 28th Southeastern Magnetic Resonance Conf., Tuscaloosa, AL, October 10-12, 1996.

Cross, T.A.; Cotten, M.; Tian, F.; Xu, F. and Hu, W., *Trytophan, the Unique Amino Acid of Membrane Proteins: A Perspective from Gramicidin and Solid State NMR*, XVIIth Intl. Conf. on Magnetic Resonance in Biological Systems, Keystone, CO, August, 1996.

Cross, T.A.; Ketchem, R.R.; Brenneman, M.; Hu, W.; Lee, K.-C.; Cotten, M.; Tian, F. and Huo, S., *High Resolution Structure & Dynamics by Solid State NMR: Gramicidin A in Hydrated Lipid Bilayers,* Dept. of Chemical Engineering, Florida State Univ. & Florida A&M Univ., April, 1996.

Cross, T.A.; North, C.L.; Hu, W.; Cotten, M. and Huo, S., *High Resolution Dynamics in a Membrane-Bound Polypeptide by Solid State NMR,* Himeji Institute of Technology, Himeji, Japan, March, 1996; Institute of Chemical Engineering, Kyoto Univ., Kyoto, Japan, March, 1996; Department of Synthetic Chemistry and Biological Chemistry, Kyoto Univ., Kyoto, Japan, March, 1996; Tokyo Univ. of Agriculture & Technology, Tokyo, Japan, March, 1996.

Cross, T.A.; Tian, F.; Hu, W.; Lee, K.-C. and Ketchem, R.R., *High Resolution Structure in Anisotropic Environments by Solid State NMR,* Natl. (Japan) NMR Meeting, Kyoto, Japan, November, 1996; Univ. of Hokkaido, Sapporo, Japan, November, 1996.

Cross, T.A.; Tian, F.; Hu, W.; Lee, K.-C. and Ketchem, R.R., *High Resolution Structure in Membranes by Solid State NMR: The Gramicidin A Channel*, Dept. of Chemistry, Ohio Univ., April, 1996.

Crow, J.E.; Parkin, D.M.; Schneider-Muntau, H.-J. and Sullivan, N.S., "The National High Magnetic Field Laboratory, An Introduction to Science and Technology Opportunities," in *Physical Phenomena at High Magnetic Fields II*, eds. Fisk, Z.; Gor'kov, L.; Meltzer, D.; Schrieffer, R. (World Scientific Publishing Co., Singapore, 1996), pp. 1-15.

Dagotto, E., *Antiferromagnetic Real-Space Scenario for the Cuprates*, Workshop on High-T_c Superconductivity, Houston, TX, March, 1996.

Dagotto, E., *High-T_c Superconductivity: A Brief Review on Photoemission Results from the Experimental and Theoretical Point of View*, Freie Universitat Berlin, Berlin, Germany, October, 1996.

Dagotto, E., *Strongly Correlated Electrons in High T_c Superconductors and Related Novel Compounds*, Weekly Physics Colloquium, Univ. of Georgia, Athens, GA, February, 1996.

Dagotto, E., *Surprises on the Way from 1D to 2D Quantum Magnets: The Novel Ladder Materials.*, Univ. of Florida, Gainesville, FL, December, 1996.

Dagotto, E.; Nazarenko, A.; Moreo, A. and Riera, J.A., *Model of Correlated Fermions with $d_{x^2-y^2}$ Superconductivity*, APS Bulletin 119 (1996); Epitome of the APS March Meeting, St. Louis, MO, March 18-22, 1996.

Dobrosavljevic, V. and Horbach, M., *Glassy Phase of the Random Field Ising Model: A 1/d Approach*, APS March Meeting, St. Louis, MO, March 18-22, 1996.

Dobrosavljevic, V. and Kotliar, G., *The Mott-Anderson Transition*, Intl. Conf. on Electron Localization and Quantum Transport in Solids, Jaszowiec, Poland, August, 1996.

Dobrosavljevic, V., *The Mott-Anderson Transition*, Rice Univ., November, 1996.

Duffy, D. and Moreo, A., *Effect of an External Magnetic Field on the Hubbard Model with Next-Nearest-Neighbor Hopping*, APS Bulletin 120 (1996); Epitome of the APS March Meeting, St. Louis, MO, March 18-22, 1996.

Dur, O.; Nakamae, S.; Schwartz, J. and Hascicek, Y.S., *Magnetoresistivity of Silver and Silver Magnesium Sheath Material for Bi-Based High Temperature Superconductor*, Applied Superconductivity Conf., August 25-30, Pittsburgh, PA, 1996.

Emmett, M.R.; Solouki, T. and Marshall, A.G., "MALDI FT-ICR MS Analysis of Luteinizing Hormone Releasing Hormone," p. 482, in *Proceedings of 44th Amer. Soc. Mass Spectrom. Ann. Conf. on Mass Spectrometry & Allied Topics*, Portland, OR, May, 1996.

Emmett, M.R.; Conrad, C.A.; Solouki, T. and Marshall, A.G., *Cytokine Analysis by High-Resolution FT-ICR Mass Spectrometry*, 1996 Soc. for Neurosciences Meeting, Washington, D.C., November, 1996.

Engel, L.W.; Li, C.-C.; Shahar, D.; Kurdak, C.; Shayegan, M. and Tsui, D.C., *Microwave Studies of Quantum Hall Effect and Insulating Phases*, Workshop on Millimeter Wave Spectroscopy of Solids, Univ. of California at Los Angeles, CA, March, 1996.

Engel, L.W.; Li, C.-C.; Shahar, D.; Tsui, D.C. and Shayegan, M., *Microwave Conductivity Resonances in 2D Electron System at Low Landau Filling*, APS March Meeting, St. Louis, MO, March 18-22, 1996.

Engel, L.W.; Shahar, D.; Kurdak, C. and Tsui, D.C., *Scaling in Quantum Hall Effect*, Localization '96, Jaszowiec, Poland, 1996.

Eyssa, Y.M.; Markiewicz, W.D. and Miller, J.R., *Quench, Thermal and Magnetic Diffusion Computer Code for Superconducting Solenoids*, Applied Superconductivity Conf., August 25-30, Pittsburgh, PA, 1996.

Fanucci, G.; Krzystek, J.; Talham, D.R. and Brunel, L.-C., *Broadband High Field EPR Spectroscopy of Canted Antiferromagnets*, 28th Southeastern Magnetic Resonance Conf., Tuscaloosa, October 10-12, 1996.

Fisk, Z., *Heavy Fermion Physics*, Physics Colloquium, Iowa State Univ., October, 1996.

Fisk, Z., *Kondo Insulators*, Physics Colloquium, Boston College, November, 1996.

Fisk, Z., *Matthias, Magnetism, and Superconductivity*, Physics Colloquium, Louisiana State Univ., May 1996; Chemistry Colloquium, Florida State Univ., September, 1996.

Fisk, Z., *New Materials*, Workshop on Condensed-Matter and Materials Physics, National Research Council, Washington, D.C., June 1996; Materials Science and Technology Colloquium, Los Alamos National Laboratory, August, 1996.

Fisk, Z., *Properties of Li-Doped La_2CuO_4*, Texas Center for Superconductivity at the Univ. of Houston 10th Anniversary Workshop, March, 1996.

Fu, R. and Bodenhausen, G., *Broadband Decoupling in NMR with Adiabatic Frequency-Modulated "Chirp" Pulses*, 37th Experimental Nuclear Magnetic Resonance Conf. (ENC), Asilomar, CA, 1996.

Fu, R.; Pelupessy, P. and Bodenhausen, G., *Broadband Cross Polarization at High Speed Magic Angle Spinning by Using Modulated "Meandering" Spin-Lock*, 38th Rocky Mountain Conf. on Analytical Chemistry, Denver, CO, 1996.

Geerts, W.; Kayatama, T.; Suzuki, Y. and Childress, J.R., *Wavelength Dependence of the Magneto-Optical Properties of the Interfaces of a Au Sandwiched (001) Fe Film*, J. Vac. Sci. Technol. B, **14**, 3176-3179 (1996).

Geerts, W.; MacKenzie, J.D.; Abernathy, C.R.; Pearton, S.J. and Schmiedel, T., *Temperature Dependence of the Electrical Transport of Carbon Doped GaN*, Mat. Res. Soc. Symp., 421 Compound Semiconductor Electronics and Photonics, 1996.

Geerts, W.; MacKenzie, J.D.; Abernathy, C.R.; Pearton, S.J. and Schmiedel, T., *Electrical Transport in p-GaN, n-InN and n-InGaN*, Solid State Electronics, **39,** 1289-1294 (1996).

Geerts, W.; MacKenzie, J.D.; Abernathy, C.R.; Pearton, S.J. and Schmiedel, T., *Temperature Dependence of the Electrical Transport of Carbon Doped GaN*, Materials Research Soc. Spring Meeting, San Francisco, CA, April, 1996; Mat. Res. Soc. Symp. Proc., **421**, 425-430 (1996).

Genio, E.B.; Ihas, G.G. and Sullivan, N.S., *Population Difference Thermometry Using Zeeman Perturbed NQR*, Bull. Am. Phys. Soc., **41**, 1671 (1996).

Genio, E.B.; Xu, J.W.; Ihas, G.G. and Sullivan, N.S., *Nuclear Relaxation Enhancement of Metallic Sb by ^{3}He at Low Temperatures*, Bull. Am. Phys. Soc., **41**, 42 (1996).

Godfrey, L.V.; Lee, D.-C.; Halliday, A.N., Jr.; Hein, J.R. and Salters, V.J.M., *Hafnium Isotope Ratios in Ferromanganse Deposits: A Record of ε_{Hf} in Seawater*, 1996.

Gor'kov, L.P. and Kumar, P., *Hole Spectrum in Three Band Model*, 10th Anniversary HTS Workshop, Houston, TX, March 12-16, 1996.

Gor'kov, L.P. and Schrieffer, J.R., *Lifshitz-Kosevich Oscillations in Superconductors at Fields Well Below Hc_2*, 76th Statistical Mechanics Conf., Rutgers Univ., Hill Center, December 15-17, 1996.

Gor'kov, L.P., *Fermi Liquid vs. Non-Fermi Liquid Features in Q1D Conductors*, Conf. on Quantum Coherence in Strongly Correlated Fermion Systems, Pisa, Italy, July 22-26, 1996.

Gor'kov, L.P., *Heavy Fermions: Theoretical*, NHMFL 1996 Three-Site Workshop, Camp Weed, October 26-27, 1996.

Gor'kov, L.P., *Non-Fermi Liquid Features in Quasi-One-Dimensional Organic Conductors Due to Their Proximity to SDW-State*, Intl. Conf. on Strongly Correlated Electron Systems, Zurich, Switzerland, August 19-22, 1996.

Guan, S. and Marshall, A.G., *Interactive Mass Spectrometry*, Analytical Poster #78, 212th Amer. Chem. Soc. Natl. Meeting, Orlando, FL, August, 1996.

Guan, S. and Marshall, A.G., *Linear Prediction Time-Domain Data Analysis for Ion Cyclotron Resonance Mass Spectrometry*, Abstract #485, Paper 987P, 47th Pittsburgh Conf. on Analytical Chem. and Applied Spectroscopy, Chicago, IL, March, 1996.

Guan, S. and Marshall, A.G., *Talking Back to Your Mass Spectrometer: Object-Oriented Real-Time Interactive Control of Trapped Ions in FT-ICR Mass Spectrometry*, Abstract #483, Paper #284, 47th Pittsburgh Conf. on Analytical Chem. and Applied Spectroscopy, Chicago, IL, March, 1996.

Guan, S.; Li, G.-Z. and Marshall, A.G., "Dependence of FT-ICR Time-Domain Signal Decay Envelope on Ion-Neutral Collision Mechanism," p. 493, in *Proceedings of 44th Amer. Soc. Mass Spectrom. Ann. Conf. on Mass Spectrometry & Allied Topics*, Portland, OR, May, 1996.

Guan, S.; Senko, M.W.; Canterbury, J.D. and Marshall, A.G., *High-Performance Fourier Transform Ion Cyclotron Resonance Mass Spectrometry Data System*, Abstract #487, Paper #121P, 47th Pittsburgh Conf. on Analytical Chem. and Applied Spectroscopy, Chicago, IL, March, 1996.

Guan, S.; Senko, M.W.; Hendrickson, C.L.; Pasa-Tolic, L.; Marto, J.A.; White, F.M. and Marshall, A.G., *High-Field Electrospray FT-ICR Mass Spectrometer for Biopolymer Analysis*, Abstract #486, Paper #122P, 47th Pittsburgh Conf. on Analytical Chem. and Applied Spectroscopy, Chicago, IL, March, 1996.

Guan, S.; Solouki, T.; Emmett, M.R. and Marshall, A.G., *MALDI FT-ICR MS for Peptide Mapping, Peptide Sequencing, and Identification and Location of Disulfide Bridges in Proteins*, Abstract #484, Paper #123P, 47th Pittsburgh Conf. on Analytical Chem. and Applied Spectroscopy, Chicago, IL, March, 1996.

Guan, S.; Xin, T.; Reinhold, B.B. and Marshall, A.G., "Internal Energy Deposition by Quadrupolar Excitation in the Presence of Collisional Cooling," p. 494, in *Proceedings of 44th Amer. Soc. Mass Spectrom. Ann. Conf. on Mass Spectrometry & Allied Topics*, Portland, OR, May, 1996.

Haik, Y.S.; Chen, C.J. and Pai, V., *Development of Biomagnetic Fluid Dynamics*, Ninth Intl. Symp. on Transport Phenomena in Thermal-Fluids Engineering, Singapore, June 25-28, 1996.

Haik, Y.S.; Chen, C.J. and Pai, V., *Magnetic Fluid Dynamics of Blood Flow*, 1996 ASCE Engineering Mechanics Conf., Fort Lauderdale, FL, May 19-22, 1996.

Hassan, A.K.; Balster-Martins, G.; Pardi, L.; Chou, L.K.; Talham, D.R.; Meisel, M.W. and Brunel, L.-C., *ESR Studies of the Haldane Spin System TMNIN*, 28th Southeastern Magnetic Resonance Conf., Tuscaloosa, AL, October 10-12, 1996.

Hazelton, D.W.; Gardner, M.T.; Weloth, J.M.; Rice, J.A.; Motowidlo, L.R.; Hascicek, Y.S.; Weijers, H.W.; Markiewicz, W.D. and Van Sciver, S.W., *HTS Insert Coils for Ultra High Field NMR Spectroscopy*, Applied Superconductivity Conf., Pittsburgh, PA, August 25-30, 1996.

Hendrickson, C.L.; Drader, J.J.; Guan, S. and Marshall, A.G., "MALDI FT-ICR Mass Spectrometry in a 20 Tesla Resistive Magnet," p. 481, in *Proceedings of 44th Amer. Soc. Mass Spectrom. Ann. Conf. on Mass Spectrometry & Allied Topics*, Portland, OR, May, 1996.

Hendrickson, C.L.; Guan, S. and Marshall, A.G., *Matrix-Assisted Laser Desorption/Ionization (MALDI) FT-ICR Mass Spectrometry in a 20 Tesla Resistive Magnet*, Analytical Poster #77, 212th Amer. Chem. Soc. Natl. Meeting, Orlando, FL, August, 1996.

Henning, P.; Cao, G. and Crow, J.E., "Anisotropy of Thermal Conductivity in Selectively Doped YBCO," in *Proceedings of 10th High T_c Superconductivity Conference*, 1996.

Heringhaus, F.; Leffers, R.; Gottstein, G. and Schneider-Muntau, H.-J., *Quantitative Correlation of Microstructure and Electrical Conductivity of a Heavily Deformed Eutectic Ag-Cu Composite*, TMS Fall Meeting, 1996.

Hershfield, S.P. and Beck, G., "Charge and Spin Current Flows in Spin Transistors and Similar Devices," in *Proceedings of the 41st Magnetism and Magnetic Materials Meeting*, p. 78, Atlanta, GA, November 11-15, 1996.

Hershfield, S.P.; Beck, G. and Zhao, H.L., "Nanostructure Magnetic Devices," in *Proceedings of the 190th Meeting of the Electrochemical Society*, p. 583, San Antonio, TX, October 6-11, 1996.

Hershfield, S.P.; Hettler, M.; Schiller, A. and Kroha, H., "The Kondo Effect in Nanostructures," in *Proceedings of Correlated Fermions and Transport in Mesoscopic Systems*, pp. 525-534, Les Arcs, France, January 20-27, 1996.

Hill, O.K.; Miller, J.R. and Toplosky, V.J., *Quench Initiation and Propagation Studies of Cable-in-Conduit Conductors for the NHMFL 45-T Hybrid*, Applied Superconductivity Conf., Pittsburgh, PA, August 25-30, 1996.

Hill, S., *A Comparison of the High Field Quantum Oscillations Observed by Electrodynamic and d.c. Transport Techniques in the Organic Superconductor κ-(BEDT-TTF)$_2$Cu(NCS)$_2$*, 13th Intl. Conf. on the Science and Technology of Synthetic Metals, Snowbird, UT, July, 1996.

Hill, S., *Cyclotron Resonance Studies of (DME-DCNQI)$_2$Cu*, 13th Intl. Conf. on the Science and Technology of Synthetic Metals, Snowbird, UT, July, 1996.

Hill, S., *High Frequency, High Magnetic Field, Studies of the Complex Conductivity in the Organic Superconductor κ-(BEDT-TTF)$_2$ Cu(NCS)$_2$*, APS March Meeting, St. Louis, MO, March 18-22, 1996.

Hill, S., *High Magnetic Field Groundstate in the Molecular Conductor η-Mo$_4$O$_{11}$*, 13th Intl. Conf. on the Science and Technology of Synthetic Metals, Snowbird, UT, July, 1996.

Hill, S., *Probing the Microwave Conductivity of Low-Dimensional Organic Conductors and Superconductors in High Magnetic Fields*, SPIE's Intl. Symp. on Optical Science, Engineering and Instrumentation, Denver, CO, August, 1996.

Hill, S., *Probing the Microwave Response of Low Dimensional Organic Conductors in High Magnetic Fields*, Workshop on Millimeter Wave Spectroscopy of Solids, Univ. of California at Los Angeles, CA, March, 1996.

Hu, J. and Schrieffer, J.R., *Two-Dimensional Electrons in Perpendicular Periodic Magnetic Fields*, APS March Meeting, St. Louis, MO, March 18-22, 1996.

Huang, X.; Panek, J. and Van Sciver, S.W., *Heat and Mass Transfer Between Two Saturated He II Baths*, ICEC16/ICMC, Kitakushu, Japan, 1996.

Ingersent, K., *From Magnetic Impurities to Heavy Fermions*, Univ. of Florida Physics Colloquium, Gainesville, FL, October 1, 1996; NHMFL Three-Site Meeting, Camp Weed, FL, October 26-27, 1996.

Ingersent, K., *Magnetic Impurities as a Probe of Gapless Fermi Systems*, APS March Meeting, St. Louis, MO, March 18-22, 1996.

Ingersent, K., *Three Kondo Impurities: A More Robust Route to Non-Fermi-Liquid Behavior?*, Workshop on Non-Fermi-Liquid Physics, Institute for Theoretical Physics, Santa Barbara, CA, June 7, 1996.

Jackson, G.S.; Guan, S. and Marshall, A.G., "Scaling Factors for Excitation Potentials in Tetragonal and Cylindrical Penning Traps," p. 505, in *Proceedings of 44th Amer. Soc. Mass Spectrom. Ann. Conf. on Mass Spectrometry & Allied Topics*, Portland, OR, May, 1996.

Jackson, G.S.; Guan, S. and Marshall, A.G., *Matrix-Shimmed Ion Traps for ICR Mass Spectrometry*, Analytical Poster #79, 212th Amer. Chem. Soc. Natl. Meeting, Orlando, FL, August, 1996.

Jackson, G.S.; Hammill, C.; Clark, R.J. and Marshall, A.G., "Generation and Catalytic Activity of $(Pt_n)^+$ Ions, n = 1-4," p. 1234, in *Proceedings of 44th Amer. Soc. Mass Spectrom. Ann. Conf. on Mass Spectrometry & Allied Topics*, Portland, OR, May, 1996.

Jackson, G.S.; White, F.M.; Hammill, C.; Clark, R.J. and Marshall, A.G., *Generation and Catalytic Activity of Pt_n^+ Ions, n = 1-4*, Inorganic Talk #409, 212th Amer. Chem. Soc. Natl. Meeting, Orlando, FL, August, 1996.

Kessler, J.; Boutemy, S.; Chen, S.; Dimapilis, D.; Miller, V.; Wei, W. and Schwartz, J., *Preparation of Dispersion-Hardened Single- and Multifilimentary $Bi_2Sr_2CaCu_2O_x$ Tapes and Wires*, Applied Superconductivity Conf., Pittsburgh, PA, August 25-30, 1996.

Ketchem, R.R.; Brenneman, M.; Hu, W.; Lee, K.-C.; Huo, S.; Quine, J.; Roux, B. and Cross, T.A., *A Complete Method for Determining Protein Structure from Solid-State NMR Orientational Data*, Annual Biophys. Soc. Meeting, Baltimore, MD, February, 1996.

Ketchem, R.R.; Brenneman, M.; Kovacs, F.; Hu, W.; Lee, K.-C.; Huo, S.; Quine, J.; Roux, B. and Cross, T.A., *Protein Structure Characterization Using Solid State NMR Orientational Data*, ENC Meeting, Asilomar, CA, March, 1996.

Kim, K. and Sullivan, N.S., *NMR Study of the Orientational Behavior of Thin Films of Molecular H_2 on BN*, Bull. Am. Phys. Soc., **41**, 1658 (1996).

Krzystek, J.; Hassan, A.K.; Pardi, L.; Goy, P.; Gross, M. and Brunel, L.-C., *A Very High Frequency / Field EPR Spectrometer*, 38th EPR Conf., Denver, CO, July, 1996.

Krzystek, J., *Millimiter and Submillimiter Wave Electron Paramagnetic Resonance Spectroscopy*; SPIE, Denver, CO, August, 1996.

Kuhns, P.L.; Kleinhammes, A.; Schmiedel, T.; Moulton, W.G.; Hughes, E.; Chabrier, P. and Bowers, C.R., *The Optical Overhauser Effect in GaAs and InP*, 28th Southeastern Magnetic Resonance Conf., Tuscaloosa, AL, October 10-12, 1996.

Lacerda, A., *Kondo Insulators in Very High Magnetic Fields*, Osaka Univ., Japan, February 8, 1996.

Lacerda, A., *Magnetotransport Experiments in $YbNi_2B_2C$*, III Prague Colloquium on f-Electron Systems, Prague, The Czech Republic, August 15-17, 1996.

Lacerda, A., *Magnetotransport Properties of Yb-Based Heavy Fermion Compounds*, Himeji Univ., Japan, February 6, 1996.

Lacerda, A., *Magnetovolume Effect in Heavy Fermion Compounds*, Kumamoto Univ., Japan, February 15, 1996.

Lacerda, A., *Strongly Correlated Electron System at Extreme Conditions*, Tsukuba Univ., Japan, February 3, 1996.

Lacerda, A., *Strongly Correlated Electron System at Extreme Conditions*, Saitama Univ., Japan, February 9, 1996.

Lacerda, A., *The National High Magnetic Field Laboratory–Los Alamos Facility: Tools and Results*, ISSP - Tokyo Univ., Japan, February 5, 1996.

Lacerda, A., *Very High Magnetic Fields—Very Low Temperatures: Tools and Results*, Univ. of Sendai, Japan, February 7, 1996.

Lacerda, A., *Very Low Temperature Experiments in Very High Magnetic Fields*, Universidade de Sao Paulo, Brazil, May, 1996.

Lang, T.; Moyland, P.L.; Sergatskov, D.A.; Adams, E.D. and Takano, Y., *Observation of Ferromagnetic Ordering in hcp ^3He*, XXI Intl. Conf. on Low Temperature Physics, Czech Republic, August, 1996.

Leal, J.P.; Marcalo, J.; Pires de Matos, A. and Marshall, A.G., *Periodicity in the Reactivity of Lanthanide Ions with Naphthalene and Mesitylene—Thermodynamic and Kinetic Trends*, 8th Sanibel Conf. on Mass Spectrometry: Metal-Containing Ions and Their Applications in Mass Spectrometry, Sanibel Island, FL, January, 1996.

Li, C.-C.; Engel, L.W.; Shahar, D.; Tsui, D.C. and Shayegan, M., *Microwave Conductivity Resonances in 2D Hole Systems*, APS March Meeting, St. Louis, MO, March 18-22, 1996.

Li, C.-C.; Engel, L.W.; Shahar, D.; Tsui, D.C. and Shayegan, M., *Microwave Resonance of 2D Holes in Wigner Solid Regime*, 12th Intl. Conf. on Application of High Magnetic Fields in Semiconductor Physics, Würzburg, Germany, 1996.

Li, G.-Z.; Guan, S. and Marshall, A.G., "Distribution and Density of Trapped Ions," p. 492, in *Proceedings of 44th Amer. Soc. Mass Spectrom. Ann. Conf. on Mass Spectrometry & Allied Topics*, Portland, OR, May, 1996.

Li, G.-Z.; Guan, S. and Marshall, A.G., "Methods for Cooling Trapped Ions or Electrons," p. 760, in *Proceedings of 44th Amer. Soc. Mass Spectrom. Ann. Conf. on Mass Spectrometry & Allied Topics*, Portland, OR, May, 1996.

Li, G.-Z.; Guan, S. and Marshall, A.G., *Sympathetic Cooling of Trapped Negative Ions by Self-Cooled Electrons in an FT-ICR Mass Spectrometer*, Analytical Poster #75, 212th Amer. Chem. Soc. Natl. Meeting, Orlando, FL, August, 1996.

Li, G.-Z.; Guan, S.; Vining, B.A. and Marshall, A.G., *Fluorescence of Trapped Mass-Selected Gas-Phase Ions*, Physical Poster #101, 212th Amer. Chem. Soc. Natl. Meeting, Orlando, FL, August, 1996.

Li, W.; Santos, I. and Marshall, A.G., "Determination of the Gas-Phase Acidities of Uracil and 5-Fluorouracil by FT-ICR MS," p. 1211, in *Proceedings of 44th Amer. Soc. Mass Spectrom. Ann. Conf. on Mass Spectrometry & Allied Topics*, Portland, OR, May, 1996.

Marshall, A.G., *Expanding Frontiers of Fourier Transform Ion Cyclotron Resonance Mass Spectrometry*, 211th Amer. Chem. Soc. Natl. Mtg., New Orleans, LA, March, 1996.

Marshall, A.G., *Fourier Transform Ion Cyclotron Resonance Spectroscopy*, 28th New Mexico Regional NMR Meeting, Socorro, NM, April, 1996.

Marshall, A.G., *Ion Games in a Magnetic Gymnasium: Attomoles to MegaDaltons*, 44th Amer. Soc. Mass Spectrom. Ann. Conf. on Mass Spectrometry & Allied Topics, Portland, OR, May, 1996.

Marshall, A.G., *Magnetic Resonance Spectroscopies*, NSF Chautauqua Meeting, Tallahassee, FL, June, 1996.

Marshall, A.G., *Tools for Determination of Biological Macromolecular Structure*, 9th Tandem Mass Spectrometry Conf., Lake Louise, Alberta, Canada, December, 1996.

Marshall, A.G.; Hendrickson, C.L. and Guan, S., *Matrix-Assisted Laser Desorption/Ionization Fourier Transform Ion Cyclotron Resonance Mass Spectrometry at 20 Tesla*, Abstract #480, Paper #126P, 47th Pittsburgh Conf. on Analytical Chem. and Applied Spectroscopy, Chicago, IL, March, 1996.

Marshall, A.G.; Jackson, G.S. and Guan, S., *Universal Ion Traps for ICR and Quadrupole Mass Spectrometry: Segmented and Optimized for Excitation, Detection and Trapping*, Abstract #482, Paper #124P, 47th Pittsburgh Conf. on Analytical Chem. and Applied Spectroscopy, Chicago, IL, March, 1996.

Marshall, A.G.; Li, G.-Z.; Guan, S. and Vining, B.A., *Fluorescence of Trapped Mass-Selected Gas-Phase Ions,* Abstract #479, Paper #284, 47th Pittsburgh Conf. on Analytical Chem. and Applied Spectroscopy, Chicago, IL, March, 1996.

Marshall, A.G.; Solouki, T. and Pasa-Tolic, L., *Structure Elucidation of Peptides by Matrix-Assisted Laser Desorption/Ionization Two-Dimensional FT-ICR MS/MS*, Abstract #481, Paper #125P, 47th Pittsburgh Conf. on Analytical Chem. and Applied Spectroscopy, Chicago, IL, March, 1996.

Maslov, D., *Quasi-Andreev Reflection and Paraconductivity in Quantum Wires*, seminars at Weizmann Inst. and Technion Univ., Israel, December 1996.

Maslov, D., *Transport Through Luttinger-Liquid Quantum Wires: The Roles of the Fermi-Liquid Reservoirs*, APS March Meeting, St. Louis, MO, March 18-22, 1996.

Maslov, D., *Transport Through Luttinger-Liquid Wires Connected to Fermi-Liquid Reservoirs*, XXXI Recontre de Moriond Conf.—Mesoscopic Transport and Strongly Correlated Electron Systems, Les Arcs, France, 1996.

Maslov, D., *Transport Through Quantum Wires*, Colloquium at Fermi Labs, Batavia, July, 1996.

McCarty, A.; Hassan, A.K.; Herbette, S.; Martins, G.B.; Furdyna, J.K. and Brunel, L.-C., *High Field Electron Paramagnetic Resonance of Cd(.7)Mn(.3)Se and Cd(.55)Mn(.45)Se*, 28th Southeastern Magnetic Resonance Conf., Tuscaloosa, AL, October 10-12, 1996.

Melik-Alaverdian, V. and Bonesteel, N.E., *Monte Carlo Comparison of Quasielectron Wave Functions,* APS March Meeting, St. Louis, MO, March 20, 1996.

Melik-Alaverdian, V.; Ortiz, G. and Bonesteel, N.E., *Monte Carlo Comparison of Quasielectron Wave Functions*, APS March Meeting, St. Louis, MO, March 20, 1996.

Miller, J.R., *Design and Development of Large-Bore Superconducting Solenoids for High-Field Hybrid Magnet Systems,* 1996 U.S./Japan Workshop on High-Field Superconductor Materials, Brookhaven National Laboratory, 1996.

Miller, J.R., *Large Magnet Systems at the NHMFL: Present and Future,* Intl. Workshop on High Magnetic Fields: Industry, Application, and Technology, Tallahassee, FL, February 28-March 1, 1996.

Miller, J.R., *Low Temperature Superconductivity—State of the Art and Applications,* Educational Institute for Superconductivity Conf. (EIS '96), Washington, D.C., 1996.

Miller, J.R., *Nb_3Sn CiCCs for the 45-T Hybrid: Design, Development, Manufacturing, Processing, and Characterization,* Low-Temperature Superconductor Workshop, Napa, CA, 1996.

Miller, J.R.; Miller, G.E.; Eyssa, Y.M.; Kenney, W.J.; Hill, O.L.; Kenney, S.J.; Painter, T.A.; Toplosky, V.J. and Windham, C.L., *Development and Testing of Low Resistance Nb_3Sn Joints for Cable-in-Conduit Conductors*, Applied Superconductivity Conf., Pittsburgh, PA, August 25-30, 1996.

Miranda, E.; Dobrosavljevic, V. and Kotliar, G., *Disorder-Driven Non-Fermi Liquid Behavior in Kondo Alloys*, APS March Meeting, St. Louis, MO, March 18-22, 1996; Non-Fermi Liquid Physics in Metals Conf., Santa Barbara, CA, June 17-21, 1996; Workshop on Perturbative Methods for Strongly Interacting Electrons, Brasilia, Brazil, June 24-28, 1996.

Miranda, E.; Dobrosavljevic, V. and Kotliar, G., *Kondo Disorder: A Possible Route Towards Non-Fermi Liquid Behavior*, 1996 NHMFL Three-Site Workshop, Live Oak, FL, October 26-27, 1996.

Miranda, E.; Dobrosavljevic, V. and Kotliar, G., *Non-Fermi Liquid Behavior as a Consequence of Kondo Disorder*, Intl. Conf. on Strongly Correlated Electron Systems - SCES '96, Zurich, Switzerland, August 19-22, 1996.

Moreo, A.; Hallberg, K. and Horsch, P., *Critical Behavior of the S=3/2 Heisenberg Chain*, APS Bulletin 279 (1996); Epitome of the APS March Meeting, St. Louis, MO, March 18-22, 1996.

Moyland, P.L.; Lang, T.; Adams, E.D.; Stewart, G.R. and Takano, Y., "Nuclear Antiferromagnetic Ordering in $PrBe_{13}$," in *Proceedings of the 21st Intl. Conf. on Low Temperature Physics*, Prague, August 1996; *Czechoslovak Journal of Physics*, **46**, Supl. S4, 2199-2200 (1996).

Musfeldt, J.L.; Li, G. and Wang, Y.J., *Spectroscopic Studies of Spin-Peierls Materials in a Magnetic Field*, 13th Intl. Conf. on the Science and Technology of Synthetic Metals, Snowbird, UT, July, 1996.

Musfeldt, J.L.; Wang, Y.J.; Poirier, M. and Jandl, S., *An Infrared Investigation of the Broken Symmetry Ground State in $GeCuO_3$*, APS March Meeting, St. Louis, MO, March 18-22, 1996.

Musfeldt, J.L.; Wang, Y.J.; Jandl, S.; Poirier, M.; Revcolevschi, A. and Dhalenne, G., *An Infrared Investigation of the Broken Symmetry Ground State in $GeCuO_3$*, APS March Meeting, St. Louis, MO, 754 (1996).

Nakamae, S. and Schwartz, J., *Thermal Conductivity of $Bi_2Sr_2CaCu_2O_x$ Superconductors in High Magnetic Fields*, Applied Superconductivity Conf., Pittsburgh, PA, August 25-30, 1996.

Ng, H.K.; Love, B.; Cope, C.J.; Wang, Y.J.; Yuen, T. and Lin, C.L., *Increase Conductivity in the Modified Huesler Alloy UNiSn with Application of Magnetic Field*, 41st Annual Conf. on Magnetism & Magnetic Materials, EE-03 (1996).

Pai, V.; Haik, Y.S. and Chen, C.J., *Bio-Magnetic Fluid Dynamics*, 1996 ASME Fluids Engineering Division Summer Meeting, San Diego, CA, July 7-11, 1996.

Painter, T.A.; Miller, J.R.; Miller, G.E.; Kenney, W.J.; Hill, O.L.; Kenney, S.J.; Toplosky, V.J.; Windham, C.L.; Bascunan, J. and Devernoe, A.L., *Processing of the 45-T Hybrid Magnet Nb_3Sn Outsert Coils*, Applied Superconductivity Conf., Pittsburgh, PA, August 25-30, 1996.

Panek, J.; Huang, X. and Van Sciver, S.W., *Heat and Mass Transfer in Two-Phase Helium II*, ASME Intl. Congress and Exposition, Atlanta, GA, 1996.

Pardi, L., *Application of High Field EPR Spectroscopy in Molecular Magnetism*, Laboratoire Louis Brillouin, Saclay, France, May, 1996.

Pardi, L.; Brunel, L.-C.; Redijk, J. and Hulsbergen, F.B., *Direct Measurement of Zero Field Splitting of Divalent Nickel in a One-Dimensional System by High Frequency - EPR Spectroscopy*, 38th EPR Conf., Denver, CO, July, 1996.

Pilla, S. and Sullivan, N.S., *First Order Phase Transitions in Orientational Ordering of Monolayers of N_2 on Graphite Studied by Monte Carlo Techniques*, Bull. Am. Phys. Soc., **41**, 192 (1996).

Prestemon, S. and Lienau, J.J., *Application of the Spectral Collocation Method to Flows with Two Inhomogeneous Dimensions*, 6th Intl. Symp. on Flow Modelling and Turbulence Measurements, Tallahassee, FL, 1996.

Reinhold, B.B.; Costello, C.E.; Guan, S. and Marshall, A.G., *Internal Energy Deposition by Quadrupolar Excitation in the Presence of Collisional Cooling*, Analytical Poster #74, 212th Amer. Chem. Soc. Natl. Meeting, Orlando, FL, August, 1996.

Reinhold, B.B.; Helin, J.; Ngoka, L.; Ye, S.; Reinhold, V.; Costello, C.E. and Marshall, A.G., "Fragmentation Pathways of Cationized Permethylated Maltoheptaose under Diverse Conditions," p. 1247, in *Proceedings of 44th Amer. Soc. Mass Spectrom. Ann. Conf. on Mass Spectrometry & Allied Topics*, Portland, OR, May, 1996.

Riera, J.A.; Dagotto, E.; Sandvik, A. and Moreo, A., *Spin Dynamics of Hole Doped Y_{2-x} Ca_x Ba Ni O_5*, APS Bulletin 735 (1996); Epitome of the APS March Meeting, St. Louis, MO, March 18-22, 1996.

Roach, J.F.; Sanger, P.A.; Hartman, D. and Miller, J.R., *Electrical Testing of Large Scale IR and D Dummy Coil for TPX Magnet Insulation Design Verification*, Applied Superconductivity Conf., Pittsburgh, PA, August 25-30, 1996.

Salters, V.J.M. and Longhi, J., *Partitioning of Trace Elements During Primary Melting of MORB Mantle*, Goldschmidt Conf., Heidelberg, Germany, 1996.

Salters, V.J.M. and Longhi, J., *Trace Element Partitioning During the Initial Stages of Melting Beneath a Mid-Ocean Ridge,* AGU Fall Meeting, San Francisco, CA, December, 1996.

Salters, V.J.M. and White, W.M., *Geochemical Reference Points from the Hf Isotopes,* AGU Fall Meeting, San Francisco, CA, December, 1996.

Sandhu, P.S. and Brooks, J.S., "Lattice Effects on the dHvA Oscillations and Magnetic Breakdown in Quasi-Two Dimensional Organic Conductors," in *Proceedings of the 13th Intl. Conf. on the Science and Technology of Synthetic Metals*, Snowbird, UT, July, 1996.

Sarrao, J.L., *Resonant Ultrasound Spectroscopy, Hole Doping and the Structural Phase Transition in La_2CuO_4*, Physics Colloquium, Univ. of Michigan, November 1996; Physics Colloquium, Clemson Univ., October 1996; Physics Colloquium, Iowa State Univ., April, 1996.

Sarrao, J.L., *Unusual Elastic Properties of Pure and Doped La_2CuO_4 as Probed by Resonant Ultrasound Spectroscopy*, 131st Meeting of the Acoustical Soc. of America, May, 1996.

Sarrao, J.L.; Benton, C.L.; Fisk, Z.; Lawrence, J.M.; Mandrus, D.; Chen, Y.Y. and Thompson, J.D., *$YbIn_{1-x}Ag_xCu_4$: Crossover from First-Order Valence Transition to Heavy Fermion Behavior*, APS March Meeting, St. Louis, MO, March 18-22, 1996.

Sarrao, J.L.; Torelli, M.E. and Fisk, Z., *Lithium Doping in La_2CuO_4 and La_2NiO_4*, Materials Research Soc. Fall Meeting, Boston, MA, 1996.

Schiller, A. and Ingersent, K., *Renormalization-Group Study of a Magnetic Impurity in a Luttinger Liquid*, APS March Meeting, St. Louis, MO, March 18-22, 1996.

Schiller, A., *Systematic 1/d Corrections to the Infinite-Dimensional Limit of Correlated Lattice Electrons*, APS March Meeting, St. Louis, MO, March 18-22, 1996.

Schneider-Muntau, H.-J.; Boenig, H.J.; Campbell, L.J.; Eberl, K.R.; Eyssa, Y.M.; Parkin, D.M.; Pernambuco-Wise, P.; Schillig, J.B. and Sims, J.R., "Design Status of the US 100 Tesla Non-Destructive Magnet System," in *Proceedings of the Megagauss VII Conf.*, 1996.

Schrieffer, J.R., *(1) Recent Advances in High Temperature Superconductivity; (2) Novel Concepts in Condensed Matter Physics; (3) Ward's Identity and Vertex Corrections in Spin Fluctuation Systems*, Lectures at Tohoku Univ., Japanese Phys. Soc. and in Kyoto, March 28-April 8, 1996.

Schrieffer, J.R., *High Temperature Superconductivity,* Colloquium, Michigan State Univ., April 16, 1996.

Schrieffer, J.R., *Superconductivity as an Example of the Scientific Process,* Distinguished Lecture Series, Michigan State Univ., April 16, 1996.

Schrieffer, J.R., *Erotic Materials and Fundamental Concepts: Writing Volume II of Condensed Matter Physics*, 50th Anniversary Argonne National Lab., September 18, 1996.

Schrieffer, J.R., *Exotic Condensates and Excitations in Condensed Matter Systems*, Colloquium Seoul Natl. Univ., Seoul, Korea, June 10, 1996.

Schrieffer, J.R., *Future Science, Who Will Benefit, Who Will Pay?,* FSU Foundation, Tallahassee, FL, October 4, 1996.

Schrieffer, J.R., *Novel Concepts in Condensed Matter Physics*, Colloquium, UCSB January 23, 1996; Inauguration Conf. of the Asian Pacific Center for Theoretical Physics, Seoul, Korea, June 4, 1996.

Schrieffer, J.R., *Spectral Properties of Quasi Particle Excitations Induced by Magnetic Moments in Superconductors*, Seminar, CNRS, Laboratoire Louis Neel, Grenoble France, October 15, 1996.

Schrieffer, J.R., *The Creative Process: How Does Science Really Work?,* NSF Alliance for Minority Participation Workshop, Tallahassee, FL, July 22, 1996.

Schrieffer, J.R., *The Spin Deformation Potential and the Suppression of the Nearly Antiferromagnetic Fermi Liquid Mechanism of High Temperature Superconductivity,* Intl. Conf. on Advanced Materials and Devices, Kangwon-Do. Korea June 11, 1996.

Schrieffer, J.R., *Spin Deformation Potential Theorem for NAFL Scheme of HTS and Supression of T_c in this Approach,* APS March Meeting, St. Louis, MO, March 18, 1996.

Schrieffer, J.R., *The Role of Vertex Corrections to the Pairing Interaction in Spin Fluctuations Superconductors,* 10th Anniversary HTS Workshop on Physics, Materials & Applications, Houston, TX, March 12, 1996.

Schwartz, J., *Towards a Practical High-T_c Superconducting Conductor*, Florida State Univ. Materials Research and Technology Center, 1996.

Schwartz, J.; Amm, B.C.; Garmestani, H.; Hilton, D.K. and Hascicek, Y.S., *Mechanical Properties and Strain Effects in $Bi_2Sr_2CaCu_2O_x/AgMg$ Composite Conductors*, Applied Superconductivity Conf., Pittsburgh, PA, August 25-30, 1996.

Schwartz, J.; Fischer, V.; Godfrey, M.I.; Hascicek, Y.S.; Hilton, D.K.; Kessler, J.; Miller, V.; Shoaff, P.V., Jr.; Van Sciver, S.W.; Wei, W. and Weijers, H.W., "High Temperature Superconductivity Research and Development at the National High Magnetic Field Laboratory," in *Proceedings of the 7th U.S.-Japan Workshop on High T_c Superconductors*, Tsukuba, Japan, 1996.

Senko, M.W.; Hendrickson, C.L.; White, F.M.; Quinn, J.P.; Marto, J.A.; Pasa-Tolic, L.; Guan, S. and Marshall, A.G., "Electrospray Ionization Fourier Transform Ion Cyclotron Resonance Mass Spectrometry at 9.4 Tesla," p. 485, in *Proceedings of 44th Amer. Soc. Mass Spectrom. Ann. Conf. on Mass Spectrometry & Allied Topics*, Portland, OR, May, 1996.

Senko, M.W.; Hendrickson, C.L.; White, F.M.; Quinn, J.P.; Marto, J.A.; Pasa-Tolic, L.; Guan, S. and Marshall, A.G., *Electrospray Ionization Fourier Transform Ion Cyclotron Resonance Mass Spectrometry at 9.4 Tesla*, Analytical Poster #76, 212th Amer. Chem. Soc. Natl. Meeting, Orlando, FL, August, 1996.

Shoaff, P.V., Jr.; Hascicek, Y.S.; Schwartz, J. and Van Sciver, S.W., *An Investigation of the Characterization and Development of HTS Joints in BSCCO 2212/Ag Composites*, Applied Superconductivity Conf., Pittsburgh, PA, August 25-30, 1996.

Smith, M.R. and Van Sciver, S.W., *Observed Pressure Distribution and Drag on a Sphere in Flowing He I and He II*, APS Division of Fluid Mechanics Meeting, 1996.

Smith, M.R.; Eyssa, Y.M. and Van Sciver, S.W., *Design of a Superconducting Magnetic Suspension System for a Liquid Helium Flow Experiment,* Applied Superconductivity Conf., Pittsburgh, PA, August 25-30, 1996.

Soghomonian, V.; Bird, M.D.; Eyssa, Y.M.; Murphy, P.; Rosanske, R.; Schneider-Muntau, H.-J. and Cross, T.A., *NMR at Very High Field (24 T) in Resistive Magnets: Results and Challenges*, Experimental NMR Conf., Asilomar, CA, March, 1996; AMPERE Congress, Canterbury, England, September, 1996.

Solouki, S.; Emmett, M.R.; Guan, S. and Marshall, A.G., "Presence and Location of Disulfide Bonding in Biologically Active Peptides/Proteins by Multistage Fragmentation: A MALDI FT-ICR Mass Spectral Analysis," p. 1347, in *Proceedings of 44th Amer. Soc. Mass Spectrom. Ann. Conf. on Mass Spectrometry & Allied Topics*, Portland, OR, May, 1996.

Solouki, T.; Reinhold, B.B.; Costello, C.E.; O'Malley, M.; Guan, S. and Marshall, A.G., "Structural Analysis of Polysaccharides and Peptides by MALDI FT-ICR MS," p. 1125, in *Proceedings of 44th Amer. Soc. Mass Spectrom. Ann. Conf. on Mass Spectrometry & Allied Topics*, Portland, OR, May, 1996.

Solouki, T.; Reinhold, B.B.; Costello, C.E.; O'Malley, M.; Guan, S. and Marshall, A.G., *High-Resolution Matrix-Assisted Laser Desorption/Ionization (MALDI) FT-ICR Mass Spectrometry of Oligosaccharides*, Biological Poster #21, 212th Amer. Chem. Soc. Natl. Meeting, Orlando, FL, August, 1996.

Stern, L.A.; Amundson, R.G.; Baisden, W.T. and Wang, Y., *CO_2 Fluxes from Soils Is in Oxygen Isotope Equilibrium with Surface Soil Water*, Fall Meeting of Amer. Geophysical Union, San Francisco, CA, EOS Transactions, Amer. Geophysical Union (abstract), **77**, F109-F110 (1996).

Sullivan, N.S., *Molecular Spectroscopy at Very High Magnetic Fields*, Workshop on Molecular Properties at High Magnetic Fields, NHMFL, Gainesville, October 24-25, 1996.

Sullivan, N.S., *NMR Study of the Orientational Behavior of Molecular Hydrogen Films on Hexagonal BN*, Bull. Am. Phys. Soc., **41**, 374 (1996).

Sullivan, N.S., *Nuclear Magnetic Resonance Spectrometers*, Encyclopedia of Scientific Instrumentation, 1995-96.

Sullivan, N.S., *Ortho-Para Hydrogen at Low Temperature*, Encyclopedia of Nuclear Magnetic Resonance, J. Wiley & Sons, NY, 1996.

Sullivan, N.S.; Pilla, S. and Kim, K., *Cryomagnetic Magnetic Resonance Spectrometers*, in Recent Research Developments in Cryogenics, Research Signpost, India, 1996.

Summers, L.T.; Walsh, R.P. and Miller, J.R., *Thermal and Operating Strain Effects on the Critical Current of High-Current, High-Field Cable-in-Conduit Conductors (CICC) for the NHMFL Hybrid Magnet,* Applied Superconductivity Conf., Pittsburgh, PA, August 25-30, 1996.

Tian, F. and Cross, T.A., *Dipolar Oscillations in Membrane-Bound Polypeptides,* ENC Meeting, Asilomar, CA, March, 1996.

Tian, F.; Cotten, M.; Busath, D. and Cross, T.A., *Solid State NMR of Gramicidin A to Study Channel Selectivity and Gramicidin Analogs to Probe the Functional Roles of Tryptophan*, Annual Biophys. Soc. Meeting, Baltimore, MD, February, 1996.

Torelli, M.E.; Sarrao, J.L. and Fisk, Z., *Magnetic and Transport Properties of Doped Half-Heusler Alloys*, APS March Meeting, St. Louis, MO, March 18-22, 1996.

Van Sciver, S.W. and Smith, M.R., "Realization of a 10^7 Reynolds Number Helium Flow Facility," in *Proceedings of the Intl. Workshop on Ultra High Reynolds Number Flows*, Brookhaven, NY, 1996.

Van Sciver, S.W. and Welton, S.J., *Analysis and Characterization of Saturated Bath He II Heat Exchangers*, ICEC16/ICMC, Kitakushu, Japan, 1996.

Van Sciver, S.W., *He II Cooling for Large Superconducting Magnets*, Intl. Workshop on High Magnetic Fields: Industry, Materials and Technology, Tallahassee, FL, February 28-March 1, 1996.

Van Sciver, S.W.; Bartholomew, K. and Welton, S.J., *The Cryogenic System for the NHMFL Hybrid Magnet*, NIFS Symp. on Cryogenic Systems for Large Superconducting Applications, Toki-city, 1996.

Van Sciver, S.W.; Baudouy, B.J.P. and Bartholomew, K., "Enthalpy AC Loss Measurement Technique Using He II," in *Proceedings of the 4th Intl. Conf. on Cryogenics* (Cryogenics '96) Prague, Czech Republic, 1996.

Vining, B.A.; Li, G.-Z.; Solouki, T.; Guan, S.; Marshall, A.G. and Vincent, J., "Characterization of Low Molecular Weight Chromium-Binding Substance by MALDI FT-ICR MS," p. 1423, in *Proceedings of 44th Amer. Soc. Mass Spectrom. Ann. Conf. on Mass Spectrometry & Allied Topics*, Portland, OR, May, 1996.

Walsh, R.P., "Use of Strain Gages for Low Temperature Thermal Expansion Measurements," in *Proceedings of the ICMC Kitakyushu*, Japan Conf., 1996.

Walsh, R.P.; Summers, L.T. and Miller, J.R., "The 4 K Tensile and Fracture Toughness Properties of a Modified 316LN Conduit Alloy," in *Proceedings of the ICMC Kitakyushu, Japan Conf.,* 1996.

Wang, A.; Xu, F.; Vaughn, J.B. Jr. and Cross, T.A., *Conformational Interconversion of a Polypeptide Induced by "Catalytic" Solvent*, Annual Biophys. Soc. Meeting, Baltimore, MD, February, 1996.

Wang, Y.; Amundson, R.G. and Trumbore, S., "The Impact of Climate and Land Use Change on C Turnover in Soils," in *Proceedings of the Fourth Intl. Symp. on the Geochemistry of the Earth's Surface*, 327-330 (1996).

Wang, Y.J. and McCombe, B.D., *Resonant Electron Optical Phonon Interaction with Barrier AlAs-like LO Phonons in GaAs/AlGaAs MWQs*, APS March Meeting, St. Louis, MO, 590 (1996).

Wang, Y.J.; Nickel, H.A.; McCombe, B.D.; Peeters, F.M.; Hai, G.Q.; Shi, J.M.; Devreese, J.T. and Wu, X.G., *Resonant Magnetopolaron Effects in GaAs/AlGaAs MQWs at High Magnetic Fields*, 12th Intl. Conf. on the Application of High Magnetic Fields, Wurzburg, Germany, Wep 50, 1996.

Ward, B.; Dodson, B.; Talham, D.R.; Chaparala, M.; Granroth, G.E. and Meisel, M.W., *Search for the Possible Existence of the Haldane Gap in S = 2 Materials*, Bull. Am. Phys. Soc., **41**, 334 (1996).

Wei, W.; Sun, Y.R.; Schwartz, J.; Goretta, K.C.; Balachandran, U. and Bhargava, A., *Preparation and Properties of Nanosize TiO_2 and MgO-Doped $Bi_2Sr_2CaCu_2O_x$ Tapes*, Applied Superconductivity Conf., Pittsburgh, PA, August 25-30, 1996.

Weijers, H.W.; Van Sciver, S.W., *et al.*, *Bi-2212 Insert Coils for 1-T Class Insert Coils*, Applied Superconductivity Conf., Pittsburgh, PA, August 25-30, 1996.

Whitaker, H.L.; Martins, G.B.; Pardi, L.; Hassan, A.K.; Cao, G. and Brunel, L.-C., *Study of Linewidth and g-Anisotropy of $Y_{1-x}R_xB_2C_3O_{6+\delta}$ Using X-Band and D-Band EPR*, 28th Southeastern Magnetic Resonance Conf., Tuscaloosa, AL, October 10-12, 1996.

White, F.M.; Marto, J.A. and Marshall, A.G., "An External Source 7 Tesla FT-ICR Mass Spectrometer with Electrostatic Ion Guide," p. 1167, in *Proceedings of 44th Amer. Soc. Mass Spectrom. Ann. Conf. on Mass Spectrometry & Allied Topics*, Portland, OR, May, 1996.

Wolters, Ch.; Amm, K.M.; Knoll, D.J.; Peterson, S.C. and Schwartz, J., *Synthesis of (Hg, Re) $Ba_2Ca_2Cu_3O_x$ Superconductors by a Two-Step Method*, Applied Superconductivity Conf., Pittsburgh, PA, August 25-30, 1996.

Xiao, L.Y. and Van Sciver, S.W., *Intrinsic Stability of High T_c Superconducting Tapes Including the Effect of Anisotropic J_c*, Applied Superconductivity Conf., Pittsburgh, PA, August 25-30, 1996.

Xu, F.; Wang, F.; Vaughn, J.B. Jr. and Cross, T.A., *The Solvent Effects on the Conformational Interconversion of a Polypeptide and Their Implications for Membrane Proteins in the Lipid Environment,* Annual Biophys. Soc. Meeting, Baltimore, MD, February, 1996.

Xu, M.; Li, W.; Guan, S.; Marshall, A.G. and Dougherty, R.C., "Inverted Region Behavior in Gas-Phase Electron-Transfer Reactions," p. 112, in *Proceedings of 44th Amer. Soc. Mass Spectrom. Ann. Conf. on Mass Spectrometry & Allied Topics*, Portland, OR, May, 1996.

Young, D.R.; Sarrao, J.L.; Fisk, Z.; Mandrus, D. and Ramirez, A.P., *Magnetic and Transport Properties of Pure and Doped FeSi*, APS March Meeting, St. Louis, MO, March 18-22, 1996.

Zhang, Z.; Guan, S. and Marshall, A.G., *Quantitation of H/D Exchange in Peptides and Proteins: Deconvolution of Natural Isotopic Abundance Distributions by Least Squares and Maximum Entropy Methods*, Biological Poster #19, 212th Amer. Chem. Soc. Natl. Meeting, Orlando, FL, August, 1996.

Zhang, Z.; Guan, S. and Marshall, A.G., "Deconvolution of Natural Isotopic Abundance Patterns by Least Squares and Maximum Entropy Methods," p. 366, in *Proceedings of 44th Amer. Soc. Mass Spectrom. Ann. Conf. on Mass Spectrometry & Allied Topics*, Portland, OR, May, 1996.

Zhang, Z.; Li, W.; Guan, S. and Marshall, A.G., "Higher-Order Structure of Gas-Phase Peptides from Gas-Phase H/D Exchange Experiments," p. 1061, in *Proceedings of 44th Amer. Soc. Mass Spectrom. Ann. Conf. on Mass Spectrometry & Allied Topics*, Portland, OR, May, 1996.

Zhang, Z.; Li, W.; Guan, S. and Marshall, A.G., *Higher-Order Structure of Gas-Phase Peptides from Gas-Phase H/D Exchange Experiments*, Biological Poster #20, 212th Amer. Chem. Soc. Natl. Meeting, Orlando, FL, August, 1996.

Zhang, Z.; Senko, M.W.; Li, M.; Dillon, S.; Logan, T.M.; Guan, S. and Marshall, A.G., *Protein Molecular Weight to 1 Da by ^{13}C, ^{15}N Double-Depletion and FT-ICR Mass Spectrometry*, Tenth Symp. of the Protein Soc., San Jose, CA, August, 1996.

Zhang, Z.; Guan, S. and Marshall, A.G., *Quantitation of H/D Exchange: Deconvolution of Natural Isotopic Abundance Distributions by Least Squares and Maximum Entropy Methods*, Tenth Symp. of the Protein Soc., San Jose, CA, August, 1996.

Zhang, Z.; Li, W.; Li, M.; Logan, T.M.; Guan, S. and Marshall, A.G., *Higher-Order Structure and Dynamics of FK506-Binding Protein Probed by Backbone Amide Hydrogen/Deuterium Exchange and Electrospray Ionization Fourier Transform Ion Cyclotron Resonance Mass Spectrometry*, Tenth Symp. of the Protein Soc., San Jose, CA, August, 1996.

Zhang, Z.; Li, W.; Li, M.; Logan, T.M.; Guan, S. and Marshall, A.G., *FK506 Binding Protein Conformation from Protein Amide Hydrogen Exchange Determined by Electrospray FT-ICR Mass Spectrometry*, Biological Poster #22, 212th Amer. Chem. Soc. Natl. Meeting, Orlando, FL, August, 1996.

Zibold, A.; Liu, H.L.; Tanner, D.B. and Wang, J.Y., *Optical Studies on Semiconducting Cuprates at High Magnetic Field*, Bull. Am. Phys. Soc. **41**, 728 (1996); APS March Meeting, St. Louis, MO, March 18-22, 1996.

Zindler, A. and Salters, V.J.M., *MORB Melting Revisited*, Geophysical Union Fall Meeting, San Francisco, CA, 1996.

Zindler, A., *Convective Isolation of the Lower Mantle: A Geochemical Update*, Amer. Geophysical Union Fall meeting, San Francisco, CA, 1996.

Zindler, A.; Salters, V.J.M.; Bourdon, B. and Elliott, T.E., *Plumes and Plums in the MORB Mantle,* Goldschmidt Conf., Heidelberg, Germany, 1996.

Zindler, A.; Salters, V.J.M.; Elliott, T.E. and Bourdon, B., *MORB Melting Revisited,* AGU Fall Meeting, San Francisco, CA, December, 1996.

Zou, H. and Zindler, A., *Constraints on the Degree of Dynamic Partial Melting and Source Composition Using Concentration Ratios in Magmas*, Goldschmidt Conf., Heidelberg, Germany, 1996.

Related Activities

Awards, Honors, Services

Nick Bonesteel received a Sloan Research Fellowship from the Alfred P. Sloan Foundation.

Russ Bowers received the National Science Foundation Career Award.

Louis-Claude Brunel served on four National Institutes of Health review panels. He also served on the Advisory Committee of Pacific Northwest National Laboratory.

Zachary Fisk was elected to the National Academy of Sciences.

Alan G. Marshall was selected to receive the 1997 Maurice F. Hasler Award, given by the Spectroscopy Society of Pittsburgh.

Don Parkin received the 1996 Los Alamos Distinguished Performance Award.

David Reitze was named a 1996 Cottrell Scholar, awarded by the Research Corporation.

Robert Schrieffer was appointed by President Clinton to serve on the Committee on the National Medal of Science.

Book Chapters

Cerling, T.E. and Wang, Y., "Stable Carbon and Oxygen Isotopes in Soil CO_2 and Soil Carbonate: Theory, Practice, and Application," in *Mass Spectrometry of Soils*, eds., Boutton, T.W. and Yamasaki, S.I., (Marcel Dekker, Inc., New York, NY, 1996), pp. 113-131.

Cross, T.A., "Orientational Constraints for Defining High Resolution Structure: The Gramicidin Channel," in *Encyclopedia of Nuclear Magnetic Resonance*, eds. Grant, D.M. and Harris, R.K., (John Wiley & Sons, New York, NY, 1996), pp. 2234-2238.

Ketchem, R.R.; Roux, B. and Cross, T.A., "Computational Refinement Through Solid State NMR and Energy Constraints of a Membrane Bound Polypeptide," in *Membrane Structure and Dynamics*, eds. Merz, K.M. and Roux, B., (Birkhauser, Boston, MA, 1996), pp. 299-322.

Book Reviews

Guan, S. and Marshall, A.G., review of *Mass Spectrometry in the Biological Sciences*, eds. Burlingame, A.L. and Carr, S.A., Humana Press, Totowa, NJ, 1996, review published in *Appl. Spectrosc.*, 50 (9), 18A-22A (1996).

Refereed Papers Republished in Reprint Collections

Comisarow, M.B. and Marshall, A.G., "Fourier Transform Ion Cyclotron Resonance Spectroscopy," republished in *J. Mass Spectrom*, **31**, 586-587 (1996).

Comisarow, M.B. and Marshall, A.G., "Frequency-Sweep Fourier Transform Ion Cyclotron Resonance Spectroscopy," republished in *J. Mass Spectrom*, **31**, 588-589 (1996).

Patent Awarded

Fu, R. and Bodenhausen, G., *Method and Apparatus for Broadband Decoupling in Nuclear Magnetic Resonance with Chirp Pulses*. US Patent No: 5,581,182. December 3, 1996.

Patents Pending

Hascicek, Y.S. and Belenli, I., *Self Insulating Substrate Tape for Magnet Making from High Temperature Superconducting Conductors*, 1996.

Hascicek, Y.S.; Schneider-Muntau, H.-J. and Van Sciver, S.W., *High Temperature Superconducting Thin Film Magnets*, 1996.

Wolters, Ch.; Schwartz, J. and Amm, K.M., *Process for Preparing Mercury-Barium-Calcium-Copper-Oxide Based Superconductor Materials*, 1996.

Inventions

Hilton, D.K.; Weijers, H.W.; Hascicek, Y.S.; Van Sciver, S.W. and Schwartz, J., *A Novel Lorentz Force Tensile Test and Fatigue Apparatus*, 1996.

Hascicek, Y.S. and Schneider-Muntau, H.-J., *Coaxial Current Down Leads for Magnets and Insert Probes*, 1996.

Hascicek, Y.S., and Van Sciver, S.W., *Laser Sewing for Superconducting Joints Between Superconducting Tapes*, 1996.

Hascicek, Y.S.; Van Sciver, S.W. and Schneider-Muntau, H.-J., *Unidirectional Cyclic Hot Pressing of BSCCO/Ag Tape Conductors*, 1996.

Hascicek, Y.S. and Kleinhammes, A., *Direct Laser Patterned Deposition (DLPD)*, 1996.

Hascicek, Y.S., *In-Situ Laser Surface Processing of High Temperature Spray Insulating Materials*, 1996.

Hascicek, Y.S., *Rotating Heat Treatment Process for Wind and React Magnets Built from Bare HTS Tapes*, 1996.

Grants

New Grants

PI: C.R. Abernathy
Grant Title: Evaluation of Electrical and Thermal Limits in III-Nitrides Electronics
Agency: Electric Power Research Institute
Project Dates: 9/10/96 - 12/31/96
Award Amount: $101,949

PI: C.R. Abernathy
Grant Title: Materials & Device Processing Improvements in III-V Nitrides
Agency: U.S. Air Force
Project Dates: 7/15/96 - 2/14/97
Award Amount: $148,848

PI: C.R. Abernathy
Grant Title: Synthesis & Characterization of A1GAT1AS
Agency: U.S. Air Force
Project Dates: 7/15/96 - 7/14/99
Award Amount: $101,949

PI: C.R. Abernathy
Grant Title: Synthesis & Characterization of INT1P & INT1AS
Agency: U.S. Air Force
Project Dates: 2/15/96 - 2/14/99
Award Amount: $108,664

PI: A. Angerhofer
Grant Title: Special Board Allocation to Provide Matching for NSF Academic Infrastructure Program Award
Agency: UF Division of Sponsored Research
Project Dates: 12/13/96 - 6/30/97
Award Amount: $218,494

PI: A. Angerhofer
Grant Title: Upgrade & Development of Advanced EPR/ENDOR/ODMR Instrumentation
Agency: NSF
Project Dates: 9/15/96 - 8/31/98
Award Amount: $540,167

PI: C.R. Bowers
Grant Title: Enhanced Sensitivity NMR Studies of Nanostructured Electronic Materials
Agency: NSF
Project Dates: 5/1/96 - 4/30/00
Award Amount: $137,500

PI: L.C. Brunel, P.G. Fajer
Grant Title: Consortium for the Development of a Continuous Nanosecond and Subnanosecond Transient EPR High Field Spectrometer
Agency: NSF
Dates of Grant: 9/1/96-8/31/98
Award Amount: $472,000

PI: Y.M. Eyssa
Grant Title: Investigation Fatigue Properties of Possible Conductor Materials to be Used on the Design Production of a 2 HZ, 30 T Split Pair
Agency: The Regents of the University of California
Dates of Grant: 8/1/96-9/1/97
Award Amount: $125,325

PI: S.P. Hershfield
Grant Title: Hershfield-Special Board Allocation
Agency: UF Division of Sponsored Research
Project Dates: 2/13/96 - 6/30/97
Award Amount: $30,000

PI: S.P. Hershfield
Grant Title: Nanoscale Devices & Novel Engineered Materials
Agency: U.S. Air Force
Project Dates: 8/14/96 - 6/14/97
Award Amount: $137,253

PI: A. Lacerda
Grant Title: Strongly Correlated Electron Systems at Extreme Conditions
Agency: NSF
Dates of Grant: 5/1/96-6/30/96
Award Amount: $2,500

PI: W.P. Beyermann (Univ. of CA, Riverside), *A. Lacerda*, P.C. Canfield (Ames Laboratory)
Grant Title: Fermi-Liquid and Non-Fermi-Liquid Properties in Weakly Hybridized 4f Intermetallic Compounds
Agency: NSF
Dates of Grant: 4/96-3/99
Award Amount: $284,000

PI: S.J. Pearton
Grant Title: Compound Semiconductor Processing
Agency: Sandia National Laboratories
Project Dates: 6/26/96 - 12/25/96
Award Amount: $25,000

PI: S.J. Pearton
Grant Title: Nanoscale Devices & Novel Engineered Materials
Agency: U.S. Air Force
Project Dates: 8/14/96 - 6/14/97
Award Amount: $838,747

PI: D.H. Reitze
Grant Title: Coherent Control of Charge Carrier Motion in Semiconductor Heterostructures
Agency: Research Corporation
Project Dates: 5/15/96 - 5/14/01
Award Amount: $50,000

PI: V.J.M. Salters
Grant Title: A HF-Isotope Study of Mantle Materials
Agency: NSF
Dates of Grant: 8/1/96-7/31/98
Award Amount: $100,000

PI: V.J.M. Salters
Grant Title: Collaborative research: Experimental Determination of Trace Element Distributions between Melts and Mantle Phases at P,T and X Relevant to MORB Genesis
Agency: NSF
Dates of Grant: 11/1/96-11/30/97
Award Amount: $56,534

PI: J.R. Schrieffer
Grant Title: Administrative Support to 1996 President of APS
Agency: American Physical Society (Research Foundation)
Dates of Grant: 1/1/96-12/31/96
Award Amount: $7,909

PI: J.R. Schrieffer
Grant Title: Theory of Strongly Correlated Electron Systems
Agency: NSF
Dates of Grant: 7/1/96-6/30/97
Award Amount: $135,000

PI: J. Schwartz
Grant Title: Hot Rolling of Bismuth-Based Superconductors
Agency: University of Chicago (ANL)
Dates of Grant: 5/20/96-5/19/97
Award Amount: $19,920

PI: J. Schwartz
Grant Title: Control of Carbon Induced Dimensional Instabilities in Ag/BiSrCaCuO Conductors
Agency: Naval Research Laboratory
Dates of Grant: 7/31/96-7/30/97
Award Amount: $50,000

PI: J. Schwartz
Grant Title: Micro and Superconducting Properties of Bulk Hg-Ba-Ca-Cu-O on Metallic Surfaces
Agency: NSF
Dates of Grant: 2/15/96-1/31/97
Award Amount: $195,305

PI: N.S. Sullivan
Grant Title: Dynamical Properties of Frustrated Molecular Solids
Agency: NSF
Project Dates: 9/96-8/99
Award Amount: $300,000

PI: S.W. Van Sciver
Grant Title: Liquid Helium Fluid Dynamics Studies
Agency: U.S. Dept. of Energy
Dates of Grant: 1/1/96-12/31/96
Award Amount: $205,000

PI: A. Zindler, V.J.M. Salters, W.M. Landing, P.C. Ragland
Grant Title: The Acquisition of a High Resolution Inductive Coupled Plasma Mass Spectrometer
Agency: NSF
Dates of Grant: 8/1/96-7/31/99
Award Amount: $267,500

PI: A. Zindler
Grant Title: U-Th Systematics of Primitive Icelandic Basalts: Building a Foundation for Interpreting U-Th Disequilibrium in MORBs
Agency: NSF
Dates of Grant: 5/1/96-4/30/98
Award Amount: $300,000

Continuing Grants

PI: M.D. Bird
Grant Title: Magnetically Damped Furnace-Bitter Magnet Coil
Agency: NASA
Dates of Grant: 8/14/95-11/1/96
Award Amount: $89,373

PI: J.R. Childress
Grant Title: NSF Young Investigation
Agency: NSF
Project Dates: 8/1/94 - 7/31/97
Award Amount: $66,720

PI: T.A. Cross
Grant Title: Correlations: Structure-Dynamics-Function in Gramicidin
Agency: NIH
Dates of Grant: 1/1/95-2/29/96
Award Amount: $219,881

PI: T.A. Cross, *et al.*
Grant Title: Joint Study of Polymer Structural Analysis by New Solid State NMR Method
Agency: Japanese Ministry of Education, Science & Culture
Date of Grant: 4/94-3/96
Award Amount: 5.7M Yen

PI: T.A. Cross
Grant Title: Protein Stability: Catalytic and Non-Catalytic Solvent
Agency: NIH
Dates of Grant: 8/1/93-7/31/96
Award Amount: $348,244

PI: T.A. Cross
Grant Title: Ultra-High Resolution Structure and Dynamics of Bilayer Bound Polypetides
Agency: NSF
Dates of Grant: 1/1/94-12/31/96
Award Amount: $345,000

PI: E. Dagotto, A. Moreo
Grant Title: Photoemission Spectra, d-Wave Superconductivity and Other Properties of High T_c Electronic Models
Agency: NSF
Dates of Grant: 11/95-11/98
Award Amount: $51,000/year

PI: Z. Fisk
Grant Title: Collaborative Research on Lanthanum Bases Cuprates and Kondo Insulators
Agency: University of California
Dates of Grant: 4/1/95-3/31-96
Award Amount: $30,104

PI: Z. Fisk
Grant Title: Interactions and Coherence in Lathanide Metallic Compounds
Agency: NSF
Dates of Grant: 5/15/95-1/31/98
Award Amount: $240,000

PI: Z. Fisk
Grant Title: Study of Materials and Electronic Properties of d-Electron Systems
Agency: NEDO
Dates of Grant: 4/1/94-3/31/96
Award Amount: $78,253

PI: S.P. Hershfield
Grant Title: Nanoscale Device & Novel Engineered Materials
Agency: U.S. Air Force
Project Dates: 12/15/95 - 8/14/96
Award Amount: $112,335

PI: S.P. Hershfield
Grant Title: National Young Investigator Award
Agency: NSF
Project Dates: 7/1/93 - 7/31/98
Award Amount: $62,500

PI: A.G. Marshall, S. Guan, S.C. Foster
Grant Title: FT/ICR/MS: Techniques Development and Non-Biological Applications
Agency: NSF
Dates of Grant: 5/1/94-4/30/96
Award Amount: $377,643

PI: A.G. Marshall, S. Guan
Grant Title: FT Mass Spectrometry for Biomolecule Analysis
Agency: NIH
Dates of Grant: 7/1/94-6/30/97
Award Amount: $451,283

PI.: A.G. Marshall, S. Guan, J.R. Eyler
Grant Title: National High Field FT-ICR Mass Spectrometry Facility
Agency: NSF
Dates of Grant: 9/1/94-6/30/96
Award Amount: $2,400,000

PI: J.R. Miller
Grant Title: HTS Current Lead Assembly Test
Agency: Badcock and Wilcox
Dates of Grant: 6/1/95-1/1/97
Award Amount: $18,920

PI: S.J. Pearton
Grant Title: Nanoscale Devices & Novel Engineered Materials
Agency: U.S. Air Force
Project Dates: 12/15/95 - 8/14/96
Award Amount: $671,565

PI: S.J. Pearton
Grant Title: Role of Light Impurities (H.O.C.) in III-V Nitrides
Agency: NSF
Project Dates: 4/1/95 - 3/31/98
Award Amount: $80,000

PI: V.J.M. Salters
Grant Title: Collaborative Research: Hf and Pb Isotope Ratios in Seawater Indicators of Paleo Hydrothermal Activity
Agency: NSF
Dates of Grant: 7/1/94-6/30/96
Award Amount: $78,618

PI: H.-J. Schneider-Muntau
Grant Title: Cryogen Test
Agency: Allegheny Ludlow Corporation
Dates of Grant: 10/1/94-12/31/99
Award Amount: $10,554

PI: J.R. Schrieffer, M.A. Novotny, L. Gor'kov
Grant Title: Theoretical Studies of Magnetic Systems
Agency: U.S. Dept. of Energy
Dates of Grant: 8/1/94-7/31/96
Award Amount: $90,000

PI: J. Schwartz
Grant Title: Stability of High-T_c Superconducting Conductors
Agency: Naval Research Laboratory
Dates of Grant: 3/10/94-5/21-96
Award Amount: $125,000

PI: S.W. Van Sciver
Grant Title: Heat Transfer Coefficient in Liquid Helium
Agency: Badcock and Wilcox
Dates of Grant : 10/13/94-12/31/97
Award Amount: $52,000

PI: S.W. Van Sciver
Grant Title: Liquid Helium Feasibility Experiments
Agency: Naval Undersea Warfare Center
Dates of Grant: 10/6/95-4/6/96
Award Amount: $40,000

PI: A. Zindler
Grant Title: Technician Support for L-DGO Solid Source Isotope Facility: Phase I
Agency: NSF
Dates of Grant: 7/1/94/2/29/96
Award Amount: $10,800

PI: A. Zindler, A.L. Odom, V.J.M. Salters
Grant Title: The Acquisition of a High Abundance Sensitivity Thermal Ionization Mass Spectrometry
Agency: NSF
Dates of Grant: 9/15/94-8/31/96
Award Amount: $244,265

RESEARCH REPORTS BY CATEGORY

Appendix A

RESEARCH REPORTS BY AUTHOR

Appendix B

D

E

F

G

H

I

J

K

PUBLICATIONS BY AUTHOR

Appendix C

G

H

I

N

O

P

Q

R

S

T

U

V

W

X

Y

Z

USERS & PROJECTS

Appendix D

NHMFL - DC High Field Facility

USER	INSTITUTION	FUNDING	PROJECT
Agosta, C.	Clark Univ.	State of FL	Transport and Penetration Depth in BETS Based Organic Conductors
Coffey, T.*	Clark Univ.		
Ivanov, S.*	Clark Univ.		
Aronson, M.	Univ. of Michigan	DoE	High Pressure Fermi Surface of SmB_6
Tozer, S.	NHMFL		
Fisk, Z.	FSU		
Aronson, M.	Univ. of Michigan	DoE	Magnetoresistance of EuB_6
Fisk, Z.	FSU		
Chaparala, M.◊	NHMFL		
Cooley, J.*	Univ. of Michigan		
Sarrao, J.◊	NHMFL		
Berkowitz, A.	UC, San Diego	NSF	High Field and Low Temperature Characterization of Magnetic Oxide Nanoparticles
Kodama, R.*	UC, San Diego		
Makhlouf, S.	UC, San Diego		
Tronc, E.	Univ. Pierre et Marie Curie		
Berkowitz, A.	UC, San Diego	NSF	Magnetic Properties of Single Molecule Magnets
Aubin, S.*	UC, San Diego		
Eppley, H.	Univ. of Indiana		
Christou, G.	Univ. of Indiana		
Spagna, S.	Quantum Design		
Sager, R.	Quantum Design		
Bowers, C.R.	UF	State of FL	Dynamics of Optical Dynamic Nuclear Polarization in GaAs and InP
Moulton, B.	FSU		
Kleinhammes, A.◊	NHMFL		
Kuhns, P.	NHMFL		
Hughs, E.	UF		
Schmiedel, T.◊	NHMFL		
Brandt, B.	NHMFL	NSF/NHMFL	Magnetoresistance of Cernox Temperature Sensors
Liu, D.*	FSU		
Courts, S.S.	Lake Shore Cryo., Inc		

*◊ Postdoc * Graduate Student # Undergraduate Student*

USER	INSTITUTION	FUNDING	PROJECT
Brooks, J.	FSU	NSF	^{77}Se NMR Study of Spin Density Wave States of the Molecular Crystal $(TMTSF)_2PF_6$
Moulton, B.	FSU		
Valfells, S.*	Boston Univ.		
Kuhns, P.	NHMFL		
Kleinhammes, A.◊	NHMFL		
Uji, S.	NRIM		
Brooks, J.	FSU	NSF	Electronic Properties of Novel Molecular Conductors in High Magnetic Fields
Uji, S.	NRIM		
Hill, S.◊	NHMFL		
Qualls, J.*	FSU		
Sandhu, P.S.*	NHMFL		
Szabo, T.*	NHMFL		
Stalcup, T.*	NHMFL		
Valfells, S.*	Boston Univ.		
Brooks, J.	FSU	NSF	Fermi Surface Study of $(ET)_2KHg(SCN)_4$ by NMR
Moulton, B.	FSU		
Hill, S.◊	NHMFL		
Valfells, S.*	Boston Univ.		
Szabo, T.*	NHMFL		
Uji, S.	NRIM		
Kleinhammes, A.◊	NHMFL		
Kuhns, Phil	NHMFL		
Brooks, J.	FSU	NSF	FTIR Studies on Mo_4O_{11} and $(BEDT\text{-}TTF)I_3$: Field and Temperature Dependence
Wang, Y.-J.◊	NHMFL		
Szabo, T.*	NHMFL		
Brooks, J.	FSU	NSF	Uniaxial Stress Study of a Bechgaard Salt
Harris, J.	Stanford Univ.		
Qualls, J.*	NHMFL		
Chaikin, P.M.	Princeton Univ.	NSF	Heat Capacity Study of Phase Transition in $(TMTSF)_2ClO_4$
Scheven, U.	Princeton Univ.		
Immer, C.*	FSU		
Hannahs, S.	NHMFL		
Chaparala, M.	NHMFL	NSF/NHMFL	Orientation Dependent Torque and Transport on Layered Superconductors

◊ Postdoc * Graduate Student # Undergraduate Student

USER	INSTITUTION	FUNDING	PROJECT
Chen, C.	FAMU-FSU College of Eng.	State of FL	Effects of Magnetic Fields on Biological Fluids
Pai, V.*	FAMU-FSU College of Eng.		
Haik, Y. *	FAMU-FSU College of Eng.		
Cheong, S.W.	AT&T Bell Labs	AT&T	Field and Pressure Effects on the Interplay Among Charge, Spin, and Lattice in Doped Manganese Perovskites
Batlogg, B.	AT&T Bell Labs		
Tozer, S.	NHMFL		
Hwang, H. *	AT&T Bell Labs		
Clark, W.G.	UCLA	NSF	NMR Studies of Correlated Electron Systems
Zheng, G.-Q.	Osaka Univ.		
Brown, S.E.	UCLA		
Tanaka, K.	UCLA		
Moulton, B.	FSU		
Kuhns, P.	NHMFL		
Courts, S.S.	Lake Shore Cryo., Inc	Lake Shore	Magnetoresistance RuO Temperature Sensors
Lui, D.*	FSU		
Brandt, B.	NHMFL		
Cross, T.	FSU	NSF/NHMFL	Development of Higher Homogeneity Resistive Magnet Capabilities
Rosanske, R.	FSU		
Soghomonian, V.◊	NHMFL		
Sabo, M.	NHMFL		
Murphy, P.	NHMFL		
Crow, J.	NHMFL	NSF/NHMFL	Magnetization Studies of Itinerant Electron Systems at High Magnetic Fields
Shepard, M.*	FSU		
Wolters, C.◊	NHMFL		
Crow, J.	NHMFL	NSF/NHMFL	Magnetoresistance Studies of Itinerant Electron Systems
Cao, G.◊	NHMFL		
McCall, S.	NHMFL		
Guertin, R. P.	Tufts Univ.		
Crow, J.	NHMFL	NSF/NHMFL	Righi-Leduc Effect in Doped YBCO
Cao, G.◊	NHMFL		
Henning, P.*	FSU		
DeLong, L.	Univ. of Kentucky	NSF	Torque Measurements on Anisotropic Intermetallic Compounds
Sechovsky, V.	Charles Univ., Prague		
Havela, L.	Charles Univ., Prague		
Prokes, K.	Charles Univ., Prague		

◊ Postdoc * Graduate Student # Undergraduate Student

USER	INSTITUTION	FUNDING	PROJECT
Douglas, E.P.	LANL	LANL	Polymer Processing
Benicewicz, B.	LANL		in High Magnetic
Smith, M.	LANL		Fields
Du, R.R.	Univ. of Utah	Univ. of Utah	Angular Dependent
Zudov, M.*	Univ. of Utah		Quantum Hall
Simmons, J.	Sandia Nat'l. Labs		Measurements Around
Chui, H.C.	Sandia Nat'l. Labs		n=3/2
Fisk, Z.	FSU	NSF/NHMFL	Magnetic Field and
Sarrao, J.	NHMFL		Pressure Studies of
Lacerda, A.	LANL		Pure and Doped
Immer, C. *	FSU		$YbInCu_4$, $YbZnCu_4$, $YbInNi_4$
Fortune, N.	Smith College	Smith College	Quasi-Low
Kobayashi, Y.*	Smith College		Dimensional Collective Phenomena in Molecular Conductor
Furdyna, J.	Univ. of Notre Dame	NSF	Far Infrared
Wang, Y.◊	NHMFL		Transmission Studies of ZnSe Superlattices
Furdyna, J.	Univ. of Notre Dame	NSF	Investigation of Spin
Schmiedel, T.◊	NHMFL		Interactions in
Pareek, A.*	Univ. of Notre Dame		MnSe/ZnSe
Yin, A.*	Univ. of Notre Dame		Superlattice at High
Dobrowolska, M.	Univ. of Notre Dame		Magnetic Fields
Goodrich, R.G.	Louisiana State Univ.	DoE	Fermi Surface in
Vuillimen, J.	Univ. of Arizona		Highly Correlated
Haanappel, E.◊	NHMFL/LANL		Systems
Hall, Donovan*	Louisiana State Univ.		
Goodrich, R.G.	Louisiana State Univ.	DoE	Landau Quantum
Lowndes, D.	Oak Ridge Nat'l. Lab.		Oscillations in
Hall, D.*	Louisiana State Univ.		Superconductors
Graybeal, J.	UF	UF	Infrared Reflectence
			Measurement in Li Doped Lanthanum Copper Oxides

*◊ Postdoc * Graduate Student # Undergraduate Student*

USER	INSTITUTION	FUNDING	PROJECT
Grossinger, R.	Vienna Univ. of Tech.	Austrian	The
Kou, X.C.	Vienna Univ. of Tech.	Science	Magnetocrystalline
de Boer, F.	Univ. of Amsterdam	Foundation	Anisotropy and the
			Magnetic Intersublattice Exchange Interaction in the Rare-Earth Transition-Metal Intermetallics
Guillot, M.	Service Nat'l. des Champs Intenses	CNRS of France	Magnetic and Magneto Optical (Faraday Rotation) Studies of Magnetic Insulators
Halperin, W.	Northwestern Univ.	NSF	Flux Melting Phase
Reyes, A.	Northwestern Univ.		Transition by NMR
Hammel, C.	LANL		
Martindale, J.	Ohio State		
Kuhns, P.	NHMFL		
Kleinhammes, A.◊	NHMFL		
Mitrovic, V.	Northwestern Univ.		
Bachman, H.N.*	Northwestern Univ.		
Hammel, P.C.	LANL	DoE	NMR Study of
Moulton, B.	FSU		Magnetic Properties
Pennigton, C.	Ohio State Univ.		of $YBa_2Cu_3O_7$ near
Smith, J.L.	LANL		T_c
Hults, W.	LANL		
Kuhns, P.	NHMFL		
Kleinhammes, A.◊	NHMFL		
Hascicek, Y.	NHMFL	NSF/NHMFL	Critical Current vs.
Shaoff, P.	NHMFL		Field and Strain of
Osman, D.*	NHMFL		Bismuth 2212 Joints
Hascicek, Y.	NHMFL	NSF/NHMFL	Field Dependence of
Boutemy, B.	NHMFL		the Critical Current
Howton, J.	NHMFL		Density of Sheathed
Osman, D.*	NHMFL		Dip-Coated Monocore
Hilton, D.*	NHMFL		Tape
Hascicek, Y.	NHMFL	NSF/NHMFL	Magnetoresistance of
Osman, D.*	NHMFL		Ag and Ag Alloys as
Howton, J.	NHMFL		Sheathing to High T_c Superconducting Wire

*◊ Postdoc * Graduate Student # Undergraduate Student*

USER	INSTITUTION	FUNDING	PROJECT
Jones, E.D.	Sandia Nat'l. Labs	Sandia Labs	Magneto Polarons in
Yokoi, H.	Nat'l. Inst. of Mat. & Chem. Res.		CdTe/CdMnTe
Tozer, S.	NHMFL		
Schmiedel, T.◊	NHMFL		
Mirecki-Millinchick, J.◊	Sandia Nat'l. Labs.		
Jones, E.D.	Sandia Nat'l. Labs	Sandia Labs	Pressure Dependent
Yokoi, H.	Nat'l. Inst. of Mat. & Chem. Res		Determination of Conduction and
Tozer, S.	NHMFL		Valence Band Masses
Schmiedel, T.◊	NHMFL		in n-Type InGaAs/GaAs
Mirecki-Millinchick, J.◊	Sandia Nat'l. Labs		
Kang, W.W.	Univ. of Chicago	Packard	Pressure Dependence
Hannahs, S.	NHMFL	Foundation	of Magnetotransport
Haddon, R.	Bell Labs/AT&T		in Organic Conductors
Kang, W.W.	Univ. of Chicago	Packard	Sonoluminesence
Young, J.*	Univ. of Chicago	Foundation	at High Magnetic
Cho, H.	Univ. of Chicago		Fields
Schmiedel, T.◊	NHMFL		
Kang, W.W.	Univ. of Chicago	Packard	Spin Effects in the
Hannahs, S.	NHMFL	Foundation	Quantum Hall
Young, J.*	Univ. of Chicago		Effect
Gossard, A.	UC, Santa Barbara		
Palm, E.	NHMFL		
Landee, C.	Clark Univ.	State of FL	Magnetization of
Turnbull, M.	Clark Univ.		S=1/2, Low Exchange
Albrecht, A.*	Clark Univ.		Strength, Heisenberg Antiferromagnets in 2D
Manlief, M.	Am. Superconductor	Am. Supercon.	High Temperature
Schwartz, J.	NHMFL		Superconductor Coil
Amm, B.*	FSU		Performance
Hilton, D.*	NHMFL		
Brandt, B.	NHMFL		
Maple, M.B.	UC, San Diego	DoE	Non-Fermi Liquid
Aronson, M.	Univ. of Michigan		Scaling in
Chau, R.*	UC, San Diego		$UCu_{5X}Pd_{x}$
Wolters, C.◊	NHMFL		(x=1,1.5)

◊ Postdoc ** Graduate Student* *# Undergraduate Student*

USER	INSTITUTION	FUNDING	PROJECT
Maple, M.B.	UC. San Diego	DoE	Superconducting
Andrade, M.	IPAPS, UC San Diego		Transition
Han, Suengho	IPAPS. UC San Diego		Measurements T_c and H_c
Marken, K.	Oxford Supercon Tech	Oxford Super-conducting	Critical Current as a Function of
McKinnell, J.	Oxford Supercon Tech	Technology	Temperature,
Hong, S.	Oxford Supercon Tech		Magnetic Field,
Cowey, L.	Oxford Supercon Tech		and Strain in High
Dai, W.	Oxford Supercon Tech		Field Superconducting
Henges, R.	Oxford Supercon Tech		Materials
Tatum, J.	Oxford Supercon Tech		
Ting, S.	Oxford Supercon Tech		
Markiewicz, D.	NHMFL	NSF / NHMFL	Critical Current
Bonney, L.◊	NHMFL		Testing of
Dixon, I.	NHMFL		Superconductors
Dougherty, J.	NHMFL		for Development of
Pickard, K.	NHMFL		900 MHz NMR Magnets
Marshall, A.	FSU	NSF	FT-ICR Mass
Guan, S.	NHMFL		Spectometry in a 20 T
Drader, J.*	Univ. of Texas, Austin		Water-Cooled
Hendrickson, C.	NHMFL		Magnet
McCombe, B.D.	SUNY , Buffalo	ONR	Resonant Magneto
Wang, Y.-J.◊	NHMFL		Polaron Effects with
Nickel, H.*	Research Foundation of SUNY		Interface Phonons in GaAs/AlGaAs
Peeters, F.	Univ. of Antwerp		Quantum Wells
Schaff, W.	Cornell		
McElfresh, M.W.	Purdue Univ.	State of FL	Phase Diagram of Deoxygenated
Moloni, K.	Purdue Univ.		YBCO Thin Films
Li, S.*	Purdue Univ.		
Overhauser, A.	Purdue Univ.		
Meisel, M.W.	UF	State of FL	Magnetization Study
Talhan, D.	UF		of s=2 Linear Chain
Ward, B.	UF		Heisenberg
Chou, L.*	UF		Antiferromagnet
Granroth, G. *	UF		
Moulton, B.	FSU	NSF/NHMFL	Development of
Kleinhammes, A.◊	NHMFL		Probe for Condensed
Kuhns, P.	NHMFL		Matter NMR

*◊ Postdoc * Graduate Student # Undergraduate Student*

USER	INSTITUTION	FUNDING	PROJECT
Moulton, B.	FSU	NSF/NHMFL	NMR on La_2CuO_4
Kleinhammes, A.◊	NHMFL		Doped with Li
Kuhns, P.	NHMFL		or Na
Musfeldt, J.L.	SUNY, Binghamton	SUNY, Bing.	Spectroscopic
Wang, Y.-J.◊	NHMFL		Studies of,
Li, G.F.*	SUNY, Binghamton		Spin-Peierls
Lee, J.*	SUNY, Binghamton		Materials
Naughton, M.	SUNY, Buffalo	NSF	Fluctuation
Chaparala, M.◊	NHMFL		Magnetization
Ulmet, J.P.	SNCMP		Studies of High
Hope, A.*	SUNY, Buffalo		Temperature
Lee, I.J.*	SUNY, Buffalo		Superconductors
Naughton, M.	SUNY, Buffalo	NSF	Magnetic Anisotropy
Hope, A.*	SUNY, Buffalo		of Y(Pr)BaCuO
Maple, M.B.	UC, San Diego		
Gajewski, D.*	UC, San Diego		
Leone, M.*	SUNY, Buffalo		
Petrou, D.*	SUNY, Buffalo		
Naughton, M.	SUNY, Buffalo	NSF	Magnetization
Lee, I.*	SUNY, Buffalo		Studies of $(ET)_2TlHg(SeCN)_x$
Naughton, M.	SUNY, Buffalo	NSF	Magnetization Study
Chaikin, P.	Princeton Univ.		of Molecular Metals
Laukhin, V.	SUNY, Buffalo		
Hope, A.*	SUNY, Buffalo		
Ng, H.-K.	FSU	FSU	Infrared Spectroscopy
Cope, P.	Wilmad Glass		of Highly Correlated
LaSalle, A.	LANL		Electron Compounds
Nurmikko, A.V.	Brown Univ.	NSF	Spectroscopy of
Song, Y.S.*	Seoul Nat'l. Univ.		Blue-Green
Zhou, H.	Brown Univ.		Semiconductor Light
Schmiedel, T.◊	NHMFL		Emitting Heterostructures
Painter, T.	NHMFL	NSF/NHMFL	Critical Current
Berry, M.	NHMFL		Measurements and Time Constant Measurements of Nb_3Sn Cable

*◊ Postdoc * Graduate Student # Undergraduate Student*

USER	INSTITUTION	FUNDING	PROJECT
Park, Y. W.	Seoul Nat'l. Univ.	Korea Science	Magneto
Hannahs, S.	NHMFL	& Eng.	Thermoelectric
Song, Y. S.	Seoul Nat'l. Univ.	Foundation	Power of Doped
Choi, E. S.*	Seoul Nat'l. Univ.		Polyacetylene and High T_c Superconductor
Petrou, A.	SUNY, Buffalo	NSF	Investigation on
Salib, M.	SUNY, Buffalo		X-Crossing in
Luo, H.*	SUNY, Buffalo		GaAs/AlAs Multiple
Kioseoglou, G.*	SUNY, Buffalo		Quantum Well
Hoetly, J.*	SUNY, Buffalo		Structures
Stoltz, S.*	SUNY, Buffalo		
Schmiedel, T.◊	NHMFL		
Petrou, A.	SUNY, Buffalo	NSF	Magneto
Schmiedel, T.◊	NHMFL		Luminescence of
Salib, M.*	SUNY, Buffalo		n-Type
Kioseoglou, G.*	SUNY, Buffalo		ZnSe/ZnCdMnSe
Furdyna, J.	Univ. of Notre Dame		Quantum Wells
Luo, H.	SUNY, Buffalo		
Petrou, A.	SUNY, Buffalo	NSF	Optically Detected
Salib, M.*	SUNY, Buffalo		Resonances Using FIR Laser
Popovic, D.	City College of CUNY/NHMFL	NSF	Magnetotransport in Quantum Wells
Dunford, R.	CUNY, Brooklyn College		
Pollack, F.	CUNY, Brooklyn College		
Streit, D.	TRW Electronic Systems		
Wojiowicz, M.	TRW Electronic Systems		
Ramierez, A.	Lucent Technologies	Lucent	Magnetization
Chaparala, M.◊	NHMFL	Technologies	Measurements of YMo_2O_7
Schmiedeshoff, G.M.	Occidental College	State of FL	Upper Critical Field of UBe_{13}
Stewart, G.	UF		
Schneider, D.	Technische Universitat Braunschweig	NSF/NHMFL	Nonparabolicity of the Conduction Band
Wang, Y.-J.◊	NHMFL		in Highly n-Doped
Tank, B.	Technische Universitat Braunschweig		InGaAsP
Berfuss, K.	Technische Universitat Braunschweig		

◊ Postdoc ** Graduate Student* *# Undergraduate Student*

USER	INSTITUTION	FUNDING	PROJECT
Schneider-Muntau, H.	NHMFL	NSF/NHMFL	Magnetothermal Conductivity of
Gottstein, G.	RWTH Technical Univ.		Ag-Cu Wires
Heringhaus, F. *	RWTH Technical Univ./NHMFL		
Schwartz, J.	FSU	NSF	Critical Current and
Nakamae, S.*	FSU		Magnetothermal
Burkhardt, E.*	FAMU-FSU College of Eng.		Conductivity of Bi-2212
Amm, K.*	FAMU-FSU College of Eng.		Superconductors
Schwartz, J.	FSU	NSF	Development of High
Hascicek, Y.	NHMFL		Strength Conductors
Dur, O.*	NHMFL		for High Field NMR
Boutemy, B.	NHMFL		Magnets
Boutemy, S.*	NHMFL		
Schwartz, J.	NHMFL	NSF	Microstructure and
Amm, K.*	FAMU-FSU College of Eng.		Superconducting Properties of Bulk
Wolters, C.◊	NHMFL		Hg-Ba-Ca-Cu-O on Metallic Surfaces
Sessoli, R.	Universita Degli Studi di Firenze	NSF/NHMFL	Magnetic Aniostropy of an Octangular
Chaparala, M.◊	NHMFL		Iron (III) Cation
Shayegan, M.	Princeton Univ.	NSF	Angular Dependence
Manoharan, H.*	Princeton Univ.		of Two Dimensional
Papadakis, S.*	Princeton Univ.		Holes in Magnetic Fields
Shivaram, B.	Univ. of Virginia	NSF	Sound Propagation
Ulrich, V.*	Univ. of Virginia		in Heavy Electron
Hinks, D.	Argonne Nat'l Lab.		Materials
Shivaram, B.	Univ. of Virginia	NSF	Unconventional
Ulrich, V.	Univ. of Virginia		Superconductivity
Dorsey, B.*	Univ. of Virginia		and Magnetism in
Wang, H.*	Univ. of Virginia		Heavy Electron
Drake, D.*	Univ. of Virginia		Metals
Chaparala, M.◊	NHMFL		
Singleton, J.	Oxford Univ.	Eng. &	Investigation of
House, A.	Oxford Univ.	Physical	Angular Dependent
Blundell, S.	Oxford Univ.	Sciences	Magnetoresistance
Honold, M.*	Oxford Univ.	Res. Council, UK	Oscillations in Organic Molecular Metals

◊ Postdoc ** Graduate Student* *# Undergraduate Student*

USER	INSTITUTION	FUNDING	PROJECT
Smet, J.	Max-Planck Institute, Stuttgart	Max-Planck Institute	Quasi Classical Dynamics of
Von Klitzing, K.	Max-Planck Institute, FKF		Composite Fermions
Weiss, D.	Max-Planck Institute, Stuttgart		
Coleridge, P.	Nat'l. Research Center, UK		
Stewart, G.	UF	State of FL	Magnetization of
Andraka, B.	UF		Spin Fluctuation
Thomas, S.	UF		Systems in High
Lumpe, H.*	Univ. of Augsburg		Magnetic Fields
Kim, J.J.	Univ. of Central FL		
Chaparala, M.◊	NHMFL		
Summers, L.	NHMFL	NSF/NHMFL	Investigation of the
Walsh, R.	NHMFL		Effect of Applied
Haslow, M.	NHMFL		Strain on the Critical
Bednar, N.	NHMFL		Current of Cable-in-
Miller, J.	NHMFL		Conduit Conductors for the 45 T Hybrid Magnet
Summers, T.	NHMFL	NSF	Magnetoresistance
Gottstein, G.	RWTH Technical Univ.		of High Strength CuAg
Herringhaus, F.*	NHMFL		
Lutzler, M.	Hoesch Stahl		
Tanner, D.	UF	NSF	Investigation of
Wang, Y.-J.◊	NHMFL		Magnetic Phase
Zibold, A.◊ Liu, H.*	UF		Transition Spin-Flop Phase C60 Magnons
	UF		
Tanner, D.	UF	NSF	Magnetotransmittance
Zibold, A.*	UF		and Reflectance;
Liu, H.*	UF		Investigation of Superconducting Carrier Density and Magnon Excitations
Tanner, D.	UF	NSF	Midgap Infared
Wang, Y.-J.◊	NHMFL		Absorption in the
Zibold, A.◊	UF		Insulating Phases of
Liu, H.*	UF		the Cuprate
Laveigne, J.*	UF		Superconductors

*◊ Postdoc * Graduate Student # Undergraduate Student*

USER	INSTITUTION	FUNDING	PROJECT
Taylor, P.C.	Univ. of Utah	NSF	High Magnetic Field
Hari, P.	Univ. of Utah		NMR Studies of
Moulton, B.I	FSU		Chalcogenide
Kuhns, P.	NHMFL		Glasses
Kleinhammes, A.◊	NHMFL		
Tozer, S.	NHMFL	NSF/NHMFL	Magnetoresistance
Hannahs, S.	NHMFL		Studies of $(TMTSF)_2PF_6$ and Related Salts at High Pressures
Tsui, D.C.	Princeton Univ.	NSF & AFOSR	Fractional Quantum Hall Effect
Stormer, H.L.	AT&T Bell Labs		
Du, R.R.	Univ. of Utah		
West, K.	AT&T Bell Labs		
Pfieffer, L.	AT&T Bell Labs		
Yeh, A.*	Princeton Univ.		
Van Sciver, S.	FAMU-FSU College of Eng.	NSF/NHMFL	Bi-2212 Coil Critical Current as a Function
Ousman, D.*	NHMFL		of Applied Field and
Hazelton, D.	IGC Inc.		Quench Behavior
Weijers, H.*	NHMFL		
Von Klitzing, K.	Max-Planck Institute, FKF	Max-Planck Institute	Magnetic Modulation in the Fractional
Smet, J.	Max-Planck Institute, Stuttgart		Quantum Hall Regime
Weiss, D.	Max-Planck Institute, Stuttgart		
Vuillemin, J.J.	Univ. of Arizona	State of FL	Fermi Surface
Goodrich, R.	Louisiana State Univ.		Parameters in Highly Correlated Systems
Welp, U.	Argonne Nat'l. Lab.	DoE / NSF	Magnetic Anisotropy
Fendrich, J.	Argonne Nat'l. Lab.		and Resistivity of $YBa_2Cu_3O_2$
Woo, J.-C.	Seoul Nat'l. Univ.	Korean	Magnetic Field
Kim, D.	Seoul Nat'l. Univ.	Ministry of Ed	Dependence of
Koh, H.S.*	Seoul Nat'l. Univ.		Anti-Stokes
Woo, D.H.	Seoul Nat'l. Univ.		Luminescence in
Rhee, S.J.*	Seoul Nat'l. Univ.		Asymmetric Double Quantum Wells

◊ Postdoc ** Graduate Student* *# Undergraduate Student*

USER	INSTITUTION	FUNDING	PROJECT
Woo, J.-C.	Seoul Nat'l. Univ.	Korean	Photoluminescence
Kim, D.W.	Seoul Nat'l. Univ.	Ministry of Ed	(PL) and PLE
Koh, H.S.*	Seoul Nat'l. Univ.		
Kim, W.S.*	Seoul Nat'l. Univ.		
Kim, D.H.*	Seoul Nat'l. Univ.		
Kim, Y.S.*	Seoul Nat'l. Univ.		
Kim, Y.M.*	Seoul Nat'l. Univ.		
Wu, Y.	Univ. of NC	NSF	High Field NMR
Poon, J.	Univ. of Virginia		Studies of Quasicrystalline and Amorphous Metallic Alloys
Yeh, N.-C.	Cal Tech	NSF	Magnetic Field Tuned
Samoilov, A.*	Cal Tech		Superconductor to
Konczykowski, M.	Ecole Polytechnique		Insulator Transitions
Tsuei, C.	IBM Watson Research Center		in Amorphous Superconductors
Yokoi, H.	Nat'l. Inst. of Mat. & Chem. Res.	Japan	Pressure and Magnetic Field
Takeyama, S.	Himeji Institute of Technology		Effects on Localization by Free
Tozer, S.	NHMFL		Excitation Magneto
Schmiedel, T.◊	NHMFL		Polarons
Fujiwara, S.	NIMR		
Kossut, J.	Polish Academy of Science		
Sayama, K.	NIMR		
Zuo, F.	Univ. of Miami	State of FL	Magneto-Transport in
			$(BEDT\text{-}TTF)_2CuCNS$

NHMFL - Pulse Field Facility

USER	INSTITUTION	FUNDING	PROJECT
Alexander, J.*	New Mexico Tech.	DoE	Data Acquisition
Lacerda, A.H.	LANL	NHMFL	Programming
Arko, A.J.	LANL	DoE	dHvA in Heavy
Cornelius, A.◊	LANL	DoE	Fermion Systems
Smith, J.L.	LANL	DoE	
Aronson, M.	Univ. of Mich.	NSF/DoE	EuB_6
Lacerda, A.H.	LANL	NHMFL	
Cooley, J.C.*	Univ. of Mich.	NSF/DoE	
Sarrao, J.L.	NHMFL/FSU	NHMFL	
Fisk, Z.	NHMFL/FSU	NHMFL/FSU	

*◊ Postdoc * Graduate Student # Undergraduate Student*

USER	INSTITUTION	FUNDING	PROJECT
Baggio-Saitovitch, E.	CBPF	Brazil	$Ce(Ru_{1-x}\ Fe_x)^2Ge_2$
Fontes, M.B.	CBPF	Brazil	
Bud'ko, S.L.	CBPF	Brazil	
Sampaio, L.C.	CBPF	Brazil	
Guimaraes, A.P.	CBPF	Brazil	
Continentino, M.A.	UFF	Brazil	
Hundley, M.F.	LANL	DoE	
Lacerda, A.H.	LANL	NHMFL	
Beyermann, W.P.	UC Riverside	NSF	$Pr_{1-x}\ La_xPb_3$
Yatskar, A. *	UC Riverside	NSF	
Bud'ko, S.L.	Ames Labs.	DoE	
Canfield, P.C.	Ames Labs.	DoE	
Lacerda, A.H.	LANL	NHMFL	
Brooks, J.S.	NHMFL/FSU	NSF	Quantum Limit of
Qualls, J.S.*	NHMFL/FSU		Low Dimensional
Engel, L.W.	NHMFL/FSU	NHMFL	Metals
Clark, R.G.	U. New S. Wales	Australia	
Dzurak, A.S.	U. New S. Wales	Australia	
Kane, B.E.	U. New S. Wales	Australia	
Miura, N.	Univ. Tokyo	Japan	
Rickel, D.G.	NHMFL	NHMFL	
Goettee, J.D.	LANL	DoE	
Canfield, P.C.	Ames Labs.	DoE	$HoNi_2B_2C$
Cho, B.K.*	Iowa State Univ.		
Lacerda, A.H.	LANL	NHMFL	
Clark, R.G.	U. New S. Wales	Australia	Transport
Kane, B.E.	U. New S. Wales	Australia	Measurements in
Dzurak, A.S.	U. New S. Wales	Australia	Extreme Fields
Brooks, J.S.	NHMFL/FSU	NSF	
Engel, L.W.	NHMFL/FSU	NSF	
Miura, N.	Univ. Tokyo	Japan	
Yokoi, H.	NIMCR	Japan	
Rickel, D.G.	NHMFL	NHMFL	
Goettee, J.D.	LANL	DoE	

*◊ Postdoc * Graduate Student # Undergraduate Student*

USER	INSTITUTION	FUNDING	PROJECT
Harrison, N.◊	LANL	NHMFL	(BEDT-
Mielke, C.H.◊	LANL	NHMFL	$TTF)_2KHg(SCN)_4$
Lacerda, A.H.	LANL	NHMFL	
Rickel, D.	NHMFL	NHMFL	
Honold, M.M.	Oxford Univ.	U. K.	
Singleton, J.	Oxford Univ.	U. K.	
Kurmoo, M.	Royal Ints.	U. K.	
Day, P.	Royal Ints.	U. K.	
Jardim, R.	USP	Brazil	$Pr_{1-x}Ba_xMnO_3$
Cohenca, C.H.#	USP	Brazil	
Torikachvili, M.S.	San Diego State	NSF/DoE	
Lacerda, A.H.	LANL	NHMFL	
Jardim, R.	USP	Brazil	$LnNiO_3$
Escote, M.T.#	USP	Brazil	
Torikachvili, M.S.	San Diego State	NSF/DoE	
Lacerda, A.H.	LANL	NHMFL	
Jones, E.D	Sandia Nat'l. Labs	DoE	Pressure/Field
Kim, Y.◊	NHMFL	NHMFL	Studies of Single
Perry, C.H.	Northeastern Univ.	NHMFL	Quantum Wells,
Tozer, S.W.	NHMFL	NHMFL	(InGaAs-GaAs)
Rickel, R.G.	NHMFL	NHMFL	
Kim, Y.◊	NHMFL	NHMFL	Photoluminescence
Perry, C.H.	Northeastern Univ.	NSF/DoE	
Rickel, D.	NHMFL	NHMFL	
Simmons, J.	Sandia Nat'l. Labs	DoE	
Jones, E.D.	Sandia Nat'l. Labs	DoE	
Klem, J.F.	Sandia Nat'l. Labs	DoE	
Lacerda, A.H.	LANL	NHMFL	Kondo Insulators
Goettee, J.D.	LANL	DoE	
Smith, J.L.	LANL	DoE	
Schmiedeshoff, G.	Occidental Col.	DoE	
Canfield, P.C.	Ames Labs	DoE	
Lacerda, A.H.	LANL	NHMFL	$RESb_2$
Mielke, C.H.◊	LANL	NHMFL	
Harrison, N.◊	LANL	NHMFL	
Bud'ko, S.	Ames Labs	DoE	
Canfield, P.C.	Ames Labs	DoE	

◊ Postdoc ** Graduate Student* *# Undergraduate Student*

USER	INSTITUTION	FUNDING	PROJECT
Lacerda, A.H.	LANL	NHMFL	$YbNi_2B_2C$
Yatskar, A. *	UC Riverside	NSF	
Mielke, C.H.◊	LANL	NHMFL	
Beyermann, W.P.	UC Riverside	NSF	
Laukhin, V.N.	Inst. Chem. Phys.	NSF	Magnetoresistance
Naughton, M.J.	SUNY, Buffalo	NSF	and Quantum
Haanappel, E.◊	LANL	NHMFL	Osc. in BEDT-TTF
Lee, K-S.	ETRI	Korea	GaAs/(Al,Ga)As
Kim, Y.◊	NHMFL	NHMFL	Quantum Wells
Maple, M.B.	UC San Diego	NSF/DoE	$Y_{1-x}U_xPd_3$
Dickey, R.P.*	UC San Diego	NSF/DoE	
Gajewski, D.A.*	UC San Diego	NSF/DoE	
deAndrade, M.C.◊	UC San Diego	NSF/DoE	
Maple, M.B.	UC San Diego	NSF/DoE	$Nd_{1.85}Ce_{0.15}CuO_{4\pm\delta}$
Dickey, R.P.*	UC San Diego	NSF/DoE	
Hermann, J.◊	UC San Diego	NSF/DoE	
deAndrade, M.C.◊	UC San Diego	NSF/DoE	
Jiang, W.	Univ. of Maryland		
Mao, S.N.	Univ. of Maryland		
Green, R.L.	Univ. of Maryland		
Mielke, C.H.◊	LANL	NHMFL	dH-vA in $SmSb_2$
Lacerda, A.H.	LANL	NHMFL	
Salo, L. #	S. Plains College	SERS	
Canfield, P.C.	Ames Labs.	DoE	
Bud'ko, S.L.	Ames Labs.	DoE	
Mielke, C.H.◊	LANL	NHMFL	Molecular Metals
Harrison, N.◊	LANL	NHMFL	
Agosta, C.C.	Clark Univ.	Air Force	
Lacerda, A.H.	LANL	NHMFL	
Montenegro, F.C.	UFPE	Brazil	$Fe_xZn_{1-x}F_2$
Lima, K. #	UFPE	Brazil	
Torikachvili, M.S.	San Diego State	NHMFL	
Lacerda, A.H.	LANL	NHMFL	

*◊ Postdoc * Graduate Student # Undergraduate Student*

USER	INSTITUTION	FUNDING	PROJECT
Movshovich, R.	LANL	DoE	CePtPb
Lawrence, J.M.	UC Irvine	NSF/DoE	
Hundley, M.F.	LANL	DoE	
Neumeier, J.	LANL	DoE	
Thompson, J.D.	LANL	DoE	
Lacerda, A.H.	LANL	NHMFL	
Fisk, Z.	NHMFL/FSU	NHMFL/FSU	
Nakotte, H.◊	LANL	DoE	$UCu_{3.5}Al_{1.5}$
Lacerda, A.H.	LANL	NHMFL	
Torikachvili, M.S.	San Diego State	NHMFL	
Bruck, E.	Amsterdam Univ.	Netherlands	
Prokes, K.*	Amsterdam Univ.	Netherlands	
de Boer, F.R.	Amsterdam Univ.	Netherlands	
Perry, C.H.	Northeastern Univ.	NHMFL	Semiconductor
Kim, Y.◊	NHMFL	NHMFL	Heterostructures
Rickel, R.G.	NHMFL	NHMFL	
Rickel, D.	NHMFL	NHMFL	Mag. of CuAg Wires
Campbell, L.J.	NHMFL	NHMFL	
Rickel, D.	NHMFL	NHMFL	40 T Long Pulse
Pernambuco-Wise, P.	NHMFL	NHMFL	
Campbell, L.J.	NHMFL	NHMFL	
Safar, H.	Univ. of Chicago	NSF	$YBa_2Cu_3O_7$
Lopez, D.◊	IBM		
Krusin-Elbaum, L.	IBM		
Maley, M.P.	LANL	DoE	
Salamon, M.B.	Univ. of Illinois	NSF/DoE	Hall Measurements
Jaime, M.◊	Univ. of Illinois	NSF/DoE	
Hardner, H.	Univ. of Illinois	NSF/DoE	
Emin, D.	Sandia Nat'l. Labs	DoE	
Rubenstein, M.	Naval Research	DoD	
White, P.	Univ. of Illinois	NSF/DoE	
Lacerda, A.H.	LANL	NHMFL	

*◊ Postdoc * Graduate Student # Undergraduate Student*

USER	INSTITUTION	FUNDING	PROJECT
Schmiedeshoff, G.M.	Occidental Col.	DoE	$LuNi_2B_2C$
Lacerda, A.H.	LANL	NHMFL	
Buford, M.C.#	Univ. NC	DoE	
Braje, T.#	UF	DoE	
Canfield, P.C.	Ames Labs.	DoE	
Smith, J.L.	LANL	DoE	
Schmiedeshoff, G.M.	Occidental Col.	DoE	$U_{1-x}Th_xBe_{13}$
Torikachvili, M.S.	San Diego State	DoE	
Lacerda, A.H.	LANL	NHMFL	
Buford, M.C.#	Univ. NC	DoE	
Smith, J.L.	LANL	DoE	
Schmiedeshoff, G.M.	Occidental Col.	DoE	$ThBe_{13}$
Torikachvili, M.S.	San Diego State	DoE	
Lacerda, A.H.	LANL	NHMFL	
Smith, J.L.	LANL	DoE	
Tessema, G.X.	Clemson Univ.	NSF	Low Dimensional
Kuh, J.*	Clemson Univ.	NSF	Metals
Mengistu, E.H.	Clemson Univ.	NSF	
Skove, M.J.	Clemson Univ.	NSF	
Safar, H.	Univ. of Chicago	NSF	
Mielke, C.H.◊	LANL	NHMFL	
Lacerda, A.H.	LANL	NHMFL	
Thompson, J.D.	LANL	DoE	$Ce_3Bi_4Pt_3$
Modler, R.◊	LANL	DoE	
Moshopoulou, E.◊	LANL	DoE	
Canfield, P.C.	Ames Labs.	DoE	
Fisk, Z.	NHMFL/FSU	NHMFL/FSU	
Triscone, G.◊	UC San Diego	NSF/DoE	$Bi_2Sr_2CaCu_2O_8$
Maple, M.B.	UC San Diego	NSF/DoE	
Zettl, A.	UC Berkeley	NSF	Josephson Vortex
Fuhrer, M.S.*	UC Berkeley	NSF	
Ino, K.	Tsukuba	Japan	
Oka, K.	Tsukuba	Japan	
Nishihara, Y.	Tsukuba	Japan	

◊ Postdoc ** Graduate Student* *# Undergraduate Student*

NHMFL - NMR Facility

USER	INSTITUTION	FUNDING	PROJECT
720 MHz NMR (Varian)			
Meersman, T. Bodenhausen, G.	NHMFL NHMFL	NHMFL	Transverse Relaxation in Coupled Spin Sytems
Jeannerat, D. Bodenhausen, G.	NHMFL NHMFL	NHMFL	Accurate Determination of Scalar Coupling Constants
Peng, C. Bodenhausen, G.	NHMFL NHMFL	NHMFL	Automated Spectral Analysis
Vincent, S.J.F. Zwahlen, C. Bodenhausen, G.	NHMFL NHMFL NHMFL	NHMFL	Suppression of Spin Diffusion in Nuclear Overhauser Spectroscopy
Murali, N. Bolton, P.H.	NHMFL Wesleyan Univ.	NHMFL NSF, NIH	Molecular Alignment in High Field
Logan, T.M. Murali, N.	FSU/NHMFL NHMFL	FSU	Suppressing ^{13}C-^{1}H Dipolar Cross-Relaxation in NOESY Spectra of Proteins
Logan, T.M.	FSU/NHMFL	NIH, Petroleum Research Fund	Structural Characterization of Peptides
Trewhella, J.	LANL	LANL	Study of Complexes Formed by Ca^{2+} Binding Proteins and Their Regulatory Targets
500 MHz NMR (Varian)			
Logan, T.M. Bonneau, R.	FSU/NHMFL FSU	Petroleum Research Fund	Rapid Amide Exchange in Unfolded Proteins
Logan, T.M.	FSU/NHMFL	NIH	Structure Determination of Mutant FKBP Proteins
Logan, T.M. Callihan, D.	FSU/NHMFL FSU	NIH, Petroleum Research Fund	Peptide Mimics of Unfolded Proteins
Cross, T.A. Xu, Feng	FSU/NHMFL FSU	NIH	Peptide - Solvent Interactions

*◊ Postdoc * Graduate Student # Undergraduate Student*

USER	INSTITUTION	FUNDING	PROJECT
Cross, T.A.	FSU/NHMFL	NIH	Peptide Structure in
Xu, Feng	FSU		Organic Solvents
Robert, J.	Univ. S. Fla		Study of Poly Peptides and Proteins
Gochin, M.	UC, San Francisco	NIH(GMS)	Use of Paramagnetic Shifts in NMR for Structure Determination
Bodenhausen, G.	NHMFL/FSU	NHMFL	Broadband Decoupling
Gochin, M.	UC, San Francisco		of Paramagnetic
Fu, R.	NHMFL	NHMFL	Macromolecules
600 MHz Wide Bore - NMR (BRUKER)			
Kinsey, S.	FSU/NHMFL	NSF	NMR Studies of
Ellington, R.	FSU/NHMFL		Lactate Permeation Mechanisms in Single Cell Bundles
Combs, C.	FSU/NHMFL	NSF	NMR Studies of the
Ellington, R.	FSU/NHMFL		Impact of Severe Acidosis on Cellular Energetics
Combs, C.	FSU/NHMFL	NSF	NMR Studies of
Kinsey, S.	FSU/NHMFL		Mitochondrial Sulfide
Ellington, R.	FSU/NHMFL		Oxidation
Doeller, J.	Univ. Alabama, Birmingham		
Kraus, D.	Univ. Alabama, Birmingham		
Kinsey, S.	FSU/NHMFL	NASA	Studies of Water and
Locke, B.	FSU/NHMFL		Diffusion in Gels
Moreland, T.	FSU/NHMFL		
300 MHz Wide Bore & Narrow Bore			
Bodenhausen, G.	NHMFL/FSU	NHMFL	Study of Enzyme
Post, C.B.	Purdue Univ.		C0-factor Complex
Burgner, J.W.	Purdue Univ.		
Zwahlen, C.	NHMFL	NHMFL	
Vincent, S.J.F.	NHMFL	NHMFL	
Bodenhusen, G.	NHMFL	NHMFL	Study of Chemical
Roe, D.C.	DuPont	DuPont	Exchange and
Fu, R.	NHMFL	NHMFL	Membrane
Zwahlen, C.	NHMFL	NHMFL	Properties
Vincent, S.J.F.	NHMFL	NHMFL	

*◊ Postdoc * Graduate Student # Undergraduate Student*

USER	INSTITUTION	FUNDING	PROJECT
Bodenhausen, G.	NHMFL/FSU	NHMFL	Study of a New DNA
Bolton, P.H.	Wesleyan Univ.		Structure
Zwahlen, C.	NHMFL	NHMFL	
Vincent, S.J.F.	NHMFL	NHMFL	
Bodenhusen, G.	NHMFL/FSU	NHMFL	Study of DNA
Leroy, J. L.	Ecole Polytech., France		Tetrad
Gueron, M.	Ecole Polytech., France		
Zwahlen, C.	NHMFL	NHMFL	
Vincent, S.J.F.	NHMFL	NHMFL	
Bodenhusen, G.	NHMFL/FSU	NHMFL	Study of Proteins
Logan, T.M.	FSU	NHMFL	Using Isotopically
Zwahlen, C.	NHMFL	NHMFL	(^{13}C, ^{15}N)
Vincent, S.J.F.	NHMFL	NHMFL	Enriched Proteins
Zwahlen, C.	NHMFL	NHMFL	Study of Calcium
Vincent, S.J.F.	NHMFL	NHMFL	Binding Protein by
Malliavin, T.	Univ. Montpellier I, France	CNRS	NMR
Bodenhusen, G.	NHMFL/FSU	NHMFL	Study of Peptides
Logan, T.M.	FSU	NHMFL	
Jeannerat, D.	NHMFL	NHMFL	
Bodenhausen, G.	NHMFL/FSU	NHMFL	Study of Taxol
Holton, R.A.	FSU	FSU	
Meersmann, T.	NHMFL	NHMFL	
Jeannerat, D.	NHMFL	NHMFL	
Peng, C.	NHMFL	NHMFL	
Bodenhausen, G.	NHMFL/FSU	NHMFL	Computer Analysis of
Yuan, C.	Chinese Academy of Sciences		NMR Spectra
Zheng, C.	Chinese Academy of Sciences		
Peng, C.	NHMFL	NHMFL	
Berhault, P.	CEA, France	CEA, France	Study of Lewis X
Desvaux, H.	CEA/NHMFL	CEA/NHMFL	Analog
Birlirakis, N.	CEA, France	CEA, France	
Rubinstenn, G.	ENS, France	Univ. Paris, VI	
Sinay, P.	ENS, France	Univ. Paris, VI	
Lippens, G.	Pasteur Institute, France	CNRS	Study of Cyclic Glucan
Desvaux, H.	CEA/NHMFL	CEA/NHMFL	

*◊ Postdoc * Graduate Student # Undergraduate Student*

USER	INSTITUTION	FUNDING	PROJECT
Bodenhausen, G.	NHMFL/FSU	NHMFL	Transmission Line Probe
Rosanske, D.	FSU	FSU	
Gullion, T.	FSU	FSU	
Schaefer, J.	Washington Univ.		
Fu, R.	NHMFL	NHMFL	
Bodenhausen, G.	NHMFL/FSU	NHMFL	Instrumentation for Studying Quadrupolar Nuclei
Gullion, T.	FSU		
Samoson, A.	Estonian Academy of Science	NATO	
Fu, R.	NHMFL	NHMFL	
Grant, D.M.	Univ. Utah	Univ. Utah	Investigation of Coupled Relaxation in Methyl Groups
Mayne, C.	Univ. Utah	Univ. Utah	
Chenon, M.T.	Univ. Utah	Univ. Utah	
Smith, S.A.	NHMFL	NHMFL	
Mayne, C.	Univ. Utah	Univ. Utah	Multi-Mode Relaxation in Molecules with Strong Scalar Coupling
Smith, S.A.	NHMFL	NHMFL	
Smith, S.A.	NHMFL	NHMFL	Relaxation and Exchange Effects in NMR Experiments
Bodenhausen, G.	NHMFL/FSU	NHMFL	
Skrynnikov, N.	McGill Univ., Montreal		

NHMFL - EMR Facility

USER	INSTITUTION	FUNDING	PROJECT
Talham, D.R.	UF	NHMFL	Broadband High Field AFMR Spectroscopy of Layered Antiferromagnets
Fanucci, G.	UF		
Krzystek, J.	NHMFL		
Brunel, L.C.	NHMFL/FSU		
Krzystek, J.	NHMFL	NHMFL and HFSO	DPPH as a Standard for High Frequency EPR Spectroscopy
Sienkiewicz, A.	Pol. Acad. Sci.		
Pardi, L.	NHMFL		
Brunel, L.C.	NHMFL/FSU		
Hoffman, B.M.	Northwestern U.	NHMFL	Multifrequency High Field EPR of Mn(III) Porphyrazines
Krzystek, J.	NHMFL		
Goldberg, D.P.	Northwestern U.		
Brunel, L.C.	NHMFL/FSU		
Brunel, L.C.	NHMFL/FSU	NHMFL	High Field ESR Studies of Pure and Zn Doped $CuGeO_3$
Hassan, A.	NHMFL/FSU		
Martins, G.	NHMFL		
Pardi, L.	NHMFL		
Cao, G.	NHMFL/FSU		
Delia, A.	NHMFL		
Laukamp, M.	FSU/NHMFL		
Dagotto, E.	FSU/NHMFL		

*◊ Postdoc * Graduate Student # Undergraduate Student*

USER	INSTITUTION	FUNDING	PROJECT
Meisel, M. Hassan, A. Pardi, L. Martins, G. Chou, L. Talham, D.R. Brunel, L.C.	UF NHMFL/FSU NHMFL NHMFL UF UF NHMFL/FSU	NHMFL	ESR Studies of the Haldane Spin System TMNIN
Maniero, A.L. Brunel, L.C. Brustolon, M. Chis, V.	NHMFL NHMFL/FSU Univ. of Padova Univ. of Padova	CNR Italy and NHMFL	A New Radical Detected by HF-EPR, ENDOR and Pulsed EPR in a Room Temperature Irradiated Single Crystal of Glycine
Furdyna, J. McCarty, A. Hassan, A. Herbette, S. Martins, G. Pardi, L. Brunel, L.C.	U. Notre Dame NHMFL/FSU NHMFL/FSU INSA, Toulouse NHMFL NHMFL NHMFL/FSU	NHMFL	High Field Electron Paramagnetic Resonance of $Cd_{0.7}Mn_{0.3}Se$
Dagotto, E. Martins, G. Hassan, A. Pardi, L. Brunel, L. C. Riera, J.	FSU/NHMFL NHMFL NHMFL/FSU NHMFL NHMFL/FSU Inst. Fisica Rosario	NHMFL	Rapid Suppression of the Spin Gap in Zn-Doped $CuGeO_3$ and $SrCu_2O_3$
Dagotto, E. Martins, G. Laukamp, M. Riera, J.	FSU/NHMFL NHMFL NHMFL Inst. Fisica Rosario	NHMFL	Local Enhancement of Antiferromagnetic Correlations by Nonmagnetic Impurities
Dagotto, E. Martins, G. Riera, J.	FSU/NHMFL NHMFL Inst. Fisica Rosario	NHMFL	Many-Body Basis-Set Reduction Applied to the Two-Dimensional t-J Model with Holes
Brunel, L.C. Whitaker, H. Martins, G. Pardi, L. Hassan, A. Cao, G.	NHMFL/FSU NHMFL/FSU NHMFL NHMFL NHMFL/FSU NHMFL/FSU	NHMFL	EPR Study of Linewidth and g-Anisotropy of $Y_{1-x}R_xBa_2Cu_3O_{6+\delta}$
Gatteschi, D. Pardi, L. Benelli, C.	Univ. of Florence NHMFL Univ. of Florence	Univ. of Florence	High Field EPR Spectra of a Tetranuclear Cluster

*◊ Postdoc * Graduate Student # Undergraduate Student*

USER	INSTITUTION	FUNDING	PROJECT
Gatteschi, D. Pardi, L. Sessoli, R. Caneschi, A. Brunel, L.C.	NHMFL NHMFL Univ. of Florence Univ. of Florence NHMFL/FSU	Univ. of Florence	Ferrimagnetic Resonance in a Molecular Based Magnetic Material
Brunel, L.C. Pardi, L. Redijk, J. Hulsbergen, F.U.	NHMFL/FSU NHMFL Univ. of Neimegen Univ. of Neimegen	NHMFL	Direct Measurement of Zero Field Splitting in a One-Dimensional Heisenberg Antiferromagnet, by HF
Dalal, N.S. Cage, B. Hassan, A. Pardi, L. Krzystek, J. Brunel, L.C.	FSU FSU NHMFL/FSU NHMFL NHMFL NHMFL/FSU	NHMFL	High-Field EPR Spectroscopy of Low-Dimensional Magnetic Systems: The Role of Exchange Effects and g-Strain in Determining Spectral Resolution

NHMFL - ICR Facility

USER	INSTITUTION	FUNDING	PROJECT
Laude, D.A. Drader, J.J.*	Univ. Texas, Austin Univ. Texas, Austin	NSF ICR Facility	6 T In-Bore ESI
McLafferty, F.W. Kelleher, N.L.* Siegel, M.M.	Cornell Univ. Cornell Univ. Wyeth-Ayerst	NSF ICR Facility	9.4 T ESI of Large Proteins
Costello, C. Reinhold, B.B.◊	Boston Univ. Boston Univ.	NSF ICR Facility	Oligosaccharide Identification and Sequencing
Eyler, J.R. Nawrocki, J.* Wigger, M. Benner, S.	UF UF UF UF	NSF ICR Facility	9.4 T ESI of Peptide Combinatorial Library
Eyler, J.R. Milgram, E.*	UF UF	NSF ICR Facility	ICP/FT-ICR
Rice, J.A. Brown, T.L.* Laude, D.A. Robinson, J.M.*	South Dakota St. South Dakota St. Univ. Texas, Austin Univ. Texas, Austin	NSF ICR Facility	9.4 T ESI of Humic Substances

*◊ Postdoc * Graduate Student # Undergraduate Student*

USER	INSTITUTION	FUNDING	PROJECT
Gaskell, S. **Naito, Y.◊**	Univ. Manchester Univ. Manchester	NSF ICR Facility	Mechanism of Peptide Cleavage
Wood, T.D. Dufresne, C.P.*	SUNY, Buffalo SUNY, Buffalo	NSF ICR Facility	9.4 T ESI of G-6-Kinase
Hunt, D.F. Marto, J.A.◊	Univ. Virginia Univ. Virginia	NSF ICR Facility	Peptide Sequencing
Amster, I.J. Taylor, P.K.* Kulkarni, S.S.*	Univ. Georgia Univ. Georgia Univ. Georgia	NSF ICR Facility	9.4 T ESI of Noncovalent Multimeric Proteins
Griffey, R.H. Greig, M.J. Laude, D.A. Robinson, J.M.*	ISIS Pharmaceutical ISIS Pharmaceutical Univ. Texas, Austin Univ. Texas, Austin	NSF ICR Facility	9.4 T ESI of Oligonucleotides
Vala, M. Ekern, S.◊	UF UF	NHMFL	Photodissociation of Proposed Interstellar Molecules

*◊ Postdoc * Graduate Student # Undergraduate Student*

KEY PERSONNEL & COMMITTEES

Appendix E

NHMFL Key Personnel

Jack Crow, Director
Don Parkin, Co-Principal Investigator, LANL
Neil Sullivan, Co-Principal Investigator, UF
Hans Schneider-Muntau, Deputy Director
Robert Schrieffer, Chief Scientist

National High Magnetic Field Laboratory
Florida State University
1800 E. Paul Dirac Dr.
Tallahassee, FL 32310
(904) 644-0311

Continuous Field Facilities
Tallahassee, FL
Bruce Brandt
(904) 644-4068
brandt@magnet.fsu.edu

Pulsed Field Facilities
Los Alamos, NM
Laurence Campbell
(505) 667-1482
ljc@lanl.gov

Magnetic Resonance Facilities
Tallahassee, FL
(904) 644-1933
Louis-Claude Brunel (EMR)
brunel@magnet.fsu.edu
Alan Marshall (ICR and NMR)
marshall@magnet.fsu.edu

Gainesville, FL
Thomas Mareci (MRI/S)
(352) 392-3375
thmareci@csbnmr.health.ufl.edu

Ultra-High B/T Facility
Gainesville, FL
Jian-sheng Xia
(352) 392-8869
jsxia@phys.ufl.edu

NHMFL Committees

External Advisory Committee

Members of the External Advisory Committee are appointed by the Chancellor of the State University System. The committee reviews and evaluates overall performance and provides recommendations to the Chancellor. It meets at least annually.

Eric Jones, Chair
Sandia National Laboratories

Theoren Smith
IBM-Watson Research Center

Peter Roemer
Advanced Mammography Systems

Donald Gubser
Naval Research Laboratory

George Crabtree
Argonne National Laboratory

Brian Maple
University of California at San Diego

Carl Rosner
Intermagnetics General Corporation

Ray Shaw
Varian Associates, Inc.

Eric Oldfield
University of Illinois at Urbana-Champaign

Raymond Orbach
University of California at Riverside

Peter Wyder
High Field Magnet Laboratory, Grenoble, France

Representative of
Southeastern University Research Association (SURA)

Users' Committee

Members of the Users' Committee are appointed by the Director in consultation with the National Science Foundation and the NHMFL user community. The committee provides guidance on the needs and policies related to the development and utilization of the magnet laboratory's facilities and equipment in support of the users.

Mike Naughton, Chair
SUNY Buffalo

David Awschalom
University of California at Santa Barbara

James Brooks
Florida State University and National High Magnetic Field Laboratory

Paul Chaikin
Princeton University

Gil Clark
University of California at Los Angeles

Naresh Dalal
West Virginia University

Roy Goodrich
Louisiana State University

Clive Perry
Northeastern University

Horst Störmer
AT&T Bell Laboratories

Stan Tozer
National High Magnetic Field Laboratory

Regitze Vold
University of California at San Diego

Eric Zuiderweg
University of Michigan

Research Program Committee

The Research Program Committee (RPC) is charged with promoting the NHMFL In-House Research Program (IHRP) and with encouraging the highest quality research among members of the NHMFL research community. The committee evaluates research opportunities available to the NHMFL and recommends programs for the use of facilities and resources of the NHMFL. The RPC oversees the IHRP, encourages the formation of collaborative research efforts, establishes worldwide channels for communication, and identifies cutting-edge high magnetic field research programs. The committee, through its chair, administers the funding of the IHRP. Members of the RPC also participate in the Users Program proposal review and evaluation.

NHMFL/FSU

James Brooks
Zachary Fisk
Lev Gor'kov
Alan Marshall
Stan Tozer
Stephan von Molnar

NHMFL/UF

John Graybeal, Chair
Kevin Ingersent
Thomas Mareci

NHMFL/LANL

Alan Bishop
Chris Hammel
Joe Thompson

Executive Committee

The NHMFL Executive Committee is charged with reviewing and advising on numerous issues including organization, staffing, resource allocation, and budgeting. Members take into account the objectives and mission of the laboratory, external reviews, and internal evaluations of the overall program. The committee is chaired by the Director of the NHMFL.

Jack E. Crow, Director

Don Parkin, Co-Principal Investigator, LANL

Neil Sullivan, Co-Principal Investigator, UF

J. Robert Schrieffer, Chief Scientist

Hans Schneider-Muntau, Deputy Director and Director of Magnet Science and Technology

Laurence Campbell, Director of Pulsed Field Facility

Bruce Brandt, Director of Continuous Fields Facility

John Graybeal, Chair of Research Program Committee

Louis-Claude Brunel, Center for Interdisciplinary Magnetic Resonance (CIMAR) Representative

Jim Ferner, Chief Administrative Officer

Janet Patten, Director of Public and Governmental Relations